

# International Journal on Advances in Intelligent Systems



The *International Journal on Advances in Intelligent Systems* is Published by IARIA.

ISSN: 1942-2679

journals site: <http://www.ariajournals.org>

contact: [petre@aria.org](mailto:petre@aria.org)

Responsibility for the contents rests upon the authors and not upon IARIA, nor on IARIA volunteers, staff, or contractors.

IARIA is the owner of the publication and of editorial aspects. IARIA reserves the right to update the content for quality improvements.

Abstracting is permitted with credit to the source. Libraries are permitted to photocopy or print, providing the reference is mentioned and that the resulting material is made available at no cost.

Reference should mention:

*International Journal on Advances in Intelligent Systems, issn 1942-2679*  
*vol. 8, no. 3 & 4, year 2015, [http://www.ariajournals.org/intelligent\\_systems/](http://www.ariajournals.org/intelligent_systems/)*

The copyright for each included paper belongs to the authors. Republishing of same material, by authors or persons or organizations, is not allowed. Reprint rights can be granted by IARIA or by the authors, and must include proper reference.

Reference to an article in the journal is as follows:

<Author list>, "<Article title>"  
*International Journal on Advances in Intelligent Systems, issn 1942-2679*  
*vol. 8, no. 3 & 4, year 2015, <start page>:<end page> , [http://www.ariajournals.org/intelligent\\_systems/](http://www.ariajournals.org/intelligent_systems/)*

IARIA journals are made available for free, proving the appropriate references are made when their content is used.

Sponsored by IARIA

[www.aria.org](http://www.aria.org)

Copyright © 2015 IARIA

**Editor-in-Chief**

Freimut Bodendorf, University of Erlangen-Nuernberg, Germany

**Editorial Advisory Board**

Josef Noll, UiO/UNIK, Norway

**Editorial Board**

Jemal Abawajy, Deakin University - Victoria, Australia

Sherif Abdelwahed, Mississippi State University, USA

Habtamu Abie, Norwegian Computing Center/Norsk Regnesentral-Blindern, Norway

Siby Abraham, University of Mumbai, India

Witold Abramowicz, Poznan University of Economics, Poland

Imad Abugessaisa, Karolinska Institutet, Sweden

Arden Agopyan, CloudArena, Turkey

Leila Alem, The Commonwealth Scientific and Industrial Research Organisation (CSIRO), Australia

Panos Alexopoulos, iSOCO, Spain

Vincenzo Ambriola, Università di Pisa, Italy

Junia Anacleto, Federal University of Sao Carlos, Brazil

Razvan Andonie, Central Washington University, USA

Cosimo Anglano, DiSIT - Computer Science Institute, Università del Piemonte Orientale, Italy

Richard Anthony, University of Greenwich, UK

Avi Arampatzis, Democritus University of Thrace, Greece

Sofia Athenikos, IPsoft, USA

Isabel Azevedo, ISEP-IPP, Portugal

Costin Badica, University of Craiova, Romania

Ebrahim Bagheri, Athabasca University, Canada

Fernanda Baiao, Federal University of the state of Rio de Janeiro (UNIRIO), Brazil

Flavien Balbo, University of Paris Dauphine, France

Suliaman Bani-Ahmad, School of Information Technology, Al-Balqa Applied University, Jordan

Ali Barati, Islamic Azad University, Dezful Branch, Iran

Henri Basson, University of Lille North of France (Littoral), France

Carlos Becker Westphall, Federal University of Santa Catarina, Brazil

Ali Beklen, Cloud Arena, Turkey

Petr Berka, University of Economics, Czech Republic

Julita Bermejo-Alonso, Universidad Politécnica de Madrid, Spain

Aurelio Bermúdez Marín, Universidad de Castilla-La Mancha, Spain

Lasse Berntzen, Vestfold University College - Tønsberg, Norway

Michela Bertolotto, University College Dublin, Ireland

Ateet Bhalla, Independent Consultant, India  
Freimut Bodendorf, Universität Erlangen-Nürnberg, Germany  
Karsten Böhm, FH Kufstein Tirol - University of Applied Sciences, Austria  
Pierre Borne, Ecole Centrale de Lille, France  
Christos Bouras, University of Patras, Greece  
Anne Boyer, LORIA - Nancy Université / KIWI Research team, France  
Stainam Brandao, COPPE/Federal University of Rio de Janeiro, Brazil  
Stefano Bromuri, University of Applied Sciences Western Switzerland, Switzerland  
Vít Bršlica, University of Defence - Brno, Czech Republic  
Dumitru Burdescu, University of Craiova, Romania  
Diletta Romana Cacciagrano, University of Camerino, Italy  
Kenneth P. Camilleri, University of Malta - Msida, Malta  
Paolo Campegnani, University of Rome Tor Vergata, Italy  
Marcelino Campos Oliveira Silva, Chemtech - A Siemens Business / Federal University of Rio de Janeiro, Brazil  
Ozgu Can, Ege University, Turkey  
José Manuel Cantera Fonseca, Telefónica Investigación y Desarrollo (R&D), Spain  
Juan-Vicente Capella-Hernández, Universitat Politècnica de València, Spain  
Miriam A. M. Capretz, The University of Western Ontario, Canada  
Massimiliano Caramia, University of Rome "Tor Vergata", Italy  
Davide Carboni, CRS4 Research Center - Sardinia, Italy  
Luis Carriço, University of Lisbon, Portugal  
Rafael Casado Gonzalez, Universidad de Castilla - La Mancha, Spain  
Michelangelo Ceci, University of Bari, Italy  
Fernando Cerdan, Polytechnic University of Cartagena, Spain  
Alexandra Suzana Cernian, University "Politehnica" of Bucharest, Romania  
Sukalpa Chanda, Gjøvik University College, Norway  
David Chen, University Bordeaux 1, France  
Po-Hsun Cheng, National Kaohsiung Normal University, Taiwan  
Dickson Chiu, Dickson Computer Systems, Hong Kong  
Sunil Choenni, Research & Documentation Centre, Ministry of Security and Justice / Rotterdam University of Applied Sciences, The Netherlands  
Ryszard S. Choras, University of Technology & Life Sciences, Poland  
Smitashree Choudhury, Knowledge Media Institute, The UK Open University, UK  
William Cheng-Chung Chu, Tunghai University, Taiwan  
Christophe Claramunt, Naval Academy Research Institute, France  
Cesar A. Collazos, Universidad del Cauca, Colombia  
Phan Cong-Vinh, NTT University, Vietnam  
Christophe Cruz, University of Bourgogne, France  
Beata Czarnacka-Chrobot, Warsaw School of Economics, Department of Business Informatics, Poland  
Claudia d'Amato, University of Bari, Italy  
Sérgio Roberto P. da Silva, Universidade Estadual de Maringá - Paraná, Brazil  
Mirela Danubianu, "Stefan cel Mare" University of Suceava, Romania  
Dragos Datcu, Netherlands Defense Academy / Delft University of Technology, The Netherlands  
Antonio De Nicola, ENEA, Italy  
Claudio de Castro Monteiro, Federal Institute of Education, Science and Technology of Tocantins, Brazil  
Noel De Palma, Joseph Fourier University, France

Zhi-Hong Deng, Peking University, China  
Stojan Denic, Toshiba Research Europe Limited, UK  
Vivek S. Deshpande, MIT College of Engineering - Pune, India  
Sotirios Ch. Diamantas, Pusan National University, South Korea  
Leandro Dias da Silva, Universidade Federal de Alagoas, Brazil  
Jerome Dinet, Univeristé Paul Verlaine - Metz, France  
Jianguo Ding, University of Luxembourg, Luxembourg  
Yulin Ding, Defence Science & Technology Organisation Edinburgh, Australia  
Alexiei Dingli, University of Malta, Malta  
Mihaela Dinsoreanu, Technical University of Cluj-Napoca, Romania  
Ioanna Dionysiou, University of Nicosia, Cyprus  
Roland Dodd, CQUniversity, Australia  
Nima Dokoohaki, Royal Institute of Technology (KTH)-Kista, Sweden  
Suzana Dragicevic, Simon Fraser University- Burnaby, Canada  
Mauro Dragone, University College Dublin (UCD), Ireland  
Marek J. Druzdzel, University of Pittsburgh, USA  
Carlos Duarte, University of Lisbon, Portugal  
Raimund K. Ege, Northern Illinois University, USA  
Jorge Ejarque, Barcelona Supercomputing Center, Spain  
Larbi Esmahi, Athabasca University, Canada  
Simon G. Fabri, University of Malta, Malta  
Umar Farooq, Amazon.com, USA  
Mehdi Farshbaf-Sahih-Sorkhabi, Azad University - Tehran / Fanavaran co., Tehran, Iran  
Anna Fensel, Semantic Technology Institute (STI) Innsbruck and FTW Forschungszentrum Telekommunikation Wien, Austria  
Stenio Fernandes, Federal University of Pernambuco (CIn/UFPE), Brazil  
Oscar Ferrandez Escamez, University of Utah, USA  
Agata Filipowska, Poznan University of Economics, Poland  
Ziny Flikop, Scientist, USA  
Adina Magda Florea, University "Politehnica" of Bucharest, Romania  
Francesco Fontanella, University of Cassino and Southern Lazio, Italy  
Panagiotis Fotaris, University of Macedonia, Greece  
Enrico Francesconi, ITTIG - CNR / Institute of Legal Information Theory and Techniques / Italian National Research Council, Italy  
Rita Francese, Università di Salerno - Fisciano, Italy  
Bernhard Freudenthaler, Software Competence Center Hagenberg GmbH, Austria  
Sören Frey, Daimler TSS GmbH, Germany  
Steffen Fries, Siemens AG, Corporate Technology - Munich, Germany  
Somchart Fugkeaw, Thai Digital ID Co., Ltd., Thailand  
Naoki Fukuta, Shizuoka University, Japan  
Mathias Funk, Eindhoven University of Technology, The Netherlands  
Adam M. Gadomski, Università degli Studi di Roma La Sapienza, Italy  
Alex Galis, University College London (UCL), UK  
Crescenzo Gallo, Department of Clinical and Experimental Medicine - University of Foggia, Italy  
Matjaz Gams, Jozef Stefan Institute-Ljubljana, Slovenia  
Raúl García Castro, Universidad Politécnica de Madrid, Spain

Fabio Gasparetti, Roma Tre University - Artificial Intelligence Lab, Italy  
Joseph A. Giampapa, Carnegie Mellon University, USA  
George Giannakopoulos, NCSR Demokritos, Greece  
David Gil, University of Alicante, Spain  
Harald Gjermundrod, University of Nicosia, Cyprus  
Angelantonio Gnazzo, Telecom Italia - Torino, Italy  
Luis Gomes, Universidade Nova Lisboa, Portugal  
Nan-Wei Gong, MIT Media Laboratory, USA  
Francisco Alejandro Gonzale-Horta, National Institute for Astrophysics, Optics, and Electronics (INAOE), Mexico  
Sotirios K. Goudos, Aristotle University of Thessaloniki, Greece  
Victor Govindaswamy, Texas A&M University-Texarkana, USA  
Gregor Grambow, University of Ulm, Germany  
Fabio Grandi, University of Bologna, Italy  
Andrina Granić, University of Split, Croatia  
Carmine Gravino, Università degli Studi di Salerno, Italy  
Michael Grottko, University of Erlangen-Nuremberg, Germany  
Vic Grout, Glyndŵr University, UK  
Maik Günther, Stadtwerke München GmbH, Germany  
Francesco Guerra, University of Modena and Reggio Emilia, Italy  
Alessio Gugliotta, Innova SPA, Italy  
Richard Gunstone, Bournemouth University, UK  
Fikret Gurgen, Bogazici University, Turkey  
Maki Habib, The American University in Cairo, Egypt  
Till Halbach Røssvoll, Norwegian Computing Center, Norway  
Jameleddine Hassine, King Fahd University of Petroleum & Mineral (KFUPM), Saudi Arabia  
Ourania Hatzi, Harokopio University of Athens, Greece  
Yulan He, Aston University, UK  
Kari Heikkinen, Lappeenranta University of Technology, Finland  
Cory Henson, Wright State University / Kno.e.sis Center, USA  
Arthur Herzog, Technische Universität Darmstadt, Germany  
Rattikorn Hewett, Whitacre College of Engineering, Texas Tech University, USA  
Celso Massaki Hirata, Instituto Tecnológico de Aeronáutica - São José dos Campos, Brazil  
Jochen Hirth, University of Kaiserslautern, Germany  
Bernhard Hollunder, Hochschule Furtwangen University, Germany  
Thomas Holz, University College Dublin, Ireland  
Władysław Homenda, Warsaw University of Technology, Poland  
Carolina Howard Felicíssimo, Schlumberger Brazil Research and Geoengineering Center, Brazil  
Weidong (Tony) Huang, CSIRO ICT Centre, Australia  
Xiaodi Huang, Charles Sturt University - Albury, Australia  
Eduardo Huedo, Universidad Complutense de Madrid, Spain  
Marc-Philippe Huget, University of Savoie, France  
Chi Hung, Tsinghua University, China  
Chih-Cheng Hung, Southern Polytechnic State University - Marietta, USA  
Edward Hung, Hong Kong Polytechnic University, Hong Kong  
Muhammad Iftikhar, Universiti Malaysia Sabah (UMS), Malaysia  
Prateek Jain, Ohio Center of Excellence in Knowledge-enabled Computing, Kno.e.sis, USA

Wassim Jaziri, Miracl Laboratory, ISIM Sfax, Tunisia  
Hoyoung Jeung, SAP Research Brisbane, Australia  
Yiming Ji, University of South Carolina Beaufort, USA  
Jinlei Jiang, Department of Computer Science and Technology, Tsinghua University, China  
Weirong Jiang, Juniper Networks Inc., USA  
Hanmin Jung, Korea Institute of Science & Technology Information, Korea  
Ilya S. Kabak, "Stankin" Moscow State Technological University, Russia  
Eleanna Kafeza, Athens University of Economics and Business, Greece  
Hermann Kaindl, Vienna University of Technology, Austria  
Ahmed Kamel, Concordia College, Moorhead, Minnesota, USA  
Rajkumar Kannan, Bishop Heber College(Autonomous), India  
Fazal Wahab Karam, Norwegian University of Science and Technology (NTNU), Norway  
Dimitrios A. Karras, Chalkis Institute of Technology, Hellas  
Koji Kashihara, The University of Tokushima, Japan  
Nittaya Kerdprasop, Suranaree University of Technology, Thailand  
Katia Kermanidis, Ionian University, Greece  
Serge Kernbach, University of Stuttgart, Germany  
Nhien An Le Khac, University College Dublin, Ireland  
Reinhard Klemm, Avaya Labs Research, USA  
Ah-Lian Kor, Leeds Metropolitan University, UK  
Arne Koschel, Applied University of Sciences and Arts, Hannover, Germany  
George Kousiouris, NTUA, Greece  
Philipp Kremer, German Aerospace Center (DLR), Germany  
Dalia Kriksciuniene, Vilnius University, Lithuania  
Markus Kunde, German Aerospace Center, Germany  
Dharmender Singh Kushwaha, Motilal Nehru National Institute of Technology, India  
Andrew Kusiak, The University of Iowa, USA  
Dimosthenis Kyriazis, National Technical University of Athens, Greece  
Vitaveska Lanfranchi, Research Fellow, OAK Group, University of Sheffield, UK  
Mikel Larrea, University of the Basque Country UPV/EHU, Spain  
Philippe Le Parc, University of Brest, France  
Gyu Myoung Lee, Liverpool John Moores University, UK  
Kyu-Chul Lee, Chungnam National University, South Korea  
Tracey Kah Mein Lee, Singapore Polytechnic, Republic of Singapore  
Daniel Lemire, LICEF Research Center, Canada  
Haim Levkowitz, University of Massachusetts Lowell, USA  
Kuan-Ching Li, Providence University, Taiwan  
Tsai-Yen Li, National Chengchi University, Taiwan  
Yangmin Li, University of Macau, Macao SAR  
Jian Liang, Nimbus Centre, Cork Institute of Technology, Ireland  
Haibin Liu, China Aerospace Science and Technology Corporation, China  
Lu Liu, University of Derby, UK  
Qing Liu, The Commonwealth Scientific and Industrial Research Organisation (CSIRO), Australia  
Shih-Hsi "Alex" Liu, California State University - Fresno, USA  
Xiaoqing (Frank) Liu, Missouri University of Science and Technology, USA  
David Lizcano, Universidad a Distancia de Madrid, Spain

Henrique Lopes Cardoso, LIACC / Faculty of Engineering, University of Porto, Portugal  
Sandra Lovrencic, University of Zagreb, Croatia  
Jun Luo, Shenzhen Institutes of Advanced Technology, Chinese Academy of Sciences, China  
Prabhat K. Mahanti, University of New Brunswick, Canada  
Jacek Mandziuk, Warsaw University of Technology, Poland  
Herwig Mannaert, University of Antwerp, Belgium  
Yannis Manolopoulos, Aristotle University of Thessaloniki, Greece  
Antonio Maria Rinaldi, Università di Napoli Federico II, Italy  
Ali Masoudi-Nejad, University of Tehran, Iran  
Constandinos Mavromoustakis, University of Nicosia, Cyprus  
Zulfiqar Ali Memon, Sukkur Institute of Business Administration, Pakistan  
Andreas Merentitis, AGT Group (R&D) GmbH, Germany  
Jose Merseguer, Universidad de Zaragoza, Spain  
Frederic Migeon, IRIT/Toulouse University, France  
Harald Milchrahm, Technical University Graz, Institute for Software Technology, Austria  
Les Miller, Iowa State University, USA  
Marius Minea, University POLITEHNICA of Bucharest, Romania  
Yasser F. O. Mohammad, Assiut University, Egypt  
Shahab Mokarizadeh, Royal Institute of Technology (KTH) - Stockholm, Sweden  
Martin Molhanec, Czech Technical University in Prague, Czech Republic  
Charalampos Moschopoulos, KU Leuven, Belgium  
Mary Luz Mouronte López, Ericsson S.A., Spain  
Henning Müller, University of Applied Sciences Western Switzerland - Sierre (HES SO), Switzerland  
Susana Munoz Hernández, Universidad Politécnica de Madrid, Spain  
Adrian Muscat, University of Malta, Malta  
Bela Mutschler, Hochschule Ravensburg-Weingarten, Germany  
Deok Hee Nam, Wilberforce University, USA  
Fazel Naghdy, University of Wollongong, Australia  
Joan Navarro, Research Group in Distributed Systems (La Salle - Ramon Llull University), Spain  
Rui Neves Madeira, Instituto Politécnico de Setúbal / Universidade Nova de Lisboa, Portugal  
Toàn Nguyễn, INRIA Grenoble Rhone-Alpes/ Montbonnot, France  
Andrzej Niesler, Institute of Business Informatics, Wroclaw University of Economics, Poland  
Kouzou Ohara, Aoyama Gakuin University, Japan  
Jonice Oliveira, Universidade Federal do Rio de Janeiro, Brazil  
Ian Oliver, Nokia Location & Commerce, Finland / University of Brighton, UK  
Michael Adeyeye Oluwasegun, University of Cape Town, South Africa  
Sigeru Omatu, Osaka Institute of Technology, Japan  
Sascha Opletal, University of Stuttgart, Germany  
Fakri Othman, Cardiff Metropolitan University, UK  
Enn Õunapuu, Tallinn University of Technology, Estonia  
Jeffrey Junfeng Pan, Facebook Inc., USA  
Hervé Panetto, University of Lorraine, France  
Małgorzata Pankowska, University of Economics, Poland  
Harris Papadopoulos, Frederick University, Cyprus  
Laura Papaleo, ICT Department - Province of Genoa & University of Genoa, Italy  
Agis Papantoniou, National Technical University of Athens, Greece

Thanasis G. Papaioannou, École Polytechnique Fédérale de Lausanne (EPFL), Switzerland  
Andreas Papasalouros, University of the Aegean, Greece  
Eric Paquet, National Research Council / University of Ottawa, Canada  
Kunal Patel, Ingenuity Systems, USA  
Carlos Pedrinaci, Knowledge Media Institute, The Open University, UK  
Yoseba Peña, University of Deusto - DeustoTech (Basque Country), Spain  
Cathryn Peoples, University of Ulster, UK  
Asier Perillos, University of Deusto, Spain  
Christian Percebois, Université Paul Sabatier - IRIT, France  
Andrea Perego, European Commission, Joint Research Centre, Italy  
Mark Perry, University of Western Ontario/Faculty of Law/ Faculty of Science - London, Canada  
Willy Picard, Poznań University of Economics, Poland  
Meikel Poess, Oracle, USA  
Agostino Poggi, Università degli Studi di Parma, Italy  
R. Ponnusamy, Madha Engineering College-Anna University, India  
Dorin Popescu, University of Craiova, Romania  
Stefan Poslad, Queen Mary University of London, UK  
Wendy Powley, Queen's University, Canada  
Radu-Emil Precup, "Politehnica" University of Timisoara, Romania  
Jerzy Prekurat, Canadian Bank Note Co. Ltd., Canada  
Didier Puzenat, Université des Antilles et de la Guyane, France  
Sita Ramakrishnan, Monash University, Australia  
Elmano Ramalho Cavalcanti, Federal University of Campina Grande, Brazil  
Juwel Rana, Luleå University of Technology, Sweden  
Martin Randles, School of Computing and Mathematical Sciences, Liverpool John Moores University, UK  
Christoph Rasche, University of Paderborn, Germany  
Ann Reddipogu, ManyWorlds UK Ltd, UK  
Ramana Reddy, West Virginia University, USA  
René Reiners, Fraunhofer FIT - Sankt Augustin, Germany  
Paolo Remagnino, Kingston University - Surrey, UK  
Sebastian Rieger, University of Applied Sciences Fulda, Germany  
Andreas Riener, Johannes Kepler University Linz, Austria  
Ivan Rodero, NSF Center for Autonomic Computing, Rutgers University - Piscataway, USA  
Joel Rodrigues, Instituto de Telecomunicações / University of Beira Interior, Portugal  
Alejandro Rodríguez González, University Carlos III of Madrid, Spain  
Paolo Romano, INESC-ID Lisbon, Portugal  
Agostinho Rosa, Instituto de Sistemas e Robótica, Portugal  
José Rouillard, University of Lille, France  
Paweł Różycki, University of Information Technology and Management (UITM) in Rzeszów, Poland  
Igor Ruiz-Agundez, DeustoTech, University of Deusto, Spain  
Michele Ruta, Politecnico di Bari, Italy  
Melike Sah, Trinity College Dublin, Ireland  
Francesc Saigi Rubió, Universitat Oberta de Catalunya, Spain  
Abdel-Badeeh M. Salem, Ain Shams University, Egypt  
Yacine Sam, Université François-Rabelais Tours, France  
Ismael Sanz, Universitat Jaume I, Spain

Ricardo Sanz, Universidad Politecnica de Madrid, Spain  
Marcello Sarini, Università degli Studi Milano-Bicocca - Milano, Italy  
Munehiko Sasajima, I.S.I.R., Osaka University, Japan  
Minoru Sasaki, Ibaraki University, Japan  
Hiroyuki Sato, University of Tokyo, Japan  
Jürgen Sauer, Universität Oldenburg, Germany  
Patrick Sayd, CEA List, France  
Dominique Scapin, INRIA - Le Chesnay, France  
Kenneth Scerri, University of Malta, Malta  
Adriana Schiopoiu Burlea, University of Craiova, Romania  
Rainer Schmidt, Austrian Institute of Technology, Austria  
Bruno Schulze, National Laboratory for Scientific Computing - LNCC, Brazil  
Wieland Schwinger, Johannes Kepler University Linz, Austria  
Hans-Werner Sehring, T-Systems Multimedia Solutions GmbH, Germany  
Paulo Jorge Sequeira Gonçalves, Polytechnic Institute of Castelo Branco, Portugal  
Sandra Sendra Compte, Polytechnic University of Valencia, Spain  
Kewei Sha, Oklahoma City University, USA  
Roman Y. Shtykh, Rakuten, Inc., Japan  
Robin JS Sloan, University of Abertay Dundee, UK  
Vasco N. G. J. Soares, Instituto de Telecomunicações / University of Beira Interior / Polytechnic Institute of Castelo Branco, Portugal  
Don Sofge, Naval Research Laboratory, USA  
Christoph Sondermann-Woelke, Universitaet Paderborn, Germany  
George Spanoudakis, City University London, UK  
Vladimir Stantchev, SRH University Berlin, Germany  
Claudius Stern, University of Paderborn, Germany  
Mari Carmen Suárez-Figueroa, Universidad Politécnica de Madrid (UPM), Spain  
Kåre Synnes, Luleå University of Technology, Sweden  
Ryszard Tadeusiewicz, AGH University of Science and Technology, Poland  
Yehia Taher, ERISS - Tilburg University, The Netherlands  
Yutaka Takahashi, Senshu University, Japan  
Dan Tamir, Texas State University, USA  
Jinhui Tang, Nanjing University of Science and Technology, P.R. China  
Yi Tang, Chinese Academy of Sciences, China  
John Terzakis, Intel, USA  
Sotirios Terzis, University of Strathclyde, UK  
Vagan Terziyan, University of Jyvaskyla, Finland  
Ioan Toma, STI Innsbruck/University Innsbruck, Austria  
Lucio Tommaso De Paolis, Department of Innovation Engineering - University of Salento, Italy  
Davide Tosi, Università degli Studi dell'Insubria, Italy  
Raquel Trillo Lado, University of Zaragoza, Spain  
Tuan Anh Trinh, Budapest University of Technology and Economics, Hungary  
Simon Tsang, Applied Communication Sciences, USA  
Theodore Tsiligiridis, Agricultural University of Athens, Greece  
Antonios Tsourdos, Cranfield University, UK  
José Valente de Oliveira, University of Algarve, Portugal

Eugen Volk, University of Stuttgart, Germany  
Mihaela Vranić, University of Zagreb, Croatia  
Chieh-Yih Wan, Intel Labs, Intel Corporation, USA  
Jue Wang, Washington University in St. Louis, USA  
Shenghui Wang, OCLC Leiden, The Netherlands  
Zhonglei Wang, Karlsruhe Institute of Technology (KIT), Germany  
Laurent Wendling, University Descartes (Paris 5), France  
Maarten Weyn, University of Antwerp, Belgium  
Nancy Wiegand, University of Wisconsin-Madison, USA  
Alexander Wijesinha, Towson University, USA  
Eric B. Wolf, US Geological Survey, Center for Excellence in GIScience, USA  
Ouri Wolfson, University of Illinois at Chicago, USA  
Yingcai Xiao, The University of Akron, USA  
Reuven Yagel, The Jerusalem College of Engineering, Israel  
Fan Yang, Nuance Communications, Inc., USA  
Maribel Yasmina Santos, University of Minho, Portugal  
Zhenzhen Ye, Systems & Technology Group, IBM, US A  
Jong P. Yoon, MATH/CIS Dept, Mercy College, USA  
Shigang Yue, School of Computer Science, University of Lincoln, UK  
Constantin-Bala Zamfirescu, "Lucian Blaga" Univ. of Sibiu, Romania  
Claudia Zapata, Pontificia Universidad Católica del Perú, Peru  
Marek Zaremba, University of Quebec, Canada  
Filip Zavoral, Charles University Prague, Czech Republic  
Yuting Zhao, University of Aberdeen, UK  
Hai-Tao Zheng, Graduate School at Shenzhen, Tsinghua University, China  
Zibin (Ben) Zheng, Shenzhen Research Institute, The Chinese University of Hong Kong, Hong Kong  
Bin Zhou, University of Maryland, Baltimore County, USA  
Alfred Zimmermann, Reutlingen University - Faculty of Informatics, Germany  
Wolf Zimmermann, Martin-Luther-University Halle-Wittenberg, Germany

**CONTENTS**

*pages: 233 - 244*

**Pictogram Creation with Sensory Evaluation Method Based on Multiplex Sign Languages**

Naotsune Hosono, Keio University, and Oki Consulting Solutions, Japan  
Hiromitsu Inoue, Chiba Prefectural University of Health Sciences, Japan  
Miwa Nakanishi, Keio University, Japan  
Yutaka Tomita, Keio University, Japan

*pages: 245 - 254*

**Effects of Boundary Damping on Natural Frequencies in Bending Vibrations of Intelligent Vibrissa Tactile Systems**

Carsten Behn, Ilmenau University of Technology, Germany  
Christoph Will, Ilmenau University of Technology, Germany  
Joachim Steigenberger, Ilmenau University of Technology, Germany

*pages: 255 - 265*

**On the Potential of Grammar Features for Automated Author Profiling**

Michael Tschuggnall, Institute for Computer Science, University of Innsbruck, Austria  
Günther Specht, Institute for Computer Science, University of Innsbruck, Austria

*pages: 266 - 277*

**An Analysis to Improve Voltage Stability in Smart Grids by Regulating Active Power in Intelligent Buildings**

Abid Ahmad Khan, University of Applied Sciences Darmstadt, Germany  
Michael Massoth, University of Applied Sciences Darmstadt, Germany  
Torsten Wiens, University of Applied Sciences Darmstadt, Germany

*pages: 278 - 287*

**Practical Aspects of Ontology-Based Analysis and Reasoning for Law Information Represented in Textual Form**

Raoul Schönhof, HLRS (High Performance Computing Center Stuttgart), Germany  
Axel Tenschert, HLRS (High Performance Computing Center Stuttgart), Germany  
Alexey Cheptsov, HLRS (High Performance Computing Center Stuttgart), Germany

*pages: 288 - 299*

**Designing a Low-Cost Web-Controlled Mobile Robot for Ambient Assisted Living**

Yvon Autret, University of Brest, France  
David Espes, University of Brest, France  
Jean Vareille, University of Brest, France  
Philippe Le Parc, University of Brest, France

*pages: 300 - 309*

**Innovation and Creativity in the HCI classroom**

Alma Leora Culén, University of Oslo, Norway

*pages: 310 - 323*

**Human-Machine Cooperation Loop in Game Playing**

Maciej Świechowski, Systems Research Institute, Polish Academy of Sciences, Poland

Kathryn Merrick, School of Engineering and Information Technology, University of New South Wales, Australia

Jacek Mańdziuk, Faculty of Mathematics and Information Science, Warsaw University of Technology, Poland

Hussein Abbass, School of Engineering and Information Technology, University of New South Wales, Australia

*pages: 324 - 338*

**Designing for Experienced Simplicity. Why Analytic and Imagined Simplicity Fail in Design of Assistive Technology**

Suhas Govind Joshi, Department of Informatics, Faculty of Mathematics and Natural Sciences, University of Oslo, Norway

*pages: 339 - 346*

**Predicative Recursion, Diagonalization, and Slow-growing Hierarchies of Time-bounded Programs**

Emanuele Covino, Dipartimento di Informatica, Università di Bari, Italy

Giovanni Pani, Dipartimento di Informatica, Università di Bari, Italy

*pages: 347 - 373*

**Service Recommendation Using Machine Learning Methods Based on Measured Consumer Experiences Within a Service Market**

Jens Kirchner, Karlsruhe University of Applied Sciences, Linnaeus University, Germany/Sweden

Andreas Heberle, Karlsruhe University of Applied Sciences, Germany

Welf Löwe, Linnaeus University, Sweden

*pages: 374 - 384*

**Simulation of Emergence of Local Common Languages Using Iterated Learning Model on Social Networks**

Makoto Nakamura, Japan Legal Information Institute, Graduate School of Law, Nagoya University, Japan

Ryuchi Matoba, Department of Electronics and Computer Engineering, National Institute of Technology, Toyama College, Japan

Satoshi Tojo, School of Information Science, Japan Advanced Institute of Science and Technology, Japan

*pages: 385 - 397*

**A Novel Chemistry-inspired Approach to Efficient Coordination of Multi-mission**

## **Networked Objects**

Mahmoud ElGammal, Virginia Polytechnic Institute and State University, USA  
Mohamed Eltoweissy, Virginia Military Institute, USA

*pages: 398 - 412*

### **Unmanned Aerial Systems as Tools to Assist in Digitalized Decision Making**

Tapio Saarelainen, Army Academy, Finland

*pages: 413 - 425*

### **Structural Adaptation for Self-Organizing Multi-Agent Systems: Engineering and Evaluation**

Thomas Preisler, HAW Hamburg, Germany  
Wolfgang Renz, HAW Hamburg, Deutschland  
Tim Dethlefs, HAW Hamburg, Germany

*pages: 426 - 436*

### **Pedestrian Detection with Cascaded Part Model for Occlusion Handling**

Yawar Rehman, Hanyang University, South Korea  
Irfan Riaz, Hanyang University, South Korea  
Fan Xue, Hanyang University, South Korea  
Piao Jingchun, Hanyang University, South Korea  
Jameel Ahmed Khan, Hanyang University, South Korea  
Shin Hyunchul, Hanyang University, South Korea

*pages: 437 - 447*

### **Improving Energy Awareness Integrating Persuasive Game, Feedback, and Social Interaction into the Novel Ener-SCAPE Application**

Diego Arnone, Engineering Ingegneria Informatica S.p.A., Italy  
Alessandro Rossi, Engineering Ingegneria Informatica S.p.A., Italy  
Marzia Mammina, Demetrix S.r.l., Italy  
Enrico Gabriele Melodia, Pidiemme Consulting S.r.l., Italy  
Sandra Elizabeth Jenkins, Massachusetts Institute of Technology, USA

*pages: 448 - 457*

### **Round-Trip Engineering Approach to Keep Activity Diagrams Synchronized with Source Code**

Keinosuke Matsumoto, Osaka Prefecture University, Japan  
Ryo Uenishi, Osaka Prefecture University, Japan  
Naoki Mori, Osaka Prefecture University, Japan

*pages: 458 - 466*

### **Considerations for Proposed Compatibility Levels for 9-150 kHz Harmonic Emissions Based on Conducted Measurements and Limits in the United States**

Elizabeth Devore, Auburn University, USA  
Adam Birchfield, Auburn University, USA  
Mark Halpin, Auburn University, USA

*pages: 467 - 482*

**Evaluation of an Integrated Testbed Environment for the Web of Things**

Mina Younan, Minia University, Egypt

Sherif Khattab, Cairo University, Egypt

Reem Bahgat, Cairo University, Egypt

*pages: 483 - 493*

**Quality of Service Based Event Stream Processing Systems in Smart Grids**

Orleant Epal Njamen, Grenoble INP, LIG, France

Lourdes Martinez, Grenoble INP, LIG, France

Christine Collet, Grenoble INP, LIG, France

Genoveva Vargas-Solar, CNRS, LIG-LAFMIA, France

Christophe Bobineau, Grenoble INP, LIG, France

*pages: 494 - 506*

**Map-Cache Synchronization and Merged RLOC Probing Study for LISP**

Vladimír Veselý, Brno University of Technology, Czech Republic

Ondřej Ryšavý, Brno University of Technology, Czech Republic

## Pictogram Creation with Sensory Evaluation Method Based on Multiplex Sign Languages

Naotsune Hosono  
Keio University,  
Oki Consulting Solutions  
Tokyo, Japan  
naotsune@mx-keio.net

Hiromitsu Inoue  
Chiba Prefectural University  
of Health Sciences,  
Chiba, Japan  
cal32840@topaz.plala.or.jp

Miwa Nakanishi  
Keio University  
Kanagawa, Japan  
miwa\_nakanishi@ae.keio.ac.jp

Yutaka Tomita  
Keio University  
Kanagawa, Japan  
tomita@z3.keio.ac.jp

**Abstract**— Human sign languages are originally designed for use by hearing impaired people, and they include semantic expressions in their scope. This paper discusses an original method to create pictograms based on multiplex local sign languages with the concept of “Context of Use” on dialogue, by applying Multivariate Analysis (MVA). Since pictograms are universal communication tools, Human-Centred Design (HCD) and context analysis with a Persona model are applied. The experiments consist of three steps with seven phases. The first step is to measure the similarity of a selected word among seven different local sign languages using MVA. The second step is to guide a pictogram designer to create a new common pictogram, by exploiting results from the first step result. The final step is to validate the newly created pictogram with MVA. Under the cycle of HCD, pictogram designers will summarize the expression of several local sign languages using this method. The acquisition of this experience is to be included as a pictogram design guideline within the context of universal communications, such as emergency and traveling situations. Through the proposed method, the relationship between selected words and local sign languages are initially explained by sensory evaluation of the subjects. The outcome of pictograms or icons of this experiment are implemented on smartphones with a touch panel. The final system is evaluated by hearing impaired subjects and foreigners, to compare qualitative measures of effectiveness, efficiency, and satisfaction based on context of use.

**Keywords**- *Context of Use; Computer Human Interface; Human-Centred Design; Pictogram; Universal Communication; Sensory Evaluation; Smartphone.*

### I. INTRODUCTION

Quite often a designer must face the challenge of developing a new machine or software without any guidelines. Often only conventional design processes provide a starting point, where the process tends to start from an initial perception of needs. The target specification are then created and measured only by the experts of the area. The original design resources are derived from proprietary technologies (Seeds). Then, subsequent experimental and manufacturing development stages are based on this predetermined specification. The prototype machine is developed to meet mass production standard of value engineering (VE) within resource constraints. This initial machine tends to be an origin or source of mass-production

version neglecting market needs. Finally, the machine is refined and shipped to a predetermined market. This introduction into a market may be the first opportunity that the end users have to examine and determine the efficiency of the machine. Necessary feature requests and candid feedback from end users (Needs) are only available to the designers after once the machine has been introduced into the real market.

Because of the initial lack of a specific requirement balance, computer based interface designers are required to measure and analyze the value of users’ comfort level [1]. In order to improve such long an expensive cycles, the International Standard Organization (ISO) proposed an international standard (IS) 9241-210 for Human-Centred Design [2]. This standard is a revision of IS 13407, which was prepared by ISO/TC159 in June 1999 [3] and provides requirements and recommendations for human-centred design principles and activities throughout the life cycle of computer-based interactive systems. It is intended to be used by the manager of the design processes, and is concerned with ways in which both hardware and software components of interactive systems can enhance human-system interaction. The application of human factors and ergonomics to interactive systems design enhances effectiveness, efficiency, and improves human working conditions. The benefits can include: increased productivity, enhanced quality of work, reduction in support and training costs and improves user satisfaction. The aim of IS is to help those responsible for managing hardware and software design processes, and to identify and plan effective and timely Human-centred design (HCD) activities. It complements existing design approaches and methods. The major additional portion is that IS 9241-210 includes User Experience (UX) concept with emotional factors [4].

However, the above mentioned IS does not provide detailed coverage of the method and technologies for determining the design. Because of the lack of a specific requirement balance, computer based interface designers are required to measure and analyze the value of users’ comfort levels. Because of generally scarce resources, designers must trade-off various elements of basic requirements by themselves. In the initial stages of development, designers will have little or no direct experience in developing a specific outcome to meet the exact requirement of icons or pictograms.

Sense, feeling, impression, and emotion are words of subjective notions, and deeply relate to happiness, anger, sorrow and enjoyment that are fundamental factors of UX. Sensory analysis [5] provides the basis for an examination of organoleptic attributes of a product by the sensory organs. This paper explores a sensory analysis method and discusses a method to create pictograms or icons to be used not only by hearing impaired, but also hearing people required to interpret a variety of local sign languages, with the concept of context of use on dialogue and Multivariate Analysis (MVA) [6].

The structure of this paper is as follows. Section II described the research motivation, which arises with hearing impaired people issues in the face of emergencies. Simple and easy to use pictograms or icons are assumed to provide a basis for an efficient language-independent communication tool. In Sections III, IV, and V, the design of pictograms or icons is discussed, by applying sensory evaluation methods. The validity of the newly created pictograms or icons is discussed in Section VI, where the outcome of the results is implemented on a smartphone with touch panel. Then the efficiency of the system is evaluated by hearing impaired and foreign subjects. Section VII summarizes conclusions.

## II. RESEARCH PURPOSE AND ISSUES

The purpose of this research is to develop a method to create meaningful pictograms or icons [7] referring to several local sign languages [8]. Sign language (SL) is basically a communication method from one person to another for hearing impaired persons. A significant difference between sign language and vocal language is that characters are represented by a hand shape. Since there is no uniform SL in reality, and each SL expression is not exactly the same, and can vary from country to country because of their native cultures. Whereas sensory related expressions of SL such as happiness, angry, sorrow and enjoyment are tend to be universal regardless cultures. Those sensory related words are closely relating to UX.

The main factors of almost all sign languages consist of the hand shape, location, movement and additional face expressions. However, there is a dilemma that SL is a language with motion whereas pictograms or icons are static. The development and learning of current sign languages and their expression has drawn a lot of attention from both signers and sign language designers. Then hand shapes and locations are drawn by an animation and movements are done by arrows referring to a snapshot of the related local sign languages [9-20]. With this background, this paper discusses a method to create icons and pictograms by choosing and selecting the common features among several sign languages for a designer who has little experience. In this study, the referring seven sign languages are;

- A: American Sign Language (ASL)
- B: British Sign Language (BSL)
- C: Chinese Sign Language (CSL)
- E: Spanish Sign Language (ESL)
- F: French Sign Language (FSL)
- J: Japanese Sign Language (JSL)
- K: Korean Sign Language (KSL)

## III. RESEARCH PROCEDURES

This research scope covers not only linguistic studies of sign language but also HCD and context of use, since pictograms or icons are universal communication tools. The research was started in order to investigate the context of universal communication through local sign languages. HCD [2, 3] is based on the context of use [21], which is organized by four factors; "user," "product," "task," and "environment" in use for goal (Figure 1). HCD and context analysis using the Persona model by Alan Cooper [22] are applied in this research.

With this framework, the following three steps with seven phase research procedures are developed;

Step1:

Phase 1: Concept Generation

Phase 2: Persona Model and Scenario Creation

Phase 3: Key words extraction on the situations

Phase 4: Initial Sensory Evaluation with Seven Local Sign Languages

Step 2:

Phase 5: Summarized Pictogram Design.

Step 3:

Phase 6: Second Sensory Evaluation with Seven Local Sign Languages with a Summarized Pictogram to prove the outcome

Phase 7: Conclude the Method

### Phase 1: Context Generation

Based on the framework described above, two context situations have been selected: 1) emergencies and 2) travelling.

Alan Cooper proposed the Persona Model related to HCD, where several situations representing Personas are imagined to be in certain contexts in order to simulate and find how they will behave. This method is highly accepted by manufacturers in the creation of new product plans and has also been applied to service science.

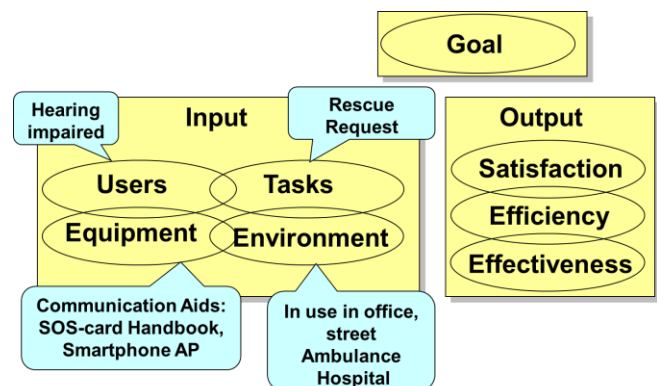


Figure 1. Context of use of ISO 9241-11

### Phase 2: Persona Model and Scenario Creation

The first step is to create Personas by applying the Persona Model under HCD. A created Persona is a hearing impaired person in a situation where he suffers from a sudden illness while commuting in the morning, and is carried to the hospital by an ambulance (Figure 2).

Diary like scenarios underlying Personas are described from discussions with colleagues utilizing the Brain Storming Method. These scenarios mainly pay attention to

the dialogues between the target Persona and people surrounding them. The main goal of the target Persona is to describe his emergency situation in order to solicit help. The scenario of the hearing impaired person in an emergency consists of about 600 words (equivalent to 3000 Japanese characters).

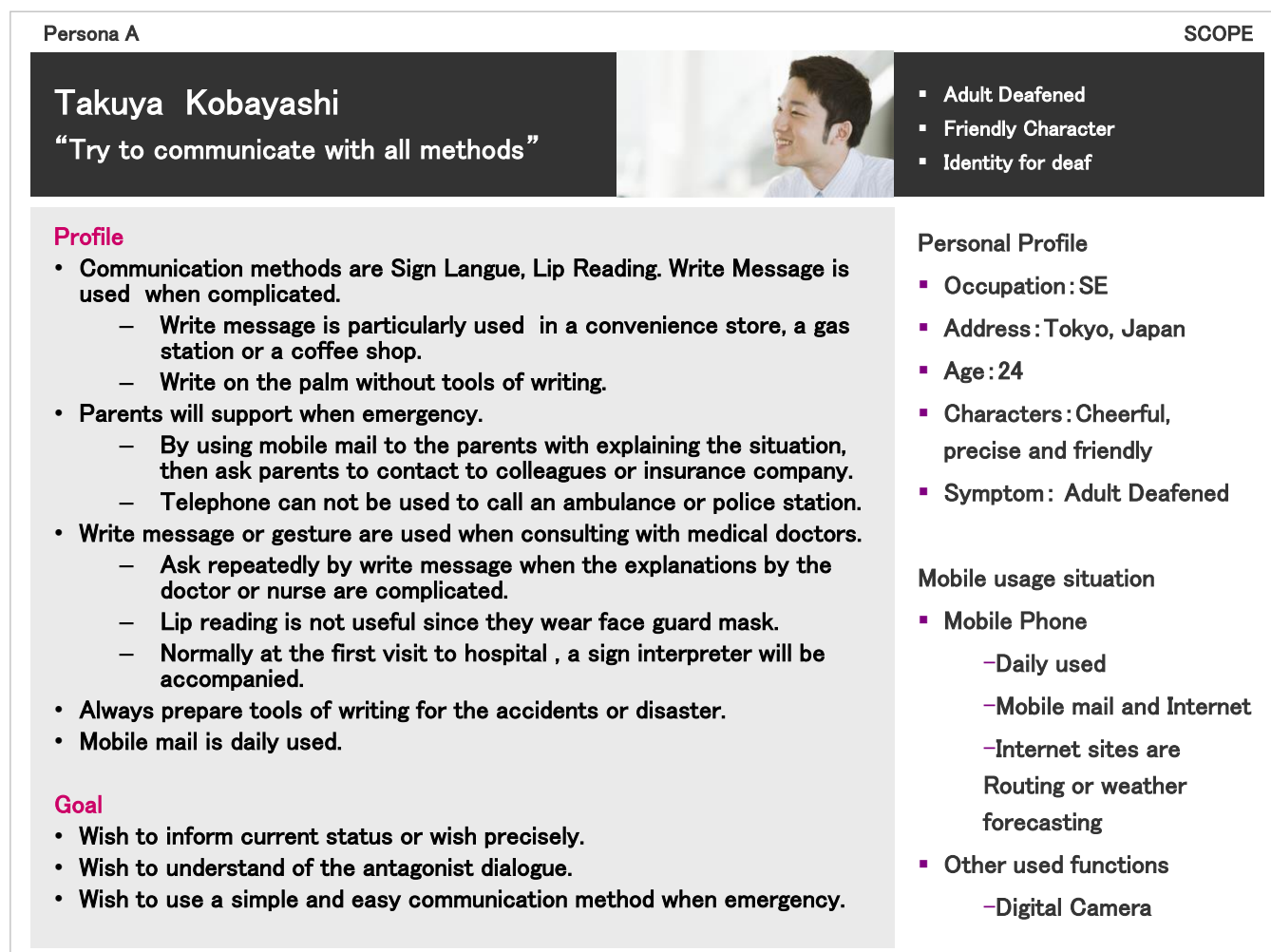


Figure 2. An Example of Persona Model

### Phase 3: Key word extraction on the situations

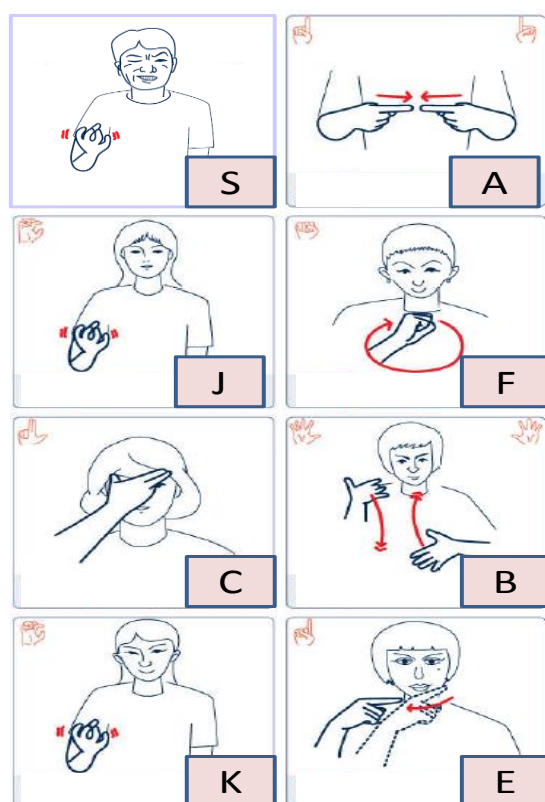
The former phase is focused upon dialogues with several subjects and refers to observations from the view point of the provider and the receiver under the dialogue principle [23].

In this phase, the goal is to extract words that are fundamentally essential to establish the dialogues of the scenarios. In the context of a Persona in such an emergency situation, the most commonly used words are determined. In this case, 37 words were selected and categorized by the Brain Storming Method. Selected words are essential to the dialogues of the scenarios. The categorized 37 words were as follows;

- Ten greeting words that trigger the initial dialogues: thank you, hello, goodbye, indeed, yes, no, I am deaf, do not understand, sorry, please do.
- The next step of the dialogues start commonly with seven interrogative pronoun words: where ?, how much ?, how many ?, when ?, what ?, which one ?, who ?.

- Twelve associated reply words for interrogative pronouns are: toilet, country, numeric (0, 1, 2, 3, 5, and 10), yesterday, today, tomorrow, name.
- Three essential adjectives are: painful, different, expensive.
- Five essential verbs are: want to, go, come, buy, reserve.

A word “Painful” is a typical example among the selected seven words; Thank you, Goodbye, When? Where? Painful, Expensive, and Toilet through the Brain Storming Method by co-authors, representatives of the fire brigade and hearing impaired architects. This paper explains the development of our method by a selected word: “Painful” as a representative, since it closely relates to the usage context and UX concept and coincides to the survey results of Tokyo Fire Department and Keio University hospital (introduced in the next section).



#### Abbreviations:

- A: American Sign Language (ASL)
- J: Japanese Sign Language (JSL)
- F: French Sign Language (FSL)
- C: Chinese Sign Language (CSL)
- B: British Sign Language (BSL)
- K: Korean Sign Language (KSL)
- E: Spanish Sign Language (ESL)
- S: Summarized and newly designed pictogram

Figure 3. Sign Language Figures of “Painful”

*Phase 4: Initial Sensory Evaluation with Seven Local Sign Languages*

The overall research is initially focused on the creation of pictograms or icons to support dialogues, since the fundamentals of sign language are hand shape, location and motion. References are made to a collection of animation figures, extracted from seven local sign languages used by deaf architect. This architect provided enthusiastic support to the research by supplying and permitting reference to the database. The seven local sign languages are of American, British, Chinese, French, Korean, Japanese, and Spanish [8].

In the experiments, the subjects are first shown an expression with the collection of animation figures extracted from seven local sign languages (Figure 3). Subsequently, the subjects are informed of the meaning of the sign, and then they are requested to vote with 19 tokens to express which of the seven different local sign language expressions (samples) best coincides with the original image. They are asked to use all 19 tokens, but that they are permitted eventually zero voting on some samples (Figures 4 and 5).

This sensory evaluation method can easily make relative comparisons between the seven expressions of local sign languages and is more effective than the Ordering Method or Pair Comparison Method. Correspondence Analysis (CA) of MVA by IBM SPSS Statistics Ver.18 [24] is then applied.

The outcome is plotted on a plane such as similar local sign languages are plotted close together. The outcome of CA of MVA is fundamentally no name of Eigenvalue axes. Because of the characteristics of CA, the subjects who have general and standard ideas are positioned in the centre, whereas those who have extreme or specialized ideas are positioned away from the centre of position (0.0). The center crossing point of the first and second Eigenvalues is also called “centre of the gravity” or “average”. Then CA establishes a way to graphically examine the relationship between local sign languages and subjects [25].

Figure 6 is an example of an outcome chart where “painful” is plotted. Focusing on Subject No.3 and looking at the voting sheet, the image of “painful” by the subject will be appropriate to Spanish Sign Language (ESL) and American Sign Language (ASL) since the subject put more tokens on ESL and ASL than other sign languages. In the plot chart of CA, the subject is observed to have extreme or specialized ideas from other subjects, since the subject plot position is remote from the centre in Figure 7. In practice, the subject is then positioned closed to Spanish Sign Language (ESL) and American Sign Language (ASL) whereas far away from French Sign Language (FSL), British Sign Language (BSL), Japanese Sign Language (JSL), Korean Sign Language (KSL), or Chinese Sign language (CSL).

On the other hand, in Figure 8, Subject No.8 is positioned centre, since the subject voted equally on all the sign languages of ESL, ASL, FSL, BSL, JSL, KSL and CSL (cf. Subject No.3). Hence, the above two plots provide examples of CA with the relationships between subjects and samples (sign languages), and explains the relations both between subjects to other subjects and between sign languages and other sign languages. Figure 9 shows the position of Subject.

	●	●						
	●	●	●	●	●			
	●							
	●	●	●					
	●	●						
	●	●	●	●	●			
	●							

Figure 4. Inquiry Sheet Example of “Painful”



Figure 5. A View of Experiment by the Subject

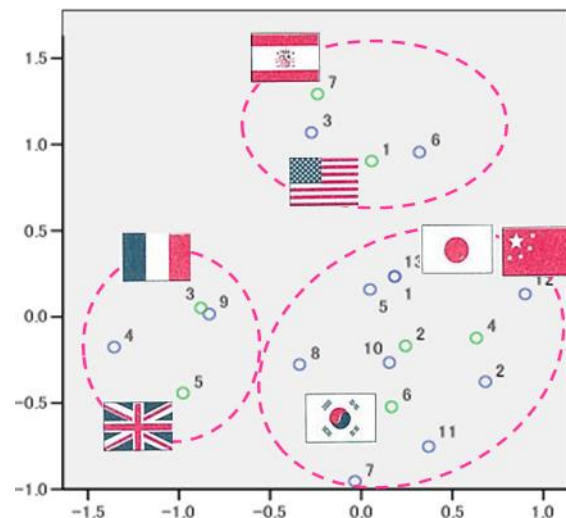


Figure 6. A Plot of “Painful” with 7 Sign Languages

No.3 is an outlier with respect to all other subjects and thus it is concluded that the subject idea is extreme or has specialized ideas compared with the others.

The first experiment subjects are 13 people in their twenties, including nine science course students, and four humanity course students. Some have experience living overseas and sign language interpreting. The reason to exclude hearing impaired people in subjects is that they are biased their own sign language. After voting with the tokens, all the subjects are asked about their confidence level using the Semantic Differential (SD) method [5].

#### Phase 5: Summarized Pictogram Design

The analysis of an outcome CA plot chart of “painful” is shown in Figure 6; with seven sign languages (SL), voted subjects create three clusters of “FSL and BSL”, “ASL and ESL”, “JSL, KSL and CSL” sign languages.

Following the cycle process of HCD [2, 3], an original designer is asked to summarize and design an original pictogram for JSL, KSL and CSL by reflecting of the outcome by the sensory evaluation mentioned above. Then the newly designed pictogram, which is “S” in Figure 10, is added to the previous seven local sign languages.

#### Phase 6: Second Sensory Evaluation with Seven Local Sign Languages with a Summarized Pictogram to prove the outcome

The first experiment is done with seven sign languages. The subject is permitted up to seven tokens for each sign language, for a total of 49 possible votes. Each subject is given 19 tokens, which is about 40% of total 49 voting locations. The second experiment is done with seven sign languages, plus one newly created sign language. Then the total voting locations becomes 56. Each subject is given 23 tokens, which are again about 40% of total 56 voting location.

After subjects are informed of the intended sign meaning, they are requested to vote with 23 tokens, which of the eight different local sign language expressions including the newly designed language, which has a pictogram “S” as show in Figure 10. This process was the same as the first sensory evaluation step of phase 4, and the Correspondence Analysis of Multivariate Analysis (MVA) by SPSS is once again performed [24].

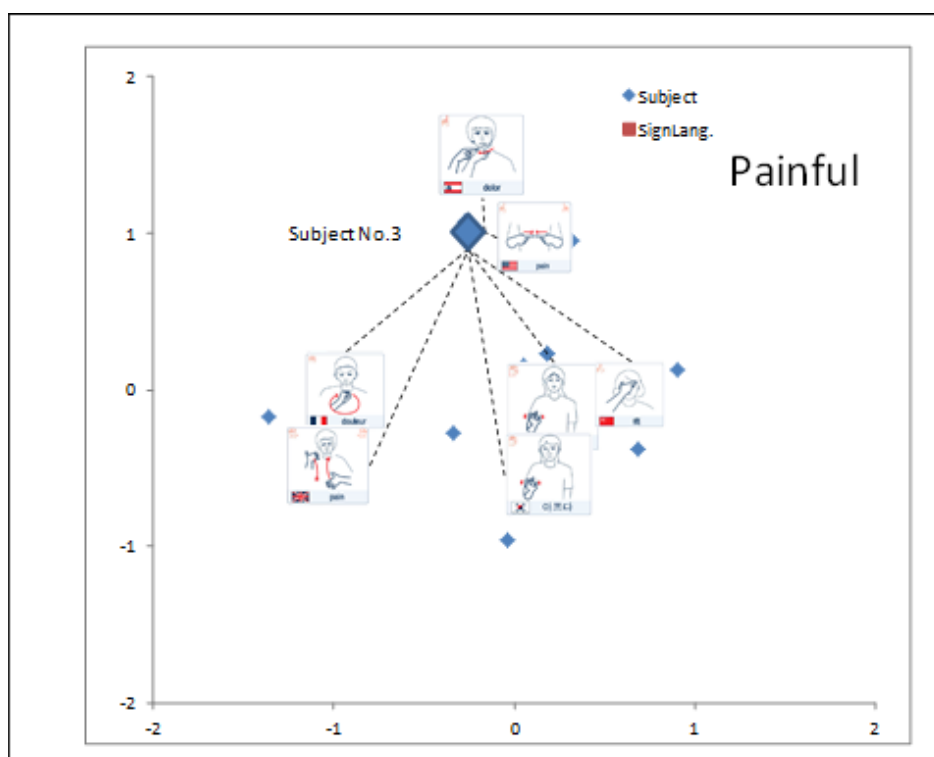


Figure 7. Subject 3 is plotted near to ESL and ASL

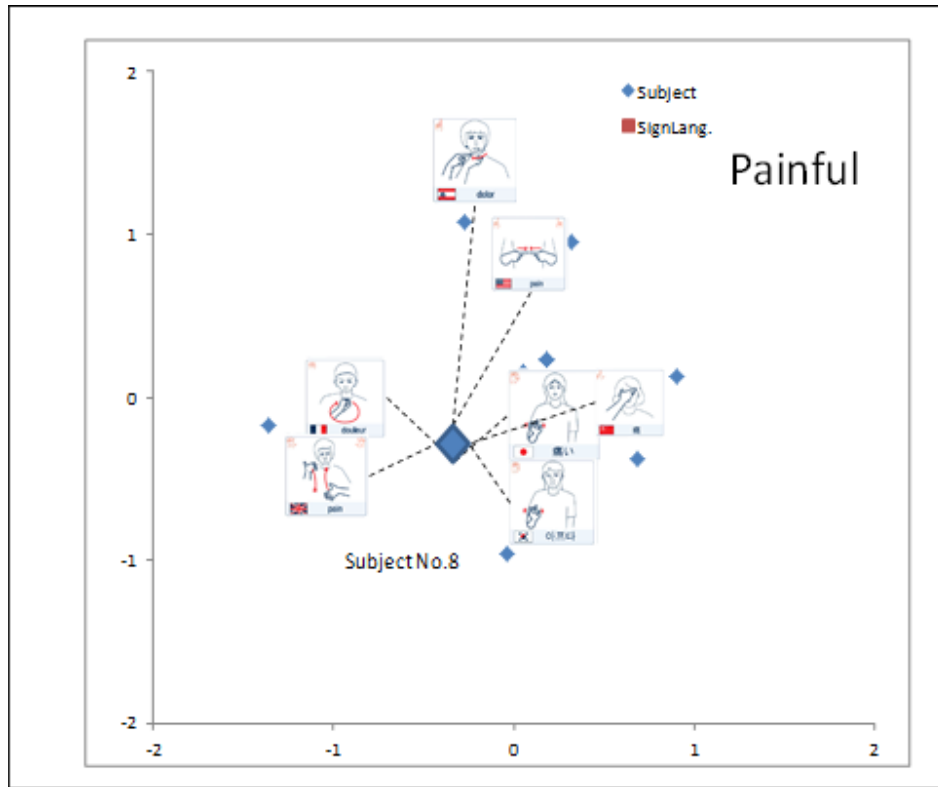


Figure 8. Subject 8 is plotted further from all SL's

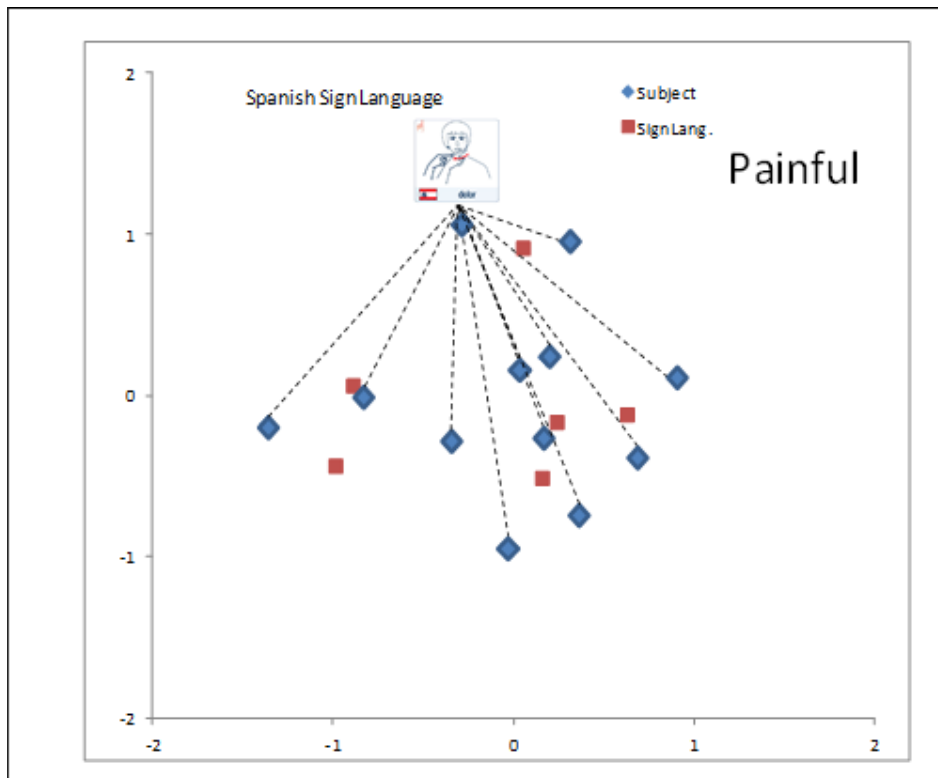


Figure 9. Subject 3 is plotted further from all other Subjects

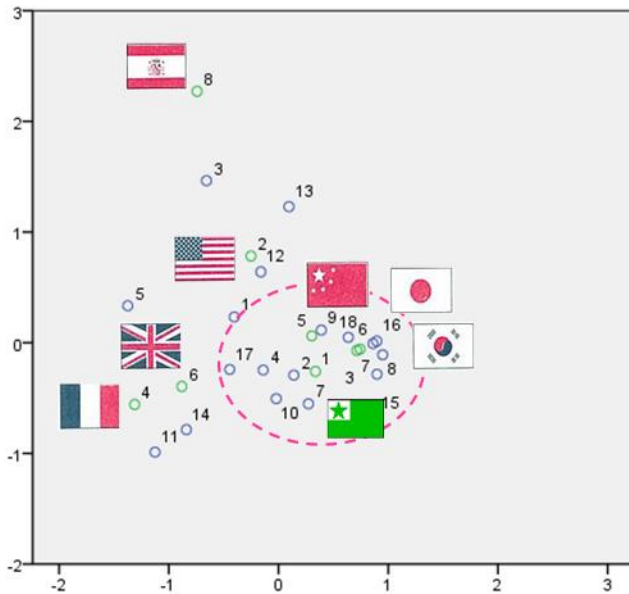


Figure 10. A Supplementary Treatment Plot of “Painful” with 7+1 Sign Languages, where S is a summarized one.

The outcome, including the newly designed pictogram, is plotted with other seven local sign languages in order to measure whether the newly created pictogram is representative of the dominant cluster. The second experiment subjects are 20 engineering department students in their twenties including two female students. Almost all except three are different subjects from the first experience. After voting by the tokens, all the subjects are again asked of their confidence level using the Semantic Differential (SD) method [5]. Figure 10 is an example of outcome chart where “painful” is plotted. The newly designed symbol with a coloured green flag will represent JSL, KSL and CSL sign languages since it is plotted closer to those three sign languages. Whereas FSL, BSL, ASL and ESL are plotted further down.

In order to demonstrate the outcome more precisely, supplementary treatment of MVA by SPSS is also applied by adding a newly designed supplementary category to the seven sign languages (active categories). Supplementary categories do not influence the analysis but are represented in the space defined by the active categories. Supplementary categories play no role in defining the dimensions. These versions of the plots are similar in seven sign languages and those created from summarized pictogram experiments.

*Phase 7: Concluding the Method*

Phase 4 explains how to determine similarity amongst seven sign languages. Then the newly created icon or pictogram provides a basis to measure the similarity. Phase 7 explains how that outcome is confirmed, since it plotted closed to the referred sign languages.

Table I. Complains Survey of Tokyo Fire Department and Keio Hospital

	Tokyo Fire Dept. 290,471	Keio Univ. Hospital 2,421
Pain problems	30.10%	38.30%
unconsciousness	11.20%	15.90%
breath trouble	8.40%	5.10%
fever	8.10%	2.30%
vertigo	6.60%	6.50%
convulsion	5.40%	3.00%
vomit	4.80%	2.50%
hard of standing	4.60%	2.40%
malfunction in cardiac and lung	N/A	2.30%
injury	N/A	21.60%
others	20.80%	0.10%

Contents of Keio Univ. Pain Data  
 - Stomachache: 22.7%  
 - Headache: 19.7%  
 - Lumbago, backache: 11.9%

Comparing the two outcomes of Phase 4 (Figure 6) with seven local sign languages and of Phase 5 (Figure 10) with seven local ones plus one, one can conclude the following,

- Seven summarized pictograms are created for seven aggregated words respectively such as “painful.”
- Then newly designed pictograms by a designer are all positioned in the centre of the related local sign languages cluster.
- Even though most subjects are different in the first and second experiments, the outcome plot patterns by CA hold similar patterns in space.
- the oriental sign languages of JSL, KSL and CSL are plotted closely together.
- The outcome is confirmed by Supplementary Treatment of MVA by SPSS.

IV. CONCEPT AND SYSTEM DESIGN OF THE SMARTPHONE WITH TOUCH PANEL

The data of patient issues collected by Tokyo Fire Department (TFD, 290,471 patients) and Keio University hospital (2,421 patients) were analyzed (Table I). The collected data were not only hearing impaired, but all kind patients. From both datasets, more than 30% of complaints were determined to be about pain problems. Ten selected patient complaint items were pain/ache/grief, unconsciousness, difficulty breathing, fever, faintness, convulsions, vomiting, difficulty standing and walking, cardiopulmonary problems and external injury.

The “Context of Use” referring to ISI9241-11 [21] is composed of four factors: user, product, task and environment for the goal. At the time when a designed is to create icons or pictograms, it is necessary to bear in mind how such symbols are to be used under the context; otherwise the outcomes will be hard to be recognized by the users. They must be useful, effective and particularly

efficient for both the hearing impaired and language dysfunction people and foreigners. Here the research intended to particularly focus on the communication method [23] of complaint of pain/ache/grief by hearing impaired patients.

The pain or ache sources were assumed to be positioned in either the head, face, chest, back, belly, waist, arm/hand and leg/foot. In addition, three ache depths come from surface skin, visceral and bone. The hearing impaired and language dysfunction people complaint of pain/ache/grief and external injury was to be drawn by pictograms and icons that were easy to understand, even in emergency situations with help of minimum selected key words with MVA. Aching places were drawn in two dimensions. Ache depth and severe pain were in the third dimension. The hearing impaired and people will simply touch the designated icon or pictogram to communicate to support people in such emergency situation by ubiquitously carrying a smartphone with touch panel.

The modern smartphones with touch panel are primarily equipped the following functions 1) tap to select, 2) double tap to do scaling, 3) drag to jump, 4) flick or swipe to move next page, 5) pinch in/out with double fingers, 6) accelerate sensor to position upright, 7) photo browsing to display icons or pictograms, 8) backlight for dark place usage, 9) GPS/Wi-Fi positioning, and 10) wireless function to download the new contents and applications.

The framework is implemented on the smartphones of with touch panel applying functions above such as iOS and Android devices to enable hearing impaired or language dysfunction people to communicate the remote supporter place of the nearest fire brigade in such urgent situations through the ICT clouds. The smartphone with touch panel will produce a text message for e-mail through simply tapping on icons or pictograms. The mail text is to be instantly sent to the remote supporters.

Currently, 31 screen contents on the smartphone are implemented by the Software Development Kit (SDK) of MIT APP Inventor [26] and distributed onto Android touch panel terminal by DeployGete [27] for the evaluation (Figure 11). JAVA and Eclipse are used for the detailed programming part. It is also implemented on iOS using Objective-C with Xcode. The screen transition process is based on the telephone dialogues of the command console of the Kasuga Onojo Nakagawa Fire Department in Fukuoka Prefecture. The overall process is analyzed and drawn by Freeplane by Mind Mapping [28]. The touch panel includes the cognitive design method on Automated Teller Machine (ATM) for elderly people since under such an urgent situation, people would be upset and find it hard to communicate just like a cognitive decline [29, 30]. The repertoire of possible actions is as follows:

- (1) Simple selection with limited choices
- (2) Explicit sliding at the time of screen change
- (3) Step by step procedures after selection

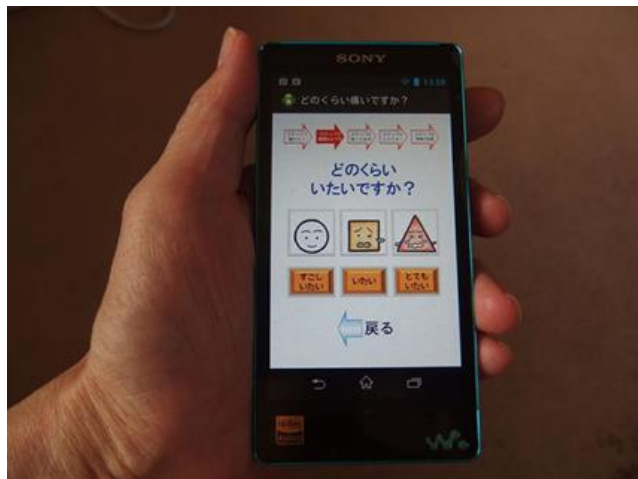


Figure 11. Pictograms on the Smartphone with Touch Panel representing Degree of Pains



Figure 12. The Evaluation Experiment Scene by the Hearing Subjects

## V. EXPERIMENTAL EVALUATION

The proposed smartphone with touch panel was evaluated by hearing impaired people in a manner similar to the usability test under the working hypothesis related to desire of communication outcome. The communication method for hearing impaired people or language dysfunction depended only on the sign language. Nowadays, since hearing impaired people are starting to use smartphones with text messaging. This improves their communication behaviour and quality of life (QOL) [31].

The five tasks were prepared to compare performance with and without a service to call ambulance and fire brigades. This evaluation focused on efficiency by comparing two task groups; those that apply tapping icons or pictograms on the smartphone, and those that send text message by e-mail by means of personal computer (PC) key board. The evaluation test was performed by four hearing

impaired subjects as described in the following five tasks. All experiment instructions are introduced to hearing impaired subjects by a sign interpreter (Figure 12). Subjects are permitted to use memo notes.

- Task-1: Fire report by tapping icons on the smartphone.  
This scenario was that “The forest is on fire. I recognize a flame but no smoke. I am safe since I am away from the fire spot. There was no injury. Please help”.
- Task-2: Fire report by e-mail text message  
The scenario was “This building is on fire. My floor is different from the fire spot. I cannot recognize flame but see smoke. There were some injuries. Please help”.
- Task-3: Ambulance request by e-mail text message  
The scenario was “Please call ambulance since I was run over by a car. I am middle aged male. I am conscious but my leg is broken and bleeding. It is quite painful. Please send an ambulance soon”.
- Task-4: Ambulance request by tapping icons on the smartphone  
The scenario was “My daughter is severely sick. She is a pregnant adult. She may have a preterm birth. She is conscious but indicates severe pain in the belly. She was once suffering from gallstones. Please send an ambulance soon”.
- Task-5: Interviews after four tasks  
An exercise to fill out a personal data sheet such as name, address, age and issues of input methods by a soft key board or hand writing.

## VI. EVALUATION RESULTS

The results must be analyzed under “the Context of Use” [21] whose result was measured by the effectiveness, efficiency, and satisfaction. This evaluation focused particularly on the efficiency with comparing two task groups, and found applying tapping icons or pictograms on the smartphone was about three times quicker than text message by e-mail (Table II).

It is natural that simple tapping icons input must be quicker than text input, however, the purpose of the evaluation is to measure how much quicker on the speed ratio utilizing smartphone comparing to text e-mail. In practice, it must be much quicker than three times since to input texts by telephone dials of ten keys is more complicated comparing to PC keyboard. For instance, it is necessary to push the “2” button three times to input single “c” character in 3G type mobile phones. The smartphones are equipped the soft keyboard on the touch panel. However, the character array is the same as PC keyboard, key widths are narrow and sometimes without any feedback. The current technology is not really effective yet.

During interviews after the evaluation, many hearing impaired people pointed out that this smartphone service would ease their predicted mental anguish during any emergency. This concept is closely aligned to the Satisfaction in the Context of Use or User Experience (UX) [4].

Table II. The Evaluation Result on Efficiency

Subjects	Task-1	Task-2	Task-3	Task-4
MKS	12"82	3'40"07	2'45"28	53"26
YNY	24"20	1'34"08	2'23"72	59"85
SZKM	19"52	1'54"84	2'02"72	49"72
SZKK	20"87	1'06"68	2'01"68	N/A
Average	19"35	2'03"92	2'18"35	54"28

## VII. CONCLUSION

This paper consists of two parts. The first part of this paper discusses a method to extract the summarized expression of several local sign languages in order to draw pictograms or icons by applying the sensory evaluation with MVA. The experiments consist of three steps. The first step is to select a pictogram as a majority common expression upon a word among seven local sign languages. Considering this first step, this method seems valid in practice since oriental sign languages, Japanese, Chinese and Korean are similar by historical background, and in fact and they emerge as similar to each other. The second step is to confirm that the experimental characteristics of the pictogram represent the meaning of the word. The final step is to validate the newly created pictogram by MVA. Since almost all of the newly designed pictograms were positioned close to the cluster it can be concluded that they were representative of the clusters.

In the example of the concept of “painful” taken from seven sign languages, and analysis with the supplementary treatment of MVA, the newly designed pictogram was close to those oriental sign languages since it was plotted close to those sign languages on the plane. The last part of this paper discussed how the use of the outcome of pictograms or icons of this experiment was implemented on a modern smartphone with a touch panel display for computer-human interaction. Through the proposed method, the relationship between selected words and local sign languages were initially explained by sensory evaluation by the subjects. Under the cycle of HCD, the pictogram designer will perform to summarize the expression of several local sign languages by this method. We showed how the acquisition of user experience can provide design guidance, for instance, in the context of emergency and traveling situations.

In order to show stability and repeatability, the experiments were done twice. The first one was to confirm the similarity among seven sign languages for any selected word. The second experiment was done with different subjects, in order to demonstrate independence of outcome. This is confirmed in the second experimental results. By applying the method, the selected seven words; Thank you, Goodbye, When? Where? Painful, Expensive, and Toilet were analyzed. All the summarized outcomes were positioned close to the referred ones on the plot. The results of the second experiment confirmed the outcome design by

supplementary treatment of the CA procedure. The proposed method was quite an original one and thus provided one of the guidelines to create pictograms by referring to several sign languages. The relevant methods can be considered as a ranking method and a pair comparison method. A ranking method is relatively simple, however, when increasing the number of items to more than ten, it becomes hard to do ranking in middle: e.g., the seventh or eighth is hard to distinguish. A pair comparison method requires a large number of comparisons, e.g., 45 comparisons for ten items [5].

The second part of this paper introduces an experiment to implement the outcome of icons or pictograms on the smartphones with touch panel. At the beginning they were printed in the form of a booklet to be used the communications between hearing impaired and hearing people as well as between foreigners and Japanese. The suffixes were created and translated into English, Spanish, Korean, Chinese and Portuguese for the foreign people use referring to nationality population composition in Japan. The results by the foreign people with the booklet were that the time to collaborate was 20% shorter and the messages of the dialogue were 20% more precise than simple gesture communication. In practice, the booklet was published 6,000 copies and currently mounted on several ambulances in the local fire departments to aid to collaborate between the hearing impaired patient and emergency response personnel. The current prototype terminal was implemented on the smartphone with touch panel. The system then connects over a network to remote supporters of the nearest fire brigade. It was implemented on both iOS by Apple and Android mobile terminals with GPS positioning technology.

The outcome of this research will be proposed to the Japanese government to make easily available, and to be used such a crisis for urgent communication or to be used during the next Olympics, to be held in the year of 2020 in Tokyo.

#### ACKNOWLEDGMENT

This research is supported and funded by the Project organized by Fire and Disaster Management Agency under Ministry of Internal Affairs and Communications (MIC) of Japan. The original idea of the booklet was proposed by a hearing impaired architect, Mr. M. Suzuki. A collection of local sign language database is supplied and permitted for research use by Mr. M. Akatsuka of Architectural Association of Japanese DEAF (AAJD). Dr. H. Akatsu of Oki Electric Ind. Co., Ltd. introduced the cognitive design method on ATM for elderly people. Mr. T. Inaba and Mr. F. Miyajima of Kasuga Onojo Nakagawa Fire Department in Fukuoka Prefecture and Mr. M. Nishijima of Oki Consulting Solutions Co., Ltd. for the implementation on the smartphone in this research. Special thanks to Prof. Dr. R. Goebel, Alberta University, Canada who supported to perform the native check of the article.

#### REFERENCES

- [1] N. Hosono, H. Inoue, Y. Nagashima, and Y. Tomita, "Sensory Evaluation Method to create Pictograms based on Multiplex Sign Languages," in Proc. ACHI, 2013, pp. 13-16, Nice, France.
- [2] International Organization for Standardization: ISO9241-210: 2010, "Ergonomic requirements for Office Work with Visual Display Terminals (VDTs)." Available from: [http://www.iso.org/iso/home/store/catalogue\\_tc/catalogue\\_detail.htm?csnumber=52075](http://www.iso.org/iso/home/store/catalogue_tc/catalogue_detail.htm?csnumber=52075), 2015.11.8.
- [3] International Organization for Standardization: ISO9241-210 (former ISO13407:1999), "Ergonomics Human-centred design processes for interactive systems," 2010.
- [4] R. Hartson and P.S. Pyla, "The UX Book: Process and Guidelines for Ensuring a Quality User Experience," Morgan Kaufmann Publishers, 2012.
- [5] H. Inoue, "Sensory Evaluation," Juse-P, ISBN978-4-817-9435-0, Japanese version, 2013.
- [6] A. Field, "Discovering Statistics Using SPSS 3rd edition," Sage Publications, 2009.
- [7] W. Horton, "The Icon Book," John Wiley & Sons, Inc., 1994.
- [8] M. Akatsuka, "Seven Sign Languages for Tourists: Useful Words and Expressions," Chinese-Japanese-American Working Group, 2005.
- [9] N. Hosono, M. Suzuki, S. Hori, and Y. Tomita, "SOS Placard for the Hearing Disabled," in Proc. IEA2006, Maastricht, Netherlands.
- [10] N. Hosono, M. Suzuki, S. Hori, and Y. Tomita, "SOS Placard in Universal Use," The 2nd International Conference for Universal Design, IAUD, Kyoto, Japan, 2006.
- [11] N. Hosono, M. Suzuki, R. Kimura, H. Miki, and Y. Tomita, "Emergency Communication Service on Mobile Phone for Universal Ubiquitous Use," in Proc. AHFE2008, Las Vegas, USA.
- [12] N. Hosono, H. Miki, M. Suzuki, and Y. Tomita, "Urgent Collaboration Service for Inclusive Use," in Proc. HCII2009, San Diego, USA.
- [13] N. Hosono, H. Inoue, H. Miki, M. Suzuki, and Y. Tomita, "Universal Communication through Touch Panel," in Proc. AHFE2010, Miami, USA.
- [14] N. Hosono, H. Inoue, H. Miki, M. Suzuki, Y. Nagashima, and Y. Tomita, "Universal Communication Service for Inclusive Use," in Proc. SICE2010, Taipei, Taiwan.
- [15] N. Hosono, H. Miki, M. Suzuki, and Y. Tomita, "Universal Communication System for Urgent Use," in Proc. IAUD 2010, Hamamatsu, Japan.
- [16] M. Hirayama, M. Suzuki, and N. Hosono, "An Emergency Communication Pad for Hearing Impaired Persons," ICCIT 2010, Seoul, Korea.
- [17] N. Hosono, H. Inoue, and Y. Nagashima, "Context Analysis of Universal Communication through Local Sign Languages applying Multivariate Analysis," ICCHP2010, Vienna, Austria.
- [18] N. Hosono, H. Inoue, H. Miki, M. Suzuki, Y. Nagashima, Y. Tomita, and S. Yamamoto, "Service Science Method to create Pictograms referring to Sign Languages," in Proc. HCII2011, Orland, USA.
- [19] N. Hosono, H. Inoue, H. Miki, M. Suzuki, Y. Nagashima, Y. Tomita, and S. Yamamoto, "Service Service Method to create Pictograms referring to Sign Languages," in Proc. HCII2011.
- [20] N. Hosono, F. Miyajima, T. Inaba, M. Nishijima, M. Suzuki, H. Miki, and Y. Tomita, "The Urgent Communication System for Deaf and Language Dysfunction People," in Proc. HCII2013, Las Vegas, USA.

- [21] International Organization for Standardization, ISO9241-11, "Ergonomic requirements for Office Work with Visual Display Terminals (VDTs), Guidance on usability," 1998.
- [22] A. Cooper, "About Face 3," Wiley, 2007.
- [23] International Organization for Standardization, ISO9241-110, "Ergonomic requirements for Office Work with Visual Display Terminals (VDTs), Dialogue principles," 2006.
- [24] SPSS, "Categories in Statistical Package for Social Science ver.18," 2009.
- [25] N. Hosono, H. Inoue, and Y. Tomita, "Sensory Analysis Method applied to develop Initial Machine Specification," Measurement, vol. 32, pp. 7-13, 2002.
- [26] MIT, "APP Inventor," Available from: <http://appinventor.mit.edu/>, 2015.11.8.
- [27] Deploygate, Available from: <https://deploygate.com/>, 2015.11.8.
- [28] Freeplane, Available from: [http://freeplane.sourceforge.net/wiki/index.php/Main\\_Page](http://freeplane.sourceforge.net/wiki/index.php/Main_Page), 2015.11.8.
- [29] H. Akatsu, A. Komatsubara, "Auditory and Visual Guidance for Reducing Cognitive Load," in Proc. HCII 2007, Beijing, China.
- [30] H. Akatsu, H. Miki, and N. Hosono, "Designing Adaptive ATM based on universal design," in Proc. The 2nd International Conference for Universal Design, IAUD, Kyoto, Japan, 2006, pp.793-800, Kyoto, Japan.
- [31] H. Miki, and N. Hosono, "Universal Design with Information Technology," Japanese version, Maruzen, 2005.

# Effects of Boundary Damping on Natural Frequencies in Bending Vibrations of Intelligent Vibrissa Tactile Systems

Carsten Behn  
Christoph Will

Department of Technical Mechanics  
Ilmenau University of Technology, Germany  
Email: carsten.behn@tu-ilmenau.de  
christoph.will@tu-ilmenau.de

Joachim Steigenberger

Institute of Mathematics  
Ilmenau University of Technology, Germany  
Email: joachim.steigenberger@tu-ilmenau.de

**Abstract**—This paper is devoted to the analytical investigations of transversal vibrations of beams, which exhibit discrete, viscoelastic, rotational and translational supports. The special structure of the beam models is caused by the consideration of animal vibrissae. Vibrissae are tactile hairs (of a tactile sense organ), which complement the audible and visual sense. There exist different types of these tactile hairs, where we do not want to distinguish the various types, because the tenor of our investigations is from biomimetics and bionics. Rather, we are interested in the special design of a vibrissa from the mechanical point of view. In contrast to many works from literature, which focus on (quasi-) static bending investigations, we try to investigate and to determine the effects of the special design of a vibrissa (e.g., viscoelastic supports due to the follicle sine complex and due to the skin) on the dynamic behavior, especially on the spectrum of (natural) frequencies. The knowledge of dynamical characteristics is important for the design of artificial sensors. We present various beams with different supports (clamped and pivoted with discrete viscoelastic couplings), which are to model the biological tissues. This is new in literature and is different from existing researches. We focus on investigations of the natural frequency spectra of various systems. A close examination of vibrissa-like beam models with boundary damping exhibits features that are unlike in comparison to classical vibration systems.

**Keywords**—Bending beam vibrations; boundary damping; natural frequency; bio-inspired sensor; vibrissa.

## I. INTRODUCTION & MOTIVATION

This paper contributes to the development of intelligent tactile sensors and extends the results in the INTELLI 2014 paper [1]. There is a great interest in tactile sensors, since they have advantages in contrast to other sensor types. They are superior to optical sensors as in noisy environments (e.g., dark, murky water or in smoky air), and also cheaper in manufacture and use.

In the technical development, engineers often use biological systems as an inspiration. A tactile sensor system, which attracted attention in recent years, is the *animal vibrissa* found on, e.g., rats and mice. These hair-like sensors serve for the exploration of the environment, the animals use them, e.g., to detect outer objects, to distinguish between different surfaces, or to recognize surface textures, respectively.

For the functional understanding and analytical investigations, there are already various mechanical models for a

vibrissa to explain the technical acquisition of information. In contrast to various works from literature [2] [3] [4] [5] [6], we focus on investigations of the vibrissa dynamics in this paper. For this, we utilize the *classical Euler-Bernoulli beam*, which is often used to analyze systems in technical disciplines like automotive engineering (e.g., power train vibration) and microsystems technologies (e.g., cantilever vibration). In recent years, this classical model is used to model and to understand effects of vibrissa sensor systems in biomechanics [7]. This is also the background of the work presented in the paper. Due to the biological paragon, we set up various mechanical models and analyze them in an analytical and numerical way.

The scope of the present paper is to contribute to the mechanical modeling of a technical vibrissa as tactile sensors for the distance detection. In later application of object localization and distance detection, we try to determine the natural frequency spectrum due to an obstacle contact (modeled as a sudden bearing to the beam, hence, sudden change of boundary conditions) and its shift (compared to the scenario of no contact) to calculate the distance of the obstacle to the base of the artificial vibrissa, see also [8] and [9].

But, in contrast to literature, we incorporate spring and damping elements as in [1], representing the biological tissue of animal skin and support of the vibrissa. This is rarely done in literature. Hence, we extend the results in [10].

For this, we start an introduction to the biological paragon, describing its functionality, presenting the state of art in modeling of hair-like sensor systems, and introduce the analytical treatment of transverse vibrations of beams due to [11] in the following and present the investigations of various vibrissa models.

## II. THE PARAGON FROM BIOLOGY: VIBRISSAE

A paragon of (biological and artificial) tactile sensor systems is the animal vibrissae. Vibrissae are tactile hairs, can be found on, e.g., mice and rats, and complement the audible and visual sense. Mice and rats use their vibrissae (in the mystacial pad) to acquire information about their surroundings. The vibrissa itself (made of dead material) is mainly used as a lever for the force transmission. But, in contrast to ordinary hairs, vibrissae are stiffer and have a (assumed hollow) conical shape [12]. The mystacial vibrissae are arranged in an array of columns and rows around the snout, see Figure 1.

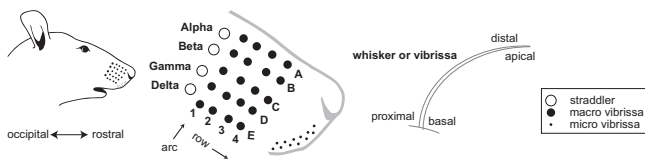


Figure 1. Schematic drawing of the mystacial pad, [12].

Each vibrissa is embedded in and supported by its own follicle-sinus complex (FSC). The FSC is characterized by its exceptional arrangement of blood vessels, neural connections and muscles. It is presumed that the rodents can control the viscoelastic properties of the vibrissa's support by regulating the blood supply to the sinus (like a blood sac) [13]. The functionality of these vibrissae vary from animal to animal and is best developed in rodents, especially in mice and rats [14]. The detection of contact forces is made possible by the pressure-sensitive mechanoreceptors in the support of the vibrissa (i.e., FSC). These mechanoreceptors are stimulated due to the vibrissa displacements in the FSC. The nerves transmit the information through several processing units to the Central Nervous System (CNS). The receptor cells offer the fundamental principle 'adaptation' [15] [16] [17] [18]. The muscle-system, see Figure 2 (adapted from [13] [19] [20] [21]) enables the rodents to use their vibrissae in two different ways (modes of operation):

- In the *passive mode*, the vibrissae are being deflected by external forces (e.g., wind). They return to their rest position passively — thus without any muscle activation, just via the fibrous band.
- In the *active mode*, the vibrissae are swung back-and forward by alternate contractions of the intrinsic and extrinsic muscles (with different frequencies and amplitudes). By adjusting the frequency and amplitude of the oscillations, the rodents are able to investigate object surfaces and shapes amazingly fast and with high precision [22].

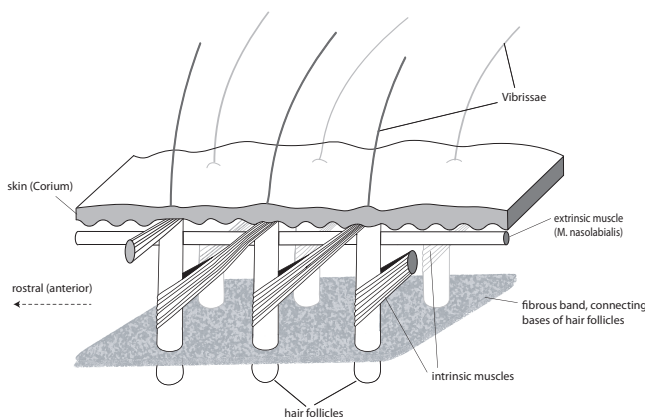


Figure 2. Schematic drawing of neighboring mystacial follicles [16].

Therefore, this biological sensor system is highly interesting for applications in the field of autonomous robotics, since tactile sensors can offer reliable information, where conventional sensors fail.

But, how the animals convert these multiple contacts with single objects into coherent information about their surroundings is still unclear. And it is not of main interest from our point of view: the tenor of our investigations is from bionics. The main focus is not on "copying" the solution from biology/animality, rather on detecting the main features, functionality and algorithms of the considered biological systems to implement them in (here: mechanical) models and to develop ideas for prototypes. We have to proceed in several steps, where step 1 to step 4 are usually of iterative manner, [18]:

1. analyzing live biological systems, e.g., here tactile hair system,
2. quantifying the mechanical and environmental behavior: identifying and quantifying mechanosensitive responses (e.g., pressure, vibrations) and their mechanisms as adaptation,
3. modeling live paradigms with those basic features developed before,
4. exploiting corresponding mathematical models in order to understand details of internal processes and,
5. coming to artificial prototypes (e.g., sensors in robotics), which exhibit features of the real paradigms.

Therefore, we present the state of art in modeling such sensor systems in the following.

Starting point and motivation of the following investigations are multiple **hypotheses** concerning the **functionality of the vibrissa**:

- The elasticity and the conical shape of the hair are relevant for the functionality of the vibrissa [2].
- The viscoelastic properties of the support (see the FSC) are controlled by the blood pressure in the blood sinus [13] [23].
- The vibrissae are excited with or close to their resonance frequencies during the active mode [24] [25].

Following these hypotheses, the primary tasks now are:

- to investigate the influence of elasticity and conical shape on the vibration characteristics of the vibrissa by analyzing its natural frequency spectrum;
- to analytically examine innovative models of a flexible vibrissa with a viscoelastic support, which fit the real object and its support better than models in literature.

### III. STATE OF ART IN MODELING HAIR-LIKE SENSORS

An intensive literature overview of technical vibrissa models has been given in [16].

In the majority of papers found in literature, the development of innovative technical whiskers was poorly based on mechanical models of the vibrissa. In order to analyze the mechanical and especially the dynamical behavior of the vibrissa, the physical principles of the paradigm have to be identified. Therefore, abstract technical models, which describe the biological example in detail and are suitable to be analyzed using engineering and scientific methods, are sought.

Usually, two types of models are used to analyze the mechanical behavior of the vibrissa:

- *Rigid body models* form the vibrissa as a stiff, inelastic body. Such models have the advantage of a simple mathematical description and solution. Furthermore, these models can easily be used to analyze the influence of varying viscoelastic supports. However, neglecting the inherent elasticity of the vibrissa implies a questionable oversimplification of the biological example.
- *Continuum models* are closer to the biological paradigm, as the tactile hair is implemented as an elastic beam. They are thus able to take the inherent dynamical behavior and the bending stiffness of the biological vibrissa into account.

Some approaches to the modeling of the biological paragon vibrissa use rigid body models, in which a rod-like vibrissa is supported by a combination of spring and damping elements modeling the viscoelastic properties of the follicle-sinus complex. However, all the rigid body models can only offer limited information about the functionality of the biological sensory system. Therefore, we focus on continuum models and deal with bending problems of continuous beam systems. In the following, we summarize the relevant models of [16] without any valuation:

- Birdwell et al. analyzed the bending behavior in [2]. They set up a simple model, which is analyzed in a linearly way, i.e., the investigations are only valid for small deflections. An important feature therein was the incorporation of the conical shape to the bending behavior. They stated that this fact from biology is not negligible. Moreover, they found out that the Young's modulus of natural vibrissae varies, but they were still neglecting the support's compliance. Further on, they determined the clamping torques for a vibrissa model, which is only valid for small deflection. In this context, they found out that influence of the natural pre-curvature of the vibrissa is negligible, which is rather obvious from the mechanical point of view.
- Scholz and Rahn set up a model for profile sensing with an actuated vibrissa in [26]. They realized an active mode of a vibrissa, scanned various obstacle contours and reconstructed the shape in the following way: the one-sided clamped vibrissa was moved along an object, the clamping reaction were measured and then used for a numerical integration method to determine the shape of the deflected vibrissae, which form an envelope of the object. These results were improved from, first, a fully analytical way in [5] and then, secondly, in [6] were the authors present a reconstruction algorithm, which uses noise corrupted measurement data to reconstruct the object shape. A test rig for an experimental verification is presented in [26] and [27]. All these works focussed a one-sided clamped technical vibrissa where the support's compliance is also neglected.
- The groups of Neimark et al. [24] and Andermann et al. [25] set up a model for the determination of the support's influence on the resonance properties of natural vibrissae. The present experimental measurements of vibrissae's resonance frequencies (with dubious results during numerical evaluations, because

a constant Young's modulus is used for all vibrissae. Their finding was a massive influence of the support on the resonance frequencies. Furthermore, they determined only of the first frequencies of the vibrissae. Analyzing the transduction and processing of the frequency provoked stimuli to the CNS, hence the resonance frequencies contain relevant information.

Most of the models in literature, in particular the rigid body models, are just results of anatomic investigations. They do not directly aim at bionic applications. Further on, some models are very exact, but too complex to gain deeper insight the system to identify the essential mechanical elements.

On the other hand, in particular, concerning continuum beam models, the level of mathematical investigations is rather low:

- linear bending theory with very simple conclusions,
- mixing of linear and nonlinear theories, and
- using boundary-value problems (BVP, the describing partial differential equation in combination with the boundary conditions of the analyzed model), which do not match the real objects sufficiently.

This was the reason that we started to investigate bending beam vibrations of technical vibrissae exhibiting a support compliance. First models were analyzed in [16] and presented in [1]. Focussing on our tenor and in order to do the investigations in an analytical way, we neglect the conical shape with respect to the complex structure of the arising partial differential equation. We focus on cylindrical beams.

First models with various elastic supports are presented in Figures 3 and 4.

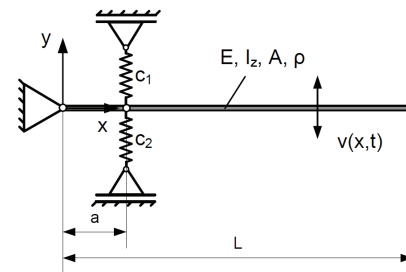


Figure 3. Pivoted vibrissa beam model with modeled skin support (one level of elasticity), [16].

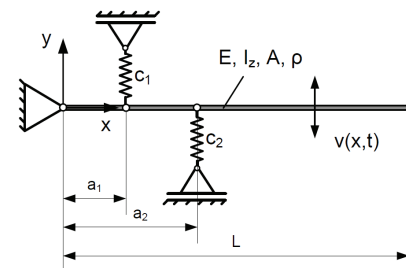


Figure 4. Pivoted vibrissa beam model with two levels of elasticity (FSC and skin), [16].

These models present a cylindrical pivoted beam with various elastics couplings (modeling the compliance of the FSC and skin). The arising BVP could be treated analytically in parts. But, the 'pivot' is at the base, this does not match reality.

Therefore, consider the model in Figure 5. The pivot is shifted, but the system is still undamped. Finally, we developed the model given in Figure 6.

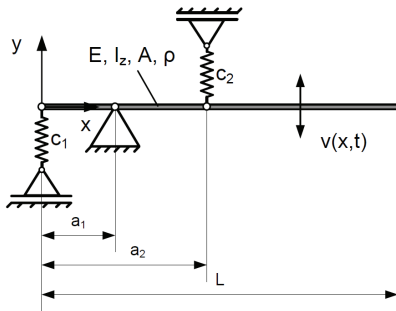


Figure 5. Undamped vibrissa beam model with modeled skin and FSC support, [16].

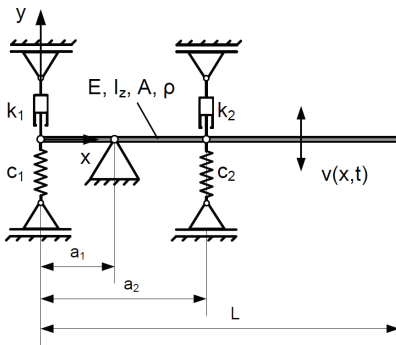


Figure 6. Damped vibrissa beam model with modeled skin and FSC support, [16].

In [1], we summarized for these models

- ⊖ Neglecting the conical shape of the vibrissa
- ⊕ Consideration of the support's compliance
  - at skin level
  - at the level of the FSC
- ⊕ Finding: massive influence of the support on the natural frequencies
- ⊕ Finding: influence of damping elements in the support
  - ↪ massive for the 1<sup>st</sup> natural frequency
  - ↪ but: unlike behavior of the natural frequencies (increasing frequencies if the system is damped, this contradicts the classical assertions)

#### IV. GOAL AND ARRANGEMENT OF THE FOLLOWING WORK

As mentioned above, we try to make the vibrissa models more realistic to the biological paradigm, but not too complex as the models in Figures 3 to 6. We present various approaches to implement and to determine the basic features of animal vibrissae as mentioned in Section II. Here, we will focus on

the mechanical properties and the dynamic behavior of the vibrissa beam models. The processing of the stimulus and the corresponding analysis of different control strategies are **not** discussed here. Furthermore, the investigations are addressed to a single vibrissa – the interaction between the different vibrissae in the mystacial pad is **not** taken into account. We just want to investigate the unlike behavior of the natural frequencies of these technical vibrissae as pointed out above.

To do this, we start with the classical differential equation for small bending vibrations of beams (linear Euler-Bernoulli theory) in the next Section V. We end up that section with an illustrating example in deriving the frequency spectrum.

Then, we set up and analyze various vibrissa beam models with different supports using discrete and continuously distributed spring and damping elements to mimic tissues of FSC and skin in Sections VI, VII and VIII. Following [24], we focus on the determination of the natural frequency spectrum of such beams analytically and numerically, while varying the viscoelastic properties of the support to check if some unlike behavior of the spectrum occurs. We will **not** focus on static bending problems in the following.

#### V. INTRODUCTION TO TRANSVERSAL VIBRATIONS OF BEAMS

The classical differential equation for small bending vibrations of beams (linear Euler-Bernoulli theory) is the basis of the investigations. Let us start with the following example: a one-sided clamped beam with elastic support (spring stiffness  $c$ ) at the end, see Figure 7. The beam has length  $L$ , Young's modulus  $E$ , density  $\rho$ , constant cross section area  $A$  and second moment of area  $I_z$ . We are seeking for the first five *natural frequencies*.

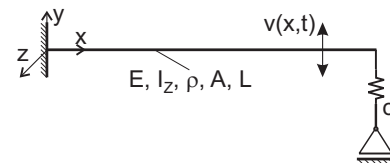


Figure 7. One-sided clamped beam with elastic end support.

**Remark V.1.** We focus on the first five natural frequencies of the spectrum because of

1. *mathematical reasons: the first three to five natural frequencies will form a good approximation basis of the Fourier series of the solution made by the method of separation of variables; and*
2. *physical meanings – higher natural frequencies are too large, whereas only lower ones are perceptible by means of tactile sense.*

The well-known equation of motion for free vibrations of a beam with small deformations, as in Figure 7, is [11]:

$$\ddot{v}(x, t) + k^4 v''''(x, t) = 0, \quad \text{with } k^4 := \frac{E I_z}{\rho A}, \quad (1)$$

where the function  $v(x, t)$  describes the vertical displacement at point  $x$  and at time  $t$ .

The partial differential equation (PDE) (1) and the following boundary conditions

- ①:  $v(0, t) = 0 \forall t \geq 0$
- ②:  $v'(0, t) = 0 \forall t \geq 0$
- ③:  $v''(L, t) = 0 \forall t \geq 0$
- ④:  $v'''(L, t) E I_z - c v(L, t) = 0 \forall t \geq 0$

form a BVP. Now, we apply the *method of separation of variables*, i.e., we are seeking for special solutions of structure

$$v(x, t) = X(x) \cdot T(t) \quad \forall (x, t). \quad (2)$$

Substitution into (1) yields two ordinary differential equations (ODEs)

$$\frac{\ddot{T}(t)}{T(t)} = -\mu^2, \quad (3)$$

$$-k^4 \frac{X''''(x)}{X(x)} = -\mu^2. \quad (4)$$

The general solution of (3) is

$$T(t) = \underline{B}_1 e^{i\mu t} + \underline{B}_2 e^{-i\mu t}, \quad \underline{B}_1, \underline{B}_2 \in \mathbb{C}. \quad (5)$$

The solution of (4) is:

$$X(x) = C_1 \cos(\lambda x) + C_2 \sin(\lambda x) + C_3 \cosh(\lambda x) + C_4 \sinh(\lambda x). \quad (6)$$

with  $C_1, C_2, C_3, C_4 \in \mathbb{C}$  and

$$\lambda^4 := \frac{\mu^2}{k^4}, \quad k^4 := \frac{E I_z}{\rho A}. \quad (7)$$

This shape solution (6) together with the formulated four boundary conditions form an eigenvalue problem (EVP) in the following. We get  $\forall t \geq 0$

- ①  $T(t) (C_1 + C_3) = 0$
- ②  $T(t) \lambda (C_2 + C_4) = 0$
- ③  $T(t) \lambda^2 (-C_1 \cos(\lambda L) - C_2 \sin(\lambda L) + C_3 \cosh(\lambda L) + C_4 \sinh(\lambda L)) = 0$
- ④  $E I_z T(t) \lambda^3 (C_1 \sin(\lambda L) - C_2 \cos(\lambda L) + C_3 \sinh(\lambda L) + C_4 \cosh(\lambda L)) - c T(t) (C_1 \cos(\lambda L) + C_2 \sin(\lambda L) + C_3 \cosh(\lambda L) + C_4 \sinh(\lambda L)) = 0$

$T(t)$  drops and a system of homogenous linear equations results with a coefficient matrix (8).

Since we are seeking for non-trivial solutions, we claim the singularity of the coefficient matrix:  $\det(M) = 0$ . Introducing a ratio of elasticity

$$\gamma_c := \frac{c}{c_S} = \frac{c}{\frac{E I_z}{L^3}} = \frac{c L^3}{E I_z}$$

we obtain the characteristic eigenvalue equation

$$\lambda^3 L^3 (1 + \cosh(\lambda L) \cos(\lambda L)) + \gamma_c (\cosh(\lambda L) \sin(\lambda L) - \cos(\lambda L) \sinh(\lambda L)) = 0 \quad (9)$$

**Remark V.2.** Before solving (9) we check it in setting

- $c = 0$ : we get  $1 + \cosh(\lambda L) \cos(\lambda L) = 0$ , which forms the eigenvalue equation of an one-sided clamped / free end beam in Figure 8;
- $c \rightarrow +\infty$ : we get  $\cosh(\lambda L) \sin(\lambda L) - \cos(\lambda L) \sinh(\lambda L) = 0$ , which arises for a clamped beam with bearing in Figure 9.

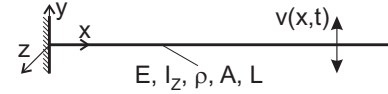


Figure 8. One-sided clamped beam with free end.

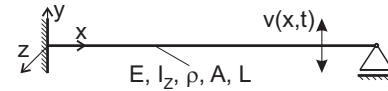


Figure 9. One-sided clamped beam with bearing.

Now, we present some numerical calculations. We choose  $\gamma_c = 1$  and derive the natural frequencies of a steel beam and of a B2 vibrissa, see Figure 1, using the following parameters:

- steel beam:  $E = 210$  GPa,  $\rho = 7850 \frac{\text{kg}}{\text{m}^3}$ ;
- B2 vibrissa:  $E = 2.3$  GPa,  $\rho = 238.732 \frac{\text{kg}}{\text{m}^3}$ ;
- geometric parameters:  $d = 0.2$  mm,  $I_z = \frac{\pi}{64} d^4$ ,  $A = \frac{\pi}{4} d^2$ ,  $L = 40$  mm.

The following Table I presents the first five eigenvalues  $\lambda_j$ , natural frequencies  $\omega_j$  in rad/s and frequencies  $f_j$  in Hz for a steel beam and a B2 vibrissa.

TABLE I. Calculation for  $\gamma_c = 1$ .

$j$	$\lambda_j$	steel beam		B2 vibrissa	
		$\omega_j$	$f_j$	$\omega_j$	$f_j$
1	2.010 $\frac{1}{L}$	653.008	103.929	843.189	62.369
2	4.704 $\frac{1}{L}$	3576.197	569.169	4617.724	341.566
3	7.857 $\frac{1}{L}$	9977.433	1587.958	12883.248	952.955
4	10.996 $\frac{1}{L}$	19544.181	3110.553	25236.203	1866.685
5	14.138 $\frac{1}{L}$	32305.127	5141.521	41713.630	3085.496

Increasing  $\gamma_c$  leads to increasing  $\omega_j$ , see also [1]. In the following, we increase the level of complexity.

## VI. VIBRISSA MODEL 1: TRANSLATIONAL VISCOELASTICITY

To clarify the unlike effects of the foregoing subsection, we deal with a 'simple' problem to investigate the influence of discrete damping elements. We consider a cylindrical, one-sided clamped beam, which is viscoelastically supported at the end, see Figure 10, which forms a subsystem of the complex one presented in Figure 6.

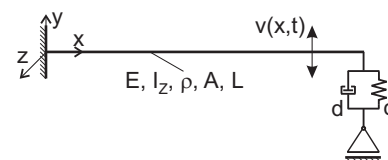


Figure 10. Clamped beam with viscoelastic end support.

$$M(\lambda) := \begin{pmatrix} 1 & \vdots & 0 & \vdots & 1 & \vdots & 0 \\ \dots & \dots & \dots & \dots & \dots & \dots & \dots \\ 0 & \vdots & \lambda & \vdots & 0 & \vdots & \lambda \\ \dots & \dots & \dots & \dots & \dots & \dots & \dots \\ \cos(\lambda L) \lambda^2 & \vdots & \sin(\lambda L) \lambda^2 & \vdots & \cosh(\lambda L) \lambda^2 & \vdots & \sinh(\lambda L) \lambda^2 \\ \dots & \dots & \dots & \dots & \dots & \dots & \dots \\ EI_z \sin(\lambda L) \lambda^3 & \vdots & -EI_z \cos(\lambda L) \lambda^3 & \vdots & EI_z \sinh(\lambda L) \lambda^3 & \vdots & EI_z \cosh(\lambda L) \lambda^3 \\ -c \cos(\lambda L) & \vdots & -c \sin(\lambda L) & \vdots & -c \cosh(\lambda L) & \vdots & -c \sinh(\lambda L) \end{pmatrix} \quad (8)$$

Equation (1) together with the boundary conditions

$$\begin{aligned} v(0, t) &\equiv 0 \\ v'(0, t) &\equiv 0 \\ v''(L, t) &\equiv 0 \\ EI_z v'''(L, t) - d \dot{v}(L, t) - c v(L, t) &\equiv 0, \end{aligned}$$

forms a BVP.

The handling of the last boundary condition results in

$$EI_z X'''(L) - c X(L) = \pm i d \lambda^2 k^2 X(L).$$

All conditions lead to a coefficient matrix (not listed here for brevity) of the homogenous systems whose singularity yields the eigenvalue equation (EVEQ):

$$\begin{aligned} \det(A(\lambda)) &= -EI_z \lambda^3 \\ &- EI_z \cos(\lambda L) \cosh(\lambda L) \lambda^3 \\ &\pm i d k^2 \sin(\lambda L) \cosh(\lambda L) \lambda^2 \\ &- c \sin(\lambda L) \cosh(\lambda L) \\ &\mp i d k^2 \cos(\lambda L) \sinh(\lambda L) \lambda^2 \\ &+ c \cos(\lambda L) \sinh(\lambda L) = 0. \end{aligned} \quad (10)$$

**Remark VI.1.** At this stage, we could check this equation in concluding well-known eigenvalue equations: setting  $\{d = 0, c = 0\}$  we get the EVEQ of system in Figure 8, or  $\{d = 0, c > 0\}$  of model in Figure 7, or  $\{d = 0, c \rightarrow +\infty\}$  of model in Figure 9, all results in the equations presented in [11] or [28].

Introducing the dimensionless parameters

$$\begin{aligned} c^* &:= \frac{c}{EI_z} \\ d^* &:= \frac{L d}{\sqrt{\rho A E I_z}}, \end{aligned}$$

we determine the first three natural frequencies in varying  $c^*$  and  $d^*$ . (From now, we drop the notation ‘\*’ as a mark for a dimensionless parameter for brevity.) We get the following Figures 11 to 13.

For fixed  $c$  and varying  $d$ , there are parameter ranges of  $c$  where we get an expected and unexpected behavior of the first natural frequency, see Figure 11:

- $c \in [0, 17]$ : the natural frequency breaks down to zero for increasing  $d$ ;
- $c \in [18, 23]$ : first, the natural frequency increases and then breaks down to zero;

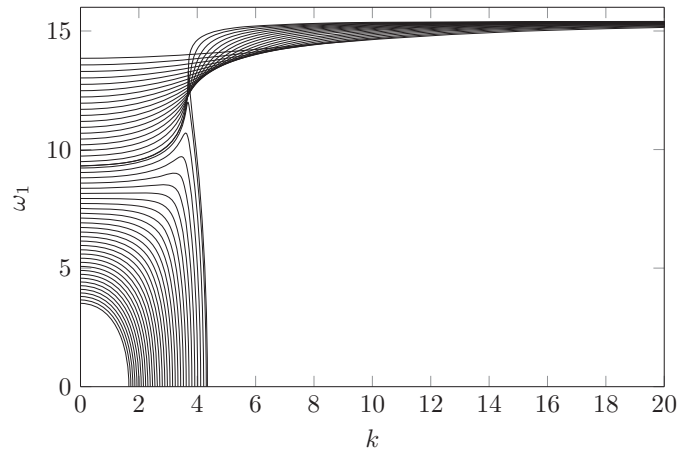


Figure 11. First natural frequency of the beam model  $\omega_1$  in  $\sqrt{\frac{EI_z}{\rho A L^4}}$  in dependence on  $c$  and  $d$ .

- $c > 23$ : the natural frequency just increases.

On the other hand, for fixed  $d$  and varying  $c$ , we observe the following:

- $d \in [0, 3.5]$ : increasing  $c$  leads to an increase of the natural frequency;
- $d > 3.5$ : an increase of  $c$  results first in a decrease and then in an increase of the natural frequency.

This may explain the behaviors of the natural frequencies described above and presented in [1], which contradicts the classical assertions.

Similar effects can be observed in Figures 12 and 13.

## VII. VIBRISSA MODEL 2: ROTATIONAL VISCOELASTICITY

Since the vibrissa system in Figure 10 forms not really a bio-inspired vibrissa system, we soften the clamping to a bearing with a torsional spring and damper element, see Figure 14.

The boundary condition have changed to

$$\begin{aligned} v(0, t) &\equiv 0 \\ EI_z v''(0, t) - c_t v'(0, t) - d_t \dot{v}'(0, t) &\equiv 0 \\ v''(L, t) &\equiv 0 \\ v'''(L, t) &\equiv 0. \end{aligned}$$

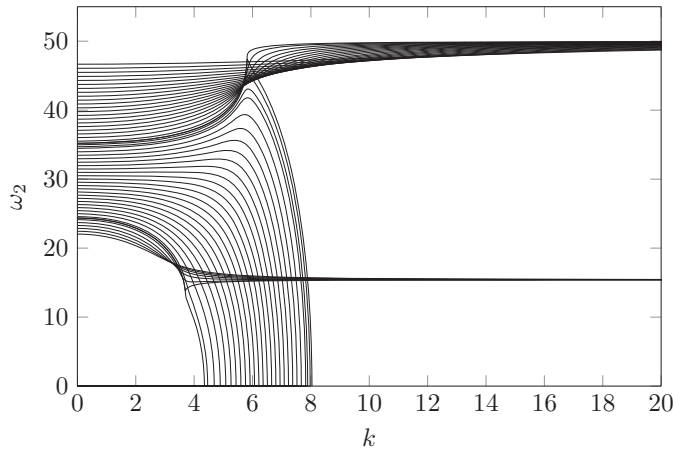


Figure 12. Second natural frequency of the beam model  $\omega_2$  in  $\sqrt{\frac{E I_z}{\rho A L^4}}$  in dependence on  $c$  and  $d$ .

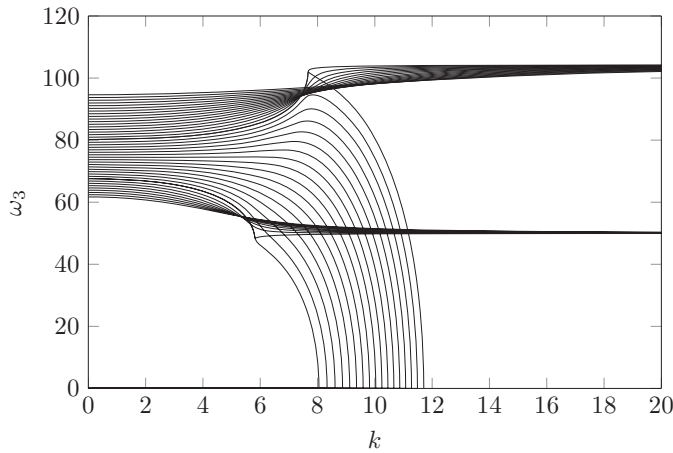


Figure 13. Third natural frequency of the beam model  $\omega_3$  in  $\sqrt{\frac{E I_z}{\rho A L^4}}$  in dependence on  $c$  and  $d$ .

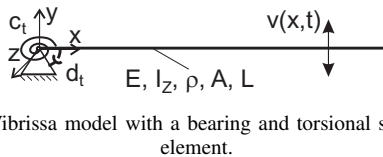


Figure 14. Vibrissa model with a bearing and torsional spring-damper element.

Introducing the dimensionless parameters

$$c_t^* := \frac{c_t}{EI_z/L}$$

$$d_t^* := \frac{d_t}{L\sqrt{\rho A EI_z}},$$

we determine the first three natural frequencies in varying  $c_t^*$  and  $d_t^*$ . (Once again, we omit the notation ‘\*’ for brevity.) We get the following EVEQ:

$$\lambda (\cos(\lambda) \sinh(\lambda) \sin(\lambda) \cosh(\lambda)) (\cos(\lambda) \cosh(\lambda) + 1) (c_t \pm i \lambda^2 d_t) = 0. \quad (11)$$

Solving this EVEQ in  $\lambda$  and determination of the corresponding natural frequencies we get the natural frequency behavior presented in Figures 15 to 17.

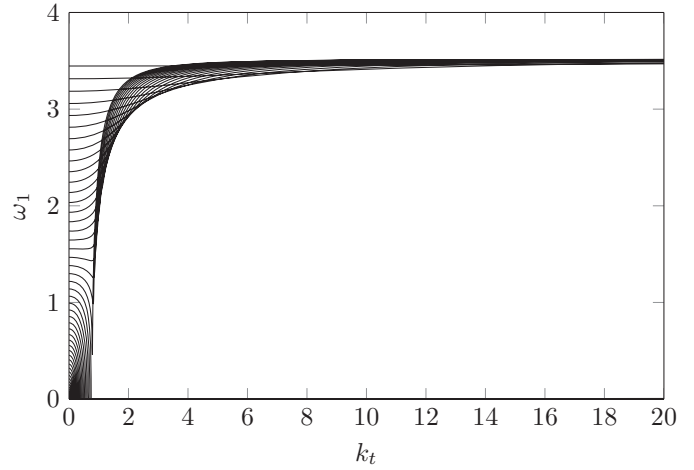


Figure 15. First natural frequency of the beam model  $\omega_1$  in  $\sqrt{\frac{E I_z}{\rho A L^4}}$  in dependence on  $c_t$  and  $d_t$ .

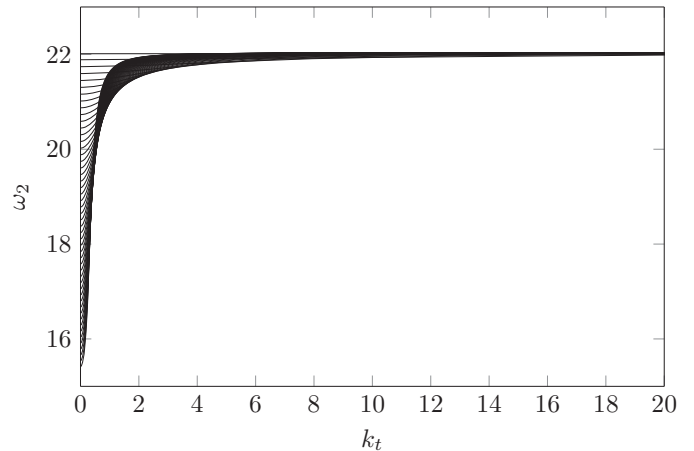


Figure 16. Second natural frequency of the beam model  $\omega_2$  in  $\sqrt{\frac{E I_z}{\rho A L^4}}$  in dependence on  $c_t$  and  $d_t$ .

One can clearly see that only the first natural frequency exhibit a similar unlike behavior, because some curves break down to zero. If  $c_t$  has a special value, then if  $c_t$  and / or  $d_t$  increases to infinity, the natural frequency  $\omega_1$  tends to the first natural frequency of system in Figure 8. This behavior can be seen in observing  $\omega_2$  in Figure 16 and  $\omega_3$  in Figure 17 from the very beginning, which is a typical behavior of natural frequencies.

### VIII. VIBRISSA MODEL 3: TRANSLATIONAL AND ROTATIONAL VISCOELASTICITY

Now, we use the model of Section VII and combine it with an additional support mimicking a sudden obstacle contact modeled as a translational viscoelastic support, see Figure 18.

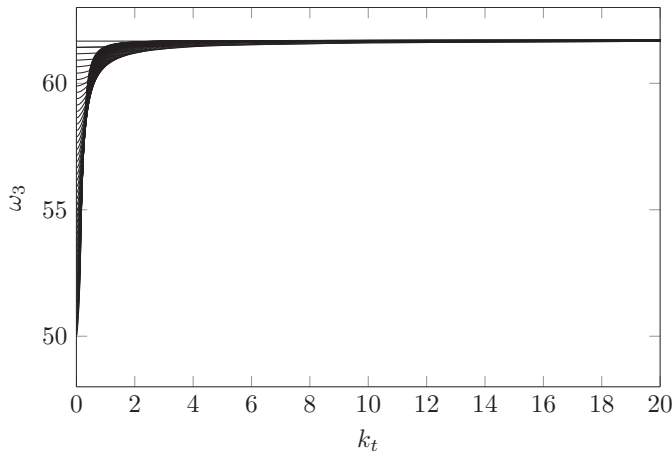


Figure 17. Third natural frequency of the beam model  $\omega_3$  in  $\sqrt{\frac{E I_z}{\rho A L^4}}$  in dependence on  $c_t$  and  $d_t$ .

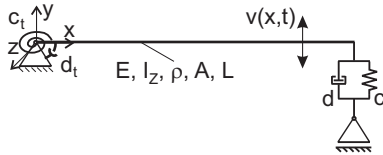


Figure 18. Vibrissa model with object contact: torsional spring-damper-bearing and viscoelastic end support.

We suppose that the vibrissa contacts the object with the tip, as in [8] and [9], such that model consideration is valid. Now, the upcoming calculation shall later provide the determination of the shift of the spectrum of natural frequencies to determine the distance to the object. For this, we need to have a reliable determination of the spectrum, still exhibiting unlike effects described above.

The boundary condition are now

$$\begin{aligned} v(0, t) &\equiv 0 \\ E I_z v''(0, t) - c_t v'(0, t) - d_t \dot{v}'(0, t) &\equiv 0 \\ v''(L, t) &\equiv 0 \\ E I_z v'''(L, t) - d \dot{v}(L, t) - c v(L, t) &\equiv 0. \end{aligned}$$

Performing the same procedure in deriving the EVEQ as above, we get

$$\begin{aligned} &\lambda^3 \left\{ \lambda (\cosh(\lambda) \sin(\lambda) - \sinh(\lambda) \cos(\lambda)) \right. \\ &\quad \left. - (c_t \pm i d_t \lambda^2) (1 + \cosh(\lambda) \cos(\lambda)) \right\} \\ &\quad \left. - (c \pm i d \lambda^2) \left\{ \lambda \sinh(\lambda) \sin(\lambda) \right. \right. \\ &\quad \left. \left. + (c_t \pm i d_t \lambda^2) (\cosh(\lambda) \sin(\lambda) - \sinh(\lambda) \cos(\lambda)) \right\} = 0. \end{aligned} \quad (12)$$

Several investigations / scenarios are conceivable. We only focus on the following two cases:

- Case 1: a parameter dependence of the natural frequencies on the 'FSC' support parameters  $c_t$  and  $d_t$  is performed, where we choose  $c = 1$  and  $k = 1$  fix.

- Case 2: a dependence of the natural frequencies on the 'contact' parameters  $c$  and  $d$  is analyzed, where we choose  $c_t = 100$  and  $d_t = 20$ .

In Case 1, we get describe a soft object contact with the chosen parameters. Hence, we have the possibility to do comparison to Section VII. One can clearly see the similarity of Figures 15 to 17 with Figures 19 to 21.

Here are more parameter studies necessary to get more familiar with this system. If we use such a system in later experiments, we could be able to detect not only the distance to an object (as done in [9]) but also the compliance of the object.

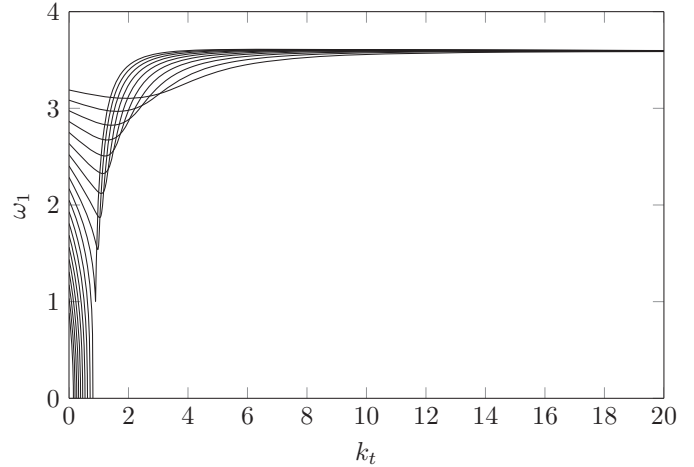


Figure 19. First natural frequency of the beam model  $\omega_1$  in  $\sqrt{\frac{E I_z}{\rho A L^4}}$  in dependence on  $c_t$  and  $d_t$ .

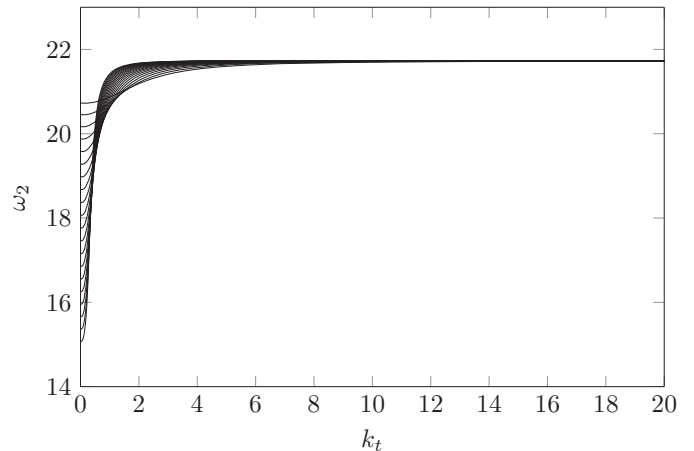


Figure 20. Second natural frequency of the beam model  $\omega_2$  in  $\sqrt{\frac{E I_z}{\rho A L^4}}$  in dependence on  $c_t$  and  $d_t$ .

In Case 1, we get describe a soft object contact with the chosen parameters. Hence, we have the possibility to do comparison to Section VII. One can clearly see the similarity of Figures 15 to 17 with Figures 19 to 21.

Here are more parameter studies necessary to get more familiar with this system. If we use such a system in later

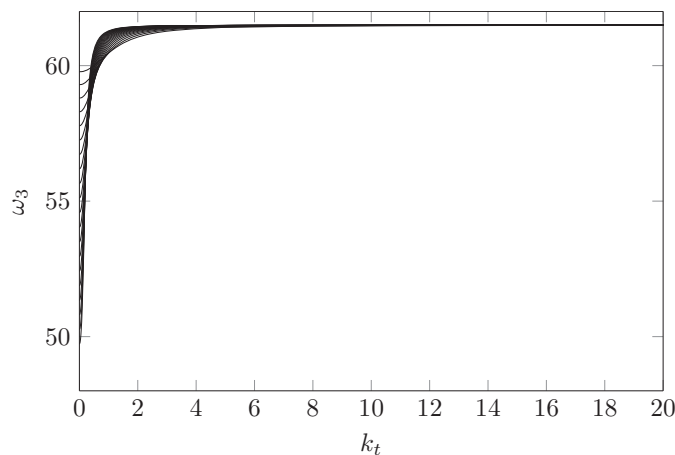


Figure 21. Third natural frequency of the beam model  $\omega_3$  in  $\sqrt{\frac{E I_z}{\rho A L^4}}$  in dependence on  $c_t$  and  $d_t$ .

experiments, we could be able to detect not only the distance to an object (as done in [9]) but also the compliance of the object.

In Case 2, we focus on a ‘hard’ bearing (or nearly a clamping), so that comparison to Section VI can be done. We have a similar behavior of the natural frequencies if someone inspects Figures 11 to 13 with Figures 22 to 24.

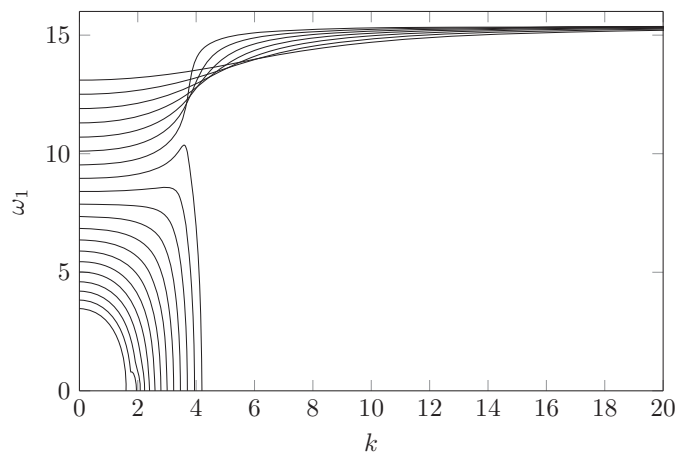


Figure 22. First natural frequency of the beam model  $\omega_1$  in  $\sqrt{\frac{E I_z}{\rho A L^4}}$  in dependence on  $c_t$  and  $d_t$ .

Summarizing, the unlike behavior appears also in combined systems and is not a numerical feature. More investigation should be done, before coming to real prototypes of artificial vibrissa-like sensors.

## IX. CONCLUSION

The goal of this contribution was to present the theoretical context needed to examine the mechanical and in particular the dynamical characteristics of the biological vibrissa. Moreover, these theoretical aspects were to be interpreted with respect to the biological vibrissa, as well as for a technical implementation of it. Inspired by this biological sensory system, several types of mechanical models were

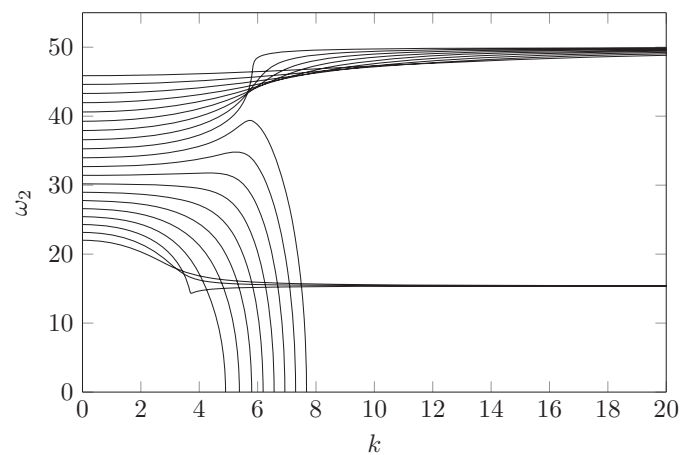


Figure 23. Second natural frequency of the beam model  $\omega_2$  in  $\sqrt{\frac{E I_z}{\rho A L^4}}$  in dependence on  $c_t$  and  $d_t$ .

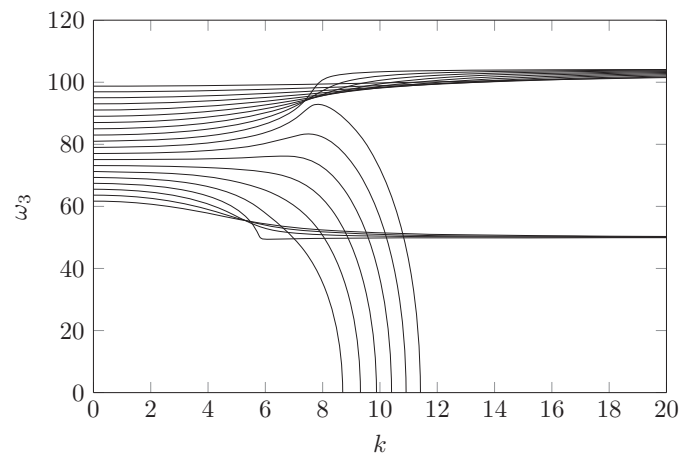


Figure 24. Third natural frequency of the beam model  $\omega_3$  in  $\sqrt{\frac{E I_z}{\rho A L^4}}$  in dependence on  $c_t$  and  $d_t$ .

developed based on findings in the literature.

The second focus was on the modeling of the vibrissa as a *continuous system*: bending vibrations of beams. There, the main focus of the studies lay on the examination of the influence of the tactile hair compliance and the viscoelastic support on the oscillation characteristics of the vibrissa. The conical form was neglected until now.

The influence of the viscoelastic support of the vibrissa has been examined using various abstract models, in which the vibrissa was modeled as a thin, cylindrical, flexible beam. The viscoelastic properties of the FSC and the skin were implemented by using spring and damping elements.

The damping element significantly increased the complexity of the differential equations and led to a surprising phenomenon: there exist some natural frequencies, which break down to zero for a certain range of parameters. This fact is well-known in 1-DoF systems (i.e., strong damping, creeping behavior). The study demonstrated that the oscillation behavior of an elastic beam differs remarkably from the behavior of such

a classical system:

- The natural frequencies may increase with growing boundary damping.
- For specific damping parameter values, the natural frequencies grow for decreasing boundary stiffness.

This behavior also occurred in other developed vibrissa-like sensor systems, which are much closer to the real paradigm, also in context of an object contact.

But, theories gained from the simplified linear Euler-Bernoulli theory are only valid for small deflections and deformations. If one considers a vibrissa beam in passive mode, then it may be questionable if this theory is really qualified for the investigations, see large bending deformations. Inspecting these vibrissa configurations, one could clearly observe that the vibrissa in passive mode suffers large deformations. Hence, the linear Euler-Bernoulli theory is not qualified to determine the natural frequencies since it describes the bending behavior for small deformations. We have to turn to a nonlinear theory – Timoshenko theory or nonlinear Euler-Bernoulli theory. We will arrive at more realistic models and description of these models, which then are closer to the biological paradigm. An approach is done in [29].

However, we are focussing on long, slender beams, whereby shear forces may have less influence. So, we shall focus on the nonlinear Euler-Bernoulli theory in future work. Additionally, we shall include the conical shape and a pre-curvature of the beam, neglected until now.

The first works, setting up a prototype of these investigations, can be found in [9] and [27].

#### REFERENCES

- [1] C. Behn, C. Will, and J. Steigenberger, "Unlike Behavior of Natural Frequencies in Bending Beam Vibrations with Boundary Damping in Context of Bio-inspired Sensors," in *Proceedings INTELLI 2014: The Third International Conference on Intelligent Systems and Applications*, Sevilla (Spain), June 2014, IARIA, pp. 75–84.
- [2] A. Birdwell et al., "Biomechanical Models for Radial Distance Determination by the Rat Vibrissal System," *The Journal of Neurophysiology*, vol. 98, pp. 2439–2455, 2007.
- [3] D. Kim and R. Möller, "Biomimetic whiskers for shape recognition," *Robotics and Autonomous Systems*, vol. 55, no. 3, pp. 229–243, 2007.
- [4] C. Tuna, J. H. Solomon, D. L. Jones, and M. J. Hartmann, "Object shape recognition with artificial whiskers using tomographic reconstruction," in *IEEE International Conference on Acoustics, Speech and Signal Processing (ICASSP)*, pp. 2537–2540, 2012.
- [5] C. Will, J. Steigenberger, and C. Behn, "Object Contour Reconstruction using Bio-inspired Sensors," in *Proceedings 11th International Conference on Informatics in Control, Automation and Robotics (ICINCO 2014)*, Vienna (Austria), September 2014, SciTePress, pp. 459–467, 2014.
- [6] C. Will, J. Steigenberger, and C. Behn, "Quasi-static object scanning using technical vibrissae," in *Proceedings 58th International Scientific Colloquium*, Ilmenau (Germany), September 2014.
- [7] S. Hirose, S. Inoue, and K. Yoneda, "The whisker sensor and the transmission of multiple sensor signals," *Advanced Robotics*, vol. 4, no. 2, pp. 105–117, 1989.
- [8] N. Ueno, M. M. Svinin, and M. Kaneko, "Dynamic contact sensing by flexible beam," *IEEE/ASME Trans. Mechatronics*, vol. 3, no. 4, pp. 254–264, 1998.
- [9] D. Baldeweg, C. Will, and C. Behn, "Transversal Vibrations of Beams in Context of Vibrissae with Foundations, Discrete Supports and Various Sections," in *Proceedings 58th International Scientific Colloquium*, Ilmenau (Germany), September 2014.
- [10] H. Pierson, J. Brevick, and K. Hubbard, "The effect of discrete viscous damping on the transverse vibration of beams," *Journal of Sound and Vibration*, vol. 332, pp. 4045–4053, 2013.
- [11] W. Weaver, S. P. Timoshenko, and D. H. Young, *Vibration Problems in Engineering*. John Wiley & Sons Inc., Chichester, 1990.
- [12] D. Voges et al., "Structural characterisation of the whisker system of the rat," *IEEE Sensors Journal*, vol. 12, no. 2, pp. 332–339, 2012.
- [13] J. Dörfel, "The musculature of the mystacial vibrissae of the white mouse," *Journal of Anatomy*, vol. 135, pp. 147–154, 1982.
- [14] T.-E. Jin, V. Witzemann, and M. Brecht, "Fiber Types of the Intrinsic Whisker Muscle and Whisking Behavior," *The Journal of Neuroscience*, vol. 24, no. 13, pp. 3386–3393, 2004.
- [15] D. R. Soderquist, *Sensory processes*. Sage Publications, Thousand Oaks, 2002.
- [16] C. Behn, "Mathematical Modeling and Control of Biologically Inspired Uncertain Motion Systems with Adaptive Features," Habilitation thesis, Faculty of Mechanical Engineering, Ilmenau University of Ilmenau, Germany, 2013.
- [17] C. Behn, "Modeling the Adjustment of Receptor Cells via Adaptive  $\lambda$ -Stabilizing-Control," *Journal of Mechatronics*, vol. 2, no. 4, pp. 275–290, 2014.
- [18] C. Behn, "Modeling, Analysis and Control of Mechanoreceptors with Adaptive Features," in *Informatics in Control, Automation and Robotics – Lecture Notes in Electrical Engineering (LNEE)*, vol. 325, J.-L. Ferrier et al. (eds.), Springer International Publishing, Switzerland, pp. 349–366, 2015.
- [19] J. Dörfel, "The innervation of the mystacial region of the white mouse – A topographical study," *Journal of Anatomy*, vol. 142, pp. 173–184, 1985.
- [20] L. E. Wineski, "Facial morphology and vibrissal movement in the golden hamster," *Journal of Morphology*, vol. 183, pp. 199–217, 1985.
- [21] S. Haidarliu, E. Simony, D. Golomb, and E. Ahissar, "Muscle Architecture in the Mystacial Pad of the Rat," *The Anatomical Record*, vol. 293, pp. 1192–1206, 2010.
- [22] M. J. Hartmann and J. H. Solomon, "Robotic whiskers used to sense features: Whiskers mimicking those of seals or rats might be useful for underwater tracking or tactile exploration," *NATURE*, vol. 443, p. 525, 2006.
- [23] K. Carl, *Technische Biologie des Tasthaar-Sinnessystems als Gestaltungsgrundlage für taktile stiftführende Mechanosensoren, Technical biology of the vibrissa sensor system as design principles for tactile mechanosensors*. PhD thesis, Universitätsverlag, Ilmenau, 2009.
- [24] M. A. Neimark, M. L. Andermann, J. J. Hopfield, and C. I. Moore, "Vibrissa Resonance as a Transduction Mechanism for Tactile Encoding," *The Journal of Neuroscience*, vol. 23, no. 16, pp. 6499–6509, 2003.
- [25] M. L. Andermann, J. Ritt, M. Neimark, and C. I. Moore, "Neural Correlates of Vibrissa Resonance: Band-Pass and Somatotopic Representation of High-Frequency Stimuli," *Neuron*, vol. 42, pp. 451–463, 2004.
- [26] G. Scholz and C. Rahn, "Profile Sensing With an Actuated Whisker," *IEEE Transactions on Robotics and Automation*, vol. 20, pp. 124–127, 2004.
- [27] C. Will, J. Steigenberger, and C. Behn, "Bio-inspired Technical Vibrissae for Quasi-static Profile Scanning," accepted for *Informatics in Control, Automation and Robotics Lecture Notes in Electrical Engineering (LNEE)*, Springer, 2016.
- [28] D. Gross, W. Hauger, W. Schnell, and P. Wriggers, *Technische Mechanik: Band 4 Hydromechanik, Elemente der Höheren Mechanik, Numerische Methoden, Technical Mechanics: Volume 4 Hydromechanics, higher mechanics, numerical methods*. Springer, Berlin, 2002.
- [29] J. H. Solomon and M. J. Hartmann, "Extracting object contours with the sweep of a robotic whisker using torque information," *The International Journal of Robotics Research*, vol. 29, pp. 1233–1245, 2010.

# On the Potential of Grammar Features for Automated Author Profiling

Michael Tschuggnall and Günther Specht

Databases and Information Systems

Institute of Computer Science, University of Innsbruck, Austria

{michael.tschuggnall, guenther.specht}@uibk.ac.at

**Abstract**—The automatic classification of data has become a major research topic in the last years, and especially the analysis of text has gained interest due to the availability of huge amounts of online documents. In this paper, a novel style feature based on grammar syntax analysis is presented that can be used to automatically profile authors, i.e., to predict gender and age of the originator. Using full grammar trees of the sentences of a document, substructures of the trees are extracted by utilizing pq-grams. The mostly used patterns are then stored in a profile and serve as input features for common machine learning algorithms. An extensive evaluation using a state-of-the-art test set containing several thousand English web blogs investigates on the optimal parameter and classifier configuration. Promising results indicate that the proposed feature can be used as a standalone, significant characteristic to automatically predict the gender and age of authors. Finally, further evaluations incorporating other commonly used word-based features like the number of stop words, the type-token-ratio or different readability indices strengthen the high potential of grammar analysis for automated author profiling.

**Keywords**—Author Profiling; Text Classification; Grammar Trees; Textual Features; Machine Learning.

## PREFACE

The following article extends previous work on profiling the gender and age of authors [1].

## I. INTRODUCTION

With the advent of the internet in general and recently especially with social media, users frequently use the numerous possibilities to compose and post text in various ways. Considering current statistics [2] estimating 70 billion pieces of content shared via Facebook or 190 million short messages posted on Twitter every day, the amount of shared textual information is huge. Although the authors of the latter examples are generally known, the information is most often restricted to a user name. Moreover, there also exist cases like anonymized blogs where every information concerning the originator is hidden intentionally.

In contrast to traditional authorship attribution approaches [3] that try to assign one of several known candidate authors to an unlabeled document, the author profiling problem deals with the extraction of useful meta information about the author. Often this information includes gender and age of the originator [4][5][6], but also other demographic information like cultural background or psychological analyses are examined in recent approaches [7][8]. Where the mining of such information can be applied very well to commercial applications by knowing the percentages of gender and age commenting on a new product release for example, it is also

of growing importance in juridical applications (*Forensic Linguistics*) [9], where, e.g., the number of possible perpetrators can be reduced. Moreover, especially nowadays in the area of cybercrime [10], recent approaches investigate the content of e-mails [11], suicide letters or try to automatically expose sexual predators from chat logs [12].

In this paper, a novel style feature to automatically extract the gender and age of authors of text documents is presented and compared to other common text features. Using results of previous work in the field of intrinsic plagiarism detection [13] and authorship attribution [14], the assumption that individual authors have significantly different writing styles in terms of the syntax that is used to construct sentences has been reused. For example, the following sentence extracted from a web blog:

*"My chair started squeaking a few days ago and it's driving me nuts."* (S1)

could also be formulated as

*"Since a few days my chair is squeaking - it's simply annoying."* (S2)

which is semantically equivalent but differs significantly according to the syntax as can be seen in Figure 1. The main idea of this work is to quantify those differences by calculating grammar profiles using pq-grams of full grammar trees, and to evaluate how reliable a prediction of an authors meta information is when solely this grammar feature is used. Given the grammar profiles, the prediction of gender and age, respectively, is then examined by utilizing modern machine learning approaches like support vector machines, decision trees or Naive Bayes classifiers. Finally, the results gained from pure grammar analysis are complemented with and compared to other commonly used lexical features like the type-token-ratio or different readability indices.

The rest of this paper is organized as follows: Section II recaps the concept of pq-grams as a fundamental basis of this work, while Section III explains the profiling process in detail. An extensive and promising evaluation using a comprehensive test set of web blogs is presented in Section IV. In order to put the results into perspective, Section V integrates and evaluates commonly used word-based features. Finally, related work is summarized in Section VI and conclusions including future work are outlined in Section VII.

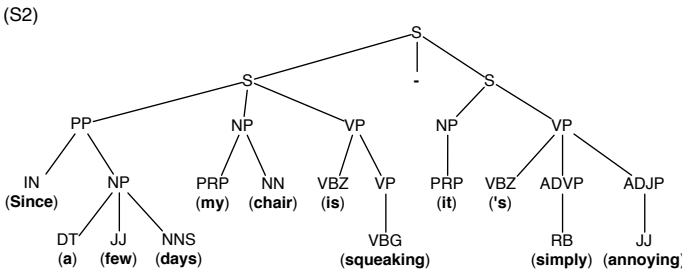
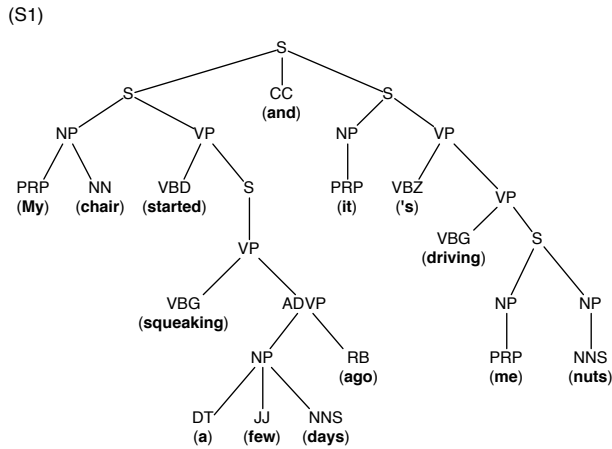


Fig. 1. Grammar Trees of the Semantically Equivalent Sentences (S1) and (S2).

## II. PRELIMINARIES: PQ-GRAMS

Similar to n-grams that represent subparts of given length  $n$  of a string, pq-grams extract substructures of an ordered, labeled tree [15][16]. The size of a pq-gram is determined by a stem ( $p$ ) and a base ( $q$ ) like it is shown in Figure 2. Thereby  $p$  defines how much nodes are included vertically, and  $q$  defines the number of nodes to be considered horizontally. For example, a valid pq-gram with  $p = 2$  and  $q = 3$  starting from PP at the left side of tree (S2) shown in Figure 1 would be [PP-NP-DT-JJ-NNS] (the concrete words are omitted).

The pq-gram index then consists of all possible pq-grams of a tree. In order to obtain all pq-grams, the base is shifted left and right additionally: If then less than  $p$  nodes exist horizontally, the corresponding place in the pq-gram is filled with \*, indicating a missing node. Applying this idea to the previous example, also the pq-gram [PP-IN-\*\*\*\*] (no nodes in the base) is valid, as well as [PP-NP-\*\*\*\*-DT] (base shifted left by two), [PP-NP-\*DT-JJ] (base shifted left by one), [PP-NP-JJ-NNS-\*] (base shifted right by one) and [PP-NP-NNS-\*\*\*\*] (base shifted right by two) have to be considered. As a last example, all leaves have the pq-gram pattern [leaf\_label-\*\*\*\*\*].

Finally, the pq-gram index is the set of all valid pq-grams of a tree, whereby multiple occurrences of the same pq-grams are also present multiple times in the index.

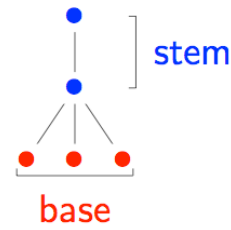


Fig. 2. Structure of a pq-gram Consisting of Stem  $p = 2$  and Base  $q = 3$ .

## III. PROFILING AUTHORS USING PQ-GRAM INDICES

The number of choices an author has to formulate a sentence in terms of grammar structure is rather high, and the assumption in this approach is that the concrete choice is made mostly intuitively and unconsciously. Previous work (e.g., [13]) and evaluations shown in Section IV reinforce that solely grammar syntax represents a significant feature that can be used to categorize authors.

Basically, the profiling of a given text using pq-grams works as follows:

- 1) At first the text is parsed and split into single sentences using common sentence boundary detection algorithms, which is currently implemented with *OpenNLP* [17]. Each sentence is then analyzed by its grammar, i.e., a full syntax tree is calculated using the *Stanford Parser* [18]. For example, Figure 1 depicts the grammar trees resulting from analyzing sentences (S1) and (S2), respectively. The labels of each tree correspond to a part-of-speech (POS) tag of the Penn Treebank set [19], where, e.g., *NP* corresponds to a noun phrase, *DT* to a determiner or *JJS* to a superlative adjective. In order to examine the building structure of sentences only like it is intended by this work, the concrete words, i.e., the leaves of the tree, are omitted.
- In case of ambiguity of grammar trees, i.e., if there exist more than one valid parse tree for a sentence, the tree with the highest probability estimated by the parser is chosen.
- 2) Using the grammar trees of all sentences of the document, the pq-gram index is calculated. As shown in Section II all valid pq-grams of a sentence are extracted and stored into a pq-gram index. By combining all pq-gram indices of all sentences, a pq-gram profile is computed which contains a list of all pq-grams and their corresponding frequency of appearance in the text. Thereby the frequency is normalized by the total number of all appearing pq-grams. As an example, the five mostly used pq-grams using  $p = 2$  and  $q = 3$  of a sample document are shown in Table I. The profile is sorted descending by the normalized occurrence, and an additional rank value is introduced that simply defines a natural order which is used in the evaluation (see Section IV).
- 3) Finally, the pq-gram profiles including occurrences and ranks are used as features that are applied to common

TABLE I  
EXAMPLE OF THE FIVE MOSTLY USED PQ-GRAMS OF A SAMPLE DOCUMENT.

pq-gram	Occurrence [%]	Rank
NP-NN-***	2.68	1
PP-IN-***	2.25	2
NP-DT-***	1.99	3
NP-NNP-***	1.44	4
S-VP-***-VBD	1.08	5

machine learning algorithms. This step is explained in detail in Section IV.

#### IV. EVALUATION

Basically, the prediction of gender and age of the author of a text document is made by machine learning algorithms. Independent of the classifier used (see Section IV-D), the input consists of a large list of features with appropriate values and a corresponding classification class. The class is used to train the algorithms if the document is part of the training set, as well as for evaluating if the document is part of the test set. Details on the usage of training and test sets, respectively, and on the test corpus in general are explained in Section IV-C.

##### A. Features

The features that have been used as input for the classifiers consist of the pq-gram profiles described previously. Thereby, each pq-gram represents a feature. To examine the significance of the concrete percentage of occurrence compared to the plain rank, a pq-gram-rank feature has been added additionally.

A small example of a feature list including the correct gender and age classification is depicted in Table II. If a document does not contain a specific feature, i.e., a pq-gram, the feature value for the pq-gram as well as for the corresponding rank is set to  $-1$ . For example, the author of document C didn't use the structure [PP-IN-\*\*\*] to build his/her sentences, so therefore the according feature values are set to  $-1$ .

TABLE II  
EXAMPLE OF A FEATURE LIST SERVING AS INPUT FOR CLASSIFICATION ALGORITHMS.

Feature	Doc. A	Doc. B	Doc. C
NP-NN-***	2.68	1.89	2.84
NP-NN-***-RANK	1	6	2
PP-IN-***	2.25	0.24	-1
PP-IN-***-RANK	2	153	-1
NP-DT-***	1.99	2.11	1.23
NP-DT-***-RANK	3	2	11
...	...	...	...
correct gender	male	female	male
correct age	20s	10s	30s

Depending on the evaluation setup shown subsequently the number of attributes to be handled by the classification algorithms range between 7,000 and 20,000.

##### B. Evaluation Setup

The computation of the feature list is an essential part of the approach. Basically, it depends on the assignment of  $p$  and  $q$ , respectively, that is used for the extraction of pq-grams from sentences. For example, by using  $p = 1$  and  $q = 0$  the pq-grams would be reduced to single POS tags. Nevertheless, based on results in previous work such configurations have been excluded as they led to insufficient results. The range of both stem and base of pq-grams has been evaluated in the range between 2 and 4, conforming to the size of n-grams that are used in other efficient approaches in information retrieval (e.g., [20]).

Considering the huge amount of possible features, especially if  $p + q > 6$ , the maximum number of sentences per text sample ( $s_{max}$ ) as well as the maximum number of pq-grams in a profile ( $pq_{max}$ ) have been limited. Accordingly, only the first 200 sentences of each document have been processed. The final pq-gram profile has then been sorted descending by the rank and limited to the 500 mostly used patterns.

Finally, three different feature sets have been used as input for the machine learning algorithms: the percentage of occurrence of each pq-gram, the rank of each pq-gram, and a combination of both occurrence-rate and rank.

An overview of all settings that have been evaluated can be seen in Table III.

TABLE III  
PARAMETER SETUP USED FOR THE EVALUATION.

Parameter	Assignment
$p, q$	2 - 4
$s_{max}$	200
$pq_{max}$	500
input feature set	occurrence-rate, rank, combined

##### C. Test Set

The approach has been evaluated extensively using a state-of-the-art test set created by Schler et. al [6], containing thousands of freely accessible English web blogs. For this evaluation, a subset of approximately 12,000 randomly selected blogs have been used<sup>1</sup>, whereby for each blog entry the gender as well as the age of the composer is given.

Regarding the latter, the ages are clustered into three distinct groups, as defined by the original test set [6]: 13-17 (=10s), 23-27 (=20s) and 33-42 (=30s). The five-year gap between each group is thereby added to gain higher distinguishability. The corpus is fairly balanced with respect to gender, but has a majority in the 20s group and a minority in the 30s group. A detailed information about the class distribution is shown in Table IV. Because of the fact that simply predicting the majority class in all cases would lead to an accuracy of, e.g., 53% for male, the baseline which should be exceeded is set accordingly to 53% for gender, 47% for age and 25% for gender+age profiling, respectively.

<sup>1</sup>in the base study of this work [1] only 8,000 blogs have been used, which led to similar, but slightly different evaluation results

TABLE IV  
TEST DATA DISTRIBUTION.

	female	male	sum
10s	18%	19%	37%
20s	22%	25%	47%
30s	7%	9%	16%
Sum	47%	53%	

Each blog consists of at least 200 English words and has been textually cleaned in the original test data, i.e. all unnecessary whitespace characters and HTML tags etc. have already been removed. Hyperlinks have been replaced by the word 'urlLink'. Nonetheless, because this approach depends on the calculation of grammar trees, the latter tags have been manually removed for the evaluation, as the computation of grammar trees would be falsified.

#### D. Classifiers

Aside from the parameter settings the accuracy of the profiling process depends on the classification algorithm that is used in combination with the set of features that are applied. Therefore, to determine the best working algorithm for this approach, several commonly used methods have been tested. Using the WEKA toolkit as a general framework [21], the following classifiers have been utilized:

- Naive Bayes classifier [22]
- Bayes Network using the K2 classifier [23]
- Large Linear Classification using LibLinear [24]
- Support vector machines using LIBSVM with nu-SVC classification [25]
- A k-nearest-neighbours classifier (kNN) using  $k = 1$  [26]
- A pruned C4.5 decision tree [27]

#### E. Results

All possible settings, i.e., combinations of assignments of  $p$  and  $q$  with classifiers, have been evaluated on the test set using a 10-fold cross validation. For each classifier the best results for predicting the gender, age and both gender and age combined are shown in Table V. The detailed results for each feature set is depicted, as well as the concrete sub results for the individual classes. Note that the average value is weighted, i.e., adjusted to the test data distribution.

In general, the results could significantly exceed the corresponding baselines, which manifests that solely the grammar of authors - analyzed with syntax trees and pq-grams - serves as a distinct feature for author profiling.

Despite of the class to predict, the support vector machine framework *LibSVM* and the large linear classification *LibLinear* worked best, whereas the kNN classifier and the C4.5 decision tree produced worse results. Also, for all classifiers the best accuracies could be achieved by using small values for  $p$  and  $q$ , i.e.,  $p = q = 2$  in most cases. Finally, the best scores except for gender+age profiling result from the using the combined occurrence-rate and rank feature set.

1) *Gender Results:* The best result using  $p = 2$  and  $q = 2$  could be achieved with *LibSVM*, leading to an accuracy of about 68%. It utilizes the combined feature set, whereby males could be identified with 69%. Although the prediction rate is a little worse than those of other approaches (e.g., [6] achieves 80% over the full test set using several style and content features), the result is promising as here only the proposed feature is evaluated and the baseline of 53% could be surpassed clearly.

2) *Age Results:* Using an identical setting, the maximum accuracy of about 65% results again from using *LibSVM* and the combined feature set. In general, the accuracy for the prediction of the age groups 10s and 20s are very solid, but all classifiers except the Bayes approaches have problems predicting the 30s group. For example, the best configuration achieved a rate of nearly 72% for 10s and 69% for 20s, respectively, but could only predict 18% correctly in the eldest group.

A reason for this may be the unbalanced distribution of the test data, which contains only a small amount of 30s text samples compared to the other groups. It might be the case that the classifiers would have needed more samples to construct a proper prediction model. Even though the unbalanced test set is an immediate consequence of the original test data distribution ([6]), future work should try to create a smaller, but equally distributed test set in order to examine the source of the problems occurring in the 30s classification.

As with gender, the age results also significantly exceed the baseline of 43%. By incorporating other commonly used features (Section V exemplary adds some lexical features) it can be assumed that a higher accuracy can be achieved (e.g., [4] could reach 77% for age profiling).

3) *Gender+Age Results:* For this problem, the combinations of gender and age, i.e., six classes, had to be predicted. The baseline coming from the majority class *male-20s* is 25% and could also be surpassed using the *LibLinear* classifier. By reusing the previous assignments  $p = 2$  and  $q = 2$ , an accuracy of 40% could be achieved using the occurrence-rate feature set. In contrast to the isolated gender and age prediction, the combined feature set never led to the highest accuracies for any classification algorithm.

Due to visibility reasons the details for the individual sub results have been omitted in the table. Nonetheless, the experimental data shows that the combined gender and age classification also suffers from predicting the male/female classes of the 30s age group correctly.

4) *Confusion Matrices:* A visualization of the confusion matrices is presented in Figure 3, while a detailed analysis of the best working classifications is shown in Table VIII in the Appendix. When predicting the gender, the number of false-positives for *females* is slightly higher than for *males*. On the other side, the classification of age groups had massive problems concerning the 30s group, where only 11.5% have been labeled correctly. The vast majority of this group has been

TABLE V  
EVALUATION RESULTS IN PERCENT FOR PROFILING GENDER, AGE AND GENDER+AGE.

Classifier	p	q	Feature Set									Max
			Occurrence-Rate			Rank			Combined			
			male	female	w. avg	male	female	w. avg	male	female	w. avg	
Naive Bayes	2	2	64.7	65.3	65.0	65.3	65.4	<b>65.3</b>	65.0	65.3	65.1	65.3
BayesNet	2	2	64.7	65.3	65.0	65.3	65.4	<b>65.4</b>	65.0	65.3	65.1	65.4
LibLinear	2	3	69.4	65.6	<b>67.6</b>	68.5	64.5	66.7	68.6	64.9	66.9	67.6
<b>LibSVM</b>	2	2	68.2	64.1	66.3	67.2	63.2	65.3	69.4	65.7	<b>67.7</b>	<b>67.7</b>
kNN	2	2	61.6	56.9	<b>59.4</b>	59.9	55.6	57.8	60.6	56.0	58.5	59.4
C4.5	2	3	61.5	57.0	59.4	62.1	57.4	59.9	62.2	58.0	<b>60.2</b>	60.2

(a) Results for Gender Prediction.

Classifier	p	q	Feature Set											Max	
			Occurrence-Rate				Rank				Combined				
			10s	20s	30s	w. avg	10s	20s	30s	w. avg	10s	20s	30s		w. avg
Naive Bayes	2	2	67.4	50.2	40.3	54.3	67.7	50.4	40.9	<b>54.7</b>	67.9	49.3	41.0	54.2	54.7
BayesNet	2	2	67.4	50.0	40.2	54.1	67.4	50.0	40.2	54.1	67.8	49.1	41.0	<b>54.2</b>	54.2
LibLinear	2	2	68.6	65.8	25.8	<b>61.6</b>	67.2	64.0	24.9	60.0	68.2	64.1	29.8	60.6	61.6
<b>LibSVM</b>	2	2	71.2	69.0	16.8	64.4	69.5	67.4	18.0	62.8	71.8	69.1	18.0	<b>64.7</b>	<b>64.7</b>
kNN	2	3	58.0	57.2	27.5	<b>52.9</b>	55.5	56.4	27.0	51.5	56.5	57.3	26.7	52.3	52.9
C4.5	2	2	60.4	57.3	27.9	<b>53.8</b>	58.0	54.7	23.9	51.0	60.1	56.1	28.5	53.0	53.8

(b) Results for Age Prediction.

Classifier	p	q	Feature Set			Max
			Occurrence-Rate	Rank	Combined	
Naive Bayes	2	2	35.9	<b>36.8</b>	36.0	36.8
BayesNet	2	2	35.9	<b>36.6</b>	35.9	36.6
<b>LibLinear</b>	2	2	<b>40.1</b>	38.7	39.5	<b>40.1</b>
LibSVM	2	4	<b>39.2</b>	38.6	39.0	39.2
kNN	2	3	<b>31.9</b>	31.3	31.5	31.9
C4.5	3	3	<b>31.5</b>	29.7	31.1	31.5

(c) Results for Gender+Age Prediction.

predicted as 20s, which represents also the majority group of the test set.

As already mentioned, a possible explanation might be the unbalanced test set. This is reinforced by the fact that mostly all false-positives of the 10s group have also been labeled as 20s. But what also seems plausible is the hypothesis that the grammar of 13-17 (10s) year olds differs significantly from that of 23-27 (20s) year olds, where on the other hand, the grammatical style of the latter is similar to 33-42 (30s) year olds. Intuitively, this seems reasonable when looking at sample documents, but future work should investigate further to verify or falsify this assumption.

It can be seen clearly that while the classification works reasonably for the gender and age classes 10s and 20s, respectively, the approach faces problems attributing the 30s class. Accordingly, this can be seen in subfigures (b) and (c), where all columns and rows containing the latter class have not been classified correctly.

Summarizing, Figure 4 illustrates the evaluation results for all three classification problems using the different feature sets. As can be seen, all baselines could be exceeded.

## V. COMPARISON OF GRAMMAR FEATURES AND COMMON WORD-BASED FEATURES

In order to put the previous results into perspective, they have been compared to the outcomes of commonly used

word-based features. The features incorporated are explained in Section V-C, and subsequently Section V-B presents the accuracy gained by using only those features on the same data set. Finally, an evaluation incorporating both the grammar features and the lexical features is presented in Section V-C.

### A. Incorporated Word-Based Features

Because the previously introduced grammar feature operates only on parse trees, the focus for selecting additional features has been laid on any metrics incorporating information on the usage of words, i.e., the vocabulary. In concrete, the following 18 features have been used:

- number of stop words<sup>2</sup>, e.g., used in [28], [29], [30]
- number of function and specific words, e.g., used in [31], [32]
  - auxiliary verbs
  - conjunctions
  - determiners
  - prepositions
  - pronouns
  - quantifiers
  - General Service List (GSL)<sup>3</sup> [33]
- vocabulary richness, e.g., used in [34], [35], [36]

<sup>2</sup>gained from <http://xpo6.com/list-of-english-stop-words/>, visited August 2015

<sup>3</sup>gained from <http://www.sequencepublishing.com>, visited August 2015

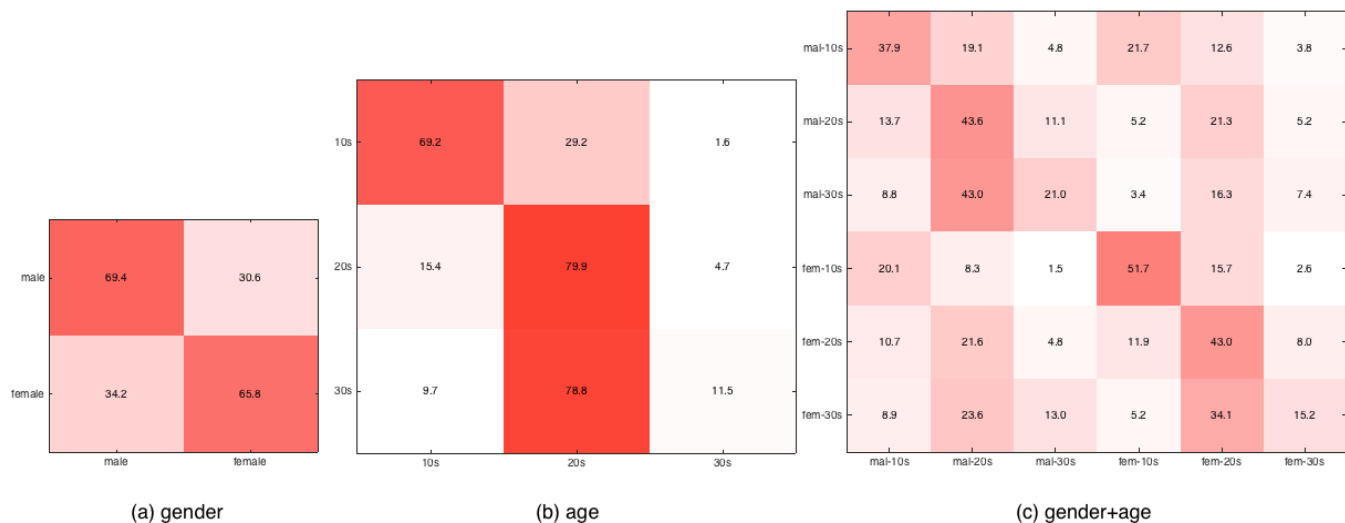


Fig. 3. Confusion Matrices for Profiling Gender, Age and Gender+Age with Grammar.

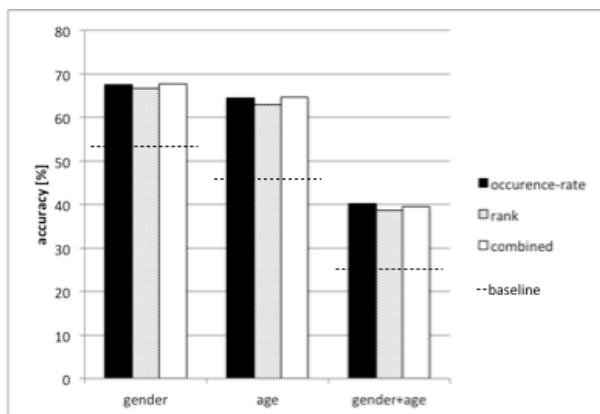


Fig. 4. Summarizing Evaluation Results Using Different Feature Sets.

- type-token-ratio
- Honore's H measure [37]
- hapax legomena
- hapax dislegomena
- readability metrics, e.g., used in [38], [39]
  - Flesch Reading Ease [40]
  - Flesch-Kincaid Reading Grade [41]
  - SMOG index [42]
  - Automated Readability Index (ARI) [43]
  - Gunning Fog index [44]
  - Coleman-Liau index [45]

### B. Feature Evaluation

In order to measure the impact of the selected word-based features when added to the grammar features, the textual features have been evaluated in isolation at first. The result using the same classifiers can be seen in Table VI. For each predicted class, the best accuracy could be gained by the *LibLinear* classifier. Obviously, it can handle the small number

of features (18 compared to several thousands) much better than all other algorithms and thus performed significantly better. In case of gender and the combined gender+age classes, nearly identical results as with pure grammar analysis could be achieved. The result for the age class is also comparable, although slightly inferior to the grammar approach. Interestingly and similar to the previously shown grammar results, the correctness of the 30s group is very low also with the word-based features (and nearly zero in the *LibLinear* case).

### C. Combining Grammar and Word-Based Features

In a final evaluation, the grammar features have been enriched with the word-based features. Thereby the latter have been combined with the different grammar feature sets, i.e., the occurrence-rate (WB + Occurrence-Rate), rank (WB + RANK) and the combined set (WB + Combined). The detailed results are presented in Table VII, and a visualized summary of the best results for all examined evaluations using word-based-only, grammar-only and all combined features is depicted in Figures 5-7 in the Appendix. It can be seen that for all three classes the grammar results could be improved as expected - nevertheless, the performance gain is relatively low as discussed later.

Identical to the pure grammar evaluation, the best results for the gender and age classes are produced by the *LibSVM* framework, and the combined gender+age profiling worked best with *LibLinear*, respectively. Also, the same pq-gram values, i.e.,  $p = q = 2$  have been used in all cases, leading to best results when all available word-based features as well as all grammar features have been utilized. While the identification of males and females is relatively balanced, the 30s-age group has again been detected at a significant lower accuracy.

Although the grammar results could be enhanced by incorporating word-based features, the best accuracies are only slightly improved. At first, this indicates that the proposed

TABLE VI  
EVALUATION RESULTS USING ONLY WORD-BASED FEATURES.

Classifier	male	female	w. avg
NaiveBayes	62.2	61.9	62.0
BayesNet	62.2	61.9	62.0
<b>LibLinear</b>	70.1	64.6	<b>67.6</b>
LibSVM	61.4	53.9	58.0
kNN	61.5	57.0	59.4
C4.5	64.8	61.6	63.3

(a) Gender

Classifier	10s	20s	30s	w. avg
NaiveBayes	61.6	54.2	32.2	53.2
BayesNet	61.6	54.2	32.3	53.2
<b>LibLinear</b>	69.3	67.9	0.3	<b>62.8</b>
LibSVM	65.4	59.0	30.7	57.0
kNN	61.2	57.6	29.1	54.2
J48	62.3	59.8	19.9	55.1

(b) Age

Classifier	w. avg
NaiveBayes	32.4
BayesNet	32.3
<b>LibLinear</b>	<b>41.9</b>
LibSVM	40.2
kNN	31.8
C4.5	32.5

(c) Gender+Age

grammar features are very informative on its own. On the other hand, the reason for the relatively low improvement could be a result of the imbalance of the number of features, i.e., the 18 word-based features compared to the several thousand features resulting from calculating and synchronizing snippets of grammar trees. In order to improve performance, future work should therefore investigate on balancing both types of features, e.g., by applying attribute selection prior to classification. It can be assumed that a lot of the produced grammar features are dispensable, and that a reduction of features leads to better performances of the classification algorithms.

## VI. RELATED WORK

The profiling of authors falls under the problem class usually referred to as text categorization [46], whereby an often applied concept is the utilization of different machine learning algorithms based on a previously selected set of features. The main problem types are differentiated between single-label and multi-label classification problems, respectively. Within the single-label text categorization problem the gender and age of the author of a text document has been analyzed frequently. Thereby the first attempts to distinguish between women and men were motivated by sociological studies (e.g., [47]). With the progress in text categorization and authorship attribution, many approaches also tried to automatically detect meta-information like the gender and age of authors, most often by reusing or adapting stylometric features that have been used in other fields. Beside, this core information also many other characteristics have been profiled, including the level of education, the geographical origin or psychological types like extrovertism or neuroticism. In the following, some examples of current profiling approaches are given.

*Gender and Age:* Probably the best approach that can be directly compared to the results presented in this paper is described in [6]. It leads to slightly better results, but incorporates also many other features that have not been considered in this approach. The fact that grammar-only analyses can lead to nearly similar results is thus promising. The approach is based on the work of [48] that analyzes the gender of the author and also automatically distinguishes between fiction and non-fiction documents, the web blog corpus created by Schler et al. - which is also used in this work - has been created to classify gender and age based on many style and content features [6]. Beside basic features like the frequencies of

function words, pronouns, determiners or the average number of words per post, also blogwords (neologisms) like 'lol', 'haha' or 'ur' as well as the frequency of hyperlinks have been analyzed. With a proposed so-called *Multi-Class Real Winnow* learning algorithm, the gender of the authors of the web blogs could be profiled with an accuracy of 80%, and the age with an accuracy of 76%, respectively. Similarly to the results described in this work, the authors also report significant problems discriminating mid-twenty year olds from mid-thirty year olds.

An extension to the previous work that additionally attempts to classify the language and personality of a writer has been proposed in [4] by utilizing taxonomies of POS tags combined with other style and content-specific features. By using a Bayesian Multinomial Regression learning algorithm [49] on the same web blog corpus, 76% accuracy on gender and 77% accuracy on age could be gained.

Two new feature sets using POS tag patterns are proposed in [50] to enhance current state-of-the-art profiling approaches. In simplified terms, the frequencies of POS- $n$ -grams (where  $n$  is not fixed) are collected, rated in terms of significance and used as features if some conditions hold. An evaluation performed also on a (different) blog corpus, the effectiveness of the two new features has been tested. The best result using a support vector machine and incorporating the large number of nearly 24,000 features could enhance the previously described result of Schler et al. by 8%, i.e., reaching 88% on their data set.

In [51], the authors try to automatically expose the gender of writers of Twitter messages by incorporating the huge amount of over 15 million features. The origins of the features are thereby quite simple and can be categorized into character {1-5}-grams and word {1-2}-grams of the actual tweets, complemented by the corresponding  $n$ -grams of the user's profile information. As expected, the best result could be gained by using the full name  $n$ -grams, reaching an accuracy of 89%.

An interesting approach that also analyzes the gender of web blog authors is presented in [7]. Besides commonly used features in the field of text categorization the focus has been laid on blog-specific features. The approach thereby considers the usage of background colors, emoticons like ;-) or :-D, punctuation marks or fonts. It is shown that the prediction of gender can be enhanced by using these features. Moreover, as a result from the experiment, a list of words which occur in

TABLE VII  
EVALUATION RESULTS IN PERCENT BY COMBINING GRAMMAR AND WORD-BASED FEATURES

Classifier	p	q	Feature Set									Max
			WB + Occurrence-Rate			WB + Rank			WB + Combined			
			male	female	w. avg	male	female	w. avg	male	female	w. avg	
Naive Bayes	2	2	64.6	65.4	65.0	65.1	65.3	<b>65.2</b>	65.0	65.3	65.2	65.2
BayesNet	2	2	64.6	65.4	65.0	65.1	65.4	<b>65.3</b>	65.0	65.3	65.2	65.3
LibLinear	2	3	70.3	66.5	<b>68.5</b>	69.7	66.0	68.0	69.1	65.6	67.4	68.5
<b>LibSVM</b>	2	2	69.6	65.5	67.7	68.8	64.9	66.9	70.3	66.9	<b>68.7</b>	<b>68.7</b>
kNN	2	2	61.6	57.3	<b>59.6</b>	59.8	55.7	57.9	60.7	56.4	58.6	59.6
C4.5	3	3	61.4	56.8	59.2	61.2	57.1	59.3	61.7	58.0	<b>60.0</b>	60.0

(a) Results for Gender Prediction.

Classifier	p	q	Feature Set												Max
			WB + Occurrence-Rate				WB + Rank				WB + Combined				
			10s	20s	30s	w. avg	10s	20s	30s	w. avg	10s	20s	30s	w. avg	
Naive Bayes	2	2	68.0	50.1	40.3	<b>54.5</b>	67.9	50.0	40.3	54.5	68.0	49.2	40.7	54.2	54.5
BayesNet	2	2	68.0	50.0	40.2	<b>54.4</b>	67.9	49.9	40.4	54.5	68.0	49.0	40.6	54.1	54.5
LibLinear	2	2	69.7	66.0	27.5	<b>62.2</b>	69.0	64.8	26.3	61.2	69.3	64.4	30.3	61.2	62.2
<b>LibSVM</b>	2	2	72.1	69.2	16.4	64.8	70.3	68.0	18.1	63.5	72.2	69.3	17.8	<b>64.9</b>	<b>64.9</b>
kNN	2	3	57.9	57.3	27.7	<b>52.9</b>	55.8	56.4	26.5	51.5	56.6	57.5	27.2	52.5	52.9
C4.5	2	2	60.2	57.7	26.9	<b>53.7</b>	59.1	53.4	26.7	51.1	60.2	56.4	27.6	53.3	53.7

(b) Results for Age Prediction.

Classifier	p	q	Feature Set			Max
			WB + Occurrence-Rate	WB + Rank	WB + Combined	
Naive Bayes	2	2	35.7	<b>36.3</b>	36.0	36.3
BayesNet	2	2	35.7	<b>36.2</b>	35.9	36.2
<b>LibLinear</b>	2	2	<b>41.3</b>	40.3	40.3	<b>41.3</b>
LibSVM	2	3	<b>39.1</b>	38.2	37.5	39.1
kNN	2	3	<b>32.0</b>	31.3	31.5	32.0
C4.5	2	2	<b>31.3</b>	30.8	30.4	31.3

(c) Results for Gender+Age Prediction.

male but rarely/not in female blogs (e.g., "psst", "income" or "wasup") and vice versa (e.g., "muah", "jewelry" or "kissme") is presented. On the other side, examples of the most gender-discriminant words of the study are: "peace", "shit", "yo", "man", "fuck", "damn".

*Other Information:* Many studies (e.g., [52]) have analyzed the five psychological traits: neuroticism, extraversion, openness, agreeableness and conscientiousness. Thereby one key problem for verifying such approaches is the lack of test data, i.e., the ground truth is always manually created and thus subjective to some extent. For example, for the evaluation in [53] psychology students have been asked to write a random essay within 20 minutes, whereby the categorization of personality has been made by filling out an additional questionnaire. In another paper [54] web blogs have been psychologically and gender-wise analyzed. Here, 71 bloggers have been asked to submit previously written text, and to additionally fill out a sociobiographic questionnaire as well as an online implementation of a psychological categorization test. By inspecting only eight different POS frequencies like the number of nouns, adjectives or articles, every personality trait of the authors could be predicted with an accuracy of 50-60% in this study.

English emails have been profiled into ten classes including gender, age, geographic origin or level of education as well as into the five psychological traits in [55]. The authors

use several character-level, lexical and structural features and report a similar accuracy for gender classification as the outcome presented in this work, but show a worse result for age classification. But it has to be stressed that emails are typically significantly shorter than blogs, and thus the result should not be compared directly.

With the recent rise of social media networks, also content such as chat lines, Facebook postings or tweets have been analyzed and automatically profiled. It is shown (e.g., in [5]) that a well-defined set of style and content features can be used to expose meta information of chat logs. In a recent workshop [56], participants also gained good results for profiling gender, age and the personality of Twitter users by applying several types of features sets. Nevertheless, the authors in [57] show that the application of common text categorization techniques using natural language processing is challenging - but possible - when facing highly limited data sets.

The analysis of grammar trees with pq-grams has also been used in previous work, where it has been shown that the grammar of authors is also a feasible criteria to intrinsically expose plagiarism [13], attribute authors to unlabeled text documents [14] and to automatically decompose a multi-author document [58].

VII. CONCLUSION AND FUTURE WORK

In this paper, a novel feature that can be used to automatically profile the author of a text document is presented. Based on full grammar trees, it utilizes substructures of these trees by using pq-grams. State-of-the-art machine learning algorithms are finally applied on pq-gram profiles to learn and predict the gender and age of the originator. An extensive evaluation using a state-of-the-art test set shows that pq-grams can be used as significant features in text classification, whereby gender and age can be predicted with an accuracy of 68% and 65%, respectively.

An extensive evaluation compared the outcome of the proposed grammar features with the performance of a selected set of commonly used word-based metrics like the type-token-ratio or frequencies of stop words. Results show that - in isolation - the pq-gram features perform better than the word-based statistics, and that the best performance can be achieved by combining all features. In order to reduce the large number of features resulting from grammar trees, future work should investigate whether a prior attribute selection algorithm can further improve accuracies.

Evaluation results showed that the approach has problems predicting the 30s age group. Although hypothesis explaining the problem have been stated, they should be verified or falsified in detail by utilizing a different test set.

In order to build a reliable text classification approach, the grammar feature should be combined with other commonly used style and content feature sets, besides the exemplarily selected word-based features used in this work. In addition to the utilization of other common lexical, syntactic or complexity features, detailed metrics of vocabulary or neologisms should be considered, especially when analyzing online content. Moreover it should be investigated whether the proposed feature is also applicable to shorter text samples such as chat logs or even single-line Twitter postings. The approach could additionally also benefit from applying sentiment analysis.

Finally, research should also examine whether pq-gram profiles are also exploitable to other languages, especially as syntactically more complex languages like German or French may lead to even better results due to the higher amount of grammar rules available.

APPENDIX

In this section alternative result views are presented.

TABLE VIII  
CONFUSION MATRICES OF THE BEST RESULTS FOR GENDER AND AGE PROFILING.

	classified as [%]		classified as [%]		
	male	female	10s	20s	30s
male	69.4	30.6	69.2	29.2	1.6
female	34.2	65.8	15.4	79.9	4.7

(a) Gender

	classified as [%]		
	10s	20s	30s
10s	69.2	29.2	1.6
20s	15.4	79.9	4.7
30s	9.7	78.8	11.5

(b) Age

	classified as [%]					
	mal-10s	mal-20s	mal-30s	fem-10s	fem-20s	fem-30s
mal-10s	37.9	19.1	4.8	21.7	12.6	3.8
mal-20s	13.7	43.6	11.1	5.2	21.3	5.2
mal-30s	8.8	43.0	21.0	3.4	16.3	7.4
fem-10s	20.1	8.3	1.5	51.7	15.7	2.6
fem-20s	10.7	21.6	4.8	11.9	43.0	8.0
fem-30s	8.9	23.6	13.0	5.2	34.1	15.2

(c) Gender And Age

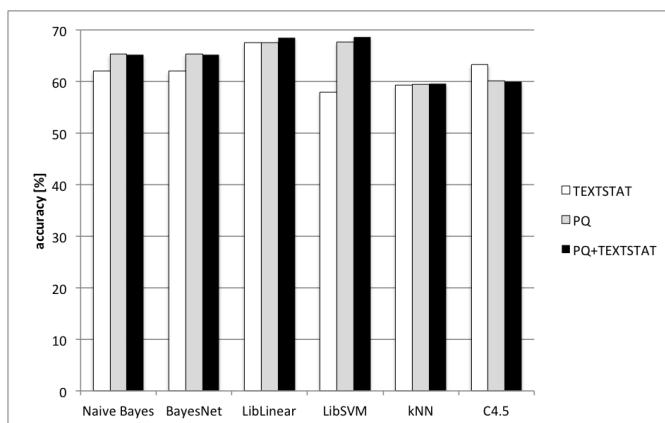


Fig. 5. Best Evaluation Results For Gender Using All Features.

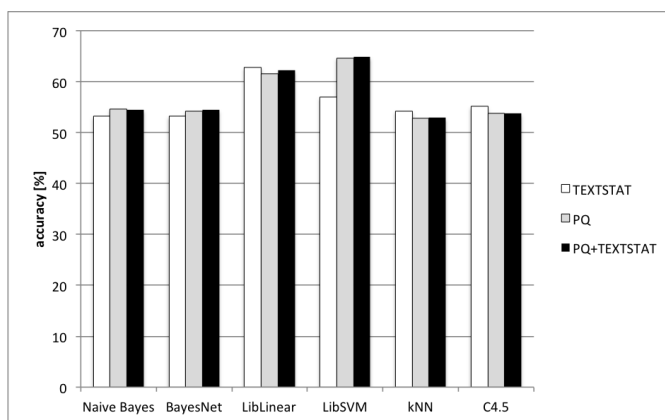


Fig. 6. Best Evaluation Results For Age Using All Features..

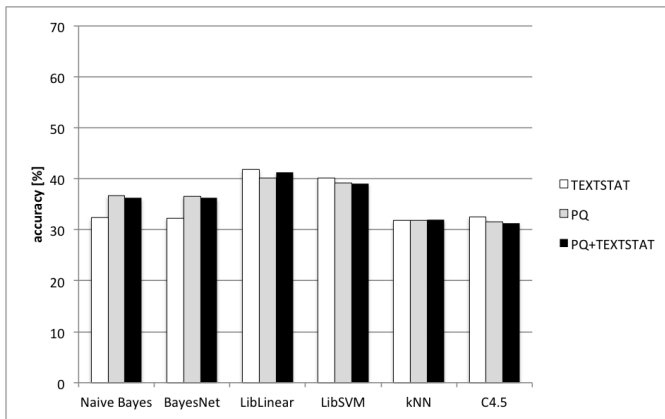


Fig. 7. Best Evaluation Results For Gender+Age Using All Features.

## REFERENCES

- [1] M. Tschuggnall and G. Specht, "What grammar tells about gender and age of authors," in *Proceedings of the 4th International Conference on Advances in Information Mining and Management (IMMM)*, Paris, France, July 2014, pp. 30–35.
- [2] "Statistic Brain Research Institute," <http://www.statisticbrain.com/social-networking-statistics>, visited February 2014.
- [3] E. Stamatatos, "A Survey of Modern Authorship Attribution Methods," *J. Am. Soc. Inf. Technol.*, vol. 60, no. 3, pp. 538–556, Mar. 2009.
- [4] S. Argamon, M. Koppel, J. W. Pennebaker, and J. Schler, "Automatically Profiling the Author of an Anonymous Text," *Commun. ACM*, vol. 52, no. 2, pp. 119–123, Feb. 2009.
- [5] L. Flekova and I. Gurevych, "Can We Hide in the Web? Large Scale Simultaneous Age and Gender Author Profiling in Social Media," *Notebook Papers of CLEF 13 Labs and Workshops*, 2006.
- [6] J. Schler, M. Koppel, S. Argamon, and J. W. Pennebaker, "Effects of Age and Gender on Blogging," in *AAAI Spring Symposium: Computational Approaches to Analyzing Weblogs*, 2006, pp. 199–205.
- [7] X. Yan and L. Yan, "Gender Classification of Weblog Authors," in *AAAI Spring Symposium: Computational Approaches to Analyzing Weblogs*, 2006, pp. 228–230.
- [8] J. Noecker, M. Ryan, and P. Juola, "Psychological Profiling Through Textual Analysis," *Literary and Linguistic Computing*, 2013.
- [9] J. Gibbons, *Forensic Linguistics: An Introduction to Language in the Justice System*. Blackwell Pub., 2003.
- [10] S. Nirxhi and R. Dharaskar, "Comparative Study of Authorship Identification Techniques for Cyber Forensics Analysis," *International Journal*, 2013.
- [11] E. E. Abdallah, A. E. Abdallah, M. Bsoul, A. F. Otoom, and E. Al-Daoud, "Simplified Features for Email Authorship Identification," *International Journal of Security and Networks*, vol. 8, no. 2, pp. 72–81, 2013.
- [12] G. Inches and F. Crestani, "Overview of the International Sexual Predator Identification Competition at PAN-2012," in *CLEF (Online Working Notes/Labs/Workshop)*, 2012.
- [13] M. Tschuggnall and G. Specht, "Using Grammar-Profiles to Intrinsically Expose Plagiarism in Text Documents," in *NLDB*, 2013, pp. 297–302.
- [14] —, "Countering Plagiarism by Exposing Irregularities in Authors Grammars," in *EISIC, European Intelligence and Security Informatics Conference, Uppsala, Sweden*, 2013, pp. 15–22.
- [15] N. Augsten, M. Böhlen, and J. Gamper, "The pq-Gram Distance between Ordered Labeled Trees," *ACM Transactions On Database Systems (TODS)*, vol. 35, no. 1, p. 4, 2010.
- [16] S. Helmer, N. Augsten, and M. Böhlen, "Measuring Structural Similarity of Semistructured Data Based on Information-theoretic Approaches," *The VLDB Journal—The International Journal on Very Large Data Bases*, vol. 21, no. 5, pp. 677–702, 2012.
- [17] The Apache Software Foundation, "Apache OpenNLP," <http://incubator.apache.org/opennlp>, visited February 2014.
- [18] D. Klein and C. D. Manning, "Accurate Unlexicalized Parsing," in *Proceedings of the 41st Annual Meeting on Association for Computational Linguistics - Volume 1*, ser. ACL '03, Stroudsburg, PA, USA, 2003, pp. 423–430.
- [19] M. P. Marcus, M. A. Marcinkiewicz, and B. Santorini, "Building a Large Annotated Corpus of English: The Penn Treebank," *Computational Linguistics*, vol. 19, pp. 313–330, Jun. 1993.
- [20] E. Stamatatos, "Intrinsic Plagiarism Detection Using Character n-gram Profiles," in *CLEF (Notebook Papers/Labs/Workshop)*, 2009.
- [21] M. Hall et al., "The WEKA Data Mining Software: an Update," *ACM SIGKDD explorations newsletter*, vol. 11, no. 1, pp. 10–18, 2009.
- [22] G. H. John and P. Langley, "Estimating Continuous Distributions in Bayesian Classifiers," in *Proceedings of the Eleventh conference on Uncertainty in artificial intelligence*. Morgan Kaufmann Publishers Inc., 1995, pp. 338–345.
- [23] G. F. Cooper and E. Herskovits, "A Bayesian Method for the Induction of Probabilistic Networks From Data," *Machine learning*, vol. 9, no. 4, pp. 309–347, 1992.
- [24] R.-E. Fan, K.-W. Chang, C.-J. Hsieh, X.-R. Wang, and C.-J. Lin, "LIBLINEAR: A Library For Large Linear Classification," *The Journal of Machine Learning Research*, vol. 9, pp. 1871–1874, 2008.
- [25] C.-C. Chang and C.-J. Lin, "LIBSVM: a Library for Support Vector Machines," *ACM Transactions on Intelligent Systems and Technology (TIST)*, vol. 2, no. 3, p. 27, 2011.
- [26] D. Aha and D. Kibler, "Instance-Based Learning Algorithms," *Machine Learning*, vol. 6, pp. 37–66, 1991.
- [27] J. R. Quinlan, *C4.5: Programs for Machine Learning*. Morgan Kaufmann Series in Machine Learning, 1993.
- [28] F. Mosteller and D. Wallace, *Inference and Disputed Authorship: The Federalist*. Addison-Wesley, 1964.
- [29] D. I. Holmes, "The evolution of stylometry in humanities scholarship," *Literary and Linguistic Computing*, vol. 13, no. 3, pp. 111–117, 1998.
- [30] S. Argamon, M. Šarić, and S. S. Stein, "Style mining of electronic messages for multiple authorship discrimination: First results," in *Proceedings of the 9th International Conference on Knowledge Discovery and Data Mining (SIGKDD)*. Washington, DC, USA: ACM, August 2003, pp. 475–480.
- [31] R. Zheng, J. Li, H. Chen, and Z. Huang, "A framework for authorship identification of online messages: Writing-style features and classification techniques," *Journal of the American Society for Information Science and Technology*, vol. 57, no. 3, pp. 378–393, 2006.
- [32] M. Koppel and J. Schler, "Exploiting stylistic idiosyncrasies for authorship attribution," in *Proceedings of the 18th International Joint Conference on Artificial Intelligence*, vol. 69, Acapulco, Mexico, August 2003, pp. 72–80.
- [33] W. Michael, "A general service list of english words," 1953.
- [34] C. U. Yule, *The Statistical Study of Literary Vocabulary*. Cambridge University Press, 1943.
- [35] C. E. Chaski, "Empirical evaluations of language-based author identification techniques," *Forensic Linguistics*, vol. 8, pp. 1–65, 2001.
- [36] F. J. Tweedie and R. H. Baayen, "How variable may a constant be? measures of lexical richness in perspective," *Computers and the Humanities*, vol. 32, no. 5, pp. 323–352, 1998.
- [37] A. Honoré, "Some simple measures of richness of vocabulary," *Association for literary and linguistic computing bulletin*, vol. 7, no. 2, pp. 172–177, 1979.
- [38] W. Daelemans and V. Hoste, "Stylene: an environment for stylometry and readability research for dutch," 2013.
- [39] G. Lynch, "A supervised learning approach towards profiling the preservation of authorial style in literary translations," *Proceedings 25th COLING*, pp. 376–386, 2014.
- [40] R. Flesch, "A new readability yardstick," *Journal of applied psychology*, vol. 32, no. 3, p. 221, 1948.
- [41] J. P. Kincaid, R. P. Fishburne Jr, R. L. Rogers, and B. S. Chissom, "Derivation of new readability formulas (automated readability index, fog count and flesch reading ease formula) for navy enlisted personnel," DTIC Document, Tech. Rep., 1975.
- [42] G. H. McLaughlin, "Smog grading: A new readability formula," *Journal of reading*, vol. 12, no. 8, pp. 639–646, 1969.
- [43] R. Senter and E. Smith, "Automated readability index," DTIC Document, Tech. Rep., 1967.
- [44] R. Gunning, "{The Technique of Clear Writing}," 1952.
- [45] M. Coleman and T. L. Liao, "A computer readability formula designed for machine scoring," *Journal of Applied Psychology*, vol. 60, no. 2, p. 283, 1975.

- [46] F. Sebastiani, "Machine Learning in Automated Text Categorization," *ACM computing surveys (CSUR)*, vol. 34, no. 1, pp. 1–47, 2002.
- [47] N. Besnier, "Language and affect," *Annual Review of Anthropology*, vol. 19, no. 1, pp. 419–451, 1990.
- [48] M. Koppel, S. Argamon, and A. R. Shimoni, "Automatically Categorizing Written Texts by Author Gender," *Literary and Linguistic Computing*, vol. 17, no. 4, pp. 401–412, 2002.
- [49] A. Genkin, D. D. Lewis, and D. Madigan, "Large-scale bayesian logistic regression for text categorization," *Technometrics*, vol. 49, no. 3, pp. 291–304, 2007.
- [50] A. Mukherjee and B. Liu, "Improving Gender Classification of Blog Authors," in *Proceedings of the 2010 Conference on Empirical Methods in NLP*. Association for Computational Linguistics, 2010, pp. 207–217.
- [51] J. D. Burger, J. Henderson, G. Kim, and G. Zarrella, "Discriminating gender on twitter," in *Proceedings of the Conference on Empirical Methods in Natural Language Processing (EMNLP)*. Edinburgh, UK: Association for Computational Linguistics, July 2011, pp. 1301–1309.
- [52] S. Argamon, S. Dhawle, M. Koppel, and J. W. Pennebaker, "Lexical predictors of personality type," in *Proceedings of the Joint Annual Meeting of the Interface and the Classification Society of North America*, St. Louis, Missouri, USA, June 2005.
- [53] J. W. Pennebaker and L. A. King, "Linguistic styles: Language use as an individual difference," *Journal of Personality and Social Psychology*, vol. 77, no. 6, p. 1296, 1999.
- [54] S. Nowson, J. Oberlander, and A. J. Gill, "Weblogs, genres and individual differences," in *Proceedings of the 27th Annual Conference of the Cognitive Science Society*. Stresa, Italy: Citeseer, July 2005.
- [55] D. Estival, T. Gaustad, S. B. Pham, W. Radford, and B. Hutchinson, "Author Profiling for English Emails," in *Proceedings of the 10th Conference of the Pacific Association for Computational Linguistics*, 2007, pp. 263–272.
- [56] F. Rangel, P. Rosso, M. Potthast, B. Stein, and W. Daelemans, "Overview of the 3rd author profiling task at pan 2015," in *Proceedings of CLEF*, 2015.
- [57] C. Peersman, W. Daelemans, and L. Van Vaerenbergh, "Predicting Age and Gender in Online Social Networks," in *Proceedings of the 3rd international workshop on Search and mining user-generated contents*. ACM, 2011, pp. 37–44.
- [58] M. Tschuggnall and G. Specht, "Automatic decomposition of multi-author documents using grammar analysis," in *Proceedings of the 26th GI-Workshop on Grundlagen von Datenbanken*. Bozen, Italy: CEUR-WS, October 2014.

## An Analysis to Improve Voltage Stability in Smart Grids by Regulating Active Power in Intelligent Buildings

Abid Ahmad Khan, Michael Massoth and Torsten Wiens

Department of Computer Science  
Hochschule Darmstadt — University of Applied Sciences  
Darmstadt, Germany  
{abid.a.khan | michael.massoth | torsten.wiens}@h-da.de

**Abstract**—This paper describes an approach to minimize the uneven effect of voltage and power in smart buildings and on electrical networks. The idea is to analyze and improve the voltage variation in intelligent buildings and in electrical networks. In a second step, the actual power consumption and power reserves of selected Smart Homes is calculated and regulated by a control application using Next Generation Network technology. In the last step, stationary storages for improving the stability of the smart systems are discussed and evaluated. The analysis is performed by considering multiple scenarios in smart power grids. We consider intelligent buildings (Smart Homes) based on Next Generation Network components. These components are applied as a communication and integration platform between the smart phones of the Smart Home owners and the building control system, as well as the energy supplier of the smart power grid. The Session Initiation Protocol and the Presence Service are used to build a performant and scalable system based on open source software. The Smart Home appliances are based on the KNX bus, a secure and trustful architecture by which the user can remotely monitor and control his house or facility from anywhere in the world.

**Keywords**—Energy Management; Home Automation; Smart Power Grid; Next Generation Network; Presence Service.

### I. INTRODUCTION

The work at hand is an extended version of our paper “Stability Improvement Solution of the Smart Power Grid by an Analysis of Voltage Variation in Intelligent Buildings” [1].

Intelligent power grids form the core of the future power supply. As a part of smart cities, smart buildings, home area networks (HAN) are composed of devices that communicate with each other, can communicate data to utilities (or other energy service providers) and can respond to signals sent by these remote entities. An overarching vision of the Smart Grid holds that providing consumers with information about their energy usage will support an array of electricity pricing models and enable customers to better control their use of electricity. Smart thermostats, smart meters, real-time dynamic pricing and next-day energy information feedback to electricity users play an important role in this intelligent energy management infrastructure. Every part of our energy environment will be connected to each other and may be

controlled from central points with the given rights, to exchange both energy and information. The actual intelligence is supplied by the IT-supported structure and control tactics, especially to match fluctuating Smart Grids, which are supposed to guarantee stable power supplies within the European Norms. For the stability of a Smart Grid system, there are two main criteria: First, the power generation has to match the demand at any time and has to hold a reserve (e.g., battery storage) for immediate outages. Second, the grid has to provide sufficient capacities for voltage stabilization at every point in time. According to our particular status, all countries need to simplify the smart cities and adjust their parameters in order to fit their own features.

#### A. Purpose and Relevance

The purpose and contribution of this paper is to investigate various issues regarding voltage and power instabilities of Next Generation Network (NGN) based smart building systems from uncertain energy sources, and to suggest solutions based on exemplary calculations.

Our previous work presented a novel approach for a performant, scalable, secure and trustworthy interaction between intelligent homes, control managers and energy suppliers of the smart grid [1]. Our work also described energy management mechanisms by load balancing tactics that include manual and automated control of equipment in smart homes, using NGN technologies based on the Session Initiation Protocol (SIP) and its Presence Service. Based on these ideas, a near-real-time push solution has been implemented, using the IP Multimedia Subsystem (IMS) to remotely monitor and control Home Automation systems via mobile devices with open source software [2][3].

According to the latest report by GTM Research, the U.S. home energy management market is forecasted to be worth more than USD 4 billion by 2017 [4]. This forecast shows the business opportunities and relevance of our proposed ideas for home control and energy management services. According to this source, the sectors with the largest potential for saving energy are buildings and mobility.

#### B. Structure of the paper

Following this introduction, Section II shows related work for the suitability of our previous idea to implement a control solution based on NGN technology. In Section III,

the instability problem and two important use cases are presented. The overall system design is described in Section IV. The calculation for the first solution is discussed and evaluated in Sections V and VI. Section VII gives power and energy consumption statistics for the second solution. The components used to analyze the solution are presented in Section VIII. Section IX gives an outlook on future work and concludes the paper.

## II. RELATED WORK

Many companies and institutions are working on solutions for energy efficient management of buildings. But only a few of them are working on a complete solution that relies exclusively on open standards. Most of the systems focus on the inside- or outside-systems of the building. Many control and automation system devices are usually installed at the low-voltage part of the grid. They have more capabilities in controlling electrical energy consumption of consumers [5][6][7][8]. In our previous work, we presented the idea to connect the technology of NGN to Smart Homes. The next step is to use SIP with all its benefits as the main communication protocol and connect it to a KNX bus system. The general architecture is depicted in Figure 1.

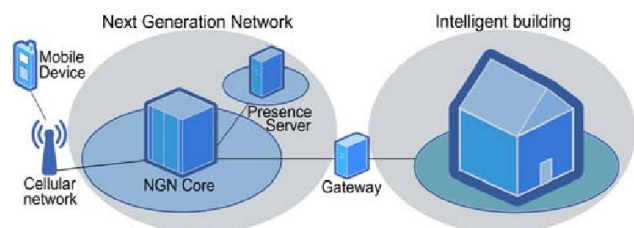


Figure 1. General architecture.

The NGN infrastructure that has been prototypically set up at our project consists of an IP Multimedia Subsystem (IMS) in its center. The IMS is a control architecture based on SIP, designed by the wireless standards body 3rd Generation Partnership Project (3GPP). It aims to standardize access to different networks. The core functionality of the IMS is to operate and manage multimedia sessions of various types in NGN infrastructures, ranging from simple telephone calls to multi-participant video conferencing and many more applications. Therefore, all communication is based on the Internet Protocol (IP).

An important functionality of the IMS is the Presence Service. This service was originally specified to manage and track the online status of all connected multimedia units. The basic idea in our project was to use the Presence Service to store the status of sensors and actors of Smart Homes instead. Advantageous about this idea is that the effort for setup and implementation of our demonstrator system is reduced, since most of the major functionality maps quite simply from IMS to home automation. Also, means to enable secure communication are already included or may be added at a relatively limited expense.

This idea enables to represent different home automation appliances as users to the outside world. Each appliance can set its own current status, or the status can be monitored by the central instance. Thus, it is possible to register a mobile device at the SIP network, and in this way at the Presence Service. The status information of the different home automation appliances can also be viewed on mobile devices, such as smart phones.

The IMS is connected via a gateway to a KNX bus system. The gateway translates control messages from SIP to KNX, and vice versa. The KNX bus installation is connected to different types of actors and sensors. Actors are appliances that perform different actions, for example switching lights on or off. They provide their activity status and are able to receive telegrams from physical switches. Sensors are appliances that can detect different conditions, e.g., temperature or brightness. They are capable of sending KNX messages (so-called KNX telegrams) to specific actors or software tools.

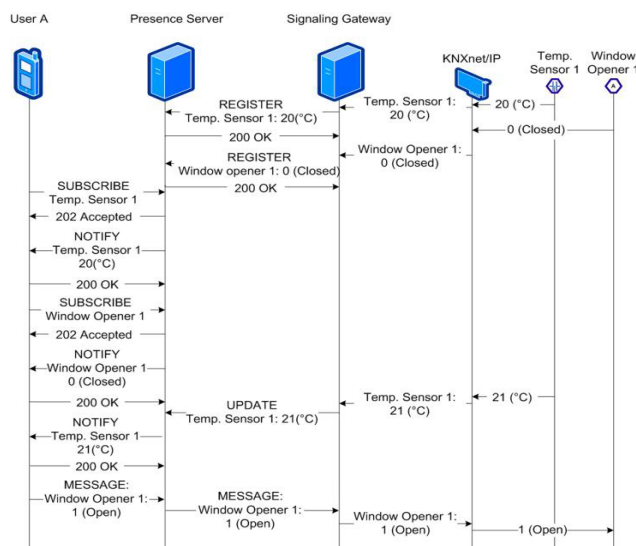


Figure 2. Signal flow in system.

The signaling gateway is the main part of this concept and has been prototypically implemented. The signaling gateway is used to control the whole infrastructure that is connected to it. It also provides various interfaces to the outside world, for example, for the connection of mobile devices, on which the smart grid management component runs that is part of the ideas described in the paper at hand.

This software service connects the KNX bus to the IMS network, as mentioned. Figure 2 shows a typical signal flow in the system. The sensors and actors on the right are connected through a KNXnet/IP device to the signaling gateway. The signaling gateway is connected to the presence server. User A (which may be any kind of IP enabled device) is connected to the Presence Server. The SIP protocol is used to communicate between the participants as shown. At first, the participants are set up using the REGISTER command. To transfer status

messages and to store and manage the status data at the Presence Service, SUBSCRIBE, NOTIFY and UPDATE messages are used.

Using a KNXnet/IP connector device, KNX telegrams are transferred to an IP network. The telegrams are packed into the payload of UDP packets and are sent over the network. Thus, one function of the signaling gateway is to receive these IP packets sent by the KNXnet/IP device. Furthermore, the information contained in the telegram has to be extracted. The telegram may consist of sensor values or other status messages of different home automation appliances. The KNXnet/IP device is also able to receive IP packets from the IP network and to send the containing telegram to the KNX bus. Thus, in order to control appliances that are associated with the bus installation, the signaling gateway has to have the ability to generate KNX telegrams (see Figure 3).

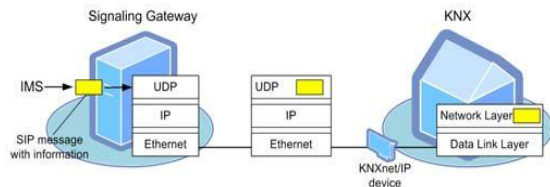


Figure 3. Basic System Architecture.

#### A. System security

It is necessary to ensure a secure connection to the mobile device, a secure authentication for the user and a generally secured environment that is up to current standards. The original KNX standard, which historically dates back to a predecessor from the 1980s, did not offer sufficiently secure communication environments. Here, our security approach is introduced that secures the end-to-end network communication of the system. For all connections, SIP Security (SIPS) is used, applying Transport Layer Security (TLS) and the Secure Real-Time Transport Protocol (SRTP). SRTP is used for securing Voice and Video-Data connections. TLS is used for exchanging signaling messages (e.g., for authentication and registration). TLS is a hybrid encryption protocol for secure data connections over the Internet. In the OSI reference model, TLS acts at the transport layer. Within SIPS, TLS takes care of the following security tasks:

- Bidirectional authentication of communication endpoints
- Exchanging shared secrets
- Cryptographic encoding of data to be transferred
- Securing the integrity of transferred SIP messages

We measure the security of the selected approach according to the four pillars of information security [9].

- Confidentiality
- Integrity
- Availability
- Authenticity

As described above, SIPS is using the protocols TLS and SRTP for secure communication. TLS uses a high security encoding and therefore grants high confidentiality. The TCP/IP protocol ensures integrity by adding a checksum to each message. Authenticity is granted by using an authentication with credentials.

#### III. USE CASES FOR SMART ENERGY MANAGEMENT

The focus of this paper is to analyze the problem of voltage and power variation in NGN based smart homes, using our project infrastructure described above. In order to meet today's power system requirements, it is necessary to apply regulation in order to keep the voltage in the permitted voltage range for the distribution grids on the low voltage and middle voltage levels. The consumption of electrical power causes the voltage to drop at the junction point of the smart buildings, whereas an injection of power will make it rise. This overshoot-and-dip-effect increases with the power and the distance of the smart buildings to the substation. If the voltage drops or rises too much, the distribution system operator has to take countermeasures. This is because the end users' appliances and electrical devices are designed for a certain voltage range defined by European norms (EN50160:2007, [10]). The amplitude of the supply voltage is defined in this norm (see Table I). It is defined in the norms that the magnitudes of the low voltage and high voltage should be in the given range.

TABLE I. AMPLITUDE OF SUPPLY VOLTAGE

<b>Voltage Magnitude</b>	LV: $U = 230V$ MV: "by convention"
<b>Voltage Magnitude Variations</b>	LV, MV: $\pm 10\%$ for 95% week

#### A. Use case UC1: Insufficient or lack of renewable energy

In our previous work, we discussed the following use cases. In use case UC1, the power consumption in the city and the load on the distribution grid reaches its maximum level. During the same time frame, the feed-in of renewable energy is diminishing to the minimum, e.g., because of wind calm or the lack of sun radiation. Figure 4 illustrates this situation.

After further analysis of this topic, we found that in times of high load, the voltage at the terminals might fall below 0.9 p.u. (red line, equivalent to 207V), which would be a voltage magnitude violation according to the European norm. This dip effect increases with the power and the distance of the smart houses to the substation. The typical instrument to counteract this effect is the application of tap-changer transformers, because the end users appliances and electrical devices are designed for a certain voltage range, as defined by the norm. This lack of electric power shall be balanced with an optimum approach, at least partly by the intelligent buildings of the city.

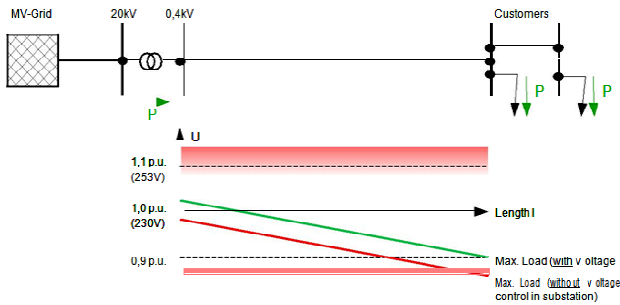


Figure 4. Maximum load scenario.

In order to do that, the lack of energy is signaled by the power providers towards the owners of intelligent buildings in the city by means of usual communication technologies.

The house owners can then react by turning off domestic appliances (e.g., white goods), set air conditioning units or heat pumps to eco-mode and deactivate charging stations for electric cars and vehicles. Therefore, the energy supply within the city could be balanced in a better way by the swarm behavior of the intelligent consumers by deactivating power loads. This is one of the core ideas of our previous and current work.

*B. Use case UC2: Surplus or excess of renewable energy*

In our previous work, we also discussed use case UC2. The power consumption and load in the city reaches its lowest level. During the same time frame, the renewable energy is fed into the power grid at maximum levels because of strong winds or strong sun radiation. Figure 5 illustrates this situation.

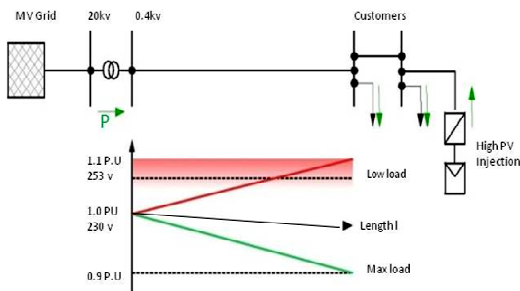


Figure 5. Low load scenario.

This is likely to occur in time periods when the injection of photo voltaic (PV) is high and the load on the net is low, typically during the morning hours. The high PV injection shown here is meant to illustrate the idea of getting more power from the grid to the consumer. An injection of power may make the voltage at the terminals rise up to 1.1 p.u. (red line, equivalent to 253V), which is also a possible voltage level violation to the European norm. This overshoot effect increases with the power and the distance of the smart houses to the substation. If the voltage rise gets too high, the distribution system operator also has to take counter measures, because the end users appliances and electrical

devices are designed for a certain voltage range only (as mentioned above). Again, this surplus or excess of electric power shall be used with optimum approach by the intelligent buildings of the city. In order to do that, the surplus of energy is again signaled by the energy suppliers towards the owners of the intelligent buildings in the city. The house owners with our smart phone application can then react by turning on additional power loads such as domestic appliances (e.g., white goods, air conditioning units or heat pumps), as well as electric cars and vehicles. Also in this case, the energy supply within the city could be balanced by the swarm behavior of the intelligent consumers.

IV. CONCEPT AND OVERALL SYSTEM DESIGN

The core concept is to minimize the uneven effect of smart buildings on electrical networks and on the smart power grid by analyzing and controlling the load profile of the intelligent buildings. The use of information technology allows an improvement on the electricity's transport from the power grid, with power system stability to consumer consumption integration. The idea is to balance loads in power grids by using KNX-enabled Smart Homes and a communication infrastructure as described above. The advantages of NGN are used to build a communication platform between mobile devices and an intelligent building with a home automation solution.

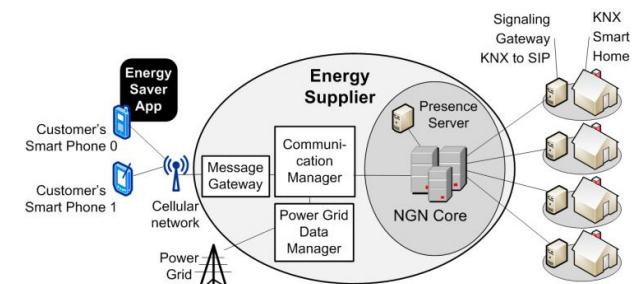


Figure 6. Control system with smart loads L9.....L20.

Figure 6 depicts the smart loads and their control system architecture. For simplicity, the loads are named L 9, 10, 19, 20. To analyze the facts related to smart homes and power networks, we used an integrated engineering tool for the power system calculations. The following features are provided by "Dig SILENT Power Factory" [11]: It has been designed as an advanced integrated and interactive software package dedicated to electrical power system and control analysis in order to achieve the main objectives of planning and operation optimization. Some of these functions are load flow, stability calculation and modal analysis. To design a distribution model of a smart home electrical network and a power grid, the following steps have been applied that include the external grid, transformers, bus-bars etc. (see Figure 7).

At first, an external grid (medium voltage) was connected to the bus-bar (B1). The specific bus-bar was

connected to a transformer (step-down), the parameters being 120/20 kV. The low-voltage side was connected to the bus-bar (B2). At the high-voltage end of Transformers T1...T3 line, one end was connected to B3 and the other end to the consumer (load), the line-line voltage being 400V and 230V line-ground.

There is a total of 12 smart houses and 23 “normal” houses, loads being 1.14 kW each, with a power factor of 0.95 to bus-bar B3. The transmission line of B3 is 5 km in length. The resistance value for each kilometer of B3 is 0.2215 Ohm, with a reactance of 0.037 Ohm, which are standard values. When voltage is applied to the transmission line of (B3), due to different loads, the voltage in the simulation sags from 400V to 343V. The voltage of 343V does not comply with the norms: According to these, there may be a  $\pm 10\%$  voltage magnitude variation of the reference voltage.

The distribution grid model consists of five transmission lines, three transformers 0.4 kV, four photo voltaic generators (PV cell) and one motor (battery). Every load at the consumer end could be “1 to n” number of customers. Three transmission lines are connected to one bus-bar, which is connected to one transformer (20/0.4 kV). The other two transmission lines are connected to a separate bus-bar, which is connected to another transformer (20/0.4 kV).

Now, there are mainly two tasks: Energy balancing and operational control. Both tasks are closely linked, since the power that is generated at different places and times in the grid must be evacuated and transported. According to the German Energy Industry Act, the power from internal Renewable Energy Sources (RES) generators must be evacuated [12]. For a further coverage of 30% RES, contracts for RES outside the grid have been made. However, forecast and reality do not always match, neither on the generation nor on the load side [13].

### V. EVALUATION AND ANALYSIS OF OUTPUT PLOTS

The scenario being displayed in Figure 8 shows the high load connection. It shows a voltage dip after each smart load.

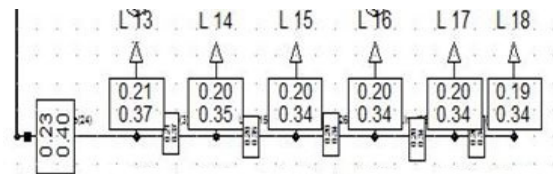


Figure 8. Transmission line with max load smart homes.

In Figure 9, the scenario being displayed is high load. On the X-axis the distance in kilometers is displayed, the Y-axis shows the voltage (unit: p.u.).

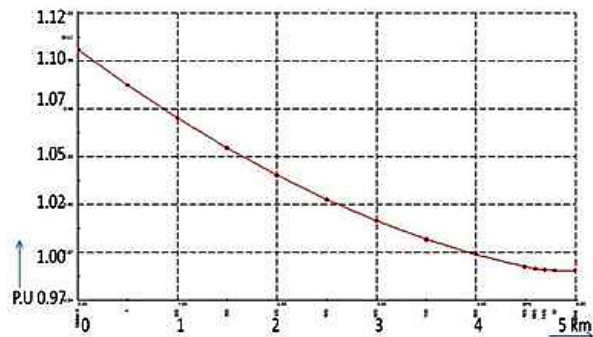


Figure 9. Voltage drop across supply line, high load at terminals.

Let us assume that the voltage has dropped from 1 p.u. to 0.97 p.u., which is equivalent to 207V at the end of the line. The graph shows that when high smart loads are connected to a transmission line, there will be a voltage drop

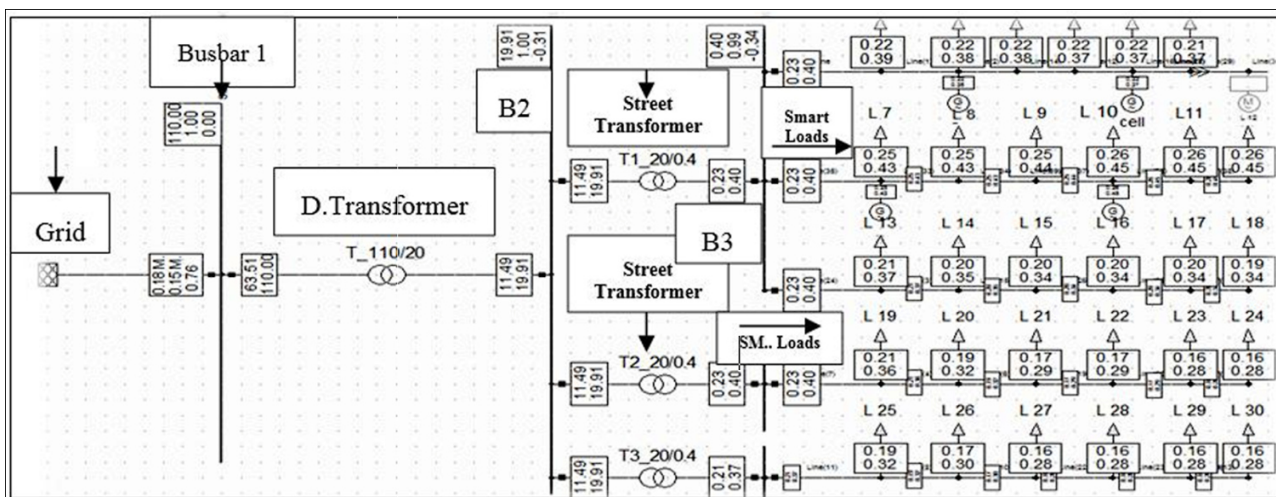


Figure 7. Transmission from grid to consumer end.

at the consumer end, so that the effect is increasing when the distance to substation increases. Line-to-line and line-to-phase voltages are drastically reduced. Here, the voltage variations are also violating the norms, since the voltage should be within the 10% range. Usually, tap-changer transformers are used by distribution system operators as the typical instrument to counteract this effect. The technique is to choose another tap winding so that the voltage in the substation increases, which also affects the terminal voltage. However, they can only be operated in a load-free state, which is a great disadvantage. If the voltage is supplied by the grid, the feed-in of renewable energy is diminishing to the minimum and the consumer is in the high load state, the voltage at the transmission line is decreased. This has to be improved to a standard that complies with the norms. Electrical appliances may be damaged if the voltage levels are not kept within the specified range. The electrical appliances at households cannot bear such decreases in voltage. More current will be drawn by the appliances, causing higher expenses and affecting the efficiency of these appliances.

In the following, a scenario for high PV injection is described (Figure 10). Each load is connected to bus-bar B3 (0.4 kV). Every alternate load is connected via a generator to smart houses.

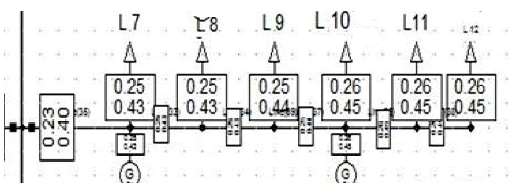


Figure 10. Transmission line with smart homes delivering excess power.

In Figure 11, the scenario being displayed is a high integration of in-feed electrical power by a high PV injection. On the X-axis the distance in kilometers is displayed, the Y-axis shows the voltage (unit: p.u.).

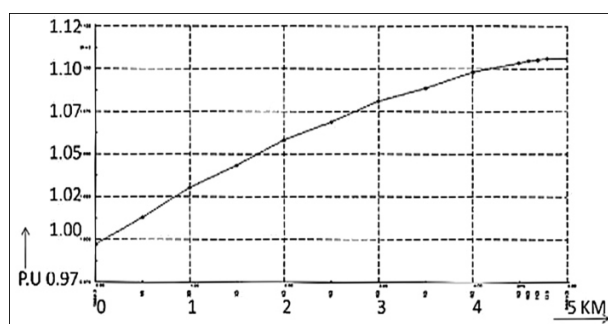


Figure 11. High photo voltaic generation violates voltage criteria.

Figure 11 shows the results of our simulation when the voltage goes up from 1.0 p.u. to 1.10 p.u. (equivalent to 253V) at the end of the line. Due to the power injection by the generators (PV panels) on the specific loads, which are connected to that generator, the effect will be distributed

and the voltage is increased after every kilometer. Because of this injection of power, the transmission line voltage went high. The system voltage shows an overshoot from the normal range, therefore violating the norms, when excess power is available. In this scenario, balancing should be applied. Here, the PV generators are replaced with asynchronous generators just to implement the idea. The active power of each generator is 4.5 kW, the reactive power is 0 MVar, and the consumer is considered as normal households. Now the voltage is supplied by the grid, and the generator injection is applied with the consumer having a lower load. The voltage at the transmission line increases (overshoots), and now it has to be lowered to the standard given by the norms. The electrical appliances at the households cannot bear such an increase of voltage. Damage could be caused to the appliances and also affect the efficiency of these appliances.

### VI. CALCULATION AND EVALUATION

The purpose of the calculations given in this section is to find the actual power that is needed to minimize the uneven effect of our smart houses, in order that an optimal control and balancing technique can be applied.

Voltages with  $U=230V$  are used as a reference. Concerning the given voltage magnitude variations, the admissible voltage range for the LV consumer is  $207V < ULV < 253V$ . The terminal voltage is subject to the line impedance  $R, X$  and the apparent power, as shown in Figure 12.

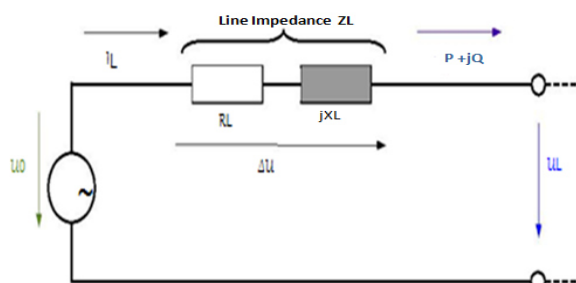


Figure 12. Equivalent circuit of supply line with line impedance.

Figure 12 shows the equivalent circuit of a supply line with the voltage  $U_0$  at the substation, and  $U_L$  at the junction point of the load. The apparent power  $S = P + jQ$  is injected and flows towards the junction point. The voltage  $\Delta U$  drops across the line impedance  $Z_L = R_L + jX_L$  and can be defined as [14]:

$$U = U_0 - U_l = I \cdot R_l \cdot jX_l \tag{1}$$

Figure 13 shows the voltage across a supply line in the low voltage grid. The flow of the active power  $P$  is directed from the MV-grid downwards through the MV/LV transformer, over a stub line, towards the customers. In the following, a calculation of different scenarios (high/low load, high/low PV injection) is presented.



Figure 13. Single line distribution.

$$\text{Apparent power: } S = P + (j \cdot Q) \quad (2)$$

Let  $Q = 0$ , then  $S = P$ . Number of smart loads = 12.

$$P/\text{Customer at any specific time} = 1.14 \text{ kW} \cdot 12 = 13.68 \text{ kW}$$

$$\text{Voltage at load: } U_a = U_0 \pm U_k \quad (3)$$

$$\text{Difference voltage} = U_k$$

The voltage at the customer end is in question:  $U_a = ?$

Supply Voltage:  $U_0 = 230\text{V}$  (Line-Earth),

$$P [\text{W}] = U [\text{V}] \cdot I [\text{A}]$$

$$\text{Current: } I = \frac{P}{V} = 13.68 \text{ kW} / 230 \text{ V} \quad (4)$$

$$I = 59.4 \text{ A}$$

$$\text{The change in voltage is: } U_k = I \cdot Z_k \quad (5)$$

$$U_k = I_k \cdot Z_k$$

$$Z_k = R_k + (j \cdot X_k)$$

Resistance =  $0.207 \Omega / \text{km}$ ,

Reactance  $X_k = 0.0804 \Omega/\text{km}$ , Distance =  $5 \text{ km}$ .

$$Z_k = \sqrt{0.5748} = 0.758155 \cdot 5 = 3.79 \Omega \quad (6)$$

$$U_k = I_k \cdot Z_k = 59.4 \cdot 3.79 = 225.17 \text{ V} \quad (7)$$

Calculations of specific power:

$$U_k = I_k \cdot U = I \cdot Z_k$$

$$U_a = U_0 \pm U_k = 230\text{V} - 225.17 \text{ V} = 4.83 \text{ V}$$

$$P_{\text{specific}} = 4.83 \cdot 59.4 = 286.9 \text{ W} \quad (8)$$

This power is needed to stabilize the transmission line (Figure 14).

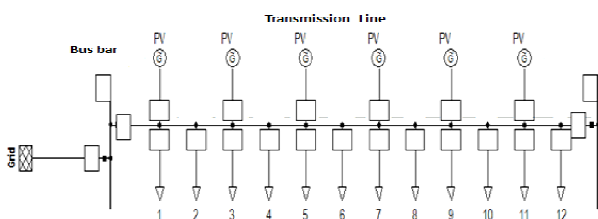


Figure 14. Unloaded transmission line.

Now, the excessive and deficit of power is calculated:

$$U_a = U_0 \pm U_k = 230 \text{ V} - 205 \text{ V} = 25 \text{ V}$$

$$P = 1.485 \text{ kW} \quad (9)$$

$$U_a = U_0 \pm U_k = 230 \text{ V} - 253 \text{ V} = -23 \text{ V}$$

$$P = -1.366 \text{ kW} \quad (10)$$

The important results for the first solution are:

- Equation (9) indicates the power needed to be fed into the system in order to balance the uneven effect of voltage caused due to a high load at the consumer end.
- Equation (10) indicates the power value needed to be taken out of the system in order to balance the uneven effect of voltage caused due to low load and surplus power at the consumer end.
- Equations (9) and (10) also indicate that if the storage battery system of same power capacity is added to the system, it will balance the load profile in both cases, charging when surplus energy is available and discharging when energy is less than the required limit.

Figure 15 contains loads, PV generators and a battery system, which defines the balanced load profile. Low load and high load scenarios are balanced with regulating the power by integration of battery storage systems.

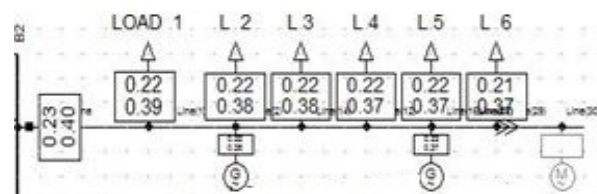


Figure 15. Stabilized voltage scenario.

In Figure 16, the scenario being displayed is balanced power. Again, on the X-axis the distance in kilometers is displayed, the Y-axis shows the voltage (unit: p.u.).

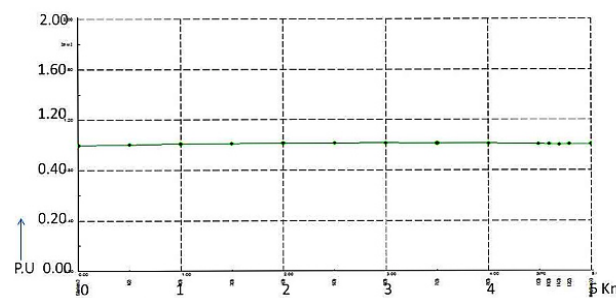


Figure 16. Stabilized voltage scenario.

The above graph indicates the balanced voltage values with high load and high in-feed from PV generators with an integration of battery systems.

VII. POWER AND ENERGY CONSUMPTION, SECOND SOLUTION

In this section, we will discuss some power consumption statistics in detail and find out how our NGN based network can minimize the problem. We will discuss two use cases here. The power usage data will be collected in dynamic power environment, which varies with the utilization.

A. Residential environment

For instance, we look at a two person living room apartment. Before we start with the power and energy consumption analysis, we must have a rough idea about the consumption of power and energy among the individuals in the residential environment. The full system power consumption is divided into two components: Static or constant power, which is independent of system activity, and dynamic power, which varies with the utilization [15]. The data that we have collected leads us to come up with a synopsis of power and energy used among the two persons at peak hours (see Figure 17).

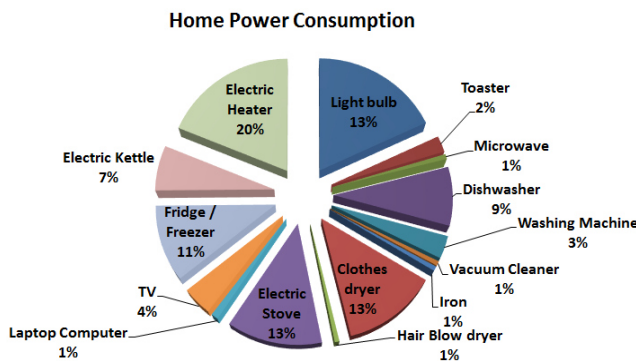


Figure 17. Power and energy consumption in residential environment.

The above power consumption statistical graph is for a high-load residential environment, where an excessive number of appliances is in use by the residents. So, for the simplification of our calculation, we will use the ideal case as given in Table II. In this table, the values are depending on the variable time.

It can be constant and variable according to the different profile of the individuals. It also depends on the type and number of appliances that are being used at certain points in time. Power consumption per day for pure resistive loads (from the above figure and calculation):

- Light bulb, heaters, smart devices = 1550 W
- Energy per day for same loads = 5.4 kWh
- Energy per month for same loads=162 kWh

TABLE II. POWER CONSUMPTION OF DIFFERENT APPLIANCES

Items	Quantity	Power consumption (W)	Operational time (h)	Energy (kWh)
Light bulb	4	40	6	0.96
Electric Stove	1	1500	1	1.5
Electric Heater	1	1500	2	3.0
Fridge /Freezer	1	100	24	2.4
TV	1	80	1	0.08
Washing Machine	1	200	1	0.2
Cloth dryer	1	2000	0.5	1.0
Smart Devices	6	10	24	1.44

It should be kept in mind that these values are taken in a normal two person ideal residential environment. These values vary with different profiles and different household appliances. This example of normal households is given to illustrate the idea of analyzing how load profiling is taking part to regulate the power system networks in different levels [16].

Now we discuss the given example in more detail. We take a specific time interval between (5pm to 10pm) when all of the house appliances are in operating mode, meaning that the house residents are using most of the appliances at this specific time. So, this will be about load calculation in peak hours. At the same time, our Smart Home communication infrastructure is providing the information to the house owner by a graphical user interface panel, installed at the same premises. Alternatively, the information is passed through our smart phone android application to the user. The house owner will have the possibility to minimize or regulate the power consumption profile by switching off the high power rating device or appliance.

An example for a random user: If he turns off a specific appliance, for instance a heater, at peak hours - how much effect will be observed after this specific action? Let us assume that he is reducing the load by 20% at peak hours. Similarly, if ten users are using the same control technique for their smart homes, they are reducing a considerable amount of load, which obviously sends a positive effect to the energy suppliers. The energy supply within the city could be balanced in a better way by the swarm behavior of the intelligent consumers by de-activating power loads.

The active power per customer taken in the above calculation is for simulation and to analyze the effect of power and voltage variation in electricity networks. Now again, we will use the ideal case values as above and analyze the effect of our control action on our power and energy statistics.

In the calculations, power reduction and energy differences in the defined time is given.

$$\begin{aligned} \text{Power reduction Total} - \text{Spec} &= 5,430 - 1,550 \\ &= 3,880 \text{ W} \end{aligned}$$

$$\begin{aligned} \text{Energy difference in } 0.3h &= 1,550 \text{ W} \cdot 0.3h \\ &= 0.46 \text{ kWh} \end{aligned}$$

$$\text{Energy difference for 5 appliances} = 2.3 \text{ kWh}$$

$$\begin{aligned} \text{Energy difference per day} &= 10.58 - 2.3 \text{ kWh} \\ &= 8.28 \text{ kWh} \end{aligned}$$

In the same manner, the same control technique of our smart KNX architecture affects different environments [17]. Now, we will take another use case for power consumption statistics.

**B. Office in a business environment**

Now follows a power consumption analysis of an office in a business environment, taking into account the broad spectrum of workflows of the office environment and including different appliances in the office. To deal with power consumption, the components used in the business office system should be known that are responsible for the consumption of power. Also, the recourses that are been used in the same scenario should be taken into account. All these power measurements are taken in real time. To overcome the repetition of the measuring part, we came up with estimated data and the calculation of power consumption.

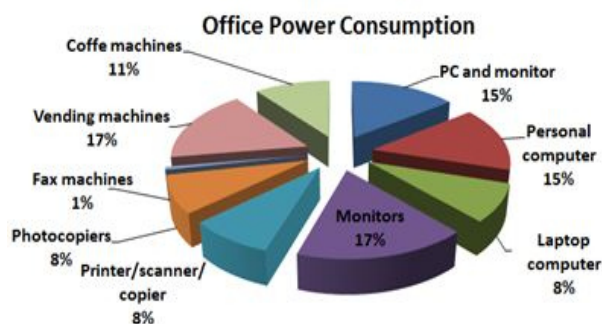


Figure 18. Power and energy consumption in a business environment.

This provides us with the parameters we want to observe. This approach also focuses on benchmarking the computer system in order to achieve an overall overview of the energy consumed by the computer system in the office. So, in the end we have the infrastructure of the power consumption used in the business environment in a real-time scenario [18].

For the simplification of our calculation, we will use the ideal case as given in Table III. In this table, the values depend on the variable of time. It can be constant and variable according to the different profile of individuals.

TABLE III. POWER CONSUMPTION OF DIFFERENT OFFICE APPLIANCES

Items	Peak rating	No of Items	Time (h)	Power (W)	Energy (KWh)
PC and monitor	300	30	7	63000	63
Laptop computer	100	10	4	4000	4
Monitors	200	5	8	8000	8
Printer/scanner/copier	50	5	4	1000	1
Fax machines	130	10	0.3	390	0.39
Vending machines	3000	2	8	48000	48
Coffee machines	1000	1	5	5000	5

Power consumption per day for specific loads (from the above figure and calculation):

- Coffee machine = 1 kW
- Energy per day for same load = 5 kWh
- Energy per month for same load = 150 kWh

It should be kept in mind that these values are taken in a normal, “ideal” office environment. These values vary with different profiles and different equipment or appliances. The given example of normal loads again illustrates the idea to analyze how load profiling is taking part to regulate the power system networks in different levels.

Now we discuss the given example in more detail. Again, we look at a specific time interval (between 5pm to 10pm) when all of the office equipment or appliances are in operating mode. This means that the office workers use most of the devices at this specific time, leading to a load calculation for peak hours. At the same time, our KNX-enabled office [19] communication infrastructure is providing the information for the office energy operator by a graphical user interface panel, installed at the same premises, or the information is passed through our smart phone application. The operator will have the possibility to minimize or regulate the power consumption profile by turning off the high power rating device or appliance. Example: A specific appliance, for instance a coffee machine, is used for 3 hours instead of 5 hours, at peak load. How much effect will be observed after this specific action? Let us assume there will be a reduction of the load by 11% (see Figure 13) at peak hours. Similarly, if ten users are using the same control technique for a “smart” office, they

are reducing the load by a considerable amount, which obviously sends a positive effect to the energy suppliers of the city. This could be balanced in a better way by the swarm behavior of the intelligent consumers by deactivating power loads. The active power per customer taken in the above calculation is used for simulation and analyzing the effect of power and voltage variation in the electricity networks. Again, we will use the ideal case values as above and analyze the effect of our control action on our power and energy statistic [20].

$$\text{Energy difference in 2h} = 1000 \text{ W} \cdot 2\text{h} = 2 \text{ kWh}$$

$$\text{Energy difference for 5 appliances} = 10 \text{ kWh}$$

$$\begin{aligned} \text{Energy difference per day} &= 129.39 - 10 \text{ kWh} \\ &= 119.39 \text{ kWh} \end{aligned}$$

### VIII. COMPONENTS

The following section introduces the components that are needed for the proposed analysis and calculation. The following parts of the Power Factory workspace are visible.

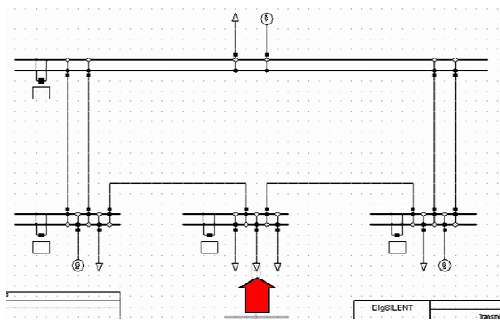


Figure 19. Transmission grid, single line diagram.

The distribution grid (see Figure 19) is fed by an external grid element. The transmission grid has a load element in the middle that represents the distribution grid, as depicted in Figure 20 by the red arrow. In order to connect the two grids, we have to remove the external net object in the distribution grid, and the middle load element in the transmission grid.

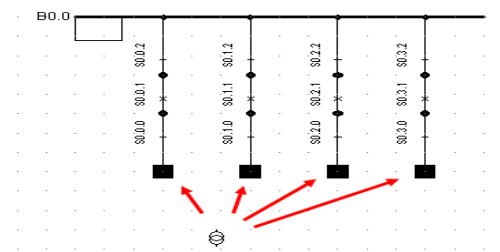


Figure 20. Transformer connected to the single busbar system.

To create a 110/33 kV transformer and to connect the 110 kV double busbar system with the 33 kV busbar, the terminals (busbars) of the substations are to be connected with two winding transformers. To draw the first transformer, the upper terminal at the position is suggested by the background pattern. The transformer is now connected to the terminal at that position. The middle terminal makes the second connection (see Figures 20 and 21).

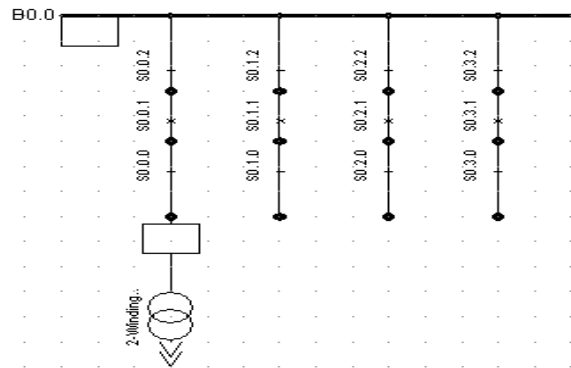


Figure 21. Two winding transformer connection.

A load flow calculation may be started from the main menu of Power Factory. For the intended load flow calculation, the following options need to be set: Calculation Method = AC Load Flow, balanced, positive sequence. All other options on the basic options page need to be disabled. The load flow calculation is not executed to resolve the error. One should first find the element for which the error was reported. With the Power Factory output window, the error can be corrected and the load flow calculated again.

Then, the calculation shows that the load flow solving algorithm has found one area (separated area) in the whole system and chosen the external grid element as a reference element. The single line graphic in Figure 21 shows the results of the load flow in the result boxes.

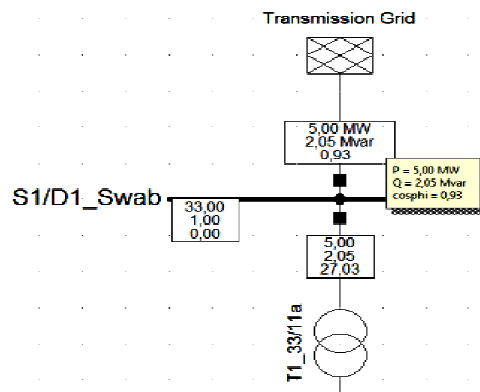


Figure 22. Results of the load flow calculation.

## IX. FUTURE WORK AND CONCLUSION

We are concluding this work by stating that our smart home KNX control architecture solution is secure and trustworthy for the solution of current challenges in the field of optimal smart grids. Capable of energy efficient management for intelligent buildings, our simulation provides the important values, which estimate the values of power that can balance the uneven effect of voltage in both cases. An interesting alternative is the integration of battery backup systems. Already a proven technology for uninterrupted power supply (UPS) units, they become increasingly interesting for applications in power systems. They cannot only be used for energy balancing purposes, but can also serve as primary and secondary control reserves.

Actually, this concept is not new: A battery-based system was built in Germany for voltage and frequency stabilization for the supply of the island network used in West Berlin in 1986. The 17 MW plant was to go through an entire charge and discharge cycle twice per day [21]. Keeping in view that if emerging renewable energy sources act as separate generation, they cannot balance the existing energy demand. It is necessary that RES will be integrated in the existing power grid.

Our results evaluate the following important conclusions: In case of high loads and a lack of power, and in case of excessive power and low loads, we have to manage a certain amount of power that can balance the effect. This could be done by reducing or raising the load with our load management and control solution.

In the power statistics (Section VII), the collected data will help us to create a power model, as the power model would be the most efficient and effective way to replicate the workload on the different users in the business environment dealing with real time data. Advancements are required in the existing power management systems.

The software being used for simulation purposes in this work is a limited version, in which only small networks can be analyzed. For future work, voltage variations are to be looked upon with specific actual loads as presented in Section VII at larger scales. This will be done with an extended version of the software, allowing to simulate a whole city as a grid model [22]. The number of transmission lines will be increased as well as the number of parameters for the distribution grid. Thus, we will have the knowledge to give an intelligent idea within this remarkable field of study.

## ACKNOWLEDGMENT

This work has been performed within the project "Smart Home Control" at Hochschule Darmstadt (University of Applied Sciences). The authors would like to acknowledge the support of the Energy Lab at the University for giving access to the Dig Silent software and Albrecht JUNG GmbH & Co. KG for their contribution of KNX actors, sensors and other KNX home automation devices and kind support.

## REFERENCES

- [1] A. Khan, T. Wiens, and M. Massoth, "Stability Improvement Solution of the Smart Power Grid by an Analysis of Voltage Variation in Intelligent Buildings," (SMART 2014), IARIA, 2014, pp. 13-19, ISSN: 2308-3727, ISBN: 978-1-61208-363-6.
- [2] T. Wiens and Michael Massoth, "Trustful interaction between intelligent building control and Energy suppliers of the smart power Grid," in Proceedings of the 2nd International Conference on smart system, devices and technology (SMART 2013), IARIA, 2013, pp. 46-51, ISSN: 2308-3727, ISBN: 978-1-61208-282-0.
- [3] M. Massoth et al., "Ubiquitous Smart Grid Control Solution based on a Next Generation Network as Integration Platform," in Proceedings of the 1st International Conference on Smart Grids, Green Communications and IT Energy-aware Technologies (ENERGY 2011), IARIA, 2011, pp. 173-178, ISSN: 2308-412X, ISBN: 978-1-61208-136-6.
- [4] "Genentech Media. Home Energy Management Systems," [Online]. Available from: <http://www.greentechmedia.com>, 2013-2017.
- [5] D. Tsiamitros, D. Stimoniari, N. Poulakis, M. A. Zehir, A. Batman, M. Bagriyanik, A. Özdemir and E. Dyalynas, "Advanced Energy Storage and Demand-Side Management in Smart Grids using Buildings Energy Efficiency Technologies," 5th IEEE PES Innovative Smart Grid Technologies Europe (ISGT Europe), Istanbul, Oct 2014, pp. 632-637, ISBN: 978-1-4799-7721-5.
- [6] R. Acker and M. Massoth, "Secure Ubiquitous House and Facility Control Solution," Fifth International Conference on Internet and Web Applications and Services (ICIW 2010), IARIA, 2010, pp. 262-267, ISBN 978-0-7695-4022-1.
- [7] M. Liska, M. Ivanic, V. Volcko, P. Janiga, "Research on Smart Home Energy Management System," Institute of Power and Applied Electrical Engineering, Slovak University of Technology in Bratislava, Slovakia, 2015.
- [8] B. Asare-Bediako, P. F. Ribeiro, and W. L. Kling, "Integrated Energy Optimization with Smart Home Energy Management Systems," 3rd IEEE PES Innovative Smart Grid Technologies Europe (ISGT Europe), IEEE, 2014, pp. 1-8, ISBN: 978-1-4673-2595-0, ISSN: 2165-4816.
- [9] A. Menezes, P. van Oorschot, and S. Vanstone, "Handbook of Applied Cryptography (Discrete Mathematics and Its Applications), CRC Press, 1996.
- [10] Deutsches Institut für Normung, „DIN EN 50160.“ Available from: <http://www.leonardo-energy.org/good-practice-guide/standard-en-50160>, 2015.
- [11] Dig Silent, "Dig Silent Power Factory, Version 14.23 software". [Online]. Available from: <http://www.digsilent.de/>
- [12] Bundesministerium des Inneren, „Energiewirtschaftsgesetz," [Online]. Available from: [http://www.gesetze-im-internet.de/bundesrecht/Energy\\_Act\\_\[2005\]/gesamt.pdf](http://www.gesetze-im-internet.de/bundesrecht/Energy_Act_[2005]/gesamt.pdf), 2005.
- [13] AsianPower & EnergyFront, "Smart Grid. [Online]," Available from: <http://my.reset.jp/~adachihayao/indexE100319.htm>, 2012.
- [14] L. Petry, "Renewable energies - Master of Electrical Engineering (Power)". University of Applied Sciences Darmstadt, 2011.
- [15] A. K. Tao Jiang, "LAYERED GREEN PERFORMANCE," GAMES, <http://dl.acm.org/citation.cfm?id=2039447.2039651>, 2010.
- [16] M. Liserre, T. Sauter and J. Y. Hung, "Future Energy Systems: Integrating Renewable Energy Sources into the Smart Power Grid through Industrial Electronics," Industrial Electronics Magazine, Vol. 4, Issue 1, IEEE, 2010, ISSN: 1932-4529.
- [17] KNXAssociation, "KNX Standard. [Online]," Available from: <http://www.knx.org/knx-standard/standardisation>, 2015.
- [18] tED magazine, "Special Report. [Online]," Available from: [http://www.tedmag.com/news/news-room/special-report/Special-Report/Special-Report-\[1-22-2009\]](http://www.tedmag.com/news/news-room/special-report/Special-Report/Special-Report-[1-22-2009]), 2014.

- [19] P. Kundur and J. Paserb, "Definition and Classification of Power System Stability," IEEE Transactions on Power Systems, Vol. 19, IEEE, 2004, pp. 1387-1401, ISSN: 0885-8950.
- [20] G. M. Shafiullah, "Potential challenges: Integrating renewable energy with the Smart Grid," in Proceedings of the IEEE Universities Power Engineering Conference (AUPEC), 2010, pp. 1-6, ISBN 978-1-4244-8379-2.
- [21] T. H. Fiedler, "Mobile and Immobile Components in Modern Power Grids for Improving Stability," Faculty of Electrical Engineering, IOSUD, 2010.
- [22] IEEE Task Force on Harmonics Modeling and Simulation, "Modeling and simulation of the propagation of harmonics in electric power networks, Part I. Concepts, models, and simulation techniques," IEEE Transactions on Power Delivery 11, IEEE, 1996, pp. 452-465.

## Practical Aspects of Ontology-Based Analysis and Reasoning for Law Information Represented in Textual Form

Raoul Schönhof, Axel Tenschert and Alexey Cheptsov  
High Performance Computing Center Stuttgart,  
University of Stuttgart  
Stuttgart, Germany  
e-mail: raoul.schoenhof@b-f-u.de, tenschert@hls.de, cheptsov@hls.de

**Abstract**—Legal domain is an important source of information and includes diverse law texts, court decisions, etc., which is dominated by documents collected in natural language. There is a great demand for the automatic analysis of the legal information in everyday work of lawyers and other people dealing with laws, for which the ontology-based knowledge representation would be of a great advantage. Unfortunately, the current semantic and ontology based technologies cannot be easily applied for the analysis of legal texts due to a certain complexity of those. We present a strategy that allows different categories of tools, such as those for ontology creation, syntactical analysis of texts collected in natural language, and others to interoperate in order to achieve a common goal – creation of domain-specific ontologies and performing complex reasoning over them. A model that can be applied for the legal system knowledge representation is proposed and its implementation for the German Civil Law System in form of an ontology is discussed. The model allows the creation of a common ontology spanning over the knowledge contained in diverse laws, thus paving the way towards a wide adoption of semantic technologies by the experts in the law domain.

**Keywords**—Knowledge Representation; Law Texts; Ontology; RDF; Big Data; Rule-Set.

### I. INTRODUCTION

This paper deals with the technologies presented in our previous work [1] for legal knowledge representation as Resource Description Framework (RDF) ontologies and discusses practical aspects of their application by means of the existing analysis tools. Working with highly unstructured and ambiguous data is a major challenge when solving many research, industrial, and societal issues. The knowledge required for tackling those challenges is contained in most cases in the documents that are represented as natural texts, e.g., in books, journal articles, websites, files on the disc, etc. The information extraction from those sources requires a deep knowledge of the content as well as the understanding of the domain-specific terminology. However, the major challenge is the automation of the knowledge discovery process.

A law system can be considered as an important source of information that has to be retrieved in form of a digital knowledge base with the goal to perform reasoning over a

number of interrelated information sources of the distributed nature. The knowledge base has to be built and treated dynamically from the changing data sources. For example, in Germany, 553 federal laws and many more federal state ones have appeared in the time between 2009 and 2013 [2]. Everyday, hundreds of new court decisions are made, which have a potential to influence the interpretation of the statements contained in laws.

Semantic technologies offer well-established tools for treating the legal knowledge in unstructured and dynamic data sets by retrieving the content as a structured (and thus analyzable) ontological representation. As compared with the other domains that rely on plain texts as the major source of information, the law data offer a well-defined terminology and a clear, systematic structure. Center of the law system is the German Civil Code (in German terminology "Bürgerliches Gesetzbuch" or shortly BGB). It manages and defines fundamental and general issues. The paragraphs are numbered ongoing through the entire BGB. Most of the single paragraphs are broken down into articles, sub articles and half sentences or numbers (see Figure 1). Despite the semi-structured nature of the law texts, several previous attempts to treat law information (cf. [3], [4]) by means of ontologies were not very successful as they were based on abstract model with a static structure, which made their use in practice very limited.

Our approach is different – we aim to develop a system that is able to automatically and on-the-fly build the ontological representation of the information contained in dynamic data sources and enabling reasoning over it. The goal of reasoning is to understand and analyse the information based on multiple sources, such as laws and previous court verdicts. As a use case, the German law system is considered. The law texts are explored and structured using the techniques such as Resource Description Framework Syntax (RDFS) [5] and Web Ontology Language (OWL) [6] for the ontology extraction and further use in an automated reasoning process. Using the proposed tool set, the experts of the problem domain will be able to consider a much wider spectrum of documents than available to them currently.

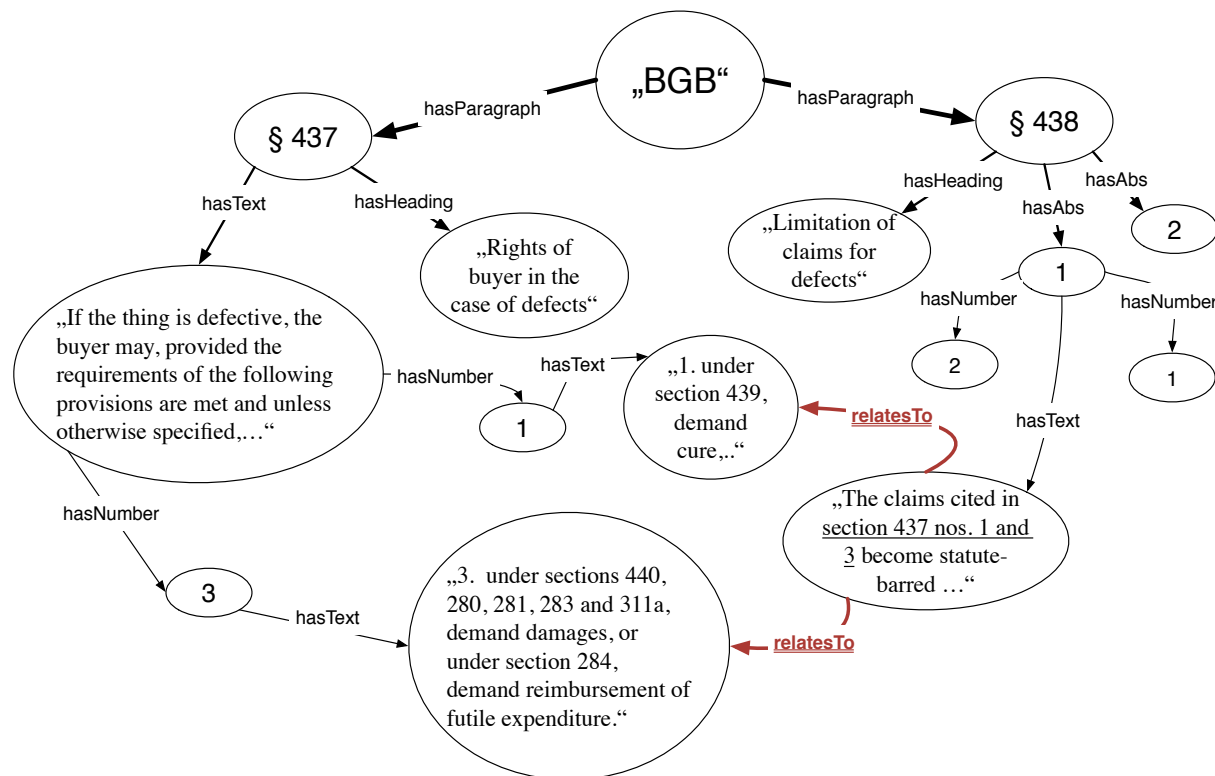


Figure 1. Example of connections in legal text

The remainder of the paper is organized as follows: Section II gives an overview of the German legal system and explains briefly, supplied by an example, how different laws can interact with one another. Section III demonstrates the capability of semantic web technologies in the field of law by means of a little use case. Section IV introduces the system design and shows how legal knowledge ontologies could be generated from natural texts found in law collections by using computer linguistic tools. Finally, Section V deals with the future tasks as well as the assets and drawbacks.

## II. EXEMPLARY SCENARIO

The information contained in individual laws only make value when considered across all other regulations of a law system related to the given case. However, the analysis of cross-references between multiple laws is often complicated by several factors, such as complex structure, use of abstract wording and specialized terminology, number of related laws, etc. For example, the BGB is divided into five chapters; each chapter manages a special legal domain. The first chapter is called General Part, which is the result of the repetition reduction. It contains mostly definitions and general rules of law; these are used in the chapters two to five. The second chapter is called Law of Obligations. It contains rules of law to any kind of contract and defines the most common contracts, for example the purchase

agreement. This chapter is followed by the Law of Property, the Family Law and the Law of Succession. Especially the separation between more general rules of law and specialized rules of law makes it possible that two rules of law regulate one situation in different ways. In such cases, the more general rule of law is displaced by a more specialized one or a younger rule of law displaces the older rule of law. Therefore, rules of law interact constantly with each other.

Let us illustrate the dependencies between laws based on the following example (§ 437 BGB and § 438 BGB of the Sales Convention [7]):

§ 437 BGB : “If the thing is defective, the buyer may, provided the requirements of the following provisions are met and unless otherwise specified, 1. under section 439, demand cure, 2. revoke the agreement under sections 440, 323 and 326 (5) or reduce the purchase price under section 441, and 3. under sections 440, 280, 281, 283 and 311a, demand damages, or under section 284, demand reimbursement of futile expenditure.” [7].

§ 438 I BGB: “The claims cited in section 437 nos. 1 an 3 become statute-barred 1. in thirty years, if the defect consists a) a real right of a third party on the basis of which return of the purchased thing may be demanded, or



purchase agreement states, among others, the seller is obligated to deliver the *thing*. Obviously, a reasoning algorithm can not match the entity *bicycle* to the entity *thing*, required for § 433 I [7]. By adding additional information from dictionaries or encyclopedias, it is possible to bridge this gap between *bicycle* and *thing*. These connections are represented through orange arrows. In a similar way, the entities *Henry* and *Peter* can be abstracted to the entities *buyer* and *seller* via the entity *person* and their names. As result (blue arrows), the entities *Henry*, *bicycle* and *Peter* can now be matched to the entities *buyer*, *thing* and *seller*. Furthermore, the purple relation *is\_obligated\_to\_deliver* is applicable between the entity *Peter* and *bicycle*.

In this simple use case, the system reports back, that Peter is obligated to deliver the bicycle. The user benefits from a fast and simple way to get informative hints, in the field of law.

#### IV. STATE OF THE ART

The information extraction from natural texts, in the context of our research goals, is based on three pillars: Linguistic, Computer Science, and Law. The first two pillars offer technologies while the third one represents an use case. In the following subsections, we concentrate on technological challenges of the analysis technologies.

##### A. Information Retrieval Systems for Ontology Generation

The amount of information is constantly increasing but only available in an unstructured format. Mostly, the information is hiding in natural language texts. There have been numerous approaches to retrieve information from documents and texts, deriving an RDFS/OWL graph. To the most popular approaches belong Text2Onto [10], OntoLearn/OntoLearn Reloaded [11], OntoMiner [12] and OntoLT [13][14]. The OntoMiner approach analyzes regularities from HTML Web documents. A substantial disadvantage is the requirement of a handpicked set of web sites within the admired field of interest. The output taxonomy is strictly hierarchical, which is appropriate to classify entities, but it cannot find a considerable amount of relations between entities inside a level in the hierarchy. Interconnections are necessary performing complex reasoning tasks. The same situation looms with regards to the OntoLearn Reloaded approach. Much more promising is the approach of Text2Onto and OntoLT. Text2Onto combines machine learning strategies with basic NLP methods [10], particularly tokenization, lemmatizing and shallow parsing, allowing the application to analyze a natural language text more detailed. Testing Text2Onto has demonstrated, that the retrieved amount of information was not enough, with regards to the field of interest. Beside Text2Onto, even OntoLT was using NLP technology, above the task of named-entity-recognition, to generate semantic networks. Hereby, OntoLT was using predefined mapping rules for every desired annotation tag. OntoLT then

constructs an OWL ontology according to the given mapping rules. According to our knowledge, OntoLT has not been extended since 2007.

The presented approach affiliates this concept of grammatical-driven information retrieval, implements state of the art NLP tools and expands it by considering grammatical dependencies for information retrieval to achieve a higher precision and applying it to the field of law. Using dependencies for information retrieval, the approach benefits by additional information about the semantic content of text [15]. Our approach is based on three pillars: Linguistic, Computer Science, and Law. The first two pillars offer technologies while the third one a use case. In the following subsections, we concentrate on technological challenges of the analysis technologies.

##### B. Linguistic Tools and Syntax Theories

P. G. Otero [15] presents an approach for exploiting human-written text by computers, according to which it is necessary to examine the structure of each sentence considering the dependency syntax. In the last decade, the linguistic tool development has been established very well, especially with regard to grammatical parsers. For example, the Stanford NLP Group offers a comprehensive toolset for various aspects of grammatical sentence parsing [16]. For our goals, we took a closer look at four types of computer linguistic tools: i) constituency parsers, based on the generative grammar, ii) dependency parsers, based on the dependency grammar, iii) named entity recognizers, used for locating and classifying entities in text, and iv) sentence splitters.

**Constituency Parser.** Constituency parsers are based on the idea of splitting a sentence in functional units called constituents [17]. The resulting tree of superior and subordinated constituents generates a tree-like structure, which is mapped as an Augmented Transition Network (ATN) [18]. ATN offers a flexible and scalable technology to represent the grammatical structure of sentences. It disassembles a sentence into constituents (see Figure 3) and tags them. A very common constituency parser is the Stanford Parser [19]. It supports various languages, including English, German, Chinese, and Arabic. An example of ATN for the sentence "*A computer is a machine.*" is shown in Figure 3, by using the constituent tags from the Penn Treebank Project [20][21]. The sentence (S) is divided in two "sub-constituents", here the noun phrase (NP) and the verbal phrase (VP). These contain either atomic words or other constituents. Here, the determiner (DT) "*A*", the noun (NN) "*computer*", the verb (VBZ) "*is*", the noun "*machine*" represent atomic words, whereas "*A computer*" or "*a machine*" form a noun phrase. In combination with a verb, the constituent VBZ and NP, here "*is a machine*", form a verbal phrase.

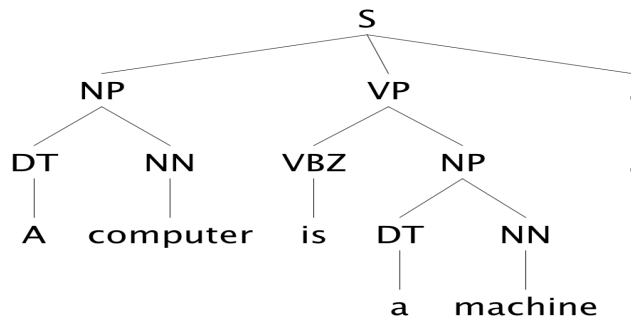


Figure 3. ATN Example based on Stanford Parser GUI

**Dependency Parser.** Dependency parsers [22] are based on the dependency grammar [23], which focuses on relationships between words and their functional role within a sentence [23]. Relations can be represented in a form of a directed graph, which makes it possible to derivate a hierarchy [23]. Because the structure of the hierarchy is only depending on the grammatical syntax, it is also possible to conclude to the semantic [15], e.g., Figure 3 shows an example sentence with its dependencies and constituents.

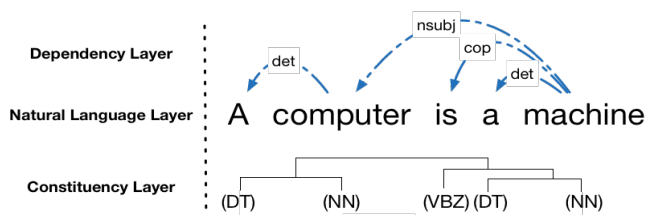


Figure 4. Grammatical structure of a sentence

The dependencies in a sentence are presented as a tree of connected word tags being knots. Hereby, the dependency tags *det*, *nsbj* and *cop* stand for *determiner*, *nominal subject* and *copula* [24] and provide additional information about the type of grammatical relations. Basically, this pattern is representative for a sentence of the type "*Object*  $\rightarrow$  *Subject*". Figure 4 shows the resulting dependency pattern. The abstract pattern helps finding sentences with the known information structure. The identified words then need to be transferred into a more machine-recognizable format. This is not only useful for identification of classes and their subclasses but also with regard to the "valence theory" [22]. Origin of this theory is the empirical knowledge of the structure-determining characteristic of verbs as presented by L. Tesnière [25]. According to this and exposed by H. M. Mueller et al. [23] and V. Ágel [26][25], each word or word group is typically associated with a verb in the sentence. Therefore, dependencies could also help identifying the actions (= verbs) of individuals in the sentence.

**Named Entity Recognition.** Named Entity Recognizers (NER) are tools to identify typical non-context related individuals, e.g., locations ("Berlin", "Hong Kong"), organizations ("UNICEF", "NASA") or person names ("Lisa", "Rouven"). Therefore, NERs, like the Stanford

NER, are using Conditional Random Fields (CRFs) to identify entities [27]. With regards to our approach, NERs are not essential but an improvement area to gather additional information helping to find some individuals, which could not be found by only focusing on ATN-trees or dependency structures.

**Sentence Splitting.** Typically, a text contains many sentences; in order to analyze them, they have to be separated. This task is performed by sentence splitters. One of the most popular sentence splitters is provided by A Nearly-New Information Extraction System (ANNIE) [28] - a software package of the GATE project. This splitter can distinguish between a full stop and any other point.

### C. Working with Information

While ATN, NER, and other dependency parsers can derive some useful information about the texts' structure, the ontology languages facilitate information representation. Ontologies can be leveraged to text to identify classes, individuals, or even properties in them. Alongside with that, ontology-based analysis frameworks provide tools that allow for querying the retrieved information.

#### 1) Web Ontology Language

OWL provides a framework to store and handle information by ontologies [6]. OWL is based on the RDF [29] and equipped with an additional vocabulary [30]. Each OWL ontology can represent different kinds of information, e.g., classes, individuals or properties. While classes express abstract concepts, individuals are existing members of one or more classes. The relations between other individuals are defined by their properties. Therefore, OWL is predestinated to use ontologies with reasoning algorithms. [6]

#### 2) Semantic Web Rule Language

As a special sub language of OWL, the SWRL represents abstract rules associating OWL individuals to any desired OWL class. Special forms of these rules are built-in relations. These rules consist of an antecedent, called "*body*", and a consequence, called "*head*". Several OWL individuals of an ontology can hereby be associated with another class [31]. This enables the use of very complex rules. A little example to illustrate: "*If a device contains a CPU, then it is a computer*". Therefore, an individual of the class "*device*" is defined as "*computer*" if this individual is connected to another individual of the class "*CPU*" by the object property "*hasContain*". The resulting SWRL Rule would be (1).

$$\begin{aligned} & \text{device}(?x) \wedge \text{hasContain}(?x, ?y) \wedge \text{CPU}(?y) \\ & \Rightarrow \text{computer}(?y) \end{aligned} \quad (1)$$

## V. SYSTEM ARCHITECTURE

As we proposed in [1], the current framework is defined by three components, the Sentence Processing Unit, the Ontology Generator and the Reasoner, shown in Figure 5. In this respect, we have improved our primary system architecture mentioned in 2014 [1][32]. In the first step, natural language texts from different sources like Wikipedia, law texts or from a given use case are loaded to the Sentence Processing Unit.

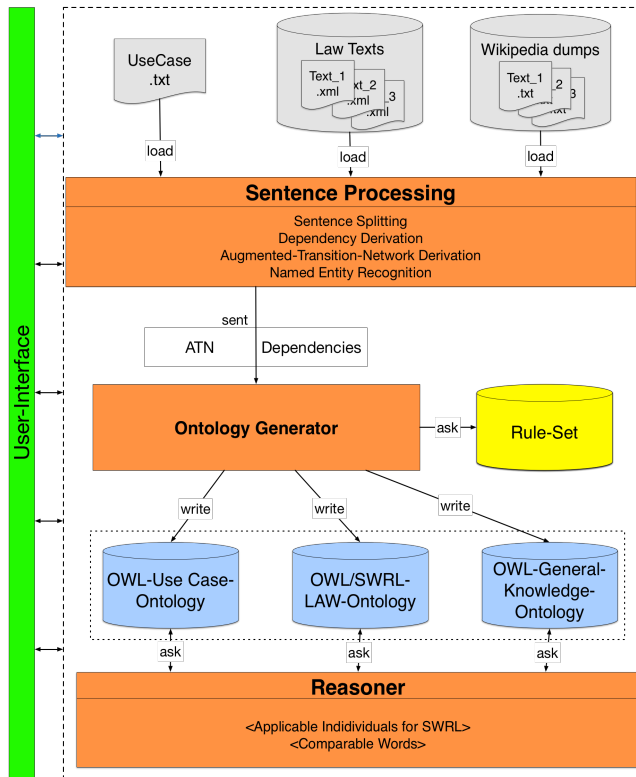


Figure 5. System Architecture

The first component represents the Sentence Processing Unit. The Sentence Processing Unit splits up the text to its sentences and divaricates the grammatical structure as an ATN and a dependency network. It is basically a conglomeration of different language processing tools containing the sentence splitter from ANNIE/GATE [28], the dependency and constituency parser from the Stanford NLP Group [19][22], as well as a Named Entity Recognizer [27]. The second component is the Ontology Generator with its Rule-Set (see Figure 5). It builds three OWL models out of natural texts. The first ontology contains the information about the questionable use case (OWL - Use Case Ontology). The second one contains the laws, respectively the legal prerequisites, represented as SWRL Rules (OWL/SWRL - LAW Ontology). The third ontology contains general knowledge, mainly about classes and subclasses (OWL - General - Knowledge). Finally, the third component is the reasoning process, respectively the reasoner. Hereby, the reasoner tries to match the given

information based on the Use Case Ontology with the rules from the LAW Ontology. Because laws are written in a notional way, it is necessary to establish a connection between the individual of the use case and the SWRL rule. The General Knowledge Ontology provides this connection. The strict separation between the Use Case Ontology and the General Knowledge Ontology is necessary because the correctness of the given information in a random use case cannot be assumed.

### A. Sentence Processing

Starting point is the raw data, which contains texts with one or many sentences. The source of the texts might be Wikipedia [33], law texts [34], or any other texts related to the topic of our use case. These texts have to be processed, so the sentence structure, defined as pattern  $p$ , can be mapped. Each pattern  $p \in P = \{d, A\}$  is represented by a subset of dependencies  $d \in D = \{s, p, o\}$  and an ATN  $A$ . Hereby,  $d$  is described by triples, consisting of a subject  $s$ , a predicate  $p$  and an object  $o$ . While  $s$  and  $o$  are words,  $p$  belongs to a dependency tag, also shown in Figure 4. Therefore, each text passes through the ANNIE sentence splitter of the text-engineering tool GATE [28]. The constituent and dependency parsers then analyze the isolated sentences. Afterwards, the atomic words will be exchanged against their lemma projecting the numerous variants of a concept to a single lemma. Therefore, the complexity of the dictionary is reduced.

### B. Information Retrieval

Information about the content of the given law texts have to be extracted and added to the model, which is one of the most challenging tasks. Of an extraordinary interest is the identification of concepts in the encyclopedia text files, the law books or the particular rule as well as its heading. For instance, one of these concepts is "statute-barred" in § 438 I BGB, shown in Figure 1. The concept identification uses statistical extraction methods as well as pattern-based methods. Especially latter methods are predestinated to identify cross references, which are common in law texts. Because of the circumstance that some rules refer to another rule and some rules prohibit the applicability of another rule, the pattern based method has to distinguish between these two cases. Subsequent to the information extraction, the identified concepts are added as OWL triples to the initial model.

Naturally, these methods will just help to identify entities but they will not be able to extract a very large amount of information, e.g., the relation between a number of entities. Therefore, additional tools have to be used. Meanwhile, there are various text engineering tools, which are capable to extract information out of natural text; for instance, Text2Onto [10] and Gate [35] with the OWLExporter plug-in [36] as well as Protégé [37] with its plug-in OntoLT [38].

Beside these tools, the Stanford Natural Language Processing Group (SNLPG) at the University of Stanford developed a broad range of computer linguistic tools including a part-of-speech (POS) tagger to break sentences down into their lemma and mark them with their part of speech [39]. SNLPG also provides a special Named Entity Recognizer to find and classify salient nouns, e.g., the noun "London" as a location [27]. Furthermore, a sentence parser, e.g., Stanford Parser [19], is provided, which can be used to identify dependencies between words in a sentence.

The information extraction will be done as follows. Firstly, each sentence of the initial RDF ontology will be passed to the POS-tagger. It splits each sentence into single words and figures out, which part of speech may be present, e.g., whether it is a noun, a verb or an adjective. Also, the POS-tagger references from the words in a sentence to their lemmas. The lemma of nouns are added as isolated entities to the RDF model. After the sentence is tagged by the POS-tagger, the information about the part of speech is used by the Stanford Parser to generate a parsing tree. Dependency parsing is based on a parsing tree that represents a grammatical structure of a sentence, e.g., such as shown in Figure 4 for a part of § 437 BGB as ATN including the dependencies [7].

This parser allows it to detect references between verb and noun phrases. These references will be used as properties in the RDF model. Unfortunately, there is no German language support for the Stanford Dependency Parser [22]. Thus, an alternative is necessary, which could be the Zurich Dependency Parser for the German language (ParZu) [40]. Output of the dependency parsing process may be considered as directed graph, consisting of the words as node and the dependencies as edges. These edges are tagged with the dependency type, e.g., nominal subject (nsubj), providing additional information about the specific type of relation.

### C. Ontology Generator & Rule-Set

The Ontology Generator translates a given sentence into a machine-recognizable OWL ontology, based on its pattern. The resulting OWL ontology is representing the base for any reasoning attempts. Hereby, the Ontology Generator compares the grammatical structures of a given sentence from a set of predefined grammatical patterns, called Rule-Set, to derive the OWL ontologies mentioned in Figure 5. If a pattern could be identified, the Ontology Generator converts the words as OWL Classes, OWL Individuals or SWRL Rules and interconnects them. The axioms are stored in different OWL ontologies. This is essential because the given information from a use case do not have to be true. One of the most difficult tasks is the development of the Rule-Set. This set contains patterns of

typical sentence structures, as well as corresponding instructions. They can be described as follows:

Let  $rs \in RS = \{p, i\}$  be the Rule-Set, which contains pattern and instruction  $i$ . The instruction describes the connection between the words as and OWL model, by generating OWL's Classes, Individuals, and Predicates. Because of the complexity of natural language, the patterns cannot exist statically (therefore, one pattern for each type of sentence) but must be composed from different rules. This process could be demonstrated at the following example.

Let us apply that Rule-Set to the text mentioned in Figure 3 ("a computer is a machine"). The first rule  $rs_1(p_1, i_1)$  contains pattern  $p_1$  (see Figure 6) that describes a noun (e.g., *computer*) referencing to another noun (e.g., *machine*) using the dependency *nominal subject*. In addition to the dependency structure,  $p_1$  also contains the constituencies.

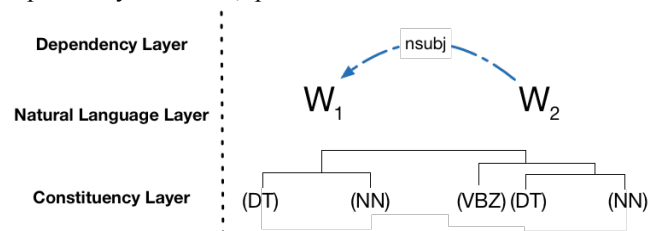


Figure 6. Pattern of  $rs_1$

The corresponding instruction  $i_1$  defines the first noun as a subclass of the second one:

$$i_1 := \text{SubClassOf}(\text{Computer}, \text{Machine}) \quad (2)$$

Now, let us add another rule  $rs_2(p_2, i_2)$  to our Rule-Set specifying the connection between two nouns by means of the dependency "compound", like shown in Figure 4. The pattern is typical for compound nouns like "computer system" or "street light".

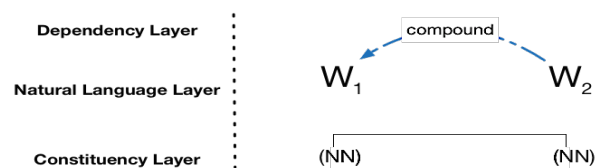


Figure 7. Pattern of  $rs_2$

The instruction for this rule will be the following:

$$i_2 := \text{Class}(\text{Computer-System}) \quad (3)$$

Now, when trying to apply these both rules  $rs_1$  and  $rs_2$  to a more complex sentence like "A computer system is a machine", we will see that none of them alone is able to cope with the more complex grammatical structure of the new text. Therefore, the Ontology Generator must be able to combine existing rules to more complex rules, based on the simple patterns discussed above. To handle the mentioned sentence, it is necessary to combine  $rs_1$  and  $rs_2$ , shown in Figure 8.

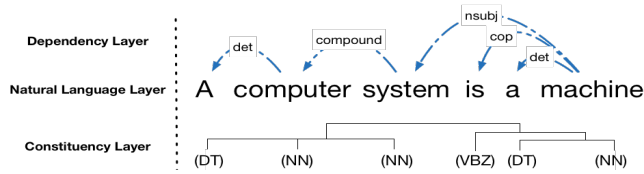


Figure 8. Joint pattern of  $rs_1$  and  $rs_2$

Now, the corresponding instruction  $i_3$  defines the first two nouns as a subclass of the second one:

$$i_3 := \text{SubClassOf}(\text{Computer-System}, \text{Machine}) \quad (4)$$

Hereby, the selection of several applicable rules follows the principle of speciality, according to which a more complex rule takes precedence over a combination of more simple ones. The described patterns exist currently just in hard-coded form, containing a handful of rules, to proof the concept. Later, numerous rules will be derivated by automated or semi-automated machine learning algorithms.

Our approach was implemented in an early stage system to prove the proposed concept (see Figure 2). Hereby, the system contains the sentence processing unit as well as the Ontology Generator with a hardcoded Rule-Set. The given Rule-Set is capable to find and connect entities consisting of two nouns as well as simple sentences containing a simple subject-verb-object combination (see Figure 6). We defined a simple test set containing 41 sentences, as shown in Figure 9, and tested it for a small hardcoded Rule-Set (about five Rules). A more complex scenario, such as mentioned by Li et al. [41], will be a future work. Here, the given sentences are typically stating one entity as a subclass of another entity or connecting two entities by a verb. Beside grammatically correct sentences, the set contains also a grammatically malformed sentence (see Figure 9, no. 41). The resulting OWL ontology graph is shown in Figure 10. It contains gathered classes, individuals as well as object properties. So, for example, the individual "Henry" belongs

- |  |   |   |
|--|---|---|
| 1. Ferraris are red cars.  | 15. A person is a human being.                    | 29. Tool development is a challenge.              |
| 2. A car is a vehicle.   | 16. A teacher is a person who teaches.            | 30. A cow is an animal.                           |
| 3. A truck is a vehicle.   | 17. Peter Miller is a teacher.                    | 31. A Ferrari is a fast and expensive sports car. |
| 4. If a person buys a thing, than this person becomes the owner. | 18. A bicycle is a vehicle.                       | 32. A coca-cola is a drink.                       |
| 5. Karl sells his washing machine.                               | 19. Henry is a professor.                         | 33. A vehicle is a transportation machine.        |
| 6. A machine is a device.  | 20. A professor is a kind of teacher.             | 34. A Porsche is a sports car from Germany.       |
| 7. A device is a thing.  | 21. A vehicle is a thing.                         | 35. A document is a thing.                        |
| 8. A washing machine is a machine.                               | 22. A Ferrari is a car and a vehicle.             | 36. A contract is a document.                     |
| 9. Fritz buys a washing machine.                                 | 23. Stuttgart is located in Germany.              | 37. A dog is an animal.                           |
| 10. A purchase agreement is a contract.                          | 24. Stuttgart is a city.                          | 38. Henry sells the bicycle.                      |
| 11. A student is a person.                                       | 25. A cabrio and a van are special types of cars. | 39. Peter Miller buys a bicycle.                  |
| 12. A computer is a device.                                      | 26. Germany is a country in Europe.               | 40. Peter Miller drives a truck.                  |
| 13. A coffee is a drink.   | 27. Europe is a continent.                        | 41. A continent is a big. (malformed)             |
| 14. A thing is a thing.  | 28. A person is a human.                          |   |

Figure 9. Example sentences

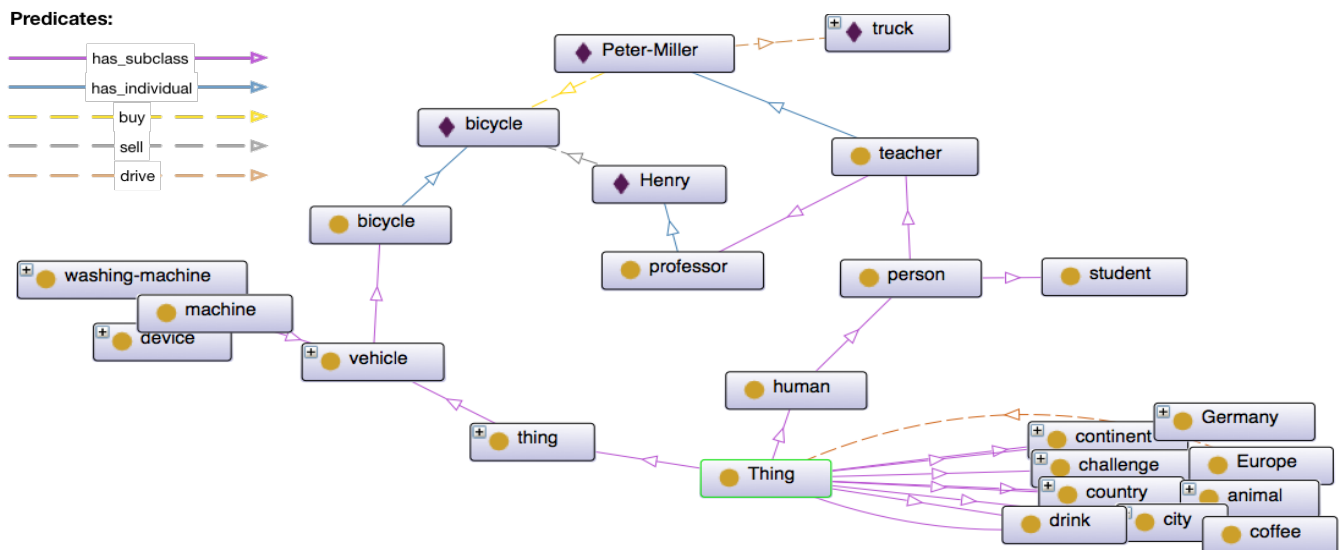


Figure 10. Resulting Ontology from the example sentences shown in Protégé [37]

to the Class "Professor". It has to be mentioned, that it is not mandatory to connect an individual just to one class. Basically an allocation to several other classes would be valid too, as long as there are no disjunctions between the chosen classes. The individual "Henry" could also be a "professor" and a "student" the same time. The given ontology shows every type of object predicate by the arrow's colour. Noticeable is the ability to distinguish between the ill-formed sentence no. 41, which is not represented in the ontology, and the well-formed ones, e.g., sentence no. 28 (see Figure 9).

#### D. Reasoner

The main task of the reasoner is the identification of connections between the given case and the law ontology. Therefore, the reasoner has to find a conclusive path through the OWL networks. The results of the Ontology Generator are, depending of the input source, three OWL ontologies (see Figure 5). The record information, like individuals and their actions, is represented in the use case ontology. Information about the laws is given in the law ontology, mainly as classes and SWRL Built-in Rules. The last ontology is the General Knowledge Ontology, which is extracted from wikidump files [33]. It bridges the missing links between the particular use case and the abstract rules from the law books through additional information. Beside the General Knowledge Ontology, the reasoner will also be connected to several already existing knowledge bases, which provide more additional information like lexical-semantic information from GermaNet [42] or OpenCyc [43]. With regards to the example shown in Section III, the following example shall illustrate the interaction.

If an individual named "bicycle" is given in the Use Case Ontology as well as a SWRL rule requiring an individual of the class "thing"; the General Knowledge Ontology contains necessary information about the hyperclasses of "bicycle". One of them is the hyperclass "thing". Therefore, the individual of the class "bicycle" can be used for a SWRL rule, which requires an individual of the class "thing".

When working with large amount of information by converting texts from natural language into an OWL model, it is likely to find an inconsistency. This circumstance is not only the result of potential mistakes in the information extraction process, but also inducted by contradictory statements in a text. The difficulty becomes obvious with regards to paragraph 90a of the German Civil Code [7]. It declares that animals are not things even though laws for things shall be applicable for animals as well. Therefore, the reasoning process will have to work with such types of inconsistencies. This problem could be solved by creating and solving two ontologies in parallel, where just one critical statement at a time is given. The result of this type of reasoning would not be a logical but a conclusive solution.

## VI. CONCLUSION

In this paper, we proposed a system for knowledge extraction and analysis from text presented in the domain of law. The system was demonstrated on a typical use case scenario from this domain. Furthermore, we showed how semantic ontologies can improve the information extraction and enable reasoning over the complex knowledge contained in the texts. As a proof-of-concept, a prototype of the analysis system was implemented, equipped with a hard coded rule set. The prototype was used to identify i) abstract concepts as OWL classes, ii) persons and specific entities as OWL individuals, and iii) verbs as OWL object properties correctly. The resulting ontology was tested with the Pellet reasoner [44] and further, the use of the presented approach for handling simple unstructured texts was performed successfully. The advantages of this system design are obvious; it benefits from its high degree of automation enabling the fast adaption to a constantly changing law system. In addition, the OWL ontology is reusable, once generated. Also, the system can be modified adapting to different countries and law systems. Future tasks will focus on several issues like implementing the reasoner and enhancing the presented approach by not only considering isolated sentences but extending the sentence analysis by broadening its scope and applying it on paragraphs as a whole and full texts. Hereby, interferences between sentences will be considered by implementing the Stanford Deterministic Coreference Resolution System [45]. In addition, the currently hard coded rule set will become a flexible more complex one containing a wide range of rules customized to the given context through adapting automated methods composed by making use of machine learning concepts and algorithms for generating tailor made rules. The current Rule-Set represents a small prototype, containing a small set of rules, to proof the concept. It will be the future task, to enlarge the Rule-Set, allowing the ontology generator to handle sentence complexities which are usual in natural language text. After the rule set is more complex, approximately several hundreds of rules, and flexible, a detailed evaluation, especially a precision and recall test like a F-score, will be done. Besides the full text analysis and the enhanced rule set generation the presented approach will be extended by taking into account external knowledge bases like OpenCyc [43] or GermaNet [42] for improving the general knowledge ontology and thus providing the reasoner with additional information regarding different languages and meaning of terms. Furthermore, the ontology has to be validated by a test set, which does not exist yet. The third challenge is how inevitably emerging logical inconsistencies shall be handled by the reasoner. It will be future work to address this challenge and to develop the algorithms to create a logical net of statements, definitions and connections in order to solve a simple case automatically.

## ACKNOWLEDGMENT

Authors would like to thank the consortium of the EU-ICT research project DreamCloud (Dynamic Resource Allocation in Embedded and High-Performance Computing) [46] as well as the EU-ICT research project JUNIPER (Java platform for hIgh PERformance and Real-time large scale data management) [47] for the support with the Java platform and first prototype of our software system development.

## REFERENCES

- [1] R. Schönhof, A. Tenschert, and A. Cheptsov, "Towards Legal Knowledge Representation System Leveraging RDF," The Eighth International Conference on Advances in Semantic Processing, pp. 13-16, Italy 2014, ISBN: 978-1-61208-355-1.
- [2] Statistic of the Bundestag, 09.04.2014, p. 5: [http://www.bundestag.de/blob/196202/860ee459a5e1d085fd796e376ef3bdd3/kapitel\\_10\\_01\\_statistik\\_zur\\_gesetzgebung-data.pdf](http://www.bundestag.de/blob/196202/860ee459a5e1d085fd796e376ef3bdd3/kapitel_10_01_statistik_zur_gesetzgebung-data.pdf) (retrieved: 06, 2014).
- [3] L. Mehl, "Automation in the Legal World from the Machine Processing of Legal Information to the "Law Machine"," Teddington Conference 1958.
- [4] G. Sartor, P.Casanovas, M. A. Biasiotti, and M. Fernández-Barrera, "Approches to Legal Ontologies," Springer Press, ISBN 978-94-007-0119-9.
- [5] About RDFS: [w3.org/TR/rdf-schema/](http://www.w3.org/TR/rdf-schema/) (retrieved: 08, 2015).
- [6] About OWL: <http://www.w3.org/TR/owl2-overview> (retrieved: 02, 2015).
- [7] N. Mussett, Federal Ministry of Justice and consumer protection Germany, "German Civil Code BGB," Date: 27.07.2011, published in: [http://www.gesetze-im-internet.de/englisch\\_bgb/](http://www.gesetze-im-internet.de/englisch_bgb/); Federal Ministry of Justice and consumer protection, Germany: <http://www.gesetze-im-internet.de/bgb/xml.zip> (retrieved: 06, 2014).
- [8] About UCC: [law.cornell.edu/ucc/2/](http://www.law.cornell.edu/ucc/2/) (retrieved: 08, 2015).
- [9] About Wikipedia: [wikipedia.de](http://www.wikipedia.de) (retrieved: 08, 2015).
- [10] P. Cimiano and J. Völker, "Text2Onto A Framework for Ontology Learning and Data-driven Change Discovery," Change Discovery, Institute AIFB, University of Karlsruhe 2005.
- [11] P. Velardi, S. Faralli, and R. Navigli, "OntoLearn Reloaded: A Graph-based Algorithm for Taxonomy Induction," Computer Linguistics, Vol. 39, No. 3, August 2013, pp. 665-707.
- [12] H. Davulcu, S. Vadrevu, and S. Nagarajan, "OntoMiner: Bootstrapping and Populating Ontologies From Domain Specific Web Sites," The First International Workshop on Semantic Web and Databases, 2003, pp. 24-33.
- [13] P. Buitelaar, D. Olejnik, and M. Sintek, "OntoLT: A Protégé Plug-In for Ontology Extraction from Text," International Semantic Web Conference (ISWC), 2003, pp. 31-44.
- [14] P. Buitelaar, D. Olejnik, and M. Sintek, "A Protégé Plug-In for Ontology Extraction from Text Based on Linguistic Analysis," First European Semantic Web Symposium (ESWS), Heraklion, Greece, May 2004.
- [15] P. G. Otero, "The Meaning of Syntactic Dependencies," Linguistik online, Vol. 35, Issue 3, 2008, ISSN 1615-3014.
- [16] Stanford NLP Tools: <http://nlp.stanford.edu/software/index.shtml> (retrieved: 02, 2015).
- [17] A. Carnie, "Syntax - A Generative Introduction," Third Edition, chapter 1 - 3, Published by Wiley-Blackwell 2013, ISBN 978-0-470-65531-3.
- [18] W. A. Woods, "Transition network grammars for natural language analysis," Communications of the ACM, Vol. 13, Issue 10, p. 591-602, Oct. 1970.
- [19] The Stanford Parser: <http://nlp.stanford.edu/software/lex-parser.shtml> (retrieved: 02, 2015).
- [20] M. P. Marcus, B. Santorini, and M. A. Marcinkiewict, "Building a Large Annotated Corpus of English: The Penn Treebank," Computational Linguistics - Special issue on using large corpora, Vol. 19, pp. 313-330, June 1993.
- [21] A. Bies, M. Ferguson, K. Katz, and R. MacIntyre, <http://www.sfs.uni-tuebingen.de/~dm/07/autumn/795.10/ptb-annotation-guide/root.html> (retrieved: 03, 2015).
- [22] The Stanford Dependency Parser: <http://nlp.stanford.edu/software/standoff-dependencies.shtml> (retrieved: 02, 2015).
- [23] H. M. Mueller, "Arbeitsbuch Linguistik," Second Edition, Published by Ferdinand Schoeningh 2009, ISBN 978-8252-21969-0.
- [24] About Dependencies: [http://nlp.stanford.edu/software/dependencies\\_manual.pdf](http://nlp.stanford.edu/software/dependencies_manual.pdf) (retrieved: 02, 2015).
- [25] L. Tesnière, "Eléments de syntaxe structurale," Librairie C. Klincksieck, Paris, 1959, Translation: U. Engel: L. Tesnière - "Grundzüge der strukturalen Syntax," Published by Klett-Cotta Stuttgart, 1980, ISBN 3-12-911790-3.
- [26] V. Ágel, "Valenztheorie," Published by Narr Tuebingen, 2009, ISBN 3-8233-4978-3.
- [27] About Stanford NER: [nlp.stanford.edu/software/CRF-NER.shtml](http://nlp.stanford.edu/software/CRF-NER.shtml).
- [28] About GATE/ANNIE: <https://gate.ac.uk/sale/tao/splitch6.html> (retrieved: 02, 2015).
- [29] About RDF: [www.w3.org/RDF/](http://www.w3.org/RDF/) (retrieved: 03, 2015).
- [30] About OWL: <http://www.w3.org/TR/owl-features> (retrieved: 02, 2015).
- [31] About SWRL: <http://www.w3.org/Submission/SWRL> (retrieved: 02, 2015).
- [32] R. Schönhof, A. Tenschert, and A. Cheptsov, "Information Extraction from Unstructured Texts by means of Syntactic Dependencies and Constituent Trees," The Ninth International Conference on Advances in Semantic Processing, France 2015, ISBN: 978-1-61208-420-6.
- [33] About Wiki Dumps: <https://dumps.wikimedia.org/backup-index.html> (retrieved: 02, 2015).
- [34] Law texts: [http://www.gesetze-im-internet.de/Teilliste\\_translations.html](http://www.gesetze-im-internet.de/Teilliste_translations.html) (retrieved: 02, 2015).
- [35] The Gate Project: <https://gate.ac.uk/> (retrieved: 06, 2014).
- [36] The OWLExpporter Project: <http://www.semanticsoftware.info/owlexporter> (retrieved: 06, 2014).
- [37] The Protégé Project: <http://protege.stanford.edu/> (retrieved: 06, 2014).
- [38] The OntoLT Project: <http://olp.dfki.de/OntoLT/OntoLT.htm> (retrieved: 12, 2015).
- [39] The Stanford POS Tagger: <http://nlp.stanford.edu/software/tagger.shtml> (retrieved: 06, 2014).
- [40] The Zurich Dependency Parser for German: <http://kitt.cl.uzh.ch/kitt/parzu/> (retrieved: 06, 2014).
- [41] T. Li, T. Balke, M. De Vos, K. Satoh, and J. A. Padget, "Detecting Conflicts in Legal Systems," Y. Motomura, A. Bulter, D. Bekki (Eds.), New Frontiers in Artificial Intelligence: JSAI-isAI 2012 Workshops, Revised Selected Papers, LNAI 7856, pp. 174 -- 189 (2013).
- [42] GermaNet Homepage: <http://www.sfs.uni-tuebingen.de/GermaNet/> (retrieved: 06, 2014).
- [43] Cycorp Homepage: <http://www.cyc.com/> (retrieved: 06, 2014).
- [44] About the Pellet Reasoner: <https://www.w3.org/2001/sw/wiki/Pellet> (retrieved: 12, 2015).
- [45] K. Raghunathan, H. Lee, S. Rangarajan, N. Chambers, M. Surdeanu, D. Jurafsky, and C. Manning, "A Multi-Pass Sieve for Coreference Resolution," EMNLP-2010, Boston, USA 2010.
- [46] About DreamCloud: <http://www.dreamcloud-project.org> (retrieved: 12, 2015).
- [47] About JUNIPER: [www.juniper-project.org](http://www.juniper-project.org) (retrieved: 12, 2015).

# Designing a Low-Cost Web-Controlled Mobile Robot for Ambient Assisted Living

Yvon Autret, David Espes, Jean Vareille and Philippe Le Parc

Université Européenne de Bretagne, France

Université de Brest

Laboratoire en Sciences et Techniques de l'Information (LabSTICC UMR CNRS 6285)

20 av. Victor Le Gorgeu, BP 809, F-29285 Brest, France

Email: {yvon.autret, david.espes, jean.vareille, philippe.le-parc}@univ-brest.fr

**Abstract**—In this paper, we focus on a Web-controlled mobile robot for home monitoring, in the context of Ambient Assisted Living. The key point is low-cost as dependent person have often tiny budget. The robot is built from standard components to reduce the cost of the hardware. A large part of the system is deported to the Internet to minimize the required software on the robot. Two low-cost positioning systems are also provided to make the robot more usable. The first one uses Received Signal Strength Indicators (RSSI), and the second one uses Infrared (IR) LEDs and an IR webcam. The result is a small robot that can be used inside or outside the house.

**Keywords**—Mobile robot; Home monitoring; Ambient Assisted Living; Web control; WebSocket; RSSI positioning; IR positioning.

## I. INTRODUCTION

This paper is an extension of [1] published in UBI-COMM2014. Web-controlled mobile devices are more and more used in ubiquitous environments [2][3][4][5]. Small monitoring robots such as the WowWee Rovio can be used [6]. Web control is not really new, but recent improvements of network performance has led to the emergence of Service Robotics [7]. Services Oriented Architectures (SOA) [8] start to be used to control physical devices [9].

Our aim is to use these approaches to control mobile home robots designed for Assisted Ambient Living (AAL) environments. For us, a typical application is helping elderly people who live in their houses and have sometimes some difficulties to move. A mobile home robot carrying a camera could help them monitoring their house either indoors or outdoors. The mobile home robot could also be used by care helpers or relatives, as a moving phone to communicate with the inhabitants of a house, or as a monitoring device.

In such an AAL environment, the total cost of the mobile home robot is the first key point. It must be kept as low as possible especially if it is an AAL environment for elderly people who often have tight budgets. This means that the mobile home robot must be built by using low-cost commercial components. Moreover, we always keep in mind that mechanical failures are unavoidable and reliability is a major key point. The basic mobile home robot design must be as simple as possible, while remaining flexible enough to carry sophisticated sensors.

The second main key point is software and network configurations. The mobile home robot should be plug and play. This means that software and network configurations should be reduced as much as possible. Deporting a part of the system to the Internet can be a solution if it helps to get a reliable plug and play system.

The third key point is security and access control. A Web-controlled mobile home robot can be used from anywhere in the world, but the interior of a house must not be seen by unauthorized users. It is necessary to avoid any intrusive access. More, in case of network failure, the mobile home robot should also be able to properly stop its current action and wait for a new order.

The fourth key point is the autonomy of the battery. The robot should have an autonomy close to one hour when moving, and automatically come back to a charging dock when the battery is low.

Another important aspect is the positioning of the mobile platform. Even if it is considered in this paper that the mobile home robot is remotely controlled all the time, i.e., not autonomous, having a rough idea of his position in the house could be helpful in several situations and could be used to improve user experience.

In this paper, the second section presents a mobile home robot solution based on a commercial low-cost robot and we discuss the advantages and the disadvantages. This lead us to the design of a mobile home robot built from commercial components such as a low-cost robotic platform and a smartphone to control it. In the third part, we present the distant control system and its performance. In the fourth part, we present two solutions for a low-cost positioning system, one using the Received Signal Strength Indicator, another using IR LEDs and cameras. The paper finishes by a conclusion and some perspectives.

## II. DESIGNING A HOME ROBOT FOR AN AAL ENVIRONMENT

The first question to tackle with, is the AAL environment. Are people we plan to help totally dependent, or do they only suffer of little dependency? Scales are available to estimate the degree of dependency of old people. One well known is the "Bristol Activities of Daily Living Scale" [10]. It is a 20-item survey, proposed to measure the ability to perform daily activities as preparing a meal. The score goes from 0 (independent) to 60 (totally dependent). Our objective is to provide robots for people having a rather small score, around 15 points. Plugging or disconnecting a device like a mobile phone, preparing alone a meal, feeding a pet, should be feasible tasks. We target people for whom one device more at home is not a huge problem.

The second question to tackle with, is the usages of the mobile home robot (use-cases):

- 1) The old or dependent person may use the robot to project themselves in their home. It means that with a simple terminal (tablet or mobile), they can control the robot to see what is happening in another room (or floor). For example, they can check whether a noise is normal or what their pet is doing.
- 2) The family or the carers could take the control of the robot to discuss with the old or dependent person
- 3) The family or the carers could also use the robot to verify some properties such as doors or windows are closed, gas is off and so on... These checks could be crucial in case of person suffering for example of light Alzheimer disease.
- 4) The family or the carers may also take the control in case of emergency to understand the situation very quickly and to be able to react in a proper manner.

In the next section, we will first describe the context of use, that we will briefly analyze, then we will list the requirements, and finally we will suggest several useful extended abilities.

#### A. Context of use and requirements

Basically the context of use is composed by a dependent person, the home, a telephone and an Internet connection, and the availability of electricity of course. Our purpose is to give services that contribute to the well being and can help, minimizing the modifications of the home.

Generally, dependent people living at home need a service of tele-assistance paid by subscription. This service is provided using a telephone basis, a wristband or a neck pendant. In case of emergency, for example, a fall of the dependent person, it is expected that he or she presses on the button of the worn accessory to call for help. The alarm is automatically relayed by a transmitter connected to the phone line, that calls the managing organization where someone reacts, questioning the dependent person in the aim to diagnose the problem. The usage of wireless transmission between the wristband or the pendant and the transmitter induces constraints like a maximal distance that could be reduced by the presence of obstacles or a difference of altitude. A one floor home without thick walls is preferred. This system is only used in case of emergency, although the phone line could be used for a wide range of new services, especially through Internet.

The classical services of tele-assistance are not usable to maintain the social links and to help the dependent person in a run-of-river manner. There are remaining problems like the localization of the person in case of problem, and the visual evaluation of its state.

Obviously, the presence of the telephone line permits a high rate access to Internet, using ADSL for example, at little extra cost. A second dedicated box for the ambient assistance could be connected to the first one, that would be able to offer extended wireless connectivity, like Bluetooth, ZigBee, IR, 3G/4G, etc. a storage space and the software for the data transmission and data processing. The issues are how to exploit this connectivity to solve the problems previously described, and what for devices and components are needed to insure the expected services. The social interactions are mainly performed in presence. The nowadays technologies allow the extension of the sense of presence, it means that for a lot of situations, a telepresence could be enough. The aim of such

telepresence is to introduce a mobile telepresence in the home "where you are and when you need it", rather than making actions in place of the people, because they are not totally dependent, and they need more conversations, advices and stimulations, than acting help. The mobility could be achieved at least through three ways: by a smartphone worn by the person, by a device carried by a mobile platform, or by devices installed in each room of the home. The first option is not suitable here because the smartphones are designed for valid people able to use one arm while they are walking. The third option avoids the problem of the discontinuous power supply of the devices, is reliable because the failure of one of the sensors implies only a partial disability of the services, but needs some work in the home, and is heavy intrusive. The second option needs no work in the home, is cheaper and less intrusive, but needs to recharge the mobile device, and is less reliable. So, we have chosen to develop of the second option. Nevertheless, the three options are not antinomic.

A low cost robot could be a device added to the emergency-calling service, less intrusive than fixed cameras. The audio and video streams should be secured, using https or a VPN.

The required properties are:

- the telepresence services should be available where the person is, and when requested,
- the telepresence services could be activated remotely,
- the sensors are carried by a mobile platform,
- the dependent person could decide to activate it or not,
- the recharging is not automatic,
- when empty, the mobile platform asks to be charged, that stimulates the person to perform this action,
- the autonomy is sufficient to need only one charge per day in normal use, two charges maximum,
- the device is highly maintainable,
- the hardware maintenance could be done by people with a moderate knowledge in robotics, like caregivers or daily visitors, e.g., postmen.
- a modular design that permits replacements of subsystems instead the standard exchange of the whole,
- the software maintenance and the reconfiguration could be made remotely.
- the life span of the mobile platform should reach the life span of a car (or a pet),
- the price should be small in comparison to the annual cost of the subscriptions (phone, emergency-calling service), and within the mean price of a smartphone (€300),

When activated:

- the system is able to listen and transmit the sound,
- the system is able to watch (day and night),
- the mobile platform is able to move over all the kind of floor,
- it is able to cross flat obstacles like carpets,
- it is able to follow the person,
- the maximum mass should be smaller than that of a walker ( $\leq 3$  kg).

The features of our proposal are: a size of two shoes, a mass of 1.15 kg, an autonomy depending on the traveling distance, at least 30 minutes but could be a day for a quiet usage. A low cost robot cannot carry heavy batteries, many computers and a lot of sensors. We prefer a modular approach with standard and cheap components easy to associate. Each component does not bring radical novelty, but the robot could offer new services, that will be the novelty. Currently, the robot is more a platform that permits development of services using the resources of the embedded systems and those of the servers and the clients. Maintaining the permanence of the services is a crucial issue that we propose to solve using a modular approach both for the hardware as well for the software. We would like to test the flexibility and the agility of the "applications store" model of use.

The question of the acceptability cannot be avoided. We do not target to give a great autonomous behavior to the robot, because if the robot would decide itself to move, it could disturb the people present and induce a thought as "someone is watching me without my authorization". The behaviors like those of a pet are also not targeted.

Beyond the possibilities mentioned above, several extended functionalities could be added. The computational power embedded could allow to implement learning algorithms, based for instance on reduced simulated neural networks. Many recent smartphones include a voice recognition, that uses neural networks. We could add a sound analyzer in real time that would listen to the breathing of the person for the detection of apneas, or would detect an intrusion. One of the most important improvement would be an accurate localization and positioning system. Such an ability would open the door to useful characterization of the environment inside the home, like tribo-analysis of the floor, liquid detection, obstacle detection and 3D modelization. Another usage would be the localization and observation of a pet.

In Section II-B, commercial home robots are described and evaluated, while in Section II-C an alternative proposal is presented.

### B. Commercial home robots

Several commercial robots are available. We present here a short description of four of them:

- The Miobot [11] robot is rather small (about 10 cm long) and fast (3.5 m/s). It has a built-in Bluetooth connection and must be connected to a local central computer to be web-controlled. Even if it was not really designed for that, it can carry a small camera or other sensors.
- Another interesting robot is the WowWee Rovio [6]. It includes a mobile base, a mobile camera and a Wi-Fi connection. Its size is 30 x 35 x 33 cm. It can be remotely controlled from anywhere in the world. When the battery is low, it is supposed to come back automatically to its charging dock. Its total cost is about €300, which is acceptable for our purpose. The WowWee Rovio is an interesting robot for an AAL environment, but it is not an open robot and it is difficult to add new features. In case of failure, the WowWee Rovio is also difficult to repair.

For example, such a common operation as replacing batteries, requires soldering.

- The Jibo social robot [12] should be available soon, may be by the end of 2015, and should cost about €500. It is about 28cm tall and 15cm wide. Its face consists of a touchscreen and interaction is possible by poking it. It is designed to recognize the faces of the family members. It cannot move but can be motor-driven through 360 degrees. Thus, it could be a very interesting robot to monitor, not a whole house, but a room.
- The Romo [13] robot uses a smartphone to control the motors. It can be remotely controlled from anywhere by using the smartphone connectivity. When used as a toy, it can perform autonomous missions. When controlled remotely, it provides an interesting telepresence functionality. The physical separation of the smartphone and the mechanical base makes it easy to repair. The mobile base costs about €130, but the price of a smartphone (minimum Iphone 4S - €250) should be added, which lead to a minimal total cost of €380.

We can now examine the previous robots to see if they are suitable. The first key point is the camera, which is essential. The second essential key point is web-control.

Another main key point is the cost. It is difficult to evaluate the maximal possible cost of a home robot. However, it can be seen that commercial robots about €300 can be sold. €500 robots can also be sold if they are very well designed and powerful. We think that we must remain cautious for more expensive robots. Thus, we will consider that a €300 robots remains acceptable in an AAL environment where people often have narrow budgets.

The selling price is not the only thing that must be taken into account. The robots may have breakdowns and repairing must remain cheap. This is difficult to achieve if the robot is not modular. More, the technology evolves and a robot may rapidly become out of age. For example, a given robot may become useless if a new positioning technology is discovered. We think that replacing the whole robot because one component has become obsolete is not a good solution. The robot should be easily upgraded at minimal cost. For example, if the mechanical base is still suitable, there is no reason to replace it. From our point of view, the lifetime should reach at least five or ten years.

Automatic battery charging is an interesting, but not essential key point. In an AAL environment we can guess that the robot will not be used continuously. It should be used a limited number of times every day, and each use should last minutes rather than hours. Above, we supposed that the person using the robot is able to plug the battery to recharge it. Charging batteries once a day should be sufficient, and performed by the inhabitants.

Positioning capabilities are also mentioned in Table I. Rovio gets a "yes/no" as it is designed to get back automatically to its base station, but it does not know where it is.

In Table I, we can see that some common commercial robots already take into account most of those key points except positioning. However, modularity is very weak. In the

TABLE I. Comparison of commercial low-cost robots

	Miabot	Rovio	Jiho	Romo
Camera	no	yes	yes	yes
Web control	no	yes	yes	yes
Price $\leq$ €300	N/A	yes	no	no
Ease to repair, modularity	no	no	no	yes
Automatic battery charging	no	yes	yes	no
Positioning	no	yes/no	no	no

next section we will focus on that point to propose a fully modular robot, based on a smartphone, a control module and a mechanical base.

### C. Using a smartphone, a control module, and a mechanical base

Using a smartphone as in [13], may help simplifying the building of a modular home robot. The smartphone is usually reliable and includes a webcam, Wi-Fi, Bluetooth and a touch screen. Wi-Fi will provide Web-control capabilities. Bluetooth will make it possible to control the mechanical base. The webcam is not perfect for our purpose. It consumes much power and highly reduces the autonomy. Thus, we prefer an additional, independent and external infrared webcam (IR). The whole system will be more modular without really increasing the total cost because a very cheap smartphone can be used to handle only Wi-Fi and Bluetooth. More, we will see later that an external IR camera is very useful to implement a positioning system. It also provides night vision.

The touch screen provided by the smartphone is an important part of the robot because it can provide information about the state of the robot. It is useless when everything is working. When something goes wrong, it is useful to show failures in a user interface. The touch screen will also be used to set the initial configuration (Wi-Fi, Bluetooth, and the distant server address).

An open mechanical robotic platform, which includes two tracks has been used. It is a 4WD Rover 5 from RobotBase. Its size is close to that of the WowWee Rovio. When powered, it can move forward or backward and turn. The maximum speed is 0.3 m/s. That speed is optimal in an AAL environment. It does not frighten inhabitants, and a standard room can be crossed in about 10 seconds. The Rover 5 is strong enough to carry up to two kilograms.

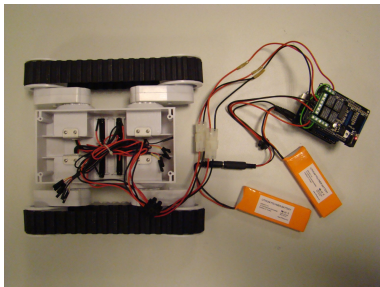


Figure 1. Components of the Web-controlled home robot.

Our control module is based on an Arduino micro-controller [14] that controls the mechanical base and communicates with the smartphone. Several Arduino shields are available to monitor the working speed and direction of the motors. We can use either a relay shield including four relays, or a motor shield based on a voltage regulator such as 78M05. An additional Arduino shield is required to allow Bluetooth communication between the Arduino and the smartphone.

The main advantage of our solution is its modularity. The home robot only includes commercial components (see Fig. 1, Fig. 2 and Fig. 3):

- A mobile Rover 5 robot used as a mechanical base (€60)
- An Android smartphone (less than €80)
- An IR Wi-Fi webcam (about €50)
- A control module including an Arduino UNO (€20), a Bluetooth shield (€10), a XBee shield (€15), and a motor command shield (€20)
- Batteries (one for the Arduino, one for the webcam, and one for the motors, 3x€15)

The control module is not yet a commercial component. Here, it is built by using commercial components that could be easily integrated on a single board. As soon as it would be done, the control module would be much cheaper, and the robot could easily be built and repaired at home. Building the robot would correspond to connecting the control module to the mechanical base, and to putting over a smartphone and a Wi-Fi webcam. This can be easily achieved if the mechanical base includes a plastic shell, plugs for the control module, and places to put the smartphone and the webcam. When a component fails, it can be easily replaced at home without replacing the whole robot. In an AAL environment, that task could be performed by caregivers.

Prices given are public prices that includes prices of the product itself but also commercial margin from the resellers. They are given here to fix ideas, but in the case of a mass production, the total cost will be lower. More we can also use an old smartphone, which has become useless or a recycled one.

The current total cost (€300), smartphone included, is comparable to that of a WowWee Rovio although our robot is a prototype. The reliability of our mobile home robot is significantly higher than that of a Rovio. In case of failure, we only need to replace one component. Moreover, the diagnosis is very easy because each component can be individually tested.

When using 2000 mAh lithium batteries, we have a 30 min autonomy when the robot is continuously moving. We have several hours of battery life when the robot is waiting for commands. Automatic battery charging is not available on our prototype, because the lack of localization procedures makes it difficult to achieve.

Apart this last point, we consider that our proposal respects constraints described above. The next part of this paper will concentrate more on software aspects.

### III. A DISTANT CONTROL SYSTEM

We propose to use a Web server to reduce home configurations and installations. The Web server will be used to control

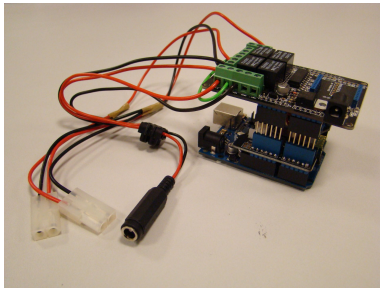


Figure 2. The Arduino command module.

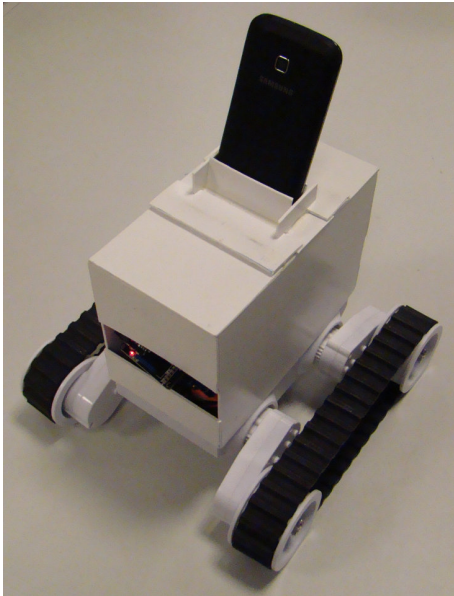


Figure 3. The Web-controlled home robot.

the robot. A user interface running on a standard Web Browser should make the robot usable without any special installation.

Using Hypertext Transfer Protocol (HTTP) is a solution to communicate with a distant server. Efficient HTTP Web servers such as Apache or Apache Tomcat are available. If the standard HTTP protocol easily handles problems such as client identification, it has severe limits when used for near real-time monitoring.

#### A. The HTTP limitations

The HTTP protocol is a stateless protocol, which was originally designed to get access to static HTML pages. Later, some web applications have implemented server-side sessions by using HTTP cookies. A Web server implementing sessions receives an HTTP request, establishes a connection with the server, executes the request, sends an HTTP response back, may keep a track of the HTTP request, and finally, releases the connection.

If a Web server is running on the robot, an identification sequence, which gives the right to monitor the robot through the Web server can be easily implemented. The communication can be secured by using the HTTPS protocol. The main problem is the execution time of a command sent to the robot.

Let us take the example of an HTTP request, which should make the robot move for several seconds. As soon as the HTTP request is received on the server, the robot starts moving. If the robot moves for more than a few seconds, the HTTP response must be sent back before the robot has finished moving. In this case, the robot can get out of control.

This is a major problem because we must monitor a robot by using commands whose execution lasts about one second. A one meter trip would require sending at least three commands to a Rover 5 moving at 1km/h. Touring a house would require hundreds of commands. When a command is sent to a distant robot, a permanent connection is required. A moving robot left unsupervised just a few seconds can be dangerous. Presence and obstacle detectors working on the robot are never 100% reliable. This means that anyone who is monitoring from the outside or inside the house must have a permanent full control of the robot through the network. Moreover, the robot should be able to detect the smallest network failure, and to automatically adapt its behavior, for example, by reducing its speed.

This means that sending HTTP requests to a Web server running on the robot is not a good solution. We must continuously send HTTP requests to the robot to be able to detect network failures. That is a misuse of HTTP. Second, establishing a new connection from outside can be time consuming and sometimes takes several seconds. That is a risk we can not take. That is why we have chosen the WebSocket solution.

#### B. Using a WebSocket server

The WebSocket protocol was standardized in 2011 [15]. The communications are established by HTTP servers, and the communications may use TCP port 80 (or 443 when using secured communications). The client is responsible for making the connection by using an URL, consisting of a protocol, host, port, path, and optionally one or more additional parameters.

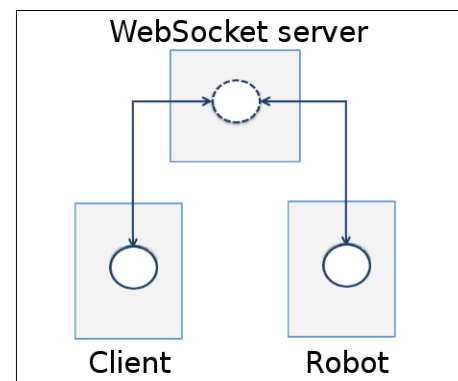


Figure 4. The WebSocket servlet.

The main advantage of WebSockets for our purpose is the fast responses coming from the server. That is due to the single connection that is established at the beginning of the communication. As soon as a connection is set, a bi-directional communication remains available. Full duplex communication over a single socket allows near real-time communication.

A standard Web browser can be used to monitor a robot through WebSockets. Most Web browsers now support WebSockets. Both the client and the robot send and receive

information to and from the Web server through WebSockets. When a command is sent from the client to the Web server by using WebSockets, as soon as it is received on the server, it can be forwarded to the robot and executed. During the execution of the command on the robot, WebSockets are still used to send periodic acknowledges from the robot to the client, and from the client to the robot.

Thus, if the robot does not receive any acknowledgment, or receive them too late, it can modify its state. For example, it can reduce its speed if the network is too slow. If the network is no more working, the robot can stop properly, and remain waiting until the network is working again.

### C. A WebSocket server

A WebSocket server greatly simplifies the installation of a Web-controlled home robot. The home robot just have to connect to the WebSocket server (Fig. 4). This does not require any special home configuration. An ordinary Wi-Fi connection can be used.

The well known Apache Tomcat Webserver now implements WebSockets. This means that we can use both the advantages of a standard Web server and those of WebSockets. A standard Tomcat application manages client and robot identification. The client uses an HTML form to ask for a robot. As soon as identification is successful on the server, a WebSocket communication becomes available between the client and the robot.

On the Tomcat server, we have a servlet to manage identification and robot allocation. We have also a WebSocketServlet to manage communication between the client and the robot.

The "manager" object is instantiated by the WebSocket server. From the robot point of view, it contains information about the client that is using the robot. From the client point of view, it contains information about the robot to control. The manager is stored as a Tomcat session object. It is a persistent object whose life duration is that of a session. A "manager" object is instantiated during the identification phase, when the client asks for a robot. Another "manager" object is instantiated when the robot connects to the WebSocket server. When the WebSocket communications are set, the "manager" objects can be retrieved and modified to help clients and robots communicate. One client is allowed to send messages to one robot, and one robot is allowed to send messages to one client.

Both the client and the robot exchange messages by sending lines of text. For example, the client sends a line containing "forward" to make the robot move forward. Parameters can also be added in the line, for example to make the robot move forward for n seconds.

### D. WebSockets on the robot

As seen above, the robot is controlled by the Arduino and the Arduino is controlled by an Android smartphone using a Bluetooth communication. We use the Tyrus API to connect the smartphone to the WebSocket server.

We use the Tyrus "ClientManager" class to set a connection between the robot and the WebSocket server. When messages come from the client, the "onMessage" method is triggered. The message is decoded and forwarded to the Arduino. During the execution of the command by the Arduino, the client and the smartphone periodically exchange messages to stop or slow

down the robot in case of network failure. This program has been tested on Android 2.3 and Android 4.

### E. WebSockets on the client

A WebSocket connection from the client to the server is only possible if the identification phase and robot selection has been successful. This is taken into account by the standard Apache Tomcat Webserver. As soon as a client is successfully registered on the distant Web server, a WebSocket connection is established. The client uses a Web page as user interface. The only thing required to use the user interface is a WebSocket compatible Browser. The user interface is managed by the distant Web server.

The Javascript "onMessage" function is triggered when a message comes from the WebSocket server. A widget such as a button in the user interface can trigger the "sendMessage" function and send commands to the robot.

### F. Performance

In this section, we present an experimentation that illustrate the usability of our system and we justify our technological choices in term of communication medium.

For the experimentation, the server is connected to the local network of the laboratory, i.e., a gigabit Ethernet network. It is hosted to a public address so any user are able to access it from anywhere using just a web browser. Beside the server, one robot is available. The robot is equipped with an Arduino board, a Bluetooth shield and a smartphone. The Bluetooth shield is fully qualified to respect the Bluetooth version 2.0. Hence, the data rate is up to 2 Mbps. The smartphone is connected to the local network through a Wi-Fi connection. The Wi-Fi card on the smartphone is compliant to the IEEE 802.11g standard. Hence, the data rate is up to 54 Mbps.

In order to show the performance of the system, we define the following performance metrics:

- the *Round-trip time between components* is the time to receive a response after sending a request without counting the delay due to other components. For example, if the Arduino board sends a request to the smartphone, the round-trip time between these both components is the delay to receive a response without counting the delays imposed by smartphone-server connection and server-user connection.
- the *End-to-end round-trip time* corresponds to the time needed to receive a response after sending a request, i.e., it is the sum of the round-trip time between the whole components of the system. The increase of the end-to-end round-trip time degrades significantly the Quality of Service of applications and the Quality of Experiment of users.

Tests have been conducted from two different locations: our laboratory (i.e., LAN access) and the Military Technical Academy of Bucharest in Romania, i.e., Internet access, located about 2500 km from the laboratory. In both cases, the server is inside our laboratory. However, due to the flexibility of our architecture, the server could be hosted in the cloud. Each 30 minutes during one week, the round-trip time between components and the end-to-end round-trip time are measured. All the results represent the average of the measured

TABLE II. END-TO-END ROUND-TRIP TIME

Protocol	End-to-end round-trip time	
	Local (inside laboratory)	Distant (Romania)
HTTP	600 ms ( $\pm 120$ ms)	730 ms ( $\pm 100$ ms)
Web Sockets	175 ms ( $\pm 60$ ms)	190 ms ( $\pm 50$ ms)

times  $\pm$  standard deviation. All times are expressed once the WebSocket connection is established.

In Table II, the end-to-end round-trip time is analyzed under two protocols (HTTP and WebSocket). The end-to-end round-trip time is an important parameter because it is the main criteria to determine if near real-time control is possible. To control a distant robot with an acceptable quality of experience, it is commonly accepted that the delay never exceeds 400 milliseconds [18]. We can see the HTTP protocol cannot guarantee the delay bound. Indeed, the time to establish the connection, to send a request and receive a response significantly exceeds the delay bound. In case a system requires the establishment of a TCP connection for each transaction, the near real-time control of the mobile robot is not possible. The WebSocket protocol is more suitable for near real-time control. Being designed to work well in the Web infrastructure, the protocol specifies that the WebSocket connection starts its life as a HTTP connection, offering backwards compatibility with no-WebSocket systems. The handshake of the WebSocket protocol has slightly the same time than the HTTP protocol. Once the connection is established, control frames are periodically sent to maintain the connection. Hence, the time is significantly reduced as compared with the HTTP protocol. For all scenarios, the end-to-end round-trip time does not exceed 300 milliseconds, which is quite acceptable to transmit QoS traffic.

TABLE III. ROUND-TRIP TIME RELATED TO ENTITY CONNECTIONS

Entity connection	Round-trip time	
	Local (inside laboratory)	Distant (Romania)
User - Server (Internet)	15 ms ( $\pm 5$ ms)	40 ms ( $\pm 5$ ms)
Server - Phone (Wi-Fi)	35 ms ( $\pm 10$ ms)	35 ms ( $\pm 10$ ms)
Phone - Robot (Bluetooth)	125 ms ( $\pm 40$ ms)	125 ms ( $\pm 40$ ms)

Table III presents the round-trip time related to robot's component inter-connections. It is interesting to see that the Internet delay, i.e., when the user is located in Romania, is almost negligible as compared with local access. Moreover, half of the Internet delay is due to the propagation time (if we assume a propagation speed of 200,000 km/s that is the common phase velocity of light in optical fibers). Nowadays, first-tier operators have 100 Gbps networks. In backbone networks, the bandwidth is so high that the transmission time of a packet is negligible.

To ensure near real-time communications, engineers have to be aware of the impact local access networks can have on the end-to-end delay. The round-trip time between both components change a lot according to the local access technology. The data rate of the Bluetooth shield is quite low (2 Mbps) in comparison to the data rate of the Wi-Fi card (54 Mbps). The time to transmit the data from the robot to the phone, or inversely, is proportional to the data rate. This is the principal factor to these delays. Moreover, Bluetooth and Wi-Fi systems are contention based systems. Bluetooth systems are based on a combination of frequency-hopping and CSMA/CA (Carrier Sense Multiple Access with Collision Avoidance) [16] methods to access to the medium. Wi-Fi systems are based on the CSMA/CA method to access to the medium. Whatever the system used, i.e., Wi-Fi or Bluetooth, the medium is shared between all the nodes belonging to the same system and other systems. The delay to access to a free medium or the retransmissions due to collisions increase the round-trip time significantly.

Connection between the phone and the server use Wi-Fi technology, as the range of Bluetooth devices is too short to allow connectivity inside a house. Unlike the connection phone-server, we have the choice between two wireless technologies (Wi-Fi and Bluetooth) to connect the phone to the robot. The choice between these technologies depends on energy consumption and response time. In order to reduce energy consumption, the use of a Bluetooth connection between the smartphone and the robot is interesting due to its low consumption. The mobile robot's operational time is limited before exhausting its battery power. Indeed, Bluetooth is much more power efficient than Wi-Fi. As mentioned by Pering et al. [17], the power consumption of Bluetooth is 10 times lower than Wi-Fi. In order to reduce response time, the use of a Wi-Fi connection between the smartphone and the robot is a more suitable solution for soft real-time systems that have relative short delay constraints. In general, the system must balance the conflicting goals of maximizing the response time and minimizing the energy consumption. To achieve these goals, the system could use the Wi-Fi card to send short delay-constrained commands to the robot and Bluetooth connection to send no delay-constrained commands.

Last versions of Bluetooth systems could also be used, as they include two specific modes of communication: Bluetooth High-Speed (BHS) and Bluetooth Low Energy (BLE). BHS is based on Wi-Fi protocol. BLE has a very low power consumption. They seem to be very good candidates for mobile near real-time systems. Due to the proposed modes of communication, near real-time applications can easily use a fast communication for short delay-constrained commands and a very low power consumption mode for no delay-constrained commands. Unfortunately, Bluetooth shields proposed by Arduino are not yet compliant with last versions of the Bluetooth protocol and do not include these features.

As we mentioned before and to provide a good user experience, the end-to-end delay is bounded at 300 ms. In our context, the use of a Bluetooth connection between the phone and the robot is the more suitable solution. Indeed, the end-to-end delay never exceeds the threshold and the energy consumption is reduced to its minimum.

#### IV. THE LOW-COST POSITIONING SYSTEM

After an introduction to positioning, we will describe the two selected positioning systems.

##### A. Introduction

The purpose of our robot, as stated in Section I, is to be used either by the dependent person or by a remote carer. Displacements inside the house may be conducted while using the video signal coming from the camera of the smartphone. Nevertheless, providing a Web interface containing a map of the house and offering the ability to choose a destination, only by a click, will be an important improvement to the users.

A localization system has then to be added on the robot, or to be developed using already embedded equipment on the robot. It should be efficient and low cost, to keep the philosophy of our approach. As the GPS system can not be used indoor, as few off the shelves solutions exist, several alternative technologies have been studied: ultrasound, cameras, infrared, Radio Frequency Identification (RFID), ZigBee, or Ultra-wideband (UWB). Some of these solutions and more are described in [19]. We do not investigate SLAM solutions [20] as our aim is not to build the environment of the robot and these solutions need lots of computations and are often based on multi-sensing.

Ultra-wideband seems to be promising, but it is still too expensive for a low-cost system. The accuracy can be better than 10cm [21].

RFID also gives an accuracy of several centimeters. As it works with an antenna checking for either active transceivers or passive tags, it is difficult to use it. Too many passive tags should be installed inside the house. In our case, a RFID positioning system could not be used as a main positioning system. It could be used to improve another positioning system.

Positioning with Ultrasound is not recommended in houses because animals can be sensitive to it.

Thus, only three main technologies remain usable for our purpose: ZigBee, cameras or infrared.

- ZigBee: The IEEE 802.15.4 standard can be used to locate a mobile device in a house. The most used method consists of using the Received Signal Strength Indicators (RSSI). That information is provided by the network and is easy to extract.
- Cameras: An optical camera can be used as a unique sensor for positioning. If the camera is on the robot, only one is required and we can expect reduce the total cost. More, there is no need for additional infrastructure.

The main problem is to analyse an image taken by the camera. Objects such as doors and windows can be detected and matched with a database containing a 3D description of a room [22]. The main difficulty will be the building of the 3D model of the house. A second approach consists of taking photos in the house, and let the system compare them to the image taken by the camera on the robot. Those approaches only rely on features of a room at one time. The recognition may easily produce errors as soon as something changes in the room, for example, the light, or the position of

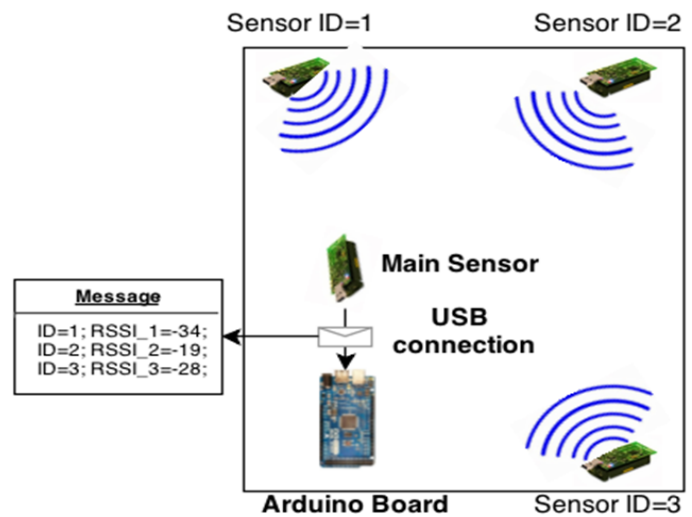


Figure 5. The positioning system.

a chair. Specific markers such as patterns or barcodes can be used in a room to improve recognition [23]. A compromise must be found between a large pattern easy to recognize, and small patterns almost invisible in the house.

Cheap cameras are available but image recognition seems to be impossible in a low-cost system.

- Infrared: Infrared light is invisible to the human eye. In a house, an infrared beacon is less intrusive than patterns such as barcodes seen above. A single IR beacon in a room may achieve room localization because IR signals do not cross walls. For meter-precision in a room, several techniques are under development. For example, cameras can be used.

In the following, we will focus on two positioning solutions. The first one will use ZigBee. The second one will use cheap IR cameras and IR emitters adapted to our problem. Our aim is to experiment well-known solutions in order to make the best proposal, fitting our requirements.

##### B. A positioning system using the Received Signal Strength Indicator (RSSI)

We designed a low-cost localization platform for 2D-positioning.

Let us assume the robot only has to monitor flat floor, i.e., the relative z-coordinate is always constant. In cases where different floors have to be monitored, a robot may be on each floor. They can communicate between them in order to extend the control in the whole habitation.

The positioning system involves 4 TelosB wireless devices. The 3 auxiliary sensors have a fixed position, being installed in strategic places of the room, in the corners for example. The places must be chosen in such way that the robot, which will have the Main Sensor attached to be in permanent Line of Sight with this sensors. This way, the communication would be done with very little interference.

Fig. 5 shows the whole system and the interaction between the components. Auxiliary sensors send messages periodically.

The main sensor do not know their position. After receiving a message from an auxiliary sensor, it gather information, such as receiver's Received Signal Strength Indicator (RSSI) and the identity of the sender. In order to optimize the energy consumption, the processing of the RSSI values is skipped in this moment, being the duty of the server application to make the necessary computations from which will result the distance approximation. Once the Main Sensor acquires a message from each of the 3 fixed sensors, it will create a data packet, which contains the 3 pairs of ID - RSSI value for each sender, and will send it through the USB interface to the Arduino board. The Arduino board forwards this message to the server that converts the raw values into physical distance, measured in meters. At this point, the server knows the distance between the main sensor and each auxiliary sensor.

In two-dimensional geometry, the trilateration technique uses three reference nodes to calculate the position of the target node. To be localized the target node should locate at the intersection of three spheres centered at each reference position. When the signal received from the reference nodes is noisy, the system is non-linear and cannot be solved. An estimation method has to be used. To get a satisfying approximation position of the mobile robot, we use the Newton-Raphson method [24]. This method attempts to find a solution in the non-linear least squares sense. The Newton-Raphson' main idea is to use multiple iterations to find a final position based on an initial guess (for example, the center of the room), that would fit into a specific margin of error.

The first results of our experiments show that RSSI values are not constant due to multipath components. Hence, the precision of our system is about 2 meters. Such a precision is sufficient to know the room where the robot is, but is insufficient to have a precise position. Our results fit with the results presented in [25]

This lack of precision leads us to propose another solution using both IR light and infrared camera.

### C. The Infrared positioning system

In the previous section, we described a well known RSSI positioning system that can tell a distant user, which room the robot is closed to, but not where is the robot in a specific room. It is an interesting information, but far from perfect. More, it significantly increases the cost. A commercial sensor costs about €80. To achieve 2D-positioning, three sensors are required. Due to the range of a sensor, i.e., 10-20 meters, the cost of the positioning system is related to the size of the house. That positioning system must be considered as optional if the cost is critical.

By only using the video sent by the robot, controlling the distant robot is a difficult task. For example, if the video shows a wall, it is often impossible to say which wall it is. If the video shows a door, it is easy to recognize a door, but often impossible to say which door it is. We need a reliable system to help the distant user.

We have been working on an Ultra-wideband system (UWB) [21]. The precision can reach two centimeters. Unfortunately, UWB transceivers are very expensive (about €400 each).

Instead, we propose to hook IR LEDs at known positions on walls of a house, and to use an infrared camera laid on the

robot to detect them, thus providing positioning. In the next sub-sections, we will show how to get a reliable detection of IR LEDs.

1) *The IR LED*: The first problem is to find an IR LED, which can be detected by using a low-cost IR camera, which produces 320x240 pixels images. A standard IR LED such as that shown in Fig. 6 is difficult to detect: when illuminating the camera from a distance of two meters, it appears on the image as a single pixel, which is almost impossible to find. To ensure that the IR beam will be visible on the image, one solution consists of using a more powerful IR LED, and concentrating the IR beam by adding a lens in front of the IR LED.



Figure 6. The standard IR LED.

We use a Mentor IR LED [26]. A 10mm lens is inserted in front of the LED, and encapsulated in a metal housing (Fig. 7). It costs about €8. The IR LED is visible in a 90 degree angle, up to several meters. If the IR LED is 2m from the camera in an angle of 30 degrees from the IR beam, we get a 5x5 pixels white rounded square on the image (Fig. 8). If the angle is close to zero, the camera is strongly illuminated and we get a 12x12 pixels white rounded square (Fig. 11).



Figure 7. The IR LED with lens.

2) *Detecting an IR LED*: An IR LED can be detected on the image up to 4m and within a 45 degree angle from the IR beam. The main problem is the image analysis. We must detect a white point in the image. The proposed solution uses XBee modules.

The IR LED is controlled by an Arduino connected to an XBee module. The whole IR LED module (Arduino, XBee and IR LED) is hooked somewhere.

As seen above, the control module on the robot includes and Arduino and an XBee module. Thus, communication is possible from the robot to the IR LED module. The robot is able to switch the IR LED ON and OFF. If the robot position must be obtained, the robot executes the following actions:

- Switch the IR LED ON, by using the XBee module to send the command
- Take a first photo
- Switch the IR LED OFF, by using the XBee module to send the command
- Take a second photo
- Compare the two images to detect the IR LED

The comparison of the two images gives the position of the LED on the image. We only have to find in the first image a group of white pixels that is absent in the second image. From the position of that group of white pixels (x, y), we can obtain an estimation of the direction of the robot (given by the x coordinate), and the distance from the wall (given by the y-coordinate).

This method is reliable under two conditions: the robot has been stopped, and nothing is moving in front of the webcam. If something is moving, the two images will be much more difficult to compare and the result not reliable.

From our point, that limitation is not a problem. The only working way to control a distant robot in a house is to make it move by steps of about one meter. A robot moving continuously is much more frightening for the inhabitants. After each step, the robot must be stopped for a short period of time, and the situation must be evaluated before the next step. As soon as the robot has been stopped, the control system on the robot can estimate the position, and send it to the distant user who can see the position and the direction of the robot. In fact, we do not obtain a precise position, but an area in which the robot is. That information is shown on a map on the user interface. By using the additional video sent by the robot, the distant user can easily guess an exact position of the robot. A simple click on the displayed map allows the distant user to give to the control system, both the exact position of the robot and the next target position.

If something or somebody is moving in front of the webcam, it is also not a problem. The robot is not an autonomous one, and when the distant user sees that something or somebody is moving in the house, the distant user should stop the robot, analyze the situation, and make sure a collision is not closed.

If there are several IR LEDs in the house, they must be numbered in such a way that the robot control system can switch them ON and OFF individually. Only one IR LED can be ON at a given time.

3) *A positioning solution by using individual IR LEDs:* Each IR LED module, including an Arduino and an XBee module, costs about 40 € when it is built by unit. Even if mass production of those modules could reduce the cost to €10 or €20, installing such devices in a whole house could be considered as too expensive.

One IR LED hooked near the door in each room, and another IR LED on the opposite wall seems to be a good compromise. At a given time, the robot control system would only have to check for only two IR LEDs. That takes about one second.

In the next sub-section, we will show a more precise positioning system, but requiring twice more LEDs.

4) *A positioning solution by using sets of two IR LEDs:* If two LEDs are hooked on a wall, the camera carried by the robot will detect two white spots on the image. The two white points will form a horizontal line if the camera is deflected towards the center of top of the door (Figs. 8 and 9).

If the camera is not deflected towards the door, but towards a point left or right to the door, the line passing through the white points on the image will be inclined (Fig. 10).

The robot position can be obtained from two white points on the image. The distance between the points gives the



Figure 8. Two IR LED on top of a door.



Figure 9. The line joining the IR LED.

distance from the LEDs. The inclination of the line passing by the two points gives the angle of vision. In fact, we measure both the horizontal and the vertical distance between the points. We directly obtained a position from those two measures. We get the distance from the wall, and the distance from a plane orthogonal to the wall and passing through a point located between the diodes.



Figure 10. The IR LED seen from aside and the line joining the IR LEDs.

The direction of the robot is obtained by comparing the center of the image to the segment center joining the two white points. the x-axis. The (0,0,0) point is on the floor, between the two IR LEDs. Doors are often 210 cm high and about 100cm wide. The camera is at a height of 40cm. The IR LED

#1 coordinates are (50,0,210), and those of IR LED #2 are (-50,0,210).



Figure 11. The IR LED, maximum illuminating.

Both on the x-axis and y-axis, one pixel image is about 2cm in the coordinate system. Thus, we can easily achieve a 10cm precision and there is no need to have a greater precision for our purpose. However, some objects may hide the IR LEDs. In this case, several sets of two IR LEDs are required on several walls.

The use of IR camera makes it possible to locate rather precisely the mobile robot, but the cost remains a question.

## V. CONCLUSION AND FUTURE WORK

The aim of this paper was to present a mobile home robot that could be helpful for old and/or dependent person. Proposing a low cost solution, using high tech components, promoting simplicity were some of the key ideas that conducted this project. We started by comparing different "off the shelves" solutions, but in our opinion, they are difficult to maintain. We chose to have a components based approach in order to improve the maintainability of our solution. We also explain the software architecture of our distant control system. As positioning could also be helpful in some circumstances, we presented 2 different low cost solutions.

In this paper, we proposed no new technologies, neither for mobile robot platform, the remote control, nor for positioning. But, we tried to show that if the right technologies are chosen, a mobile robot platform can be built and used with the respect of good properties for AAL. Our aim was clearly not to build an autonomous robot assistant, but a robotic platform that can be helpful in several cases for the old and dependent person, the relatives and the carers.

The next step will be to propose this mobile robot platform to selected users in order to get feedback and to improve all aspects of the prototype. On the hardware part, the integration of all the component of the remote control part will be a great improvement. On the software part, the development of specific applications will make it possible to propose more usages. We also want to take advantage of the good properties of cloud computing in order to provide more reliability and more flexibility. Another important objective will be to work on the interaction between the robot and all the connected objects that may be installed at home.

## REFERENCES

- [1] D. Espes, Y. Autret, J. Vareille, and P. Le Parc, "Designing a Low-Cost Web-Controlled Mobile Robot for Home Monitoring," IARIA UBICOMM 2014, The Eighth International Conference on Mobile Ubiquitous Computing, Systems, Services and Technologies, 2014, Rome, Italy, pp. 178–183.
- [2] A. Chibani, Y. Amirat, S. Mohammed, E. Matson, N. Hagita, and M. Barreto, "Ubiquitous robotics: Recent challenges and future trends," Robotics and Autonomous Systems, Volume 61, Issue 11, November 2013, pp. 1162–1172, ISSN: 0921-8890.
- [3] S. Nurmaini, "Robotics Current Issues and Trends," Computer Engineering and Applications, Vol. 2-1, March 2013, pp. 119–122, ISSN: 2252-4274.
- [4] A. Touil, J. Vareille, F. L'Herminier, and P. Le Parc, "Modeling and Analysing Ubiquitous Systems Using MDE Approach," The Fourth International Conference on Mobile Ubiquitous Computing, Systems, Services and Technologies, Florence, Italy, October 2010.
- [5] P. Le Parc, J. Vareille, and L. Marce, "Web remote control of machine-tools the whole world within less than one half-second," International Symposium on Robotics, ISR 2004, Paris, France, March 2004.
- [6] "WowWee Rovio, a Wi-Fi enabled mobile webcam," 2015, URL: [https://en.wikipedia.org/wiki/Rovio\\_\(robot\)](https://en.wikipedia.org/wiki/Rovio_(robot)) [accessed: 2015-11-20].
- [7] "Robots With Their Heads in the Clouds," IEEE Spectrum, March 2011.
- [8] "Service-Oriented Architecture (SOA) and Cloud Computing," 2015, URL: <http://www.service-architecture.com/articles/cloud-computing/> [accessed: 2015-11-20].
- [9] Y. Chen, Z. Du, and M. Garcia-Acosta, "Fifth IEEE International Symposium on Service Oriented System Engineering," Journal of Something, Nanjing, China, June 2010, pp. 151–158.
- [10] R.S. . Bucks, D.L. Ashworth, G.K. Wilcock, and K. Siegfried, "Assessment of activities of daily living in dementia: development of the Bristol Activities of Daily Living Scale," Age and Ageing, 1996, pp. 113–120.
- [11] "Introduction to the Miabots & Robot Soccer," 2015, URL: [http://eprints2.utm.edu.my/5831/1/Merlin\\_Miabot\\_Pro\\_Robot\\_Soccer\\_\(2\\_Wheels\)\\_24\\_Pages.pdf](http://eprints2.utm.edu.my/5831/1/Merlin_Miabot_Pro_Robot_Soccer_(2_Wheels)_24_Pages.pdf) [accessed: 2015-11-20].
- [12] "JIBO," 2015, URL: <http://www.jibo.com/> [accessed: 2015-11-20].
- [13] "Romo, the programmable, telepresence robot toy for kids and adult," 2015, URL: <http://www.romotive.com/> [accessed: 2015-11-20].
- [14] "The Arduino micro-controller," 2015, URL: <http://arduino.cc/> [accessed: 2015-11-20].
- [15] "The WebSocket Protocol. Internet Engineering Task Force (IETF)," 2015, URL: <http://tools.ietf.org/html/rfc6455> [accessed: 2015-11-20].
- [16] M. Oliver and A. Escudero, "Study of different CSMA/CA IEEE 802.11-based implementations," EUNICE, 1999, pp. 1–3.
- [17] T. Pering, Y. Agarwal, R. Gupta, and C. Power, "Coolspots: Reducing the power consumption of wireless mobile devices with multiple radio interfaces," Proc. ACM MobiSys, 2006, pp. 220–232.
- [18] M. C. Yip, M. Tavakoli, and R. D. Howe, "Performance Analysis of a Manipulation Task in Time -Delayed Teleoperation," Proc. IEEE/RSJ International Conference on Intelligent Robots and Systems, Taipei, Taiwan, October 2010.
- [19] D. Dardari, P. Closas, and P.M. Djuric, "Indoor tracking; theory, methods and technologies," IEEE Transaction on vehicular technology, vol. 64-4, April 2015, pp. 1263–1278.
- [20] H. Durrant-Whyte and T. Bailey, "Simultaneous localization and mapping (SLAM): Part I The essential algorithms," IEEE Robotics and Automation Magazine, vol. 13-2, June 2006, pp. 99–110.
- [21] D. Espes, A. Daher, Y. Autret, E. Radoi, and P. Le Parc, "Ultra-wideband positioning for assistance robots for elderly," 10th IASTED International Conference on Signal Processing, Pattern Recognition and Applications, SPPRA 2013, Feb. 2013, Austria.
- [22] T.K. Kohoutek, R. Mautz, and A. Donaubaauer, "Real-time Indoor Positioning Using Range Imaging Sensors," Proceedings of SPIE Photonics Europe, Real-Time Image and Video Processing, 2010, vol. 7.
- [23] A. Mulloni, D. Wgner, D.Schmalstieg, and I. Barakonyi, "Indoor Positioning and Navigation with Camera Phones," Pervasive Computing, IEEE 2009, vol. 8, pp. 22–31.

- [24] "The Newton-Raphson Method," 2015, URL: <http://www.math.ubc.ca/~anstee/math104/newtonmethod.pdf> [accessed: 2015-11-20].
- [25] T. Alhmiedat, G. Samara, and A. Salem, "An Indoor Fingerprinting Localization Approach for ZigBee Wireless Sensor Networks," *European Journal of Scientific Research*, vol. 105-2, July 2013, pp.190-202, ISSN: 1450-216X / 1450-202X.
- [26] "The Mentor M5070 IR LED," 2015, URL: [http://www.mentor-bauelemente.de/en/products/product\\_search/?s=M%205070](http://www.mentor-bauelemente.de/en/products/product_search/?s=M%205070) [accessed: 2015-11-2].

## Innovation and Creativity in HCI Education

Alma L. Culén  
University of Oslo  
Oslo, Norway  
E-mail: [almira@ifi.uio.no](mailto:almira@ifi.uio.no)

**Abstract**—The present paper explores what creative thinking and design thinking could contribute to Human-Computer Interaction (HCI) education if included as a part of the curriculum. The investigations were carried out in the context of a mixed undergraduate and graduate course in HCI. The findings indicate that design thinking contributed to increased focus on innovation and creativity, as well as prevented too early fixation on a single solution in the initial phases of HCI design processes. More openness in design processes and changes in ways of learning required stepping out of the comfort zone for some students. However, increased creativity and adaptability may still be the best long-term benefits that HCI education can offer to students when preparing them for future work practices. The paper also addresses the organization of the course that, based on the empirical evidence from the past two years, fosters such processes in HCI education.

**Keywords**—innovation; creativity; design thinking; HCI education.

### I. INTRODUCTION

This paper is an extended version of the paper [1], presented at the Advancements in Human-Computer Interaction (ACHI 2015) conference. It, like its conference version, discusses the role of innovation, design thinking, and creativity in Human-Computer Interaction (HCI) education.

HCI is an interdisciplinary field drawing from diverse disciplines, including computer science, psychology, media studies, and design. Historically, the field developed in the early 80s as a specialty area in computer science, embracing cognitive science and human factors engineering. Although it has undergone strong development over the past three decades, it is still taught at computer science departments worldwide, usually as part of the core computer science curriculum. After graduation, the students who chose HCI focus during their studies tend to pursue many different paths, ranging from seeking further education and aiming for research careers to practicing interaction design, often also in design consultancies, or working as information system developers. Preparing such students for their future work is challenging. In addition to the diversity of career paths that they can choose, they always need to relate to changing technologies, interaction modes, and interfaces. These, in turn, affect people's work and leisure practices that HCI professionals design for. So, how and what to teach HCI students that will help them to have successful carriers?

HCI students, on the one hand, need to learn appropriate theories and research methods, as well as understand state-of-the-art research and the importance of scientific rigor and relevance. However, being a profoundly interdisciplinary field, HCI does not offer any unifying core theories, so this goal is hard to achieve once and for all. For example, entering a new application domain often requires the acquisition of new knowledge, understanding of the state-of-the-art research, as well as the ability to develop domain and context specific tools, techniques, and methods. Thus, constant learning is likely to be a part of the career path.

On the other hand, students need to be able to design new technologies and interfaces, using diverse design approaches, and usually, without any formal training in design. This is, in part, why design processes in HCI often depend heavily on engaging users and other stakeholders in participatory and co-design processes, described by Muller as the third space of HCI, see [2]. Participatory approaches that involve users and stakeholders in design processes are undoubtedly valuable, but they also carry with them certain limitations. For example, HCI design practitioners, in a co-design situation, share the design responsibility with participants, whom they often rely on as domain experts. Thus, the choice of participants may influence the quality of the results. As these results (prototypes), are frequently not intended to become use artifacts, but are tied to some research objectives, this is often not seen as problematic. This focus on research objective, in contrast to making a new artifact for use, reflects the major difference in approach to design between HCI and interaction design as taught in design educations. The latter, while utilizing human-centered approach, also relies on design practices that imply more open and creative approaches to design situations, with intent to make a novel product for use. The question we started investigation for this paper was: could HCI students benefit from the inclusion of design thinking and designerly practices as part of their HCI curriculum? If so, what kind of benefits/challenges would this yield?

Drawing on insights from the work presented here and our previous work [3]–[6], this paper argues that teaching about innovation, and engaging students in creative innovation processes such as design thinking, offers one possible answer to what kind of knowledge and skills the students could be taught in HCI. Adopting this approach may be successful in a long run because, while on the road to becoming an innovator within a design team, one usually experiences creativity (one's own or that of others) and need to adapt to new situations. Creativity and adaptability may

offer greater permanent value to human-computer interaction education than many other kinds of knowledge and skills commonly considered to be part of HCI education. As reported in [5], all ten students in a graduate HCI course that made use of design thinking processes perceived themselves to be non-creative individuals at the beginning of the course. At the end of the course, all (excepting one student who felt neutral) stated that the design thinking affected them and that they now see themselves as more creative and confident in their skills. Thus, on a basic issue of whether the creativity can be taught, we can say that with proper tools and support, creativity can, at least, be nurtured [5]. We also observed an increased interest in invention among HCI students who participated in the course.

An additional indication that cultivating creativity could be a valuable asset was provided through a survey conducted at the end of a combined bachelor-master course in the fall of 2014. All design teams (18 teams in total, 3-4 students on each team) who participated in the class completed the survey. All teams reported that they now see HCI design as a creative process, and provided qualitative statements related to their experience of individual and group creativity. Some of these are presented later, in the discussion section of this paper.

In summary, the question this paper tries to answer is: what kind of knowledge and skills should be passed onto new generations of HCI students? While the complete answer remains elusive (many discussions around the HCI curriculum are already going on [7], [8]), our experience from the past two years of including design thinking and innovation (or, more precisely, increased focus on invention) in the curriculum shows that these benefit HCI students significantly. More open and creative processes seem to change how students that take part in such processes perceive themselves as HCI practitioners, and secondly, how they understand design processes, practices, and approaches to innovation.

The paper is structured as follows: the next section offers some arguments as to why HCI education should include innovation and creative thinking. In Section III, we show how these elements were introduced in a mixed bachelor-master HCI course. Discussion of the case is presented in Section IV, followed by the conclusion in Section V.

## II. FOCUSING ON INNOVATION

The ACM SIGCHI Curricula for Human-Computer Interaction defines Human-computer interaction as "*a discipline concerned with the design, evaluation, and implementation of interactive computing systems for human use and with the study of major phenomena surrounding them*", see Hewett et al. [9]. Teaching HCI typically includes the teaching of user-centered requirements analysis, design and prototyping, implementation, a design of experiments and evaluation. HCI's interdisciplinarity brings with it tensions between the breadth and the depth of teaching, diverse theories and practices, including the choice between contributing to science or to design (of new interfaces, products, services or interaction modes). Despite

these tensions, HCI education is very much alive and doing well in practice, although still without generally agreed upon curricula.

Innovation, on the other hand, is known to be hard to achieve in practice, while it is very easy to understand the need for it, and the benefits it brings, see [10]. There are various ways to define innovation. The Oslo Manual [11] defines it as: "*the implementation of a new or significantly improved product (good, or service) or process, a new marketing method, or a new organizational method in business practices, workplace organization, or external relations.*"

It is difficult to teach students to be innovative, creative and inventive. In particular, it is not easy to make good instructional frameworks for doing so. The processes related to innovation rely heavily on creativity, but also on both existing knowledge and on technical skills that are already present among the members of the design team and those whom they choose to include in the design processes. In particular, it is hard to define learning outcomes for such processes.

Within HCI, the creativity component is usually, at least partially, bypassed by two things: the framing of the process as a procedure that everyone can follow on the one hand, and relying on users and their participation in different stages of design processes on the other hand. The 'typical' design process consists of developing an understanding of the contextual domain first, and second, concretizing this understanding through practical work that involves iterative prototype design and evaluation, often in co-creation with users and other stakeholders. However, designerly and creative practices, a core activity of innovative design [12], [13] are, as already mentioned, harder to frame.

Purposefully managed innovation through design and creativity has been advocated in many different ways [14]. Design thinking is one of those options. Understanding design thinking is not straightforward. In [15, p. 13], Kimbell offers three different ways of understanding design thinking: as a cognitive style, as a general theory of design, or as an organizational resource. The last understanding lends itself well as an approach to innovation and real-life problem solving through human-centered design, employing empathy with users, rapid prototyping and abductive thinking as its main components. This understanding of design thinking has strongly impacted innovation in business, education, health and other crucial domains, see [12], [13], [16]–[18]. Many examples of how businesses and organizations could benefit from incorporating design thinking into their work and organizational processes were given in Brown's book [19], making design thinking into an efficient innovation engine emphasizing observation, collaboration, fast learning, visualization of ideas, rapid concept prototyping, synthesis and concurrent business analysis.

However, no approach solves all problems. Thus, only a few years after design thinking made a breakthrough in the world of business strategy and management, its limitations were brought forth in works such as Collins and McCullagh's works [20], [21]. The point made by

Nussbaum in [22], though, hits home best: “From the beginning, the process of design thinking was a means to deliver creativity. But in order to appeal to the business culture of process, it has on occasion been reduced to a more linear process—presumably to eliminate the mess, conflict, failure, emotions, and iteration that are part and parcel of the creative process. In a few companies, CEOs and managers accepted that mess along with the process, and real innovation took place.” In short, the core of innovation is creativity, a messy and unstructured process. By framing design thinking in a particular, linear way, the creativity becomes limited, leading, in turn, towards failure to innovate.

Simultaneously, concerns are being raised around the failure of design processes currently applied within the field of HCI to support more radical innovation [3]. In particular, HCI design processes are held to lead mainly to incremental innovation and small changes. Innovation, radical or incremental, is a much more complex process than the design and invention of new products, systems, or interaction modes. It implies also their acceptance and use by people [11]. Upon careful consideration of design practices within HCI, one could argue that invention is common. However, a very small percentage of those inventions (prototypes) ever become finished products, and an even smaller percentage is adopted and used, see [4], [23].

Design thinking is only one approach to design, but it may be the one that is particularly suitable for non-designers and for multi-disciplinary collaboration. It employs, in part, steps similar to those often proposed in HCI: it frames its process in ways that have familiar overtones to those used in HCI, see Fig. 1.

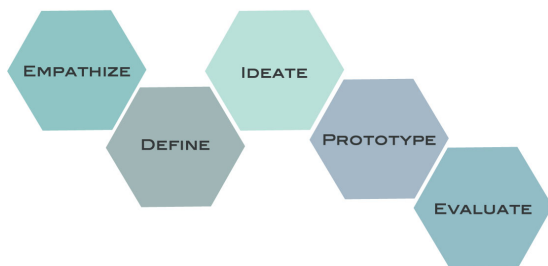


Figure 1. A process that may seem familiar to HCI students, as well as to those using design thinking. The image is adapted from [24].

Arguably, differences between design thinking and HCI should be sought by other means than comparing high-level design processes. One needs to consider differences in the assumptions, scope and aim of the design process – concerning, for instance, the role of research, the requirements specification, the questioning of assumptions, the consideration of organizational issues and the systematic exploration of design alternatives.

Design thinking stands on three main pillars: empathy with users and human-centeredness, rapid prototyping to generate a large number of alternatives in order to solve the correct problem rather than any given problem correctly (the creative part), and last, but not least, their synthesis leading

to the best viable and feasible solutions that incorporate desired values, see Fig. 2 and [17].

IDEO [25], a design and innovation consultancy, has streamlined the process shown in Fig. 1 and made a 60 minutes version of it available to all, also non-designers. Although their process appears to be simple and short, its power rests on its capacity to initiate deeper engagement with the problem space and allow for organizational changes that support the engagement and creativity initiated by those short processes.

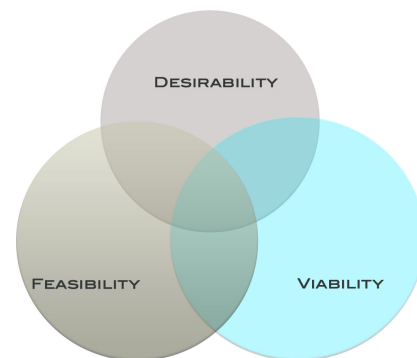


Figure 2. The solutions emerging from design thinking should be desirable, feasible and viable, i.e., belong to the intersection of the three.

As mentioned in the Introduction, HCI students need to master diverse types of knowledge and gain practical design experience. They are also expected to produce or develop new knowledge. In [26], Owen proposes a model for dual nature of knowledge production as depicted in Fig. 3.

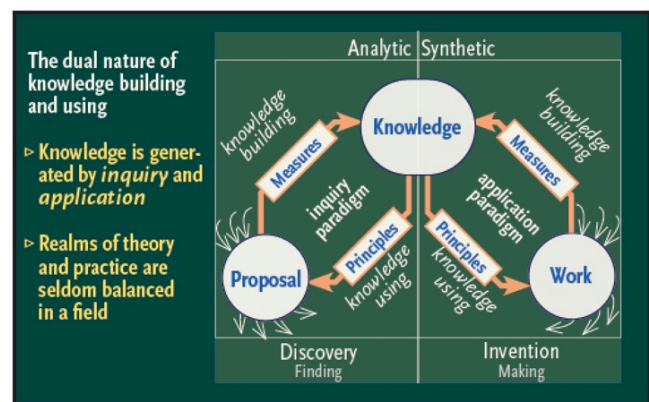


Figure 3. The dual nature of knowledge building, from Owen, [26].

Within interaction design, as practiced by HCI professionals, the research (finding, discovery) and design (prototyping, making) are often intertwined, involving knowledge of *techne* (programming, digital crafting), *episteme* (theoretical grounding) and *phronesis* (practical design knowledge). Production of new knowledge within these three (or any similar distinctions between knowledge forms) is also expected from students, especially those who are more advanced in their studies. Multiple roles that an interaction design student often assumes in any given

project (that of a researcher, a designer, a programmer, or a crafter) further obscure the clarity of what this new knowledge is. In addition, he/she may have personal biases towards, or different levels of expertise in, either research, programming or design [27].

Fig. 3 makes another important point: realms of theory and practice are seldom balanced in a field. Papadimitriou's paper [28] discusses this topic in relation to the field of databasis; it considers the relation between theory and practice in the databases, summarizing what a good theory is and how applied science looks like during the 'normal' phase (referring to Khun's view on the structure of scientific revolution [29]). Papadimitriou searches for the equivalent of the concept of 'crises' in a non-natural, applied science field. As a possible contender, he proposes the lack of connectedness between theory and practice in the field of data basis. This is visually represented by a directed graph with very few paths connecting communities focusing on theoretical knowledge and those focusing on practical knowledge. At the same time, the theoretical community, as well as the practice-based community, had strong internal connections.

Similar arguments are true for HCI and its education. If the knowledge circle in Fig. 3 was further divided into diverse knowledge forms it would become even more transparent that there are too few connections between discovery and invention. A demand that the knowledge is relevant and rigorous exists within both discovery and invention. However, different criteria of relevance and rigor apply to different knowledge forms whose purposes, processes and contexts are also different [30], [31]. Navigating this landscape is particularly challenging for a novice HCI practitioners and interaction designers, HCI students among them, who wish to use HCI design and research through design approach, see [32] and [33], and who need to address knowledge production related to all these diverse knowledge forms and establish both relevance and rigor in their work.

So, why make the teaching of HCI, even more, complicated by explicitly introducing creative thinking, using design thinking and innovation?

### III. THE CASE: TEACHING HCI WITH A CREATIVE WREE

#### A. Previous Classroom Experiences with Design Thinking

During the fall semester of 2013 two student project teams, from a combined bachelor-master course in interaction design, were introduced to design thinking. These teams worked with the design of new services for the University Library. They were introduced to design thinking and participated in workshops using service design methods and tools, such as service design cards, touch points and customer journeys, see [34].

Besides, during the same semester, a small graduate course of ten students, mentioned in the introduction, adopted the design thinking approach and studio-based teaching. There, three student groups were taught about design thinking and focused explicitly on nourishing creativity [5], [6]. They were also required to read articles

like [33], [35]–[39], to gain a deeper understanding of research through design and designerly practices. In addition, successful examples of applications of design thinking were discussed [17], as was the work reflecting on the design practice and possibilities for understanding daily practices as a design material, see [30], [40].

Experiences from both classes strongly indicated that cultivation of creative thinking and making have a potential to contribute positively to the teaching of HCI.

#### B. The Course Setup

The teaching approach that we argue for in this paper was applied in the context of a combined bachelor-master course in interaction design. The course in question teaches traditional HCI research methods, using the textbook [41], and has two prior HCI courses as prerequisites. In addition to teaching research methods through lectures and small group learning sessions, the course aims to address real-world problems by offering a semester-long project in cooperation with external, local organizations. Usually, ten or more organizations (or large, funded research projects) are involved, offering two distinct project proposals each. Students, in small design teams of 3-4, select one of the proposals, based on a first-come-first-serve basis. The project work is, thus, anchored in the real needs of local companies and organizations. Sometimes, these needs are not clearly formulated. Rather, a company wishes to renew its offerings and engages student teams in looking for new, open and creative solutions. Some student teams have experienced such open requests as challenging. The insight that demand for novel and creative solutions could be challenging was gained through observation that proposals with a narrow scope and clear goals were almost always selected first while explorative problems were chosen last.

The students in the course were further supported (or challenged) in their learning efforts as follows: they were free to make mixed master-bachelor student groups, but master students needed to have a deeper focus on knowledge and knowledge production. Thus, they were required to read, understand, and actively apply previous research related to their projects. This implied finding published research of high quality and discerning its relevance to their projects. Both master and bachelor students needed to find examples of relevant previous design work. Furthermore, all teams had regular, hour-long design feedback sessions during the conceptual design and prototyping phases of the project (usually during the first 4-5 weeks). One senior researcher and a representative of a company, for which the students were designing, were required to participate in these sessions. Also, all groups made in-class, midterm presentations of their design efforts. The presentations were open to anyone, from interested organizations to other faculty members, professional designers, and junior students. They were also available online, see [42].

The course ended with a juried competition for the best student project, again with open access to the event. An independent jury consisting of three judges, recruited among HCI, design, and pedagogy professionals, judged the

contest. Criteria for the jury were: novelty, clarity of presentation, the potential impact of the designed prototype (its relevance), validation of the prototype with users and the overall impression of the project work. This exact setup has been run for three consecutive years and has included a survey at the end of each semester. The surveys were individual and optional previously, focusing on cooperation with industry and research partners. Last year's survey was filled by all design teams and included questions about creativity, group or individual, and how design processes were affected by the introduction of creative and design thinking.

Although the course addresses real-life problems, which in non-academic settings would likely be solved by multidisciplinary teams, multidisciplinary was not always possible to achieve in the context of this university course. In other words, teams could not invite others whose expertise could contribute significantly to the quality of designs and prototypes (for example, a highly skilled programmer, designer or engineer). Multidisciplinary was anchored in the skills and knowledge that students had in addition to HCI, such as psychology, graphic design, or arts and in skills and knowledge of those that they collaborated with, such as librarians, museum professionals, software developers and others from participating organizations. Students were encouraged to understand the assemblages of skills and knowledge that they had within the team, and consequently organize work so that their skills could be used well, but also so that they could learn the most, from each other, organizations they worked with, and senior researchers.

### C. The Use of Creative Thinking and Innovation

The teams were free to choose and follow an approach of their choice, as long as they complied with general course requirements described above. The challenge was how to best support the creativity within each team. A lecture on creative thinking and design thinking was given at the start of the course, introducing concepts of assemblages of skills and practices. The idea that one can design and adopt a set of practices that support creativity was also introduced in [5]. This was further practically demonstrated and re-enforced during design sessions.

In addition, all available external opportunities were sought out and used to motivate students. For example, last year, during the fall semester, the dean of the University extended an innovation challenge to all students at the University of Oslo, whether they study science, politics, social sciences or entrepreneurship. The most innovative idea was rewarded both financially and through support for its further development. The students participating in the innovation challenge had to go through several selection rounds, until the winner was chosen. All student teams in the course were encouraged to participate. Two teams took up the challenge. This has, in addition to the usual interaction-design course work, involved making a financial proposal and a business plan for implementation of the innovative idea/proposal, and a proof of the feasibility, essentially following the idea behind Fig. 2. Students did

not have any prior experience with such processes yet managed to make a financial and business model for their ideas. Both teams were selected among the top four projects (although neither ultimately won the first place).

However, when judged independently in the context of the course and during the final competition, they won the first and the third place (from the total of 18 teams), indicating that they were highly motivated by the innovation challenge.

Each of the two teams in question consisted of four second year undergraduate students, and was supervised by a PhD student whose research focused on elderly living in a smart house. Thus, both projects addressed design for and with elderly users in that context, see [43] and [44] (projects were delivered in Norwegian, but one group also wrote a paper based on their project in English, and presented it at the HCII 2015 conference, see [45]). The latter project, see Fig. 4, developed a high fidelity interactive prototype utilizing low frequency-based technology (iBeacons) that helps elderly people with cognitive difficulties to navigate complex buildings indoors. Their system aimed to improve the well-being of elderly people and help them become more independent by introducing a familiar design on the tablet that was already in use as part of the smart house solution, and integrating it with a pre-existing aid, a walker.

The use of the smart-walker with the tablet that presented data from iBeacons, required mastery of the technology every time it was used. However, this task was made to be as simple as possible. SmartWalker enabled users with cognitive difficulties to move easier around on their own, giving them an increased degree of freedom of movement inside the complex building where they live.



Figure 4. SmartWalker: a system co-designed with elderly and based on a low frequency technology and a simple visualization of the current position in the building on a familiar tablet interface. Photos from [44].

The second project [43], see Fig. 5, focused on self-management and bodily mastery through movement, see also [46]. It involved design of an exercise system for elderly users. The system was based on a motion sensor (Kinect), and wearable technology (a glove, powered by Arduino, that enabled more precise tracking of movements). The system provided feedback on whether exercise was performed correctly, and was designed to support bodily mastery and well-being in general, and in particular for those who needed rehabilitation and training after, for example, a fall.

This project involved 26 persons, 17 elderly, 3 physiotherapists and 6 employees in diverse homes for elderly.



Figure 5. An exercise system that enables correction of movements during the exercise session. Photo from [43].

Even though these two groups have achieved very good results, they were not the only ones that pursued the goal of being innovative and creative. Some other ways in which this focus on creative thinking and innovation affected the work of the project teams, with examples, is discussed in the next section.

#### IV. DISCUSSION

The contextual differences among briefs presented to students by organizations that participated in this educational endeavor were substantial. Some teams were required to find new application domains for existing technologies, others to design new applications involving new technologies and yet others had to use old applications and old technologies, but find new ways of working with them. For example, a team had to work with the latest technology such as Google glasses and their potential use in crises situations by crisis management state bodies, such as the police, or paramedics. Another team had to work with complex web-based software used in the oil industry that required creative thinking around how to help users to customize it. What, then, about knowledge building and the best approach to it, for individuals, teams, and the class as a whole?

##### A. Arbitrage, Bricolage and Assemblages

Reflecting on alternatives and knowing why design processes involved certain tools, techniques and methods was a course requirement. This was seen as part of the knowledge production process, either in support of the scientific methods or in support of establishing reflective designerly practices, see [30]. Arbitrage was used to discuss what the ‘new knowledge’ is in each case, and how to communicate it.

Arbitrage is a concept used in economics and has to do with price negotiations where one capitalizes on striking deals that profit the most from imbalances between prices on similar items at different markets. Translated to interaction design, one might want to strike the optimal balance for similar work in terms of regarding differences in knowledge among practitioners and researchers working closely together. Over time, this strategy could increase links between research and practice in interaction design.

The issue of knowledge production has been a recent topic of discussion in interaction design and HCI communities. The discussion was concerned with how research through design in interaction design and HCI design, produces new knowledge. What forms this knowledge takes and how to frame questions around it has been a topic of a recent CHI workshop [47].

If students worked alone, arbitrage perhaps would not have been as effective, since they all have similar knowledge bases. However, the involvement of senior researchers and industry partners (most of whom are practitioners) was required, in part, to provide fertile ground for negotiations around knowledge production and design artifact created.

*Bricolage* and *assemblages* are terms used by Levi-Strauss [48], as well as by many others. We have experimented with implementing the practice of bricolage, both in the sense of using multiperspective research methods and seeing what ‘fits’ best in relation to the problem at hand, and as the practice of design and making that constrains design space in some way (in our case, material expenses needed to be minimal, and students were encouraged to use in-house resources). Assemblages of skills and practices were used as described earlier in the paper. With bricolage, also assemblages of materials were relevant. These concepts appeared to be useful in supporting creativity and a better understanding of a design practice in HCI education, see [5] and [49], while also improving students’ analytic skills.

The practical application of these concepts in design processes was not yet carried out systematically. Both the assemblages of skills and practices, as well as arbitrage, were processes that could be applied where there was true multidisciplinary within the team. Then the participants were asked to explain their approaches or demonstrate their skills so that others could gain an understanding of what those are and include them actively in the decision-making process. This process was also beneficial in terms of preventing too early fixation on any given solution, having first to get acquainted with people’s skills and practices, postponing the need to fixate on a solution fast, and instead, give time to consider the resources within the team and how these fit together. The bricolage was most relevant for projects where students were building or constructing an artifact using materials at hand and trying various techniques and methods in their work.

##### B. Design Thinking and Combining Approaches

The vast majority of teams benefited from being inspired by at least one of the three main components of design thinking: empathy with users, rapid prototyping, or abductive thinking. The use of any specific method, including design thinking, was never enforced, so teams could choose to use any component of design thinking, none or a combination of design thinking with other practices used in industry, and more traditional HCI approaches. Yet, as mentioned above, the negotiations needed to be done (arbitrage) as to which approaches fit best relative to the problem at hand.

Empathy is a multifaceted construct that includes emotional recognition, vicarious feeling, and perspective taking [50]. Empathy was ‘new’ for many HCI students. While students were used to conducting user studies, they seldom tried to take the place of a user themselves and develop empathy with users in that way (e.g. through role-playing). In part, this might be due to the perception that basing the design decisions on empathy, the ‘scientific’, objective component of the research is lost in favor of the subjective (emphatic feelings of the HCI designer). Another reason might be that the phenomenological perspective that is characteristic of the latest wave of HCI, is still lagging behind in HCI education. Regardless of the reason for empathy’s ‘newness’, once it was tried, the students understood its benefits and could apply it creatively when working with conceptual development of their solutions.

As an example, two teams were engaged in designing for better waiting room experiences in children’s wing of the hospital. Being empathetic observers in the hospital’s waiting room brought insights that whatever it was that they would end up making, it had to respect young patients’ right to have a quiet and safe (e.g., germ free) waiting room. They could engage young patients, alone or with others if desired, in technology-mediated interaction, but it had to be easy to choose a non-engagement as well. What students learned from empathic observations eliminated many of the initial ideas they had. They worked extra hard in order to find novel and engaging solutions that also meet all the above-mentioned conditions. The end results of design and research efforts were the following: the first team developed a water fountain, Fig. 6, and the second team a dress-up game. The LED lit fountain was controlled by in-air hand gestures, enabled by the Leap Motion sensor, not requiring any physical contact. It was fun to play with, nice to look at, and it had a pleasing and very soft sound, see Fig. 6 and [51]. The breakthrough for this group was achieved after they experienced empathy with young patients and understood how to translate this empathy, together with other findings, into a design opportunity.



Figure 6. The water fountain project. Photos from [51].

The second team utilized the Kinect motion sensor to support their dress-up game, again requiring no physical contact with any objects in the room. The game, see Fig. 7, could be played by a single child, or by multiple participants. In the stand by mode, it was non-intrusive and easy to ignore. Attention was paid to special situations, such as players in a wheel chair, and players with otherwise different movements (for example, slower than usual, as a result of fatigue).



Figure 7. A dress-up game for young patients waiting for an appointment, see [52].

Rapid prototyping, the second pillar of design thinking, was also frequently used. Once students understood that they were to generate many simple prototypes, not just one or two, they found that communication of ideas became easier and clearer, in particular when group members had different backgrounds and levels of knowledge.

The following case demonstrates how the two teams working with service design for the University Library went about rapid prototyping. A workshop was organized by one master degree student, and apart from the two teams, two researchers, one designer and eight librarians attended the workshop. The participants were divided into two groups and engaged in bricolage and rapid prototyping, see Fig. 8.

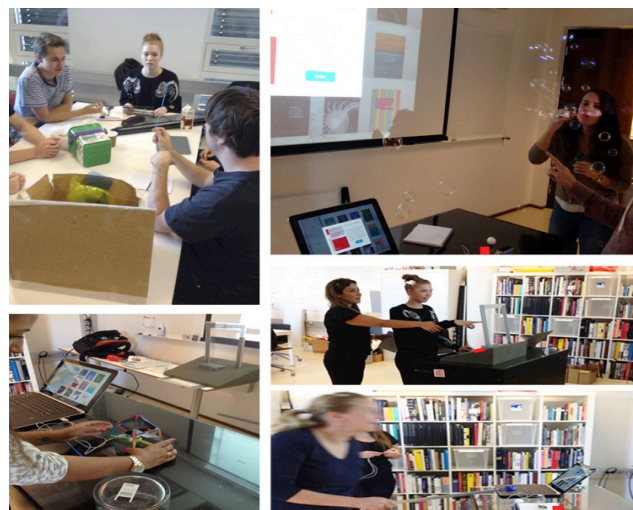


Figure 8. Making rapid prototypes of an intermediary surface in order to enable better precision when using LEAP motion for selection of books, see [53].

Everyone was to make as many prototypes as possible in the given timeframe. The problem they worked with had to do with reducing precision problems arising from the gesture-based selection when using the LEAP motion, in a multi-user situation. The second and longer part of the workshop was dedicated to discussion related to the prototypes made. The library experts could at once provide information on existing services, and how each of

prototypes could fit with the existing services (or not), discussing the viability of proposals.

The last pillar of design thinking, abductive reasoning, was used to discuss how good parts of some of the prototypes could be combined to make a better prototype. The feasibility of diverse prototypes was a prominent part of this discussion. Abductive thinking and the ability to ‘see’ design opportunities by combining aspects of diverse proposals may be something that comes easier to people within design disciplines, rather than those using analytic way of thinking. The participating student teams clearly benefitted from being a part of this process, at least by gaining an understanding of what rapid prototyping and abductive thinking involve, as well as the relevance of concepts presented in Fig. 2.

### C. Survey results

A short questionnaire, consisting of three questions only, was conducted after the initial 4 weeks of instruction, during which time the students were encouraged to remain open, not to “jump” to a particular solution, but instead, to take the time to feel the discomfort of not having a solution yet, and actually exploring the options. 30 students answered the questionnaire.

The first question was phrased as follows: *“In the design process you now have started, how did you feel about the request to keep the process open and resist the desire to use the first opportunity to define your solution and work towards accomplishing it”*. These are some answers to the question: *“I believe that this is more enjoyable and challenging. However, it can be tempting to jump right into solving a problem, and it is important to try to avoid this”*. *“It is difficult to keep yourself from starting to implement the first idea that one comes upon. One also thinks that if the solution is good enough, then one saves time and money by jumping over, maybe, an unnecessary process”*. *“Curious, hesitant at first”*. *“I actually think it is exciting. You know – the part of the process when everything can happen. I love being creative and I love creating ideas. For our group’s work, my strategy was to make use of the small sketchbook our supervisor gave us. I used it to sketch ideas even if it was very early in the process”*. These answers reflect a willingness to engage in open processes. They sometimes expressed the discomfort and sometimes the joy of having an opportunity to do so.

The second question was phrased as follows: *“Can you think of anything that instructors could do to help you with keeping the process open and creative?”* Some of the answers here indicate a worry that they will somehow not have enough time to do the “real work”, or lack of understanding of how they can accomplish all the goals laid out for the course: *“Even more real-life examples”*, or *“being clear about how much/what is expected of us”*, *“creative tools”*.

The last question was open, requesting *“Any comments on creativity in design processes?”* Most people did not answer this one, or answered it with a simple *“I like it”*. Some other comments included: *“It is hard, without knowing the defined possibilities”*, *“Tips about places one*

*can find inspiration”*, *“Background differences are good”* and *“look to choreographers – they have an idea they want to explore – each dancer contributes with their movement material”*. This last remark expresses the same idea behind discussing the assemblages of skills, practices and materials.

At the end of the last semester, all teams filled a questionnaire, providing 18 sets of answers. Two questions were related to creativity:

- 1) Do you think that the kind of work you did in this course is also creative?
- 2) What do you think about group creativity?

All teams answered the first one in affirmative. As for the second question, here are some of the answers (the answers were given in English, as presented, only the very last statement was translated from Norwegian): *“It really helps. Quite often you have some ideas, but you need help to be able to explain them. So in our group we really understood how each other was thinking, and we could really help each other describe and realize our ideas and creativity.”* Another team expresses it as follows: *“We have a group of different people with different ways of thinking, stirred together in a creative pot, it’s awesome”!* The third considers that the *“group work increases creativity”*. The two most cautious expressions were the following two: *“We feel that the group works very well together, although this experience may vary”*, and *“Very good! Perhaps a bit too creative and ambitious”*.

### D. Analysis

During the past three years, much experience was accumulated with project-based courses such as the one described in this paper. Lots of anecdotal evidence as to what works and what does not has been gathered and best efforts made to design a course that teaches HCI with a focus on creativity and innovation. Clearly, both theory and practice needed to be well represented in such a course. Things are not made easier by the lack of theory as to how interaction design produces new knowledge [47], what makes a prototype novel [54] or how to bridge (connect) diverse theoretical concepts and theoretical concepts and practice (see Fig. 3). Arbitrage (facilitated by a senior researcher or designer) helps discuss, understand and choose tools and methods that fit the context and design space. It is difficult to build directly on design and creativity in HCI due to the lack of design knowledge and frequently experienced insecurity among students in their capacity to be creative. Creativity is often confused with being artistic. However, through the work with the course, we see evidence that designerly practices, including bricolage and design thinking, are highly relevant tools for supporting creativity among students, conducting projects in the described setting. Multidisciplinarity is important, considerations of different practices often open up for new ways to be creative and learn in the process. The multidisciplinary exchange is facilitated well by looking at group composition and assembling all skills and practices in a short session at the start of the work on a project, which also facilitates getting to know other members of the project

team. Students' answers to questionnaires confirm these findings.

The class as a whole learns to trust the process by having common presentations and demonstrations during the semester. Hearing and learning about different approaches, but also experiencing the results they produce, is very important. The close contact with the outside institutions, and a senior researcher or designer (often a PhD student), helps keep the processes within the framework of the course, as well as it utilizes their tacit or scientific knowledge for moving forward their work and learning through both classes and designerly practices.

## V. CONCLUSION

The aim of this paper has been to inquire into the interplay between innovation, design thinking and creativity as educational channels that stand out as alternative or complementary to the ones traditionally used by HCI educators. The framework for learning about innovation, design thinking and creativity was introduced and explained. This setup has been repeated for the past two years and may be repeated by others. The concepts that have been helpful in the cultivation of creativity were assemblages of skills and practices within multidisciplinary settings, empathy, rapid prototyping and abductive thinking. At the same time, care was taken not to reduce working with them as a specific procedure. Rather, tools, methods and techniques needed to be reflected over and chosen in accordance with the problem at hand. Experimenting with, or, at least, negotiating choices of research methods and techniques was encouraged.

Further research is required regarding other frameworks and practices for supporting creativity and innovation in HCI curriculums, including a comparative analysis of outcomes.

The achievements and learning outcomes in the course described here has kept improving over the last three years, as frameworks for supporting innovation and creativity got better and clearer described. The students' understanding of processes has also increased over time. These findings indicate that design thinking contributed to increased focus on innovation and creativity, as well as helping to keep design processes wider and more open for a longer period, fostering increased flexibility and adaptability in learning processes. Added creativity and adaptability may be the best long-term goals that HCI education can add to its curriculums when preparing students for future work practices.

## ACKNOWLEDGMENT

Many people deserve profound gratitude for helping with this work. All representatives from different participating organizations, designers and other professionals, as well as Ph.D. students, who helped with supervising student teams, have my deep gratitude. Finally, gratitude goes to all the students in the course for their work and for their efforts to try new ways of doing things that they were familiar with. In particular, gratitude is due for taking time to participate in surveys and interviews.

## REFERENCES

- [1] A. L. Culén, "HCI Education: Innovation, Creativity and Design Thinking," in Proceedings of ACHI 2015, The Eighth International Conference on Advances in Computer-Human Interactions, 2015, pp. 125–130.
- [2] M. J. Muller, "Participatory design: the third space in HCI," in The Human-computer Interaction Handbook, Hillsdale, NJ, USA: L. Erlbaum Associates Inc., 2003, pp. 1051–1068.
- [3] A. L. Culén and A. Følstad, "Innovation in HCI: What Can We Learn from Design Thinking?," in Proceedings of the 8th Nordic Conference on Human-Computer Interaction: Fun, Fast, Foundational, New York, NY, USA, 2014, pp. 849–852.
- [4] A. L. Culén, "Scaffolding Sustainability in the Academic HCID Practice," in Proceedings of the International Conference on Interfaces and Human Computer Interaction, 2014, pp. 45–54.
- [5] S. Finken, A. L. Culén, and A. A. Gasparini, "Nurturing Creativity: Assemblages in HCI Design Practices," in Proceedings of DRS 2014, Umeå, 2014, pp. 1204–1217.
- [6] A. L. Culén, H. N. Mainsah, and S. Finken, "Design Practice in Human Computer Interaction Design Education," in Proceedings of ACHI 2014, The Seventh International Conference on Advances in Computer-Human Interactions, 2014, pp. 300–306.
- [7] E. F. Churchill, A. Bowser, and J. Preece, "Teaching and Learning Human-computer Interaction: Past, Present, and Future," *Interactions*, vol. 20, no. 2, pp. 44–53.
- [8] L. Bannon, "Reimagining HCI: Toward a More Human-centered Perspective," *Interactions*, vol. 18, no. 4, pp. 50–57, Jul. 2011.
- [9] T. T. Hewett, R. Baecker, S. Card, T. Carey, J. Gasen, M. Mantei, G. Perlman, G. Strong, and W. Verplank, "ACM SIGCHI Curricula for Human-Computer Interaction," ACM, New York, NY, USA, 1992.
- [10] G. C. O'Connor, "Major Innovation as a Dynamic Capability: A Systems Approach," *J. Prod. Innov. Manag.*, vol. 25, no. 4, pp. 313–330, 2008.
- [11] Luxembourg, The Measurement of Scientific and Technological Activities Oslo Manual: Guidelines for Collecting and Interpreting Innovation Data. OECD publishing, 2005.
- [12] T. Brown and J. Wyatt, "Design Thinking for Social Innovation (SSIR)," *Stanford Social Innovation Review*, 2010.
- [13] T. Brown, "Design Thinking," *Harv. Bus. Rev.*, vol. 86, no. 6, p. 84, 2008.
- [14] B. von Stamm, *Managing Innovation, Design and Creativity*, 2 edition. Chichester, UK; Hoboken, NJ: Wiley, 2008.
- [15] L. Kimbell, "Rethinking design thinking: Part I," *Des. Cult.*, vol. 3, no. 3, pp. 285–306, 2011.
- [16] N. Cross, "Designerly ways of knowing," *Des. Stud.*, vol. 3, no. 4, pp. 221–227, 1982.
- [17] R. L. Martin, *The Design of Business: Why Design Thinking is the Next Competitive Advantage*. Harvard Business Press, 2009.
- [18] A. L. Culén and M. Kriger, "Creating Competitive Advantage in IT-Intensive Organizations: A Design Thinking Perspective," in *HCI in Business*, F. F.-H. Nah, Ed. Springer International Publishing, 2014, pp. 492–503.
- [19] T. Brown, *Change by design: how design thinking can transform organizations and inspire innovation*. New York, NY: HarperCollins Publishers, 2009.
- [20] H. Collins, "Can Design Thinking Still Add Value?," *Des. Manag. Rev.*, vol. 24, no. 2, pp. 35–39, Jun. 2013.

- [21] K. McCullagh, "Stepping Up: Beyond Design Thinking," *Des. Manag. Rev.*, vol. 24, no. 2, pp. 32–34, Jun. 2013.
- [22] B. Nussbaum, "Design Thinking Is A Failed Experiment. So What's Next?," *Co.Design*, 2012. [Online]. Available: <http://www.fastcodesign.com/1663558/design-thinking-is-a-failed-experiment-so-whats-next>. [Accessed: 01-Dec-2015]
- [23] P. K. Chilana, A. J. Ko, and J. Wobbrock, "From User-Centered to Adoption-Centered Design: A Case Study of an HCI Research Innovation Becoming a Product," in *Proceedings of the 33rd Annual ACM Conference on Human Factors in Computing Systems*, New York, NY, USA, 2015, pp. 1749–1758.
- [24] M. K. Collias, "Unpacking Design Thinking: Define," *Knowledge Without Borders*. [Online]. Available: <http://knowwithoutborders.org/unpacking-design-thinking-define/>. [Accessed: 01-Dec-2015].
- [25] "IDEO | A Design and Innovation Consulting Firm." [Online]. Available: <http://www.ideo.com/>. [Accessed: 24-Oct-2014].
- [26] C. Owen, "Design thinking: Notes on its nature and use," *Des. Res. Q.*, vol. 2, no. 1, pp. 16–27, 2007.
- [27] A. L. Culén, S. Joshi, and A. Atif, "HCID: Who is an interaction designer?," in *Proceedings of the 2nd International Conference for Design Education Researchers*, Oslo, Norway, 2013, vol. 4, pp. 1924–1937.
- [28] C. H. Papadimitriou, "Database Metatheory: Asking the Big Queries," *SIGACT News*, vol. 26, no. 3, pp. 13–30, Sep. 1995.
- [29] T. S. Kuhn, *The Structure of Scientific Revolutions*, 3rd Edition, 3rd edition. Chicago, IL: The University of Chicago Press, 1996.
- [30] D. A. Schön, *The reflective practitioner: How professionals think in action*, vol. 5126. Basic books, 1983.
- [31] J. Dewey, *Logic - The Theory of Inquiry*. S.I.: Saerchinger Press, 2007.
- [32] D. Fallman, "Why research-oriented design isn't design-oriented research: On the tensions between design and research in an implicit design discipline," *Knowl. Technol. Policy*, vol. 20, no. 3, pp. 193–200, 2007.
- [33] J. Zimmerman and J. Forlizzi, "Research Through Design in HCI," in *Ways of Knowing in HCI*, J. S. Olson and W. A. Kellogg, Eds. Springer New York, 2014, pp. 167–189.
- [34] A. L. Culén and A. Gasparini, "Find a Book! Unpacking Customer Journeys at Academic Library," in *The Seventh International Conference on Advances in Computer-Human Interactions*, 2014, pp. 89–95.
- [35] J. Zimmerman, E. Stolterman, and J. Forlizzi, "An analysis and critique of Research through Design: towards a formalization of a research approach," in *Proceedings of the 8th ACM Conference on Designing Interactive Systems*, 2010, pp. 310–319.
- [36] D. Fallman, "Design-oriented Human-computer Interaction," in *Proceedings of the SIGCHI Conference on Human Factors in Computing Systems*, New York, NY, USA, 2003, pp. 225–232.
- [37] E. Goodman, E. Stolterman, and R. Wakkary, "Understanding interaction design practices," in *Proceedings of the SIGCHI Conference on Human Factors in Computing Systems*, New York, NY, USA, 2011, pp. 1061–1070.
- [38] J. Löwgren and J. L. E. Stolterman, *Thoughtful Interaction Design: A Design Perspective On Information Technology*. MIT Press, 2004.
- [39] B. K. Chakravarthy and J. Krishnamoorthi, "Innovation By Design."
- [40] L. Kuijter, A. de Jong, and D. van Eijk, "Practices As a Unit of Design: An Exploration of Theoretical Guidelines in a Study on Bathing," *ACM Trans Comput-Hum Interact*, vol. 20, no. 4, pp. 21:1–21:22, Sep. 2008.
- [41] D. J. Lazar, D. J. H. Feng, and D. H. Hochheiser, *Research Methods in Human-Computer Interaction*. John Wiley & Sons, 2010.
- [42] "Project presentations - INF2260 - Fall 2014," 2014. [Online]. Available: <http://www.uio.no/studier/emner/matnat/ifi/INF2260/h14/presentations/>. [Accessed: 01-Sep-2015].
- [43] "Motus - Kampen Omsorg+ - INF2260 - Høst 2014 - Universitetet i Oslo." [Online]. Available: <http://www.uio.no/studier/emner/matnat/ifi/INF2260/h14/presentations/kampen2/index.html>. [Accessed: 01-Dec-2015].
- [44] "SmartWalker - Indoor Navigation for Elderly - INF2260 - Høst 2014 - Universitetet i Oslo." [Online]. Available: <http://www.uio.no/studier/emner/matnat/ifi/INF2260/h14/presentations/kampen1/smartwalker---indoor-navigation-for-elderly.html>. [Accessed: 19-Jan-2015].
- [45] M. Källström, S. Berdal, and S. Joshi, "Designing an Indoor Navigation System for Elderly People's Capabilities," in *Human Aspects of IT for the Aged Population. Design for Everyday Life*, vol. 9194, 2015, pp. 435–445.
- [46] A. L. Culén, S. Finken, and T. Bratteteig, "Design and Interaction in a Smart Gym: Cognitive and Bodily Mastering," in *Human Factors in Computing and Informatics*, A. Holzinger, M. Ziefle, M. Hitz, and M. Debevc, Eds. Springer Berlin Heidelberg, 2013, pp. 609–616.
- [47] K. Höök, P. Dalsgaard, S. Reeves, J. Bardzell, J. Löwgren, E. Stolterman, and Y. Rogers, "Knowledge Production in Interaction Design," in *Proceedings of the 33rd Annual ACM Conference Extended Abstracts on Human Factors in Computing Systems*, New York, NY, USA, 2015, pp. 2429–2432.
- [48] C. Lévi-Strauss, *The Savage Mind*. University of Chicago Press, 1966.
- [49] A. L. Culén, H. N. Mainsah, and S. Finken, "Design, Creativity and Human Computer Interaction Design Education," *J. Adv. Life Sci.* V 6 N 34 2014, vol. 6, no. 3&4, 2014.
- [50] A. A. Gasparini, "Perspective and Use of Empathy in Design Thinking," in *ACHI 2015*, 2015.
- [51] J. Berggren, G. Schistad, and T. Borge, "UTAIN - Interactive fountain." 2014.
- [52] "KlePå - INF2260 - Høst 2014 - Universitetet i Oslo." [Online]. Available: <http://www.uio.no/studier/emner/matnat/ifi/INF2260/h14/presentations/KleP%C3%A5/>. [Accessed: 01-Dec-2015].
- [53] A. L. Culén and A. A. Gasparini, "HCI and Design Thinking: Effects on Innovation in the Academic Library," in *Proceedings of the International Conferences on Interfaces and Human Computer Interaction 2015*, 2015, pp. 3–10.
- [54] M. Wiberg and E. Stolterman, "What Makes a Prototype Novel?: A Knowledge Contribution Concern for Interaction Design Research," in *Proceedings of the 8th Nordic Conference on Human-Computer Interaction: Fun, Fast, Foundational*, New York, NY, USA, 2014, pp. 531–540.

## Human-Machine Cooperation Loop in Game Playing

Maciej Świechowski\*, Kathryn Merrick†, Jacek Mańdziuk‡§, Hussein Abbass†

\*Systems Research Institute, Polish Academy of Sciences, Warsaw, Poland

Email: m.swiechowski@ibspan.waw.pl

†School of Engineering and Information Technology, University of New South Wales, Canberra, Australia

Email: (k.merrick, h.abbass)@adfa.edu.au

‡Faculty of Mathematics and Information Science, Warsaw University of Technology, Warsaw, Poland

§School of Computer Engineering, Nanyang Technological University, Singapore

Email: j.mandziuk@mini.pw.edu.pl

**Abstract**—This paper presents a new concept for human-machine iterative cooperation based on the Upper Confidence Bounds Applied to Trees method. Analysis of such human-computer cooperation may potentially lead to pertinent insights related to performance improvement of both the human subject and an artificial agent (machine) during certain kinds of strategic interactions. While the experiments described in this paper refer to the so-called General Game Playing (being a certain embodiment of multi-game playing) the overall idea of proposed human-machine cooperation loop extends beyond game domain and can, in principle, be implemented in the form of a flexible general-purpose system applicable to cooperative problem solving or strategic interactions of various kinds. The concept proposed in this study is evaluated by means of a direct involvement of human subjects in specifically defined cooperative environment, which provides vast opportunity to learn from and cooperate with an artificial game playing agent under the certain rules of cooperation. The choice of games is seemingly important to this kind of experiment. Although the participants played better with the assistance of the machine in some of the games, they lost the track in subsequent matches when the assistance was (intentionally) no longer available. Possible reasons for such an activity pattern are discussed in the conclusions. Three design iterations showing evolution of the experiment setup are presented in the paper. The analysis of cooperative and non-cooperative matches reveals different patterns for each chosen game characterized by various levels of advantage gained by means of cooperation.

**Keywords**—human-machine cooperation; human learning, game playing; UCT algorithm.

### I. INTRODUCTION

In this paper, we extend the finding and ideas proposed in our previous conference paper [1] devoted to human-machine cooperation in General Game Playing [2]. Based on the outcomes of the initial experimental studies presented in [1], a new refined experimental setup and new extended experimental results are proposed in this paper. The conclusions listed in [1] are revisited, strengthened and better motivated.

General Game Playing (GGP), by some researchers claimed to be one of the ‘grand AI challenges’ in games and a step towards machine manifestation of possessing human-like intelligence [3], [4], gained recently a lot of attention due to popularization of the annual world-wide General Game Playing Contest organized by people affiliated with Stanford Logic Group at Stanford University [5]. This event is currently the most prominent embodiment of the multi-game playing idea, which aims to create systems capable of playing a variety of games (as opposed to agents that can only play single games).

Hence, the design, study and verification of approaches that allow for cooperation between humans and GGP agents is an important research avenue and complementary research stream to the mainstream research activities. We believe that analysis of such human-computer cooperation may potentially lead to pertinent insights related to performance improvement of both the human subject and an artificial agent (machine) during certain kinds of strategic interactions.

In this study, we continue our attempts to building a system that would enable effective cooperation between human subject and machine player by means of iterative strategic cooperation. We borrowed the concept of cooperation from [6] stating that it takes place when two systems cause each other to modify their behavior to achieve some mutual advantage. Since our focus is on human-machine cooperative loop, we do not explicitly discuss in the paper the principles of cooperation between humans. The readers interested in this area may be willing to consult [7], or [8] as a starting point.

The particular type of strategic interaction considered in this research is collaborative game playing. The type of machine cooperators will be a GGP [2] agent based on the Monte Carlo Tree-Search (MCTS) method. The MCTS is used as the main routine of the strongest state-of-the-art GGP players and is also widely applied to other games such as Go [9] or Arimaa [10] as well as other areas of Artificial Intelligence (AI), including decision problems based on Partially Observable Markov Decision Processes [11], [12], [13], Dynamic Vehicle Routing Problems [14] or Risk-Aware Project Scheduling [15], [16].

The paper reports on several human user studies performed to validate the proposed approach to human-machine cooperation. We will start with presentation of two pilot experiments performed with the two following aims: (1) verification (in terms of effectiveness, clarity, user-friendliness) of the experimental setup for human-machine cooperation and (2) providing preliminary verification of our research hypothesis. Next, we will present a large-scale experiment, in which the disadvantages and pitfalls of the preliminary design were (to a large extent) eliminated. Clearly, apart from providing the circumstances for potentially successful cooperation, we are also interested in measuring the effects of such cooperation, i.e., verify to which extent it affects/improves the average quality of play.

While human-machine interaction [17] has been a hot research topic in various domains outside the game area, e.g., in aviation [18], complex products design [19] or surgery [20],

surprisingly in games the task of creating strong machine players appeared to be challenging enough *per se* [9], [21], [22]. Consequently, to the best of our knowledge, except for our initial study [1], there has not been any related work concerning human-machine cooperation neither in GGP nor in the MCTS game-playing framework. We believe that the way we approach the problem of cooperation can contribute to the area of general knowledge-free and learning-based methods in games [23] and beyond this area, since we can examine the way humans learn from machines and *vice versa* provide a basis for development of automatic or semi-automatic methods by which machines can learn from humans how to play games (or solve problems in a more general perspective).

The remainder of the paper is organized as follows: the next two sections contain brief descriptions of GGP, MCTS and our cooperation platform within the MCTS framework. In Section IV the research hypotheses are formulated. Section V describes the two particular setups tested in the two pilot studies and summaries the main outcomes and conclusions that stemmed from these studies. Sections VI and VII present the new refined experimental setup and the outcomes of this main experiment, respectively. The last section is devoted to conclusions and directions for future work.

## II. INTRODUCTION TO GENERAL GAME PLAYING AND MONTE CARLO TREE SEARCH

In this section, a brief introduction to the General Game Playing and Monte Carlo Tree Search is provided. In particular, the way MCTS is applied to GGP is discussed in more detail, since the machine cooperator is actually a GGP player that relies on MCTS scheme enhanced by a bunch of local, lightweight heuristics.

### A. GGP Preliminaries

GGP is a trend in AI which involves creating computer systems, known as GGP agents, capable of playing a variety of games with a high level of competence. The range of games playable within the GGP framework consists of any finite deterministic game. Unlike specialized playing programs, GGP systems do not know rules of the games being played until they actually start. The concept of designing universal game playing agents is also known as multi-game playing or metagaming, but as stated in the introduction, we refer to the Stanford's definition of GGP [2], which is the most recent one. The official GGP Competition, which is *de facto* the World Championship Tournament, is also part of the GGP specification. The machine player used in this research is our entry in the latest installment of the competition (2014). Borrowing from the GGP terminology, we will use the term *play clock* for the time (in seconds) available to make a move by a player. In addition to *play clock*, there is also *start clock*, which is the time spanning from starting the match until the first move is to be played. During the *start clock* players may think and do any kind of meta-gaming prior to the actual game start. To enable matches between our GGP program and humans, we had to slightly loosen the official specification. For instance, GGP agents are normally penalized for not responding with a legal move in time by having the move chosen for them at random. In our scenario, human participants can think about moves as long as they want to without any penalty and the machine players always respond

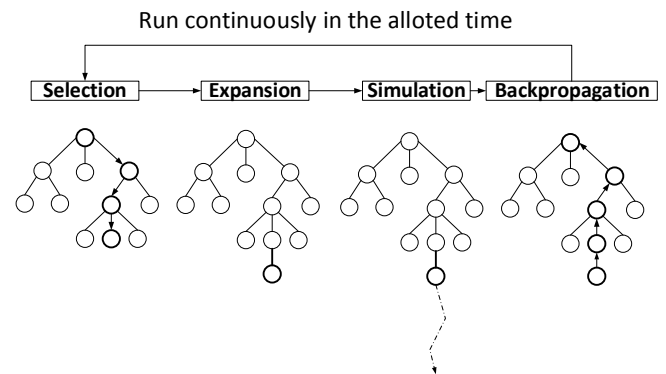


Figure 1. The four phases of Monte Carlo Tree Search algorithm. The algorithm is repeated until the allotted time runs out.

in time. In GGP, the rules of the games to play are a real-time input parameter written in a specialized language called Game Description Language (GDL) [24]. We will not go into details of this language other than it is relatively slow to interpret in a program, therefore, it required to set the *play clocks* to a relatively long time.

### B. The Tree-Search Algorithms Used

MCTS is an algorithm for searching a game tree in a quasi-random fashion in order to obtain as accurate an assessment of game states as possible. In general, the assessment is computed statistically as the average score -  $Q$  - which is defined by the total score of simulations going through a state divided by the number of visits to that state. The total score is a sum of the outcomes of simulations. For all games considered in this article, the value of 1.0 denotes a win, 0.5 denotes a draw and 0.0 denotes a loss in a single simulation. The input to the method is the current game state. Then, the algorithm gradually searches the game tree starting from the current state in a series of iterations adding one node in each of them. An iteration, depicted in Figure 1, consists of the following four steps:

- 1) **Selection.** Start from the root and go progressively down. In each node, choose the child node according to a given selection policy until reaching a leaf node.
- 2) **Expansion.** If a state contained in the leaf node is not terminal, choose an action that would fall out of the tree. Allocate a new child node associated with that action.
- 3) **Simulation.** Starting from a state associated with the newly expanded node, perform a full game simulation (i.e., to a terminal state).
- 4) **Backpropagation.** Fetch the result of the simulated game. Update statistics (average scores, numbers of visits) of all nodes on the path of simulation, starting from the newly expanded node up to the root node.

In the classical MCTS implementations, the selection policy of child nodes in step 1) is either uniform (each child can be selected with equal probability) or greedy (a child with the highest score hitherto, i.e., the most promising one, is selected). A significant improvement over the pure MCTS is the Upper Confidence Bounds Applied to Trees (UCT) algorithm [25], which allows for maintaining a balance between the

exploration and exploitation ratio in the selection step. Instead of sampling each action uniformly or greedily, the following scheme is advised:

- 1) **Selection.** If there are child nodes not yet selected (in previous simulations) choose one of them at random. Otherwise, select child node  $a^*$  according to the following formula:

$$a^* = \arg \max_{a \in A(s)} \left\{ Q(s, a) + C \sqrt{\frac{\ln[N(s)]}{N(s, a)}} \right\} \quad (1)$$

where  $s$  is the current state;  $a$  is an action in this state;  $A(s)$  is a set of actions available in state  $s$ ;  $Q(s, a)$  is an assessment of performing action  $a$  in state  $s$ ;  $N(s)$  is a number of previous visits to state  $s$ ;  $N(s, a)$  is a number of times an action  $a$  has been sampled in state  $s$ ;  $C$  is the exploration ratio constant.

In summary, the input to the UCT method is the current state. Then, the algorithm gradually searches the game tree starting from the current state in a series of simulations adding one node in each of them. Actions within the built part of the tree (the selection phase) are chosen according to Equation (1) whereas actions outside of the tree (the simulation phase) are chosen quasi-randomly with the help of lightweight heuristics (for the sake of clarity of the presentation, we will not get into details here but interested readers may consult our papers [26], [27]). Nodes store the average players' scores obtained in the process of these iterations.

In contrast to all the variations of min-max alpha-beta search, the MCTS is an aheuristic, anytime and relatively easy to parallelize method. Aheuristic means that there are no game-specific knowledge required (heuristics) so the method can be applied in general domains. The min-max-based search needs the heuristic unless the tree can be search thoroughly. Moreover, the algorithm can be stopped at virtually anytime and still give the currently best answer. It asymptotically converges to the perfect play although the convergence can be very slow. The quality (or accuracy) of the answer is a function of time allocated for the process. Finally, it is considerably easy to parallelize because many simulations can be run in parallel.

In order to illustrate the way the MCTS algorithm works, let us consider a game between two MCTS-based machine players in a well-known game of Connect-4. In each step, each of the players was allotted 7 second for a move. Four interesting steps were selected from the played game. Figure 2 shows snapshots of the game board taken in these four steps (after the move was performed). The statistics computed for each available action (move) just prior to the presented game positions are provided below in the text. Please note that  $Q$  and  $N$  denote the UCT parameters from Equation (1). The boundary values of  $Q$  are equal to 0 (expected loss for red) and 100 (expected victory for red), respectively.

In step 1, two moves putting stones in the middlemost columns, i.e., 4 and 5, were clearly the best for the red player.

STEP 1

[Drop in column 1]	Q: 50.0	N: 2319
[Drop in column 2]	Q: 53.3	N: 3294
[Drop in column 3]	Q: 58.4	N: 6743
[Drop in column 4]	Q: 61.7	N: 12829
[Drop in column 5]	Q: 61.4	N: 11896
[Drop in column 6]	Q: 57.4	N: 5677

[Drop in column 7]	Q: 52.5	N: 3017
[Drop in column 8]	Q: 50.8	N: 2522

In step 3, the best strategy for red was to continue putting stones in the middle and block the blue player:

STEP 3

[Drop in column 1]	Q: 56.1	N: 6263
[Drop in column 2]	Q: 55.9	N: 6036
[Drop in column 3]	Q: 54.4	N: 4882
[Drop in column 4]	Q: 59.3	N: 11395
[Drop in column 5]	Q: 59.7	N: 12208
[Drop in column 6]	Q: 53.1	N: 4094
[Drop in column 7]	Q: 55.4	N: 5601
[Drop in column 8]	Q: 53.9	N: 4552

In step 15, the highest  $Q$  value was equal to 55.6, which means that the red player was slightly more likely to win, but the MCTS/UCT algorithm does not see any path leading to a very strong position (very likely victory) of this player (and of the other, as well):

STEP 15

[Drop in column 1]	Q: 55.6	N: 44908
[Drop in column 2]	Q: 46.0	N: 4945
[Drop in column 3]	Q: 47.1	N: 5788
[Drop in column 4]	Q: 44.8	N: 4241
[Drop in column 5]	Q: 47.0	N: 5737
[Drop in column 6]	Q: 43.7	N: 3679
[Drop in column 7]	Q: 44.8	N: 4205
[Drop in column 8]	Q: 43.4	N: 3547

Finally, in step 41, three out of four actions were assigned  $Q = 100$  meaning that they lead to a victory for red. Only the last action resulted in an immediate win, but the length of a winning path makes no difference to the MCTS/UCT assessment.

STEP 41

[Drop in column 2]	Q: 100.0	N: 2567553
[Drop in column 3]	Q: 26.3	N: 259
[Drop in column 7]	Q: 100.0	N: 2567833
[Drop in column 8]	Q: 100.0	N: 2681408

### III. COOPERATION IN THE MCTS/UCT FRAMEWORK

The machine cooperater used in this paper is an adapted MiNI-Player [26], [27], [28] - a GGP tournament-class program equipped with additional features to enable cooperation. The cooperation is accomplished mainly by means of statistics provided by the machine to help humans choose which move to play. During both cooperative and non-cooperative plays, it is always a human who makes the final choice. When the statistics are presented, i.e., in the cooperative mode, it is up to the participant whether or not to take advantage of them.

The second means of cooperation is by permitting interference with the MCTS/UCT. At this point, we need to clarify that there are two versions of the program participants operate with: with and without cooperation. Both possibilities are embedded in the same (common) program and the cooperation option is either enabled or switched off. In this way, we propose an interactive process of building the game tree, while playing the game, involving both the machine and human. In the original MCTS/UCT, the same four-phase algorithm is repeated all the

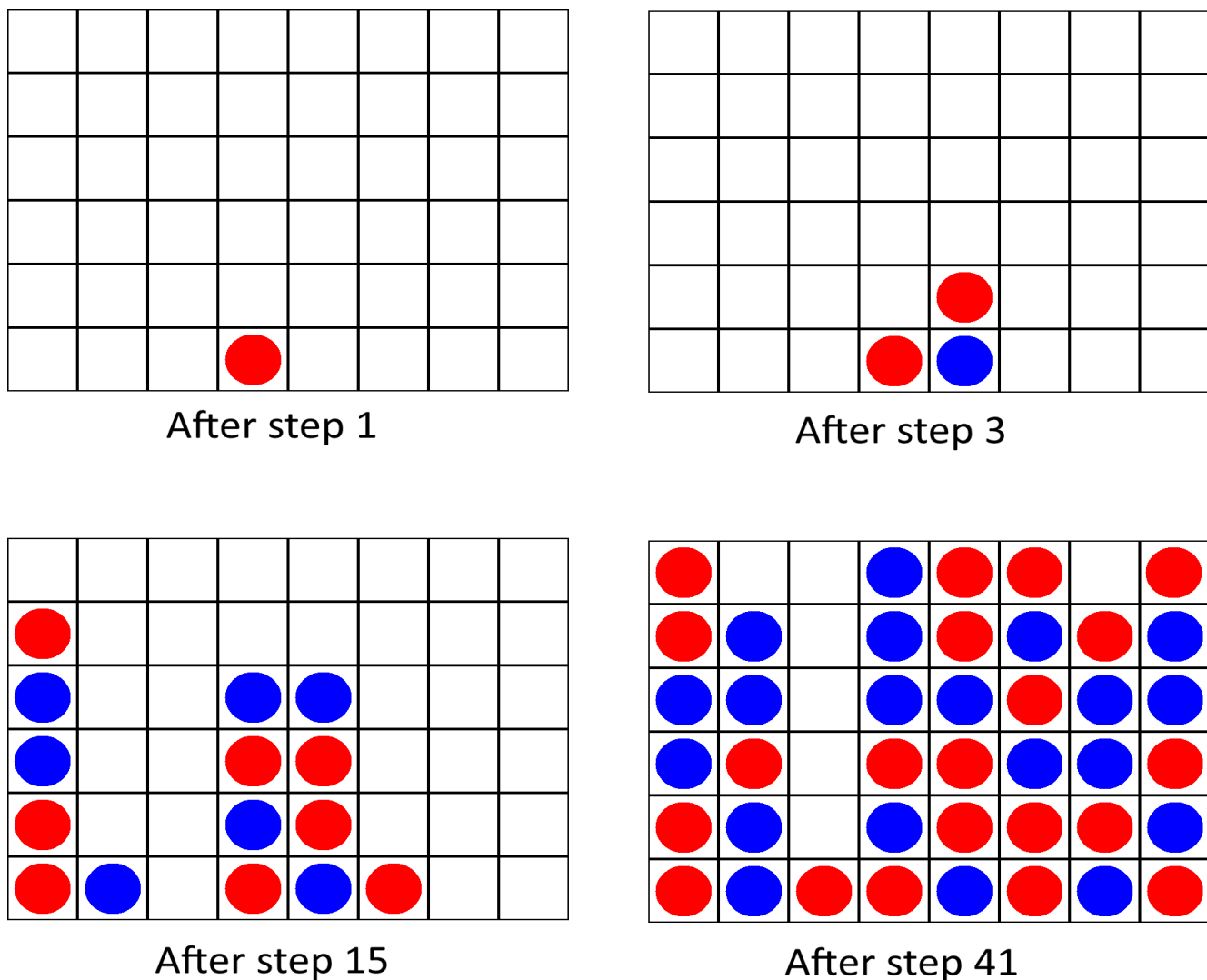


Figure 2. Board states after moves 1,3,15, and 41 extracted from a game between two MCTS-based computer playing programs in Connect Four.

time during the *play clock*. For cooperative purposes we split this time into three equal intervals  $T1 + T2 + T3 = \textit{play clock}$ . Between any two consecutive intervals (T1 and T2 or T2 and T3) humans can interact with the MCTS/UCT based on statistics presented to them. The statistics include: each action  $a$  available to the player to make a move with the  $Q(s,a)$  and  $N(s,a)$  values from (1). These values are scaled to the [0%, 100%] interval to be more readable by the participants. The final statistic is the actual number of simulations which ended with a win, draw and loss for the subject, respectively. The MCTS/UCT can be directed by the human in two ways: enabling/disabling actions available in the current state or toggling priorities of the actions on/off. If an action is disabled, the MCTS/UCT will ignore this action in the selection step, which means that no simulations will start with a disabled action. Changing the priority is equivalent to changing the value of the  $C$  parameter in (1) from 1 to 10. Participants are allowed to make any number of the aforementioned interventions at each step and once they are done, they click the simulate button to submit all of them in one batch and observe how the statistics have changed. By doing so, they can help the machine to focus

on the most promising actions and avoid presumably wasteful computations. In this way, the human→machine cooperation happens. On the other hand, the feedback from the machine supports or questions the above-mentioned human player's choices. The machine→human cooperation is naturally accomplished by means of providing human player with all moves-related statistics calculated by the machine during simulations and allowing human to react accordingly. The reaction can be realized either by setting up particular actions in the simulation phase or making a particular move in the played (real) game. Since there are three simulation phases before each move played in a game, the cooperation happens, *de facto*, in a loop.

Our experimental design is justified by the two following observations. First of all, in many well-established games, it has been found that the experts can intuitively discard unpromising actions and focus on the few best ones. Such behavior is manifested by human playing experience and intuition and is one of the aspects in which humans are better than machines despite having comparably "less computational power". Provided that the human choice is correct, the process can converge faster to the optimal play. The introduction of

action priority is a similar, but slightly weaker, modification to the MCTS/UCT algorithm. The second observation (or assumption) we made is that the cooperation has to be easy for participants to understand. Therefore, we avoided asking them to set the internal parameters of the algorithm or to deal with more complicated operations on the tree structure. In fact, the participants do not even need to know that the tree exists.

#### IV. RESEARCH HYPOTHESIS

In order to better focus the study on performance of human-machine cooperation, we formulated the following research hypothesis: **a human cooperating with a machine GGP agent is a better player than human or machine agent individually.** We write this thesis in a shortened form of  $H + M > M$  and  $H + M > H$ , where  $H$  denotes a human player;  $M$  denotes a machine player and  $M + H$  denotes a hybrid player comprising a cooperating machine and human.

We attempt to verify this hypothesis in a devoted experiment or at least make a step towards such a verification. The main research question is whether a mutually beneficial cooperation can originate and develop between human and machine players. In order to verify the above-listed hypotheses, we gathered samples from people playing without any machine assistance ( $H$  vs.  $M$ ) and with such assistance ( $H+M$  vs.  $M$ ). The first case involves a human simply playing a match against MINI-Player [26], [27], [28]. The second case involves a human playing against the same opponent but this time with assistance of a “friendly” GGP agent (a clone of MiNI Player) running in the background. Before we move to the experiment setup, let us discuss the meaning of all possible outcomes:

- **$H + M > M$**  If also  $H + M > H$  holds, then we can say that there are truly mutual benefits of the cooperation.
- **$H + M > H$**  Humans with machine assistance play better than those without.
- **$H + M = M$**  Humans do not improve the level of play of machines.
- **$H + M = H$**  Humans do not make any quantifiable positive use of the machine assistance.
- **$H + M < M$**  Humans not only do not benefit from machine assistance, but also degrades the machine playing performance.
- **$H + M < H$**  The machine assistance is deceptive to humans thus decreasing their quality of play.

#### V. PILOT STUDIES

This section reports on the results of two pilot studies that we have run to refine our experimental setup as well as to gather preliminary evidence regarding the research hypothesis. In particular, we present a technical setup and provide the profile of the human players participating in the experiment.

Since a well-played game is time consuming, we limited the number of games a single person can play to three. The experiment was performed separately for each human subject, so no information could be exchanged in the process, e.g., looking how other people play. The program participants used to play, and the opponent program were run on the same computer, both having access to two physical CPU cores. We set the *play clock* for the two machines (the cooperator and adversary) to 30 seconds in the first pilot study and 9 seconds

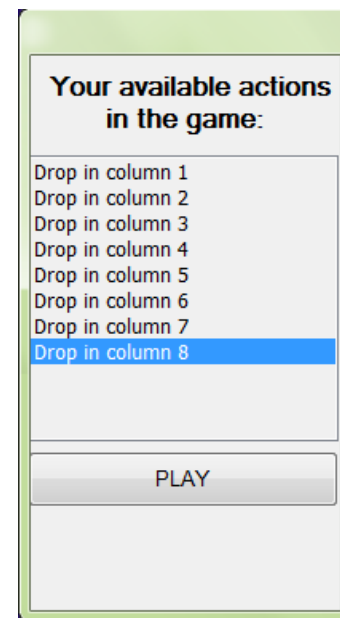


Figure 3. The window used to choose an action during a game.

in the second one. In order to avoid time-outs resulting from the human player, we discarded the concept of random moves if a player fails to respond in time. The matches were played only during weekdays anytime from the morning to the late afternoon. The age of participants varied from 21 to 30 with only one exception of 31 to 40. Most of them were PhD students of computer science.

In the experiment, three games were used but one of them, namely Tic-Tac-Chess, was discarded after the Pilot Study 1 as it appeared to be too biased in favor of the player making the first move. Descriptions as well as screenshots of all the games can be found in the Appendix. Figures 7, 8, and 9 show screenshots of the program operated by participants for Inverted Pentago, Nine Board Tic-Tac-Toe and Tic-Tac-Chess respectively, the three games played in Pilot Studies.

The user interface consisted of three windows: the action window, the board window and the cooperation window. The action window is presented in Figure 3. It displays moves available to the participant and contains a button for making an actual (i.e., not simulated) move in the game. The board window presents the current game state (board) - please refer to the Appendix for some examples. Finally, the cooperation window, depicted in Figure 4, provides the statistics from simulations and enables the cooperation options which were discussed in Section III. The only difference, in terms of the user interface, between cooperative and non-cooperative games is that in the latter case, the cooperation window is not shown.

##### A. Pilot Study 1

We gathered 6 human participants for the first pilot study. They were divided into two groups of 3 people each. These two groups formed our two samples of data: playing with machine assistance ( $H+M$ ) and without ( $H$ ). During the experiment, we started each game with a short training session. We also gave participants a transcript explaining what they are asked to do and how the user-interface works. When participants

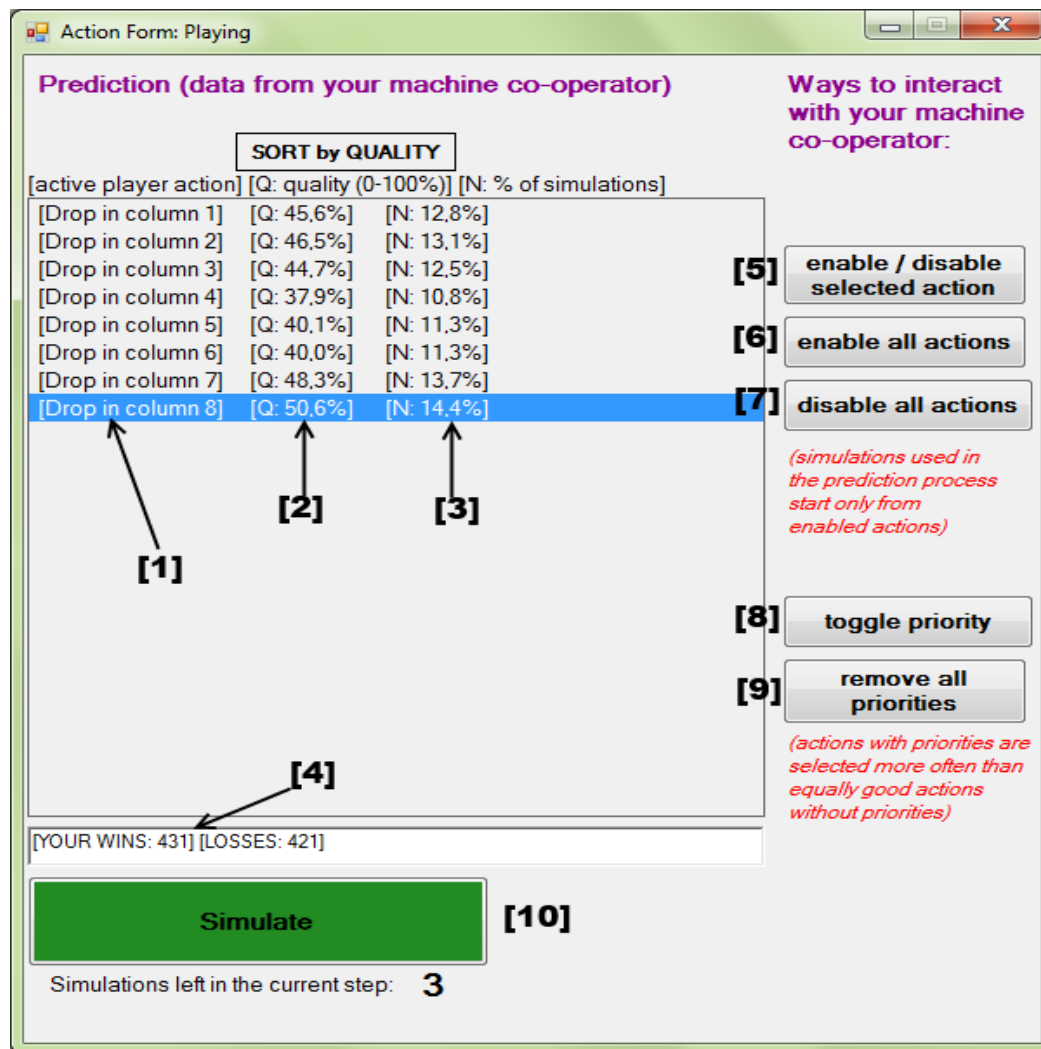


Figure 4. The window human players used to cooperate with the machine player. [1] - action name; [2] - the quality of an action (Q) computed by the MCTS/UCT algorithm, shown as a percentage chance of winning the game by the human player; [3] - the percentage of simulations (relative to the total number of simulations), in which a particular action was investigated; [4] - this field, after selecting an action, it shows the number of simulations which ended with wins, draws and losses, respectively, from the human player's perspective; [5][6][7] - an interface for disabling and enabling actions to be used in the simulations; [8][9] - an interface for managing priorities of actions (to make them used more frequently than they would be used otherwise, i.e. without priority settings); [10] - when participants were satisfied with the selection of the enabled actions and priority assignments, they would click this button to run a batch of simulations.

were ready, they started playing a serious (i.e., not training) game and when they finished all three matches they were asked to complete a short questionnaire to obtain a profile of the subjects. The assignment of human players to games was based on the *Latin square design* [29] with 3 games, 6 participants and two playing modes, i.e., with machine assistance being switched ON or OFF. Using this design, the minimum required number of participants for a full experiment is 12, but in the pilot study we stopped at 6 participants.

### B. Pilot Study 2

At this point, we decided to revisit the experimental setup slightly and continue the experiment, called pilot study 2, to mitigate some problems that arose. Instead of asking people to play each game once, we asked them to play one game three times in order to enable learning by experience. The first match played includes a training session. The training session

was extended to be a full match to let participants learn from their mistakes in endgames (late phases), which are often the most tricky to play. It is also often the case that people learn how to play better from the way they lost.

As mentioned above, we excluded Tic-Tac-Chess from the set of games for giving too much advantage to the first player to have a turn. As a consequence, each subject lost their match very quickly in the same way leaving us with no relevant data to work on. Although there exist certain strategies to avoid a quick loss, it is unlikely to be seen by players unfamiliar with the game. Having only one type of game per participant, we modified the players' assignment in such way that we have all combinations of participants playing at least one of the three consecutive matches with the co-operation of the machine.

In order to deal with the problem of long experiments, which was mainly caused by the simulation time needed to get meaningful results, we decided to write highly-optimized

dedicated interpreters for rules of the chosen games. We were able to reduce the *play clock* just to 9 seconds.

### C. Results of Pilot Studies

Numerical outcomes and human players' behavior during the experiments allowed us to make the following observations:

- The score between samples is even.
- All games appear to be very demanding for participants.
- There were no wins for Inverted Pentago and for Tic-Tac-Chess (discarded in the pilot study 2). There were 2 wins for Nine Board Tic-Tac-Toe, one with the cooperation and one without.
- The main reason for poor performance as specified by subjects in the questionnaire and communicated right after the end of the experiment was the lack of experience in playing given games. The rotations in Pentago were commonly mentioned as something being particularly difficult.
- Despite understanding the role of the program and the advice provided to them, the participants often seemed not to have desire to cooperate. If they had an assumption about which action was the best, they just opted to play it instead of investing time for more simulations.
- The participants seemed to enjoy playing the game but some stress was caused by the level of difficulty and the expectation to win.

Figure 5 shows the average scores (0 meaning loss, 50 meaning draw and 100 meaning victory) obtained by the cooperating participants (H+M) and non-cooperating participants (H) against the machine in Inverted Pentago whereas Figure 6 shows the same data for Nine Board Tic-Tac-Toe. Vertical error bars denote 95% confidence intervals. The X axis denotes game step (ply). The error bars overlap so the results cannot be used yet to formally verify the hypothesis.

There were not enough participants in the pilot study to make any statistically significant claims. However, the trend so far is that the participants who did not cooperate played slightly better average games. This is reflected in the **H vs M** curve, starting from step 10, being above the **H + M vs M** one. However, both curves eventually meet at a common point, which means that the average game results of both samples are even and equal to zero (which means a loss). The same properties are valid in the Nine Board Tic-Tac-Toe game. Because in the pilot studies, the participants rarely and quite chaotically used the cooperation possibilities, a conclusion that cooperation does not help would be an overstatement. The sample is too small, the participants would use the provided statistics when already behind in the game and because the cooperation options were shown only every second move, the machine was not able to help with a coherent line of actions.

## VI. REFINED EXPERIMENT

### A. Changes after Pilot Studies

Based on the lessons learnt from the pilot studies we have made a list of desirable changes to be introduced before moving to the final phase of the experiment. Among various

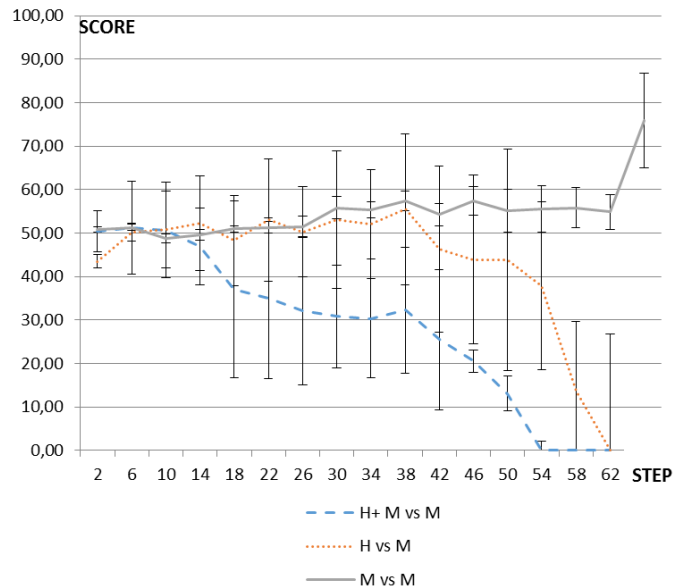


Figure 5. Graph showing the average scores obtained by the cooperating participants (H+M) and not cooperating participants (H) against the machine in Inverted Pentago.

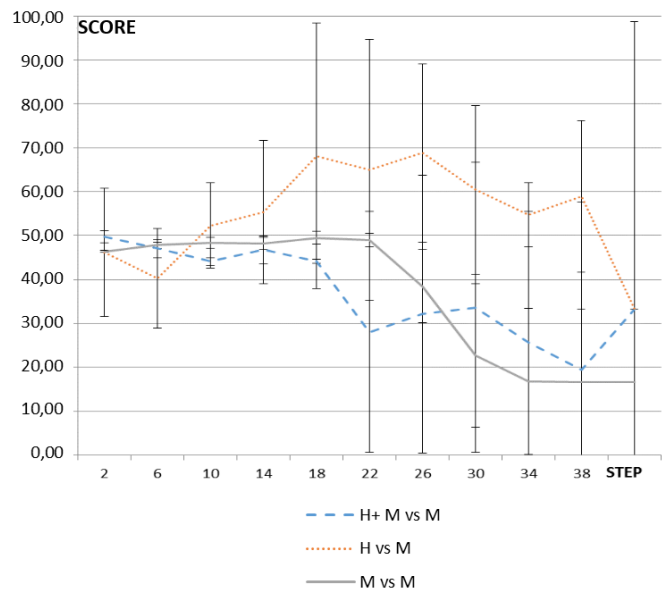


Figure 6. Graph showing the average scores obtained by the cooperating participants (H+M) and not cooperating participants (H) against the machine in Nine Board Tic-Tac-Toe.

observations the following four points seem to be the most relevant.

- In order to have a chance to observe any progress in playing, each subject should play a given game more than three times, preferably at least five. We have to make room for more learning possibilities as it turned out that three games were not enough to learn how to play previously unknown game well (e.g., Inverted Pentago or Nine Board Tic-Tac-Toe).

With more repeats we can also slightly reduce (though not eliminate) the effect of personal predispositions.

- The cooperation options should definitely be shown all the time for players playing with the help of a machine.
- Actions' priorities should be removed and only the mechanism of enabling and disabling actions should be left as the latter has more influence on the game tree and should be used more often. We have to make sure that all the participants understand why and when it is beneficial to disable actions.
- Participants should be asked to play two games with the machine cooperation in the middle (e.g., the second and the third ones) to be able to observe, in the remaining games, the effects of learning from those (supervised) games.

We analyzed the average outcomes of matches for the H + M vs. M and H vs. M samples of data as well as the average evaluation observed by the machine in every 4 steps of games. The 95% confidence intervals were computed using the t-student test. The results showed that the number of participants in the pilot study is not enough to make any significant claims regarding the hypothesis. Therefore, our plans shifted towards investigating how participants cooperate and whether they can learn the game faster by playing with machine assistance.

### B. Setup of the Experiment

All the changes enumerated in the previous paragraph were pursued in the refined setup. In terms of the user interface two changes were introduced: firstly, the toggle priority button was removed (since it was very rarely used in previous experiments) and secondly, the statistics (the cooperation window) were shown permanently in the cooperation mode. Making the statistics always visible had been identified as a crucial requirement in order to support continuous cooperation loop. We have managed to gather 11 people who agreed to participate in three game sessions of our experiment. All of them were computer science or mathematics students, without any competitive backgrounds in games. None of them knew the games chosen for the experiment. Such a candidate profile, i.e., analytic mind capable of learning quickly unknown games, was deemed appropriate for our experiment. Ultimately, the attendance varied from 9 to 10 people at the same time. Consequently, we do not have full statistics for some people.

Each session was carried out in a computer lab starting by a detailed explanation of the experiment and rules of the current game to play. We ensured that there was no communication and information exchange between the subjects during the experiment.

Three games have been prepared, one for each session, i.e., Nine Board Tic-Tac-Toe in session 1, Cephalopod in session 2 (see Appendix for a description of this new game and Figure 10 for its visualization in our system) and Inverted Pentago in session 3. Each game has been tested for opening balance between the playing sides, i.e., whether one the players is favored over the other one because of them making move in the first/second turn. There are many ways how to check such a property and we decided to repeat hundreds of matches between two machine players and observe the average score.

TABLE I. Games used in respective sessions of the refined experiment. The *Participant* column denotes which player (the first turn or the second turn) participants played as.

Session	Game	Participant	Balance
1	Nine Board TTT	2nd	1st slightly favored
2	Cephalopod	2nd	Practically fair
3	Inverted Pentago	2nd	2nd slightly favored

The setup of games and outcomes related to balance were as shown in Table I.

During a session, we asked each subject to play at least five matches. The first five were mandatory meaning that the participants had agreed to play those beforehand. Each match after the fifth one was optional and some participants took this opportunity to play one or two more games.

In the first session, half of the participants played the second and the third game (out of the mandatory five) in the cooperation with the machine. The other matches were played without the cooperation.

In the second session, those who had not played with the cooperation before, were asked to play games two and three with the cooperation. The main idea was to observe whether any learning process occurs. We could compare whether the cooperating people play the respective games better than the non-cooperating ones as well as whether any effects of learning can be noticed in games played after the cooperation (game fourth and onward). We assumed that playing with the machine assistance at some point may speed-up the learning process.

Finally, in the third session all participants played games two and three in the cooperation in order to gather more samples in this mode.

The average game lasted about 35 minutes and the average five-game session took about 3 hours. We expected this time to be long enough to build up some experience in playing particular games.

## VII. RESULTS OF THE REFINED EXPERIMENT

We present an overview of how each game ended in Tables II, III, and IV for Nine Board Tic-Tac-Toe (session 1), Cephalopod (session 2) and Inverted Pentago (session 3), respectively. The first thing to notice is that players with the machine assistance, therefore, theoretically on a favored position, did not win any match of Nine Board Tic-Tac-Toe whereas there have been wins for players who did not cooperate. Though, nobody was able to win more than two matches.

The only three games won by participants in Cephalopod happened to be in the cooperation mode, however, only in the first assisted games. Nobody out of those three winners was able to repeat a victory, even in the cooperation mode. Since the second assisted games were carried out using the same setup as in the first ones, we consider this "concentration of wins" as a pure coincidence. Overall, this game has proven to be very difficult although it is relatively unbiased when it comes to starting position balance.

In the third session, with Inverted Pentago as the game of choice, participants were playing slightly favored roles, i.e., second to go. In such a setup, in majority of the played moves,

TABLE II. Results of matches of Nine Board Tic-Tac-Toe. In the first column, there are identifiers of participants used cohesively for all games. The respective  $G_i$  column denotes  $i$ -th played game. 100 denotes a win of the participant, 50 denotes a draw, whereas 0 denotes a loss. Scores with stars to them were obtained in games played with the cooperation of the machine player.

Subject	$G_1$	$G_2$	$G_3$	$G_4$	$G_5$	$G_6$	$G_7$
1	0	0*	0*	0	0	-	-
2	0	0*	0*	0	0	-	-
3	0	0*	0*	0	0	-	-
4	0	0*	0*	0	0	-	-
5	0	0*	0*	0	0	-	-
6	0	0	100	0	0	-	-
7	100	100	0	0	0	-	-
8	100	0	0	100	0	-	-
9	0	0	0	0	0	0	100
10	-	-	-	-	-	-	-
11	0	100	0	0	0	0	-

TABLE III. Results of matches of Cephalopod. Please refer to Table II for the cells' interpretation.

Subject	$G_1$	$G_2$	$G_3$	$G_4$	$G_5$	$G_6$	$G_7$
1	0	0	0	0	0	-	-
2	0	0	0	0	0	-	-
3	0	0	0	0	0	-	-
4	0	0	0	0	0	0	0
5	0	0	0	0	0	0	0
6	0	0*	0*	0	0	-	-
7	0	0*	0*	0	0	-	-
8	0	100*	0*	0	0	-	-
9	0	100*	0*	0	0	-	-
10	0	100*	0*	0	0	-	-
11	-	-	-	-	-	-	-

TABLE IV. Results of matches of Inverted Pentago. Please refer to Table II for the cells' interpretation.

Subject	$G_1$	$G_2$	$G_3$	$G_4$	$G_5$	$G_6$	$G_7$
1	0	100*	50*	0	0	-	-
2	0	50*	50*	0	0	-	-
3	0	100*	0*	0	0	-	-
4	0	50*	50*	0	0	-	-
5	0	100*	100*	0	0	-	-
6	-	-	-	-	-	-	-
7	0	100*	0*	0	0	-	-
8	0	50*	100*	0	0	-	-
9	0	50*	100*	0	0	-	-
10	0	100*	50*	0	0	-	-
11	-	-	-	-	-	-	-

one does not have to do anything more to win than just to follow the machine cooperators suggestion. The only won or drawn games indeed happened to be in the cooperation mode. The main reason for that was the strength of the machine cooperators. When not played in the cooperation mode, all games were lost.

Analysis of the results shows that the cooperation is significantly helpful in Inverted Pentago. It may be beneficial for Cephalopod as well, but the sample is not big enough to make such a claim. What definitely stands out is that no learning patterns can be observed. Players who won (or drew) once were not able to repeat this result convincingly.

In order to facilitate the detailed analysis of results let us introduce a concept of the rank of a move by means of the machine evaluation, i.e., based on the average score  $Q$  computed by the UCT algorithm using Equation (1). The rank

of 1 means that the move is the best according to the machine, i.e., has the highest  $Q$ . The rank of 2 denotes the second best (the second highest  $Q$ ) and so on. Those ranks were logged for each played move in all matches, even in games without the cooperation because the machine still computed all the statistics without showing them to players. The average and median ranks were then computed for a match and next aggregated for all matches with and without the cooperation.

Tables V and VI show some aggregated statistics gathered separately for games played with and without cooperation. It could be seen from Table V that players were generally choosing moves that were highly ranked in the cooperation mode, especially in Nine Board TTT and Inverted Pentago. Please recall that the *MedRank* and *AvgRank* indicators are the averages (over subjects) from median and average ranks, respectively, based on moves played in each game. Both these indicators are significantly lower, with 95% confidence, than their counterparts computed for matches without cooperation.

These average scores show that lower ranks do not necessarily translate into better outcomes since the game-related starting bias should also be taken into consideration when analysing these move-ranking statistics. Since the machine opponent is slightly favored at the beginning of Nine Board Tic-Tac-Toe games, a human player should disagree with the machine evaluation, at least at some point, to give themselves a chance to turn the game into their favor. If they do not, the machine playing the slightly favored role against itself has a very high chance for winning. That is why there have been more wins in Inverted Pentago, in which the situation is the opposite.

Table VI presents how many times (in game steps) the chosen move was within the 15% margin of the best move by means of machine evaluation, in which case we call it a *good move*. The average number of game steps is included for reference. We also introduce a concept of a mistake which occurs when the played move is evaluated at least 20% worse than the previously played one. As shown in Table VI, the average number of such mistakes per game varied from 0.3 (Inverted Pentago, cooperation) to 7.8 (Cephalopod, no cooperation), which is - most probably - the main reason for so many losses in this game.

The notion of good moves and mistakes is more accurate for Cephalopod and Inverted Pentago since, as stated above, the machine's assessment of moves is higher in these games than in Nine Board Tic-Tac-Toe, which favors the opponent's role. Nevertheless, in NB TTT, the number of mistakes is significantly higher in the cooperative mode, which means that subjects chose to disagree with the machine helper at some point, but eventually lost all the games, anyway.

Another statistic shows that the cooperative games took more steps to finish what may suggest that they were more balanced until the game reached the conclusion phase.

It is worth underlying that participants used the cooperation options actively, when playing in this mode, almost in every step of every game. The differences in median and average move ranks, which can be read from Table V, suggest that participants also actively used the information provided by the machine player. However, without asking participants explicitly whether a particular play was a result of the machine suggestion, we cannot be sure whether this claim is true. On the

TABLE V. Selected averaged statistics grouped for each game for both cooperation modes. *MedRank* and *AvgRank* denote median and average ranks of moves taken by players, respectively. The ranking is defined by the machine evaluation of moves, e.g., the highest evaluated move has the rank equal to 1. These values are averaged among all matches played for the respective (game, cooperation mode) pair, therefore medians can be non-integer numbers. The last column denotes the average score from 0 (loss) to 100 (win). For each value, the 95% confidence intervals are shown in brackets.

Game	MedRank		AvgRank		AvgScore	
	Coop	NoCoop	Coop	NoCoop	Coop	NoCoop
NB TTT	1.2 (± 0.2)	2.3 (± 0.3)	1.7 (± 0.3)	2.6 (± 0.2)	0 (± 0.0)	16.3 (± 11.1)
Cephalopod	1.3 (± 0.3)	3.5 (± 0.3)	2.3 (± 0.6)	5.1 (± 0.2)	30 (± 29.9)	0 (± 0.0)
Inv. Pentago	1.1 (± 0.2)	5.1 (± 0.4)	2.0 (± 0.4)	6.8 (± 0.5)	66.7 (± 15.8)	0 (± 0.0)

TABLE VI. Selected averaged statistics grouped for each game and for both cooperation modes. *AvgLength* denotes the average number of steps required to complete the games. The *GoodMoves* column denotes the number of steps in which participants played a move with the machine evaluation not lower than the highest evaluated move by more than 15%. The last column denotes the number of steps in which the played move had at least 20% lower evaluation than the previously played one (likely to be a mistake leading to a loss). For each value, the 95% confidence intervals are shown in brackets.

Game	AvgLength		GoodMoves		Mistakes	
	Coop	NoCoop	Coop	NoCoop	Coop	NoCoop
NB TTT	19.1 (± 1.3)	17.5 (± 0.9)	18.1 (± 1.3)	16.5 (± 1.0)	3.5 (± 0.6)	1.8 (± 0.3)
Cephalopod	39.8 (± 2.4)	37.2 (± 0.9)	37.8 (± 2.9)	30.7 (± 1.1)	5.0 (± 2.2)	7.8 (± 0.6)
Inv. Pentago	35.9 (± 0.1)	30.8 (± 1.7)	35.8 (± 0.2)	27.5 (± 1.9)	0.3 (± 0.3)	3.0 (± 0.9)

other hand, posing such a question after each move would have been very disturbing for them, so we had refrained ourselves from that option.

### VIII. CONCLUSIONS AND DIRECTIONS FOR FUTURE RESEARCH

In this paper, the MCTS/UCT algorithm is used as a tool for introducing cooperation between humans and machines during strategic interaction. The particular embodiment of such a cooperation is General Game Playing framework, which is represented in our experimental setup and used in the experiments conducted with human subjects. The MCTS/UCT algorithm has a desirable property that it is able to exploit the raw computational power of machines by running a continuous simulation-based assessment of game states. The method can be regarded as a machine learning approach. The algorithm can, in principle, be steered by the human input to improve its learning rate, although, we have not been able as yet to convincingly justify this claim.

Balancing the proper games difficulty is crucial to this kind of experiment. Certainly, for the cooperation to make sense, humans should not dominate over machines. Furthermore, on the one hand, games have to be difficult enough for humans so as human players should consider statistics computed by the machine as a valuable source of knowledge about the game. On the other hand, however, games cannot be too difficult because unexperienced humans will lose in the vast majority of matches played against the machine without gaining any real

experience/knowledge about how to play the game, at least in the non-cooperation mode.

The initial goal of our experiment was to verify the  $H + M > M$  and  $H + M > H$  hypotheses. It turned out that proving any of these two claims with statistical significance requires many more human participants and much more data. Additionally, successful cooperation between human and machine does not necessarily have to be measured solely by means of the average score achieved in played games. One of the interesting factors indirectly supporting the existence of such cooperation could be, for instance, the observable existence of the learning process emerging in the proposed human-machine cooperation loop.

When looking at the games played in cooperation with the machine player in Nine Board Tic-Tac-Toe, Cephalopod and Inverted Pentago, one can see three different activity patterns. In Nine Board Tic-Tac-Toe, the machine assistance does not really help. In Cephalopod, it has some positive impact, because the only games won by participants involved cooperation. In the last game, people played significantly better with machine assistance. However, in all three cases, no effects of learning could actually be spotted. Even in the case of Inverted Pentago, where many of the games in the cooperation mode ended up well, none of the participants was capable to win or even draw afterwards when played without cooperation. Major differences in the results shapes suggest that the hypotheses  $H + M > M$  and  $H + M > H$  are very sensitive to the choice of game and, therefore, hard to prove or disprove in general case. On a general note, the results show that experimental outcomes which involve human subjects are often inconsistent and drawing any firm conclusion requires much more time and effort than in the case of machine-based experiments.

Our future plans are concentrated on revisiting the experimental environment to make it more learning-friendly for the human subjects. It seems that the basic statistics of actions which are provided to them are not sufficient to *really understand and learn how to play the game*. The participants should learn game-related concepts and patterns and memorize more from the played games than they do in the current setup. They should be able to understand why certain actions are good or bad. In order to learn how to play a game well, the participants probably need more time per session and more sessions separated by a one-two day breaks (i.e., organized in different days). Apparently, it is hard for humans to learn how to play a new non-trivial game during one session only.

Our conclusions, which revolve around the importance of the proper selection of games, in a natural way lead towards the next research steps. It is very likely that not only “pure” difficulty but also other characteristics of games may be decisive in building a successful cooperation framework. Investigation of such features across various games and measuring the extent to which they affect the effectiveness of cooperation is one of the crucial objectives of our future research. The problem is multi-dimensional where “pure” game difficulty is only one of the dimensions. The game difficulty, fairness and interestingness may be measured analytically, e.g., by analyzing the number and the complexity of game rules or game states, or experimentally, based on the outcomes of games with either human players, or specifically designed artificial agents [30]. A similar problem was approached in [31]

from the automatic game design perspective, where the authors proposed 57 computable characteristic features of games such as uncertainty, drama, lead change, permanence, completion, duration, momentum, etc. While the goal of [31] was to find *interesting* games, we believe that similar research principles apply in the quest for *cooperation-friendly* games.

#### APPENDIX GAMES DESCRIPTIONS

**Inverted Pentago** is a game played on a 6x6 board divided into four 3x3 sub-boards (or quadrants). Taking turns, the two players place a marble of their color (either red or blue) onto an unoccupied space on the board, and then rotate any one of the sub-boards by 90 degrees either clockwise or anti-clockwise. A player wins by making their opponent get five of their marbles in a vertical, horizontal or diagonal row (either before or after the sub-board rotation in their move). If all 36 spaces on the board are occupied without a row of five being formed then the game is a draw. Participants play as blue and are the second player to have a turn.

**Nine Board Tic-Tac-Toe.** In nine board tic-tac-toe, nine 3x3 tic-tac-toe boards are arranged in a 3x3 grid. Participants play as 'O' and are the second player to have a turn. The first player may place a piece on any board; all moves afterwards are placed in the empty spaces on the board corresponding to the square of the previous move. For example, if a piece was placed were in the upper-right square of a board, the next move would take place on the upper-right board. If a player cannot place a piece because the indicated board is full, the next piece may be placed on any board. Victory is attained by getting 3 in a row on any board. If all boards are full without any player having a line-of-three, then the game ends with a draw.

**Tic-Tac-Chess** is a game played on a 7x7 board. Players start with one piece marked by a red or blue square in their respective starting location. Participants are the second player to have a turn. The starting locations are outside the movable area of the board, which is defined by the inner 5x5 square. On their turn, each player may move a piece as though it were a Chess knight or capture with a piece as though it were a Chess king. Capturing is possible only with pieces belonging to the center 5x5 square. Pieces from the starting locations do not disappear when moved, so moving a piece from the starting location effectively spawns a new one on a destination square. The first player to get three pieces in a row, column, or diagonal in the center 3x3 square wins. Participants play as blue and are the second player to have a turn.

**Cephalopod** is a game played on a 5x5 board. Taking turns, the two players place a die of their own colour (either white or black) onto an empty cell on the board. Immediately after the die is placed, the capturing conditions are checked and enforced if apply. The placement is capturing if and only if: (1) - the currently added die is horizontally or vertically adjacent (so no more than four neighbours are possible) to at least two dice and (2) - the sum of the pip counts on those adjacent dice is six or less. In both cases it does not matter what colours the adjacent dice are. If the die placement is capturing, then all the horizontally and vertically adjacent dice are removed from the board and the new dice is set to show the sum of the pip counts of the captured dice. Capturing are mandatory only when placing a die onto a square where capturing conditions

apply. The game terminates when the board is full. The player who controls more dice wins. Draws and ties are impossible. Participants play as black and are the second player to have a turn.

#### ACKNOWLEDGMENT

M. Świechowski would like to thank the Foundation for Polish Science under International Projects in Intelligent Computing (MPD) and The European Union within the Innovative Economy Operational Programme and European Regional Development Fund. The research was financed by the National Science Centre in Poland, grant number DEC-2012/07/B/ST6/01527. This initial studies and the pilot experiments were performed while Maciej Świechowski and Jacek Mańdziuk were visiting UNSW Canberra. The ethics approval number granted from the university is A14-09.

#### REFERENCES

- [1] M. Świechowski, K. Merrick, J. Mańdziuk, and H. Abbas, "Human-Machine Cooperation in General Game Playing," in The Eighth International Conference on Advances in Computer-Human Interactions (ACHI 2015). IARIA, 2015, pp. 96–100.
- [2] M. R. Genesereth, N. Love, and B. Pell, "General Game Playing: Overview of the AAAI Competition," *AI Magazine*, vol. 26, no. 2, 2005, pp. 62–72.
- [3] J. Mańdziuk, "Towards Cognitively Plausible Game Playing Systems," *IEEE Computational Intelligence Magazine*, vol. 6, no. 2, 2011, pp. 38–51.
- [4] —, "Computational intelligence in mind games," in *Challenges for Computational Intelligence*, ser. Studies in Computational Intelligence, W. Duch and J. Mańdziuk, Ed. Springer Berlin Heidelberg, 2007, vol. 63, pp. 407–442.
- [5] "Stanford General Game Playing," 2014, URL: <http://games.stanford.edu/> [accessed: 2015-11-25].
- [6] C. P. Hoc J-M. and H. E., Eds., *Expertise and Technology: Cognition & Human-computer Cooperation*. Psychology Press, 2013.
- [7] M. Argyle, *Cooperation (Psychology Revivals): The Basis of Sociability*. Routledge, 2013.
- [8] K. R. Olson and E. S. Spelke, "Foundations of Cooperation in Young Children," *Cognition*, vol. 108, no. 1, 2008, pp. 222–231.
- [9] S. Gelly et al., "The Grand Challenge of Computer Go: Monte Carlo Tree Search and Extensions," *Commun. ACM*, vol. 55, no. 3, Mar. 2012, pp. 106–113, DOI: 10.1145/2093548.2093574.
- [10] O. Syed and A. Syed, *Arimaa - A New Game Designed to be Difficult for Computers*. Institute for Knowledge and Agent Technology, 2003, vol. 26, no. 2.
- [11] A. Kolobov, Mausam, and D. S. Weld, "LRTDP versus UCT for online probabilistic planning," in *Proceedings of the Twenty-Sixth AAAI Conference on Artificial Intelligence*, 2012.
- [12] T. Keller and P. Eyerich, "PROST: Probabilistic Planning Based on UCT," in *Proceedings of International Conference on Automated Planning and Scheduling*, 2012.
- [13] Z. Feldman and C. Domshlak, "On Monte-Carlo Tree Search: To MC or to DP?" in *Proceedings of ECAI-14. 21st European Conference on Artificial Intelligence*, 2014.
- [14] J. Karwowski and J. Mańdziuk, "A New Approach to Security Games," in *International Conference on Artificial Intelligence and Soft Computing (ICAISC'2015)*, ser. Lecture Notes in Artificial Intelligence. Springer-Verlag, 2015, vol. 9120, pp. 402–411.
- [15] K. Wałędzik, J. Mańdziuk, and S. Zadrozny, "Proactive and Reactive Risk-Aware Project Scheduling," in *2nd IEEE Symposium on Computational Intelligence for Human-Like Intelligence (CHILI'2014)*, Orlando, FL. IEEE Press, 2014, pp. 94–101.
- [16] K. Wałędzik, J. Mańdziuk, and S. Zadrozny, "Risk-Aware Project Scheduling for Projects with Varied Risk Levels," in *3rd IEEE Symposium on Computational Intelligence for Human-like Intelligence (CHILI'2015)*. IEEE Press, 2015, p. *in press*.

- [17] A. Klinger, *Human-Machine Interactive Systems*. Springer Science & Business Media, 2013.
- [18] B. Stevens and F. Lewis, *Aircraft Control and Simulation*. New York: Wiley, 1992, ISBN: 0-471-61397-5.
- [19] Y. H. Yin, L. Da Xu, Z. Bi, H. Chen, and C. Zhou, "A novel human-machine collaborative interface for aero-engine pipe routing," *Industrial Informatics, IEEE Transactions on*, vol. 9, no. 4, 2013, pp. 2187–2199.
- [20] C. G. Eden, "Robotically Assisted Surgery," *BJU International*, vol. 95, no. 6, 2005, pp. 908–909.
- [21] M. Buro, "The Evolution of Strong Othello Programs," in *Entertainment Computing*, ser. The International Federation for Information Processing, R. Nakatsu and J. Hoshino, Eds. Springer US, 2003, vol. 112, pp. 81–88.
- [22] F.-H. Hsu, *Behind Deep Blue: Building the Computer that Defeated the World Chess Champion*. Princeton, NJ, USA: Princeton University Press, 2002.
- [23] J. Mańdziuk, *Knowledge-Free and Learning-Based Methods in Intelligent Game Playing*, ser. Studies in Computational Intelligence. Berlin, Heidelberg: Springer-Verlag, 2010, vol. 276.
- [24] N. Love, T. Hinrichs, D. Haley, E. Schkufza, and M. Genesereth, "General Game Playing: Game Description Language specification," 2008. [Online]. Available: [http://logic.stanford.edu/classes/cs227/2013/readings/gdl\\_spec.pdf](http://logic.stanford.edu/classes/cs227/2013/readings/gdl_spec.pdf) [accessed: 2015-11-25]
- [25] L. Kocsis and C. Szepesvári, "Bandit Based Monte-Carlo Planning," in *Proceedings of the 17th European conference on Machine Learning*, ser. ECML'06. Berlin, Heidelberg: Springer-Verlag, 2006, pp. 282–293.
- [26] M. Świechowski and J. Mańdziuk, "Self-Adaptation of Playing Strategies in General Game Playing," *IEEE Transactions on Computational Intelligence and AI in Games*, vol. 6, no. 4, Dec 2014, pp. 367–381.
- [27] M. Świechowski, J. Mańdziuk, and Y.-S. Ong, "Specialization of a UCT-based General Game Playing Program to Single-Player Games," *IEEE Transactions on Computational Intelligence and AI in Games*, 2015, DOI: 10.1109/TCIAIG.2015.2391232 (*accepted for publication*).
- [28] M. Świechowski and J. Mańdziuk, "Fast Interpreter for Logical Reasoning in General Game Playing," *Journal of Logic and Computation*, 2014, DOI: 10.1093/logcom/exu058.
- [29] R. A. Bailey, *Design of Comparative Experiments*. Cambridge University Press, 2008, vol. 25.
- [30] A. Jaffe, A. Miller, E. Andersen, Y.-E. Liu, A. Karlin, and Z. Popovic, "Evaluating Competitive Game Balance with Restricted Play," in *AI-IDE*, 2012.
- [31] C. Browne and F. Maire, "Evolutionary Game Design," *Computational Intelligence and AI in Games, IEEE Transactions on*, vol. 2, no. 1, 2010, pp. 1–16.

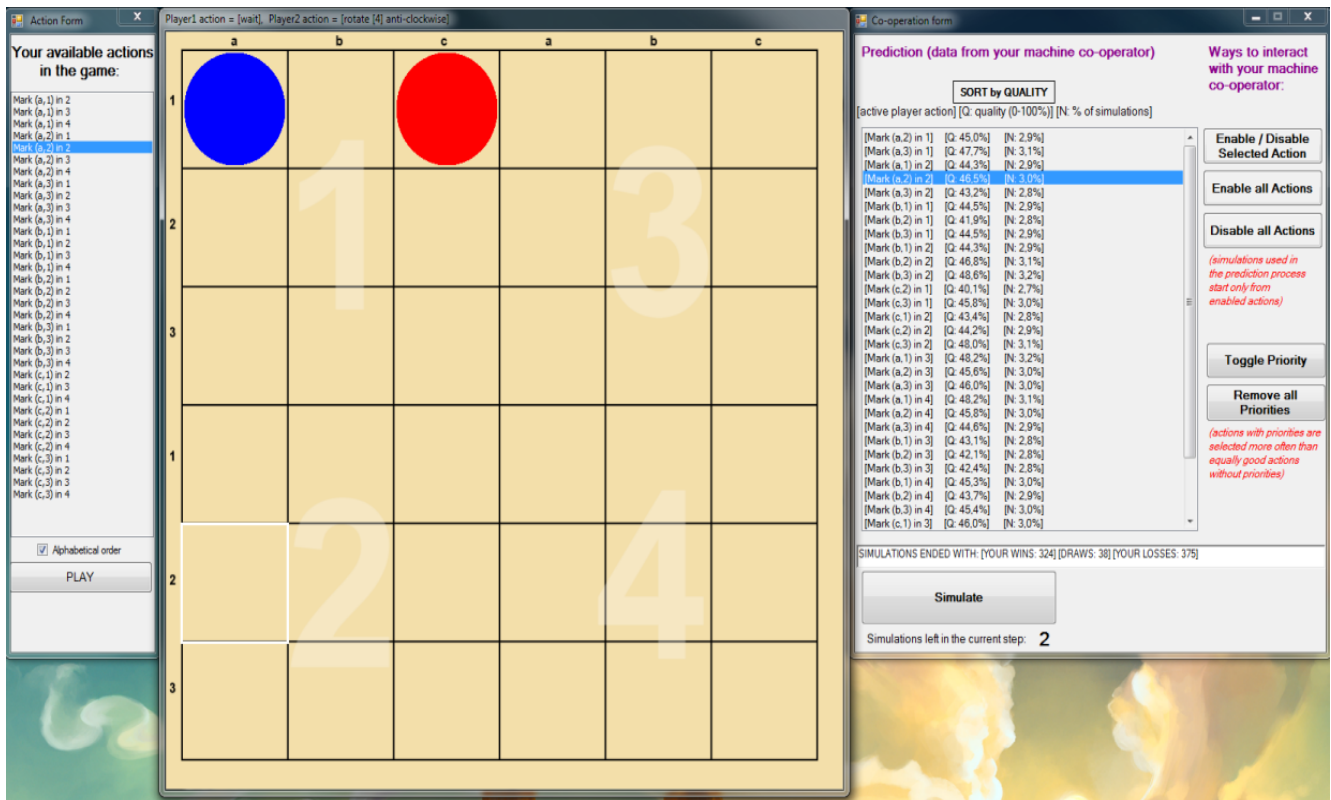


Figure 7. Screenshot of a program used to play Inverted Pentago on Windows 7 operating system (version with the cooperation).



Figure 8. Screenshot of a program used to play Nine Board Tic-Tac-Toe on Windows 7 operating system (version with the cooperation).

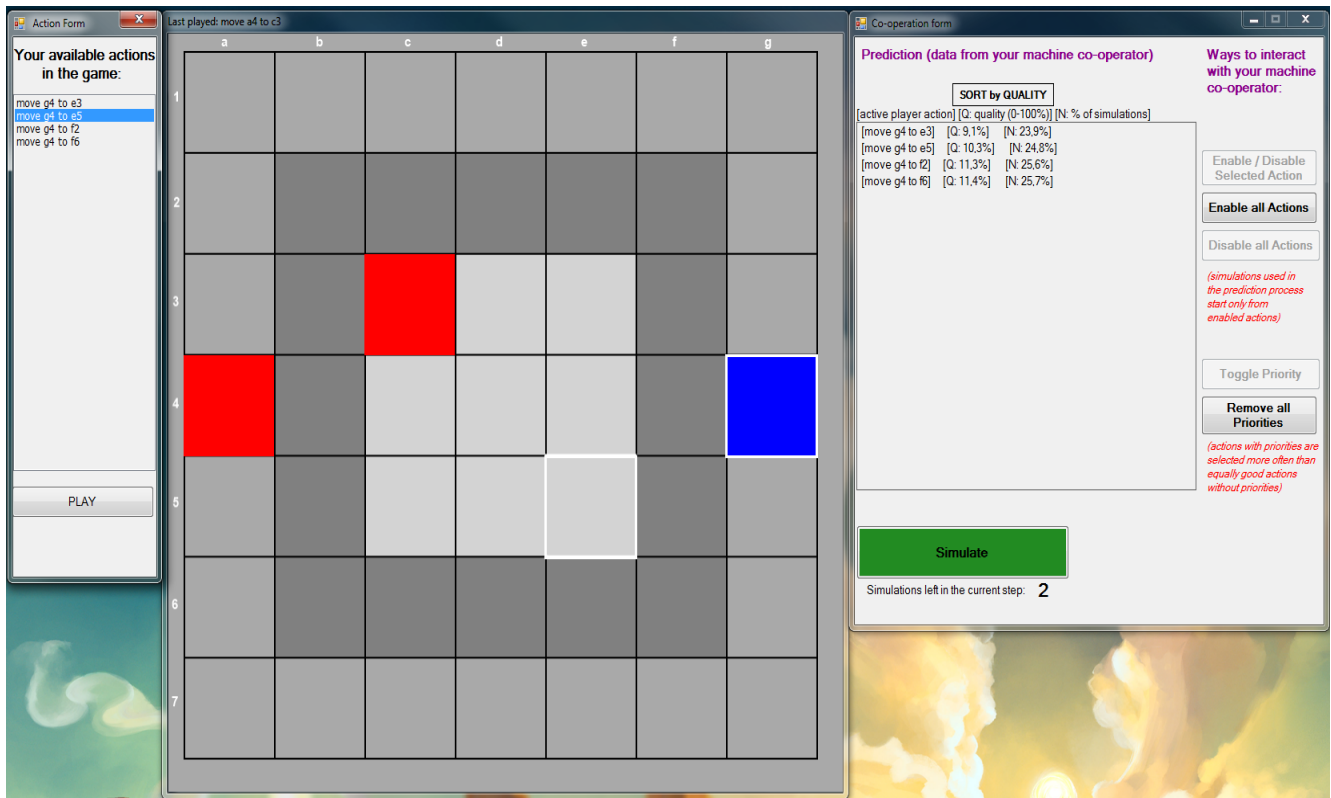


Figure 9. Screenshot of a program used to play Tic-Tac-Chess on Windows 7 operating system (version with the cooperation).

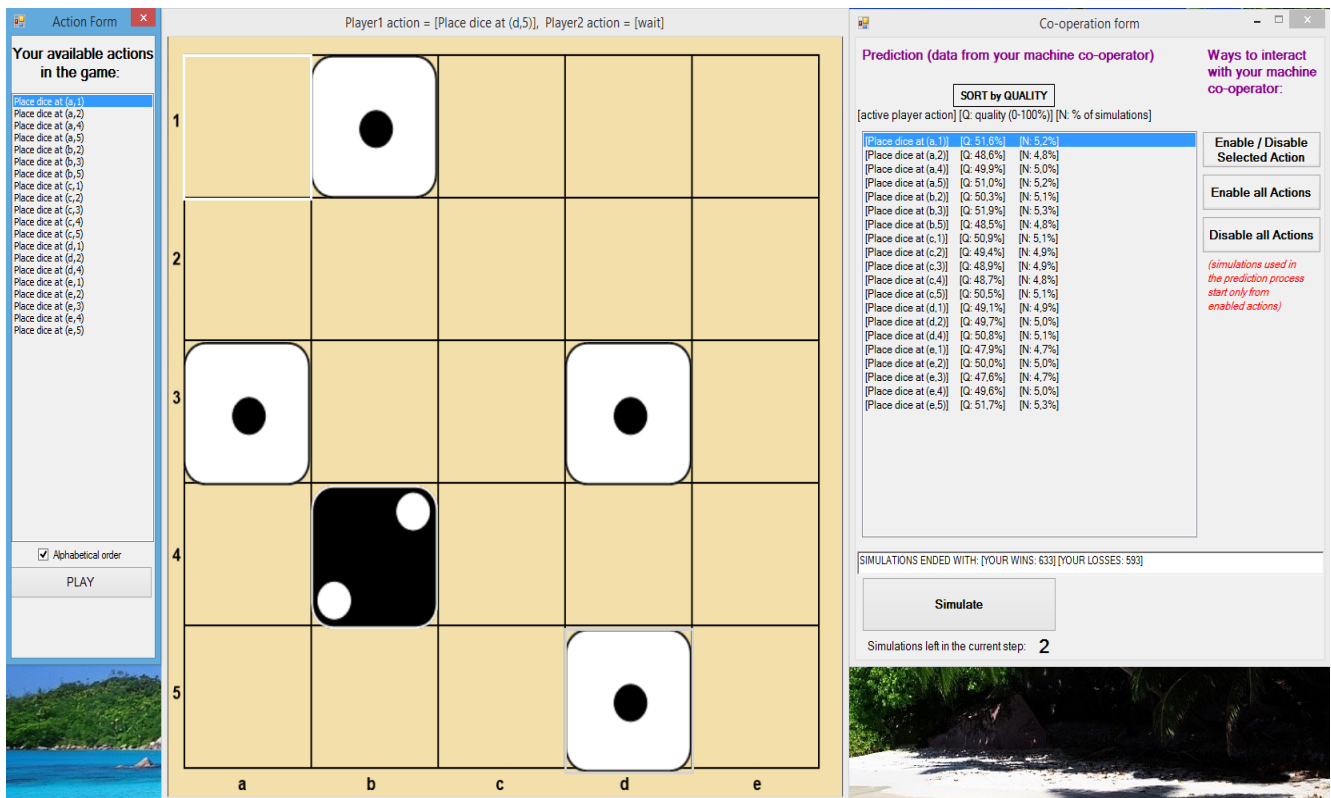


Figure 10. Screenshot of a program used to play Cephalopod on Windows 8 operating system (version with the cooperation).

## Designing for Experienced Simplicity

### Why Analytic and Imagined Simplicity Fail in Design of Assistive Technology

Suhas Govind Joshi

Department of Informatics

Faculty of Mathematics and Natural Sciences, University of Oslo

Oslo, Norway

joshi@ifi.uio.no

**Abstract**— This paper uses the design of assistive technology for elderly people as a case for exploring why analytic or imagined simplicity often end up as complicated and incomprehensible in use. Our claim is that building on *mastery* and *context* is more important than objective guidelines on simplicity. Rather than relying solely on context-detached principles that cannot guarantee simplicity in use, we introduce the term *experienced simplicity* as a way of shifting focus from how designers shape the design, to how users experience the design. Finally, we present and discuss five design implications for experienced simplicity.

**Keywords** — *simplicity; elderly; assistive technology.*

#### I. INTRODUCTION

As assistive technology is being rolled out in large scale in Norway, designers are aiming at delivering simple interactions specially adapted and tailored for the needs of elderly people. Most designers follow principles of simplicity (e.g., minimalism) in order to create a design simple enough for elderly people with reduced experience and capacities to interact with the technology. However, designing for simplicity does not guarantee simplicity in use, and our prior research has demonstrated how designs claiming to be simple can end up making life difficult [1].

One of the technological devices found in the apartment of an 84-year-old lady residing in a local care home in Oslo is an automated light sensor in her living room. Because of the small size of her apartment she sleeps with the door open, and when she turns in bed at night the sensor in the living room registers her movement and the light is activated throughout the apartment. Her solution to this was to cover the sensor with tinfoil (as illustrated in Figure 1).



Figure 1. Covering a sensor with tinfoil (Photo: S. Finken [2])

This observation exemplified how simple technology may end up making life difficult, and served as a trigger for us to explore the matter of simplicity. In this paper, we (1) investigate why existing assistive technology claiming to be simple end up as difficult in use by looking at simplicity from the perspective of the elderly users rather than the designer, and we (2) introduce *experienced simplicity* as a term that focus on the use rather than the isolated design. We discuss why it is challenging to design technology simple for others, in this particular case making assistive technology simple for the elderly users. The discussion is grounded in data gathered with three different evaluation methods spanning over 13 months. We have engaged 45 participants, including 30 elderly people with an average age of 86 years.

The paper is structured as follows. In Section II, we give an analysis of simplicity in the literature, as well as our perspective on the matter. In Sections III and IV, we outline the research context and research methods of our study before presenting the results in Section V. We end the paper with a discussion in Section VI on why simplicity is challenging through five implications for design pursuing experienced simplicity.

#### II. SIMPLICITY

##### A. Defining simplicity

In the complex world we live in, taming the complexity is one of our major goals with human-centered design [3]. Simplicity in its most elementary definition describes something with an uncomplicated quality or condition. Researchers have applied the concept of simplicity to various research studies within various disciplines of computer science. Over time, this vague definition of simplicity has made it applicable to different areas of computer science, and in several disciplines the term has evolved into an established term with a more refined and tailored use mainly applicable to that specific discipline or context. As a philosophical principle, simplicity can be differentiated into ontological simplicity, following the principle of parsimony, and syntactical (structural) simplicity, perceived as elegance [4]. Hence, the theoretical perspective of the researchers in the debate of philosophy of science can heavily influence how they perceive and apply such a term. Lee et al. [5] describes simplicity within the

area of Human-Computer Interaction (HCI) as “not only simple page layout but also interface organization, functionality, structure, and workflow and framework”. Following this definition, simplicity in HCI encompasses various elements and researchers tend to find their own perspectives and definitions to simplicity. One of the most cited authors on simplicity, Maeda [6], defines his ten laws of simplicity (reduce, organize, time, learn, differences, context, emotion, trust, failure and the one). On the other hand, Colborne [7] concentrates on only four strategies (remove, organize, hide and displace) in his discussion on simplifying devices and experiences. Simplicity has also been analyzed through the notion of minimalism by Obendorf [8] who defines four types of minimalism (functional, structural, compositional and architectural) and utilize this perspective on minimalism to discuss simplicity in HCI. However, as Picking et al. [9] points out, design principles are in general often formulated as brief guidelines that aim to cover wide areas of application and apply to multiple domains simultaneously; it is difficult to use these guidelines consistently as they rarely specify which specific design choices to make. Since laws, strategies and principles for simplicity can serve as everything from minor inspirations to governing factors, Obendorf [8] have called for more differentiated and concretized definitions of how simplicity is understood, and exactly how it influences the design outcome.

Several researchers have pointed out the importance of simplicity as a design principle in systems designed for the older population [10]-[12], however, prior studies [4] [1] suggest that perceived simplicity is context-dependent and relies heavily on the users' previous exposure. As a result, we want to expand on the definitions of simplicity currently found in the literature (summarized in Table I).

TABLE I. OVERVIEW OF DEFINITIONS OF SIMPLICITY

Related work	Definition
Lee et al. [5]	“not only simple page layout but also interface organization, functionality, structure, and workflow and framework”
Maeda [6]	Ten principles of simplicity: reduce, organize, time, learn, differences, context, emotion, trust, failure and the one.
Colborne [7]	Strategies for simplicity: remove, organize, hide and displace.
Obendorf [8]	Minimalism: functional, structural, compositional and architectural.

### B. Experienced simplicity

Our understanding of simplicity is anchored in two main elements, namely *mastery* and *context*. Both of these elements revolve around the users' experience and perception of the system in use rather than the isolated and context-detached design itself; simplicity is a characteristic of a system that manifests itself once the intended users take use of the system in its appropriate context. When using

simplicity as a design guideline, one should always envision the act of simplification resulting in positive effects on the mastery of the user in the desired context. Blindly following simplicity as a design principle, e.g., reducing or hiding elements because general rulebook on simplicity says so, ignores the true intention behind the design choice, namely disentangling the perceived complexity. We have labeled this perspective on simplicity as *experienced simplicity* as it shifts focus on simplicity from something the designer use as a guideline to something we can only confirm through user experience. A design is not simple unless the user perceives the interaction to be simple in use.

However, analyzing the simplicity laws and principles of Maeda, Colborne and Obendorf one quickly register that these laws mainly consider simplicity as context-independent. All of Colborne's four principles encourage modification to the design detached from the eventual context. Similarly, Obendorf relies on minimalism which itself does not automatically ensure systems free of complexity; it only encourages basic design with deliberate lack of decoration without discussing the perceived simplicity. From Maeda's ten laws we can extract five laws concerning the relational use of the system rather than the system itself, namely time, learn, context, emotions and trust. Only these laws reflect how we understand simplicity, i.e., rather than being a term of size, quantity or volume, it should first and foremost reflect the contextual experience. Thus, simplicity in a system is not something one adds to the design; it is something achieved once mastery is uncomplicated in its appropriate context.

Our view on simplicity aligns with the research of Eytam and Tractinsky [13] who suggest that the ability to design own complexities can be a desire among users. They define this contrast between advocated guidelines for simplicity and the observed behavior as the paradox of simplicity, and argue that simplicity is not defined in objective guidelines, but rather a quality to be understood through how the users perceive simplicity. The explicit focus on the users' side of the interaction in HCI influences how we discuss the concept of simplicity how it is a matter of more than just reducing complexity; simplification is an intricate and dynamic design principle embracing factors such as mastery and context of use as examples of decisive factors of simplicity. This is also in line with [4] who suggest that simplicity as a design principle should be a complex and flexible design paradigm rather than a simple dichotomous variable, incorporating elements such as user interface design, as well as contextual factors (for example integration to other IS). Keay-Bright and Howarth [14] focus on designing intuitive interfaces and describe simplicity not as a compromise in richness or diversity of human experience, but rather a minimal interface that empowers the users to design their own complexities that ensures mastery.

Another early supporter of our perspective is Norman who claimed that designing solely for simplicity would force a compromise on functionality [3]. He pointed out two common implicit assumptions that designers rely on: (1) that

features equals capability, and (2) that simplicity equals ease of use. He argued that this one-way logic does not have any guaranteed backwards mechanism. Thus, if we want to achieve capable and usable systems, designing for simplicity alone will not automatically deliver our desired solution: "*Features do not equal capability. Simplicity is not the same as usability. Simplicity is not the answer.*" [3].

### III. RESEARCH CONTEXT

#### A. Empirical context

This study is part of a larger long-term research project focusing on newly acquired assistive technology in local care homes in Oslo Municipality. The particular local care home involved in this study consists of 91 individual apartments for the elderly residents (with an average age of 84 years) organized with common reception, cantina and recreation room (depicted in Figure 2). There are no medical services provided, and those in need organize their own arrangements with the district home care services. However, the residents have access to basic services such as hairdressing, foot therapist, gym and cinema. The goal of the local care home is to be a smart house, for instance actively utilizing technology in order to prolong the time elderly people can remain independent in their own homes before being admitted to a nursing home.



Figure 2. The reception and common area of the local care home

Each individual apartment comes pre-installed with a set of new technologies, including automated lighting, heating and ventilation control, stove guard, electrical sockets with timers, motion sensors in all rooms, video calling, door locks with radio-frequency identification (RFID), and a customized tablet. Ever since the building opened in 2012, our research group has been present at this facility, and this local care home is an excellent arena to study existing technology. It also serves a venue where we experiment with new and alternative assistive technology.

#### B. Technology under evaluation

For the purpose of evaluation in this study, we included the tablet and some of the room control devices found in the apartments of the local care home. The initial main objective was to concentrate solely on the tablet; however, we feared that only studying this touch-based device would restrict the discussion of simplicity to an analysis of touch-screen interfaces rather than being an open discussion of how users experience simplicity in the assistive technological devices that surround them. As a result, we included a set of devices in the room, i.e., light, temperature and ventilation systems, as well as the RFID door locking system.

##### 1) Tablet

The tablet illustrated in Figure 3 comes pre-installed in all apartments and introduces a new way of arranging, planning and keeping an overview of everyday activities, as well as allowing residents to order meals from the downstairs cafeteria straight from the device. The tablet also provides basic opportunities for communication, namely telephoning and text messaging, as well as entertainment services, e.g., radio and an Internet browser. However, the tablet only comes with one mode and offers few options for customization, hence, flexibility and robustness is of great importance as it needs to support the daily activities of all residents and employees.



Figure 3. The tablet

##### 2) Room controls devices

Some of the pre-installed assistive technologies and devices in each apartment is lightning, heating and ventilation control in every room of the apartment. This includes automated motion-activated light sensors, automated thermostat and automated adjustment of ventilation. The photos in Figure 4 depicts a close-up of the heating interface as well as the RFID door locking system used to access each apartment. The door locks automatically, but opens with a RFID-card, and represents an interface few had experienced before. Since all these devices come pre-installed there is no option for the residents to utilize other interfaces or interaction methods, e.g., traditional door locks with keys or two-button light switches, and these pre-installments can all be considered a part of the "welfare package" in each apartment. As a result, they were tested

together during the evaluations, and we will refer to these devices as "room control devices" in this paper.



Figure 4. Heating control (left) and RFID door (middle)

#### IV. RESEARCH METHOD

The data for this study was gathered over a period of 13 months divided into three phases. We were motivated by prior experiences with elderly people and assistive technology [13] [14], where findings suggested that giving enough time could help avoiding or eliminating bias. Three different methods of evaluation were used during these three phases, and Figure 5 illustrates the outline of the research phases.

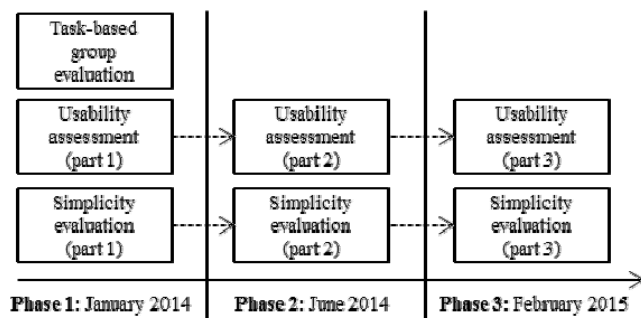


Figure 5. Outline of the research phases

We applied different methods of evaluation. This was partly motivated by methodical triangulation, although the main reason was giving the participant more than just one opportunity to express their perspectives on simplicity. Also, in order to detect any cases of reverse-halo effect, we preferred to have at least one method that was an objective and metric evaluation of performance rather than subjective assessment. The applied methods are listed in Table II.

The *task-based group evaluation* allowed the participants to freely address simplicity issues during the task walkthrough independent of schemas, heuristics or guidelines. Through the *simplicity evaluation* participants had a chance to evaluate the simplicity by grading pre-

selected factors of simplicity, and during the *usability assessment* we did not ask them, but rather observed and measured them in order to discuss simplicity through their performance. The first phase included a task-based group evaluation, a simplicity evaluation and a usability assessment. The initial plan was to conduct these three activities during the first phase and then follow up with an equivalent usability assessment after six months with the same participants and the same usability criteria. However, due to the feedback and results discovered during the second usability assessment, we chose to repeat the simplicity evaluation as well. The results from the second phase suggested that six months was not enough time to capture whether perspectives on simplicity had evolved over time. As a result, the third phase was conducted almost 13 months after the first phase, giving us enough time to reduce the selection bias such as length time bias. It also gave the participants the opportunities to experience the technology through additional stages of its lifecycle, e.g., maintenance, software updates, component replacement, and thereby attributing their assessment of simplicity to actual use over time rather than just first-impression or initial use.

TABLE II. OVERVIEW OF METHODS

#	Method	Participants Phase 1	Participants Phase 2	Participants Phase 3
A	Task-based group evaluation	22	-	-
B	Usability assessment	11	11	11
C	Simplicity evaluation	12	12	12
D	Follow-up interview	-	-	6

##### A. Task-based group evaluation

The task-based group evaluation was a part of a broad study where altogether 22 participants were engaged, namely 11 elderly users, 7 employees and 4 experts. This dataset includes several factors out of which some are not relevant for this study, although data from this evaluation has previously contributed to another study [15]. Nevertheless, the evaluation included a total of 6 sessions, 3 sessions with groups of elderly, 2 sessions with groups of employees, and 1 session with a group of HCI-experts. The employees were recruited from the local care home, and the participants represented both daytime and nighttime employees. The sessions were structured as group walkthroughs of pre-selected representative tasks where the participants were asked to grade the severity of identified issues and then engage in a plenary discussion. Examples of representative tasks were ordering a meal and signing up for activities on the tablet and controlling lighting and ventilation in the room. During this session all participants labeled issues with predefined categories. The data included in this study are those issues labeled by the participants as "simplicity" issues. All participants were free to

individually define what issues they considered to be simplicity issues.

### B. Usability assessment

The usability assessment involved 11 participants; 7 elderly residents and 4 experts. The participants were given a set of 10 representative tasks to perform while completion time and error rates were measured and the sessions photographed. The tasks are listed in Table III. The given tasks were distributed evenly between the tablet and the room control devices. Errors were counted and also divided into *deliberate errors* and *accidental errors*; the former represents errors where the user performed an action intentionally although performed the wrong action, while the latter represents unintentional actions. An example of a deliberate error is intentionally pressing the channel button on the television remote control when you want to adjust the volume because you in your best judgment consider the channel button to be the correct action for the desired outcome (i.e., adjust the volume), and you intentionally press that button. On the other hand, if you want to change the channel and while reaching for the correct button you unintentionally bump into the power button instead, then it would be a case of an accidental error.

TABLE III. OVERVIEW OF PERFORMED TASKS

Task #	Task description
Task 1	Locking and unlocking the RFID door
Task 2	Playing a game on the tablet
Task 3	Browsing on the tablet
Task 4	Sending and receiving text messages on the tablet
Task 5	Listening to radio on the tablet
Task 6	Ordering food from the cafeteria on the tablet
Task 7	Activating room control devices with movement
Task 8	Setting and adjusting the ventilation
Task 9	Turning on and off wall and ceiling lighting
Task 10	Adjusting the heating level

In the first two phases, these evaluations were carried out in the homes of 5 of the 7 participants, while 2 participants preferred to have the test conducted in an adjacent meeting room along with the experts. In the third phase, we conducted all evaluations in the meeting room. The usability assessment was repeated during the second and third phase in order to study changes in behavior, performance and satisfaction after six and thirteen months. The conditions and environmental factors were similar between the three assessments with the exception of the participants agreeing to have the evaluation along with the experts in the meeting room in the final evaluation.

### C. Simplicity evaluation

The goal of the simplicity evaluation was to provide the residents with an opportunity to evaluate the simplicity without being restricted to certain tasks (as in method A) or tied to their performance (as in method B). Hence, the participants were asked only to grade the simplicity of the tablet and the room control systems. The evaluation

included 12 elderly users in each of the three phases. All participants were given an individual oral and written explanation of each factor and was then asked to grade the simplicity factor from 1-5.

The evaluation comprised 7 factors redefined from 5 laws of Maeda coinciding with our perspective of experienced simplicity, namely the symbiotic relationship between mastery and context. The 7 elements were *intuitivity*, *organization*, *memorability*, *error rate*, *time*, *learnability* and *trust*. Intuitivity reflects the perceived easiness when first approaching the system in the given context, while learnability and memorability describes the system's ability to foster mastery and maintain it over time. With organization we did not look at organization of the interface, e.g., icon clutter, but studied how the system fitted within its context. We also included time, i.e., their experience on their own performance and error rate, i.e., how many errors they encountered, in order to study their own perspective on mastery.

### D. Follow-up interview

The usability assessment and simplicity evaluation during the third phase was accompanied with a few interviews in order to gather perspectives from both experts and elderly participants on their opinions and performance. We chose to include these interviews in the final phase as we could not interpret the rationale behind the fluctuating opinions between phase 1 and phase 2, and wanted to get some insight into this matter. The interviews included three elderly participants and three daytime employees and were conducted immediately after the evaluations.

### E. Participants

The three methods involved 45 participants altogether and the participants were divided into four user groups described in Table IV. The elderly people ( $n = 30$ ) participated in all methods during all three phases, while the usability experts ( $n = 8$ ) participated during all phases of the simplicity evaluation and the usability assessment. Finally, the employees ( $n = 7$ ) only participated in the task-based group evaluation. A few daytime employees were invited to the follow-up interviews after the evaluation in phase 3 in order to capture some of their experience since last time.



Figure 6. Elderly residents participating in the task-based group evaluation

The elderly participants were recruited among the residents at the local care home and their age ranged from 79-94 ( $\mu = 86$ ). Participants from one session are depicted in Figure 6. As a general rule, upon moving into this local care home, all residents are cognitively cleared by medical experts, i.e., possessing at least an acceptable level of cognitive and reasoning abilities. However, they all share in common that they struggle with various medical conditions, e.g., reduced motor abilities or reduced vision, and they represent a broad range of social difficulties. In addition, the cognitive abilities of the residents are not monitored regularly, and several residents, including some of our participants, developed symptoms of beginning cognitive disorder throughout the 13-month period of our study.

TABLE IV. OVERVIEW OF PARTICIPANTS

User group	User role	Use frequency	Expertise	Participated in method #	N
The elderly	End-users	Every day	(none)	A, B, C, D	30
Daytime employees	End-users and trainers	Every day	Health and domain	A, D	4
Shift work employees	End-users and trainers	Once a week	Limited domain-expertise	A	3
Usability experts	None	One-time only	HCI and usability	A, B	8

## V. RESULTS

### A. Task-based group evaluation

Out of a total of 39 identified issues, 17 were considered simplicity issues by at least one of the user groups. Each group that had identified the issue was then asked to grade the severity of the issue as *minor* (M), *serious* (S) or *critical* (C). All identified issues are listed in Table V. The *aggregated degree of seriousness* reflects the final level of seriousness assigned to the issue based on the grading of the

groups. If there were disagreements between only two groups, the most serious grading took precedence; otherwise the number of occurrences decided this aggregated degree of seriousness. Out of these 17 identified issues 5 were labeled as critical issues, 7 were categorized as serious issues, and 5 were considered minor issues. The group of elderly reported a total of 14 issues, out of which 36 % were graded as minor. The similar percentage was lower for the two other groups, respectively 25 % for the employees and 27 % for the experts. Since both the employees and experts reported fewer issues overall than the other two groups, this implies that the employees and experts regarded identified issues as more severe than the elderly, with a percentage of 75 % (employees) and 73 % (experts) graded as either serious or critical against only 64 % for the elderly participants.

We also wanted to study the balance of simplicity, i.e., identify the level of simplicity where the system was neither too simple nor too complex. As a result, we also asked the participants to differentiate between issues they considered a result of the vendor making the interface or interaction *too simple*, i.e., a matter of oversimplification, and issues they considered *too complex* and wished were further simplified. 13 issues were considered a result of oversimplification and participants expressed usability issues due to interface, language, symbols, etc., being too simple for their liking. 4 of the 5 critical and 6 of the 7 serious issues were labeled oversimplified. It should be noted that similar to the aggregated degree of seriousness, the expressed simplification desire is the aggregated evaluation of the group(s) who brought forward the issues, however, all groups answered unanimously for all issues. As a result, their individual answers are not presented similar to the degree of seriousness where we encountered variations between groups.

Most of the issues had a clear consensus on the grade of severity. Only those 3 cases where two groups addressed an

TABLE V. IDENTIFIED SIMPLICITY ISSUES

Issue #	Issue description	Aggregated degree of seriousness	Group 1 Elderly	Group 2 Employees	Group 3 Experts	Imbalance issue
1	The device screen always stays on (even in standby mode)	S	M	S	S	Too simple
5	The phone icon color is misleading	S	S	M	S	Too complex
7	There is no indicator of remaining battery	C	C	C	C	Too simple
8	There is no indication of the device being charged or already fully charged	S	-	S	-	Too simple
10	The system signals two new messages when just one message arrive	S	M	S	-	Too simple
11	The system uses separate indicators to indicate the same message	M	M	-	-	Too complex
15	There is one phone number for texting (12-digit) and another for calling	C	C	S	C	Too complex
20	The default values in text boxes are misleading and unpractical	S	S	C	S	Too simple
21	It is impossible to grad the on-screen keyboard in certain views	C	S	-	C	Too simple
24	The language is inconsistent	S	S	S	-	Too simple
25	It is too easy to delete everything	M	-	M	M	Too simple
28	The events in the calendar are not chronologically ordered	M	M	S	M	Too complex
29	The duration of phone calls is missing	S	M	-	S	Too simple
34	There is no comment feature on activities and events	M	-	-	M	Too simple
35	The language is confusing	M	S	M	-	Too simple
36	The icons are confusing	C	S	-	C	Too simple
38	The notifications are misleading	C	C	S	-	Too simple

issue and simultaneously gave it different grades did we encounter any disagreements. Rather than considering the grade of one group as more important than other, we chose instead to always use the highest grade. This was considered an acceptable solution by the participants; for example, the elderly participants labeled the highest number of issues as minor issue, but for 3 of the 5 issues that the elderly labeled as minor issues (#1, #10, #29) the aggregated grading was upgraded to serious since either the employees or the experts regarded the issue as serious. For the two remaining issues one was only reported by the elderly residents (#11) and one group disagreed with the group of elderly on the severity grade of the last issue (#28). Additionally, only in 3 cases were the issue only addressed by one group (out of which two were minor issues), and the overall consistency of the grading of the issues was therefore considered to be good.

### B. Usability assessment

The usability assessment included 10 tasks (Table III) tested by 7 elderly people and 4 experts in each of the three phases, and Figures 7-9 present the completion time and error rate for each of the tasks in all three phases. The completion time listed for each task is the average time spent by all 11 participants to complete the task, while the error rate is the average error rate for deliberate and accidental errors.

On average, the experts performed their tasks during the first phase within almost half the time of the elderly participants ( $\mu_{\text{experts}} = 173.11$  against  $\mu_{\text{elderly}} = 330.57$ ), and did so with half as many deliberate ( $\mu_{\text{experts}} = 1.82$  against  $\mu_{\text{elderly}} = 3.90$ ) and accidental ( $\mu_{\text{experts}} = 1.18$  against  $\mu_{\text{elderly}} = 3.18$ ) errors. Their standard deviation also confirms a more consistent performance throughout the 10 tasks both time wise ( $\sigma_{\text{experts}} = 11.90$  against  $\sigma_{\text{elderly}} = 36.66$ ) and error wise ( $\sigma_{\text{experts}} = 0.52$  against  $\sigma_{\text{elderly}} = 1.06$  and  $\sigma_{\text{experts}} = 0.32$  against  $\sigma_{\text{elderly}} = 0.59$ ). There is no clear consistency in how the user performs on average in each task. Between the two first phases, the completion time of four tasks decreased with an average of 9.46 seconds, while the completion time of the remaining six tasks increased with an average of 15.98 seconds. The deliberate error rate dropped for six tasks ( $\Delta\mu_{1-2} = -0.36$ ) and increased for the other four tasks ( $\Delta\mu_{1-2} = 0.46$ ). On the other hand, the accidental error rate increased for four tasks ( $\Delta\mu_{1-2} = 0.29$ ), dropped for four tasks ( $\Delta\mu_{1-2} = -0.32$ ) and remained unchanged for the remaining two tasks (#7 and #9). However, there is no correlation between which tasks that went up in deliberate or accidental error rate. Only for one of the tasks (#4) did the sum of deliberate and accidental errors decrease when the completion time decreased. For the other three tasks, where the completion time dropped (#1, #2 and #10), one increased the sum of errors by 0.14 (#1) while the two other had no change in error rate even though the completion time decreased.

Between the second and third phases, the completion time of seven tasks increased with an average of 16.45 seconds, while the 3 additional tasks demonstrated a 4.38 second drop in completion time. Interestingly, three of the four tasks that decreased in average completion time between the first and second cycle (#1, #2 and #4) flipped between the second and third evaluation and demonstrated an increase between the two final evaluations. Hence, any consistencies were even harder to identify after the third phase. This lack of pattern in performance was further strengthened by the changes in error rates. The deliberate error rate increased for 6 tasks ( $\Delta\mu_{2-3} = 0.29$ ) and dropped for the other four ( $\Delta\mu_{2-3} = -0.36$ ). Four of the six tasks that had increased in deliberate error rate since last time had previously demonstrated a negative change between the first two phases, indicating an increased performance (#1, #2, #7, #8). The accidental error rate remained unchanged for two tasks between the second and third phase (#2 and #6), increased for five tasks ( $\Delta\mu_{2-3} = 0.34$ ), and decreased for three tasks ( $\Delta\mu_{2-3} = 0.33$ ). Again, the changes were inverted for four of the five tasks compared to last time. Only for one task (#5) did we register a similar trend between the three cycles.

The average completion time for all ten tasks increased slightly between the first and second phase ( $\Delta\mu_{1-2} = 8.29$ ,  $\Delta\sigma_{1-2} = 7.36$ ) for the elderly participants. The difference between the second and third phase almost completely inverted the change between the first two phases by dropping back on both completion time and standard deviation ( $\Delta\mu_{1-2} = -14.63$ ,  $\Delta\sigma_{1-2} = -4.92$ ). The standard deviation on average completion time in the second ( $\sigma_{\text{experts}} = 8.32$  against  $\sigma_{\text{elderly}} = 29.3$ ) and third ( $\sigma_{\text{experts}} = 9.25$  against  $\sigma_{\text{elderly}} = 25.0$ ) phase still suggested that the performance of the experts was time wise more consistent throughout all ten tasks. However, the standard deviation kept dropping and between the first and third phase for the elderly participants, the change in standard deviation considering average completion time dropped from 36.6 to 25.0 seconds. This happened despite the average completion time increasing between the first two phases, and then decreasing between the two last.

The standard deviation for deliberate errors hovered around the value from the first phase for both experts and elderly users. For the experts the standard deviation from the first phase ( $\sigma_1 = 0.52$ ) changed both positively and negatively in the two following phases ( $\Delta\sigma_{1-2} = -0.14$  and  $\Delta\sigma_{2-3} = 0.08$ ). In the case of the standard deviation for the elderly participants, the changes from the first phase ( $\sigma_1 = 1.06$ ) were again both positive and negative in the successive phases ( $\Delta\sigma_{1-2} = -0.16$  and  $\Delta\sigma_{2-3} = 0.08$ ). The standard deviation for accidental errors also remained very close to its initial value after a year. For the experts, the initial value ( $\sigma_1 = 0.32$ ) decreased before the second phase ( $\Delta\sigma_{1-2} = -0.02$ ) and increased back before the third phase ( $\Delta\sigma_{2-3} = 0.05$ ). As this value is marginally higher after the third phase, we see an example of how the accidental error

count does not necessarily improve over time even for younger users. For the elderly people, changes followed a similarly fluctuating pattern as the experts. The standard deviation from the first phase ( $\sigma_1 = 0.59$ ) both decreased before the second phase ( $\sigma_{1-2} = -0.08$ ) and then increased before the third phase ( $\Delta\sigma_{2,3} = 0.12$ ). This also demonstrates a very low overall deviation from this initial value even after a year.

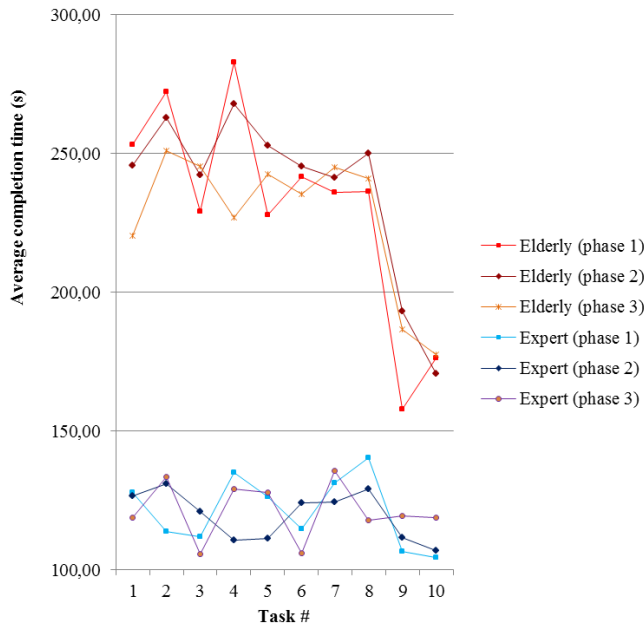


Figure 7. Overview of average completion time (s)

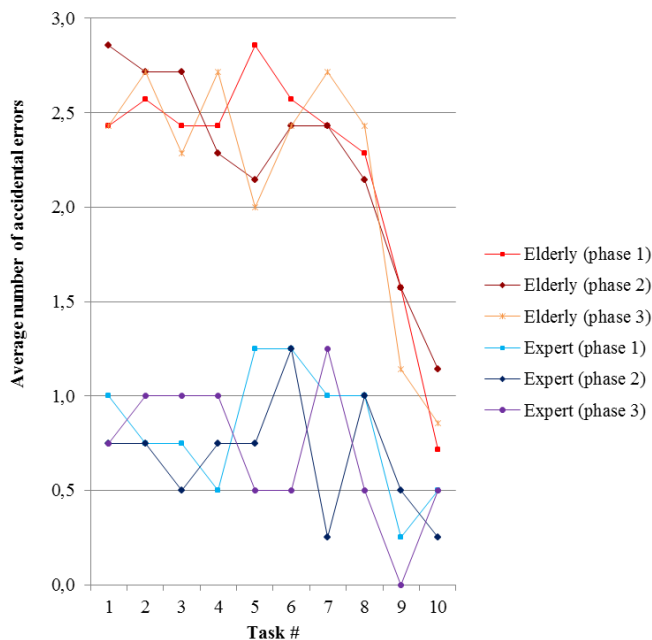


Figure 8. Overview of average number of accidental errors

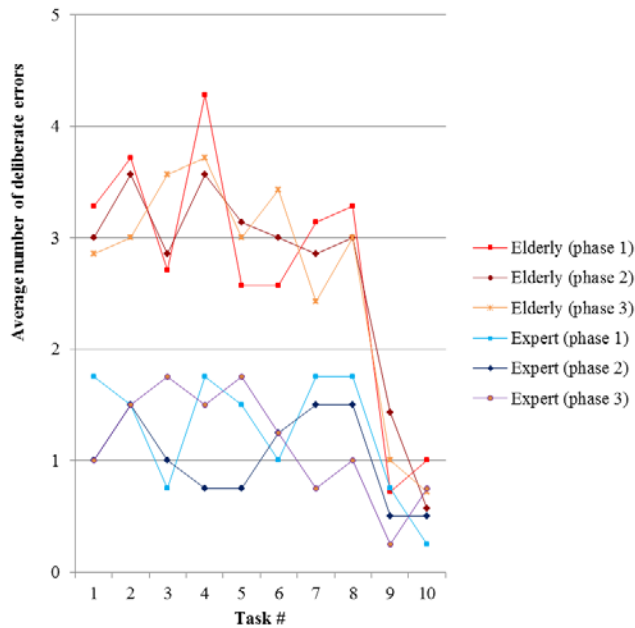


Figure 9. Overview of average number of deliberate errors

Already during the first phase, we registered that the two last tasks had the lowest completion time in both cases for all participants, as well as the lowest error rate (both deliberate and accidental) for both groups. A similar performance pattern was also registered among the experts, a group with less performance fluctuation than the elderly participants, and these were the two tasks with highest mean deviation in all three phases for both groups. These two tasks were also the only tasks where the group of elderly participants matched the performance of the experts. The average difference in completion time between elderly residents and experts in phase 1 was 110.2 seconds ( $\sigma_1 = 30.9$ ), 117.6 seconds ( $\sigma_2 = 26.4$ ) in phase 2, and 105.4 seconds ( $\sigma_3 = 18.8$ ), while the differences for task #9 and #10 were only 61.7 seconds in phase 1, 67.15 in phase 2, and 67.8 in phase 3. Similarly, the difference in deliberate error rate had an average of 1.46 ( $\sigma_1 = 0.69$ ) in phase 1, 1.68 ( $\sigma_2 = 0.73$ ) in phase 2, and 1.52 ( $\sigma_3 = 0.86$ ) in phase 3, while the differences for task #9 and #10 were only 0.48 in phase 1, 0.41 in phase 2, and 0.45 in phase 3. The accidental error rate had an average difference of 1.4 ( $\sigma_1 = 0.45$ ) for phase 1, 1.57 ( $\sigma_2 = 0.48$ ) for phase 2, and 1.47 ( $\sigma_3 = 0.53$ ) for phase 3, compared to 1.2 difference in phase 1, 0.55 in phase 2, and 0.87 for task #9 and task #10. The task order was completely randomized and the participants never saw any task numbers – only tasks. Consequently, this anomaly is not a result of learning effect but rather a sign of tasks that were significantly easier than the rest. This anomaly, alongside the fluctuating opinions on simplicity between phase 1 and 2, was the reason for introducing the follow-up interviews conducted in phase 3. The follow-up interviews helped us confirm the distinction between the eight first and the two final tasks; the participants, regardless of whether

they belonged to the elderly group or the employee group, unanimously reported the two final tasks as categorically different from the rest. The participants also unanimously rejected any learning effect as the reason behind the sudden drop in task #9 and task #10. In any case, a pattern of learning effect would have manifested itself through a more constant descending curve from tasks #1 through task #10 rather than the abrupt drop after task #8.

### C. Simplicity evaluation

Figures 10 and 11 present the results from all three phases of the simplicity evaluation. During the first phase, there were clear differences in opinion between the participants. While the average score of the 12 participants ended up on the upper half of the scale, the deviation within the data was large ( $\mu_1 = 3.4$  and  $\sigma_1 = 0.79$ ), and participant #10 gave 4.4 out of 5 on average for the seven factors of simplicity, whereas participant #11 only gave 1.7 out of 5. The average score given to each of the seven factors were much more evenly distributed with only half the deviation ( $\sigma_1 = 0.4$ ) despite some of the factors having a much higher internal deviation (e.g., memorability with  $\mu_1 = 3.0$  and  $\sigma_1 = 1.2$ ).

The second phase yielded results very similar to the first phase. There were few changes in how the users perceived and rated the seven factors with the highest factor difference between the two first phases being as low as 0.3 (intuitivity and trust), while the rest averaged at 0.15. However, almost all participants had changed their perception of simplicity since the first phase. Participant #10 and #12 both end up with an average score 0.1 below their previous average, and for some participants, e.g., participant #6 with a 0.9 difference, the change in opinion was much more evident. Five of the participants ended up giving a higher average score during the second phase ( $\Delta\mu_{1-2} = 0.53$ ), while the remaining 7 reduced their average score ( $\Delta\mu_{1-2} = -0.37$ ). Hence, even though the number of participants increasing their score between the two first evaluations is lower than those reducing it, the difference in their average score brings the total average up ( $\Delta\mu_{1-2} = 0.1$ ). While the overall perception of simplicity does not necessarily change much, the reduced deviation between participants carefully suggest that their opinions had harmonized during the six months between the two evaluations ( $\sigma_2 = 0.51$  against  $\sigma_1 = 0.79$ ).

During the third phase, we saw very few changes in the simplicity evaluation compared to the previous phase. Two factors represented the biggest changes in opinion (intuitivity and error rate) with a difference of 0.4 in both cases, while the rest had an average difference of  $<0.01$ . Yet again, we registered changes both individually and as a group, even though the average remained almost constant. The overall standard deviation between phases 2 and 3 suggested that their opinions continued its convergence ( $\sigma_2 = 0.47$ ), yet the extremities were more apparent. Participant #9 set a new record with a 1.2 positive difference between

July and February, increasing the average score from 2.7 out of 5 to 3.9 out of 5. Participant #12 also demonstrated distinct changes in opinion by dropping the average score from 4.0 to 3.1, thereby reducing the score by 0.9. The follow-up interview revealed that the participants had not changed their definition of the seven factors, only their opinion on the matter.

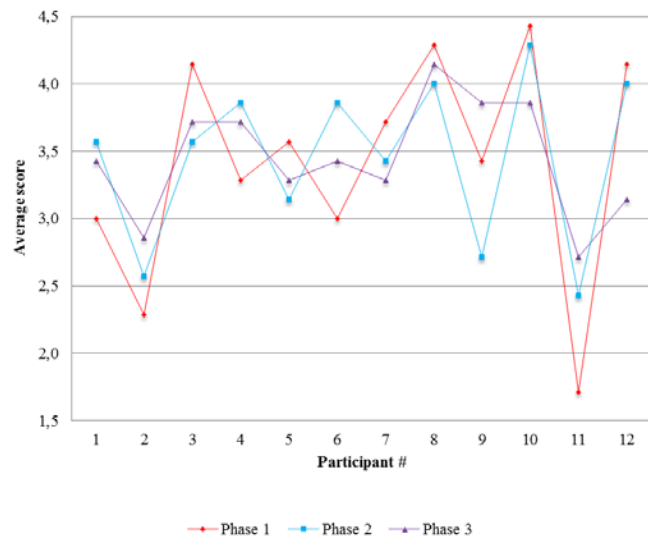


Figure 10. Average score given by each participant

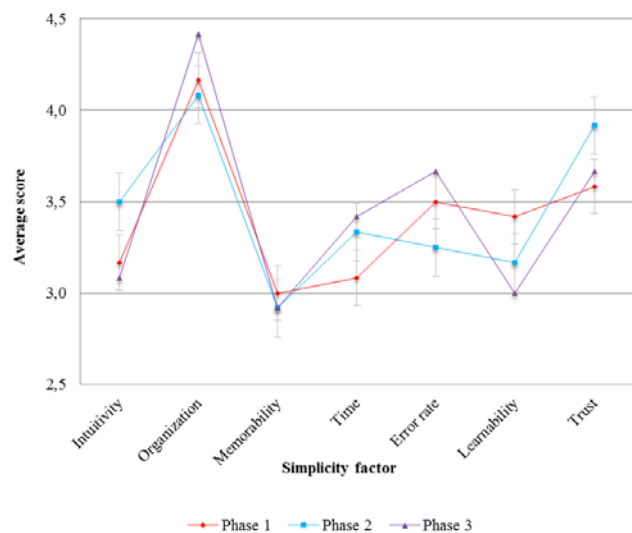


Figure 11. Average score given for each simplicity factor

## VI. UNDERSTANDING WILL BRING SIMPLICITY

### A. Designing for understanding rather than simplicity

Our main results from [1] relied on quantitative data to demonstrate how technologies intended to be simple in use were experienced as difficult. We studied the performance

and error rate in order to determine the experienced simplicity, and we demonstrated that their aggregated performance over time did not improve. However, we quickly found these usability metrics unable to capture the real essence of the problem, i.e., why the system was not perceived as simple. In general, usability metrics such as aggregated or average speed or error rate does not reflect individual experience, only performance. And there is no guaranteed correlation between an objectively good performance and a satisfactory experience. To expand on our work, we carried out a third research phase with a new cycle of usability assessment and simplicity evaluation where we followed up both activities with a short interview of the participants. Through our interviews, we attempted to capture insight on experienced simplicity of a system where we simultaneously had knowledge about their performance. This allowed us to compare their performance in relation to their perception of the simplicity, and it also provided an opportunity to ask for the reasoning behind the given grades and assessments.

One prominent example within our own empirical context was employees who would consistently outperform the elderly people, despite spending less time on the tablet. They would perform tasks faster and with fewer errors. However, they did not perceive it as simple. As the results in Table V shows, several participants found the system to be oversimplified and preventing them from performing tasks in the preferred manner, and instead drove them into a predefined pattern of use. One participant claimed that she had *"[...] learned to perform this task in a certain way because that is how it wants me to do it"*. This user in particular did not perceive the system as simple. She had written down a step-by-step guide, which she had then memorized over time. It was not a matter of simplicity that led to the fast performance, but rather her learning precise instructions by heart. When asked to perform a similar, albeit slightly different task, she was no longer performing as well. Just by switching to a task with different sequential steps she was unable to use her instructions, and she was unable to transfer the knowledge from the familiar tasks to this new task. This example illustrates how the constructed simplicity imagined by the designers does not manifest itself as a simple experience as long as the user is unable to understand the system, even though they somehow manage to get through the task. As long as the understanding of the system remains at the same level, the experienced simplicity will also remain the same.

From the elderly participants, we learned that we should be realistic on how much effort we can and should expect from elderly end-users. If even basic operations of the system require a lot of new understanding and practice, most elderly would not invest the necessary time. While the employees were able to learn the system during their work hours as a part of their profession, the elderly people would rather choose to abstain from use if the entry level threshold was set too high. This exact phenomenon has also been

captured in prior research in the same empirical context; more precisely, lack of familiarity with the features of the system led to fewer people using it [17]. Designers should not spend time on trying to make the design itself simple, but instead focus on designing for understanding and mastery which will give users an opportunity to experience simplicity as their understanding and mastery grows. Designing solely for simplicity will force a compromise on functionality. Norman also argues that by recognizing understandability as the real issue, we are halfway to the solution [3]. In fact, his three suggested principles, i.e. modularization, mapping and conceptual models, all suggest supporting user in their use indirectly by helping them better understand the system.

However, the cognitive capacities of elderly people should not be discarded. Nor should it be the default excuse for interfaces and interactions that fail to deliver simplicity. Several participants demonstrated fully functional cognitive capabilities, and for these participants it was not their mental or physical conditions that prevented them from learning. It was simply the way the tablet had been introduced. During our follow-up interviews, one participant said she still used the tablet regularly after 13 months, and knew exactly what to expect from it. However, she did not understand it. She explained that repetitions help a lot, and she knew exactly what to expect from the tablet. There were issues she could not explain, and she *"[...] knew the errors will show up, because they do every time, but knowing about them was not the same as knowing how to remove them"*. She explained that she would attend a new training course or course for intermediate users, however, no such courses existed, so she had just learned to live with the errors.

#### B. Lowering the threshold for understanding

Designing for experienced simplicity also require attention to the way the technology is introduced and taught to the users. Our initial research was supported by ethnographic studies, and one of the lessons learned from home visits was that only 23.9 % (22/92) of the residents at the care facility were actively using the tablet one year after the introduction. After two years, the number of active users had dropped to 18.5 % (17/92). The number of participants at the introductory training given by the vendor was significantly higher (56.5 %). Through follow-up interviews we could conclude that the reason behind the high dropout rate was that the entry-level threshold was too high for most people. Several elderly people had attempted to learn the basic operations of the system, yet the provided training was not enough to get them familiar and confident enough to continue the learning on their own. The instructions that came along the tablet were also not adapted to individual needs, something that made it difficult to catch up for those who felt comfortable starting after they saw how the early adopters were mastering the system.

The lack of ideal users within the context of assistive technology strongly suggests diversity in both the design of the system and in the way the user is taught to operate the system. It has also been pointed out that heterogeneous qualities can blur out if elderly people are clustered into one or only a few larger groups, and thereby end up ignoring individual needs and understanding [18]. Prior research [19] [20] have pointed out how this homogenous clustering can force user groups over on impractical or difficult alternatives, or even exclude them all together [20]. The generation of elderly people that has grown up without technology also entails diversity in both exposure and prior knowledge [21]. This also suggests a more individually tailored approach in order to help users accommodate and struggle less in order to feel a sense of mastery.



Figure 12. Group training on the left and individual training on the right

Other researchers within our empirical context have addressed this issue by developing an alternative instruction manual of the tablet aiming at a *design for all* approach. The goal was to design an instruction manual understandable for everyone regardless of skills and possible disabilities [17]. Their instruction manual was built around a task-divided design where tasks were grouped into difficulty levels, and thereby only introduced more advanced operations once the users had gained some basic skills. This made the instruction manual more dynamic as it would adapt to the learning curve of the user rather overwhelming the user by introducing all tasks at once. We carried out sessions of individual workshops and training in our prior research [22], and used a similar approach with smaller groups of people. When elderly people with limited abilities to participate in communal activities were unable to join our sessions, we brought in family members or daytime employees who could speak authoritatively on behalf of those who could not voice their own needs. Thereby their challenges and mastery progress were represented through proxy-users who could follow them up individually later. Moving from training in larger groups to smaller groups or even individual training (Figure 12) demonstrated a significant increase in the number of users. One of the quotes reported by our colleges in [17] illustrates the need to adapt the training in order to support mastery: *“I think I could have used this on my own, if someone first just once had showed me how it works”*.

## VII. DISCUSSION

### A. Ensuring familiarity and transferability

Mastery requires understanding and learning. It also relies heavily on the users' previous exposure, and design following simplicity should evoke a connection to prior experiences. Thus, the elderly users rely heavily on transferring prior skills and knowledge in order to adapt a level of understanding and learning that nurtures mastery. One of the key challenges with both systems evaluated in our study was the lack of consistent metaphors. Several elderly residents with prior experience with devices similar to those used in our evaluation were unable to utilize prior knowledge due to metaphors not being consistent; simplicity also encompasses other design principles, e.g., consistency and affordance. Actions, icons, symbols and other metaphors should mediate experiences rather than direct [13]. And the diverse backgrounds of the elderly participants made us very aware of the difficulty of reducing complex information into simplified metaphors where everyone understands both the metaphors and the symbolic meaning or feeling they encompass. This challenge has been addressed by previous studies [23] who relied on a simplified design to trigger a nostalgic effect in order to help familiarizing metaphors.

In our studies, several elderly users struggled with the tablet responding to their actions with unexpected outcomes. One example included residents trying to use prior knowledge like familiarized gestures on the tablet, e.g., pinching and dragging to zoom or sliding actions to scroll, when visiting websites during task #3 (Table III). The system being of a different operating system than what they had previously used responded differently than expected; the slider scrolled the website in the opposite direction and the pinch and drag gesture were not recognized by the system at all. During the follow-up interviews we confirmed that participants still struggled after 13 months of use as they still had not forgotten the habits of their prior interaction. For many participants, the cognitive and physical load of learning how to independently operate a piece of technology was so straining that the participants were unable to completely unlearn their prior habits, also after 13 months.

Another prominent example was the RFID doors automatically locking if they were closed, i.e., a contrast from the traditional method of locking doors, by turning a key. The doors were heavy and closed automatically, and once closed they would also lock automatically like a spring lock, only without any sound or click. It was especially confusing during the first evaluation as the elderly people still had not memorized that the redundant key hole affording use of traditional keys (Figure 4) served no purpose, and repeatedly expected the door to be locked manually with a key after closing the door, when instead the door would automatically close and lock behind them. In fact, the accidental error rate for the task involving the doors

(task #1 in Table III) was one of the tasks with highest combined average error rate and was one out of only four cases where the deliberate error rate increased between the first and second phase. This was a matter of confusion and reported as one of the main issues responsible for the degree of learnability dropping in the simplicity evaluations throughout the three phases (see Figure 11).

A third example included problems during text messaging (task #4 in Table III). When asked to send and receive text messages, several old and familiar metaphors were suddenly replaced by new unfamiliar metaphors, where the residents struggled with applying old knowledge to the new system. For instance, the phone number was not their usual phone number, nor did it resemble a traditional phone number (issue #15), and the icons used to symbolize contacts and messages were not recognized (issue #36). The task of text messaging yielded the highest number of deliberate errors during all three evaluations, and this was clearly a result of their attempt to perform actions associated with prior experience or applying old metaphors to the new system that were no longer compatible or purposeful. The number had too many digits to learn by heart, and it did not make sense for the participants to break with the standard eight-digit phone number system in Norway as their number would not be recognized as a phone number most places. Through the follow-up interview we also learned how this way of using phone numbers eliminated their close identity to their phone number. There was no way of registering the new number on their own name in any of the major phone directories, and no way of people to finding their number by entering their name.

Through these three examples we discovered that the most confusing and frustrating situations arose when the elderly users performed an action where the outcome was unclear or unfamiliar. Familiarity and transferability became strong indicators of the ability to master new systems; when actions became disconnected from their meaning, the purposefulness in the actions disappeared and mastery suddenly became a challenge.

### *B. Maintaining purposeful actions*

In order to further discuss purposeful actions, we gave the participants 6 months and then later another 7 months to familiarize themselves with the systems before asking them to evaluate the simplicity a second and third time. 4 participants (#1, #4, #6 and #11 in Figure 10) reported a higher average score during the second simplicity evaluation, suggesting a more positive attitude towards the 7 elements of simplicity we evaluated. As a result, we used the second and third phase to investigate whether this was a result of increased learning and understanding, or just a matter of increased use frequency. When discussing the mastery of the system, we need to distinguish between increased ease due to more frequent use and increased ease due to actions, metaphors and language suddenly making more sense. It was unanimously agreed upon that the

participants reported a higher score as a result of increased frequency rather than actions, metaphors and language making sense. Confusing metaphors were still confusing and over the course of 13 months participants had begun to learn certain use patterns by heart. To them, adopting strategies to avoid problems would result in less complicated interaction and improve the efficiency once memorized.

However, over time, we registered that the average score for some of these participants had normalized. Only participant #2 and #11 in Figure 10 increased their average score between the second and third phase. It was evident that time did not contribute to increased understanding of metaphors, but rather resulted in incorporated strategies and workarounds. Confusing actions, metaphors and language remained confusing even after 13 months of use, also for those reporting a higher average score, and the increased perception bloomed out of the development of personal strategies for memorizing or working around troublesome tasks. This is an important finding as patience is often considered a virtue when elderly people adapt to new technology, including in our own previous work [15] [16]. However, in this study, we observed that actions, metaphors and language confusing the ended up remaining confusing after 6 and 13 months as well; providing more time might heal all wounds, but it does not guarantee disentanglement of perplexities and disorientations.

Another argument for ensuring purposeful actions is to maintain good mapping. Natural mapping is understood as designing the interface in such a manner that the user can readily determine the relationship between the action and the outcome into the world [24]; i.e., a design where the user is able to associate cause with effect, thereby understanding expected output for provided input. For instance, the autonomy and intangibility of the automated light sensor evaluated during the usability assessment (task #9 in Table III) imposed several challenges to mapping. The physical zone in the room where movements were recognized was not clear, and there were no indications in the interface towards the intensity of the light or the duration of the light. One participant claimed that the best mapping for her was a traditional light switch where up meant on and down meant off in the middle in the room where the left switch controlled the lamp to the left and the right switch controlled the lamp to the right. Similarly, replacing traditional door keys with RFID cards to unlock doors had similar effects on the natural mapping; the users were unable to properly answer how long the door remained unlocked once the RFID card was scanned or determine the minimum required distance between the RFID card and the scanner on the door.

### *C. Adapting to evolving perceptions of simplicity*

Trier and Richter [4] argues that the application of simplicity as a design guideline requires flexibility. Between the two first phases we observed two participants undergo

changes in their overall health level. There were significant differences in their cognitive and reasoning abilities. Before the third phase, we consulted with the daytime employees and caretakers in order to confirm the appropriateness of their participation. For example, one of these participants could no longer explain the numbers on the display used to adjust heating levels (Figure 4). She had a custom color marker that indicate up and down for temperature as the up- and down-facing arrows no longer served as metaphors for increasing and decreasing the room temperature. While the arrows and display offered sufficient explanation during the first evaluation, she could no longer explain the details of the system during the second evaluation, e.g., the meaning of “1.4°C” on the display (as illustrated in Figure 4). Instead, she found that blue and red colors helped her remembering that if she pressed those buttons long enough it would eventually get colder or warmer. This exemplifies how typical aging symptoms, e.g., reduced cognitive capacities, clearly influenced both their performance and their assessment of simplicity.

Related work [10] discusses how only paying attention to physical and perceptual characteristics of elderly users end up struggling with coping with the cognitive behavioral characteristics and traits of becoming elderly. Consequently, we consider achieving simplicity among elderly people especially difficult as they undergo rapid cognitive, physical and social changes in their lives that alter their attitude and opportunities towards technology. As metaphors lose their abilities to aide us with understanding and interacting with the system, our perception of the simplicity of the system deteriorate over time. Simplicity is not a constant factor that remains the same throughout of life, but rather one of the dynamic and flexible factors that evolves along as we evolve; acquiring new knowledge, entering new contexts and adapting new technologies contribute to reshaping our view on simplicity and what we perceive as simple. Similarly, changes in our lives can contribute to complicating systems we once considered simple; it often becomes a matter not only of preference, but also a matter of limited opportunities. Over a period of 13 months the perspectives of all the elderly participants changed in both the simplicity evaluation and the usability assessment. A design offering simplicity should therefore adapt according to the changing behavior and abilities of the elderly.

Cooper et al. [25] also discuss the phenomenon where visual simplicity leads to cognitive complexity due to an unbalanced reduction. Several participants struggled with adapting to new technology due to cognitive load and preferred to rely on old knowledge and metaphors instead; they preferred familiar technologies, even those comparatively inefficient and impractical, because they could rely on habits. Examples of such desires included installing old landline telephones rather than telephoning from the tablet even though the latter was free, and using old televisions with large physical buttons instead of new flat screen television even though it involved getting out of

the couch every time to change channel. A frequent counter-argument is that this behavior is a result of their attitude towards technology in general rather than a matter of cognitive overload, however their attitude during the rest of discussions clearly suggested that they were positive towards technology but struggled with adapting to certain aspects of the system, in this particular case it was the misleading colors (#5), the two separate phone number (#15) and the confusing language (#35) that caused the perceived complexity (Table V). If those aspects of the systems are metaphors intended to bridge the gap between the system and prior experiences, achieving mastery can become difficult, sometimes even impossible. As a result, we argue that design striving for simplicity should be open to seemingly inefficient and impractical features if they evoke positive stimuli for the users, e.g., allowing them to take advantage of old habits rather than adapting new ones.

#### *D. Avoiding forcing ways of reasoning*

By oversimplifying technology, we limit the users' freedom and make decisions on their behalf by forcing them into predefined patterns of behavior that do not necessarily comply with their needs. The participants in our study disliked the predefined settings and missed working with a system that could adapt or be customized to fit their cognitive and bodily capabilities. Similar to studies of Eytam and Tractinsky [13], several participants desired the ability to design their own complexities. Our principal example was the tablet which did not offer any customization options or the option to install custom application with services that the system did not currently offer. Once one participant discovered a way to override the system and install own application, in this case a video chat application, several others asked for instruction on how to do so as well. This case exemplified how the intention of simplifying the system by removing seemingly undesired features became a restriction of the users' desires. By directing, limiting or forcing decisions on the elderly, the outcome might end up being stigmatizing rather than inspiring [26]. For the elderly people who feel they are losing control and influence over their own life, this stigma through oversimplification may further assume a role as a reinforcing factor counteracting dignity and integrity by depriving them of their opportunity and right to autonomy [15]. This may again influence the ability to learn how to operate such systems as more general suggestions on simplicity in learning advocates the use of environments where users feel good and able.

From their own results, Keay-Bright and Howarth [14] conclude that environmental factors that stimulate and encourage without prejudgment is a vital requirement for learning. Besides decelerating or even preventing the process of mastering, inhibiting learning has also proven to result in negative experiences for elderly people. The feeling of helplessness that comes with aging makes the elderly people more aware of their own dependability, and previous

findings from our studies indicated that several participants felt deprived of their independence due to oversimplified and restrictive systems limited their opportunity to function at their best level [15].

### E. Balancing the simplicity

The phenomenon of systems involving simplification measurements that end up having the opposite effect is often referred to as fake simplicity. Colborne [7] describes fake simplicity as the idea unable to ever meet its initial promise, instead just making everything unnecessarily complex and less effective. One example was the microwave of one of the participants that instead of using time or watt as input, used pictures of a pizza slice and a cup of tea to signal the duration and strength. Another example mentioned by a participant was his washing machine with only predefined programs where neither duration nor temperature was specified. Oversimplification can prevent mastery by concealing important components of the interaction thereby preventing the user from learning the relationship between action and effect. It also demonstrates how mastery requires balance. On one hand, the system needs to foster mastery through a design that is perceived as free of complexities; on the other hand, the system should encourage mastery by challenging and exciting the user and simultaneously avoiding oversimplified and condescending interfaces. Finding this balance where users are both presented with challenging tasks and at the same time provided with enough help to solve them helps us preventing that the system tips over in either direction.

During the task-based group evaluation, the participants were asked to identify simplicity issues as either too simple or too complex systems. As a result, they were asked to clarify whether it was a case of lack of simplicity or abundance of simplicity, i.e., a complex issue that could benefit from simplification or an issue that was simplified to such an extent that it had become oversimplified and demeaning. Surprisingly, 13 out of 17 issues were classified by the participants as matters of oversimplification, i.e., that the simplification of the interface or interaction resulted in either poor usability or led undesired user experiences. The most important finding from these results was that simplicity is not a principle where “one size fits all”.

One argument presented by an elderly lady for not liking the phone function of the tablet was that with tablets and mobile phones, the action of answering a call required an additional step. With a traditional land line phone, picking up the phone initiated the call, while on newer device she would first have to press an answer button and then pick up the phone, thereby complicating it for her by introducing additional step. Secondly, the internal disagreement between the groups further suggests that the elderly residents might have a different outlook on simplicity relatively compared to the two other groups, thereby demonstrating a variation not only between individuals but also between groups of individuals. What remains a matter of simplicity for the

elderly users seems to deviate from what the employees and experts consider simplicity issues further suggesting that simplicity in use is different from analytic simplicity or imagined simplicity. Achieving simplicity without simultaneously weakening the functionality is one of the great struggles of designers, and it is vital to find this point of intersection where constructive simplification suddenly begins to defeat its own end. Simplicity is not only a matter of aesthetics; it is also a matter of balanced functionality.

## VIII. CONCLUSION

In this paper, we have discussed the difference between analytic and *experienced simplicity* in the context of assistive technology. We have examined and evaluated existing assistive technology over the course of 13 months in order to study how perspectives on simplicity evolve over time. We have focused on how the users experience the technology by looking at experienced simplicity as something defined through mastery and context. As a result, central to our studies have been to understand how the sense of mastery changes over time, and whether technology aiming at being simple in use is actually experienced as simple. We have reported from three phases of evaluation involving altogether 45 participants, including 30 elderly people with an average age of 86 years. Our main discussion revolve around the difference between analytic and imagined simplicity, and how analytic simplicity usually do not manifest itself as experienced simplicity within the context of assistive technology. We also discuss how designs aiming at simplicity should focus on understandability and adaptation revolving around *mastery* and *context* through five key implications suggesting that simplicity should (1) build on familiarity and the ability to utilize old knowledge to help mastering the system; (2) ensure purposeful actions where the user can understand and learn to master the system; (3) adapt along with the evolving contextual factors; (4) avoid limiting the users to predefined patterns of behavior and allow them to use and master the system as they find appropriate; and (5) find the balance where the design is simple enough to be understood and learned, yet challenging enough to allow users to progress towards mastery. Only by doing so, we can achieve mastery in the intended context of use, which is what we believe simplicity to be.

## REFERENCES

- [1] S. G. Joshi, “When Simple Technologies Make Life Difficult,” in ACHI 2015, The Eighth International Conference on Advances in Computer-Human Interactions. Lisbon, pp. 168-177, 2015.
- [2] S. Finken and C. Mörtberg, “Performing Elderliness – Intra-actions with Digital Domestic Care Technologies,” in ICT and Society, Springer Berlin Heidelberg, pp. 307-319, 2014.
- [3] D. Norman, “Simplicity is not the answer,” Interactions, septiembre-octubre, 15(5), pp. 45-46, 2008.

- [4] M. Trier and A. Richter, "' I Can Simply ...'-Theorizing Simplicity As A Design Principle And Usage Factor," in ECIS 2013, pp. 2-3, 2013.
- [5] J. Lee, D. Lee, J. Moon, and M.-C. Park, "Factors affecting the perceived usability of the mobile web portal services: comparing simplicity with consistency," *Information Technology and Management*, 14(1), pp. 43-57, 2013.
- [6] J. Maeda, "The laws of simplicity," MIT Press, 2006.
- [7] G. Colborne, "Simple and usable web, mobile, and interaction design," New Riders, 2010.
- [8] H. Obendorf, "Minimalism: Designing Simplicity," Springer, 2009.
- [9] R. Picking, V. Grout, J. McGinn, J. Crisp, and H. Grout, "Simplicity, consistency, universality, flexibility and familiarity: the SCUFF principles for developing user interfaces for ambient computer systems," *International Journal of Ambient Computing and Intelligence (IJACI)*, 2(3), pp. 40-49, 2010.
- [10] H. Akatsu, H. Miki, and N. Hosono, "Design principles based on cognitive aging," in *Human-Computer Interaction, Interaction Design and Usability*, Springer, pp. 3-10, 2007.
- [11] F. H. A. Razak, N. A. Razak, W. A. Wan Adnan, and N. A. Ahmad, "How simple is simple: our experience with older adult users," in *Proceedings of the 11th Asia Pacific Conference on Computer Human Interaction*, ACM, pp. 379-387, 2013.
- [12] S. Sulaiman and I. S. Sohaimi, "An investigation to obtain a simple mobile phone interface for older adults," in *Intelligent and Advanced Systems (ICIAS)*, IEEE, pp. 1-4, 2010.
- [13] E. Eytam and N. Tractinsky. "The Paradox Of Simplicity: Effects Of User Interface Design On Perceptions And Preference Of Interactive Systems," in *MCIS 2010*. pp. 30, 2010.
- [14] W. Keay-Bright and I. Howarth, "Is simplicity the key to engagement for children on the autism spectrum?," *Personal and Ubiquitous Computing*, 16(2), pp. 129-141, 2012.
- [15] S. G. Joshi, "Emerging ethical considerations from the perspectives of the elderly," in *Ninth International Conference on Cultural Attitudes in computer-Human Interactions*, pp. 1-15, 2014.
- [16] S. G. Joshi and A. Woll, "A Collaborative Change Experiment: Telecare as a Means for Delivery of Home Care Services," in *Design, User Experience, and Usability. User Experience Design for Everyday Life Applications and Services*, Springer, pp. 141-151, 2014.
- [17] C. Haug and F. H. Kvam, "Tablets and elderly users: Designing a guidebook," Master thesis, Department of informatics, UiO, 2014.
- [18] S. Finken and C. Mörtberg, "Performing Elderliness—Intra-actions with Digital Domestic Care Technologies," in *ICT and Society*, Springer, p. 307-319, 2014.
- [19] A. L. Culén, S. Finken, and T. Bratteteig, "Design and interaction in a smart gym: Cognitive and bodily mastering," in *Human Factors in Computing and Informatics*, Springer, pp. 609-616, 2013.
- [20] E. Brandt, T. Binder, L. Malmberg, and T. Sokoler, "Communities of everyday practice and situated elderliness as an approach to co-design for senior interaction," in *Proceedings of the 22nd Conference of the Computer-Human Interaction Special Interest Group of Australia on Computer-Human Interaction*, ACM, pp. 400-403, 2010.
- [21] N. Wagner, K. Hassanein, and M. Head, "Computer use by older adults: A multi-disciplinary review," *Computers in human behavior*, 26(5), pp. 870-882, 2010.
- [22] S. G. Joshi and T. Bratteteig, "Assembling Fragments into Continuous Design: On Participatory Design with Old People," in *Nordic Contributions in IS Research*, Springer, pp. 13-29, 2015.
- [23] M. Nilsson, S. Johansson, and M. Håkansson. "Nostalgia: an evocative tangible interface for elderly users," in *CHI'03 Extended Abstracts on Human Factors in Computing Systems*, ACM, pp. 964-965, 2003.
- [24] D. A. Norman, "The design of everyday things," Basic books, 2002.
- [25] A. Cooper, R. Reimann, and D. Cronin, "About face 3: the essentials of interaction design," John Wiley & Sons, 2007.
- [26] L. Rosenberg, A. Kottorp, and L. Nygård, "Readiness for Technology Use With People With Dementia The Perspectives of Significant Others," *Journal of Applied Gerontology*, 31(4), pp. 510-530, 2012.

# Predicative Recursion, Diagonalization, and Slow-growing Hierarchies of Time-bounded Programs

Emanuele Covino and Giovanni Pani

Dipartimento di Informatica

Università di Bari, Italy

Email: [emanuele.covino@uniba.it](mailto:emanuele.covino@uniba.it), [giovanni.pani@uniba.it](mailto:giovanni.pani@uniba.it)

**Abstract**—We define a version of *predicative recursion*, a related programming language, and a hierarchy of classes of programs that represents a resource-free characterization of register machines computing their output within polynomial time  $O(n^k)$ , for each finite  $k$ . Then, we introduce an operator of *diagonalization*, that allows us to extend the previous hierarchy and to capture the register machines with computing time bounded by an exponential limit  $O(n^{n^k})$ . Finally, by means of a restriction on composition of programs, we characterize the register machines with a polynomial bound imposed over time and space complexity, simultaneously.

**Index Terms**—Time/space complexity classes; Implicit computational complexity; Predicative recursion; Diagonalization.

## I. INTRODUCTION

A complexity class is usually defined by imposing an explicit bound on time and/or space resources used by a Turing Machine (or another equivalent model) during its computation. On the other hand, different approaches use logic and formal methods to provide languages for complexity-bounded computation; they aim at studying computational complexity without referring to external measuring conditions or a particular machine model, but only by considering language restrictions or logical/computational principles implying complexity properties. In particular, this is achieved by characterizing complexity classes by means of recursive operators with explicit syntactical restrictions on the role of variables. In this paper, we extend the result introduced in [1] by defining a resource-free characterization of register machines computing their output within polynomial time  $O(n^k)$ , for each finite  $k$ , and exponential  $O(n^{n^k})$ ; we achieve this result by means of our version of *predicative recursion* and of a new *diagonalization* operator, and a related programming language.

One of the first characterization of the polynomial-time computable functions was given by Cobham [2], in which these functions are exactly those generated by bounded recursion on notation. The first predicative definitions of recursion can be found in the work of Simmons [3], Bellantoni and Cook [4], and Leivant [5], [6]: they introduced a ramification principle that does not require that explicit bounds are imposed on the definition of functions, proving that this principle captures the class PTIMEF. Following this approach, several other complexity classes have been characterized by

means of unbounded and predicative operators: see, for instance, Leivant and Marion [7] and Oitavem [8] for PSPACEF and the class of the elementary functions; Clote [9] for the definition of a time/space hierarchy between PTIMEF and PSPACEF; a theoretical insight has been provided by Leivant [5], [10] and [6]. All these approaches have been dubbed *Implicit Computational Complexity*: they share the idea that no explicitly bounded schemes are needed to characterize a great number of classes of functions and that, in order to do this, it suffices to distinguish between *safe* and *normal* variables (or, following [3], between *dormant* and *normal* ones) in the recursion schemes. Roughly speaking, the normal positions are used only for recursion, while the safe positions are used only for substitution. The two main objectives of this area are to find natural implicit characterizations of various complexity classes of functions, thereby illuminating their nature and importance, and to design methods suitable for static verification of program complexity.

Our version of the *safe recursion* scheme on a binary word algebra is such that  $f(x, y, za) = h(f(x, y, z), y, za)$ ; throughout this paper we will call  $x, y$  and  $z$  the auxiliary variable, the parameter, and the principal variable of a program defined by recursion, respectively. We do not allow the renaming of variable  $z$  as  $x$ , implying that the step program  $h$  cannot assign the value  $f(x, y, z)$  of the being-defined program  $f$  to the principal variable  $z$ : in other words, we always know in advance the number of recursive calls of the step program in a recursive definition. We obtain that  $z$  is a *dormant* variable, according to Simmons' [3], or a *safe* one, following Bellantoni and Cook [4]. Starting from a natural definition of constructors and destructors over an algebra of lists, we define the hierarchy of classes of programs  $\mathcal{T}_k$ , with  $k \in \mathbb{N}$ , where programs in  $\mathcal{T}_1$  can be computed by register machines within linear time, and  $\mathcal{T}_{k+1}$  are programs obtained by one application of safe recursion to elements in  $\mathcal{T}_k$ ; we prove that programs defined in  $\mathcal{T}_k$  are exactly those programs computable within time  $O(n^k)$ .

Using the definition of structured ordinals as given in [11], we introduce an operator of constructive *diagonalization*, and we extend the previous hierarchy to  $\mathcal{T}_\lambda$ , with  $\omega \leq \lambda \leq \omega^\omega$ . Programs in  $\mathcal{T}_{\alpha+1}$  are obtained by one application of safe recursion to elements in  $\mathcal{T}_\alpha$ ; if  $\lambda$  is a limit ordinal, and  $\lambda_1, \dots, \lambda_k, \dots$  is the associated fundamental

sequence, programs in  $\mathcal{T}_\lambda$  are obtained by diagonalization on the previously defined sequence of classes  $\mathcal{T}_{\lambda_1}, \dots, \mathcal{T}_{\lambda_k}, \dots$ . This allows us to harmonize in a single hierarchy of classes of programs all the register machines with computing time bounded by polynomial time  $O(n^k)$  and exponential time  $O(n^{n^k})$ , for each finite  $k$ . Similar results, achieved with different approaches, can be found in [12], [13], [14], and [15].

Then, we restrict  $\mathcal{T}_k$  to the hierarchy  $\mathcal{S}_k$ , whose elements are the programs computable by a register machine in linear space. By means of a restricted form of composition between programs, we define a polytime-space hierarchy  $\mathcal{TS}_{qp}$ , such that each program in  $\mathcal{TS}_{qp}$  can be computed by a register machine within time  $O(n^p)$  and space  $O(n^q)$ , simultaneously. Similar results are in [16] and [7], and are a preliminary step for an implicit classification of the hierarchy of time-space classes between PTIME and PSPACE, as defined in [9].

The paper is organized as follows: in Section II, we introduce the basic instructions of our language, the notion of composition of programs, and the classes of programs  $\mathcal{T}_0$  and  $\mathcal{T}_1$ ; in Section III, we recall the definition of register machine, the model of computation underlying our characterization, and we prove that programs in  $\mathcal{T}_1$  capture exactly the computations performed by a register machine within linear time; in Section IV, we define the finite hierarchy  $\mathcal{T}_k$ , with  $k \geq 1$ , and we prove that programs in this hierarchy capture the computations performed within polynomial time; in Section V, we introduce the diagonalization operator, and we extend the finite hierarchy in order to capture the computations with time-complexity up to exponential time; in Section VI, we redefine the notion of composition, and we give a characterization of classes of programs with time and space polynomial bound.

## II. BASIC INSTRUCTIONS AND DEFINITION SCHEMES

In this section, we introduce the basic operators of our programming language and the first two classes on which our hierarchy is based. The language is defined over a binary word algebra, with the restriction that words are packed into lists, with the symbol  $\odot$  acting as a separator between each word. This allow us to handle a sequence of words as a single object. The basic instructions allow us to manipulate lists of words, with some restrictions on the renaming of variables; the language is completely defined adding our version of recursion and composition of programs.

### A. Recursion-free programs and class $\mathcal{T}_0$

$\mathbf{B}$  is the binary alphabet  $\{0, 1\}$ .  $a, b, a_1, \dots$  denote elements of  $\mathbf{B}$ , and  $U, V, \dots, Y$  denote words over  $\mathbf{B}$ .  $p, q, \dots, s, \dots$  stand for lists in the form  $Y_1 \odot Y_2 \odot \dots \odot Y_{n-1} \odot Y_n$ .  $\epsilon$  is the empty word. The  $i$ -th component  $(s)_i$  of  $s = Y_1 \odot Y_2 \odot \dots \odot Y_{n-1} \odot Y_n$  is  $Y_i$ .  $|s|$  is the length of the list  $s$ , that is the number of letters occupying

in  $s$ . We write  $x, y, z$  for the variables used in a program, and we write  $u$  for one among  $x, y, z$ . Programs are denoted with the letters  $f, g, h$ , and we write  $f(x, y, z)$  for the application of the program  $f$  to variables  $x, y, z$ , where some among them may be absent.

*Definition 2.1:* The basic instructions are:

- 1) the *identity*  $I(u)$  that returns the value  $s$  assigned to  $u$ ;
- 2) the *constructors*  $C_i^a(s)$  that add the digit  $a$  at the right of the last digit of  $(s)_i$ , with  $a = 0, 1$  and  $i \geq 1$ ;
- 3) the *destructors*  $D_i(s)$  that erase the rightmost digit of  $(s)_i$ , with  $i \geq 1$ .

Constructors  $C_i^a(s)$  and destructors  $D_i(s)$  leave the input  $s$  unchanged if it has less than  $i$  components.

*Example 2.1:* Given the word  $s = 01 \odot 11 \odot 00$ , we have that  $|s| = 9$ , and  $(s)_2 = 11$ . We also have  $C_1^1(01 \odot 11) = 011 \odot 11$ ,  $D_2(0 \odot 0 \odot 0) = 0 \odot 0 \odot 0$ ,  $D_2(0 \odot 0 \odot 0) = 0 \odot 0 \odot 0$ .

*Definition 2.2:* Given the programs  $g$  and  $h$ ,  $f$  is defined by *simple schemes* if it is obtained by:

- 1) *renaming* of  $x$  as  $y$  in  $g$ , that is,  $f$  is the result of the substitution of the value of  $y$  to all occurrences of  $x$  into  $g$ . Notation:  $f = \text{RNM}_{x/y}(g)$ ;
- 2) *renaming* of  $z$  as  $y$  in  $g$ , that is,  $f$  is the result of the substitution of the value of  $y$  to all occurrences of  $z$  into  $g$ . Notation:  $f = \text{RMN}_{z/y}(g)$ ;
- 3) *selection* in  $g$  and  $h$ , when for all  $s, t, r$  we have

$$f(s, t, r) = \begin{cases} g(s, t, r) & \text{if the rightmost digit} \\ & \text{of } (s)_i \text{ is } b \\ h(s, t, r) & \text{otherwise,} \end{cases}$$

with  $i \geq 1$  and  $b = 0, 1$ . Notation:  $f = \text{SEL}_i^b(g, h)$ .

Simple schemes are denoted with SIMPLE.

*Example 2.2:* if  $f$  is defined by  $\text{RNM}_{x/y}(g)$  we have that  $f(t, r) = g(t, t, r)$ . Similarly,  $f$  defined by  $\text{RMN}_{z/y}(g)$  implies that  $f(s, t) = g(s, t, t)$ . Let  $s$  be the word  $00 \odot 1010$ , and  $f = \text{SEL}_2^0(g, h)$ ; we have that  $f(s, t, r) = g(s, t, r)$ , since the rightmost digit of  $(s)_2$  is 0.

*Definition 2.3:* Given the programs  $g$  and  $h$ ,  $f$  is defined by *safe composition* of  $h$  and  $g$  in the variable  $u$  if it is obtained by the substitution of  $h$  to  $u$  in  $g$ , if  $u = x$  or  $u = y$ ; the variable  $x$  must be absent in  $h$ , if  $u = z$ .

Notation:  $f = \text{SCMP}_u(h, g)$ .

The reason of this particular form of composition of programs will be clear in the following section, where we will show to the reader how to combine composition and recursion in order to obtain new time-bounded programs.

*Definition 2.4:* A *modifier* is obtained by the safe composition of a sequence of constructors and a sequence of destructors.

*Definition 2.5:*  $\mathcal{T}_0$  is the class of programs defined by closure of modifiers under selection and safe composition. Notation:  $\mathcal{T}_0 = (\text{modifier}; \text{SCMP}, \text{SEL})$ .

All programs in  $\mathcal{T}_0$  modify their inputs according to the result of some test performed over a fixed number of digits.

### B. Safe recursion and class $\mathcal{T}_1$

In what follows we introduce the definition of our form of recursion and iteration *on notation* (see [4] and [10]).

*Definition 2.6:* Given the programs  $g(x, y)$  and  $h(x, y, z)$ ,  $f(x, y, z)$  is defined by *safe recursion* in the *basis*  $g$  and in the *step*  $h$  if for all  $s, t, r$  we have

$$\begin{cases} f(s, t, a) &= g(s, t) \\ f(s, t, ra) &= h(f(s, t, r), t, ra), \end{cases}$$

with  $a \in \mathbf{B}$ . Notation:  $f = \text{SREC}(g, h)$ .

In particular,  $f(x, z)$  is defined by *iteration* of  $h(x)$  if for all  $s, r$  we have

$$\begin{cases} f(s, a) &= s \\ f(s, ra) &= h(f(s, r)). \end{cases}$$

with  $a \in \mathbf{B}$ . Notation:  $f = \text{ITER}(h)$ . We write  $h^{|r|}(s)$  for  $\text{ITER}(h)(s, r)$  (i.e., the  $|r|$ -th iteration of  $h$  on  $s$ ).

*Definition 2.7:*  $\mathcal{T}_1$  is the class defined by closure under simple schemes and safe composition of programs in  $\mathcal{T}_0$  and programs obtained by one application of  $\text{ITER}$  to  $\mathcal{T}_0$  (denoted with  $\text{ITER}(\mathcal{T}_0)$ ).

Notation:  $\mathcal{T}_1 = (\mathcal{T}_0, \text{ITER}(\mathcal{T}_0); \text{SCMP}, \text{SIMPLE})$ .

As we have already stated in the Introduction, we call  $x, y$  and  $z$  the auxiliary variable, the parameter, and the principal variable of a program obtained by means of the previous recursion scheme. Note that the renaming of  $z$  as  $x$  is not allowed (see definition 2.2), and if the step program of a recursion is defined itself by safe composition of programs  $p$  and  $q$ , no variable  $x$  (i.e., no potential recursive calls) can occur in the function  $p$ , when  $p$  is substituted into the principal variable  $z$  of  $q$  (see definition 2.3). These two restrictions implies that the step program of a recursive definition never assigns the recursive call to the principal variable. This is the key of the polynomial-time complexity bound intrinsic to our programs.

*Definition 2.8:* 1) Given  $f \in \mathcal{T}_1$ , the *number of components* of  $f$  is  $\max\{i | D_i \text{ or } C_i^a \text{ or } \text{SEL}_i^b \text{ occurs in } f\}$ .  
Notation:  $\#(f)$ .

2) Given a program  $f$ , its *length* is the number of constructors, destructors and defining schemes occurring in its definition. Notation:  $lh(f)$ .

### III. COMPUTATION BY REGISTER MACHINES

In this section, we recall the definition of register machine as presented in [6], and we give the definition of computation within a given time and/or space bound. We prove that programs in  $\mathcal{T}_1$  are exactly those computable within linear time.

*Definition 3.1:* Given a free algebra  $\mathbf{A}$  generated from constructors  $\mathbf{c}_1, \dots, \mathbf{c}_n$  (with *arity*( $\mathbf{c}_i$ ) =  $r_i$ ), a *register machine* over  $\mathbf{A}$  is a computational device  $M$  having the following components:

1) a finite set of *states*  $S = \{s_0, \dots, s_n\}$ ;

2) a finite set of *registers*  $\Phi = \{\pi_0, \dots, \pi_m\}$ ;

3) a collection of *commands*, where a command may be:  
a **branching**  $s_i \pi_j s_{i_1} \dots s_{i_k}$ , such that when  $M$  is in the state  $s_i$ , switches to state  $s_{i_1}, \dots, s_{i_k}$  according to whether the main constructor (i.e., the leftmost) of the term stored in register  $\pi_j$  is  $\mathbf{c}_1, \dots, \mathbf{c}_k$ ;  
a **constructor**  $s_i \pi_{j_1} \dots \pi_{j_r} \mathbf{c}_i \pi_l s_r$ , such that when  $M$  is in the state  $s_i$ , store in  $\pi_l$  the result of the application of the constructor  $\mathbf{c}_i$  to the values stored in  $\pi_{j_1} \dots \pi_{j_r}$ , and switches to  $s_r$ ;  
a **p-destructer**  $s_i \pi_j \pi_l s_r$  ( $p \leq \max(r_i)_{i=1 \dots k}$ ), such that when  $M$  is in the state  $s_i$ , store in  $\pi_l$  the  $p$ -th subterm of the term in  $\pi_j$ , if it exists; otherwise, store the term in  $\pi_j$ . Then it switched to  $s_r$ .

A *configuration* of  $M$  is a pair  $(s, F)$ , where  $s \in S$  and  $F : \Phi \rightarrow \mathbf{A}$ .  $M$  induces a transition relation  $\vdash_M$  on configurations, where  $\kappa \vdash_M \kappa'$  holds if there is a command of  $M$  whose execution converts the configuration  $\kappa$  in  $\kappa'$ . A *computation* of  $M$  on input  $\vec{X} = X_1, \dots, X_p$  with output  $\vec{Y} = Y_1, \dots, Y_q$  is a sequence of configurations, starting with  $(s_0, F_0)$ , and ending with  $(s_1, F_1)$  such that:

- 1)  $F_0(\pi_{j'(i)}) = X_i$ , for  $1 \leq i \leq p$  and  $j'$  a permutation of the  $p$  registers;
- 2)  $F_1(\pi_{j''(i)}) = Y_i$ , for  $1 \leq i \leq q$  and  $j''$  a permutation of the  $q$  registers;
- 3) each configuration is related to its successor by  $\vdash_M$ ;
- 4) the last configuration has no successor by  $\vdash_M$ .

*Definition 3.2:* A register machine  $M$  *computes* the program  $f$  if, for all  $s, t, r$ , we have that  $f(s, t, r) = q$  implies that  $M$  computes  $(q)_1, \dots, (q)_{\#(f)}$  on input  $(s)_1, \dots, (s)_{\#(f)}, (t)_1, \dots, (t)_{\#(f)}, (r)_1, \dots, (r)_{\#(f)}$ .

*Definition 3.3:* Given a register machine  $M$  and the polynomials  $p(n)$  and  $q(n)$ , for each input  $\vec{X}$  (with  $|\vec{X}| = n$ ),

- 1)  $M$  computes its output within time  $O(p(n))$  if its computation runs through  $O(p(n))$  configurations;
- 2)  $M$  computes its output in space  $O(q(n))$  if, during the computation, the global length of the contents of its registers is  $O(q(n))$ .
- 3)  $M$  computes its output with time  $O(p(n))$  and space  $O(q(n))$  if the two bounds occur simultaneously, during the same computation.

Note that the number of registers needed by  $M$  to compute a program  $f$  has to be fixed a priori (otherwise, we should have to define a family of register machines for each program to be computed, with each element of the family associated to an input of a given length). According to definitions 2.8 and 3.2,  $M$  uses a number of registers which linearly depends on the highest component's index that  $f$  can manipulate or access with one of its constructors, destructors or selections; and which depends on the number of times a variable is used by  $f$ , that is, on the total number of different copies of the registers that  $M$  needs during the computation. Both these numbers are constant values, and can be detected before the

computation occurs.

Unlike the usual operators *cons*, *head* and *tail* over Lisp-like lists, our constructors and destructors can have direct access to any component of a list, according to definition 2.1. Hence, their computation by means of a register machine requires constant time, but it requires an amount of time which is linear in the length of the input, when performed by a Turing machine.

**Codes.** We write  $s_i \odot F_j(\pi_0) \odot \dots \odot F_j(\pi_k)$  for the word that encodes a configuration  $(s_i, F_j)$  of  $M$ , where each component is a binary word over  $\{0, 1\}$ .

*Lemma 3.1:*  $f$  belongs to  $\mathcal{T}_1$  if and only if  $f$  is computable by a register machine within time  $O(n)$ .

*Proof:* To prove the first implication we show (by induction on the structure of  $f$ ) that each  $f \in \mathcal{T}_1$  can be computed by a register machine  $M_f$  in time  $cn$ , where  $c$  is a constant which depends on the construction of  $f$ , and  $n$  is the length of the input.

Base.  $f \in \mathcal{T}_0$ . This means that  $f$  is obtained by closure of a number of modifiers under selection and safe composition; each modifier  $g$  can be computed within time bounded by  $lh(g)$ , the overall number of basic instructions and definition schemes of  $g$ , i.e., by a machine running over a constant number of configurations; the result follows, since the selection can be simulated by a branching, and the safe composition can be simulated by a sequence of register machines, one for each modifier.

Step. Case 1.  $f = \text{ITER}(g)$ , with  $g \in \mathcal{T}_0$ . We have that  $f(s, r) = g^{|r|}(s)$ . A register machine  $M_f$  can be defined as follows:  $(s)_i$  is stored in the register  $\pi_i$  ( $i = 1 \dots \#(f)$ ) and  $(r)_j$  is stored in the register  $\pi_j$  ( $j = \#(f) + 1 \dots 2\#(f)$ );  $M_f$  runs  $M_g$  (within time bounded by  $lh(g)$ ) for  $|r|$  times. Each time  $M_g$  is called,  $M_f$  deletes one digit from one of the registers  $\pi_{\#(f)+1} \dots \pi_{2\#(f)}$ , starting from the first; the computation stops, returning the final result, when they are all empty. Thus,  $M_f$  computes  $f(s, r)$  within time  $|r|lh(g)$ . Case 2. Let  $f$  be defined by simple schemes or safe composition. The result follows by direct simulation of the schemes.

In order to prove the second implication, we show that the behaviour of a  $k$ -register machine  $M$ , which operates in time  $cn$  can be simulated by a program in  $\mathcal{T}_1$ . Let  $next_M$  be a program in  $\mathcal{T}_0$ , such that  $next_M$  operates on input  $s = s_i \odot F_j(\pi_0) \odot \dots \odot F_j(\pi_k)$  and it has the semantic *if state* $[i](s)$  then  $E_i$ , where *state* $[i](s)$  is a test that is true if the state of  $M$  is  $s_i$ , and  $E_i$  is a modifier that updates the code of the state and the code of one among the registers, according to the definition of  $M$ . By means of  $c - 1$  safe compositions, we define  $next_M^c$  in  $\mathcal{T}_0$ , which applies  $next_M$  to the word that encodes a configuration of  $M$  for  $c$  times. We define in  $\mathcal{T}_1$

$$\begin{cases} linsim_M(x, a) = & x \\ linsim_M(x, za) = & next_M^c(linsim_M(x, z)) \end{cases}$$

$linsim_M(s, r)$  iterates  $next_M(s)$  for  $c|r|$  times, returning the code of the configuration that contains the final result of  $M$ . ■

#### IV. THE TIME HIERARCHY

In this section, we recall the definition of the class of programs  $\mathcal{T}_1$ ; we define our hierarchy of classes of programs, and we prove the relation with the classes of register machines, which compute their output within a polynomially-bounded amount of time.

- Definition 4.1:*
- 1)  $\text{ITER}(\mathcal{T}_0)$  denotes the class of programs obtained by one application of iteration to programs in  $\mathcal{T}_0$ ;
  - 2)  $\mathcal{T}_1$  is the class of programs obtained by closure under safe composition and simple schemes of programs in  $\mathcal{T}_0$  and programs in  $\text{ITER}(\mathcal{T}_0)$ ;  
Notation:  $\mathcal{T}_1 = (\mathcal{T}_0, \text{ITER}(\mathcal{T}_0); \text{SCMP}, \text{SIMPLE})$ ;
  - 3)  $\mathcal{T}_{k+1}$  is the class of programs obtained by closure under safe composition and simple schemes of programs in  $\mathcal{T}_k$  and programs in  $\text{SREC}(\mathcal{T}_k)$ , with  $k \geq 1$ ;  
Notation:  $\mathcal{T}_{k+1} = (\mathcal{T}_k, \text{SREC}(\mathcal{T}_k); \text{SCMP}, \text{SIMPLE})$ .

*Lemma 4.1:* Each  $f(s, t, r)$  in  $\mathcal{T}_k$  can be computed by a register machine within time bounded by  $|s| + lh(f)(|t| + |r|)^k$ , with  $k \geq 1$ .

*Proof:* Base.  $f \in \mathcal{T}_1$ . The relevant case is when  $f$  is in the form  $\text{ITER}(h)$ , with  $h \in \mathcal{T}_0$ . In lemma 3.1 (step, case 1) we have proved that  $f(s, r)$  can be computed within time  $|r|lh(h)$ ; hence, we have the thesis.

Step.  $f \in \mathcal{T}_{p+1}$ . The most significant case is when  $f = \text{SREC}(g, h)$ . By the inductive hypothesis there exist two register machines  $M_g$  and  $M_h$  which compute  $g$  and  $h$  within the required time. Let  $r$  be the word  $a_1 \dots a_{|r|}$ ; recalling that  $f(s, t, ra) = h(f(s, t, r), t, ra)$ , we define a register machine  $M_f$  that calls  $M_g$  on input  $s, t$ , and calls  $M_h$  for  $|r|$  times on input stored into the appropriate set of registers (in particular, the result of the previous recursive step has to be stored always in the same register). By inductive hypothesis,  $M_g$  needs time  $|s| + lh(g)(|t|)^p$  in order to compute  $g$ ; for the first computation of the step program  $h$ ,  $M_h$  needs time  $|g(s, t)| + lh(h)(|t| + |a_{|r|-1}a_{|r|}|)^p$ . After  $|r|$  calls of  $M_h$ , the final configuration is obtained within overall time  $|s| + \max(lh(g), lh(h))(|t| + |r|)^{p+1} \leq |s| + lh(f)(|t| + |r|)^{p+1}$ . ■

*Lemma 4.2:* The behaviour of a register machine which computes its output within time  $O(n^k)$  can be simulated by a program  $f$  in  $\mathcal{T}_k$ , with  $k \geq 1$ .

*Proof:* Let  $M$  be a register machine respecting the hypothesis. As we have already seen, there exists  $next_M \in \mathcal{T}_0$  such that, for input the code of a configuration of  $M$ , it returns the code of the configuration induced by the relation  $\vdash_M$ . Given a fixed  $i$ , we write the program  $\sigma_i$  by means of  $i$  safe recursions nested over  $next_M$ , such that it iterates  $next_M$  on input  $s$  for  $n^i$  times, with  $n$  the length of the input:

$\sigma_0 := \text{ITER}(nxt_M)$  and  
 $\sigma_{n+1} := \text{RNM}_{z/y}(\gamma_{n+1})$ , where  $\gamma_{n+1} := \text{SREC}(\sigma_n, \sigma_n)$ .

We have that

$\sigma_0(s, t) = nxt_M^{|t|}(s)$ ,  $\sigma_{n+1}(s, t) = \gamma_{n+1}(s, t, t)$ , and

$$\begin{cases} \gamma_{n+1}(s, t, a) &= \sigma_n(s, t) \\ \gamma_{n+1}(s, t, ra) &= \sigma_n(\gamma_{n+1}(s, t, r), t) \\ &= \gamma_n(\gamma_{n+1}(s, t, r), t, t) \end{cases}$$

In particular, we have

$$\sigma_1(s, t) = \gamma_1(s, t, t) = \underbrace{\sigma_0(\sigma_0(\dots \sigma_0(s, t) \dots))}_{|t| \text{ times}} = nxt_M^{|t|^2}$$

$$\sigma_2(s, t) = \gamma_2(s, t, t) = \underbrace{\sigma_1(\sigma_1(\dots \sigma_1(s, t) \dots))}_{|t| \text{ times}} = nxt_M^{|t|^3}$$

By induction, we see that  $\sigma_{k-1}$  iterates  $nxt_M$  on input  $s$  for  $|t|^k$  times, and that it belongs to  $\mathcal{T}_k$ . The result follows defining  $f(t) = \sigma_{k-1}(t, t)$ , with  $t$  the code of an initial configuration of  $M$ . ■

*Theorem 4.1:* A program  $f$  belongs to  $\mathcal{T}_k$  if and only if  $f$  is computable by a register machine within time  $O(n^k)$ , with  $k \geq 1$ .

*Proof:* By lemma 4.2 and lemma 4.1. ■

We recall that register machines are polytime reducible to Turing machines; thus, the sequence of classes  $\mathcal{T}_k$  captures PTIMEF (see [6] and [12] for similar characterization of this complexity class).

## V. EXTENDING THE POLYNOMIAL-TIME HIERARCHY TO TRANSFINITE

In this section, we extend the definition of the classes of programs  $\mathcal{T}_k$ , with  $k \geq 1$ , to a transfinite hierarchy of classes; in order to do this, we recall the definition of structured ordinals and of hierarchies of slow/fast growing functions, as reported in [11]. Then, we introduce a natural slow growing function  $B$ , and we give the definition of *diagonalization* at a given limit ordinal  $\lambda$ , based on the sequence of classes  $\mathcal{T}_{\lambda_1}, \dots, \mathcal{T}_{\lambda_n}, \dots$  associated with the fundamental sequence of  $\lambda$ . A similar constructive operator can be found in [15] and [12]. We prove that this transfinite hierarchy of programs characterize the classes of register machines computing their output within time between  $O(n^k)$  and  $O(n^{n^k})$  (with  $k \geq 1$  and  $n$  the length of the input), that is, the computations with time complexity between polynomial and exponential time.

### A. Structured ordinals and hierarchies

Following [11], we denote limit ordinals with greek small letters  $\alpha, \beta, \lambda, \dots$ , and we denote with  $\lambda_i$  the  $i$ -th element of the fundamental sequence assigned to  $\lambda$ . For example,  $\omega$  is the limit ordinal of the fundamental sequence  $1, 2, \dots$ ; and  $\omega^2$  is the limit ordinal of the fundamental sequence  $\omega, \omega 2, \omega 3, \dots$ , with  $(\omega^2)_k = \omega k$ .

The *slow-growing functions*  $G_\alpha : \mathbb{N} \rightarrow \mathbb{N}$  are defined by the recursion

$$\begin{cases} G_0(n) &= 0 \\ G_{\alpha+1}(n) &= G_\alpha(n) \\ G_\lambda(n) &= G_{\lambda_n}(n). \end{cases}$$

The *fast-growing functions*  $F_\alpha : \mathbb{N} \rightarrow \mathbb{N}$  are defined by the recursion

$$\begin{cases} F_0(n) &= n + 1 \\ F_{\alpha+1}(n) &= F_\alpha^{n+1}(n) \\ F_\lambda(n) &= F_{\lambda_n}(n). \end{cases}$$

We define the *slow-growing functions*  $B_\alpha : \mathbb{N} \rightarrow \mathbb{N}$  by means of the recursion

$$\begin{cases} B_0(n) &= 1 \\ B_{\alpha+1}(n) &= n B_\alpha(n) \\ B_\lambda(n) &= B_{\lambda_n}(n). \end{cases}$$

Note that  $B_k(n) = n^k$ ,  $B_\omega(n) = n^n$ ,  $B_{\omega+k}(n) = n^{n+k}$ ,  $B_{\omega k}(n) = n^{n \cdot k}$ ,  $B_{\omega^k}(n) = n^{n^k}$ , and  $B_{\omega^\omega}(n) = n^{n^n}$ ; moreover, we have that  $B_{\alpha+\beta}(n) = B_\alpha(n) \cdot B_\beta(n)$ , and that  $G_{\omega^\alpha}(n) = n^{G_\alpha(n)} = B_\alpha(n)$ .

### B. Diagonalization and transfinite hierarchy

The finite hierarchy  $\mathcal{T}_0, \mathcal{T}_1, \mathcal{T}_2, \dots, \mathcal{T}_k, \dots$ , captures the register machines that compute their output with time in  $O(1), O(n), O(n^2), \dots, O(n^k), \dots$ , respectively. Jumping out of the hierarchy requires something more than safe recursion.

A possible approach consist in defining a kind of ranking function that counts the number of nested recursion violating our "no-bad-renaming" rule or, in general, not respecting the predicative definition of a program. A class of time-bounded register machines is associated to each level of violation. This idea was introduced in [17].

On the other hand, given a limit ordinal  $\lambda$ , we propose a new operator that *diagonalizes* at level  $\lambda$  over the classes  $\mathcal{T}_{\lambda_i}$ , that is, that selects programs in a previously defined class according to the length of the input. There is no circularity in a program defined by diagonalization, and we believe that this program isn't less predicative than a program defined by safe recursion. For instance, at level  $\omega$ , we are able to select programs in the sequence  $\mathcal{T}_i$ , where the value of  $i$  depends on the length of the input; thus, this level of diagonalization captures the class of all register machines whose computation is bounded by a polynomial. Extending this approach to next levels of structured ordinals, we are able to reach the machines computing within exponential time.

*Definition 5.1:* Given a limit ordinal  $\lambda$  with the fundamental sequence  $\lambda_0, \dots, \lambda_k, \dots$ , and given an enumerator program  $q$  such that  $q(\lambda_i) = f_{\lambda_i}$ , for each  $i$ , the program  $f(x, y)$  is defined by *diagonalization* at  $\lambda$  if for all  $s, t$  if

$$f(s, t) = \text{ITER}^{|t|}(q(\lambda_{|t|}))(s, t)$$

where

$$\begin{cases} \text{ITER}^1(p)(s, t) & = \text{ITER}(p)(s, t) \\ \text{ITER}^{k+1}(p)(s, t) & = \text{ITER}(\text{ITER}^k(p))(s, t). \end{cases}$$

and  $f_{\lambda_i}$  belongs to a previously defined class  $\mathcal{C}_{\lambda_i}$ , for each  $i$ . Notation:  $f = \text{DIAG}(\lambda)$ .

Note that the previous definition requires that  $f_{\lambda_i} \in \mathcal{C}_{\lambda_i}$ , but no other requirements are made on how the  $\mathcal{C}$ 's classes are built. In what follows, we introduce the transfinite hierarchy of programs, with an important restriction on the definition of the  $\mathcal{C}$ 's.

**Definition 5.2:** Given  $\lambda < \omega^\omega$ ,  $\mathcal{T}_\lambda$  is the class of programs obtained by

- 1) closure under safe composition and simple schemes of programs in  $\mathcal{T}_\alpha$  and programs in  $\text{SREC}(\mathcal{T}_\alpha)$ , if  $\lambda = \alpha + 1$ ;

Notation:  $\mathcal{T}_{\alpha+1} = (\mathcal{T}_\alpha, \text{SREC}(\mathcal{T}_\alpha); \text{SCMP}, \text{SIMPLE})$ .

- 2) closure under simple schemes of programs obtained by one application of diagonalization at  $\lambda$ , if  $\lambda$  is a limit ordinal, with  $f_{\lambda_i} \in \mathcal{T}_{\lambda_i}$ , for each  $\lambda_i$  in the fundamental sequence of  $\lambda$ .

Notation:  $\mathcal{T}_\lambda = (\text{DIAG}(\lambda); \text{SIMPLE})$ ;

**Lemma 5.1:** Each  $f(s, t, r)$  in  $\mathcal{T}_\lambda$  ( $\lambda < \omega^\omega$ ) can be computed by a register machine within time  $B_\lambda(n)$ .

*Proof:* By induction on  $\lambda$ . We have three cases:

- (1)  $\lambda$  is a finite number; we note that  $B_k(n) = n^k$ , and the proof follows from Lemma 4.1.

(2)  $\lambda = \beta + 1$ ; this implies that  $f \in \mathcal{T}_{\beta+1}$ , and the relevant subcase is when  $f = \text{SREC}(g, h)$ , with both  $g$  and  $h$  belonging to  $\mathcal{T}_\beta$ . By the inductive hypothesis, there exist the register machines  $M_g$  and  $M_h$  computing  $g$  and  $h$ , respectively, within time bounded by  $B_\beta(n)$ . A register machine  $M_f$  can be defined, such that it calls  $M_g$  on input  $s, t$ , and calls  $M_h$  for  $|r|$  times on input stored into the appropriate set of registers.  $M_f$  needs time  $B_\beta(n) + |r|B_\beta(n)$  to perform this computation; thus, the overall time is bounded by  $B_{\beta+1}(n)$ , by definition of  $B$ .

(3)  $\lambda$  is a limit ordinal; this means that  $f$  is defined by  $\text{DIAG}(\lambda)$ , that is  $f(s, t) = \text{ITER}^{|t|}(g(\lambda_{|t|}))(s, t)$ , with  $\lambda_i$  the fundamental sequence of  $\lambda$  and  $g(\lambda_i) = f_{\lambda_i} \in \mathcal{T}_{\lambda_i}$ . By induction on the length of the input, we have that  $f(s, a) = \text{ITER}^{|a|}(g(\lambda_{|a|}))(s, a) = s$ ; obviously, there exists a register machine computing the result within time  $B_{\lambda_{|a|}}(n)$ . As for the step case we have that

$$\begin{aligned} f(s, ta) &= \text{ITER}^{|ta|}(g(\lambda_{|ta|}))(s, ta) \\ &= \text{ITER}(\text{ITER}^{|t|}(g(\lambda_{|ta|})))(s, t); \end{aligned}$$

by inductive hypothesis, there exist a sequence of register machines  $M_{\lambda_{|ta|}}$  computing the programs  $g(\lambda_{|ta|})$ 's within time  $B_{\lambda_{|ta|}}(n)$ . We define a register machine  $M_f$  such that, on input  $s, t$  iterates  $|t|$  times  $M_{\lambda_{|ta|}}$ , within time  $B_{\lambda_{|ta|}}(n) \leq B_\lambda(n)$  ■

**Lemma 5.2:** The behaviour of a register machine which computes its output within time  $O(B_\lambda(n))$  can be simulated by a program  $f$  in  $\mathcal{T}_\lambda$ .

*Proof:* Given a register machine  $M$  respecting the hypothesis, we have already seen that there exists a program  $\text{next}_M \in \mathcal{T}_0$  such that, for input the code of a configuration of  $M$ , it returns the code of the configuration induced by the relation  $\vdash_M$ . We have three cases:

- (1)  $\lambda$  is a finite number; the proof follows from Lemma 4.2.

- (2)  $\lambda$  is in the form  $\beta + 1$ ; in this case, we define the program  $\sigma_\lambda$  as follows:

$$\sigma_{\beta+1} := \text{RNM}_{z/y}(\gamma_{\beta+1}), \text{ where } \gamma_{\beta+1} := \text{SREC}(\sigma_\beta, \sigma_\beta).$$

We have that

$$\sigma_{\beta+1}(s, t) = \gamma_{\beta+1}(s, t, t), \text{ and}$$

$$\begin{cases} \gamma_{\beta+1}(s, t, a) & = \sigma_\beta(s, t) \\ \gamma_{\beta+1}(s, t, ra) & = \sigma_\beta(\gamma_{\beta+1}(s, t, r), t) \\ & = \gamma_\beta(\gamma_{\beta+1}(s, t, r), t, t) \end{cases}$$

In particular, we have

$$\sigma_{\beta+1}(s, t) = \underbrace{\gamma_{\beta+1}(s, t, t) = \sigma_\beta(\sigma_\beta(\dots \sigma_\beta(s, t) \dots, t), t)}_{|t| \text{ times}}$$

By induction we see that  $\sigma_\beta$  iterates  $\text{next}_M$  on its input  $s$  for  $B_\beta(|t|)$  times, and that it belongs to  $\mathcal{T}_\beta$ . The result follows observing that  $\sigma_{\beta+1}$  iterates  $\text{next}_M$  for  $|t|B_\beta(|t|) = B_{\beta+1}(|t|)$  times.

- (3)  $\lambda$  is a limit ordinal. Let  $\lambda_1, \dots, \lambda_n, \dots$  the fundamental sequence associated to  $\lambda$ , and  $\sigma_{\lambda_1}, \dots, \sigma_{\lambda_n}, \dots$  the sequence of programs enumerated by  $g$ , such that  $g(\lambda_i) = \sigma_{\lambda_i} \in \mathcal{T}_{\lambda_i}$ . We define  $\gamma_\lambda$  by diagonalization at  $\lambda$ . With a fixed input  $s, t$ , we have that  $\gamma_\lambda(s, t) = \text{ITER}^{|t|}(g(\lambda_{|t|}))(s, t) = \text{ITER}^{|t|}(\sigma_{\lambda_{|t|}})(s, t)$ .

The programs  $g(\lambda_{|t|})$  are defined in  $\mathcal{T}_{\lambda_{|t|}}$ , and they iterate the program  $\text{next}_M$  on its input for  $B_{\lambda_{|t|}}(|t|)$  times; this implies that  $\gamma_\lambda$  iterates  $\text{next}_M$  for  $B_{\lambda_{|t|}}(|t|) = B_\lambda(|t|)$ , for each  $t$ . ■

**Theorem 5.1:** A program  $f$  belongs to  $\mathcal{T}_\alpha$  if and only if  $f$  is computable by a register machine within time  $O(B_\alpha(n))$ , with  $\alpha < \omega^\omega$ .

*Proof:* By lemma 5.1 and lemma 5.2. ■

## VI. THE TIME-SPACE HIERARCHY

In this section, we introduce a restricted version of the previously defined time-hierarchy of recursive programs, and we prove the equivalence with the classes of register machines, which compute their output with a simultaneous bound on time and space, following the work of [2].

### A. Recursion-free programs and class $\mathcal{S}_0$

The reader should refer to Section II for the definitions of basic instruction (the identity  $1(u)$ , the constructors  $c_i^a(s)$ , and the destructors  $d_i(s)$ ); simple schemes (the renaming  $\text{RNM}_{x/y}(g)$  and  $\text{RMN}_{z/y}(g)$ , and the selection  $\text{SEL}_i^b(g, h)$ ); and safe composition  $\text{SCMP}_u(h, g)$ . In particular, a modifier is

obtained by the safe composition of a sequence of constructors and a sequence of destructors; according to definition 2.5, the class  $\mathcal{T}_0$  is the class of programs defined by closure of modifiers under SEL and SCMP.

**Definition 6.1:** Given  $f \in \mathcal{T}_0$ , the rate of growth  $rog(f)$  is such that

- 1) if  $f$  is a modifier,  $rog(f)$  is the difference between the number of constructors and the number of destructors occurring in its definition;
- 2) if  $f = \text{SEL}_i^b(g, h)$ , then  $rog(f)$  is  $\max(rog(g), rog(h))$ ;
- 3) if  $f = \text{SCMP}_u(h, g)$ , then  $rog(f)$  is  $\max(rog(g), rog(h))$ .

**Definition 6.2:**  $\mathcal{S}_0$  is the class of programs in  $\mathcal{T}_0$  with non-positive rate of growth, that is  $\mathcal{S}_0 = \{f \in \mathcal{T}_0 | rog(f) \leq 0\}$ . Note that all programs in  $\mathcal{S}_0$  modify their inputs according to the result of some test performed over a fixed number of digits and, moreover, they cannot return values longer than their input.

### B. Safe recursion and class $\mathcal{S}_1$

As written in section 2.1, a program  $f(x, y, z)$  is defined by safe recursion in the basis  $g(x, y)$  and in the step  $h(x, y, z)$  if for all  $s, t, r$  we have

$$\begin{cases} f(s, t, a) &= g(s, t) \\ f(s, t, ra) &= h(f(s, t, r), t, ra). \end{cases}$$

In this case,  $f$  is denoted with  $\text{SREC}(g, h)$ . In particular,  $f(x, z)$  is defined by iteration of  $h(x)$  if for all  $s, r$  we have

$$\begin{cases} f(s, a) &= s \\ f(s, ra) &= h(f(s, r)). \end{cases}$$

In this case,  $f$  is denoted with  $\text{ITER}(h)$ , and we write  $h^{|r|}(s)$  for  $\text{ITER}(h)(s, r)$ .

- Definition 6.3:**
- 1)  $\text{ITER}(\mathcal{S}_0)$  denotes the class of programs obtained by one application of iteration to programs in  $\mathcal{S}_0$ ;
  - 2)  $\mathcal{S}_1$  is the class of programs obtained by closure under safe composition and simple schemes of programs in  $\mathcal{S}_0$  and programs in  $\text{ITER}(\mathcal{S}_0)$ ;  
Notation:  $\mathcal{S}_1 = (\mathcal{S}_0, \text{ITER}(\mathcal{S}_0); \text{SCMP}, \text{SIMPLE})$ ;
  - 3)  $\mathcal{S}_{k+1}$  is the class of programs obtained by closure under simple schemes of programs in  $\mathcal{S}_k$  and programs in  $\text{SREC}(\mathcal{S}_k)$ .  
Notation:  $\mathcal{S}_{k+1} = (\mathcal{S}_k, \text{SREC}(\mathcal{S}_k); \text{SIMPLE})$ .

Hence, hierarchy  $\mathcal{S}_k$ , with  $k \in \mathbb{N}$ , is a version of  $\mathcal{T}_k$  in which each program returns a result whose length is exactly bounded by the length of the input; this does not happen if we allow the closure of  $\mathcal{S}_k$  under SCMP. We will use this result to evaluate the space complexity of our programs.

**Definition 6.4:** Given the programs  $g$  and  $h$ ,  $f$  is obtained by weak composition of  $h$  in  $g$  if  $f(x, y, z) = g(h(x, y, z), y, z)$ . Notation:  $f = \text{WCMP}(h, g)$ .

In the weak form of composition the program  $h$  can be substituted only in the variable  $x$ , while in the safe composition the substitution is possible in all variables.

**Definition 6.5:** For all  $p, q \geq 1$ ,  $\mathcal{TS}_{qp}$  is the class of programs obtained by weak composition of  $h$  in  $g$ , with  $h \in \mathcal{T}_q$ ,  $g \in \mathcal{S}_p$  and  $q \leq p$ .

**Lemma 6.1:** For all  $f$  in  $\mathcal{S}_p$ , we have  $|f(s, t, r)| \leq \max(|s|, |t|, |r|)$ .

*Proof:* By induction on  $p$ . Base. The relevant case is when  $f \in \mathcal{S}_1$  and  $f$  is defined by iteration of  $g$  in  $\mathcal{S}_0$  (that is,  $rog(g) \leq 0$ ). By induction on  $r$ , we have that  $|f(s, a)| = |s|$ , and  $|f(s, ra)| = |g(f(s, r))| \leq |f(s, r)| \leq \max(|s|, |r|)$ .

Step. Given  $f \in \mathcal{S}_{p+1}$ , defined by SREC in  $g$  and  $h$  in  $\mathcal{S}_p$ , we have

$$\begin{aligned} |f(s, t, a)| &= |g(s, t)| && \text{by definition of } f \\ &\leq |\max(|s|, |t|)| && \text{by inductive hypothesis.} \end{aligned}$$

and

$$\begin{aligned} |f(s, t, ra)| &= |h(f(s, t, r), t, ra)| \\ &\leq |\max(|f(s, t, r)|, |t|, |ra|)| \\ &\leq |\max(\max(|s|, |t|, |r|), |t|, |ra|)| \\ &\leq |\max(|s|, |t|, |ra|)|. \end{aligned}$$

by definition of  $f$ , inductive hypothesis on  $h$  and induction on  $r$ . ■

**Lemma 6.2:** Each  $f$  in  $\mathcal{TS}_{qp}$  (with  $p, q \geq 1$ ) can be computed by a register machine within time  $O(n^p)$  and space  $O(n^q)$ .

*Proof:* Let  $f$  be in  $\mathcal{TS}_{qp}$ . By definition 6.5,  $f$  is defined by weak composition of  $h \in \mathcal{T}_q$  into  $g \in \mathcal{S}_p$ , that is,  $f(s, t, r) = g(h(s, t, r), t, r)$ . The theorem 5.1 states that there exists a register machine  $M_h$ , which computes  $h$  within time  $n^q$ , and there exists another register machine  $M_g$ , which computes  $g$  within time  $n^p$ . Since  $g$  belongs to  $\mathcal{S}_p$ , lemma 6.1 holds for  $g$ ; hence, the space needed by  $M_g$  is at most  $n$ .

We define now a machine  $M_f$  that, by input  $s, t, r$ , performs the following steps:

- (1) it calls  $M_h$  on input  $s, t, r$ ;
- (2) it calls  $M_g$  on input  $h(s, t, r), t, r$ , stored in the appropriate registers.

According to lemma 4.2,  $M_h$  needs time equal to  $|s| + lh(h)(|t| + |r|)^q$  to compute  $h$ , and  $M_g$  needs  $|h(s, t, r)| + lh(g)(|t| + |r|)^p$  to compute  $g$ .

This happens because lemma 4.2 shows, in general, that the time used by a register machine to compute a program is bounded by a polynomial in the length of its inputs, but, more precisely, it shows that the time complexity is linear in  $|s|$ . Moreover, since in our language there is no kind of identification of  $x$  as  $z$ ,  $M_f$  never moves the content of a register associated to  $h(s, t, r)$  into another register and, in particular, into a register whose value plays the role of recursive variable. Thus, the overall time-bound is  $|s| + lh(h)(|t| + |r|)^q + lh(g)(|t| + |r|)^p$  which can be reduced to  $n^p$ , being  $q \leq p$ .

$M_h$  requires space  $n^q$  to compute the value of  $h$  on input  $s, t, r$ ; as we noted above, the space needed by  $M_g$  for the

computation of  $g$  is linear in the length of the input, and thus the overall space needed by  $M_f$  is still  $n^q$ . ■

*Lemma 6.3:* A register machine which computes its output within time  $O(n^p)$  and space  $O(n^q)$  can be simulated by a program  $f \in \mathcal{TS}_{qp}$ .

*Proof:* Let  $M$  be a register machine, whose computation is time-bounded by  $n^p$  and, simultaneously, is space-bounded by  $n^q$ .  $M$  can be simulated by the composition of two machines,  $M_h$  (time-bounded by  $n^q$ ), and  $M_g$  (time-bounded by  $n^p$  and, simultaneously, space-bounded by  $n$ ): the former delimits (within  $n^q$  steps) the space that the latter will successively use in order to simulate  $M$ .

By theorem 5.1 there exists  $h \in \mathcal{T}_q$  that simulates the behaviour of  $M_h$ , and there exists  $g \in \mathcal{T}_p$  that simulates the behaviour of  $M_g$ ; this is done by means of  $nxt_g$ , which belongs to  $\mathcal{S}_0$ , since it never adds a digit to the description of  $M_g$  without erasing another one.

According to the proof of lemma 4.1, we are able to define  $\sigma_{n-1} \in \mathcal{S}_n$ , such that  $\sigma_{n-1}(s, t) = nxt_g^{|t|} s$ . The result follows defining  $sim(s) = \sigma_{p-1}(h(s), s) \in \mathcal{TS}_{qp}$ . ■

*Theorem 6.1:*  $f$  belongs to  $\mathcal{TS}_{qp}$  if and only if  $f$  is computable by a register machine within time  $O(n^p)$  and space  $O(n^q)$ .

*Proof:* By lemma 6.2 and lemma 6.3. ■

## VII. CONCLUSIONS AND FURTHER WORK

In this paper, we have introduced a version of safe recursion, together with constructive diagonalization; by means of these two operators, we've been able to define a hierarchy of classes of programs  $\mathcal{T}_\lambda$ , with  $0 \leq \lambda < \omega^\omega$ . Each finite level of the hierarchy characterizes the register machines computing their output within time  $O(n^k)$ ; using the natural definition of structured ordinals, and combining it with the diagonalization operator, we have that the transfinite levels of the hierarchy characterize the classes of register machine computing their output within time bounded by the slow-growing function  $B_\lambda(n)$ , up to the machines with exponential time complexity. In the last section, we have defined a hierarchy of programs with simultaneous time and space bound.

While the safe recursion scheme has been studied thoroughly, we feel that the diagonalization operator as presented in this work, or as in Marion's approach (see [12]), deserves a more accurate analysis. In particular, we believe that it can be considered as predicative as the safe recursion, and that it could be used to stretch the hierarchy of programs in order to capture the low Grzegorzczk classes (see [17] for a non-constructive approach).

## REFERENCES

[1] E. Covino and G. Pani, "A Specialized Recursive Language for Capturing Time-Space Complexity Classes," in The Sixth International Conference on Computational Logics, Algebras, Programming, Tools, and Benchmarking, (COMPUTATION TOOLS 2015), Nice, France, 2015, pp. 8–13.

[2] A. Cobham, "The intrinsic computational difficulty of functions," in Y. Bar-Hillel (ed), Proceedings of the International Conference on Logic, Methodology, and Philosophy of Science, Amsterdam. North-Holland, 1962, pp. 24–30.

[3] H. Simmons, "The realm of primitive recursion," Arch.Math. Logic, vol. 27, 1988, pp. 177–121 885.

[4] S. Bellantoni and S. Cook, "A New Recursion-Theoretic Characterization Of The Polytime Functions," Computational Complexity, vol. 2, 1992, pp. 97–110.

[5] D. Leivant, "A foundational delineation of computational feasibility," in Proceedings of the 6th Annual Symposium on Logic in Computer Science, (LICS'91), Amsterdam. IEEE Computer Society Press, 1991, pp. 2–18.

[6] —, Predicative recurrence and computational complexity I: word recurrence and polytime. Birkauer, 1994, pp. 320–343.

[7] D. Leivan and J.-Y. Marion, "Ramified recurrence and computational complexity II: substitution and polyspace," in J.Tiurny and L.Pocholsky (eds), Computer Science Logic, LNCS 933, Amsterdam. Springer Berlin Heidelberg, 1995, pp. 486–500.

[8] I. Oitavem, "New recursive characterization of the elementary functions and the functions computable in polynomial space," Revista Matematica de la Univaersidad Complutense de Madrid, vol. 10, 1997, pp. 109–125.

[9] P. Clote, "A time-space hierarchy between polynomial time and polynomial space," Math. Sys. The., vol. 25, 1992, pp. 77–92.

[10] D. Leivant, "Stratified functional programs and computational complexity," in Proceedings of the 20th Annual ACM SIGPLAN-SIGACT Symposium on Principles of Programming Languages, (POPL'93), Charleston. ACM, 1993, pp. 325–333.

[11] M. Fairtlough and S. Weiner, Hierarchies of provably recursive functions. Elsevier, Amsterdam, 1998, chapter 3, pp. 149–207.

[12] J. Marion, "On tiered small jump operators," Logical Methods in Computer Science, vol. 5, no. 1, 2009.

[13] T. Arai and N. Eguchi, "A new function algebra of EXPTIME functions by safe nested recursion," ACM Transactions on Computational Logic, vol. 10, 2009, pp. 1–19.

[14] D. Leivant, "Ramified recurrence and computational complexity III: higher type recurrence and elementary complexity," Annals of pure and applied logic, vol. 96, 1999, pp. 209–229.

[15] S. Caporaso, G. Pani, and E. Covino, "A predicative approach to the classification problem," Journal of Functional Programming, vol. 11, 2001, pp. 95–116.

[16] M. Hofmann, "Linear types and non-size-increasing polynomial time computation," in Proceedings of the 14th Symposium on Logic in Computer Science (LICS'99), Trento. IEEE Computer Society Press, 1999, pp. 464–473.

[17] S. Bellantoni and K. Niggl, "Ranking primitive recursion: the low Grzegorzczk classes revisited," SIAM Journal on Computing, vol. 29, 1999, pp. 401–4015.

# Service Recommendation Using Machine Learning Methods Based on Measured Consumer Experiences Within a Service Market

Jens Kirchner

Andreas Heberle

Welf Löwe

Karlsruhe University of Applied Sciences  
Linnaeus University  
Email: Jens.Kirchner@hs-karlsruhe.de,  
Jens.Kirchner@lnu.se

Karlsruhe University of Applied Sciences  
Moltkestr. 30, 76133 Karlsruhe, Germany  
Email: Andreas.Heberle@hs-karlsruhe.de

Linnaeus University  
351 06 Växjö, Sweden  
Email: Welf.Lowe@lnu.se

**Abstract**—Among functionally similar services, service consumers are interested in the consumption of the service that performs best towards their optimization preferences. The experienced performance of a service at consumer side is expressed in its non-functional properties. Selecting the best-fit service is an individual aspect as the preferences of consumers vary. Furthermore, service markets such as the Internet are characterized by perpetual change and complexity. The complex collaboration of system environments and networks result in various performance experiences at consumer side. Service optimization based on a collaborative knowledge base of previous experiences of other, similar consumers with similar preferences is a desirable foundation. In this article, we present a service recommendation framework, which aims at the optimization at consumer side focusing on the individual preferences and call contexts. In order to identify relevant non-functional properties for service selection, we conducted a literature study of conference papers of the last decade. The ranked results of this study represent what a broad scientific community determined to be relevant non-functional properties for service selection. We furthermore analyzed, implemented, and validated machine learning methods that can be employed for service recommendation. Within our validation, we could achieve up to 95 % of the overall achievable performance (utility) gain with a machine learning method that is focused on concept drift, which in turn, tackles the change characteristic of the Internet being a service market. Besides the comprehensive and scientific identification of relevant non-functional properties when selecting a service, this article describes how machine learning can be employed for service recommendation based on consumer experiences in general, including an evaluation and overall proof of concept validation within our framework.

**Keywords**—Service Selection; Service Recommendation; Machine Learning; Non-functional properties; Performance gain.

## I. INTRODUCTION

Service-Oriented Computing (SOC), Software as a Service (SaaS), Cloud Computing, and Mobile Computing indicate the development of the Internet into a market of services. In such an anonymous market, service consumers have little to no knowledge about the implementation of a service or the system environment around it. Service functionality can be dynamically and ubiquitously consumed. Besides the actual functionality, service consumers are interested in the performance of a service. The performance of a service is expressed in its non-functional properties (NFPs) such as response time, availability, or monetary costs. In such a service market, the same service functionality may be provided by several competing service providers. Among these functionally similar

services, service consumers are interested in the service that fits best to their (NFP) preferences. In particular, consumers are interested in the performance they experience at call side. One of the major characteristics of a service market such as the Internet is perpetual change. Entering and leaving service providers as well as the complexity of service dependencies and environments make service selection and recommendation a challenge. It seems to be impossible to foresee the exact performance of a future service call in a perpetual changing market. Static and single-sided information such as Service Level Agreements (SLAs) is not a good basis for service selection for several reasons (cf. [2]). The first reason is change in general, but also because service providers are interested to embellish the NFPs of their services in order to encourage service consumers to call their services. A further reason is the complex collaboration of various system environments and networks with incidents and coincidences. Since service consumers are interested in the best-fit experience at their side, it is desirable to base service selection on the collaborative knowledge of previous service calls of similar consumers with similar preferences and call contexts. The experienced performance at consumer side is influenced by a consumer's call context, e.g., calling time and/or location. Therefore, the performance has to be predicted based on this context. Furthermore, performance is different for different consumers who value the NFPs of a service differently. For instance, some consumers are more interested in a fast response time and rather neglect higher monetary charges than others who want to have a service for free and rather accept higher response times. Therefore, service value is individual and it has to be determined individually whether a service is actually best-fit in a specific context.

In this article, we present our service recommendation framework, which uses a collaborative knowledge base of consumption experiences of similar consumers in the past to predict the performance of services in a certain consumer-based call context in order to recommend the best-fit service candidate to a consumer, considering his/her preferences [1][2][3]. For the recommendation of services aiming at the optimization of the actual experience at consumers' side, it is important to determine, which NFPs are relevant for service selection. In order to determine these NFPs, we conducted a comprehensive literature survey of scientific conference papers of the last decade. The results of the survey revealed a ranked list of NFPs, which a broad scientific community

described to be relevant for service selection and, hence, for service recommendation. Furthermore, we analyzed two machine learning approaches for their capability to be employed for this service recommendation task. For the more suitable approach, we implemented and evaluated machine learning methods within our framework. In total, this article contributes a comprehensive evaluation of the employment of machine learning within the recommendation of services, including the discussion of the benefits and drawbacks of the general machine learning approaches within the recommendation process, their evaluation, and the implementation and validation of machine learning methods for the most suitable approach. Its results furthermore provide an overall proof of concept for the optimization of service recommendation based on previous experiences considering call contexts and consumer preferences. Moreover, we present the results of a comprehensive survey about relevant NFPs during service selection as the recommendation framework's scientific foundation.

After this introduction, the article is organized as follows: Related work to our research work is outlined in Section II. Section III introduces our service recommendation framework. It describes the relevant aspects of service recommendation in a service market as well as the necessary components. In order to clarify, which NFPs are actually relevant for service selection/recommendation, we present the results of our scientific-community-based study in Section IV. In Section V, we describe how machine learning can be employed for service recommendation based on a collaborative knowledge base. It initially describes the benefits and drawbacks of *classification*- and *regression*-based approaches within this domain. Section VI presents the evaluation of both approaches. The second part of the section then presents the initial implementation within our framework completed with tests about the achievement of the overall possible gain/benefit of the experienced performance at consumer side. Finally, Section VII concludes the article.

## II. RELATED WORK

We initially introduced the overall concept of how shared knowledge can benefit service selection/recommendation in general in [2]. In that work, we presented the framework on an abstract level and introduced the recommendation component as a black box. In this article, we describe the architecture of the recommendation component in details and evaluate the employment of machine learning methods within service recommendation aiming at the improvement of service performance experienced at consumer side. Turning measurement data into shared knowledge, it can be used for a consumer-centric optimized service recommendation within an anonymous service market.

The idea for our framework is inspired by our previous contributions on profile-guided composition of desktop applications [4][5]. This framework distributes the infrastructure needed for assessing and optimizing service calls and adopts SOA components for implementing the necessary infrastructure.

There are other considerations about service markets and sub-dependencies that our framework in general focuses and we outline in this article (cf. [6][7]). In contrast to our approach, they consider service brokers and directories as service intermediaries respectively market places for services.

In our understanding, intermediaries offer new service functionalities based on the consumption of sub-services while service brokers select the best-fit service among substitutable candidates [2]. Our approach works with NFPs as a foundation for service selection. By the definition of utility functions, consumer preferences can be calculated in order to determine the individual best-fit service instance. The authors of [8] present the results of a test saying that the impact of service attributes to customer satisfaction may change over time for e-services. As for our work, we aim at an automatic recommendation for service consumers in general. With the automation aspect, we primarily address consuming systems or services. Nonetheless, the preferences of service consumers may indeed change over time. In such a case, service consumers have to update their utility functions within our framework.

There are several approaches focusing on a quality-driven selection of services at runtime (late binding), cf. [9][10][11][12][13][14][15]. In most of these approaches, service selection is based on SLAs provided by service providers. These approaches are limited to local integration environments and lack an overall view beyond the borders of a consumer's environment. Some approaches focus on the prediction of NFPs for the detection of SLA violations such as [16]. Still, that work mainly focuses on SLAs to be the foundation for any evaluation. Another approach [17] introduces a framework that uses an SLA broker that negotiates SLAs between service consumers and service providers. During service consumption, SLA breaches are monitored. In such a case, the broker renegotiates or looks for a better service if the renegotiation fails. Although this approach also aims at the optimization of consumers' experiences, negotiation is time-consuming and does not solely focus on the benefit of service consumers' and the convergence of the negotiation remains unclear. Furthermore, optimized service recommendation is supposed to prevent or at least reduce the experience of service failures. However, when it comes to renegotiation, it is already too late and a failed or non-preferred service call is conducted. Furthermore, approaches that require service providers to participate in a single-sided optimization are questionable and they tighten the coupling of service consumers and providers, which conflicts with the decoupling idea of distributed systems. Our approach supports service consumers regardless whether providers actively participate or not and does not require any changes in implementations or architectures; it only provides an extension to the hitherto existing integration environments.

In general, we argue that SLAs are not a sufficient foundation for service selection [2] (also cf. [9][18]). Considering the profit-orientation of service providers, it is tempting for them to embellish their SLAs in order to be more attractive for consumption. Furthermore, the performances of services vary [2] and they are experienced differently due to a consumer's call context. SLAs cannot reflect such aspects since they can only reflect a provider's single-sided view. For a consumer, however, the actual performance experience matters. Also, as SLAs of consuming and providing services (e.g., compound services) depend on the SLAs of sub-providers, deviations of actual NFPs and those specified in SLAs may be propagated and spread even unintendedly and without the control of the providers.

Our framework also aims at self-optimization, which is similar to the goals of autonomic computing (cf. [19][20]).

There are other approaches that focus on self-adaptation and context-orientation affecting the process logic in SOC (cf. [21]). Our approach focuses on the substitution of similar functional services regarding differences in their performance. The approach of [22] aims at the support of the software life-cycle process. By means of aspect-oriented programming, a service provider can observe quality aspects of a software component reflected in the NFPs of a service. The idea of gaining feedback and the measurement methods are similar to ours. However, they focus on the support of service providers and developers, while we focus exclusively on service consumer support. Still, although our framework aims at the optimization at consumer side, it can also be beneficial for service providers for a consumer-oriented optimization of the implementation as well as infrastructure configuration in order to be more attractive for consumption.

Collaborative filtering (CF) approaches for service recommendation also focus on the exploitation of shared knowledge about services for the recommendation of services to similar consumers on an automated basis [18][23][24][25]. Machine learning, in general, can also be used in CF. In contrast to the filtering of external decision results in CF, our approach determines the individual best-fit service based on previously measured performance data, individual preferences, and calculated utility values. With our approach considering call context and utility function, new consumers can already benefit from existing knowledge. CF approaches also do not take into account that consumers can have different optimization goals or preferences. Only some approaches [24][25] consider differences between consumers regarding their context. In [26], the authors tackle the lack of consumer preference considerations. However, they do not take consumer context into account. The authors of [27][28] describe an approach to tackle the mentioned cold-start problem within CF. The prediction of QoS or NFP values using CF is pursued in [29]. The authors assume that consumers who experience similar NFP values for one service also experience similar NFP values for other services. Although we also assume that consumers of a similar call context experience similar NFP values for one service, we claim however that due to the complexity of the Internet and other aspects, call contexts, which affect NFPs, are independent for each service candidate. Differences in call contexts are, hence, not only related to the caller but also the respective callee. For instance, a global player (e.g., Google) may provide a single services that is implemented in a world- or continents-wide load balancing scenario. Consumers all over the world or continents may experience similar NFP values for this service, however, these consumers will then experience other (local, non-balanced) services differently. Furthermore, NFP values may change considering time aspects and other contextual differences even for a single consumer. Similarly, [30] uses the relationships between services, their providers, and service consumers for a bi-directional recommendation basing service recommendation on a satisfaction degree, which is rather subjective than objective. Furthermore, the approach requires provider information that is hidden from service consumers in the SOC domain. Our approach does not require to overcome the concepts of SOC and we base recommendation on objective measurement data. Although CF could be employed for recommending prior recommendation decisions within our recommendation framework, it is disadvantageous,

since changes in NFPs over time would not be taken into account. In contrast, within our continuous, objective recommendation knowledge updates, such changes are taken into account.

The authors of [31] use data mining methods for the discovery of services. Trust and reputation are also important aspects for the recommendation of services. Understood in a reliability context, there are approaches focusing on a trust-/reputation-based service recommendation [32][33][34][35][36]. In [33], the authors present a Knowledge-Social-Trust network model to determine the “trustworthiness of a service developer regarding specific user requirements and context” [33]. In [37], a similar concept is presented focusing on the awareness of social influence.

Within our survey, in order to determine relevant NFPs for service selection (Section IV), we discovered only a very few approaches that consider more than one NFP during service selection/recommendation. Outlined within this article, aiming at the various preferences of service consumers, service recommendation has to consider several NFPs. However, multi-NFP consideration within service recommendation is challenging due to the fact that the determination of the best-fit service instance according to service consumers’ individual preferences result in a calculation task. Furthermore, NFPs have different scales of measurement and different optimization focuses. Therefore, the complete recommendation process cannot be left to machine learning alone.

### III. RECOMMENDATION FRAMEWORK

The first part of this section introduces the optimization aspects on which we focus within our recommendation framework, which is introduced in the second part of this section.

#### A. Optimization Aspects

In the introduction of this article, we outlined major characteristics of the Internet as an anonymous service market. Services depict to be black boxes. Service consumers have little to no knowledge about the implementation, sub-dependencies, system environment, or usage load. Besides the actual functionality, service consumers only experience the performance of services. *Performance* is experienced in the NFPs of services. NFPs can be measured at consumer side (e.g., response time) or they are stated (e.g., monetary charges of consumption); they can be static or dynamic. NFPs have different scales of measurement. For example, response time is a ratio scale, while the availability for a service at a specific call moment is nominal: a service is either available or not.

The performances of services vary. The complexity of the Internet and the collaboration of various system environments and networks are not evident to consumers, which is part of the design. The limitation of resources, volatile usage and loads of these resources, and incidents in general cause dynamic performance behavior at consumer side. In our analyses of two NFPs [2][3][38], we could determine a time-based behavior of the analyzed Web services. Although service consumers cannot look behind the curtain, they can observe context-based behavior. Within our recommendation framework, we consider a service call’s context. In general, a *call context* attribute is an observable/measurable aspect at consumer side at the moment of a service call that may influence the NFPs of the called service. Examples of an open list of call context

attributes are service call date/time, location, and input size. The time stamp (also date aspects such as day of week, day of months, weekday, or weekend, etc.) of a service call can be relevant due to the load of limited resources, which cannot be determined, but experienced. For example, a Web service that provides information about TV programs can have high response times at prime time, when there is a peak load due to a lot of consumers. The location of a service consumer can also affect response times. For example, due to the network topology, service consumers within the same area (country or provider network) may experience better response times than other consumers who call from a different location because of different inter-network bandwidths. Also, whether consumers use a broadband connection or a mobile internet connection can also have an impact on the experienced performance of services. Although we consider solely non-functional aspects, the size of the input data for a service (non-functional aspect) may also influence the NFPs of a service due to functional aspects. For instance, a translation service may need more time to translate a book of several hundred pages than for a single-page document. Although there might be no difference in the transmission time, due to different processing times (processing is non-evident to consumers), service consumers experience different response times.

The third important aspect is *preference*. In general, consumers on any market have different preferences. For instance, for a specific functionality, some consumers are more interested in a fast response time and rather neglect higher monetary charges than others who want to have a service for free and rather experience higher response times. Therefore, whether a service is best-fit for a certain service consumer is an individual aspect. Functionally similar services distinguish themselves among each other in their NFPs, which are experienced at consumer side. Considering a consumer's preferences during service recommendation means considering preferences in the NFPs. As outlined above, NFPs have different scales of measurement. Furthermore, they also have different optimization functions. Recalling the examples of response time and availability above: for the ratio scale of response time, the optimization is focused towards the minimum; while the optimization focus of availability, which is nominal, is to select a service that has the highest (maximum) probability of being available. When the selection of a service instance is based on more than one NFP, NFP data has to be normalized in order to be comparable and calculable. In such a case, not all NFPs are equally important, so their importance has to be weighted and taken into account [1]. Our determination basis for the recommendation of the individually best-fit service is the calculation and comparison of a utility value. A *utility value* expresses the numerical degree of how much a service meets the preference goals of a consumer. The higher a value, the better. For the calculation of this value, we introduce the concept of utility functions. In general, *utility functions* express the mathematical relationship of the expected, normalized NFP values in order to meet the selection preferences of service consumers with a numerical output (interval scale). This definition emphasizes that in general our framework is not limited to a specific structure of utility functions. As an initial implementation, we use a weighted scoring model that expresses the impact of each normalized NFP towards a consumer's preferences. They "can be captured

in a vector of real values, each representing the weight of a corresponding quality metric [NFP]" [2]. For instance, lowest response time is more important (weighted: 60%) than lowest price (weighted: 40%) would result in a utility function  $U(ResponseTime, Price) = 0.6 \times ||ResponseTime|| + 0.4 \times ||Price||$ , where  $|| \cdot ||$  normalizes *ResponseTime* and *Price*, respectively, between 0 and 1 [2]. Within a single-tier recommendation, the experienced NFPs of services are influenced by consumer contexts. Hence, within the same call context (e.g., time, weekday, location, and type/size of input data), consumers with different preferences experience statistically similar NFPs, but the calculated utilities are different due to different utility functions.

## B. Framework Components

With the characteristics of the Internet as an anonymous service market, the focus of the design of our framework is to cope with perpetual change. Furthermore, it aims at a fully automated process without any human interaction and it is supposed to work with existing Service-Oriented Architecture (SOA) infrastructures. Due to the general design of SOA with its encapsulation aspects, services are treated as black boxes within our framework.

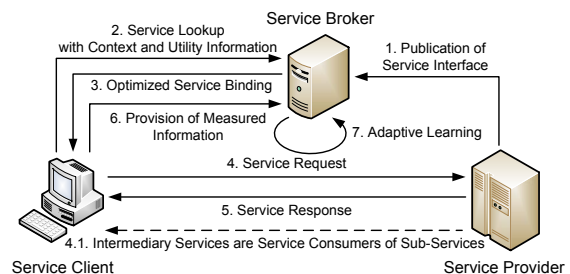


Figure 1. Enhanced SOA Model for Optimized Service Selection. [2]

For our framework, which we introduced in [2], we enhanced the traditional SOA model. The enhanced model, depicted in Figure 1, is extended by the following steps: The service lookup in step 2 is enhanced with call context and utility (preference) information. Based on this information, the service recommendation component of the broker provides in step 3 the service binding of the individually best-fit service based on the knowledge base of previous service calls of similar call contexts and similar preferences. The experienced NFPs during the actual service call in step 4 and step 5 is then submitted to the learning component of the service broker in step 6. Step 7 denotes the learning of the measurement details of the service call in order to update the knowledge base of the recommendation unit. The roles of service consumers and service providers are not always disjunct. In order to provide a certain service functionality, service providers may have further sub-dependencies and consume sub-services, which puts them in the role of a service consumer (step 4.1). Within our framework, we call such value adding services intermediary services.

The architecture of our recommendation framework is illustrated in Figure 2. Since our framework aims at the performance optimization at consumer side, the framework is logically split into a local and a central component. The local component is integrated in SOA environments (integration

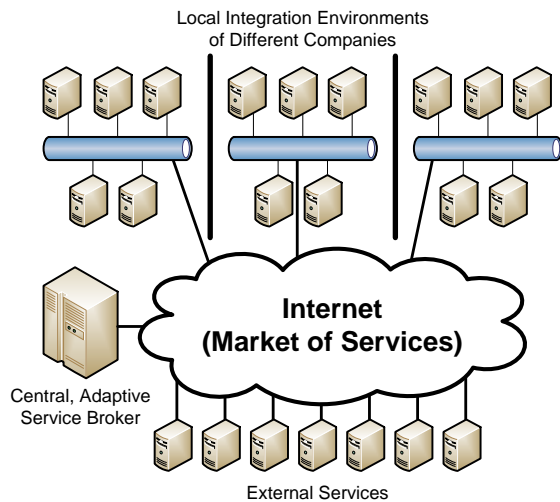


Figure 2. Architecture of Recommendation Framework.

platforms, middlewares, etc.) at consumer side. Its purpose is 1) to manage the call context and selection preferences (in the form of utility functions), 2) to manage dynamic bindings, 3) to measure the performance (NFPs) during service calls, and 4) to submit the observed information to the logically central component. Because of the automation aspect, the framework focuses on objective decision criteria in the form of measured or stated information. Hence, there is no consideration of human end-consumer ratings, which would require human interaction and that could also be rather subjective than objective, although the design could integrate such information in general. As illustrated in Figure 2, the local component is seamlessly integrated in existing infrastructures, our framework does not require any adjustment of existing implementations or systems. Through the extension of existing integration platforms, existing static bindings are replaced through dynamic bindings. Since service calls are dispatched through these integration platforms, calling components only experience optimized service performance due to the recommendation framework, but no changes in configurations or implementations.

The central component is responsible for the centralized functions. Its purpose is 1) to collect the feedback data from the local components of service consumers containing the measurement data including the call context and preference information, 2) to process and integrate the collected information into the recommendation database, 3) to recommend service candidates based on a given call context and utility function, and 4) to notify local components on dynamic binding updates. Within the illustration, the central component depicts to be a bottle neck and a single point of failure. In order to avoid these threats, the logically central component has to use distributed and high availability technologies.

In general, service recommendation aims at the optimization of performance at consumer side, which is a time-critical challenge. For the recommendation of a best-fit service, we follow two approaches. The first approach is dynamic binding. *Dynamic binding* is part of the local component, at client side. Using dynamic binding, the local component registers the desired service functionality, call context, and utility function at the central component and receives an initial best-fit service

candidate. In the event of an update, the central component notifies the local component (publish-subscribe pattern). The second concept is dynamic service calls. The *dynamic service call* concept includes the recommendation request as part of each service call. Similar to the dynamic binding, information about service functionality, call context, and utility function has to be provided. In order to tackle the time-critical drawback of service recommendation, we provide a divided architecture of the recommendation unit. The architecture of the central recommendation unit is illustrated in Figure 3. It is separated into a *foreground* and a *background model*. The knowledge preparation for service recommendation contains time-consuming tasks. The decoupling of these time-consuming tasks in the background model from the foreground model, which handles the time-critical recommendation lookups, reduces or even avoids the costs in terms of service time. The tasks in the background model are conducted asynchronously. The output of the background model is the recommendation knowledge, which is used in the foreground model. Since service recommendation within our framework is based on several aspects, which were described in the previous section, the incoming data has to be pre-processed within both models.

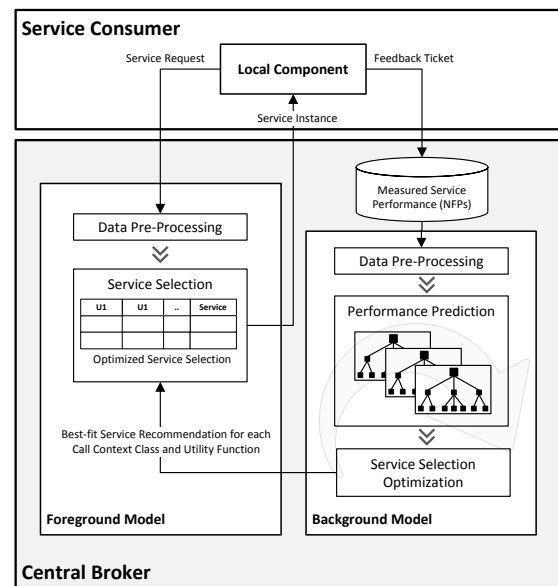


Figure 3. Foreground and Background Model Within our Framework. [1]

Based on the shared knowledge gained from the collected measurement data, the framework prepares recommendation entries with the best-fit service for each combination of call context and preference (utility function), or their cluster. For the prediction of the performance of services or the individual best-fit service, machine learning methods can be employed. Section V describes the general machine learning approaches for their employment. Finally, Section VI presents the evaluation of these machine learning approaches and methods for the employment of service recommendation as well as an initial implementation and validation within our framework. However, before we elaborate on the knowledge preparation for the recommendation task using methods of machine learning, the actual relevant NFPs have to be determined. Section IV presents the results of our literature analysis of scientific

papers in order to identify the relevant NFPs for service selection/recommendation.

#### IV. RELEVANT NFPs FOR SERVICE RECOMMENDATION

This section describes the results of our survey about relevant NFPs of services for their consumption and, hence, their selection/recommendation. It is a digest presenting the summary of the aspects that are relevant for the context of this article. The description and the detailed results of the survey can be found in the appendix.

##### A. Introduction

In order to optimize service consumption at consumer side, it is important to determine the relevant NFPs for service selection/recommendation. Furthermore, it is important to determine whether the relevant NFPs are static or dynamic. While static NFPs can be optimized once, dynamic NFPs are more difficult within service selection since they are likely to change often and require dynamic binding. Within the literature survey, the focus was set on solutions aiming at optimized service selection based on NFPs. The results of the study are based on the analysis of the scientific papers that had been published in the past ten years on conferences in the Service-Oriented Computing (SOC) or related domains. They are founded on service-selection-based conference contributions and, hence, reflect the condensed position of the scientific community in this research area within the recent years. Conference papers are a good foundation because their contributions address state of the art solutions for current problems mostly from researchers but also from industry side. The goal of the survey is to determine the relevant NFPs for service selection and whether the NFPs used within the approaches are theoretically profoundly discussed and validated in practice.

##### B. Results of the Analysis

Presenting the results of the analysis of our study, the NFPs during service selection as well as during adaptation and consumption from a consumer's perspective are analyzed according to two measures:

**Occurrence** This measure expresses the amount of conference papers that refer (mention, discussion, or validation) to a specific NFP within all relevant categorized papers.

**Count** Count represents the amount of overall references of an NFP within all relevant categorized papers. We distinguish count between absolute and relative count. *Absolute count* is the absolute amount of all references. *Relative count* is a normalization of the absolute count within a paper. It is the percentage of references to a specific NFP among all NFP references of a paper.

An NFP with a high *occurrence* can be considered to be widely accepted to be relevant, since it is referred in many papers, while *count* indicates how much text is dedicated to

an NFP in absolute terms (*absolute count*) or relatively in the papers (*relative count*). However, these two measures are not sufficient to deduct the quality of the references. In order to satisfy this aspect, we consider the quality of each NFP reference by its occurrence category, cf. Table I. Furthermore, we also differentiate between the papers regarding their semantic quality towards our finding objectives. Therefore, we categorize each paper according to its topic relevance (cf. Table II).

1) *NFPs Referred in Conference Papers*: Without any consideration of the paper and occurrence categories, we focus on the plain occurrence of NFPs in relevant papers and the plain count of the NFP references in these papers on an absolute and relative basis. In 91 % of the relevant conference papers, *response time* is mentioned (or discussed/validated). Furthermore, the ranked list continues with the following NFPs: *availability* (67 %), *reliability* (45 %), *cost* (40 %), *throughput* (35 %), and *price* (27 %). Considering the textual distribution on an absolute and relative basis, Figure 4 reveals a similar order. However, two things can be noticed: First, *response time* has the highest share among all NFP references. Furthermore, there is a big gap between the relative and absolute count for *trust*. The reason for this is related to the fact that *trust* is extensively discussed in some conference papers. Some researchers argue from their point of view that *trust* had been fiercely neglected compared to other NFPs that are also mentioned frequently in these papers. Comparing absolute and relative count, for some researchers, *trust* is a very important aspect, however for the majority, this NFP is not as relevant as others.

2) *Profoundness of the NFP References*: For further analysis, we grouped the NFPs in categories. The NFPs within their categories are listed in Table III. So far, we did not take the quality of the NFP references into account. As introduced above, we used paper and occurrence categories in order to reflect the impact quality of the papers and the references themselves into account. Figure 5 lists the grouped NFPs

TABLE I. OCCURENCE CATEGORIES

Category	Description
O-A	NFP used in service selection is <i>validated in practical or experimental context</i>
O-B	NFP used in service selection is <i>theoretically discussed in detail</i>
O-C	NFP used in service selection is <i>mentioned but not discussed</i>

TABLE II. PAPER CATEGORIES

Category	Description
P-A	Conference papers with main focus on <i>service selection/recommendation</i>
P-B	Conference papers with main focus on <i>adaptation of composite services</i>
P-C	Conference papers with main focus on <i>service computing</i> in general
P-D	Conference papers <i>without main focus</i> on either of above categories, however, in which NFPs during service selection, adaptation or consumption are mentioned or discussed
P-Z	Conference papers that do not mention NFPs of services at all or that do not fit into the above categories

TABLE III. NFP CATEGORIES

Category	NFPs
Service Time	Delay, Duration, Execution Time, Latency, Performance, Response Time, Timeliness
Service Success	Accessibility, Accuracy, Availability, Dependability, Dependency, Fault Tolerance, Reliability, Successability
Monetary Aspects	Cost, Price
Service Trust/Reputation	Privacy, Reputation, Security, Trust
Service Bandwidth	Bandwidth, Scalability, Throughput
Misc	Energy Consumption, Location, Utilization
Design Aspects	Adaptability, Composability

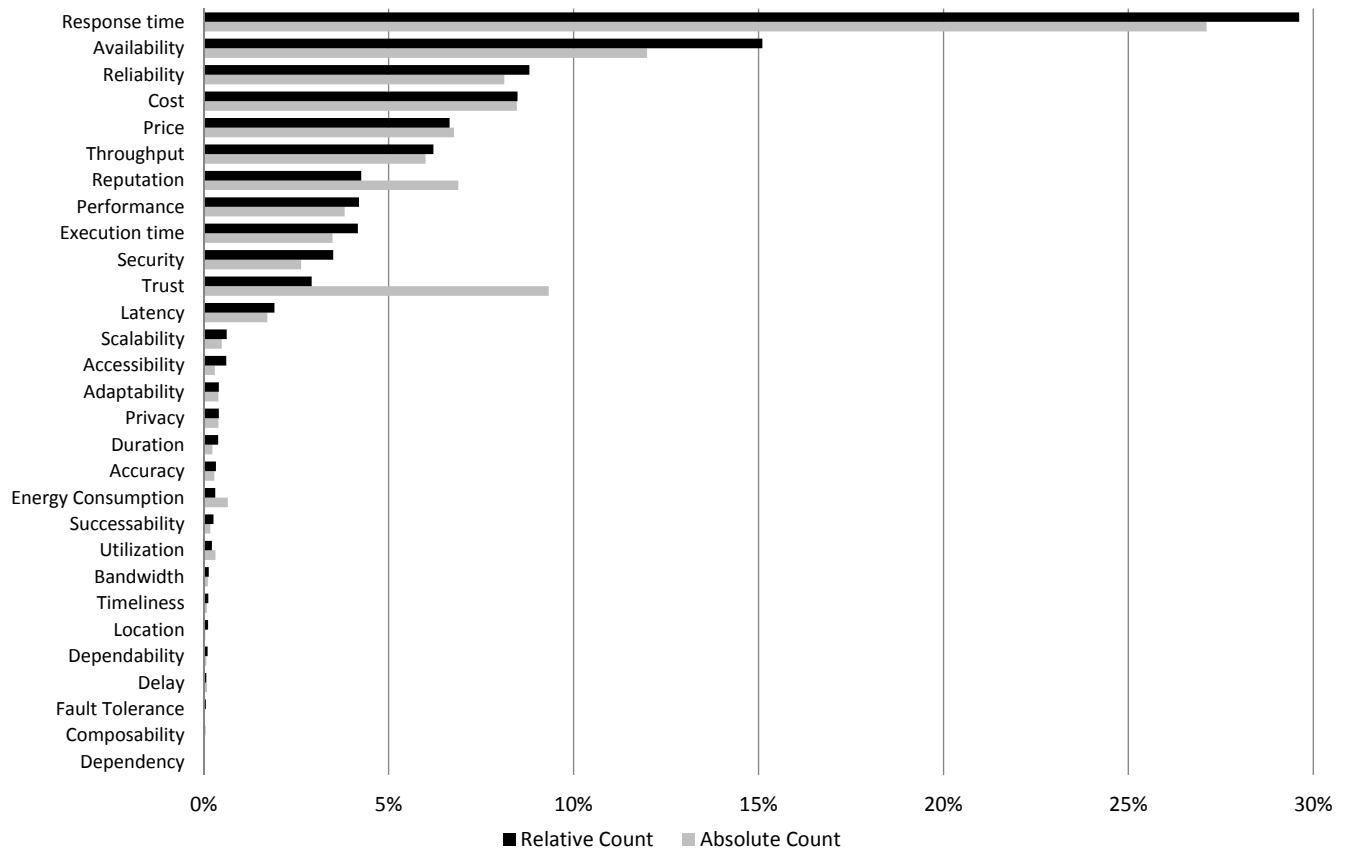


Figure 4. Overall Relative and Absolute Count of NFPs.

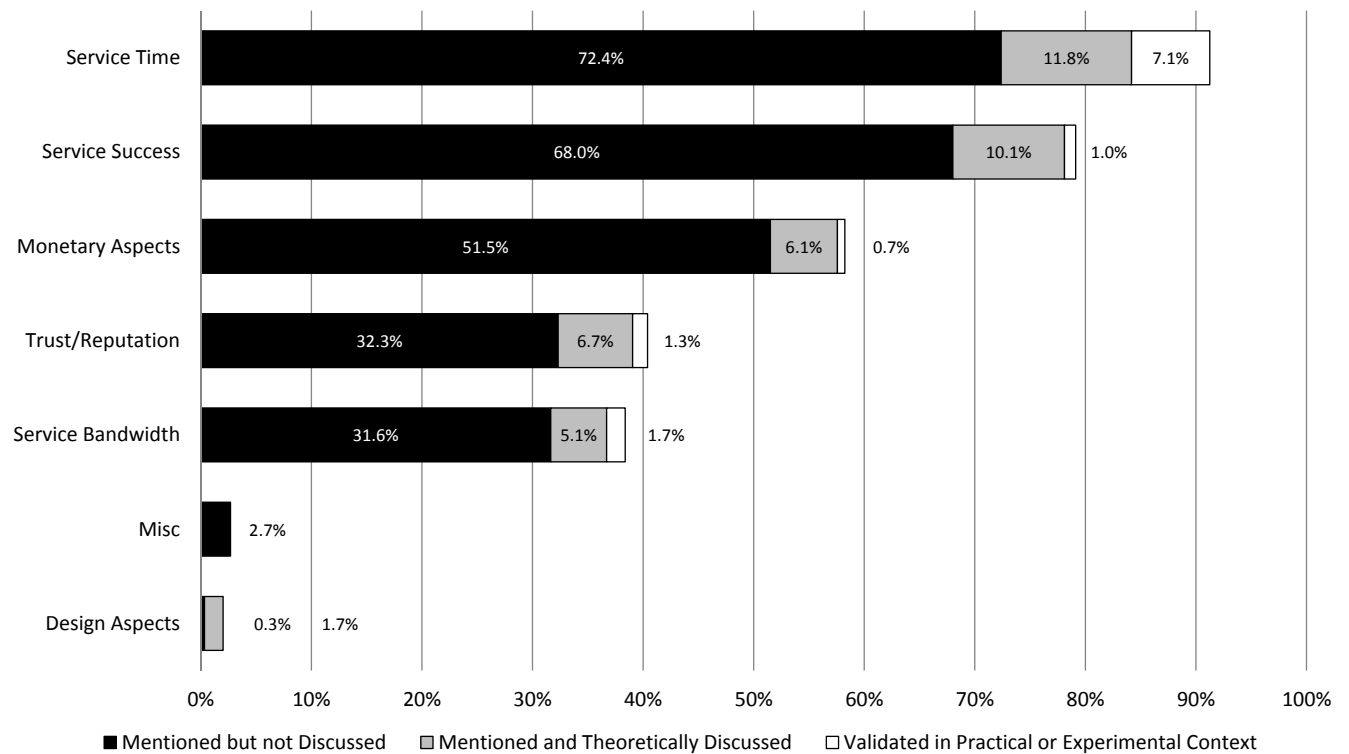


Figure 5. Paper Occurrence of Each NFP Category According to the Occurrence Categories.

regarding their paper occurrence in the form of the percental amount among all relevant papers in which the NFPs of a category occur (mentioned/discussed/validated). If a paper has two or more NFPs that belong to the same NFP category with different occurrence categories, the paper is counted in the highest occurrence category. On average over all NFP categories (disregarding the *Misc* and *Design* categories), 83 % (4 basis points deviation) of all relevant papers only mention NFPs but do not discuss them in detail. On average, 13 % (2 basis points deviation) discuss them in more detail while only 4 % (3 basis points deviation) also validate them in simulations or experiments. This means that a vast majority of relevant conference papers do not elaborate in detail on the NFPs they mention.

### C. Conclusion

As a result of this survey, we determined a list of NFP that are relevant for the selection/recommendation of services. *Response time* is determined to be the most relevant NFP for service selection. It occurs in over 90 % of all relevant categorized papers. Furthermore, with a large gap, its textual distribution with an overall share between 25 % and 30 % also verifies this relevance. The top-3 relevant NFPs are all dynamic. Within the top-6 relevant NFPs, two third of the NFPs are dynamic whereas the rest is rather static. However, *cost* and *price*, which are similar, can also be dynamic depending on the defined price models of service providers.

Considering the quality of the references within the analyzed conference papers, the results reveal that 83 % of the references only mention these NFPs without any further discussion or validation. Only 13 % of the paper occurrences discuss them and even less (4 % with a standard deviation of 3 basis points) validate them in an experimental or practical context.

As the results of a broad research-community-based survey, *response time*, *availability*, *reliability*, *cost*, *price*, and *throughput* are determined to be the top-6 of the relevant NFPs during service selection. Their mostly dynamic characteristic requires dynamic binding and a continuous learning/adaptation of the recommendation knowledge for an optimized service selection. Although response time seems to be the most important NFP among all relevant NFPs, the ranked results list confirms the importance of a multi-NFP service selection, since other NFPs still achieved a considerable relevance.

## V. EMPLOYMENT OF MACHINE LEARNING IN SERVICE RECOMMENDATION IN GENERAL

Machine learning can be employed for the recommendation unit within our framework, which we described in Section III. In general, there are two approaches for the preparation of the recommendation knowledge in the background model using machine learning methods: the prediction of a numerical or a nominal value. In machine learning, regression aims at the prediction of numerical values based on attribute values, while classification focuses on the determination of the affiliation to a certain class based on attribute values. Although both approaches fit in general, they have different focuses within the recommendation process. Figure 6 illustrates the different steps that are required for the retrieval of recommendation knowledge. The gray-shaded boxes highlight the steps for which machine learning methods are used.

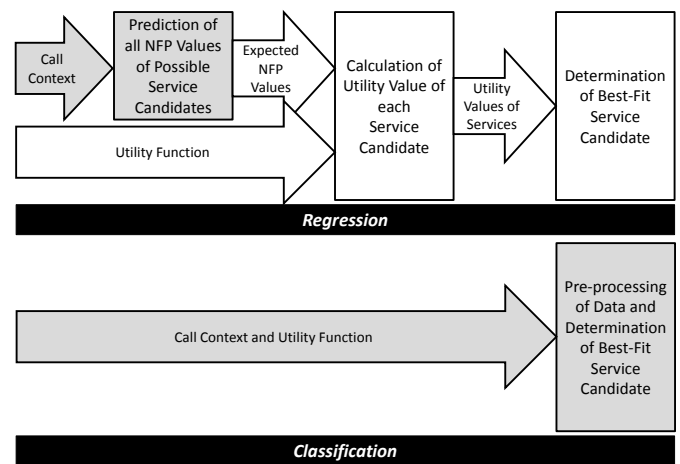


Figure 6. Learning Steps for Service Recommendation Within the Regression-/Classification-based Approach.

### A. Regression-based Approach

Within the recommendation focus, regression can be used to predict each NFP value (e. g., the expected response time and the expected degree of availability) based on call context values (e. g., calling time, weekday, and location). The gray-shaded boxes in the regression part of Figure 6 denote the actual determination of the best-fit service is not included in the learning. The drawback is that machine learning has to be conducted for each NFP individually and the actual utility value for the best-fit determination has to be calculated. However, these higher efforts have several benefits at the same time. For each NFP and call context combination, the NFP value has only to be predicted once, while the best-fit service can be calculated for each utility function individually. Furthermore, since the NFP data for all service instances are considered, the ranking of the second, third, etc. best-fit services can be used to achieve a higher overall utility gain. Underdog and quick starter strategies can also be implemented, since the performance data of service calls of the past still remain [3][38].

### B. Classification-based Approach

In general, classification focuses on the determination of the affiliation to a certain class based on attribute values. In service recommendation, consumers are ultimately interested in the selection of the best-fit service. For this, classification can be used in order to determine the best-fit service for a specific call context. With this approach, the learning method focuses directly on the best-fit determination. For this, the training set has to be pre-processed: for each combination of call context and utility function, the best-fit service has to be determined based on the measurement data. As a result, classification directly determines the best-fit service (class) within a call context and utility function combination without the consideration of the NFP values. The benefit using classification is to omit the calculation steps after prediction. Disadvantageously, however, the best-fit service has to be learned for each call context and each utility function; whereas having the NFPs predicted for a call context as an intermediate step, the best-fit service can be calculated for other utility functions without new learning. Furthermore, old

service instances are automatically not further considered and, hence, sorted out. Disadvantageously, underdogs can never prove themselves since the approach is only focused on best-fit service recommendation and non-best-fit ones are neglected or not invoked at all. Also, there is no differentiation among non-best-fit services, which is important in a non-accurate prediction in order to still create a high utility gain [3][38].

### C. Selection of Machine Learning Frameworks

In [1], we evaluated machine learning methods as well as frameworks that can be employed for our purpose. There are several aspects for the evaluation of machine learning methods such as speed, accuracy, scalability, robustness, and interpretability [39][40]. Table IV lists the requirements that we used for the selection of machine learning methods.

TABLE IV. REQUIREMENTS FOR THE SELECTION OF MACHINE LEARNING METHODS [1]

<b>Speed</b>	describes how efficient the machine learning method performs concerning the training and prediction time. Furthermore, this aspect also concerns the overall machine learning process as a 'critical path' from end-consumer side.
<b>Accuracy</b>	describes how effective the machine learning method performs: Degree of correct classification or coefficient of determination in regression [40].
<b>Scalability</b>	considers the ability of the method to be efficiently applied to a large dataset [40].
<b>Robustness</b>	describes the ability to make correct classifications and predictions, given noisy or missing data value. It also considers whether the method is able to run automatically in a changing environment [40].

In [39], the author published a comprehensive overview of established supervised machine learning techniques. This overview provides useful information for method selection, highlighting the benefits and drawbacks of each method that helped us for further evaluation. For the selection of machine learning frameworks, we focused on a Java integration ability, a high degree of automation, a strong dependence between the library and the implemented method, and a general approach being not limited to specific purposes. Furthermore, we preferred open source frameworks, which are freely available to the public [1].

Because of their extensive collection of classical machine learning methods as well as new algorithms with state of the art concepts for incremental learning, we chose Weka [41] and MOA [42]. Both frameworks provide a high degree of automation and are fully integrated in Java. Furthermore, Weka is also used by other software in this sector. The frameworks are open source and contain different methods and algorithms for pre-processing, classification, regression, clustering, association rules, visualization, and include several state of the art algorithms. Furthermore, MOA also has a focus on online algorithms processing data streams [1].

## VI. EVALUATION OF THE GENERAL CLASSIFICATION- AND REGRESSION-BASED APPROACHES

In this section, we analyze the previously outlined two general machine learning approaches, machine learning methods, and strategies for their employment within service recommendation considering optimization aspects, which were identified in Section III-A. At this point, we want to point out that since our research focus is set on the SOC domain, we do not analyze or optimize machine learning algorithms and only use them

as black boxes. We analyzed two general machine learning approaches for their capability, benefits, and disadvantages of their employment within service recommendation. Our practical assessment is based on real-world measurement data as well as simulated data in order to conduct a statistically more fine-grained analysis. Based on the evaluation of the two general approaches, the more suitable approach was then implemented and validated in our framework. For this validation in the overall recommendation framework, the three machine learning methods were implemented for their evaluation.

Outlined in Figure 6, we conducted analyses of the two general machine learning approaches using classification- and regression-based machine learning methods for their advantages and drawbacks when using them for service recommendation. This section outlines the evaluation scenario and the results of these studies.

### A. Evaluation Scenario

The analyses were described in detail in [3][38]. For more details, interested readers are referred to these references.

1) *Objectives of the Analyses:* The results in this section are summarized, based on two analyses that focused both on the evaluation of both learning approaches, however, which had different sub-objectives. The first analysis focused on a general comparison between both approaches with their methods. Furthermore, it focused on the simulation of performance data based on the real-world measurement data, in order to conduct a more fine-grained analysis. For this, we had to analyze the service profiles within the measurement data. The second analysis focused on the application of learning strategies. Furthermore, the strengths and weaknesses of each approach within certain presumed and simulated service performance profiles were focused in the analysis.

2) *Evaluation Setting:* For the conduction of the analyses, we developed a Java-based software using the Weka and MOA frameworks within the evaluation scenario. We implemented the overall recommendation process of each approach illustrated in Figure 6. For the learning task in the processes, we chose the Fast Incremental Model Tree with Drift Detection (FIMT-DD) algorithm for regression. FIMT-DD focuses on time-changing data streams with explicit drift detection [43]. For classification, we chose the implementation of a DecisionStump [44]. We chose both machine learning methods because of the requirements in Table IV as well as good results in initial pre-tests [3][38].

3) *Evaluation Criteria:* The purpose of both analyses was to evaluate the employment of both machine learning approaches for service recommendation. For their evaluation, we were interested in their overall contribution to the recommendation of best-fit services within the process illustrated in Figure 6; hence, in the benefit of the consumers.

In order to determine the benefit of the recommendation, the accuracy of predicting the best-fit service does not solely reflect the strength of an approach since the recommendation of the second best-fit might be as good as the determination of the actual best-fit if it creates a similarly high optimization benefit. Therefore, within service recommendation, the optimization aims at the experienced performance/utility gain and not at the determination accuracy of the overall best-fit. The evaluation has to take into account how good the optimization is instead

TABLE V. EVALUATION INDICATORS [3][38]

<b>RT Gain Prediction/Random</b>	This figure indicates the overall percental response time gain when using the machine learning approach including the determination of the best performing service for recommendation in comparison to a random selection of services.
<b>RT Gain Best/Random</b>	This indicator is the overall percental response time gain when continuously choosing the best performing service in comparison to a random selection of services. This is the optimum, i.e., when continuously choosing the best performing service, response time is fully minimized.
<b>Overall RT Gain Achievem.</b>	The ratio between the figures above. It indicates to what degree the response time gain of the prediction achieved the optimum.
<b>RT Ratio Prediction/Best</b>	It is the ratio between the total response times of prediction in comparison to a continuous selection of the best performing service. Since the optimum is the denominator, this figure is always $\geq 100\%$ .
<b>RT Ratio Random/Best</b>	The ratio between the total response times of a random selection in comparison to a continuous selection of the best performing service. Since the optimum is the denominator, this figure is always $\geq 100\%$ .
<b>Overall Optimization Achievement</b>	It indicates the optimization degree in percent between the response time of the worst service towards the response time of the best service for each prediction case: $\left(1 - \frac{RT_{Prediction} - RT_{Best}}{RT_{Worst} - RT_{Best}}\right) \cdot 100$
<b>Best Choice</b>	It expresses the amount in percent of the prediction of the actual best(-fit) service candidates.

of the best-fit classification accuracy. Therefore, our key figure is *performance gain* respectively *utility gain* when considering preferences. As for this analysis, the focus was set on the evaluation of the machine learning approaches. Since machine learning methods are employed for the determination of NFPs as the input for the calculation of the utility value, which is then used for the determination of the best-fit service, within the regression-based approach respectively for the determination of the actual best-fit service based on the calculation output of the utility function with the input of one or several NFPs, we could simplify the overall process and could use only one NFP for the prediction, in order to reduce unnecessary calculation overhead. In other words, since the calculation of the utility function is not part of machine learning steps within the approaches (cf. Figure 6), it could be simplified for this evaluation. Instead of determining the utility gain, we evaluated the response time gain.

Table V lists the evaluation indicators that we defined for the evaluation of both machine learning approaches. Note that the table also contains the definitions of indicators that we used in the first analysis (RT Gain Prediction/Random, RT Gain Best/Random, Overall RT Achievement, and RT Ration Random/Best) but not in the second analysis and vice versa (Overall Optimization Achievement). The main indicators of the first analysis based the evaluation on a direct comparison between each approach and random selection. However, random selection is also a simple recommendation approach. A comparison based on relative indicator values turned out to be sub-optimal. In order to get comparable indicator values, we used indicators that focus on an absolute scale in the second analysis. Therefore, they are more sufficient for comparisons between different approaches and methods.

4) *Preparation and Processing of the Datasets:* Analyzing the results of our study in [2], we could discover a pattern-based periodic behavior of the analyzed real-world Web services in natural periods of time such as differences between working days and weekends or time of day. Our hypothesis

before the conduction of this analysis was that machine learning approaches contemplating periodic behavior achieve better results. For this, additionally to the basic attributes *date*, *time*, and *response time*, we pre-calculated further attributes and provide enhanced data with focus on natural periods, which can be used by both approaches. These attributes are described in Table VI. While regression is able to focus on a time line, classification is not. However, these additional attributes allow classification to consider such natural time line based aspects for learning and prediction, such as working day or day of week.

Due to the differences between both learning approaches, further pre-processing was necessary. For classification, the dataset had to be prepared in order to train the best-fit service within each call context. In our case, for each date and time (nominal value of hour), the enhanced measurement entry with the minimum response time (desired best-fit service) remained in the dataset. So, the learning method only focused on the fastest (best) services, in which we are ultimately interested. For regression, no best-fit focus was set since the regression approach focused on the actual (NFP/response time) value prediction. However, since each NFP for each service has to be trained, the dataset had to be split for each combination of NFP and service.

After the pre-processing of each dataset (measurement or simulation), the datasets were divided into a training and a validation sub-set after pre-processing. Because of chronological aspects, the datasets could only be split into training and validation sets. *N*-fold cross validation could not be applied for that reason. While the training dataset was used for the training of the model, the validation dataset was used to validate and evaluate the prediction results of the recommendation processes. In the first analysis [3], the dataset was split in the middle. The first half of the dataset was used for learning, the second dataset was used to validate the prediction results. In contrast to initial analyses, in the second analysis [38], a sliding split point evaluation was conducted. Depending on the split point, the drawback of the initial analysis was that the analysis results varied. This was due to the varying performance profiles during the measurement period. Analyzing the measurement data, some Web services experienced temporal performance changes, which confirmed our focused aspect of the perpetual change characteristic of the Internet as a service market. In

TABLE VI. STATISTICAL ENHANCEMENT OF ATTRIBUTES [3]

<b>DayOfMonth</b>	Extracted day of month from date
<b>Hour</b>	Extracted hour from time
<b>Weekday</b>	Determined nominal day of week from date ( <i>classification only</i> )
<b>Workingday</b>	Determined whether day is a working day (Monday to Friday) ( <i>classification only</i> )
<b>RT_Xmin_AVG</b>	Response time mean of all records (chronologically) within the last 1, 2, 3, 6, 12 hours, and 1, 2, 5, 7 days
$X = \{61, 121, 181, 361, 721, 1441, 2881, 7201, 10081\}$	
<b>RT_X_AVG</b>	Response time mean of the previous <i>x</i> records (chronologically; without consideration of any other attribute)
$X = \{40, 80, 160, 240\}$	
<b>RT_X_AVG_Hour</b>	Response time mean of the previous <i>x</i> records within the same hour value (considering 1, 3, 5, 7 days of the same nominal hour)
$X = \{4, 12, 20, 28\}$	
<b>RT_X_AVG_Weekday</b>	Response time mean of the previous <i>x</i> records within the same weekday value (considering 1, 2, 4 weeks of the same nominal day of week)
$X = \{4, 8, 16\}$	

order to achieve statistically generalized results, the split point between training set and validation set was iterated on a day by day basis for each analyzed aspect. Depending on the period (and window sizes), it could result in a statistical mean of up to  $\frac{n}{24m} - 1$  iterations (for the measurement input 170 iterations per scenario), for  $n$  data entries and  $m$  data records per hour (one record for each service) [38].

5) *Learning Strategies*: Employing machine learning for the recommendation of best-fit services requires learning strategies. Within this employment, it is necessary to analyze the impact on the overall recommendation results when considering the amount of training and prediction data. In other words, how much data is necessary and beneficial for training a model, and for how long is such a trained model reliable for good service recommendation?

In the first analysis [3], there was no focus set on any learning strategy. The results of that analysis are based on a two split (50:50) conduction. The learning model was trained on the first half, while the second half was used for the validation and evaluation of the prediction results.

For the second analysis, the following learning strategies were analyzed. In order to address the research questions related to the optimal learning strategies, a prediction window of various sizes was applied to determine the optimal training/prediction interval ratio for the updates of the foreground model (Figure 3) [38].

**Incremental learning** This learning strategy continuously updates the learning model. Any strategies on changes and their impact on the model have to be dealt by the learning method such as drift detection.

**Sliding window learning** This learning strategy applies a fixed window of previous measurements for the training of the learning model.

## B. Evaluation Datasets

The machine learning approaches were analyzed and evaluated using measurement as well as simulation data. The latter focused on certain aspects during the evaluation.

1) *Measurement Data*: For both analyses, the measurement data was gained from four real-world stock quote Web services, which we already partly used in [2]. The services provide similar functionality, so they are functionally substitutable among each other. In the first analysis, the measurement dataset contained 3,223 measurement entries obtained in 34 days. The dataset in the second analysis contained 16,441 measurement entries obtained in a measurement period of 185 days. The dataset of the first analysis is also the initial subset of the second analysis. Therefore, the measurement data of the second analysis is the long term version of the dataset in the first analysis. Each entry contained the *date*, *time*, the consumed *service*, and the measured *response time* of a service call. Within each measurement period, each Web service was called on an hourly basis. If a service was not available or timed out (30,000 ms), its entry was not added to the set. Hence, up to four data entries were obtained per hour for the dataset [3][38].

2) *Simulation Data*: In contrast to measurement data, with the ability to adapt the parameters, scenarios can be simulated. The simulation of measurement data enabled to challenge machine learning approaches and to analyze their

performance in certain scenarios. Within the measured real-world Web services, the statistical characteristics showed easily distinguishable performance profiles of some services. In order to compare the strengths and weaknesses of the machine learning approaches, more challenging scenarios had to be simulated where the service profiles are harder to distinguish. In both analyses, simulation data was produced in order to analyze certain aspects. The following simulation profiles were generated [3][38]:

In the first analysis [3], the initial goal was to simulate data that closely reflects the characteristics of measured real-world Web services. With such data, it would be possible to adjust certain distinguishable profile characteristics in order to challenge the machine learning methods during the analysis. Based on the analysis of the measurement data and the observations made in [2], two simulation profiles were created [3]:

**Normal distribution profiles with similar statistical characteristics of the measured services** The visualization of the measurement data revealed that the real-world data had a massive distribution in certain intervals with diverse outliers. We presumed a normal distribution of the measurements with certain extraordinary outliers. We used the Gaussian distribution (cf. [45]) for the simulation of basic interval where most of the values occur and one with the identified outliers using the statistical mean and standard deviation of the services' intervals in order to achieve similarity [3].

**Normal distribution profiles with similar statistical characteristics of the measured services and periodicity** Additionally to the first profile, we added some periodicity to the profile in order to simulate the in [2] observed differences between certain natural time-/date-based characteristics. For this simulation, we added a periodic component to the normally distributed basis such as a working day pulse, daily periodic waves, and weekly peaks. For the simulation of working day pulse, we used the Fourier series expansion in order to produce a rectangular pulse wave (cf. Equations (1) and (3) for daily periodicity). With these periodic components additionally to the random component, we expected the classification approach to achieve better results because the additional attributes in the pre-processing aims at these natural periods. Classification is in general optimized for such periodic preparations [3].

In order to challenge both approaches, we approximated the statistical mean of all simulated services step-by-step to a defined level (target mean value). Our presumption was that the more the services approximate the statistical mean, the worse the beneficial gain results of the machine learning approaches in comparison to a random selection, since the standard deviation values in the relevant interval are close to each other. The purpose of the approximation was to evaluate, which approach tackles the challenge better and to what approximation degree machine learning approaches can still be beneficial for the recommendation task. For the challenge of the evaluated approaches and methods, the mean values of the service profiles in the first analysis were approximated in the following steps: 50 %, 75 %, 87.5 %, 93.75 %, and 100 %.

$$f(t) = \frac{\tau}{T} + \sum_{n=1}^{1000} \frac{2}{n\pi} \sin\left(\frac{n\pi\tau}{T}\right) \cos\left(\frac{2n\pi}{T}(t+p)\right) \quad (1)$$

$$f(t) = \frac{2}{\pi} \sum_{n=1}^{1000} (-1)^n \sin\left(\frac{(t+p)n2\pi}{T}\right) \quad (2)$$

$$f(t) = \sin\left(\frac{2\pi(t+p)}{T}\right) \quad (3)$$

In contrast to the first analysis, the focus of the second one was set on the explicit analysis of isolated aspects. The analyzed learning approaches with the employed machine learning methods should be challenged for their strengths and weaknesses in the following presumable scenarios. For this, the competing simulated services all had identical profiles with distinguishable differences in each focused aspect. The initially, clearly distinguishable profiles were also approximated in 10% steps in each conducted iteration until they were fully approximated in order to challenge the learning approaches and methods. In a full approximation, their profiles are identical (up to random noise) [38]:

**Normal distribution profiled data** As in the initial analysis, we assumed normally distributed response times of Web services around a mean value (with a certain standard deviation and variance). Normally distributed response time data for four services with a similar mean, standard deviation, and variance was created. These response time mean profiles of the services were initially, vertically shifted and were then approximated step by step. Fully approximated, their statistical mean is identical.

**Cyclic spikes up/down** On the basis of normally distributed response time data around the same mean value, these profiles contained cyclic/periodic spikes that go in one profile up and in the other profile down. Spikes going up simulate services that have suddenly longer response times, while spikes going down simulate sudden response time improvements. For their creation, a saw tooth generator (cf. Equations (1), (2), and [46]) in combination with an iceberg filter that are added to the basic normal distribution line was used. Again, all created services are similar. They distinguish themselves only in their horizontal shift. Fully approximated, their horizontal shift is identical.

**Acyclic spikes up/down** These profiles have several acyclic spikes and different level shifts in combination with an iceberg filter. Using several cyclic spikes with very long periods in spikes generations in combination with pulse train shifts and the iceberg filter, a complete acyclic/aperiodic behavior could be simulated. Again, all services have the same mean response time and in a fully approximated case and their spikes are overlapping.

### C. Evaluation Results

The results presented in this section are extracted from [3][38]. Interested readers are referred to these references for more details on the conduction and results of each analysis. The first analysis [3] used a two-split analysis in the middle of each input dataset for the training and test sub-sets. Additionally, each analysis scenario was re-conducted ten times

in order to achieve statistically profound results within the random components. The presented results of this analysis are mean values. In further tests, we discovered that the profiles of the measured services change and that depending on the used split point, the results of the evaluation indicators change. Therefore, we conducted a sliding split point evaluation in the second analysis [38]. While the first analysis used a split point in the middle of each input dataset, the second analysis [38] considered statistically profoundness in terms of the a sliding split point between training sets and validation sets iterated on a day by day basis.

**1) Measurement Data:** The results of the first analysis using measurement data are presented in Table VII. Within the ten iterations of which the random components (random selection) was re-conducted, the mean values and the values of the best iteration are presented for each approach. Among all indicators introduced in Table V, the most important indicator, which was also used to determine the best iteration, is *Overall RT Gain Achievement*. The second important indicator is *Best Choice Prediction*. Recall, the best choice indicator is a certain kind of accuracy, however, considering the optimization achievement within service recommendation, the actual response gain (or utility/performance gain in general) is more important, since it compares the improvement using machine learning with the overall achievable optimum, which is the RT gain when theoretically choosing always the best-performing service instance. Furthermore, it also takes the optimization degree among the recommended non-best services into account. A positive RT gain is supposed to indicate the percental response time reduction compared to a random selection. Furthermore, the table lists the amount of the selection of services that were not available at the moment of selection. When considering the figures of Table VII, please note that random components are re-conducted in each iteration, while the actual measurement data remains unchanged. The prediction and hence the recommendation results also remain unchanged in each iteration (table columns: RT ration prediction/best; non-AV section in prediction; best choice prediction). Using real-world measurement data, regression achieved better results than classification. If we compare the best choice figures for prediction in the table, we see that classification seems to have a higher accuracy. This might appear odd, when we compare the RT gain and the overall RT achievement figures. Recall, in service recommendation, accuracy is less important than the actual performance gain. The recommendation of the second best service might be in terms of RT gain almost as good as to recommend the actual best. Comparing the RT gain and best choice figure of classification and regression, we see that classification has a higher best choice, while the RT gain is better for regression. This reveals that although regression was weaker in the best choice prediction, it still achieved a higher RT gain, which shows that regression's strength is in a ranked determination, while classification does not consider any ranking. Furthermore, in 1.46% of the cases (6 times in 17 days), classification recommended a service instance that was not available at that moment. In order to verify our assumption regarding periodic strengths, we had a look at the classification model. The model based its decisions mostly on the sliding window of the previous response time values within the same nominal hour. So, our periodicity assumption was proven.

In the second analysis, the focus was set on optimal

TABLE VII. ANALYSIS RESULTS OF MACHINE LEARNING APPROACHES USING MEASUREMENT DATA [3]

		RT Gain Predict./Rand.	RT Gain Best/Rand.	Overall RT Gain Achvmt	RT Ratio Predict./Best	RT Ratio Rand./Best	Non-AV Prediction	Non-AV Random	Best Choice Prediction	Best Choice Random
Classification	Mean	66.57 %	82.33 %	80.86 %	189.17 %	565.97 %	1.46 %	4.61 %	80.09 %	24.51 %
	Best	69.76 %	84.01 %	83.03 %	189.17 %	625.66 %	1.46 %	5.58 %	80.09 %	23.05 %
Regression	Mean	75.74 %	82.44 %	91.87 %	138.16 %	569.53 %	0.00 %	4.37 %	66.99 %	25.00 %
	Best	77.78 %	83.92 %	92.68 %	138.16 %	622.05 %	0.00 %	5.58 %	66.99 %	24.27 %

TABLE VIII. DIFFERENT PREDICTION WINDOWS WITHIN INCREMENTAL LEARNING [38]

Win. Size Prediction	DecisionStump				FIMT-DD			
	Achievement		Best Choice		Achievement		Best Choice	
	mean	$\sigma$	mean	$\sigma$	mean	$\sigma$	mean	$\sigma$
1	97.10 %	6.10 %	82.26 %	22.89 %	97.04 %	3.89 %	73.35 %	21.47 %
28	96.34 %	2.23 %	72.77 %	22.94 %	97.02 %	1.60 %	72.78 %	13.59 %

TABLE IX. SLIDING WINDOW SCENARIO WITH DIFFERENT TRAINING WINDOWS [38]

Win. Size Training	DecisionStump				FIMT-DD			
	Achievement		Best Choice		Achievement		Best Choice	
	mean	$\sigma$	mean	$\sigma$	mean	$\sigma$	mean	$\sigma$
1	96.50 %	3.93 %	74.76 %	22.74 %	97.13 %	2.35 %	73.52 %	16.67 %
10	97.29 %	3.21 %	80.85 %	20.83 %	97.23 %	2.36 %	73.94 %	16.89 %
20	97.37 %	3.18 %	79.90 %	22.51 %	97.38 %	2.29 %	74.74 %	16.87 %
40	97.70 %	2.97 %	81.31 %	25.42 %	97.93 %	1.66 %	78.86 %	14.50 %
60	98.32 %	2.53 %	89.72 %	12.70 %	98.16 %	1.63 %	81.89 %	13.20 %
120	97.45 %	4.36 %	89.79 %	4.25 %	97.48 %	2.00 %	72.97 %	13.87 %

TABLE X. SLIDING WINDOW SCENARIO WITH DIFFERENT PREDICTION WINDOWS [38]

Win. Size Prediction	DecisionStump				FIMT-DD			
	Achievement		Best Choice		Achievement		Best Choice	
	mean	$\sigma$	mean	$\sigma$	mean	$\sigma$	mean	$\sigma$
1	97.86 %	4.81 %	85.61 %	17.27 %	97.48 %	3.55 %	75.76 %	21.43 %
7	97.42 %	3.52 %	83.48 %	17.33 %	97.54 %	1.95 %	75.87 %	16.27 %
14	97.31 %	2.91 %	82.06 %	18.18 %	97.56 %	1.53 %	75.87 %	12.92 %
28	97.16 %	2.22 %	79.73 %	19.52 %	97.63 %	1.16 %	76.44 %	10.71 %

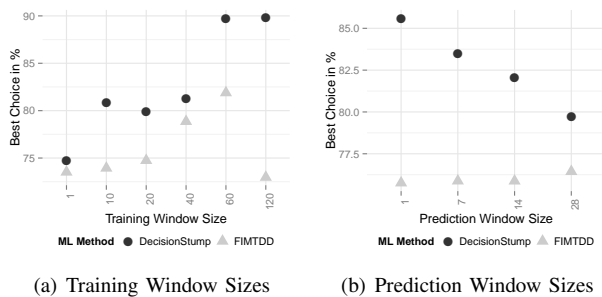


Figure 7. Best Choice Means of Different Window Sizes With Measurement Data. [38]

learning strategies and evaluation based on a longer period of measurement data as well as to equalize the results regardless any specific splitting point using the introduced sliding iterations. Tables VIII and IX focus on the evaluation of the training strategies. Table VIII shows the results of the predictions using a prediction window of 1 and 28 days and an incremental learning strategy. Tables IX and X present the results using sliding training windows. Table IX reveals the results analyzing the optimal window size for the training of the model, while Table X focuses on the optimal prediction window size. In contrast to the first analysis, in which we used a relative indicator for making comparisons to another learning approach (random selection), we used an absolute indicator to make the learning approach comparable among each other. The absolute indicator is the *Overall Optimization Achievement*. The best choice indicator remained the same. Comparing the learning strategies in the tables, the overall optimization achievement is more or less similar in all cases. This is due to the fact, that the mean response time value of the worst service is much higher than for the other services. Hence, predicting any service that is not the worst service already achieves quite a high absolute optimization achievement. Comparing on a relative basis, such as in the first analysis, results in easier distinguishable figures in such a scenario. In reality, this indicator is still significant for the general evaluation of an approach. If we directly compare the major two figures between the similar scenarios in the first and second analysis in Table VII and a prediction window of 28 days in Table VIII, the FIMT-DD-based approach could also achieve higher optimization improvements, while the best choice prediction strength of the classification-based approach could not keep its advance in a long term and iteration equalized analysis (second analysis; cf. Table VIII). However, if the prediction window size is one day, the best choice strength is still determinable. In general, a shorter prediction window size is better than a bigger one. While the classification approach gets worse in its predictions, regression-based FIMT-DD remains strong and even gets slightly better on average (illustrated in Figure 7(b)). We assume that the drift detection of this method is responsible for that. As for the training size, for both methods, the prediction results get better the bigger the training window size, up to a size of 60 days (illustrated in Figure 7(a)).

2) *Simulation Data*: Based on the measurement data, the generated data of the first analysis [3] follows a normal distribution with the same statistical means, standard deviations (both of the main base intervals), and with the same outliers of the services from the measurement data. Starting from the initial vertical level, we approximated step by step the mean values to a target value of 2,000 ms (approximation degrees are represented between 0, no approximation, and 1, full approximation). Within each approximation step, the presented results are mean values of an iteration of ten re-conductions. Tables XI

TABLE XI. ANALYSIS RESULTS OF CLASSIFICATION USING NORM. DISTR. GENERATED DATA WITH PERIODICITY (MEAN VALUES) [3]

Target Mean Value in ms	Approximation Degree	RT Gain in % Prediction/Random	RT Gain in % Best/Random	Overall RT Gain Achievement in %	RT Ratio in % Prediction/Best	RT Ratio in % Random/Best	Best Choice in % Prediction	Best Choice in % Random
2,000	0	69.21	74.89	92.40	122.64	398.33	76.60	25.34
	0.5	40.82	48.57	84.04	115.07	194.47	55.71	26.18
	0.75	29.03	38.13	76.13	114.71	161.64	43.73	23.95
	0.875	22.94	32.31	71.00	113.84	147.74	35.93	25.06
	0.9375	13.75	30.99	44.36	124.98	144.91	34.54	25.06
	1	-5.47	28.36	-19.31	147.23	139.59	32.03	26.18

TABLE XII. ANALYSIS RESULTS OF CLASSIFICATION USING NORMALLY DISTRIBUTED GENERATED DATA (MEAN VALUES) [3]

Target Mean Value in ms	Approximation Degree	RT Gain in % Prediction/Random	RT Gain in % Best/Random	Overall RT Gain Achievement in %	RT Ratio in % Prediction/Best	RT Ratio in % Random/Best	Best Choice in % Prediction	Best Choice in % Random
2,000	0	67.35	76.42	88.12	138.51	424.23	66.01	25.34
	0.5	39.17	51.28	76.38	124.85	205.25	43.73	25.06
	0.75	29.86	43.31	68.95	123.71	176.40	34.54	24.51
	0.875	23.91	37.94	63.03	122.59	161.14	35.93	24.79
	0.9375	13.53	36.98	36.59	137.21	158.69	30.36	23.95
	1	9.33	36.09	25.85	141.87	156.47	28.69	24.79

TABLE XIII. ANALYSIS RESULTS OF REGRESSION USING NORM. DISTR. GENERATED DATA WITH PERIODICITY (MEAN VALUES) [3]

Target Mean Value in ms	Approximation Degree	RT Gain in % Prediction/Random	RT Gain in % Best/Random	Overall RT Gain Achievement in %	RT Ratio in % Prediction/Best	RT Ratio in % Random/Best	Best Choice in % Prediction	Best Choice in % Random
2,000	0	50.83	74.10	68.59	189.85	386.12	38.99	24.51
	0.5	6.98	47.89	14.59	178.49	191.90	27.57	25.06
	0.75	6.28	37.53	16.74	150.03	160.09	27.85	24.51
	0.875	8.75	33.38	26.22	136.96	150.11	28.96	25.34
	0.9375	5.43	30.83	17.61	136.73	144.59	29.52	23.95
	1	3.24	28.12	11.52	134.62	139.13	25.90	25.06

TABLE XIV. ANALYSIS RESULTS OF REGRESSION USING NORMALLY DISTRIBUTED GENERATED DATA (MEAN VALUES) [3]

Target Mean Value in ms	Approximation Degree	RT Gain in % Prediction/Random	RT Gain in % Best/Random	Overall RT Gain Achievement in %	RT Ratio in % Prediction/Best	RT Ratio in % Random/Best	Best Choice in % Prediction	Best Choice in % Random
2,000	0	52.14	76.30	68.34	201.91	421.96	33.14	24.79
	0.5	23.12	51.81	44.63	159.54	207.54	26.46	24.23
	0.75	15.76	44.98	35.04	153.12	181.78	29.52	23.95
	0.875	8.33	39.78	20.94	152.23	166.08	28.13	24.23
	0.9375	0.86	37.70	2.29	159.14	160.53	24.51	25.06
	1	-3.40	35.43	-9.59	160.15	154.88	24.51	25.62

and XII present the data results of the classification-based approach, with and without periodicity on natural time periods. Tables XIII and XIV list them respectively for the regression-based approach. For both machine learning approaches, our assumptions were confirmed. The higher the approximation degree, the less the best choice prediction and the overall RT achievements. Within the approximation, the classification approach achieved now higher RT gain achievements up to a degree value of 0.9375, while within regression the figures got much worse already at a degree of 0.5. For both approaches, since the differences in the response time values between the services also decreases, the gain margin reduces and, therefore, the benefit of recommendation also decreases. Using regression in the periodic/random case, the RT gain is not much better than a random selection already at that degree. In the random-only case, it is much better. Within the generated data in contrast to the measurement data, regression lags now behind classification. The simulated periodicity was apparently not as much represented in the measurement data than expected. Furthermore, the FIMT-DD does not cope with a sinus-based (natural) periodicity. The classification-based approach could achieve better results due to the in the pre-processing focused natural periods. Nonetheless, this required further analysis. Therefore, in the second analysis [38], a focus was set on each presumed aspect (cf. the introduced simulation profiles in the previous section) individually in order to analyze the strengths and weaknesses within each aspect, but also in order to find out, which aspects can be reflected in the actual measurement data. Like the measurement data in the second analysis, the results are mean values of the sliding point iteration. Similar to the approximation of the simulation data in the first analysis, an approximation was conducted on a 10% step basis until they were identical (disregarding some random noise). The results of each approximation step reveals how good the learning approaches and scenarios can cope with the challenge that the respective scenario focused on. Figure 8 depicts the best choice results for each machine learning approach. Figure 9 shows the correspondent overall achievement figures. Since the achievement is defined relatively to the best and worst service performances and since these performances are approximated step by step, there is not much difference between both figures with their different accuracy criteria “best choice” and “overall achievement”, resp.; especially, when the approximation approaches 100%. For the cyclic and acyclic profiles, the non-best services perform equally since there is no vertical shift. Hence, the overall achievement depends only on whether finding the best choice or not. Therefore, for these profiles, there is not much difference between the best choice and the overall achievement indicators.

Before we focus on the differences between both learning approaches, we compare the differences between the different scenarios. Both approaches cope well with the normal distribution scenario. This is the only scenario approximating a vertical shift (response time mean), and both methods and their approaches get worse when the response time means are approximated. All other scenarios approximate a horizontal shift. That means that their normal distribution component is and remains similar. They only distinguish themselves in their performance spikes (response time up for worse performance; response time down for improvements). In the acyclic spike scenarios, both approaches are not able to cope with these

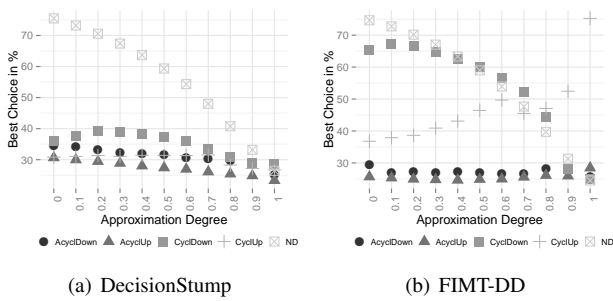


Figure 8. Best Choice Mean Using Sliding Windows Within the Scenarios. [38]

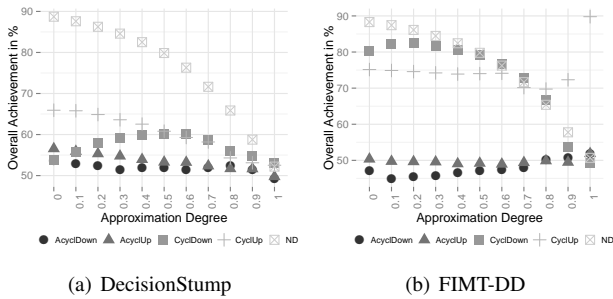


Figure 9. Overall Achievement Mean Using Sliding Windows Within the Scenarios. [38]

spikes. No matter whether the spikes go up or down, both approaches remain on a best choice rate of around 25 %, which is not much better than random selection in the first analysis. However, the DecisionStump approach achieves slightly better results. Comparing the remaining cyclic scenarios, the FIMT-DD can show its strengths (see CyclDown and CyclUp in Figures 8(b) and 10). Compared to the classification-based approach illustrated in Figure 8(a), the FIMT-DD achieves much higher best choice (and overall achievement) figures. The profiles of each service are taken into account, while this information is lost using the classification approach, which is illustrated in the charts in Figures 8 and 9. One of our question, whether it makes any difference if the spikes go up (a service gets suddenly worse) or the spikes go down (a service gets suddenly better), could be answered. According to

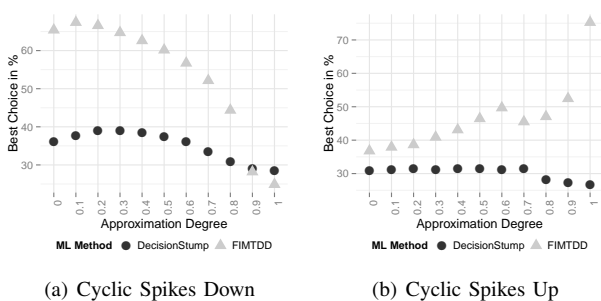


Figure 10. Best Choice Comparison Between Both Learning Methods in the Cyclic Down/Up Scenario.

the results, illustrated in the figures, it does make a difference whether the spikes go up or down. FIMT-DD is in both cases significantly better. However, services getting suddenly worse among similar services (spikes down) can be learned better than the other way around. It seems to be easier to learn an outstanding service whereas it seems to be more difficult to recognize a service getting worse within the optimization focus of similar well performing services. Having a closer look at the cyclic up illustration in Figures 8(b) and 9(b), the indicator values get better with a higher approximation degree. This seems to be odd. One explanation could be that the regression-based approach focuses on the prediction of the performance behavior of each service as a pre-step for the actual best service determination, while the classification-based approach only focuses on the direct learning of the best fit service. However, the spikes up scenario simulates the opposite. Furthermore, considering the generation of the cyclic down and up scenario, their profiles are inverted on a higher level. The differences between the results in the figures also appear to be inverted. Still, the results for this scenario require further analysis, since a total approximation of this profile and its normal distribution part should develop similarly to the fully approximated normal distribution scenario [38].

#### D. Validation of the More Suitable Approach With Machine Learning Methods in the Framework

As a result of the evaluation of the classification-based vs. regression-based approach, both approaches can be employed in general. However, the regression-based approach revealed several benefits. Therefore, for the evaluation within our framework, we focused the regression-based approach, using machine learning methods for the prediction of the performance of services. The benefit of this approach is that the estimated NFPs within a certain moment (call context) can then be used for the calculation of the utility value for different preferences. Furthermore, with this approach, a ranking between the service candidates can be conducted since it is more important to gain a higher utility than to achieve a high best-fit accuracy. With the selected regression-based approach in general, machine learning methods had to be evaluated for their NFP prediction within the overall knowledge retrieval and recommendation process. As a result, the evaluation of the recommendation process with the employment of the selected learning approach together with at least one appropriate machine learning method is also a proof of concept of the overall framework.

1) *Validation Scenario:* With the learning focus set on the prediction of NFP values, we implemented three machine learning methods in our framework for further evaluation. In contrast to the first evaluation, we also changed the training and evaluation phase to the recommendation scenario in reality. Like in reality, we used a continuous learning strategy.

After initial, various pre-tests, we selected besides FIMT-DD [43] also Naïve Bayes and Hoeffding Tree [47] for the implementation and validation within our framework [1]. The Naïve Bayes classifier is a simple probabilistic classifier based on Bayesian statistics (Bayes' theorem) with strong independence assumptions [48]. The Hoeffding tree or Very Fast Decision Tree (VFDT) is an incremental, anytime decision tree induction algorithm that is capable of learning from massive data streams, assuming that the distribution generating examples do not change over time. It exploits the fact that

TABLE XV. EVALUATION RESULTS OF THE MACHINE LEARNING METHODS NAÏVE BAYES, Hoeffding TREE, AND FIMT-DD WITHIN THE OPTIMIZED SERVICE SELECTION/RECOMMENDATION [1]

	Naïve Bayes	Hoeffding Tree	FIMT-DD
TOP1 Accuracy (in %)	58.634	59.837	69.287
TOP2 Accuracy (in %)	90.163	90.421	93.471
Mean Absolute Error (Utility)	1.656	1.660	1.049
Recommend. Table Updates	659	647	1.189

a small sample can often be enough to choose an optimal splitting attribute. This idea is supported mathematically by the Hoeffding bound, which quantifies the number of observations needed to estimate some statistics within a prescribed precision [47][49]. The FIMT-DD, which focuses on time-changing data streams with explicit drift detection [43], was again used because of its focus on drift detection. With respect to the requirements in Table IV, these methods were chosen due to their outlined characteristics (simplicity vs. incremental, anytime decision with capability of massive data streams vs. drift detection).

For the evaluation of the learning methods, the actual best-fit service instance has to be known at each call context (location, weekday, time, etc.) with each utility function. This is a challenge when it comes to a real-world validation. In reality, service calls over the Internet cannot be repeated under the exactly identical conditions as the various kinds of networks and infrastructures build complex systems with variable behavior. At a certain, unique moment, the load of a service instance's system environment and the network load or any incident are combinations of coincidences, which cannot be repeated. However, such aspects have an impact on the experienced NFPs at consumer side. For a strict validation, all service calls that are supposed to be compared had to be made at the same, identical call context, which is practically infeasible, especially when there are several competitive service instances [1].

Such a situation can only be derived within a simulation scenario, where the characteristics of NFP behavior are known for evaluation. In order to achieve such a scenario, where the validation process retrieves exactly the best-fit service instance for validation at each moment considering call context and utility function, we developed a simulator that creates NFP measurements for services based on pre-defined behavior profiles within a period. The implementation of this simulator follows a periodic behavior influenced by statistical random-based deviation. Similar to the previous simulation, the periodic behavior of the simulated Web services is based on our initial measurements and considered day/night time, weeks, month, work day, and weekend aspects. The random-based deviation is supposed to simulate unexpected incidences such as network traffic jams, high/low usage of a service's limited infrastructure [1].

For this evaluation, we focus on the machine learning within the overall recommendation process. Recall, within the regression-based approach, which we preferred for the outlined reasons, the machine learning methods are used for the prediction of the NFP values as the input for the calculation of the utility value. The amount of NFP inputs have no impact on the machine learning steps. Therefore, based on the results in Section IV, we selected the top-2 of the relevant NFPs:

response time and availability. A further advantageous aspect for their use is that their measurement scales are different and both can be measured, hence, they are variable. Furthermore, both of their measurement scales are all also used by the actual top-6 relevant NFPs: ratio scale for response time, cost, price, and throughput; nominal scale for availability and reliability. So, by their usage for the evaluation and validation, all possible measurement scales for the top-6 relevant NFPs are included in the analysis. In the appendix, Figure 18 illustrates the characteristics of the simulated response times within the whole period. Note that the line is only a visual orientation to depict the concept drift of each service instance. For the recommendation, the actual best-fit service instance at each time is important and not the averaged value of each service instance. Figure 19 (appendix) depicts the statistical value of availability with a focus on weekday and daytime periods.

2) *Results:* The evaluation results are based on the process described in Section III and Figure 6 (upper process), in which learning is only used for the prediction of the NFPs of a service. The learning of the expected NFPs is based on incremental, continuous learning with each evaluated learning method. The calculation of the individual utility values and the best-fit service determination are done in intervals and updated in the foreground model. Listed in Table XV, the results of the FIMT-DD achieved around 70 % of correct predictions on average. Note that the calculated utility ranges from 0–100. TOP 1 accuracy is the prediction accuracy of the actual best-fit service, while TOP 2 accuracy is fulfilled when predicting the best-fit or second-best-fit service.

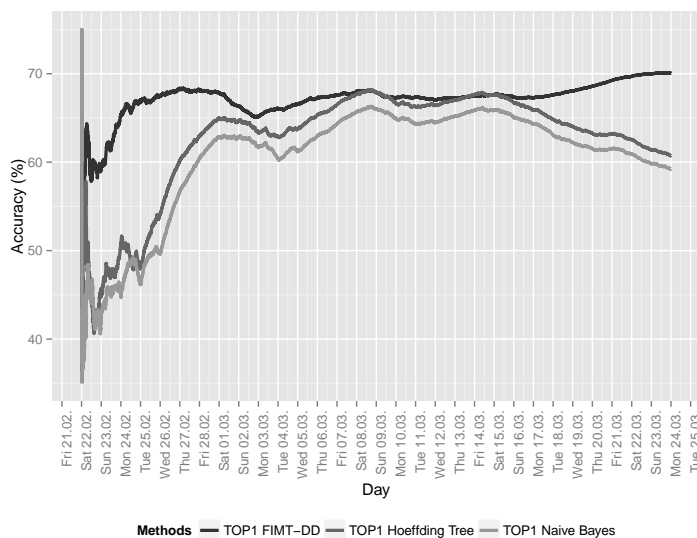


Figure 11. Service Recommendation Accuracy of the FIMT-DD, Hoeffding Tree, and Naïve Bayes Algorithm in the Course of Time. [1]

TABLE XVI. UTILITY GAIN WITH SERVICE RECOMMENDATION USING THE FIMT-DD ALGORITHM IN COMPARISON [1]

After selecting ...	Average experienced utility value	FIMT-DD comparison in percent
the FIMT-DD recommended instance	86.79	100.0 %
the perpetual best instance at each time	91.86	94.5 %
the perpetual worst instance at each time	29.22	297.0 %
the statistically best instance statically	81.96	105.9 %
an instance randomly	64.08	135.4 %

Comparing all methods, there is not much difference between Naïve Bayes and Hoeffding Tree. The FIMT-DD shows very good results. It has the highest update rate of the foreground table, which is an indication that it reacts quicker and more fine-grained on change than the other methods [1]. The cold start problem applies to service recommendation. However, good recommendation results are also supposed to be achieved with a small set of records at the beginning. Comparing the graphs in Figure 11, we can see that for the TOP 1 indicator in the overall recommendation process, the FIMT-DD quickly achieves a high accuracy in the recommendation of the best-fit service. The drift detection of the FIMT-DD seems to work at the end of the period, where some service instances change their performance behavior (see Figure 18) [1].

Figure 12 reveals more insight in the accuracy measure. The figure shows the degree of accuracy of the utility prediction. Once again, the best-fit service is the one with the highest utility value regarding a service consumer's individual preferences, which are expressed in a utility function. When comparing the prediction quality of machine learning methods within our framework, the accuracy of the NFP prediction is relevant. Since the utility value is calculated on that basis, a method is better, the closer the utility value based on the prediction is to the one based on the actual NFPs. Comparing the method's graphs, we see that for Naïve Bayes and Hoeffding Tree the predicted utility values at each time are both quite similar and do not reflect the curves of the actual values. In contrast, the graph of FIMT-DD depicts that the prediction is very close to the actual values. The intercepts of the curves show, that FIMT-DD does cope with change rapidly. In all cases, intercepts – which denote a change in the best-fit ranking – are also reflected in the prediction quite accurately [1].

For the evaluation of service recommendation in general, the actual utility gain is an important measure. Since the selection of service instances are based on several NFPs, the utility value as a basis for the individual preferences is an appropriate measure to benchmark service recommendation. In Table XVI, the average experienced utility value after the service recommendation based on the FIMT-DD algorithm is compared with other scenarios. The table reveals good results. As written above, within this evaluation scenario, the overall best and worst services can be determined at each time. Once again, such comparisons are only possible within such a scenario; this is not possible in reality. Comparing the figures, we see that the FIMT-DD-based recommendation is able to achieve 94.5 % of the maximum achievable utility value. It is 35.4 % better than a random selection approach and even 5.9 % better than the statistically best service instance when statically using it. Note, that choosing the statistically best service instance is also a kind of learning [1].

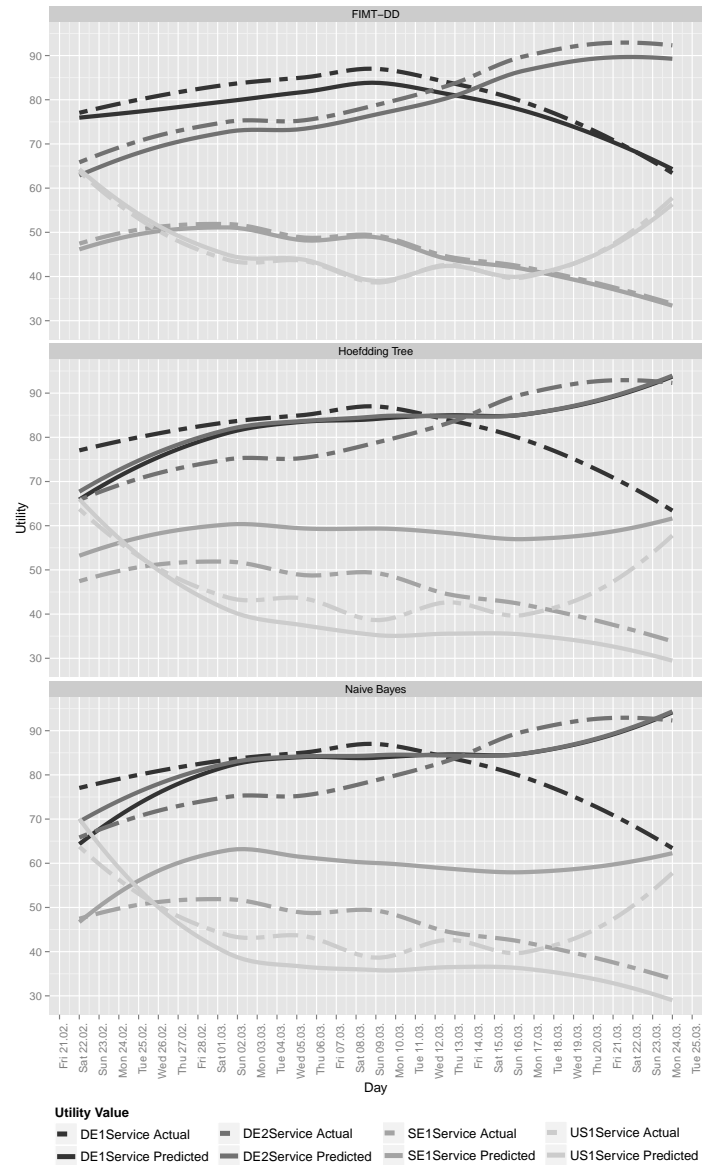


Figure 12. Detailed Overview About the Predicted and Actual Utility Values. [1]

## VII. CONCLUSION

With the introduction of our recommendation framework, we aim at the optimization of consumer experienced performance of Web services at consumer side. Thereby, our framework considers the preferences and call contexts. It uses the shared knowledge of previous service calls of other, similar consumers in order to optimize the benefit of (other) service

consumers. Furthermore, the framework does not require any changes in existing implementations or systems and does not interfere with the encapsulation concept of the distributed world.

Besides the introduction of the framework, we conducted an analysis of relevant NFPs when selecting a service among functionally equivalent candidates. The results of this survey were based on the scientific conference contributions of the last ten years. Therefore, the results reflect the condensed opinion of the scientific community in this research area about what are the relevant NFPs for service selection and, hence, for the recommendation of services. When retrieving this information, we furthermore analyzed whether the NFP candidates had been just mentioned, theoretically discussed, or even validated in a practical scenario.

Within our framework, we comprehensively evaluated the employment of machine learning methods. Initially, we analyzed the two machine learning approaches classification and regression, which aim at different aspects within the overall recommendation process. In our real-world measurement data and simulated data evaluation scenarios, we found out that both approaches can be employed for service recommendation. However, both approaches have benefits and drawbacks.

For the implementation within our framework, we employed machine learning approaches and methods for the prediction of the NFPs of services within a certain call context. The actual determination of the best-fit service is then calculated, based on the predicted NFPs. This approach has several benefits such as a ranked determination of best-fit services and the easy determination of best-fit services for new preferences for existing contexts. The first aspect aims at the fact that service consumers are interested in the increase of their individual utility. Therefore, it is not necessary to recommend always the best-fit service if the second-best-fit is determined to achieve an almost as high utility value. Since consumers' preferences can vary, the second aspect is important in order to reduce the cold-start problem.

Based on the outcome of the NFP analysis, we validated the employment of machine learning methods within our framework. Employing the FIMT-DD algorithm, we could achieve up to 95% of the overall achievable utility gain using our framework. Due to architectural- and method-based incremental learning and knowledge extraction, the strengths of this algorithm regarding drift detection could prove its capability towards perpetual change within the Internet as an anonymous service market. On the basis of our analysis of relevant NFPs within service selection, response or service time is the most important optimization aspect. However, service recommendation is time-consuming. Therefore, we optimized our framework regarding time aspects. With an architectural optimized model for speed, we reduced or even avoid the cost of service recommendation.

Summarizing all outlined aspects, our framework together with machine learning methods can be used for the optimization of service selection focusing on the benefit of service consumers addressing consumer-centric differences such as call contexts and preferences implemented in existing and prospective future real-world scenarios.

As future work, we currently analyze the application of our approach to a multi-tier scenario, comprising process

structures of composite services on each level as well as compensations and transactions. In addition to our utility-value-driven achievement validation, a direct comparison of our recommendation approach with other recommendation techniques, such as CF, is desirable for future work.

## APPENDIX I. PAPER SURVEY FOR THE DETERMINATION OF RELEVANT NFPs

In addition to the brief digest in Section IV, this section provides the design and full results of the paper survey in order to determine a ranked list of relevant NFPs during service selection.

### A. Design of the Survey

Our survey is mainly based on the "Preliminary Guidelines for Empirical Research in Software Engineering" [50][51]. With a few amendments from our side, due to context-specific conditions, the usage of these guidelines is supposed to ensure the quality of the survey and its analytical results. According to these guidelines, the clear and precise description of the objectives, the design including subjects and objects as well as the analytical process is described in this section.

1) *Objectives:* The main objective of this survey is to determine the relevant NFPs for service consumption in general and for service selection/recommendation in particular. We put a strong focus on whether or not approaches to optimized service selection based on NFPs are applicable in practice. We identified two issues helping to answer this main question.

First, what are the NFPs used in the approaches? This is interesting because of two reasons. NFPs could be statically known, like e. g., the security level of a service, or change dynamically based on input, e. g., the response time of a service. If the (majority of the) relevant NFPs is statically known, static service binding approaches are sufficient. Otherwise, dynamic service binding approaches are necessary. The latter are more complex since NFP prediction, service selection, and service binding are then runtime issues.

Second, is the approach discussed theoretically and validated in practice. This is interesting because ad-hoc approaches that are not discussed in theory might be not mature for a general application in practice and neither are theoretical approaches that have not been tested experimentally and practically.

2) *Identification of the Population:* For the conducted survey, we chose conference publications of up to ten years in the SOC context. Table XVII lists the conferences that we used with all their publications for the population of our study according to their length of existence and their size in terms of overall publications in descending order. The total amount of the processed publications was 4,407 conference papers. We believe that conferences contributions are a good basis, since a wide range of scientific approaches of a broad scientific community can be analyzed. Additionally to the scientific community, conference contributions from industry side enrich the results of the analysis with real-world applicability perspectives.

The selection of these conferences was based on our related work knowledge in this field for the past years and does not claim to include all relevant conferences. We consider papers of these conferences to be good candidates for finding answers

TABLE XVII. SELECTED CONFERENCES FOR THE POPULATION OF THE STUDY

Conference	Period
IEEE International Conference on Web Services	ICWS 2003 – 2012
International Conference on Service Oriented Computing	ICSOC 2003 – 2012
IEEE European Conference on Web Services	ECOWS 2003 – 2012
IEEE International Conference on Services Computing	SCC 2004 – 2012
ACM Conference on the Quality of Software Architectures	QoSA 2005 – 2012
IEEE Asia-Pacific Services Computing Conference	APSCC 2006 – 2012
IEEE World Congress on Services	SERVICES 2007 – 2012
European Conference on Service-Oriented and Cloud Computing	ESOCC 2012

to our main question and both sub-questions discussed before. Although we might have missed some relevant papers in this field, we believe that we obtained the condensed opinion of a broad scientific community.

3) *Process by Which the Subjects and Objects are Selected:* Our survey is based on SOC-related conference papers. For each paper, we assessed its general relevance with respect to service selection based on NFPs and the profoundness of which an approach of service selection was discussed and validated.

For the evaluation of the general relevance, each paper was classified in one of the five categories, which are listed in Table II. Category P-A to P-D are *relevant*-marked categories with graduated significance; category P-Z comprises non-relevant-marked papers.

Besides, the relevance of a paper, the profoundness of an approach to service selection is important. Is an NFP just mentioned, is it furthermore discussed in detail, or even validated in a practical or experimental context? We took account of how thoroughly an NFP is discussed and therefore how good the quality of the reference is. The referred NFPs within a paper were each classified according to the categories listed in Table I.

Since a completely manual analysis of all conference papers would have consumed too much time, we employed a more efficient two-stage approach. The first stage was an automated pre-classification of all papers into *relevant* and *non-relevant*. The second stage was a manual classification of the paper and the occurrence categories of all papers marked *relevant*.

a) *Automatic Pre-classification:* For the pre-classification of the papers, we used keyword extraction methods of computational linguistics [52]. The idea was to find a top- $k$  hit list with keywords that are highly represented only in *relevant* conference papers. Such a hit list could then be used for the automatic pre-classification of all conference papers within our survey.

When processing natural languages, there are some aspects that needed to be taken into account such as letter cases, lemmatization, acronyms, but also typographic challenges such as ligatures, and the extractions of stop words and references. Therefore, a certain pre-processing was necessary to bring the content of each conference paper into a normalized form for further processing. In order to achieve a top- $k$  hit list of relevant keywords that are salient in the majority of *relevant* conference papers, not only single keywords but also compound keywords needed to be considered. Compound (key)words can be represented in several consecutive words. The consideration of consecutive words as a compound unit is called  $n$ -grams where  $n$  is the amount of consecutive words.

For the automatic pre-classification, we analyzed  $n$ -grams up to a level of three (uni-, bi-, and trigrams).

We constructed a *gold set* of 202 randomly selected and *manually* pre-classified papers. Papers of categories P-A, P-B, P-C, and P-D were considered *relevant*. Other papers were considered *non-relevant*. Note that P-D papers do not have the main focus on the targeted topic and only discuss it in parts. Therefore, they are of less importance during the extraction of relevant keywords, since the distinguishable relevant keywords are not as highly represented as in papers that have a main focus on the targeted topics. 40 papers were manually marked *relevant* and 162 *non-relevant*. This gold set was then used for learning and validation of the pre-classification approach.

Within the gold set, each conference is almost equally represented with 4.5% on average of its overall publications. At the same time, since the conferences have diverse amounts of publications, their share in the population and in the gold set is accordingly. For the relevant-marked papers of the gold set, keyword extraction provided us with a list of relevant keywords (uni-, bi-, and trigrams). The keyword extraction was based on the Lucene [53] and the Stanford CoreNLP [54] frameworks. The keyword extraction is described in details with pre- and post-processing in Algorithm 1.

---

#### Algorithm 1 Keyword Extraction Algorithm

---

- 1: Remove URLs
  - 2: Remove references
  - 3: Substitute acronyms by their full phrases
  - 4: Substitute upper cases by lower cases
  - 5: Extract 1-grams, 2-grams, and 3-grams and their frequencies using Lucene's ShingleFilter; no  $n$ -grams starting or ending with stop words; Lemma Form of each Token using the Stanford CoreNLP framework.
  - 6: Pick the 27 most frequent 1-grams, 2-grams, and 3-grams.
  - 7: **for all**  $n \in \{1, 2\}$  **do**
  - 8:     **for all**  $m \in \{n + 1, \dots, 3\}$  **do**
  - 9:         **for all**  $kw \in n$ -gram keyword list **do**
  - 10:             **if**  $\exists kw' \in m$ -gram keyword list  $\wedge kw \subset kw'$  **then**
  - 11:                  $frequency(kw) := frequency(kw) - frequency(kw')$
  - 12:             **end if**
  - 13:         **end for**
  - 14:     **end for**
  - 15: **end for**
  - 16: Merge 1-grams, 2-grams, and 3-grams lists
  - 17: Sort merged list descendingly in updated frequencies
- 

We applied the same algorithm to the non-relevant-marked papers. Due to the small amount of relevant-marked papers in the gold set, we had to semantically revise and amend the

initial list in order to distinguish less distinctive keywords from highly relevant and distinctive ones. This left us with a top-11 hit list of relevant keywords. From a semantic aspect, the keywords are not equally important. Therefore, we manually added significance weights for each of the keywords in the list. The final keyword list with significance weights is listed in Table XVIII.

TABLE XVIII. FINAL LIST OF DISTINGUISHABLE KEYWORDS WITH THEIR CORRESPONDENT SIGNIFICANCE WEIGHT

Keyword	Weight
non-functional	0.8
response time	0.7
quality of service	0.68
service level agreements	0.68
composition	0.65
service selection	0.65
service consumer	0.4
service provider	0.4
monitor	0.3
request	0.3
resource	0.3

The automatic pre-classification of textual documents of a natural language raised a challenge (cf. [55]). Whether a document or parts of it are relevant or not depends on the determination of the actual meaning of the text. So, the relevance of a text cannot only be determined by a text's vocabulary but also its semantics in coherence with the grammatical structure. Hence, the demarcation between a *relevant* and a *non-relevant* paper is even for manual classification not an easy task due to the fact that relevance considered among all conference paper is a rather graduate characteristic.

Nonetheless, a manual conduction of all conference papers was infeasible. We tried classical classification approaches for pre-classification, but their achieved precision and recall indicators were not satisfying. The following approaches were tested and rejected: C4.5 for learning decision trees using the concept of information entropy [56], Naïve Bayesian classifier, a simple probabilistic classifier based on Bayesian statistics (Bayes' theorem) with strong independence assumptions, cf. [48], and the Multi-Nomial Bayes extension with a multinomial feature model where feature vectors represent the frequencies of features. The main problem with the classification methods was the challenge that all conference papers in this context are based on the same specific jargon.

Since the design of the second part of the study includes manual processing, we could neglect the semantic and grammatical structure of a paper. The main purpose of the automatic pre-classification was to reduce the amount of non-relevant conference papers, without sorting out relevant papers. Even for manual processing, keywords still remained a good foundation to determine relevant papers. However, we focused on their significance weight as well as their percental occurrence within a paper for which we computed a document score.

The document *score* of each paper  $p$  was computed as follows. For each paper, we computed a *keyword list*( $p$ ) applying the keyword list extraction Algorithm 1. Each keyword frequency was normalized by computing its share of all keywords in percent. The *score* of each paper  $p$  was then computed as the sum over the percentile occurrence (*pfreq*) of all its keywords

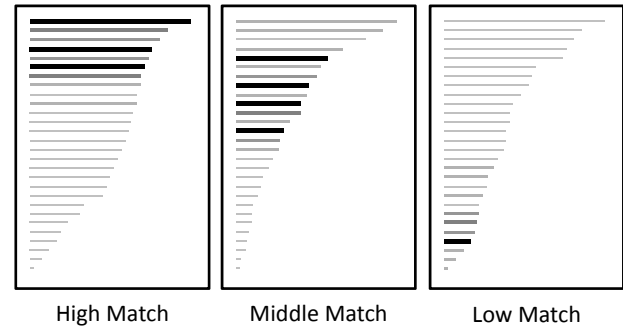


Figure 13. Descendingly Ordered Keyword (Uni-, Bi-, Trigrams) Occurrence Representations of Three Conference Papers With Different Keyword Matches.

multiplied with the manually defined significance (*sig*) of that keyword.

$$\text{score}(p) = \sum_{kw \in \text{keyword list}(p)} \text{pfreq}(p, kw) \times \text{sig}(kw)$$

Note that the significance of keywords that do not occur in the list of relevant keywords is zero.

Figure 13 illustrates the ordered top- $k$  keyword lists of three conference papers. The bulks represent keywords, their length illustrates the percentile occurrence of the respective keyword, and their saturation the keyword's significance. Obviously, the paper on the left has a higher score than the one in the middle and the one on the right. I. e., the paper on the left matches the profile of a relevant paper with higher probability than the paper on the right.

In order to deterministically classify papers as relevant or not, we learned a threshold document score. For this, we used the gold set again. The threshold value was set to the mean of the average document scores of the 40 relevant papers and the 162 non-relevant papers.

*b) Accuracy of the Automatic Pre-classification:* For the evaluation of the quality of the pre-classification algorithm, we used *precision*, *recall*, and the  $F_\beta$  *measure* (cf. [57]) from the pattern recognition and information retrieval field with the following definitions:

$$\text{precision} = \frac{|\{\text{rel.-classified papers}\} \cap \{\text{rel. papers}\}|}{|\{\text{relevant-classified papers}\}|} \quad (4)$$

$$\text{recall} = \frac{|\{\text{rel.-classified papers}\} \cap \{\text{rel. papers}\}|}{|\{\text{relevant papers}\}|} \quad (5)$$

$$F_\beta = (1 + \beta^2) \cdot \frac{\text{precision} \cdot \text{recall}}{\beta^2 \cdot \text{precision} + \text{recall}} \quad (6)$$

*Precision* scores close to 1 indicate that found papers are also relevant. *Recall* close to 1 indicates that all relevant papers are also found. The  $F_\beta$  *measure* is a geometric mean of *precision* and *recall* weighted with  $\beta$ . For our purpose, recall is more important, because the classification algorithm is supposed to sort out the non-relevant conference papers for the manual steps of the survey. It is hence less important

to have non-relevant papers remaining in the set for further processing, than sorting out too many of relevant conference papers. Therefore, recall was weighed much higher in the  $F_2$  measure ( $\beta = 2$ ).

With the above described gold set (4.584 % of population), we used two validation methods: *Leave One Out Cross-Validation* and *Two Fold Cross-Validation*. For each paper in the gold set, the former method learned the threshold on remaining papers and classifies the paper, while the latter repeatedly split the gold set randomly into two halves, learned the threshold on one half, and classified the papers in the other halves. Results are listed in Table XIX. With respect to the rather small amount of highly relevant conference papers in the gold set, we consider the figures of the *Leave One Out Cross-Validation* to be more accurate and still sufficient for further processing with manual classification.

*c) Manual Classification of Relevant Conference Papers:* From the previous automatic pre-classification of the complete population, the *relevant*-marked conference papers were the foundation for the manual processing. The main focus in this step is the semantic analysis of the papers in total and in parts. Especially, the determination of NFPs and the quality of their references (cf. Table I). But also the identification of the main focus of each conference paper (cf. Table II). For the manual analysis, we defined and conducted a strict algorithm in order to avoid bias and improve traceability of the survey.

The procedure described in Algorithm 2 was conducted as follows: For each conference paper pre-classified as *relevant* is scanned for NFPs. If an NFP is found, the quality of the occurrence is determined according to the categories listed in Table I. These categories O-A, O-B, and O-C are descendingly sorted according to their relevance. For each referred NFP, the highest category of all references for this specific NFP within the paper is chosen. Recall that occurrence categories apply individually to each referred NFP in a paper. This ensures that the reference quality of each NFP within a paper can be determined. Additionally to the occurrence category, the absolute amount of occurrences of each NFP is registered. The relative occurrence, which is the basis for later comparison and evaluation, can be calculated from the absolute occurrence. Furthermore, each manually processed conference paper is also classified according to the paper categories listed in Table II. If a paper does not contain any NFP according to the listed occurrence categories, the paper is in category P-Z. Each conference paper that mentions or discusses any NFP is at least in category P-D. However, if the abstract and the introduction of a paper focus on service selection it belongs to category P-A. If the focus is on the adaptation of composite services, it belongs to category P-B. And if the focus is on the consumption of services in general, its category is P-C. All

TABLE XIX. ACCURACY OF THE AUTOMATIC PRE-CLASSIFICATION

	Leave One Out Cross-Validation	Two Fold Cross-Validation
Precision	0.49	0.52
Recall	0.71	0.88
$F_2$ measure <sup>1</sup>	0.65	0.77

<sup>1</sup>  $\beta = 2$

#### Algorithm 2 Manual Classification Algorithm

```

1:  $P$  = set of all conference papers automatically pre-
   classified relevant
2:  $A = \emptyset$  // set of category P-A papers
3:  $B = \emptyset$  // set of category P-B papers
4:  $C = \emptyset$  // set of category P-C papers
5:  $Z = \emptyset$  // set of category P-Z papers
6:  $N = \emptyset$  // set of quadruples  $(p, i, x, c)$  of a paper ( $p$ ), an
   NFP ( $i$ ), its occurrence count ( $x$ ), and the papers highest
   occurrence category ( $c$ )
7: for all  $p \in P$  do
8:   for all found NFP  $i$  in  $p$  do
9:     if  $i$  is validated in practical or experimental context
       then
10:        $d = 'a'$ 
11:     else
12:       if  $i$  is mentioned and theoretically discussed then
13:          $d = 'b'$ 
14:       else
15:          $d = 'c'$ 
16:       end if
17:     end if
18:     if  $(p, i, *, *) \in N$  then
19:        $N = N \setminus (p, i, x, c)$ 
20:        $x = x + 1$ 
21:        $c = \max(c, d)$  // recall that 'a' > 'b' > 'c'
22:     else
23:        $x = 1$ 
24:        $c = d$ 
25:     end if
26:      $N = N \cup (p, i, x, c)$ 
27:   end for
28:   if abstract and introduction of  $p$  focus on service
       selection then
29:      $A = A \cup p$ 
30:   else
31:     if abstract and introduction of  $p$  focus on adaptation
       of composite services then
32:        $B = B \cup p$ 
33:     else
34:       if abstract and introduction of  $p$  focus on service
       consumption in general then
35:          $C = C \cup p$ 
36:       else
37:         if  $p$  mentions NFPs in a service selection, adap-
           tation, or consumption context, but without main
           focus then
38:            $D = D \cup p$ 
39:         else
40:            $Z = Z \cup p$ 
41:         end if
42:       end if
43:     end if
44:   end if
45: end for

```

remaining papers stay in category P-D.

4) *Threats to Validity*: Our survey is based on the scientific research contributions in the field of SOC of up to ten years. Therefore, the outcome does not rely on the work of a few scientists, but on the comprehensive outcome of the whole SOC research community. The results are based on quantifiable and qualifiable measures minimizing any bias. In order to achieve this, we designed a pre-classification that was fully automated and a (semi-)formal and specific manual classification procedure with a narrow interpretation scope.

However, recall is less than one. This reveals that there are probably relevant papers that are not pre-classified as such in the automated stage of our survey. Also, the population of papers is based on selected conferences that we considered to be relevant. It is possible that we missed some important papers this way. Still, since we focused on the determination of relevant NFPs based on the work of a broad scientific community, it is less important if we missed a few relevant papers.

### B. Detailed Results of the Analysis

With the outcome of the automatic pre-classification, the population set for the manual analysis was reduced to 993 conference papers (3,414 conference were pre-classified to be non-relevant); with a presumed precision of 0.49 and a recall of 0.71. Within the manual classification, described in Algorithm 2, 297 conference papers were classified among the *relevant* categories; P-A: 104, P-B: 34, P-C: 46, and P-D: 113. Presenting the results of the analysis of our study, the NFPs during service selection as well as during adaptation and consumption from a consumer's perspective are analyzed according to occurrence and count, which were both introduced in Section IV.

Recall, an NFP with a high *occurrence* can be considered to be widely accepted to be relevant, since it is referred in many papers, while *count* indicates how much text is dedicated to an NFP in absolute terms (*absolute count*) or relatively in the papers (*relative count*). As described in Section IV, these two measures are not sufficient to deduct the quality of the references. In order to satisfy this aspect, we consider the quality of each NFP reference by its occurrence category, cf. Table I. Furthermore, we also differentiate between the papers regarding their semantic quality towards our finding objectives. Therefore, we categorize each paper according to its topic relevance (cf. Table II).

1) *NFPs Referred in Conference Papers*: First, we determined a ranked list of relevant NFPs in descending order due to the amount of papers in which they occur among all relevant categorized conference papers. Figure 14 lists the relevant NFPs according to their paper occurrence without any consideration of the quality of the references (occurrence categories) or focus of the paper (paper categories; except non-relevant papers, which are in P-Z). During the manual, semantical analysis, we discovered that in virtually all papers, time-relevant NFPs were used as synonyms for response time. Therefore, in Figure 14, *response time* encompasses several expressions that are used in a synonymous meaning. Without aggregation, the synonym NFPs would occur with the following amount within all relevant conference papers: *response time*: 75.1%; *performance*: 22.2%; *execution time*: 16.5%; *latency*: 12.1%; *duration*: 3.4%; *timeliness*: 1.4%; *delay*: 1.0%. Note, since

these NFP expressions are also used synonymously within a single paper, these percentages cannot simply be added up. Figure 14 represents the correct percentage of the amount of papers that mention or discuss response time synonyms.

With the knowledge of a ranked NFP list according to the amount of papers in which an NFP is referred, we now have a closer look at the textual distribution within all references. This indicates how much text is dedicated to what NFP in comparison to all other NFP references. As outlined above, we distinguish between absolute and relative count. We argue that an absolute count is more relevant if one is interested in the absolute amount of research documentation about an NFP, while the relative count is more relevant if all papers should have the same impact on the results. Although the list in Figure 4, which lists the relevant NFPs ranked regarding their occurrence counts, is similar to the paper occurrence list in Figure 14 in its ranking, there is a big gap between the counts of response time and the other NFPs. Response time is therefore dedicated more text than the other NFPs. At least, it is more often mentioned. The full list descendingly ordered according to the relative count is depicted in Figure 4. For most NFPs, there is not much difference in the ranking between absolute and relative count. However, for *reputation* and *trust*, there is a big gap between relative count and absolute count. The reason for this is related to the fact that trust and reputation is extensively discussed in some conference papers. With the main focus on these two related NFPs, some researchers argue from their point of view that these two NFPs had been fiercely neglected compared to other NFPs that are also mentioned frequently in these papers. When comparing absolute and relative count, we notice that for some researchers, trust and reputation is a very important aspect. However, for the majority, these NFPs are not as relevant as others.

2) *Profoundness of the NFP References*: With an overview about the NFPs being widely discussed and regarding their dedicated text, we now focus on the quality of the references. As described above, we consider the paper and occurrence categories in which an NFP is mentioned or discussed.

In Figures 4 and 14, many NFPs are still closely related to each other. In order to get a better overview, for the remaining figures, we grouped all NFPs into several categories, which all represent a certain aspect. Table III lists each NFP aspect category with its containing NFPs.

In Figure 15, the occurrences of each NFP category are related to each paper category (cf. Table II). We can see that a high share of the papers (35.5% on average among the top-5 categories; 2.6 deviation) does not have its main focus on composition, adaptation, or selection of services and an (almost) equally high share of papers (37.3% on top-5 average; 2.5 deviation) focuses on service selection. Note, the listed figures in the bars are percentage points.

Within the results of the counts related to each paper category, there is a big gap between relative count and absolute count among conference papers that have the main focus on service selection for *trust/reputation*. It affirms again that some researchers put a strong focus on *trust* and *reputation* as important NFPs for service selection.

In Figure 5, the occurrences of each NFP category are related to each occurrence category (cf. Table I). When a

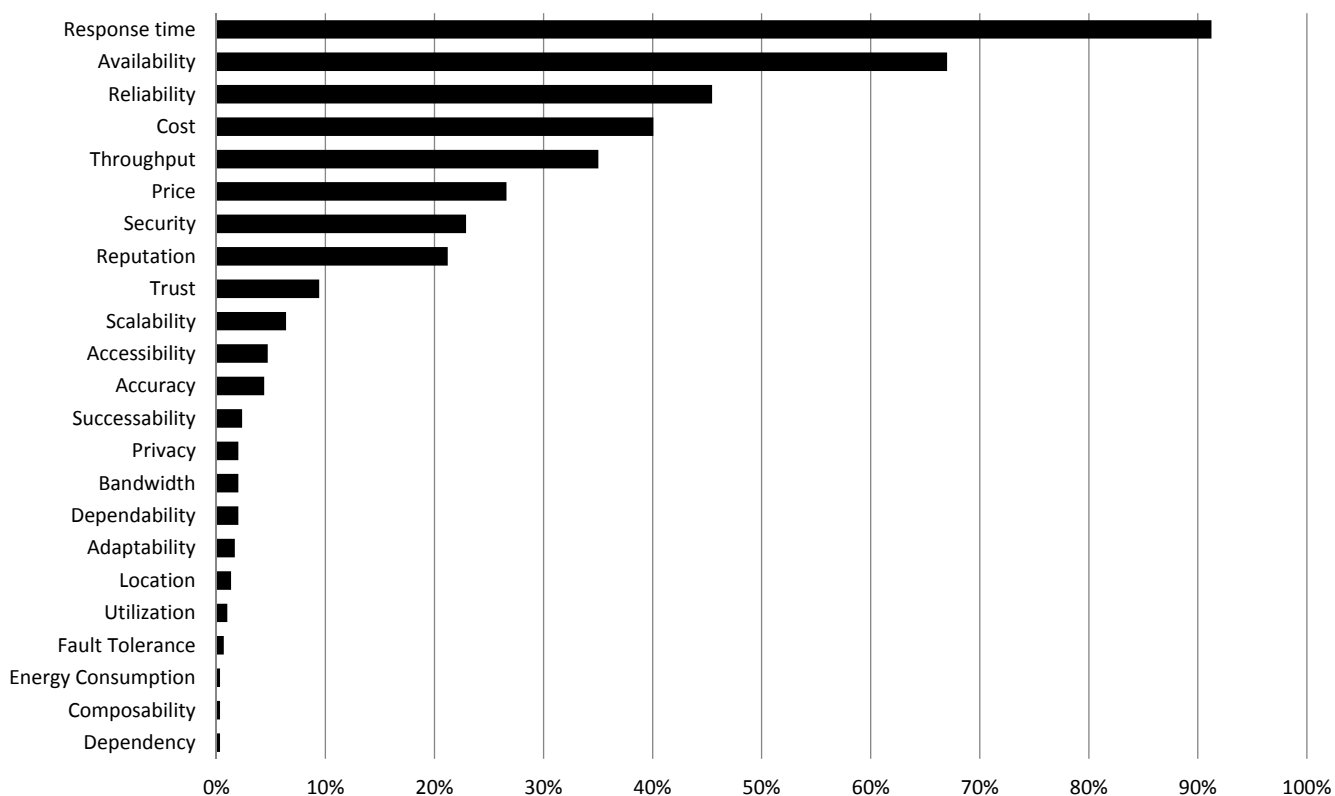


Figure 14. Paper Occurrence of Each NFP Within all Relevant Categories.

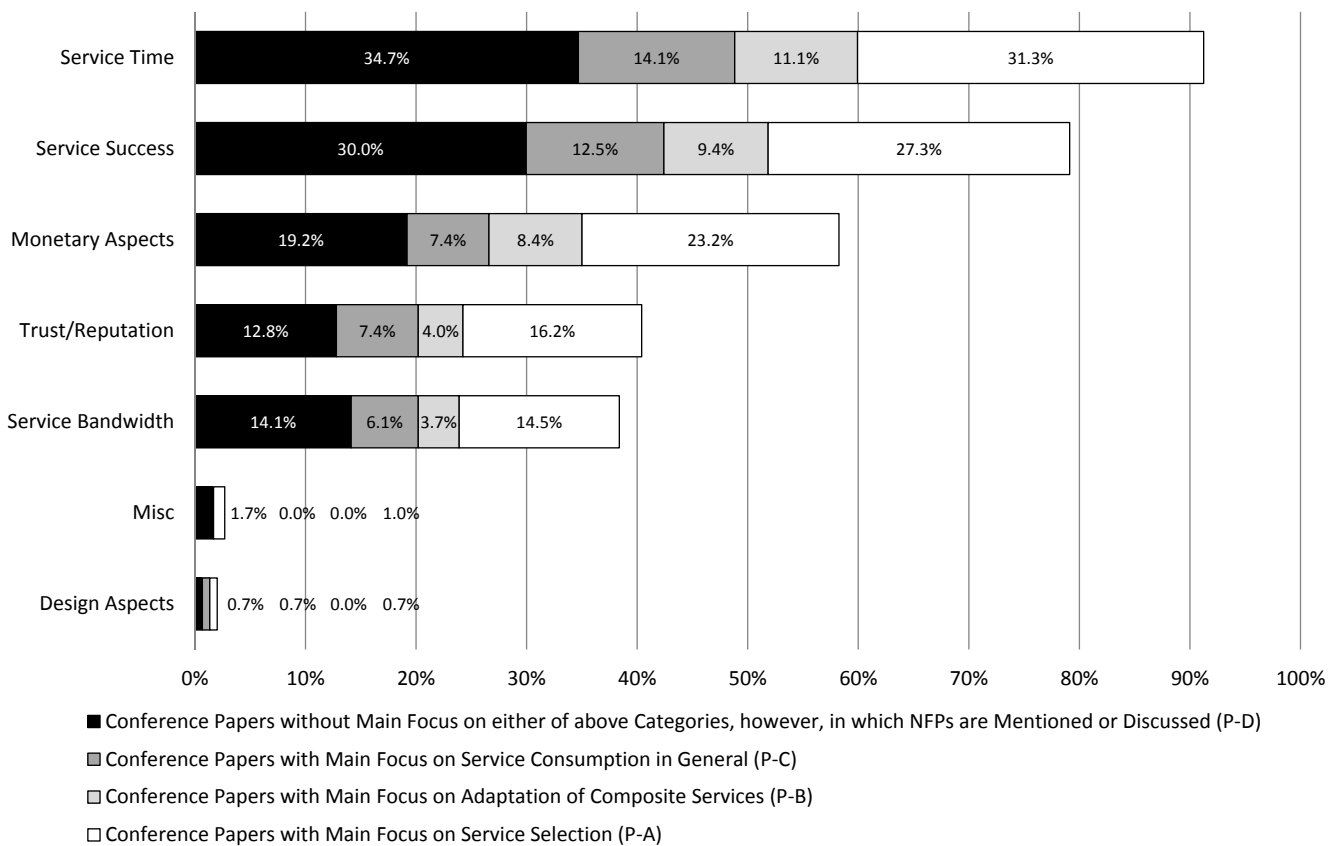


Figure 15. Paper Occurrence of Each NFP Category According to the Paper Categories.

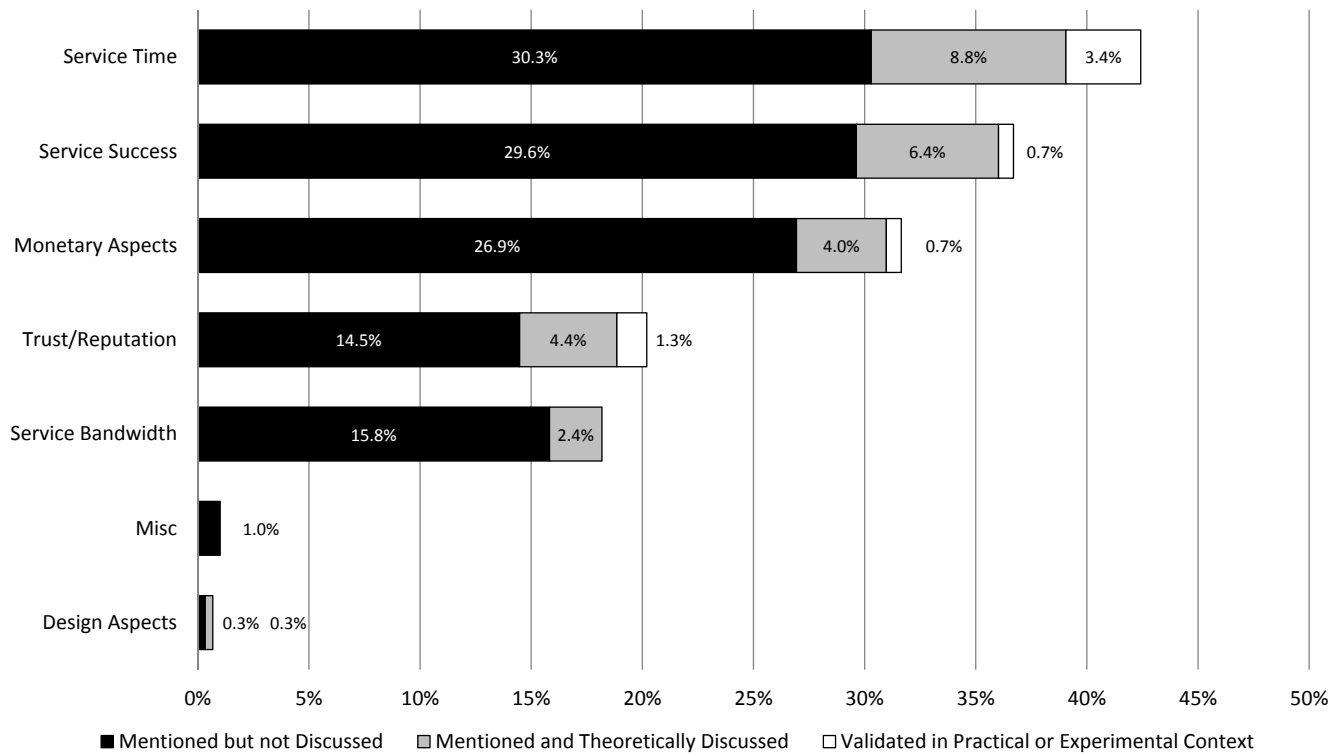


Figure 16. Paper Occurrence of Each NFP Category Within Highly Relevant Categories (P-A and P-B) According to Their Occurrence Category.

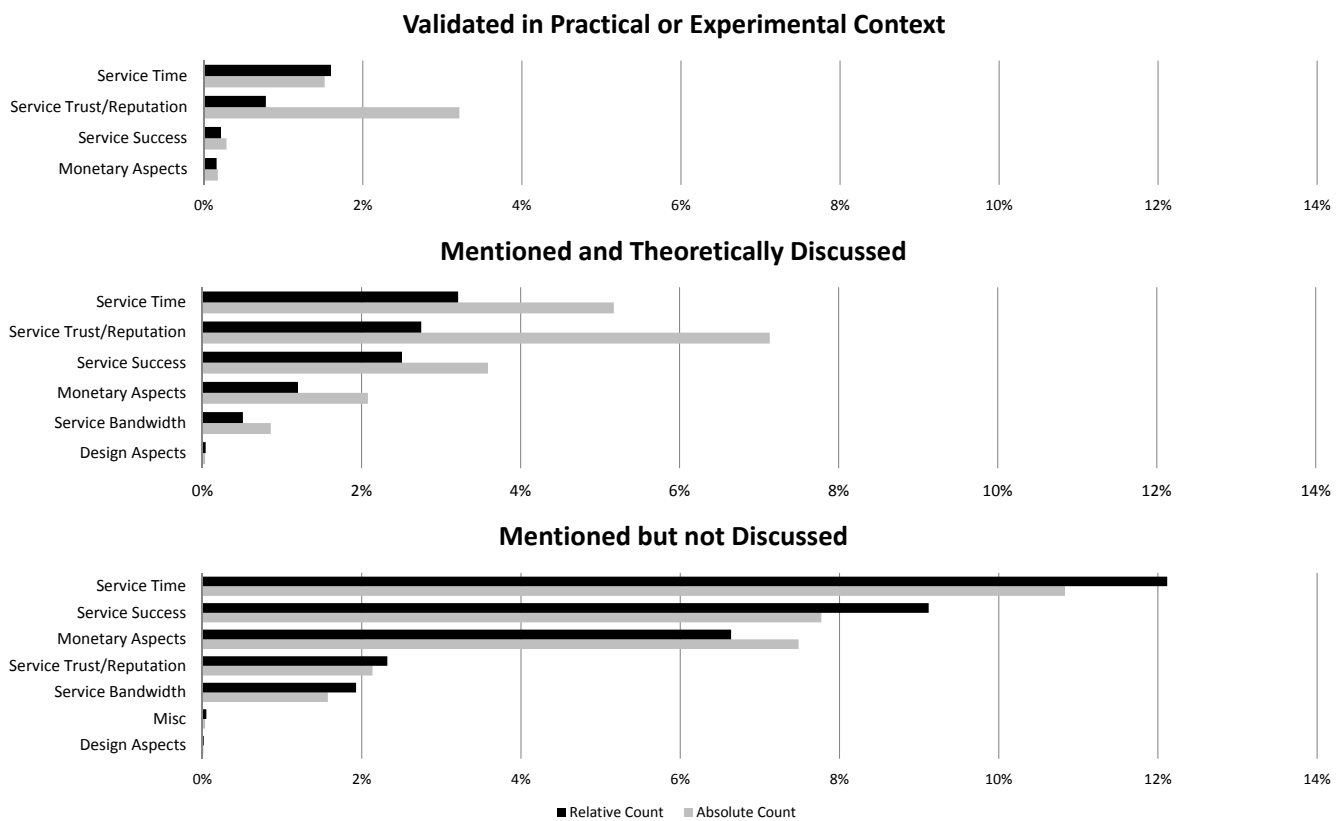


Figure 17. Overall Relative and Absolute Counts of NFPs Among Highly Relevant Categories (P-A and P-B) According to Each Occurrence Category.

paper has two or more NFPs that belong to the same NFP category with different occurrence categories, the paper is counted in the highest occurrence category. On average over all NFP categories (disregarding the *Misc* and *Design* categories), 83% of all relevant papers only mention NFPs, but do not discuss them in detail. On average, 13% discuss them in more detail while only 4% also validate them in simulations or experiments. This means that a vast majority of relevant conference papers do not elaborate in detail on the NFPs they mention.

Finally, we set the focus on highly relevant conference papers (P-A and P-B). These conference papers have a main focus on service selection/reputation or service adaptation, which is very closely related to service selection. Figure 16 shows again the overall paper occurrence per occurrence category. The overall average shares among all NFP categories (without *Misc* and *Design aspects*) are 79% for occurrence category O-C, 17% for O-B and 4% for O-A. There is only a minor difference to the mean figures of Figure 5. Still, the majority of conference papers only mention NFPs without further discussion or validation. Considering the overall counts within the highly relevant papers listed in Figure 17, the vast amount of references do not discuss an NFP in detail. Again, apart from service time, there is a big lack of validation.

#### APPENDIX II. PERFORMANCE PROFILES OF SIMULATED SERVICES FOR THE VALIDATION OF MACHINE LEARNING METHODS IN THE FRAMEWORK

For the validation of machine learning methods within our framework, we simulated the performance behavior of four services. In order to challenge the methods, their profile change over time and are, in contrast to measurement data, not easy to distinguish:

To get a situation where the validation process retrieves exactly the best-fit service instance for validation at each moment considering call context and utility function, we developed a simulator that creates service instance measurements for a certain time period based on predefined behavior profiles. The implementation of this framework follows a periodic behavior influenced by statistical random-based deviation. The periodic behavior of the simulated Web services follows our initial measurements in [2] and considers: day/night time, weeks, months, work days and weekends. The random-based deviation is supposed to simulate unexpected incidences such as network traffic jams, high/low usage of a service's limited infrastructure. The random-based influence over a period was also evidenced in our real-world service tests [2]. For a multi-NFP service selection, two NFPs were simulated, which are response time and availability [1].

Figures 18 and 19 depict an overview about the simulated NFPs. The simulated validation dataset comprises a period of 30 days and has a total set of 460,800 records (40 records/hour × 24 hours/day × 30 day × 16 unique clients). The records contain information about day, time, response time in millisecond and availability (Boolean). Within the simulation, between each record there is a time interval of 90 seconds. Figure 18 shows in a condensed form the response time of all services instances within the whole period. Note that the line is only the trend. Within the recommendation process, the actual best-fit service instance at each time is important and not the averaged value of each service instance. The line is therefore

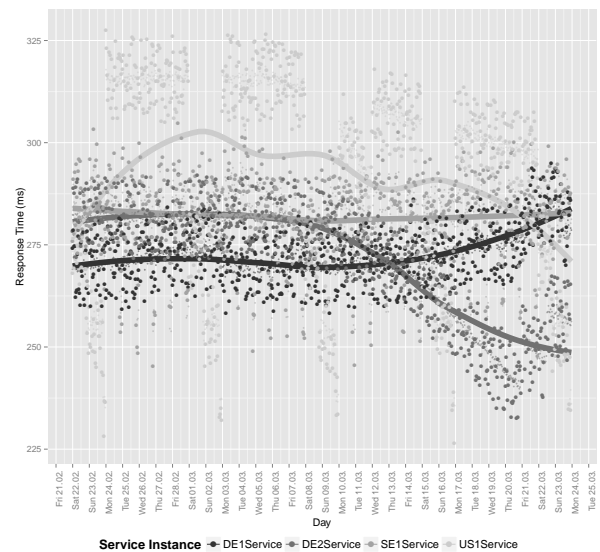


Figure 18. Overview About the Simulated Response Time of Four Service Instances and Their Trend Over the Whole Period. [1]

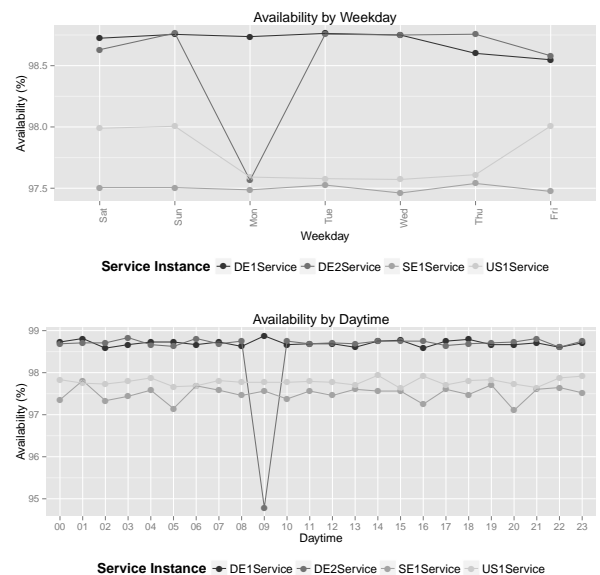


Figure 19. Overall Periodic Behavior Regarding the Availability of the Simulated Service Instances With Weekday and Daytime Aspects. [1]

only a visual orientation for us to determine the concept drift of each service instance within the period (e. g., DE2Service). Figure 19 shows the statistical value of availability with a focus on weekday and daytime periods [1].

#### REFERENCES

- [1] J. Kirchner, P. Karg, A. Heberle, and W. Löwe, "Appropriate machine learning methods for service recommendation based on measured consumer experiences within a service market," in *The Seventh International Conferences on Advanced Service Computing (SERVICE COMPUTATION)*, 2015, pp. 41–48.
- [2] J. Andersson, A. Heberle, J. Kirchner, and W. Löwe, "Service Level Achievements – Distributed knowledge for optimal service selection," in *Ninth IEEE European Conference on Web Services (ECOWS)*, 2011, pp. 125–132.

- [3] J. Kirchner, A. Heberle, and W. Löwe, "Classification vs. Regression – Machine learning approaches for service recommendation based on measured consumer experiences," in IEEE 11th World Congress on Services (SERVICES), 2015, pp. 278–285.
- [4] J. Andersson, M. Ericsson, C. Kessler, and W. Löwe, "Profile-guided composition," in 7th International Symposium on Software Composition (SC), 2008, pp. 157–164.
- [5] C. Kessler and W. Löwe, "Optimized composition of performance-aware parallel components," *Concurrency and Computation: Practice and Experience*, vol. 24, no. 5, 2012, pp. 481–498. [Online]. Available: <http://dx.doi.org/10.1002/cpe.1844>
- [6] W. van den Heuvel and M. Smits, "Transformation of the software components and Web services market," in eMergence, Proceedings of the 20th Bled eConference, 2007, pp. 246–258.
- [7] C. Legner, "Is there a market for Web services? – An analysis of Web services directories," in Proceedings of the 1st International Workshop on Web APIs and Services Mashups, 2007, pp. 29–42.
- [8] L. Nilsson-Witell and A. Fundin, "Dynamics of service attributes: a test of Kano's theory of attractive quality," *International Journal of Service Industry Management*, vol. 16, no. 2, 2005, pp. 152–168.
- [9] B. L. Duc et al., "Non-functional data collection for adaptive business processes and decision making," in MWSOC '09: Proceedings of the 4th International Workshop on Middleware for Service Oriented Computing. New York, NY, USA: ACM, 2009, pp. 7–12.
- [10] L. Zeng et al., "Monitoring the QoS for Web Services," in Service-Oriented Computing – ICSOC 2007, 2008, pp. 132–144.
- [11] L. Zeng et al., "QoS-aware middleware for Web services composition," *IEEE Trans. Softw. Eng.*, vol. 30, no. 5, 2004, pp. 311–327.
- [12] L. Zeng, B. Benatallah, M. Dumas, J. Kalagnanam, and Q. Z. Sheng, "Quality driven Web services composition," in Proceedings of the 12th International Conference on World Wide Web. ACM, 2003, pp. 411–421.
- [13] L. Li, J. Wei, and T. Huang, "High performance approach for multi-QoS constrained Web service selection," in Service-Oriented Computing – ICSOC 2007, 2008, pp. 283–294.
- [14] S. Reiff-Marganiec, H. Yu, and M. Tilly, "Service selection based on non-functional properties," in Service-Oriented Computing - ICSOC 2007 Workshops, 2009, pp. 128–138.
- [15] D. Mukherjee, P. Jalote, and M. G. Nanda, "Determining QoS of WS-BPEL compositions," in Service-Oriented Computing – ICSOC 2008, 2008, pp. 378–393.
- [16] P. Leitner, B. Wetzstein, F. Rosenberg, A. Michlmayr, S. Dustdar, and F. Leymann, "Runtime prediction of service level agreement violations for composite services," in Service-Oriented Computing. ICSOC/ServiceWave 2009 Workshops, 2010, pp. 176–186.
- [17] D. Robinson and G. Kotonya, "A runtime quality architecture for service-oriented systems," in Service-Oriented Computing – ICSOC 2008, 2008, pp. 468–482.
- [18] R. Yang, Q. Chen, L. Qi, and W. Dou, "A QoS evaluation method for personalized service requests," in Web Information Systems and Mining, ser. Lecture Notes in Computer Science. Springer Berlin Heidelberg, 2011, vol. 6988, pp. 393–402.
- [19] H. A. Müller, L. O'Brien, M. Klein, and B. Wood, "Autonomic computing," Software Engineering Institute, Carnegie Mellon University, Tech. Rep., 2006, <ftp://ftp.sei.cmu.edu/public/documents/06.reports/pdf/06tn006.pdf>; Retrieved: 25 January 2010.
- [20] M. C. Huebscher and J. A. McCann, "A survey of autonomic computing – degrees, models, and applications," *ACM Comput. Surv.*, vol. 40, no. 3, 2008, pp. 1–28.
- [21] E. Di Nitto, C. Ghezzi, A. Metzger, M. Papazoglou, and K. Pohl, "A journey to highly dynamic, self-adaptive service-based applications," *Automated Software Engineering*, vol. 15, no. 3-4, 2008, pp. 313–341.
- [22] H. van der Schuur, S. Jansen, and S. Brinkkemper, "Becoming responsive to service usage and performance changes by applying service feedback metrics to software maintenance," in Automated Software Engineering – Workshops, 2008. ASE Workshops 2008. 23rd IEEE/ACM International Conference on, 2008, pp. 53–62.
- [23] Z. Zheng, H. Ma, M. Lyu, and I. King, "QoS-aware Web service recommendation by collaborative filtering," *Services Computing, IEEE Transactions on*, vol. 4, no. 2, 2011, pp. 140–152.
- [24] M. Tang, Y. Jiang, J. Liu, and X. Liu, "Location-aware collaborative filtering for QoS-based service recommendation," in Web Services (ICWS), IEEE 19th International Conference on, 2012, pp. 202–209.
- [25] L. Kuang, Y. Xia, and Y. Mao, "Personalized services recommendation based on context-aware QoS prediction," in Web Services (ICWS), IEEE 19th International Conference on, 2012, pp. 400–406.
- [26] G. Kang, J. Liu, M. Tang, X. Liu, B. Cao, and Y. Xu, "AWSR: Active Web service recommendation based on usage history," in Web Services (ICWS), IEEE 19th International Conference on, 2012, pp. 186–193.
- [27] Q. Yu, "Decision tree learning from incomplete QoS to bootstrap service recommendation," in Web Services (ICWS), IEEE 19th International Conference on, 2012, pp. 194–201.
- [28] T. Ahmed and A. Srivastava, "A data-centric and machine based approach towards fixing the cold start problem in web service recommendation," in Electrical, Electronics and Computer Science (SCEECS), IEEE Students' Conference on, 2014, pp. 1–6.
- [29] Z. Zheng, H. Ma, M. R. Lyu, and I. King, "QoS-aware web service recommendation by collaborative filtering," *IEEE Transactions on Services Computing*, vol. 4, no. 2, 2011, pp. 140–152.
- [30] J. Cao, Z. Wu, Y. Wang, and Y. Zhuang, "Hybrid collaborative filtering algorithm for bidirectional web service recommendation," *Knowledge and Information Systems*, vol. 36, no. 3, 2013, pp. 607–627.
- [31] R. Nayak and C. Tong, "Applications of data mining in web services," in Web Information Systems – WISE. Springer Berlin Heidelberg, 2004, vol. 3306, pp. 199–205.
- [32] J. Yao, W. Tan, S. Nepal, S. Chen, J. Zhang, D. De Roure, and C. Goble, "Reputationnet: A reputation engine to enhance servicemap by recommending trusted services," in Services Computing (SCC), IEEE Ninth International Conference on, 2012, pp. 454–461.
- [33] J. Zhang, P. Votava, T. Lee, S. Adhikarla, I. Kulkumjon, M. Schlau, D. Natesan, and R. Nemani, "A technique of analyzing trust relationships to facilitate scientific service discovery and recommendation," in Services Computing (SCC), IEEE International Conference on, 2013, pp. 57–64.
- [34] K. Huang, J. Yao, Y. Fan, W. Tan, S. Nepal, Y. Ni, and S. Chen, "Mirror, mirror, on the web, which is the most reputable service of them all?" in Service-Oriented Computing, 2013, vol. 8274, pp. 343–357.
- [35] L. Li, Y. Wang, and E.-P. Lim, "Trust-oriented composite service selection and discovery," in Service-Oriented Computing, 2009, vol. 5900, pp. 50–67.
- [36] Q. He, J. Yan, H. Jin, and Y. Yang, "Servicetrust: Supporting reputation-oriented service selection," in Service-Oriented Computing, 2009, vol. 5900, pp. 269–284.
- [37] W. Chen, I. Paik, T. Tanaka, and B. Kumara, "Awareness of social influence for service recommendation," in Services Computing (SCC), IEEE International Conference on, 2013, pp. 767–768.
- [38] J. Kirchner, A. Heberle, and W. Löwe, "Evaluation of the employment of machine learning approaches and strategies for service recommendation," in Fourth European Conference on Service-Oriented and Cloud Computing (ESOCC), 2015, pp. 95–109.
- [39] S. B. Kotsiantis, "Supervised machine learning: A review of classification techniques," *Informatica*, no. 31, 2007, pp. 249–268.
- [40] J. Han and M. Kamber, *Data Mining: Concepts and Techniques*, 2nd ed. Elsevier, Morgan Kaufmann, 2006.
- [41] Machine Learning Group at the University of Waikato, "Weka – Data mining with open source machine learning software in Java," <http://www.cs.waikato.ac.nz/ml/weka/>.
- [42] University of Waikato, "MOA Massive Online Analysis," <http://moa.cms.waikato.ac.nz/>.
- [43] E. Ikonovska, J. Gama, and S. Džeroski, "Learning model trees from evolving data streams," *Data Mining and Knowledge Discovery*, vol. 23, no. 1, 2011, pp. 128–168.
- [44] Weka, "Weka Javadoc – DecisionStump," date of retrieval: 25 Oct 2014; <http://weka.sourceforge.net/doc.dev/weka/classifiers/trees/DecisionStump.html>.
- [45] M. Simons, "Java implementation of excels statistical functions norminv," <http://info.michael-simons.eu/2013/02/21/java-implementation-of-excels-statistical-functions-norminv/>; Last Retrieval: 20 June 2015.

- [46] MathWorld Team, Wolfram Research Inc., "Fourier series – triangle wave," <http://mathworld.wolfram.com/FourierSeriesTriangleWave.html>; Last Retrieval: 20 June 2015.
- [47] G. Hulten, L. Spencer, and P. Domingos, "Mining time-changing data streams," in Proceedings of the Seventh ACM SIGKDD International Conference on Knowledge Discovery and Data Mining. ACM, 2001, pp. 97–106.
- [48] E. J. Keogh and M. J. Pazzani, "Learning augmented bayesian classifiers: A comparison of distribution-based and classification-based approaches," 1999.
- [49] Weka, "Weka Javadoc – Hoeffding Tree," date of retrieval: 25 Oct 2014; <http://weka.sourceforge.net/doc.dev/weka/classifiers/trees/HoeffdingTree.html>.
- [50] B. A. Kitchenham, S. L. Pfleeger, L. M. Pickard, P. W. Jones, D. C. Hoaglin, K. El-Emam, and J. Rosenberg, "Preliminary guidelines for empirical research in software engineering," National Research Council Canada Publications Archive, 2001. [Online]. Available: <http://nparc.cisti-icist.nrc-cnrc.gc.ca/npsi/ctrl?action=rtdoc&an=8914084>
- [51] B. Kitchenham, S. L. Pfleeger, L. M. Pickard, P. W. Jones, D. C. Hoaglin, K. El-Emam, and J. Rosenberg, "Preliminary guidelines for empirical research in software engineering," Software Engineering, IEEE Transactions on, vol. 28, no. 8, Aug 2002, pp. 721–734.
- [52] R. Litschko, "Automated analysis of scientific papers using machine learning and computational linguistics," Bachelor's Thesis, Karlsruhe University of Applied Sciences, Germany, October 2013.
- [53] "Apache Lucene," <http://lucene.apache.org>.
- [54] The Stanford Natural Language Processing Group, "Stanford CoreNLP," <http://nlp.stanford.edu/software/corenlp.shtml>.
- [55] M. Bates and R. M. Weischedel, Eds., Challenges in Natural Language Processing. Cambridge University Press, 2006.
- [56] J. R. Quinlan, C4.5: Programs for Machine Learning. Morgan Kaufmann Publishers, 1993.
- [57] C. J. van Rijsbergen, Information Retrieval. Butterworth-Heinemann, 1979.

# Simulation of Emergence of Local Common Languages

## Using Iterated Learning Model on Social Networks

Makoto Nakamura

Japan Legal Information Institute,  
Graduate School of Law,  
Nagoya University  
Email: mnakamur@nagoya-u.jp

Ryuichi Matoba

Department of Electronics  
and Computer Engineering,  
National Institute of Technology,  
Toyama College,  
Email: rmatoba@nc-toyama.ac.jp

Satoshi Tojo

School of Information Science,  
JAIST,  
Email: tojo@jaist.ac.jp

**Abstract**—Thus far, there have been a variety of methodologies proposed on simulating the evolution of languages, each of which belongs to a different level of abstraction. Our goal is to provide a framework that represents the diachronic change in language by the contact among language communities. We propose an agent-based model with Kirby's iterated learning model and complex networks, putting learning agents on each node in the social network. Our proposed model is examined in three aspects: (i) the effectiveness of string-clipping, (ii) the relation between generations for learning and the number of local common languages, and (iii) the relation between network types and local common languages. A series of experiments shows that we have succeeded in modeling the actual situation of language change.

**Keywords**—Language Evolution; Language Acquisition; Iterated Learning Model; Social Network.

### I. INTRODUCTION

Thus far, simulation studies have played an important role in the field of language evolution [1] [2]. In particular, a very important function of simulation is to prove whether a prediction actually and consistently derives from a theory [3]. Thus far, there has been a variety of methodologies proposed on simulating the evolution of languages, each of which belongs to a different level of abstraction. Simulation studies for population dynamics alone include an agent-based model of language acquisition by Briscoe [4], which was developed toward a formal model of a language acquisition device. On the other hand, Nowak [5] proposed a mathematical theory of the language dynamics equation that focuses on its evolutionary aspect. The language dynamics equation is highly abstract, while an agent-based model is considered to be concrete, or less abstract.

Our goal is to provide a framework that represents the diachronic change in language by the contact among language communities. Examples are shown in the emergence of creoles in conventional linguistics and in the rapid change in Internet linguistics [6]. In fact, researchers on creoles have long known that contact speeds up language change [7] [8], in which the emergence of *pidgins* and *creoles* is one of the most interesting phenomena. Pidgins are simplified tentative languages spoken in multilingual communities. They come into being where people need to communicate but do not have a language in common. Creoles are full-fledged new languages that children

of the pidgin speakers acquire as their native languages [9]. A common view is that a pidgin or creole is a language that takes its vocabulary from one language and its grammar from another. One language, usually European landowners' in colonial situations, was the original target of language learners [10], which is reflected by a social relation between a European elite and an indigenous underclass.

The framework of language contact would be useful not only for simulating typical language changes but also for novel phenomena taking place in the cyber world. In recent decades, the evolution of the Internet technology has made it possible for users to transcend physical distance to participate in discussions with anonymous people concerning their favorite topics. They do not only exchange small bits of information, but rather seem to establish a durable channel for communication among people sharing common tastes on a bulletin board system, Twitter and so on. They often employ colloquial, rather than formal, language, and their utterances are characterized by abbreviated words and reduced grammatical complexity [11]. This phenomenon is often seen in language contact, but the time and size of the language change on the Internet are extremely fast and large [6]. Using this framework, it would be possible to deal with this rapid language change as a phenomenon of language evolution.

Simulation of the change in languages has been studied in consideration of social networks. Thus far, Nakamura et al. [12] have proposed a mathematical framework for the emergence of creoles based on the language dynamics equation. Toward a more concrete analysis, they introduced a spatial structure to the mathematical framework [13] [14], in which learning agents come into contact with neighbors according to the learning algorithm. Furthermore, the spatial structure was expanded into complex networks [15]. Their studies are based on a hypothesis about the emergence of creoles; that is, language contact is likely to stimulate creolization. However, their learning mechanisms are too simple to observe language changes from a linguistic aspect because languages are defined as similarity measures in a numeric matrix.

In this paper, we set forth two hypotheses: one is that language contact leads to the emergence of local common languages (LCLs); the other is that language divergence depends on the type of network. We test the hypotheses

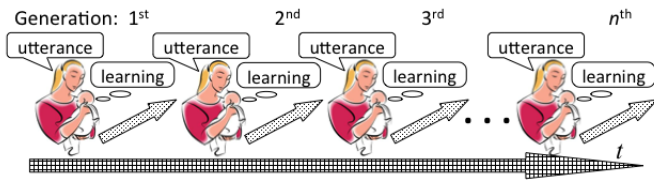


Figure 1. Iterated learning model

**Verb:** admire, detest, hate, like, love  
**Noun:** john, mary, pete, heather, gavin

e.g.) *love(mary, john)*  
 (Identical arguments are prohibited.)

Figure 2. Words used in experiment

with a simulation model parameterizing language contact with network types. We propose an agent-based model to deal with grammatical changes in the language community. Therefore, our purpose in this paper is to show a relationship between communication among learning agents and grammatical changes. We employ Kirby’s iterated learning model (ILM) [16], which shows a process of grammatical evolution through generations. This approach has often been used in simulation models concerning language evolution [17]. One important reason for this comes from its robustness against input sentences in terms of syntactic learning. As long as it is learning from a single parent, an infant agent receives sentences derived from a consistent grammar; it is possible to acquire a concise grammar. Currently, the learning situation in ILM is extended to multiple families connecting with a network. We can observe the language change, not only in a diachronic situation, i.e., in a parent-child relation, but also in a synchronic one.

Thus far, we have demonstrated a pilot version [18], where we found a problem reported by Smith and Hurford [19]; that is, in the case where learning agents potentially have more than one teacher agent, the length of syntax rules tends to increase rapidly over generations due to the addition of meaningless terminal symbols. This problem causes unnatural learning, which results in a fatal combinatorial explosion. To solve this problem, we developed a module for acceleration in ILM by string-clipping, which differs from the one for efficient learning with cognitive bias [20] [21] in that we focus on the multi-input environment.

This paper is organized as follows. In Section II, we introduce Kirby’s ILM. In Section III, we propose an agent-based model for language contact. We examine our proposed method in Section IV, and conclude in Section V.

## II. MODIFIED ITERATED LEARNING MODEL

In this section, we mention how to deal with ILM on social networks. First, we briefly explain Kirby’s ILM. Next, we introduce the modification for social networks by Matoba et al. [24] in order to avoid the combinatorial explosion, which enables the expansion of ILM.

### A. Kirby’s Iterated Learning Model

Kirby [16] introduced the notions of compositionality and recursion as fundamental features of grammar, and showed that they make it possible for a human to acquire compositional language. Figure 1 illustrates ILM. In each generation, an infant can acquire grammar in his/her mind given sample sentences from his/her mother. After growing up, the infant becomes the next parent to speak to a newborn baby with his/her grammar. As a result, infants can develop more compositional grammar through the generations. Note that the model

focuses on the grammar change in multiple generations, not on that in one generation. Also, Kirby adopted the idea of two different domains of language [25] [26] [27] [28], namely, I-language and E-language; I-language is the internal language corresponding to a speaker’s intention or meaning, while E-language is the external language, that is, utterances. In his model, a parent is a speaker agent and his/her infant is a listener agent. The speaker agent gives the listener agent a pair of a string of symbols as an utterance (E-language), and a predicate-argument structure (PAS) as its meaning (I-language). A number of utterances would form compositional grammar rules in a listener’s mind, through the learning process. This process is iterated generation by generation, and converges to a compact, limited number of grammar rules.

According to Kirby’s ILM, the parent agent gives the infant agent a pair of a string of symbols as an utterance, and PAS as its meaning. The agent’s linguistic knowledge is a set of a pair of a meaning and a string of symbols, as follows.

$$S/\text{love}(\text{john}, \text{mary}) \rightarrow \text{hjsbs}, \tag{1}$$

where the meaning, i.e., the speaker’s intention, is represented by a PAS *love(john, mary)* and the string of symbols is the utterance “hjsbs”; the symbol ‘S’ stands for the category Sentence. The following rules can also generate the same utterance.

$$\begin{aligned} S/\text{love}(x, \text{mary}) &\rightarrow \text{h } N/x \text{ sbs} \\ N/\text{john} &\rightarrow \text{j}, \end{aligned} \tag{2}$$

where the variable x can be substituted for an arbitrary element of category N.

The infant agent has the ability to generalize his/her knowledge with learning. This generalizing process consists of the following three operations [16]: *chunk*, *merge*, and *replace*.

**Chunk** This operation takes pairs of rules and looks for the most-specific generalization.

$$\begin{aligned} &\begin{cases} S/\text{love}(\text{john}, \text{pete}) \rightarrow \text{ivnre} \\ S/\text{love}(\text{mary}, \text{pete}) \rightarrow \text{ivnho} \end{cases} \\ \Rightarrow &\begin{cases} S/\text{love}(x, \text{pete}) \rightarrow \text{ivn } N/x \\ N/\text{john} \rightarrow \text{re} \\ N/\text{mary} \rightarrow \text{ho.} \end{cases} \end{aligned} \tag{3}$$

**Merge** If two rules have the same meanings and strings, replace their nonterminal symbols with one com-

mon symbol.

$$\left\{ \begin{array}{l} S/love(x,pete) \rightarrow ivn A/x \\ A/john \rightarrow re \\ A/mary \rightarrow ho \\ S/like(x,gavin) \rightarrow apr B/x \\ B/john \rightarrow re \\ B/heather \rightarrow wqi \end{array} \right. \quad (4)$$

$$\Rightarrow \left\{ \begin{array}{l} S/love(x,pete) \rightarrow ivn A/x \\ A/john \rightarrow re \\ A/mary \rightarrow ho \\ S/like(x,gavin) \rightarrow apr A/x \\ A/heather \rightarrow wqi. \end{array} \right.$$

Replace If a rule can be embedded in another rule, replace the terminal substrings with a compositional rule.

$$\left\{ \begin{array}{l} S/love(heather,pete) \rightarrow ivnwqi \\ B/heather \rightarrow wqi \end{array} \right. \quad (5)$$

$$\Rightarrow \left\{ \begin{array}{l} S/love(x,pete) \rightarrow ivn B/x \\ B/heather \rightarrow wqi. \end{array} \right.$$

In Kirby’s experiment [16], five predicates and five object words shown in Figure 2 are employed. Also, two identical arguments in a predicate like *love(john, john)* are prohibited. Thus, there are 100 distinct meanings (5 predicates × 5 possible first arguments × 4 possible second arguments) in a meaning space.

The key issue in ILM is to create a *poverty of stimulus*, which explains the necessity of universal grammar [29]. Kirby [16] modeled it as learning through bottlenecks, which are rather necessary for the learning. As long as an infant agent is given all sentences in the meaning space during learning, he/she does not need to make a compositional grammar; he/she would just memorize all the meaning-sentence pairs. Therefore, agents are given a part of sentences in the whole meaning space. The total number of utterances the infant agent receives during learning is parameterized. Since the number of utterances is limited, the infant agent cannot learn the whole meaning space, the size of which is 100; thus, to obtain the whole meaning space, the infant agent has to generalize his/her own knowledge by self-learning, i.e., *chunk*, *merge*, and *replace*. The parent agent receives a meaning selected from the meaning space, and utters it using his/her own grammar rules. When the parent agent cannot make an utterance because of a lack of grammar rules, he/she invents a new rule. This process is called *invention*. Even if the invention does not work to complement the parent agent’s grammar rules, he/she utters a randomly composed sentence.

### B. Process for String-Clipping

When an infant agent has a number of teacher agents consisting of his/her parent and neighbors, as the teacher agents have their own compositional grammar rules, they are inconsistent with each other. Although the infant agent tries to find a common chunk among utterances, it would be a short string. Since there is little probability of making a chunk from short strings, only long ones are likely to survive into subsequent generations. As a result, learning agents tend to have compositional rules with extremely long strings over generations [19].

Matoba et al. [24] proposed a clipping process in their model, which solves the above problem. This process is called

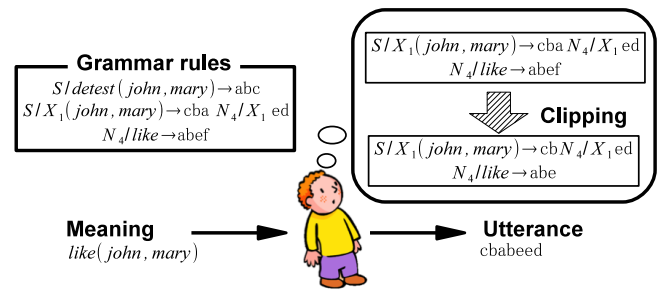


Figure 3. Image of clipping process

*backclipping*. After the learning process of the infant agent, he/she curtails symbols in his/her grammar rules from the tail of a string, unless it contains ambiguity. As a result, when the infant agent becomes the new parent agent in the next generation, the grammar set no longer contains extremely long rules.

Figure 3 illustrates the clipping process in our model. The infant agent tries to utter strings of *like(john, mary)* as shortly as possible. First, he/she chooses a grammar rule from his/her grammar set to generate an utterance of *like(john, mary)*, and deletes symbols one by one, i.e., “cba”, “ed”, “abef”. In the case of “cba”, this string does not exist in the grammar rules of the infant agent, so the infant agent executes backclipping, and the string is shortened from “cba” to “cb”. The string “cb” does not exist in the grammar rules of the infant agent, so the infant agent executes backclipping, and the string is shortened from “cb” to “c”. Since “c” exists in one of the infant’s grammar rules, “*S/detest(john, mary) → abc*”, the infant agent does not abridge it anymore, and adopts “cb” as the clipped word of “cba”. The same process is also applied to the other words. As a result, the sentence becomes shortened from “cbaabefed” to “cbabeeed”.

Of course, such phenomena occur in the real world. The deletion of part of a word constructs a new and shorter word.

e.g.) **Hamburger** → **burger**, **Influenza** → **flu**,  
**Examination** → **exam**

The position of clipping is dependent on a phonological reason [30]. Since ILM does not deal with phonological information, we need to find an alternative way to shorten strings. Nonetheless, backclipping by cutting off the final part of a word is the most common method of abbreviation in English [31].

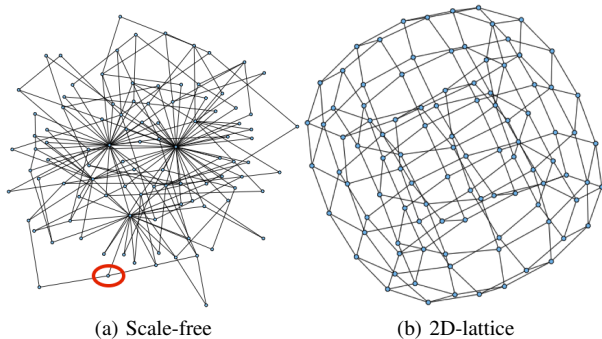
e.g.) **advertisement**, **doctor**, **laboratory**, **professor**,  
**demonstration**, **captain**

### III. AGENT-BASED MODEL FOR LANGUAGE CONTACT

In this section, we explain the agent-based model toward the emergence of local common languages (LCLs). Section III-A explains social networks for language communities. In Section III-B, we discuss the number of agents on each node in the network. We introduce a language exposure in Section III-C. Section III-D explains measuring language distance and clustering LCLs.

TABLE I. NETWORK CHARACTERISTICS

Network type ( $N_{\text{agt}} = 100$ )	Average Degree	Average shortest path
Complete graph	99.00	1.00
Star	1.98	1.98
(a) Scale-free	3.96	2.74
Small-world	4.00	4.26
(b) 2D lattice	4.00	5.05
Ring	2.00	25.25

Figure 4. Examples of networks ( $N_{\text{agt}} = 100$ )

### A. Social Networks for Language Communities

Social networks play an important role in language change, regardless of whether they are connected by an actual or virtual relationship. Some simulation studies deal with complex networks [15] [22] [23]. There are several types of networks, each of which characterizes many real-world communities.

Table I shows network characteristics, in which each value is calculated based on 100 nodes [23]. The average degree denotes the average number of edges connected to a node. The average shortest path length stands for the average smallest number of edges, via which any two nodes in the network can be connected to each other. In this paper, we examine scale-free and 2D-lattice networks.

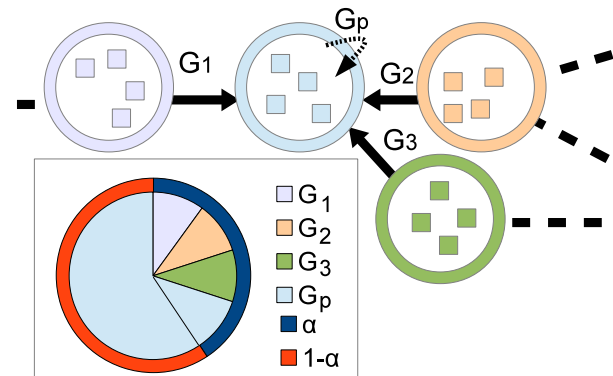
Figure 4 shows examples of networks, in which the former network is regarded as a complex network and the latter is for comparison. Agents are assigned to each node in the networks.

### B. Iterated Learning Model on a Social Network

Here, we discuss how to deal with languages in the framework of ILM on a social network. The population consists of non-overlapping generations; that is, infants at each generation are born at the same time, become parents at the same time, and die at the same time. The network is fixed through generations. The number of agents on each node depends on the model.

A group of agents on a node proceeds with learning in the following way.

- 1) In the group, there is a teacher agent, who makes utterances to all the learning agents.
- 2) Every learning agent acquires the same grammar.
- 3) At the end of a generation, one of the learning agents becomes the teacher agent in the next generation.
- 4) Repeat 1) to 3) for a certain number of generations.

Figure 5. Language input from neighbors connected in a network depending on exposure rate  $\alpha$ 

As a result, all of the agents could acquire the same grammar. In this paper, we simplify our network model so that only one learning agent resides on each node, though we suppose the network represents a much larger community.

### C. Exposure Rate $\alpha$

Nakamura et al. [12] introduced an exposure rate  $\alpha$ , which determines how often language learners are exposed to a variety of language speakers other than their parents. They modified the learning algorithm of Nowak et al. [5], taking the exposure rate into account in order to model the emergence of a creole community. They have shown that a certain range of  $\alpha$  is necessary for a creole to emerge. This parameter was further employed for the following network studies [13] [14] [15].

In some communities, a child learns language not only from his/her parents but also from other adults, whose language may be different from the parental one. In such a situation, the child is exposed to other languages, and thus may learn the most communicative language. To assess how often the child is exposed to other languages, let us divide the language input into two categories; one is from his/her parents, and the other is from other language speakers. The ratio of the latter to the total amount of language input is called an *exposure rate*  $\alpha$ . This  $\alpha$  is subdivided into smaller rates corresponding to those other languages, where each rate is in proportion to the population of the language speakers.

Figure 5 illustrates a situation of language contact where an agent receives language input from neighbors connected in a network depending on the exposure rate  $\alpha$ . The encircled agent in Figure 4a corresponds to the group of agents in the center. Here, we focus on the agent on each node due to the simplification in Section III-B. Let  $G_i$  be the language of Agent  $i$ . Suppose a child has parents who speak  $G_p$ ; he/she receives input sentences from  $G_p$  in the proportion of  $\alpha x_p + (1 - \alpha)$ , and from non-parental languages  $G_i (i \neq p)$  in the proportion of  $\alpha x_i$ , where  $x_i$  denotes a population rate of  $G_i$  speakers among the neighbors.

An infant receives a meaning-signal pair from his parent and neighbors according to the exposure rate  $\alpha$ . The number of utterances an infant receives is fixed, and he/she receives them in proportion to the language distribution for neighbors, like the pie chart shown in Figure 5.

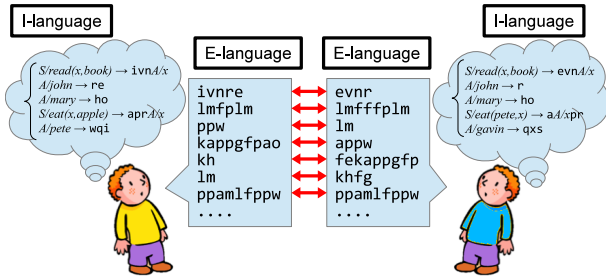


Figure 6. Calculation of distance between languages

#### D. Distance between Local Common Languages

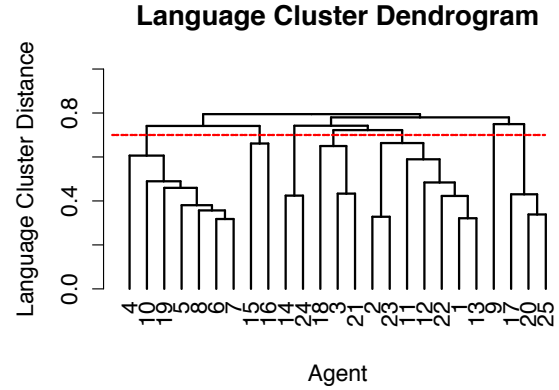
To compare between languages, we define the distance in languages by the edit distance, known as the Levenshtein distance [32]; we count the number of insertion/elimination operations to change one word into another. For example, the distance between “abc” and “bcd” becomes 2 (erase ‘a’ and insert ‘d’). Once the learning process is finished, each agent has his/her own grammar rules. In other words, each agent can enumerate all the sentences he/she can utter as E-language derived from I-language. Figure 6 depicts an image of enumeration. Note that all of the compositional grammar rules are expanded into a set of *holistic rules*, which does not include any variable, i.e., a rule consists of a sequence of terminal symbols.

Now, the comparison between a parent agent and an infant agent takes the following procedure.

- 1) Pick a grammar rule ( $g_c$ ) that is constructed by a pair of a PAS ( $p_c$ ) and an utterance ( $u_c$ ) from the child’s grammar rules ( $g_c$ ). Choose a grammar rule ( $g_p^{p_c}$ ) in which PAS ( $p_p^{p_c}$ ) is the most similar to  $p_c$  from the parent’s grammar rules ( $G_p$ ), in terms of the Levenshtein distance. If there are multiple candidates, all of them are kept for the next process.
- 2) Focus on an utterance ( $u_p^{p_c}$ ) of  $g_p^{p_c}$  and  $u_c$ , and measure a distance ( $d(u_c, u_p^{p_c})$ ) between  $u_p^{p_c}$  and  $u_c$  using the Levenshtein distance. If there are multiple candidates, choose the smallest one.
- 3) Normalize  $d$  from 0 to 1. Carry out 1) to 3) for all grammar rules of  $G_c$ . Calculate the sum of all the distances and regard the average of them as the distance of two sets of linguistic knowledge. Thus, in this case, the distance between  $G_c$  and  $G_p$  is calculated as below:

$$\text{Dist}(G_c, G_p) = \frac{1}{|G_c|} \left( \sum_{i=0}^{|G_c|} \frac{d(u_{c_i}, u_p^{p_{c_i}})}{|u_{c_i}| + |u_p^{p_{c_i}}|} \right). \quad (6)$$

Since agents independently invent languages, their acquired languages are different from each other. To classify agents into local communities by language similarity, we introduce a clustering method, recognizing a cluster as a local language community. The relationship among languages is represented by a dendrogram shown in Figure 7. The vertical axis denotes the height of the tree, which represents the language distance between two merged clusters. We employed the complete linkage method throughout the experiments. Therefore, the number of languages depends on the cutting point of the tree.

Figure 7. Clustering languages ( $N_{\text{agt}} = 25$ )

In this case, the community is regarded as having seven LCLs at the height of  $\theta = 0.7$ .

## IV. EXPERIMENTS

### A. Experimental Settings

Our purpose in the experiments is to examine how the configuration of networks affects the language change. We evaluate the method of string-clipping for high-speed processing, comparing between ILMs with and without string-clipping. In addition, we show that the more generations the simulation takes for learning, the more compositional the grammars. Likewise, the greater the number of nodes, the more network characteristics appear.

We expect LCLs to emerge depending on the types of networks and other conditions. Therefore, we examine two types of networks: Scale-free and 2D-lattice networks. Scale-free networks are drawn with BA [33] models, where the number of edges to add in each step is 2, and the power is set to 1. The generation of multiple edges is allowed. In this paper, experiments on small-world networks drawn with WS [34] models were omitted due to a lack of outstanding results.

Table II shows the list of experiments. Exp-1 is to confirm the effectiveness of string-clipping, comparing two models in the same environment without string-clipping. Since the model without string-clipping in the network becomes memory- and time-consuming through generations, the number of generations is set to 30, which is substantially lower than the former experiment [24]. To eliminate the network effect, we examine models only in the 2D-lattice network in Exp-1. Exp-2 is to observe behaviors of the model with different generations, which are set to 30, 100 and 200. Exp-3 is to observe the relation between the configuration of networks and the language change in the large scale of networks. Therefore, the number of agents is set to  $N_{\text{agt}} = 100$ , while the preceding experiments employ  $N_{\text{agt}} = 25$ .

There are some parameters for parental and infant agents in ILM. Each infant agent receives 50 sentences, while the meaning space is 100 (5 predicates  $\times$  5 possible first arguments  $\times$  4 possible second arguments). Therefore, agents need to acquire a compositional grammar for high expressivity. When

TABLE II. LIST OF EXPERIMENTS

Experiment	$N_{\text{agt}}$	Generation	Network	String-Clipping
Exp-1	25	30	2D Lattice	No
				Yes
Exp-2	25	30 / 100 / 200	2D Lattice	Yes
			Scale Free	
Exp-3	100	100	2D Lattice	Yes
			Scale Free	

a parent agent fails to derive a sentence from his/her own grammatical rules, he/she invents a holistic rule with a random string, the maximum length of which is set to 10. In the process of generating a sentence with his/her grammatical rules, parental agents randomly choose one of the candidate rules when facing a syntactic ambiguity. The agents are set to keep choosing the same rule through the generation, although on the other option agents could randomly choose a rule again.

### B. Evaluation Methods

We measure (a) the number of *local common languages* (LCLs), (b) the number of *grammar rules* and (c) *expressivity* of the grammar. (a) is calculated by setting the threshold to distinguish languages in the dendrogram to  $\theta = 0.7$ . (b) denotes the average number of grammar rules created in an agent at the final generation. (c) is defined as the ratio of the number of utterable meanings derived from the grammar rules to the whole meaning space.

Since the exposure rate  $\alpha$  activates communication with neighbors, we also expect local dialects to emerge through communication. We parameterize  $0 \leq \alpha \leq 1$ , where the larger the value  $\alpha$  is, the more frequently the neighbors speak to the infant agent. Note that, even at  $\alpha = 1$ , infants receive sentences from their parents as frequently as from one of the neighbors.

The notation of labels in Figures 8 to 13 are defined as follows:

$$\left\{ \begin{array}{c} \text{sc} \\ \text{lat} \end{array} \right\} / a \left\{ \begin{array}{c} 25 \\ 100 \end{array} \right\} / g \left\{ \begin{array}{c} 30 \\ 100 \\ 200 \end{array} \right\} / \left\{ \begin{array}{c} \text{w} \\ \text{wo} \end{array} \right\} \left\{ \begin{array}{c} \text{-lcl} \\ \text{-exp} \\ \text{-cmp} \\ \text{-lex} \end{array} \right\}, \quad (7)$$

where the first part distinguishes a network type (**scale-free** / **2D-lattice**), the second and third numerals denote the numbers of agents and generations, respectively, and ‘w’ and ‘wo’ stand for the learning methods ‘with’ and ‘without’ string-clipping. The suffixes, which are shown in Table III, denote a type of experimental result; that is, ‘-lcl’ and ‘-exp’ correspond to the number of LCLs and the degree of expressivity, respectively. The other suffixes ‘-cmp’ and ‘-lex’ show the number of grammatical rules; the former is the number of rules where the non-terminal symbol ‘S’ is put on the left-hand side, which means a compositional or holistic rule, while the latter denotes the number of lexical rules.

All the data are plotted as an average of 50 trials with 95% confidence intervals. Since scale-free networks are randomly drawn for each trial, no phenomenon peculiar to a specific network appears in the results.

TABLE III. LABEL SUFFIXES

Suffix	Definition
-lcl	Number of local common languages
-exp	Degree of expressivity (%)
-cmp	Number of rules where non-terminal symbol ‘S’ is put on left-hand side
-lex	Number of lexical rules
-prev	Language distance from previous generation

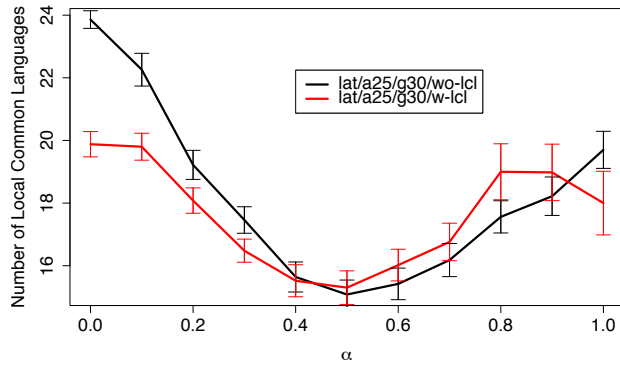
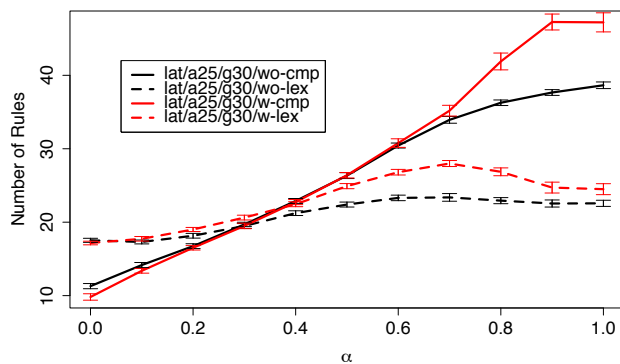
### C. Experiment 1

Figure 8 shows the experimental result of Exp-1. We first explain the characteristics of whole behaviors, focusing on ‘lat/a25/g30/wo’, the black lines, in which 25 agents in the 2D-lattice network learn languages without string-clipping in 30 generations. Figure 8a shows the number of LCLs. At  $\alpha = 0$ , every agent is isolated without connection, speaking an independent language different from each other. Therefore, the number of LCLs is almost the same as that of agents. With increasing communication with neighbors at the range  $0.1 \leq \alpha \leq 0.5$ , agents are likely to acquire common languages. As a result, the average number of LCLs decreased to 13.2 at  $\alpha = 0.5$ . However, after the low peak, LCLs increased to 19.7 at  $\alpha = 1$ . The experimental result may suggest that excessive communication at  $\alpha > 0.5$  causes language divergence. The results of LCLs form a ‘V’-shape overall.

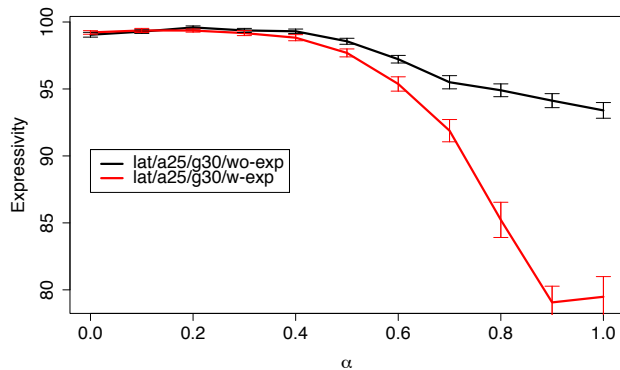
We also investigate acquired grammars. The number of grammar rules and expressivity are shown in Figures 8b and 8c, respectively. Figure 8b shows that grammars become non-compositional according to the increase of  $\alpha$ . In general, compositional rules decrease as the whole grammar gets compositional, while lexical rules increase. Although both types of rules increase, the number of compositional rules eventually exceeds the other at  $\alpha = 0.3$ , which implies that holistic rules occupy agents’ knowledge, while an ideal compositional grammar consists of one compositional rule and ten lexical rules. Figure 8c is inevitably reflected by the compositionality. The excessive language exposure negatively affects common languages.

Next, we explain the comparison between learning models with and without string-clipping. At  $\alpha = 0$ , the number of LCLs of the model with string-clipping is less than that without it. This is because the length of utterances shortens due to string-clipping, which leads to agents’ languages getting closer in language distance based on the Levenshtein distance. On the other hand, with increase of  $\alpha$ , the number of LCLs gets close to that of the model without string-clipping, and eventually the positions are reversed at  $\alpha \geq 0.5$ . The string-clipping method may become unstable in the excessive communication environment; at  $\alpha = 0.9$ , the expressivity suddenly drops to 79.1% in the model with string-clipping. Moreover, at  $\alpha = 1$ , the number of LCLs decreases from 19.0 to 18.0. At  $\alpha = 1$ , every infant agent listens to utterances equally from his/her parent and each neighbor. This uniform language sourcing may facilitate common language acquisition with string-clipping. In fact, the results are less than or insignificantly different from that of  $\alpha = 0.9$ .

With regard to 95% confidence intervals, the difference between with/without string-clipping is significant. However, the macro-scopic behaviors seem to be similar to each other

(a) Local common languages ( $\theta = 0.7$ )

(b) Grammar rules



(c) Expressivity (%)

Figure 8. Experimental results of Exp-1 with 95% confidence intervals ( $n=50$ )

as both form 'V'-shaped lines, except for the large values of  $\alpha$ . We have introduced string-clipping for computational efficiency; otherwise, a combinatorial explosion takes place in their composition of utterances after many generations. This method also supports our human behavior; that is, we do not speak sentences that are too long and beyond our presumed competency. Therefore, considering that word abbreviation

actually occurs in the real linguistic utterances, we would like to justify employing this string-clipping even for the following experiments.

#### D. Complement of Experiment 1

We examine characteristics of LCLs with Figure 9, which shows language distance from neighbors and parents for each  $\alpha$ . Our first expectation was simple: the more frequent the communication with neighbors, the larger the common language communities. If so, the experimental result should show that the greater the exposure rate  $\alpha$  is, the smaller the number of LCLs. However, as shown in Figure 8a, the relation between the exposure rate  $\alpha$  and the number of LCLs forms a 'V'-shape, where the number of LCLs reaches the lowest at  $\alpha = 0.5$ .

Figure 9a shows the average height of each branch in the dendrogram, which corresponds to clustering languages shown in Figure 7. Note that the height of the dendrogram represents the language distance between two merged clusters in the complete linkage method, meaning that a cluster consisting of 25 agents draws 24 lines of language distance. The red dashed line at 0.7 on the Y-axis denotes the threshold to distinguish languages, which means the number of lines above it corresponds to the number of LCLs. Therefore, every point of height would be below the threshold when everyone comes to speak a common language.

At  $\alpha = 0$ , since every agent learns a language only from his/her parent, all the languages spoken in the community are independent. Therefore, according to the number of grammatical rules and expressivity shown in Figures 8b and 8c, each language is sophisticated. Nevertheless, from the viewpoint of language similarity, they are far from each other.

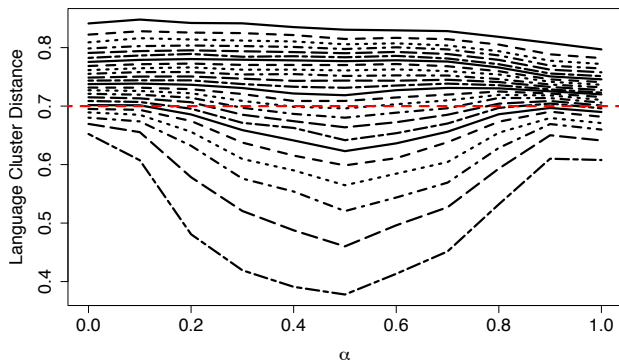
At  $0.3 \leq \alpha \leq 0.5$ , we can find some agents within a very close distance. This is because the agents learn a language mainly from their parents and a part from neighbors. We consider that these appropriate ranges of contact frequency succeed in producing some local common languages.

At  $\alpha \geq 0.9$ , although the formation in height is similar to that at  $\alpha = 0$ , the languages spoken in the community are quite different. Figure 9b shows the average language distance of agents' languages from their parental ones. While agents at  $\alpha = 0$  learn a language similar to that of their parents, the languages at large values of  $\alpha$  are far from that of the previous generation. We can regard them as diffusion due to learning from multipronged language sources. This is a reason for the 'V'-shape in Figure 8a.

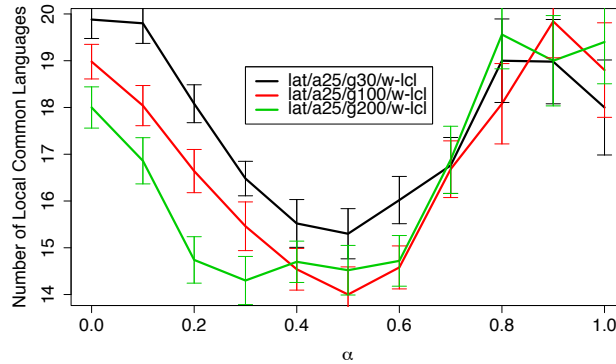
#### E. Experiment 2

The purpose in this experiment is to show an appropriate generation for grammar acquisition, taking effectiveness and computational time into account. We examined the model with a generation parameter at the range between 30, 100 and 200. Figure 10 shows the experimental results of Exp-2.

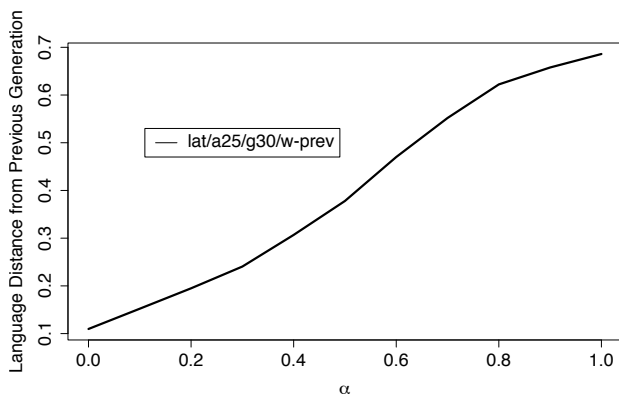
As far as the confidence intervals in Figure 10a, at the range of  $0 \leq \alpha < 0.4$ , these three results form three lines with significant difference. On the contrary, these significant differences among generation settings disappear at the range of  $\alpha \geq 0.4$ . This observation shows that the more generations there are for learning, the easier the observation of the emergence of LCLs at small values of  $\alpha$ . In other words, we



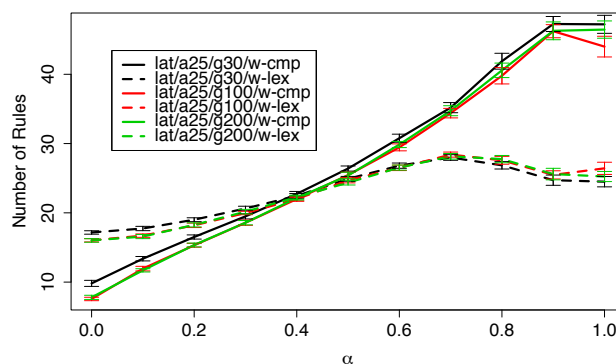
(a) Height of branches in dendrogram (lat/a25/g30/w)



(a) Local common languages ( $\theta = 0.7$ )



(b) Language distance of agents' languages from previous generation



(b) Grammar rules

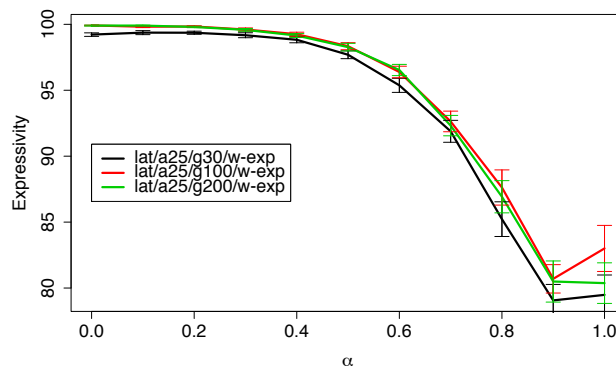
Figure 9. Language distance from neighbors and parents for each  $\alpha$

should take as much time as possible in the 2D-lattice network. However, Figures 10b and 10c show the lines are split into 30-th generation and the others.

Figure 11 shows another experimental result of Exp-2 with scale-free networks. The number of LCLs in the result of the 30-th generation is significantly greater than the others at the range of  $0 \leq \alpha \leq 0.5$ . Rather, it is clear that the results of 100-th and 200-th generations are closer to each other. The results of grammar rules and expressivity, which are omitted, showed similar characteristics as Figures 10b and 10c. Despite a little difference between the model of the 30-th generation and the others, they are significantly different from each other at the smaller values of  $\alpha$ . Taking computational time into account, the number of generations should be set to 100 in the following experiments.

### F. Experiment 3

Figure 12 shows the experimental results of Exp-3 with 100 agents in 100 generations. Looking at the result of scale-free networks (black lines), we can see a large 'S'-shape in which the number of LCLs at  $\alpha = 0.8$  is greater than that at  $\alpha = 0$ . As far as Figures 12b and 12c, agents' grammars have almost the same characteristics as that of 25 agents. This may come from the characteristics of scale-free networks.



(c) Expressivity (%)

Figure 10. Experimental results of Exp-2 with 95% confidence intervals ( $n=50$ )

Figure 13 shows language distance from neighbors (Figure 13a) and parents (Figure 13b) for each  $\alpha$ . As was shown in Section IV-D, those large values of  $\alpha$  cause language diffusion supposedly due to too many sources of language. According to the above observation, the number of lines above the threshold ( $\theta = 0.7$ ) at  $\alpha = 0.8$  must be the greatest, since the number of LCLs at  $\alpha = 0.8$  is significantly different from those at

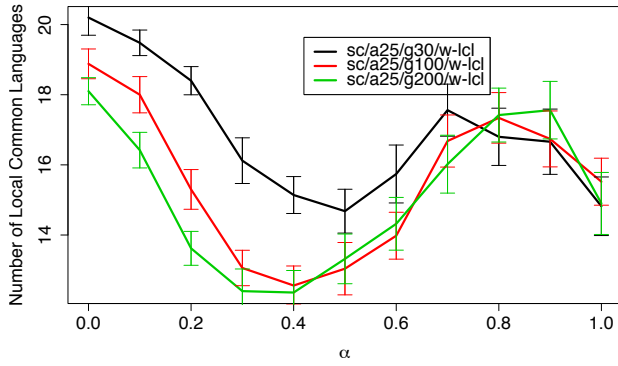
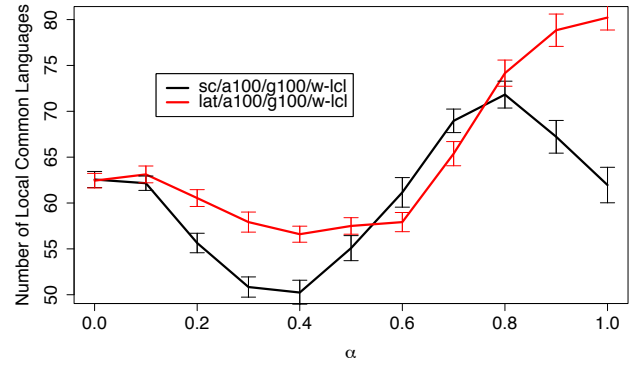


Figure 11. Local common languages ( $\theta = 0.7$ )



(a) Local common languages ( $\theta = 0.7$ )

$\alpha = 0.7$  and  $0.9$ .

We focus on the result of the 2D-lattice network (red lines). At large values of  $\alpha$ , since every agent in the 2D-lattice network is surrounded by four neighbors and his/her parent, everyone can be an influencer in the whole network. For example, an utterance by any agent can equally affect the learning of two steps away in two generations. Note that a neighbor of two steps away is far from the other in the opposite direction, which is different from Exp-1 in that the neighbors are connected in the 2D-lattice network consisting of  $5 \times 5$  vertices. As a result, the agents in such a situation may acquire not well-organized grammars, which interferes the emergence of language communities.

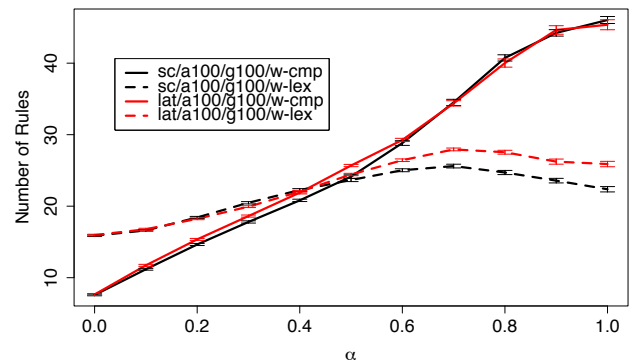
As for Figure 12a, agents in scale-free networks are likely to make local language communities at a certain range of  $\alpha$ . Although two different types of networks drew similar curves, the one by scale-free networks reached the least number of LCLs.

Therefore, we conclude confidently that the emergence of local language communities depends on network types and an appropriate communication with neighbors.

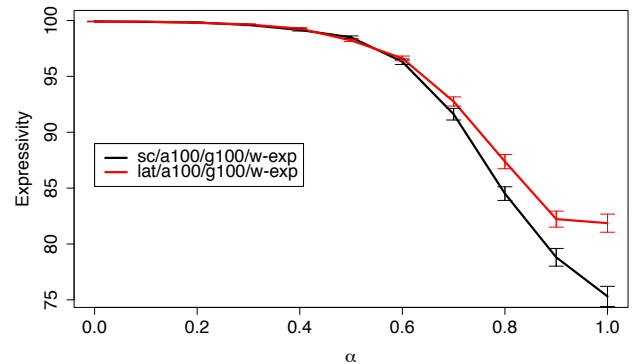
### V. CONCLUSION

In this paper, we proposed an agent-based model for language contact. We employed Kirby's iterated learning model and complex networks. Languages were measured based on the Levenshtein distance of utterances, which enabled us to show the language divergence by the clustering. Language exposure is expected to cause neighbors to communicate with each other. Overall, we succeeded in implementing a linguistic community with learning agents connected by a social network. The network model makes it possible to observe not only diachronic but also synchronic changes in grammar. We achieved implementation of a large-scale, agent-based model where 100 processes of ILM run in parallel, which contributes to the simulation study on language evolution.

Our proposed model was examined in three aspects: (i) the effectiveness of string-clipping, (ii) the relation between generations for learning and the number of local common languages, and (iii) the relation between network types and the local common languages. Through the experiments, the language



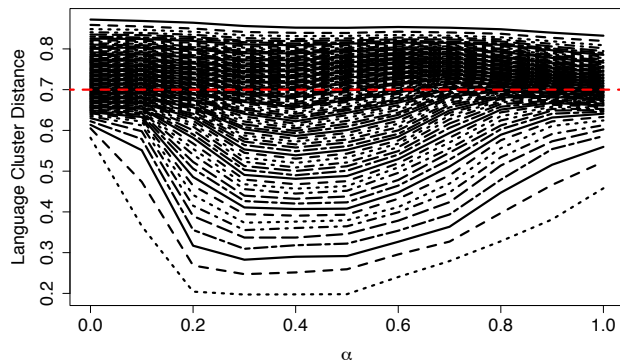
(b) Grammar rules



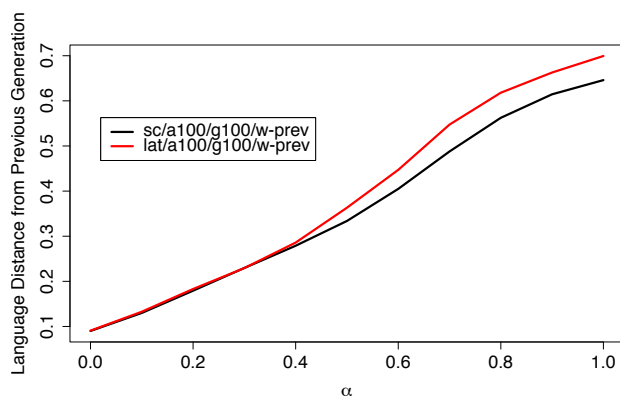
(c) Expressivity (%)

Figure 12. Experimental results of Exp-3 with 95% confidence intervals

exposure was parameterized. We confirmed that the string-clipping method works effectively for grammatical learning, but it seems unstable in the multi-input environment. The complement experiment showed that excessive communication causes language divergence, which suggests that there is an appropriate degree of exposure to other languages during learning toward the emergence of a common language. We observed that local languages are likely to emerge after generations



(a) Height of branches in dendrogram (sc/a100/g100/w)



(b) Language distance of agents' languages from previous generation

Figure 13. Language distance from neighbors and parents for each  $\alpha$ 

for learning. In addition, we confirmed that the network type affects the number of local common languages. We conclude that we succeeded in modeling the actual situation of language change through the series of experiments.

In the near future, we plan to run different types of simulations toward the framework of the diachronic change in languages by language contact. Although we employed indirect graphs for simplicity in the experiments, direct graphs with weighted edges could reflect more real-world social structures.

#### ACKNOWLEDGMENT

We would like to give a special thanks to Dr. Shingo Hagiwara from the National Institute of Technology, Toyama College, and Hiroki Sudo from JAIST for technical support. This work was partly supported by Grant-in-Aid for Young Scientists (B) (KAKENHI) No. 23700310 and No. 15K16013, Grant-in-Aid for Scientific Research (C) (KAKENHI) No. 15K00201 and No. 25330434 from MEXT Japan.

#### REFERENCES

- [1] M. Nakamura, R. Matoba, and S. Tojo, "Simulation of the Emergence of Language Groups Using the Iterated Learning Model on Social Networks," in Proceedings of the 7th International Conference on Advanced Cognitive Technologies and Applications (COGNITIVE2015), 2015, pp. 175–180.
- [2] C. Lyon, C. Nehaniv, and A. Cangelosi, Eds., *Emergence of Communication and Language*. Springer, 2007.
- [3] A. Cangelosi and D. Parisi, Eds., *Simulating the Evolution of Language*. London: Springer, 2002.
- [4] E. J. Briscoe, "Grammatical acquisition and linguistic selection," in *Linguistic Evolution through Language Acquisition: Formal and Computational Models*, T. Briscoe, Ed. Cambridge University Press, 2002, ch. 9.
- [5] M. A. Nowak, N. L. Komarova, and P. Niyogi, "Evolution of universal grammar," *Science*, vol. 291, 2001, pp. 114–118.
- [6] D. Crystal, *Internet Linguistics: A Student Guide*, 1st ed. New York, NY, 10001: Routledge, 2011.
- [7] A. Van Name, "Contributions to Creole Grammar," *Transactions of the American Philological Association*, vol. 1, 1869, pp. 123–67.
- [8] J. Holm, "Contact and change: Pidgins and creoles," in *The Handbook of Language Contact*, R. Hickey, Ed. Blackwell Publishing Ltd., 2013, ch. 12.
- [9] J. Arends, P. Muysken, and N. Smith, Eds., *Pidgins and Creoles*. Amsterdam: John Benjamins Publishing Co., 1994.
- [10] M. Sebba, *Contact Languages: Pidgins and Creoles*, ser. *Modern Linguistics*. Palgrave Macmillan, 1997.
- [11] D. Crystal, *Txtng: The Gr8 Db8*. OUP Oxford, 2008. [Online]. Available: <http://books.google.co.jp/books?id=HyNVuCXtWOC>
- [12] M. Nakamura, T. Hashimoto, and S. Tojo, "Exposure dependent creolization in language dynamics equation," in *New Frontiers in Artificial Intelligence*, ser. *Lecture Notes in Artificial Intelligence*, A. Sakurai, K. Hasida, and K. Nitta, Eds., vol. 3609. Springer, 2006, pp. 295–304.
- [13] —, "Self-organization of creole community in spatial language dynamics," in *Proceedings of 2nd IEEE International Conference on Self-Adaptive and Self-Organizing Systems (SASO2008)*, Venice, 2008, pp. 459–460.
- [14] —, "Prediction of creole emergence in spatial language dynamics," in *LATA 2009 (Proceedings of 3rd International Conference on Language and Automata Theory and Applications)*, ser. *Lecture Notes in Artificial Intelligence*, A. H. Dediu, A. M. Ionescu, and C. Martin-Vide, Eds., vol. 5457. Tarragona: Springer, 2009, pp. 614–625.
- [15] —, "Self-organization of creole community in a scale-free network," in *Proceedings of 3rd IEEE International Conference on Self-Adaptive and Self-Organizing Systems (SASO2009)*, San Francisco, 2009, pp. 293–294.
- [16] S. Kirby, "Learning, bottlenecks and the evolution of recursive syntax," in *Linguistic Evolution through Language Acquisition: Formal and Computational Models*, T. Briscoe, Ed. Cambridge University Press, 2002, ch. 6.
- [17] M. Delz, B. Layer, S. Schulz, and J. Wahle, "Overgeneralization of Verbs - the Change of the German Verb System," in *The Evolution of Language: Proceedings of the 9th International Conference (EVOLANG9)*, T. C. Scott-Phillips, M. Tamariz, E. A. Cartmill, and J. R. Hurford, Eds. World Scientific Pub Co. Inc., 2012, pp. 96–103.
- [18] M. Nakamura, S. Hagiwara, and S. Tojo, "Multilayered formalisms for language contact," in *Proceedings of WS on Constructive Approaches to Language Evolution*, Kyoto, 2012, pp. 145–147.
- [19] K. Smith and J. R. Hurford, "Language Evolution in Populations: Extending the Iterated Learning Model," in *Proceedings of ECAL03*, 2003, pp. 507–516.
- [20] R. Matoba, M. Nakamura, and S. Tojo, "Efficiency of the symmetry bias in grammar acquisition," *Information and Computation*, vol. 209, no. 3, 2010, pp. 536–547.
- [21] R. Matoba, H. Sudo, M. Nakamura, and S. Tojo, "Application of Loose Symmetry Bias to Multiple Meaning Environment," in *Proceedings of the 7th International Conference on Advanced Cognitive Technologies and Applications (COGNITIVE2015)*, 2015, pp. 62–65.
- [22] X. Castelló, V. M. Eguíluz, M. S. Miguel, L. Loureiro-Porto, R. Toivonen, J. Saramäki, and K. Kaski, "Modelling language competition: bilingualism and complex social networks," in *The Evolution of Language: Proceedings of the 7th International Conference (EVOLANG7)*, A. Smith, K. Smith, and R. Cancho, Eds. World Scientific Pub Co. Inc., 2008, pp. 59–66.

- [23] T. Gong, L. Shuai, M. Tamariz, and G. Jäger, "Studying Language Change Using Price Equation and Pólya-urn Dynamics." *PLoS One*, vol. 7, no. 3:e33171, 2012.
- [24] R. Matoba, H. Sudo, M. Nakamura, S. Hagiwara, and S. Tojo, "Process Acceleration in the Iterated Learning Model with String Clipping," *International Journal of Computer and Communication Engineering*, vol. 4, no. 2, 2014, pp. 100–106.
- [25] D. Bickerton, *Language and Species*. University of Chicago Press, 1990.
- [26] N. Chomsky, *Knowledge of Language: Its Nature, Origin, and Use*. New York: Praeger, 1986.
- [27] J. R. Hurford, *Language and Number: the Emergence of a Cognitive System*. Oxford: Basil Blackwell, 1987.
- [28] S. Kirby, *Function, Selection, and Innateness: The Emergence of Language Universals*. Oxford University Press, 1999.
- [29] N. Chomsky, *Rules and Representations*. Oxford: Basil Blackwell, 1980.
- [30] D. Jamet, "A Morphological Approach of Clipping in English. Can the Study of Clipping Be Formalized?" *Lexis*, no. 1, 2009, pp. 15–31.
- [31] A. Veisbergs, "Clipping in English and Latvian," *Poznan Studies in Contemporary Linguistics*, no. 35, 1999, pp. 153–163.
- [32] D. Jurafsky and J. H. Martin, *Speech and Language Processing: An Introduction to Natural Language Processing, Computational Linguistics, and Speech Recognition*. Upper Saddle River, NJ, USA: Prentice Hall PTR, 2000.
- [33] A.-L. Barabasi and R. Albert, "Emergence of scaling in random networks," *Science*, vol. 286, no. 5439, 1999, pp. 509–512.
- [34] D. J. Watts and S. H. Strogatz, "Collective dynamics of 'small-world' networks," *Nature*, vol. 393, 1998, pp. 440–442.

# A Novel Chemistry-inspired Approach to Efficient Coordination of Multi-mission Networked Objects

Mahmoud ElGammal

The Bradley Department of  
Electrical and Computer Engineering  
Virginia Polytechnic Institute and State University  
Blacksburg, Virginia 24061  
Email: gammal@vt.edu

Mohamed Eltoweissy\*

Department of Computer and Information Sciences  
Virginia Military Institute  
Lexington, Virginia 24450  
Email: eltoweissy@vmi.edu

**Abstract**—In this paper we present a chemistry-inspired approach for coordinating networked objects in pervasive computing environments built on the concept of *chemical affinity*. Our thesis is that by paralleling the model of interaction that takes place among atoms during a chemical reaction, a form of collective intelligence emerges among the objects in the network enabling them to achieve a common global objective while relying solely on preferences expressed on an individual basis. The main contribution of this paper is a novel implementation of a highly-parallelized chemical reaction execution engine that uses message passing to optimize reactant selection for multiple reaction rules simultaneously. In our method, objects in the chemical domain are represented using a probabilistic factor graph, where inter-reactant affinities are encoded in the factor nodes to guide bond formation among reactants. The problem of associating reactants with reaction rules is modeled as a Maximum-a-Posteriori (MAP) assignment problem, which we solve using the Max-Product Belief Propagation algorithm, allowing us to efficiently obtain a reactant-to-reaction assignment that maximizes the number of concurrent reactions. To evaluate our approach, we use simulation to assess the performance of the reaction execution engine in terms of execution speed and solution quality. Finally, we use the problem of resource-constrained task assignment among heterogeneous robots as a case study to present a concrete application of our approach.

**Keywords**—*Nature-inspired computing; Internet-of-Things; Pervasive computing; Belief propagation; Computational Chemistry.*

## I. INTRODUCTION

With the current surge in smart computing applications, researches are increasingly turning to nature-inspired computing models for ideas on how to deal with the highly dynamic nature of this new computing paradigm. In [1] we proposed a new approach to network configuration and management in pervasive computing systems inspired by the *chemical affinity* concept, which we coined *C<sub>2</sub>A<sub>2</sub>: Chemistry-inspired, Context-Aware, and Autonomic Management System for Networked Objects*. The concept behind *C<sub>2</sub>A<sub>2</sub>* is that physical and logical components of the network are mapped to the chemical domain using a layered

abstraction model. Once represented using the chemical metaphor, reaction rules are then defined to specify how reactants in the chemical domain are allowed to interact with each other, which would eventually lead to implications on the actual network. *C<sub>2</sub>A<sub>2</sub>* relied on a *reaction execution engine* that was responsible for deciding which reaction rules may be fired and which reactants should be consumed by them. The work presented herein serves as a more in-depth discussion of a significantly improved implementation of the reaction execution engine previously introduced in [1].

In our new approach, reactants and reaction rules in the chemical domain are modeled using a probabilistic factor graph, where factor nodes encode affinities between each pair of reactants, affinities between reactants and reaction rules, as well as the different constraints needed to ensure that the resulting solution constitutes a valid reactant-to-reaction assignment. The graph is constructed such that the optimal assignment of reactants to reaction rules can be obtained by solving the Maximum-a-Posteriori assignment problem [2] on the graph, which we solve by passing carefully designed messages over the graph according to the Max-Product Belief Propagation algorithm [3]. A key advantage of this approach is its ability to find a solution that maximizes the number of reaction rules that can be satisfied simultaneously, which makes it particularly suited for multi-mission pervasive computing applications.

The remainder of the document is organized as follows. In Section II, we survey some notable related works from the literature and provide an overview of the probabilistic graphical modeling techniques we rely on in later sections. In Section III, we present the implementation of our reaction execution engine. In Section IV, we analyze the performance of our approach using simulation, and validate its efficacy by applying it to a more concrete case study. Finally, in Section V, we present our conclusion and discuss future work.

## II. BACKGROUND AND RELATED WORK

In *C<sub>2</sub>A<sub>2</sub>* we leverage ideas from the fields of *bio-inspired computing* and *machine learning*. In particular, we build our work upon some of the established concepts and algorithms belonging to the subfields of *chemistry-inspired*

\*Also Affiliate Professor, The Bradley Department of Electrical and Computer Engineering, Virginia Polytechnic Institute and State University, Blacksburg, Virginia, USA.

*computing* and *probabilistic graphical modeling*<sup>1</sup> in those two research disciplines, respectively. In this section we present a rudimentary overview of these topics and discuss some important related work.

#### A. Chemistry-inspired Computing

A common feature among most, if not all, natural computing models that draw their inspiration from the chemical reaction metaphor, is that the system state is represented as a fluid in which reactants of different types move freely and interact with each other according to predefined reaction rules. Developing concrete applications based on this concept requires mature models of computation that can be used to encode real-life problems using the chemical formalism and describe programs to solve them, as well as runtime systems that can actually execute these programs. The former field of study has seen significant research activity, ushered by the  $\Gamma$  language by Banâtre et al. [4] and continued through various other works such as the Chemical Abstract Machine by Berry et al. [5], the Molecular Dynamics model by Bergstra et al. [6], Membrane Computing (P Systems) by Păun [7], and more recently in the Biochemical Tuple Spaces model by Viroli et al. [8]. Some of these works contributed incremental improvements over previous models while others offered entirely new approaches, but all have served to present the chemical metaphor as a mature and viable option for modeling computational processes, especially for applications where concurrency and self-organization are two desirable characteristics. However, despite the progress on this front, not as much attention has been given to the runtime systems on which chemical computing models can be executed [9].

The earliest runtime system for a chemical machine is perhaps the one described in [4], where an implementation of the  $\Gamma$  language on a massively parallel machine (aka the  $\Gamma$ -machine) is proposed. In order to evaluate a  $\Gamma$  program, the runtime system has to perform two tasks: (a) search for reactants that satisfy reaction conditions (in other words, determine which reactions to fire), and (b) applying the actions associated with fired reactions on the system. It can easily be shown that a roughly similar breakdown of tasks would also apply to any other runtime, not just the  $\Gamma$ -machine. The first task requires solving an  $\mathcal{NP}$ -hard optimization problem, and with  $C_2A_2$ , we attempt to put forward a practical, efficient, and scalable solution to this problem.

Existing runtime systems employ different approaches to address this problem. One approach can be described as the *search-and-match* approach, and it usually relies on some data structure that stores information about reactants and reaction rules where a search algorithm is then used to determine which reactions to fire based on the satisfiability of their premise. The implementation proposed for the  $\Gamma$ -machine in [4] falls under this category. However, it can be considered more of a proof of concept as it assumes a number of processors equal to the number of reactants, which would be faced by strict scalability limits in reality.

<sup>1</sup>For a thorough review of probabilistic graphical models, the reader is referred to [3].

Additionally, it only considers one form of reactions (more specifically, reactions that take exactly two input values and produce two output values), which would impose further constraints on the practicality of this approach. More efficient methods belonging to this category have also been proposed, such as The Chemical Machine by Rajcsányi et al. [10], which relies on the more sophisticated RETE pattern-matching algorithm [11].

Another approach that is mainly used for simulation but is also used in some runtime systems is the *computational chemistry* approach. Methods belonging to this category rely on algorithms that have long been used by theoretical chemists to solve many quantitative chemical problems using simulation with acceptable accuracy. Several algorithms have been developed under this category and which have been improving in efficiency over time, such as Gillespie's First Reaction Method [12], the Next Reaction Method by Gibson et al. [13], Slepoy et al.'s constant-time Monte Carlo algorithm for simulating biochemical reaction networks [14], ALCHEMIST [15], and others. These methods offer a statistically correct depiction of the evolution of species concentration in a chemical solution over time, which is necessary in applications that rely on accurate simulation of the laws of chemical kinetics.

These two approaches have different points of strength and weakness. The search-and-match approach can be used to model the behavior of a self-organizing system in terms of microscopic interactions among its lowest-level components, which makes it a more versatile tool for modeling a wide range of applications. On the downside, it offers limited control on the macroscopic behavior of the whole system [16]. The computational chemistry approach on the other hand offers greater control over the macroscopic behavior of the system, which allows for better overall stability and predictability, but only if the target application lends itself easily to this approach, such as the case studies given in [15], [16], [17], [18].

In  $C_2A_2$  we utilize the concept of *chemical affinity* to express the mutual attraction force between a reactant and another reactant or reaction rule, and we present an approach for reconciling the inevitably conflicting preferences of reactants to form bonds among themselves. By doing so, we aim to combine some of the advantages of the two approaches mentioned above, where the macroscopic behavior of the system is derived from the individual inclinations of reactants at the microscopic level. Furthermore, our approach maximizes the number of reaction rules that can be satisfied simultaneously, making it particularly efficient for applications requiring the execution of concurrent processes.

#### B. Probabilistic Factor Graphs

Probabilistic graphical models [3] provide a framework that enables us to encode our knowledge of how a real-world system works in a compact, machine-readable format, amenable to the application of various reasoning algorithms. Being declarative by nature, such modeling method has the advantage of separating the domain-specific knowledge needed to construct the graph from the reasoning algorithms that can be applied to it. This allows the development of

a whole host of reasoning algorithms that can manipulate the model and answer various queries about it despite being agnostic of the semantics of the real-world system it represents.

A probabilistic graphical model consists of a number of nodes, each representing a random variable, which in turn represents some aspect of the modeled system. The nodes are connected using either directed or undirected edges (as in Bayesian and Markov networks, respectively), which express how a pair of random variables interact. Assuming that we have prior knowledge of how the random variables in the graph are probabilistically interdependent (or not, in case of independent variables), our job is to reason about the most likely values of one or more variables, possibly after having observed the values of some others. In order to do that, we are often interested in calculating the joint distribution over the possible values of all random variables in the graph or a subset thereof, which can quickly become an intractable problem. For instance, in a graph containing  $N$  binary random variables, the space of possible assignments to these variables is of size  $2^N$ .

However, since most complex distributions usually contain independencies among many of their dimensions, and since the graph is essentially a representation of these independencies, we can exploit the structure inherent in the distribution by breaking it up into smaller *factors*, each having just a subset of interdependent variables in its scope. A factor  $\phi_i$  with scope  $D_i$  is a function that maps each possible assignment of the variables in  $D_i$  to a nonnegative value, essentially signifying the affinity of the random variables toward each possible joint assignment. The graph structure then becomes a factorization of the overall joint distribution  $P$  over all variables in the domain  $\mathcal{X} = \{X_1, \dots, X_n\}$ , which can now be expressed more compactly as the product of these factors:

$$P(\mathcal{X}) = \frac{1}{Z} \prod_i \phi_i(D_i) \quad (1)$$

where  $Z$  is a normalization constant (also known as the *partition function*), added in order to make  $P(\mathcal{X})$  a valid probability distribution function.

We are specifically interested in *factor graphs* – a special type of undirected probabilistic graphical models that make the factorization explicit in the graph structure. A factor graph is a bipartite graph consisting of one group of nodes that represent factors, another that represents random variables, and edges that exist only between a factor node and nodes of variables that lie in its scope. In the following sections, we discuss how we optimize reaction selection in  $C_2A_2$  by constructing a factor graph for the system and transforming the problem into one of the well-known inference problems applicable to probabilistic graphical models, which we cover next.

### C. The MAP Assignment Problem

In the MAP (*Maximum a Posteriori*) assignment problem we try to answer the following question: given a set of random variables  $\mathcal{X} = \{X_1, \dots, X_n\}$ , of which a subset  $E$  (the evidence) is observed to have the value  $e$ , what is

the *joint* assignment for the remaining variables  $W = \mathcal{X} - E$  such that  $P(W|E = e)$  is maximized?

An important thing to note is that the correct answer to this query is quite different from what could be obtained by selecting the most likely assignment for the individual members of  $W$  given the evidence, which could possibly yield an invalid solution. For instance, while the most likely independent assignments for a pair of variables  $X, Y \subset W$  given evidence  $E = e$  may be  $x$  and  $y$ , respectively, it is possible that these two assignments can never co-occur given the same evidence. Expressed more formally, there is no guarantee that  $\{\operatorname{argmax}_X P(X|e), \operatorname{argmax}_Y P(Y|e)\}$  and  $\operatorname{argmax}_{X,Y} P(X,Y|e)$  are equivalent. This adds a significant number of constraints that need to be satisfied by the solution, making MAP assignment an  $\mathcal{NP}$ -hard problem [3].

MAP inference continues to be a useful tool for solving problems in various domains, such as computer vision, speech recognition, noisy-channel coding, medical diagnosis, and many others. In all of these problems, we rely on partially observed data in conjunction with some predefined assumptions about the data model in order to estimate an unobserved quantity. As will be explained in more detail shortly, in  $C_2A_2$  we encode the *affinities* between the different objects in the network as well as the reaction rules that dictate how objects interact with each other into the factor graph devised for the system. The graph then becomes the input to a MAP assignment problem whose output determines which reactions are fired and which reactants are consumed thereby.

Owing to its intractability in large graphs, MAP inference is usually solved using one of several available heuristic algorithms. The one we are concerned with here is *Belief Propagation* [19], which we briefly discuss next before moving on to our system implementation.

### D. Belief Propagation

Belief Propagation [19] (BP) is a message-passing algorithm for performing probabilistic inference on graphical models. Given a set of factors  $\Phi$  defined over a set of random variables  $\mathcal{X}$ , we start by constructing a *cluster graph*, which is an undirected graph where each node (or cluster)  $i$  is associated with a subset of variables  $C_i \subseteq \mathcal{X}$ , and each pair of clusters  $C_i$  and  $C_j$  with shared variables are connected by an edge associated with a *sepset*  $S_{i,j} \subseteq C_i \cap C_j$ . The algorithm then progresses through a number of iterations, during which each cluster node transmits to each of its direct neighbor clusters its beliefs about the variables in their shared sepset. A message from  $C_i$  to  $C_j$  incorporates evidence collected by  $C_i$  about the variables in the sepset  $S_{i,j}$  from all its direct neighbors except  $C_j$  (which serves to avoid reinforcing a prior incorrect belief by  $C_j$ ). Provided that the graph satisfies certain properties that will be discussed later, beliefs at neighboring clusters concerning their shared sepset converge after a finite number of iterations, at which point the graph is said to have become *calibrated*. The final step consists of decoding the calibrated beliefs at every cluster to obtain the solution to our inference problem.

BP has different variants for solving different inference problems. We focus our attention on Max-Product Belief Propagation (MPBP), which can be used to solve the MAP assignment problem. In MPBP, the belief computed at cluster  $C_i$  is the *max-marginal* for the variables in its scope, which is a function that maps each possible configuration of the variables in  $Scope[C_i]$  to the unnormalized probability of the most likely joint assignment consistent with it. If the cluster graph is actually a tree, then the MAP problem can be solved exactly and the max-marginals can be computed in polynomial time. Moreover, if there is only one unique optimal assignment to the unobserved nodes, then decoding the max-marginals to obtain the solution is trivial and can be performed in  $O(N)$  [3]. Under different circumstances, the solution is only approximate, and certain measures have to be taken to guarantee convergence and simplify the final decoding step. We discuss the application of BP to our problem in more detail as well as the exact format of the messages passed on the graph in the next section where we present our system implementation.

### III. SYSTEM IMPLEMENTATION

As in other chemical computing models (e.g., [5], [20], [7]), the state of the system in  $C_2A_2$  is analogous to a chemical solution in which reactants move freely and interact with each other according to predefined reaction rules. In an actual chemical solution, Brownian motion is responsible for causing reactants to come in contact with each other, where they form different bond types at various rates that depend on their relative concentrations, the presence of certain catalysts, among other factors. In a chemical computing system, this is emulated via an algorithm that decides which reactions are triggered at what times and which reactants are consumed by them (e.g., [12], [14], [15]). In this section, we put forward an implementation of one such algorithm.

#### A. Overview

The reaction execution engine in  $C_2A_2$  is an implementation of a P System [7]. Reactions in the forward direction take the form  $ca \rightarrow cu$ , while reverse directions take the form  $cu \rightarrow ca$ . In both forms,  $a$  and  $u$  are reactant multisets, and  $c$  is a catalyst that may optionally be required in order for the reaction to be triggered.

The problem of assigning reactants to forward reactions can be seen as a clustering problem in which reaction rules play the role of exemplars while reactants (atoms and molecules) play the role of cluster members. However, one property of P Systems necessitates a slight departure from traditional clustering, which is that reactions must be performed in a maximally parallel way. Consequently, reactants are assigned to rules until no further assignments are possible, which imposes the consequence that a single rule may assume exemplarity of multiple cluster instances, all of identical structure, where the members of each instance have a one-to-one correspondence to the elements in the left-hand side multiset in the forward reaction form,  $a$ . This reformulated clustering problem can be solved by constructing a factor graph as the one shown in Figure 1, where the final reactant/reaction assignments are decided

through the iterative exchange of *affinity* values according to the BP algorithm.

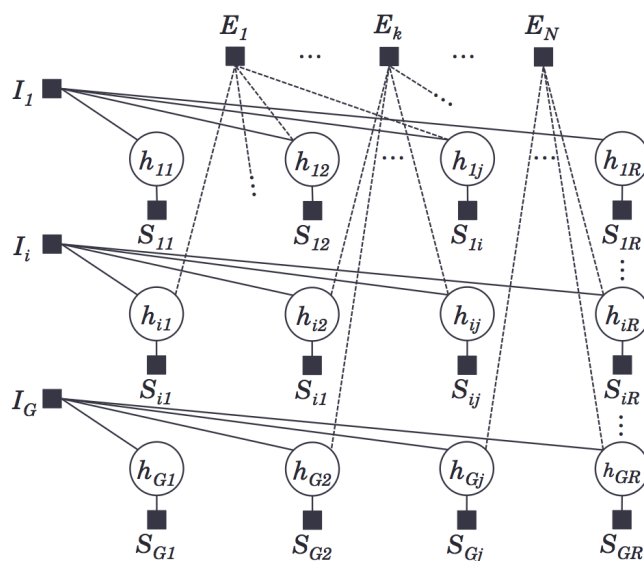


Figure 1. Factor graph of reformulated clustering problem for the reaction execution engine in  $C_2A_2$ .

#### B. Constructing the Factor Graph

In constructing the factor graph for our problem, we have extended the binary variable model for the Affinity Propagation (AP) clustering algorithm [21] presented in [22]. We assume that the system contains  $N$  reactants and  $R$  reaction rules, and the goal is to match different subsets of these  $N$  reactants with reaction rules such that each subset (henceforth called *reactant group* or just *group* for short) is congruent with the left-hand side multiset of the reaction it is matched with, and no single reactant is involved in more than one reaction.

As illustrated in Figure 1, the factor graph is 2-dimensional and is constructed such that reaction rules are organized horizontally and are indexed by the variable  $j \in \{1 \dots R\}$ , while symbols representing reactant groups are organized vertically and are indexed by the variable  $i \in \{1 \dots G\}$ . Reactant groups represent the elements of the power set over all reactants, which has a size of  $2^N$ . Obviously, this can be prohibitively large. In practice, however, reactant groups that do not appear in any reaction rules as well as those that do not satisfy a minimum affinity threshold among its members can be eliminated, reducing the size of the set by several orders of magnitude. The  $h_{ij}$  nodes are binary variables, which if set to 1 at the end of executing the message-passing algorithm indicate that group  $i$  is to be consumed by reaction  $j$ .

Because a single reactant may belong to multiple groups, if group  $i$  is assigned to rule  $j$ , we must guarantee that: (1) group  $i$  is not simultaneously assigned to any other rule  $k \neq j$ , and (2) none of the reactants in group  $i$  belong to another group consumed by a reaction. These two constraints are enforced by adding the  $I_i$  and  $E_{k \in \{1 \dots N\}}$  factor nodes, respectively. The  $S_{ij}$  factor nodes provide the initial affinity

values between each group  $i$  and reaction  $j$ . By applying equation (1) to the factor graph in Figure 1 (and ignoring the  $Z$  constant), the objective function maximized by MPBP becomes:

$$f(\{h_{ij}\}) = \prod_{mpbp}^G \prod_{j=1}^R S_{ij}(h_{ij}) \cdot \prod_{i=1}^G I_i(h_{i:}) \cdot \prod_{k=1}^N E_k(h_{::}^k)$$

where  $h_{::}^k$  denotes all the  $h_{ij}$  variables in the scope of the  $E_k$  factor. Because there are often several advantages to optimizing  $\log(f_{mpbp})$  instead [3], we use a different version of MPBP that maximizes the summation of factors in log-space instead of their product. The algorithm is called Max-Sum Belief Propagation (MSBP) which is the one we use in our implementation. The final objective function hence becomes:

$$f(\{h_{ij}\}) = \sum_{msbp}^G \sum_{j=1}^R S_{ij}(h_{ij}) + \sum_{i=1}^G I_i(h_{i:}) + \sum_{k=1}^N E_k(h_{::}^k) \quad (2)$$

The three factor types work together to produce a solution that maximizes the sum of affinities over all possible (*group, reaction*) pairs, but without violating any of the stipulated constraints. Invalid solutions are eliminated by assigning a value of  $-\infty$  to a factor when the constraint it is associated with is violated, guaranteeing a sub-optimal result for the objective function.

### C. Message Updates

We now derive the messages passed between the different nodes in the factor graph. In the max-sum algorithm, a message passed from one node to another can have one of the two forms shown in equations (3) and (4) depending on whether it flowed from a variable node  $v$  to a factor node  $f$  or in the opposite direction, respectively. In equation (3),  $\mathcal{N}(v)$  is the set of all factor nodes connected to  $v$ , while in equation (4)  $\mathcal{X}_f$  is the scope of factor  $f$ .

$$\mu_{v \rightarrow f}(val_v) = \sum_{g \in \mathcal{N}(v) \setminus f} \mu_{g \rightarrow v}(val_v) \quad (3)$$

$$\mu_{f \rightarrow v}(val_v) = \max_{\mathcal{X}_f \setminus v} \{f(\mathcal{X}_f) + \sum_{w \in \mathcal{X}_f \setminus v} \mu_{w \rightarrow f}(val_w)\} \quad (4)$$

For each variable node, a message has to be exchanged to and from all neighbor nodes for each possible assignment of the variable. Since all variables in the factor graph in Figure 1 are binary, [22] shows that we could compute the difference between the two messages associated with the two possible assignments (e.g.,  $\mu_{v \rightarrow f}(v^1) - \mu_{v \rightarrow f}(v^0)$ ) such that only one message need be sent per neighbor in each direction. Figure 2 shows a fragment of the full factor graph that illustrates all the messages involved in computing the final value of a single  $h_{ij}$  variable. We now discuss the role played by each of these messages in our application as well as the full derivation for the max-sum BP algorithm.

1) *Message from  $S_{ij}$  factor:* The  $S_{ij}$  factor represents the *reward* gained by the system when reactant group  $i$  is assigned to reaction  $j$ . The  $s_{ij}$  message, which is sent from the  $S_{ij}$  factor node to its associated  $h_{ij}$  variable node, has a constant value that represents the affinity between reactant group  $i$  and reaction  $j$ . If group  $i$  matches the input multiset

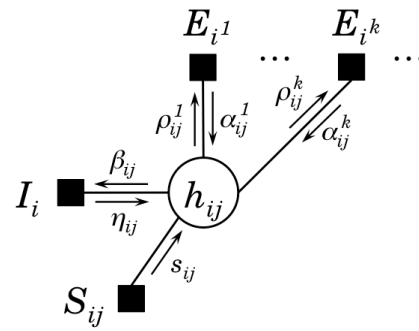


Figure 2. Factor graph fragment for computing the affiliation of reactant group  $i$  with reaction rule  $j$ .

of rule  $j$  and the group is actually assigned to the reaction, then  $S_{ij}(h_{ij})$  is set to the average affinity between the reaction and the reactants in the group. Otherwise, the pair is not candidate for matching and the factor yields a value of  $-\infty$ . In equation (6), the average is used to normalize the resulting affinity value, since reactant groups can be of different sizes.

$$S_{ij}(h_{ij}) = \begin{cases} s_{ij} h_{ij} & \text{if group } i \equiv \text{rule } j \\ -\infty & \text{otherwise} \end{cases} \quad (5)$$

$$s_{ij} = \text{avg}_k \{ \text{aff}(i^k, j) \} \quad (6)$$

2) *Messages from/to  $I_i$  factor:* The  $I_i$  factor guarantees that reactant group  $i$  is assigned to at most one reaction. Note that in equation (7), we use 0 instead of 1 when the constraint is satisfied since we are operating in log-space.

$$I_i(h_{i:}) = \begin{cases} 0 & \text{if } \sum_{j=1}^R h_{ij} \leq 1 \\ -\infty & \text{otherwise} \end{cases} \quad (7)$$

This is achieved by exchanging the  $\eta_{ij}$  and  $\beta_{ij}$  messages between the factor node and the  $h_{ij}$  node for each reaction. The derivation provided below for these two messages is similar to the original derivation for the binary model for AP in [21], but it accounts for the different structure of the factor graph in our problem, where each  $h_{ij}$  node could be connected to a varying number of  $E_k$  factors. Due to this, we use the average of the incoming  $\alpha_{ij}$  messages in the equations below instead of the summation.

- $\beta_{ij}$  message (using equation (3)):

$$\begin{aligned} \beta_{ij}(h_{ij} = 1) &= \mu_{h_{ij} \rightarrow I_i}(1) \\ &= \mu_{S_{ij} \rightarrow h_{ij}}(1) + \text{avg}_k \{ \mu_{E_k^i \rightarrow h_{ij}}(1) \} \\ &= s_{ij}(1) + \text{avg}_k \{ \alpha_{ij}^k(1) \} \end{aligned}$$

Similarly:

$$\beta_{ij}(h_{ij} = 0) = s_{ij}(0) + \text{avg}_k \{ \alpha_{ij}^k(0) \}$$

Given that each message is computed as the difference between its formulae for the two possible assignments of  $h_{ij}$ , we get:

$$\beta_{ij} = \beta_{ij}(1) - \beta_{ij}(0) = s_{ij} + \text{avg}_k \{ \alpha_{ij}^k \} \quad (8)$$

- $\eta_{ij}$  message (using equation (4)):

$$\begin{aligned} \eta_{ij}(h_{ij} = 1) &= \mu_{I_i \rightarrow h_{ij}}(1) \\ &= \max_{j' \neq j} \{I_i(h_{i1}, \dots, h_{ij} = 1, \dots, h_{iR}) \\ &\quad + \sum_{h_{ij'} \in \mathcal{N}(I_i) \setminus h_{ij}} \mu_{h_{ij'} \rightarrow I_i}(h_{ij'})\} \\ &= \max_{j' \neq j} \{I_i(h_{i1}, \dots, h_{ij} = 1, \dots, h_{iR}) + \sum_{j' \neq j} \beta_{h_{ij'}}(h_{ij'})\} \end{aligned}$$

Since we are assuming that  $h_{ij} = 1$ , the only configuration that would maximize  $\eta_{ij}(1)$  is if every other  $h_{ij'}, j' \neq j$  was set to 0, otherwise the group would be assigned to more than one reaction and  $I_i$  would yield  $-\infty$  (equation (7)).  $\eta_{ij}(1)$  then becomes:

$$\eta_{ij}(h_{ij} = 1) = \sum_{j' \neq j} \beta_{h_{ij'}}(0)$$

For  $h_{ij} = 0$ , the configuration is only valid when a unique  $h_{ij'}, j' \neq j = 1$ , in which case the  $I_i(h_{i:})$  term becomes 0, and the formula for  $\eta_{ij}(h_{ij} = 0)$  becomes a maximization over all such configurations:

$$\eta_{ij}(h_{ij} = 0) = \max_{j' \neq j} \{\beta_{ij'}(1) + \sum_{l \notin \{j, j'\}} \beta_{il}(0)\}$$

Finally,  $\eta_{ij}$  is obtained by subtracting  $\eta_{ij}(0)$  from  $\eta_{ij}(1)$ :

$$\eta_{ij} = -\max_{j' \neq j} \{\beta_{ij'}\} \quad (9)$$

3) *Messages from/to  $E_k$  factor*: The  $E_k$  factor implicitly guarantees that if a reactant group is assigned to a reaction, then no other group with any shared reactants is assigned to a reaction. This is achieved by ensuring that at most one of the  $h_{ij}$  variables attached to each  $E_k$  factor is set to 1:

$$E_k(h_{:}) = \begin{cases} 0 & \text{if } \sum_{(i,j)^k} h_{ij}^k \leq 1 \\ -\infty & \text{otherwise} \end{cases} \quad (10)$$

where  $(i, j)^k$  are the (group, reaction) indices of all the  $h_{ij}$  variables attached to  $E_k$  ( $k \in \{1 \dots N\}$ ). The  $E_k$  factor exchanges two messages with each variable it is connected to: the  $\alpha_{ij}^k$  message represents the accumulated evidence of how appropriate it would be for the  $k^{th}$  reactant in group  $i$  to partake in reaction  $j$ , while the  $\rho_{ij}^k$  message represents the accumulated evidence for the willingness of reaction  $j$  to consume the reactant, which has to take into consideration the availability of all other reactants involved in the group. In the following equations, the notation  $E_{i^k}$  denotes the  $E$  factor associated with the  $k^{th}$  reactant in group  $i$ .

- $\rho_{ij}^k$  message (using equation (3)):

$$\begin{aligned} \rho_{ij}^k(h_{ij} = 1) &= \mu_{h_{ij} \rightarrow E_{i^k}}(1) \\ &= \mu_{S_{ij} \rightarrow h_{ij}}(1) + \mu_{I_i \rightarrow h_{ij}}(1) + \text{avg}_{k' \neq k} \{\mu_{E_{i^{k'}} \rightarrow h_{ij}}(1)\} \\ &= s_{ij}(1) + \eta_{ij}(1) + \text{avg}_{k' \neq k} \{\alpha_{ij}^{k'}(1)\} \end{aligned}$$

and it can easily be shown that  $\rho_{ij}^k(h_{ij} = 0)$  would have a similar formula to  $\rho_{ij}^k(h_{ij} = 1)$ , yielding the following for  $\rho_{ij}^k$ :

$$\rho_{ij}^k = s_{ij} + \eta_{ij} + \text{avg}_{k' \neq k} \{\alpha_{ij}^{k'}\} \quad (11)$$

- $\alpha_{ij}^k$  message (using equation (4)):

Let  $H$  be the set of  $h$  variables connected to  $E_{i^k}$  except  $h_{ij}$ :  $H = \mathcal{N}(E_{i^k}) \setminus h_{ij}$ . Since  $h_{ij} = 1$ , the only configuration that ensures that the reactant is not assigned to multiple reactions is when  $h = 0 \forall h \in H$ :

$$\begin{aligned} \alpha_{ij}^k(h_{ij} = 1) &= \mu_{E_{i^k} \rightarrow h_{ij}}(1) \\ &= \max_{h \in H} \{E_{i^k}(h_{ij} = 1, H) + \sum_{h \in H} \mu_{h \rightarrow E_{i^k}}(h)\} \\ &= \max_{h \in H} \{E_{i^k}(h_{ij} = 1, H = \{0\}) + \sum_{h \in H} \rho_{h \rightarrow E_{i^k}}(0)\} \\ &= \max_{h \in H} \{0 + \sum_{h \in H} \rho_{h \rightarrow E_{i^k}}(0)\} = \sum_{h \in H} \rho_{h \rightarrow E_{i^k}}(0) \end{aligned}$$

For  $h_{ij} = 0$ , the configuration is valid when all variables in  $H$  are set to 0 as in the previous case, or when exactly one variable in  $H$  is set to 1:

$$\begin{aligned} \alpha_{ij}^k(h_{ij} = 0) &= \mu_{E_{i^k} \rightarrow h_{ij}}(0) \\ &= \max_{h \in H} \{E_{i^k}(h_{ij} = 0, H) + \sum_{h \in H} \mu_{h \rightarrow E_{i^k}}(h)\} \\ &= \max_{h \in H} \{E_{i^k}(h_{ij} = 0, h_1 = 0, \dots, h_{|H|} = 0) \\ &\quad + \sum_{h \in H} \rho_{h \rightarrow E_{i^k}}(0), \\ &\quad E_{i^k}(h_{ij} = 0, h_1 = 1, h_2 = 0, \dots, h_{|H|} = 0) \\ &\quad + \rho_{h_1 \rightarrow E_{i^k}}(1) + \sum_{h \in H \setminus h_1} \rho_{h \rightarrow E_{i^k}}(0), \dots, \\ &\quad E_{i^k}(h_{ij} = 0, h_1 = 0, h_2 = 0, \dots, h_{|H|} = 1) \\ &\quad + \rho_{h_{|H|} \rightarrow E_{i^k}}(1) + \sum_{h \in H \setminus h_{|H|}} \rho_{h \rightarrow E_{i^k}}(0)\} \end{aligned}$$

In the equation above,  $E_{i^k}(h_{:})$  is 0 for any valid configuration. By using the fact that  $a - \max(b, c) = \min(a - b, a - c)$ , the formula for  $\alpha_{ij}^k$  obtained by subtracting  $\alpha_{ij}(0)$  from  $\alpha_{ij}(1)$  becomes:

$$\alpha_{ij}^k = \min\{0, \min_{(g,r) \in (i,j)^k \setminus (i,j)} \{-\rho_{gr}^k\}\} \quad (12)$$

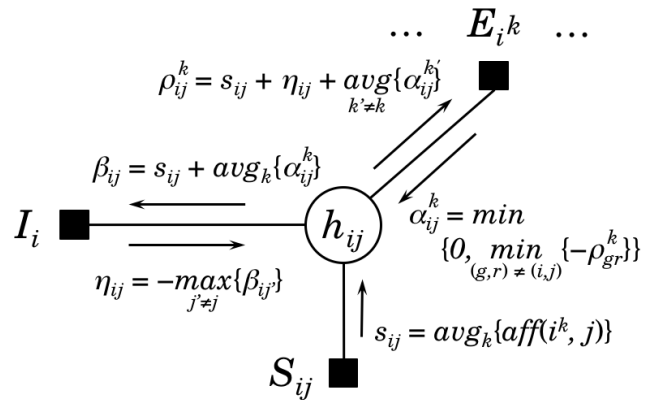


Figure 3. Messages used to compute the affiliation of reactant group  $i$  with reaction  $j$  using max-sum belief propagation.

This concludes the derivation of all messages passed over the factor graph, which are summarized in Figure 3. An important remark regarding the formulae for the  $\eta_{ij}$  and  $\alpha_{ij}^k$  messages (equations (9) and (12)) produced by the  $I_i$  and  $E_{i^k}$  factors, respectively, is that they have a

complexity of  $O(N)$  in the number of possible values for the input messages that must be processed by the factor. Typically, this step would be of exponential complexity in the number of possible assignments of the variables in the scope of the factor, but due to the constraints employed in our problem, the global solution search space could be pruned significantly via early elimination of invalid solutions locally at each factor. This should work to our advantage in terms of the overall execution cost for this implementation.

#### D. Constructing the Cluster Graph

As mentioned in Section II-D, message passing in belief propagation takes place over a *cluster graph* derived from the factor graph representation rather than directly on the latter. Different cluster graphs can be generated for the same factor graph, but for a cluster graph to be valid, it must satisfy two properties [3]:

- The *family-preservation* property, which stipulates that for each factor  $\phi$  in the original factor graph there must exist a cluster  $C$  in the cluster graph such that  $Scope[\phi] \subseteq Scope[C]$ , and
- The *running-intersection* property, which requires that for any two clusters containing a variable  $v$ , there is exactly one path between the two clusters over which information about  $v$  can be propagated.

A certain class of cluster graphs known as *Bethe cluster graphs* is guaranteed to satisfy these two properties [3]. A Bethe cluster graph is a bipartite graph where a univariate cluster is added for each variable in the factor graph, and factors are represented by multivariate clusters whose scopes include all variables in their respective factors. Edges are added only between a univariate cluster and the multivariate clusters whose scopes include the variable in question. Generating such cluster graph from the factor graph in Figure 1 is straightforward. The result is shown in Figure 4, which can be used to verify that both the family-preservation and running-intersection properties are satisfied.

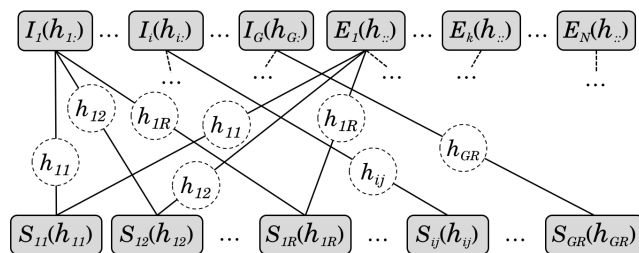


Figure 4. Cluster graph used for passing messages according to max-sum belief propagation. Univariate clusters representing each  $S_{ij}$  factor appear in the bottom row, while multivariate clusters for the  $I_i$  and  $E_k$  factors appear in the top row. Edge labels indicate the variable about which information is passed along the edge.

1) *Dealing with non-convergence*: As can be seen in Figure 4, the graph is not loop-free (e.g., the loop  $S_{11} - I_1 - S_{12} - E_1 - S_{11}$ ), which means that belief propagation is not guaranteed to converge, or to obtain the optimal variable assignment when it does converge. Obviously, the

problem of non-optimality cannot be completely eliminated. However, by ensuring that the cluster graph satisfies the running-intersection property, the quality of the approximate solution is improved as we verify in detail in Section IV. The problem of non-convergence, on the other hand, is dealt with by employing the following techniques:

- *message damping*, where the value of a message in any given iteration of the algorithm is computed as the weighted average of the new message value and its value from the previous iteration:

$$\mu_{t+1} \leftarrow d \cdot \mu_t + (1 - d) \cdot \mu_{t-1}, \quad 0 < d < 1$$

This helps reduce the chances of the message passing algorithm to oscillate indefinitely between two possible configurations.

- Terminating the message passing algorithm after having observed no improvement in the objective function (equation (2)) for a finite number of iterations. Doing so guarantees halting, but it also means that in some cases the algorithm may never find a solution. However, experimental results have shown that this only happened with an acceptably low probability, and can be remedied satisfactorily as we show in Section IV.

2) *Optimizing performance*: A significant reduction in the number of messages passed over the graph can be achieved by considering the fact that, typically, each reaction rule is compatible only with a small subset of the available reaction groups. This means that a large percentage of the  $h_{ij}$  variables in Figure 1 could never be set to 1 in a valid solution. Consequently, the beliefs about such variables in the cluster graph should remain constant throughout the execution of the algorithm, with the likelihood of  $h_{i,j} = 0$  being 1 and that of  $h_{i,j} = 1$  being 0 (or 0 and  $-\infty$  in log-domain, respectively). An optimization that we applied to our implementation in order to eliminate unnecessary message exchange with such variables is to initialize the beliefs about them in the multivariate clusters that include them in their scopes to  $belief(h_{ij}) = \{0 \rightarrow 0, 1 \rightarrow -\infty\}$  while removing the univariate clusters that represent them. This resulted in significantly faster execution times without affecting the quality of the obtained solution.

Another potentially time-consuming operation is the generation of candidate reaction groups that may be assigned to a reaction. In the case where there is a large number of instances of one or more reactants, a combinatorial explosion in the number of candidate reactant groups may occur, which can add a considerable time penalty. In order to circumvent this problem, we have used the following strategies:

- Amortizing the cost of generating candidate reactant groups by caching previous candidates and updating them upon creating or destroying reactant instances, and
- Considering only the top  $n$  reactants with the highest affinity values toward a reaction rule when updating the reactant groups candidate for consumption by the rule.

#### E. Updating the Cluster Graph

Because of the dynamic nature of applications modeled using the chemical metaphor, it is necessary to modify the

structure of the cluster graph when certain events take place, such as:

- a reactant is added or removed from the system.
- a reaction is rule is activated or deactivated due to its inputs being satisfied or unsatisfied, respectively.
- a new reaction rule is defined in the system or an existing rule removed.
- inter-reactant or reactant-reaction affinities change.

Even when no external changes are exerted on the system (such as the introduction of new reactants or reaction rules) most of these events take place by merely executing a reaction rule. Instead of reconstructing the cluster graph from scratch when one of these events occur, the graph structure is only amended accordingly. The system is said to have reached *equilibrium* when no more reactions can be executed. The pseudocode for our reaction execution engine is shown below.

```

1: procedure main()
2:  rules ← findRulesWithSatisfiedInputs()
3:  reactantGroups ←  $\phi$ 
4:  for each rule in rules do
5:    reactantGroups ← reactantGroups  $\cup$ 
      computeReactantGroupsForRule(rule)
6:  end for
7:  graph ← constructBetheClusterGraph
      (rules, reactantGroups)
8:  while true do
9:    rules ← selectReactionRulesToExecute(graph)
10:   if rules =  $\phi$  then
11:     // System reached equilibrium
12:     return
13:   end if
14:   for each rule in rules do
15:     rule.execute()
16:   end for
17:   updateAffinites()
18:   graph ← amendGraph(graph)
19: end while
20: end procedure

21: procedure selectReactionRulesToExecute(graph)
22:  // Initialize messages
23:  for each cluster in graph.multivarClusters() do
24:    for each varhij in cluster.scope() do
25:      if isCompatible(groupi, rulej) then
26:         $\mu_{S_{ij} \rightarrow cluster} \leftarrow 0$ 
27:         $\mu_{cluster \rightarrow S_{ij}} \leftarrow 0$ 
28:      else
29:         $\mu_{S_{ij} \rightarrow cluster} \leftarrow -\infty$ 
30:      end if
31:    end for
32:  end for

33:  // Execute message passing algorithm
34:  currentIteration ← 0
35:  bestObjective ←  $-\infty$ 
36:  solution ← null
37:  repeat
38:    for each edge(i – j) in graph.edges() do
39:      edge.passMessage(computeMessage(i → j))

```

```

40:    objective ← computeObjective(graph)
41:    if objective > bestObjective then
42:      bestObjective ← objective
43:      solution ← decodeSolution(graph)
44:    end if
45:  end for
46:  currentIteration ← currentIteration + 1
47:  until (calibrationError(graph) ≤ MIN_ERROR
    or currentIteration ≥ MAX_ITERATIONS
    or objective has been decreasing for
      MAX_DIVERGENT_ITERATIONS)
48:  return solution
49: end procedure

50: procedure decodeSolution(graph)
51:  for each clusterSij in graph.univarClusters() do
52:    valij ← clusterSij.valueWithMaxBelief()
53:  end for
54:  return {valij}
55: end procedure

```

#### IV. EVALUATION

In this section, we analyze the performance of our reaction execution engine and demonstrate how our proposed approach can be applied to a real-life problem, where we use the multi-agent constrained task assignment problem as a case study.

##### A. Performance Analysis

To evaluate the performance of the message-passing algorithm, we have performed over 2,500 runs using the input parameters shown in Table I, whose values were selected randomly within the indicated ranges.

TABLE I. Minimum and maximum limits used for generating random input parameters for each experiment.

Parameter	Min	Max
Num. unique reactant types	100	1,000
Num. instances of each reactant type	1	5
Num. reaction rules	1	30
Num. unique reactant types in each reaction input multiset	1	5
Reactant type multiplicity in reaction input multiset	1	# reactant instances

Depending on the parameter values generated for each run, a different number of *assignable*  $h_{ij}$  variables (henceforth referred to as *matches*) end up in the cluster graph. As mentioned in Section III-D2, this number is often much smaller than the total number of variables in the graph, and is a better estimate of the true size of the optimization problem. Therefore, it is used as a key metric in this analysis. The algorithm was implemented in Java, and all experiments were executed on the Java HotSpot<sup>TM</sup> 64-bit JVM v1.8.0\_25-b17 running on a 2.4 GHz Intel Core i5 computer with 8 GB 1067 MHz DDR3 RAM.

Figure 5 shows a scatter plot comparing the actual objective and number of matches obtained using our

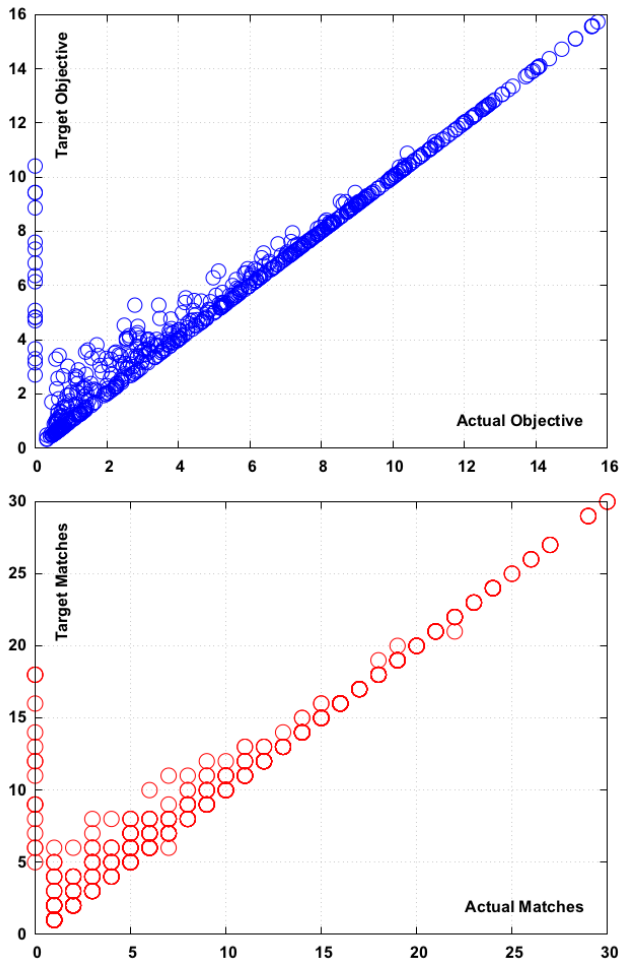


Figure 5. Scatter plot for Actual vs. Target objective (top), and number of matches (bottom).

algorithm to the same metrics when computed using a brute-force algorithm that finds the best solution using exhaustive search. The objective is computed using equation (2), and it represents the total reward gained by the system given a particular set of matches. Due to the intractability of computing the optimal solution, we have restricted comparisons with the brute-force algorithm to problems with 30 or less possible matches (which would require evaluating over 1 billion different combinations). The results in Figure 5 were obtained from over 600 runs, and they show that our algorithm matches or closely approaches the optimal solution in the majority of cases.

Figure 6 displays a break-down of the results in Figure 5. The histogram shows that our algorithm achieved 90% or more of the quality of the optimal objective in almost 77% of runs. The second largest group represents just 8% of runs, where the obtained objective lied between 50% and 70% of the optimal. In almost 2% of runs, our algorithm did not converge to any valid solution. Those runs are represented by the data points lying on the Y-axis in Figure 5. One possible circumvention in this case is to greedily select the non-conflicting matches that maximize the objective. This would usually yield an inferior solution, especially in the presence of many conflicts, but would still be preferable to

selecting no reactions at all.

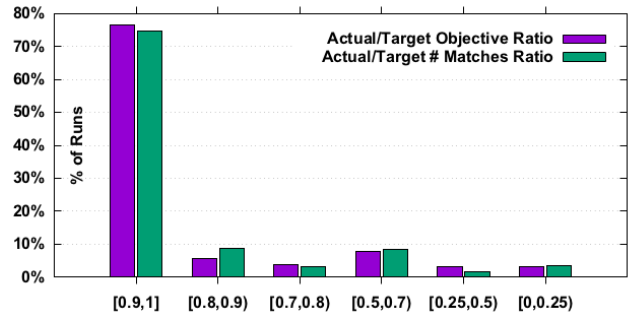


Figure 6. A break-down of the percentage of runs vs. actual/optimal solution ratio.

We now turn our attention to time performance. Figure 7 shows the number of message-passing iterations as well as the average number of messages/cluster that were needed to arrive at the solution. By combining the largest two groups in the histogram, we find that in more than 80% of runs, the best solution was found in less than 10 message-passing iterations and less than 30 message exchanges with every cluster in the graph.

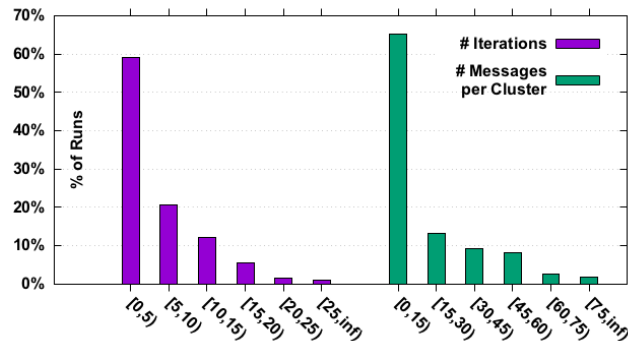


Figure 7. A break-down of the percentage of runs vs. the number of iterations and messages per cluster required to find the solution.

Figure 8 shows a comparison between the execution times of three different algorithms versus the number of possible matches in the cluster graph. In addition to the brute-force algorithm mentioned earlier, we have also added a greedy algorithm to act as a baseline for time performance. The greedy algorithm sorts all matches descendingly by reward then iterates over the sorted matches attempting the two possible assignments of each match and keeping the one that maximizes the sum of rewards.

Unsurprisingly, the message-passing algorithm is slower than the  $O(N)$  greedy algorithm, but as can be seen in Figure 8, the execution times of both algorithms remain to be within a constant factor of each other, even when the number of possible matches exceeds 500. Figure 9 focuses on the message-passing algorithm, where each data point represents the average execution time of all runs that share the same number of matches.

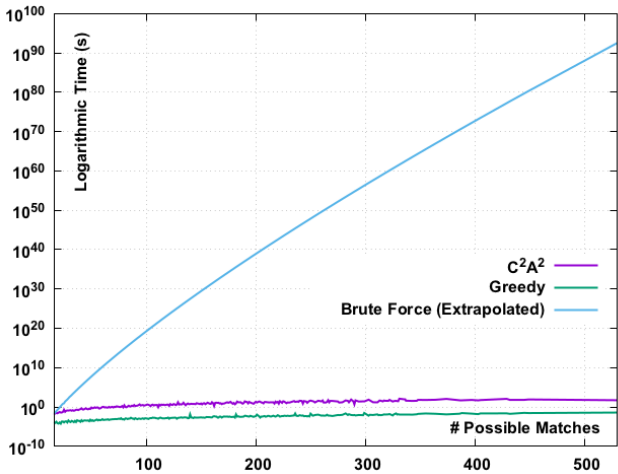
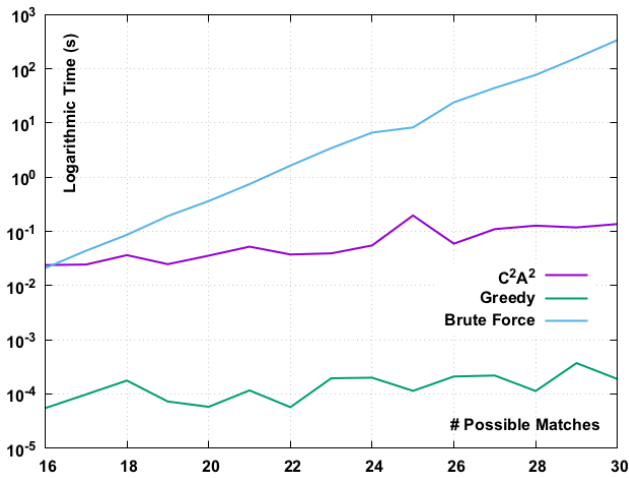


Figure 8. Logarithmic execution time vs. number of possible matches.

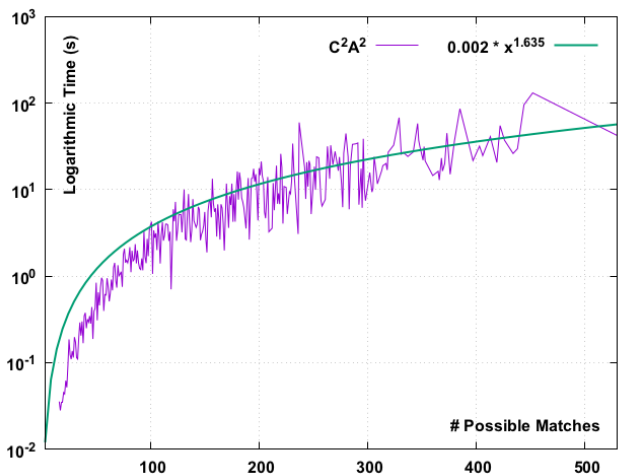


Figure 9. Execution time of message-passing algorithm vs. number of matches, showing the trend line of data points across all runs.

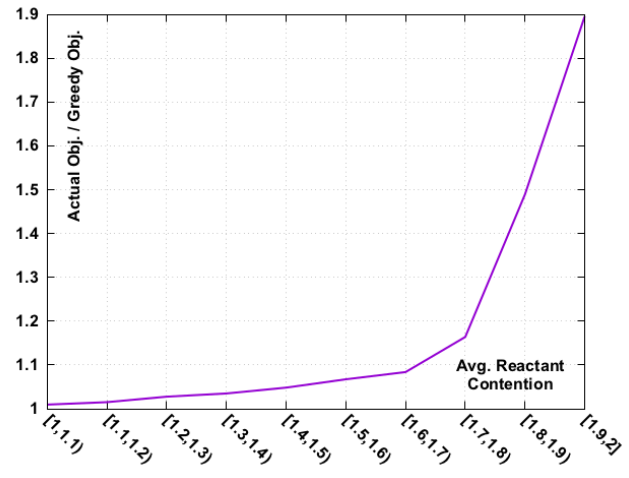


Figure 10. Reactant contention vs. improvement over greedy objective.

has an average number of reaction rules contending over it that falls within a predefined range. Figure 10 shows that the objective obtained using the message-passing algorithm improves exponentially relative to the greedy algorithm as the contention rate increases.

*B. Case Study: Resource-Constrained Task Assignment*

We now demonstrate how  $C_2A_2$  can be applied to a concrete problem in a pervasive computing setting. The case study we have chosen is the problem of resource-constrained task assignment in a multi-agent system. Different versions of this problem have been studied in the literature, each with a slightly different problem statement (e.g., [23], [24], [25], [26]). The version we are interested in here has the following problem statement: given a set of tasks  $T$  and a set of heterogeneous agents  $A$ , where each task  $t \in T$  is associated with a *demand* vector  $d_t$  that describes the requirements needed to start the execution of task  $t$ , and each agent  $a \in A$  is associated with a *supply* vector  $p_a$  that describes the capabilities of  $a$ , it is required to find an assignment  $M : A \rightarrow T$  such that:

- For each task  $t \in T$ ,  $M$  must contain an assignment associating  $t$  with a set of agents whose aggregate supply satisfies  $d_t$ .
- The assignment  $M$  should be selected such that the objective function  $f = \sum_{t \in T} w(t) - \sum_{m \in M} c(m_{a \rightarrow t})$  is maximized, where  $w(t)$  is the reward gained by the system for executing task  $t$ , and  $c(m_{a \rightarrow t})$  is the cost incurred by the system for assigning agent  $a$  to task  $t$ .

[27] shows that this problem is  $\mathcal{NP}$ -hard, and therefore finding the optimal solution is prohibitively expensive for large inputs. Several centralized and distributed heuristic algorithms have been proposed in [23], [24], [25], [26] among others. In [24], an online centralized algorithm is proposed for forming coalitions among mobile heterogeneous robots, allowing them to perform tasks that require the collaboration of multiple robots with different capabilities. A test scenario that involves 10 robots and 3 tasks is given, for which we are now going to devise a solution using  $C_2A_2$ .

Finally, as validation of the quality of the solution obtained using the message-passing algorithm, we have compared it to the greedy solution as more reaction rules contend over the same reactant. In order to do this, we have generated sets of 1,000 runs each. In every set, each reactant

The robot capabilities required in the test scenario are shown in Table II, along with baseline values for the various functional elements specific to each capability. The scenario consists of three tasks, where each task imposes two levels of constraints: (a) robot-level constraints, which must be satisfied individually by each robot involved in executing the task, and (b) coalition-level constraints, which must be satisfied by the robot coalition as a whole. The three tasks are shown in Table III. Finally, the ten robots involved in the test scenario and the different capabilities they possess are shown in Table IV.

The scenario can be modeled using the reaction rules shown below. The number of rules correspond to the number of tasks, where for each task  $t$ , a corresponding rule is responsible for producing a robot coalition,  $c_t$ , with collective capabilities that satisfy the task requirements. In each rule,  $n$  is the number of robots in the coalition ( $1 \leq n \leq 10$ ), and  $|s_i|$  is the magnitude of robot capability  $i$  possessed either by an individual robot or the whole coalition.

$$t_1 + \left( n \times r_{|s_4| \geq 1 \times \{0.8, 0.8, 0.5\}} \right) \begin{matrix} |s_1| \geq 1 \times \{0.5\} \\ |s_3| \geq 1 \times \{0.5\} \\ |s_4| \geq 2 \times \{0.8, 0.8, 0.5\} \end{matrix} \rightarrow c_1 \quad (13)$$

$$t_2 + \left( n \times r_{|s_4| \geq 1 \times \{0.8, 0.8, 0.5\}} \right) \begin{matrix} |s_4| \geq 2 \times \{0.8, 0.8, 0.5\} \\ |s_6| \geq 1 \times \{0.8, 1\} \end{matrix} \rightarrow c_2 \quad (14)$$

$$t_3 + \left( n \times r_{|s_5| \geq 12 \times \{1, 1\}} \right) \begin{matrix} |s_2| \geq 1 \times \{0.5\} \\ |s_3| \geq 2 \times \{0.5\} \\ |s_4| \geq 2 \times \{0.8, 0.8, 0.5\} \end{matrix} \rightarrow c_3 \quad (15)$$

Just like in [24], we are assuming that tasks are independent of each other, but the same concept can still be applied to dependent tasks, where a scheduler would be responsible for detecting which tasks may compete for the available resources at any given time and add the necessary reaction rules for them. The sequential scheme proposed in [24] uses a greedy heuristic to select the robot coalitions, but we will show that our concurrent solution can achieve a conflict-free assignment for all tasks with better resource utilization.

The next step is to specify the different affinity formulae that govern reaction execution, and consequently coalition formation. We consider the optimal solution to be the one that achieves the least possible surplus of unutilized capabilities, thus freeing up more robots to participate in any new tasks that may arise. Accordingly, we are going to construct the affinity formulae such that they optimize this objective. However, it can easily be shown that different definitions of optimality can be catered for by designing different affinity formulae.

We define the following affinity relationships in our solution:

- **task-to-rule affinity:** Because each rule in equations (13)-(15) is designed to produce a coalition for a particular task, the affinity between a task  $t$  and rule  $l$  is defined such that  $aff(t, l) = -\infty$  unless  $l$  produced coalition  $c_t$ :

$$aff(t, l) = \begin{cases} 0, & \text{if } output(l) = c_t \\ -\infty, & \text{otherwise} \end{cases} \quad (16)$$

- **robot-to-robot affinity:** In this particular test scenario robots have no preference as to which other robots may join them in a coalition. Therefore, affinities between all pairs of robots are set to 0.
- **robot-to-task affinity:** The affinity between robot  $r$  and task  $t$  is computed according to equation (17). If  $r$  does not satisfy the robot-level constraints of  $t$ , then  $r$  cannot join coalition  $c_t$ , and thus  $aff(r, t)$  is set to  $-\infty$ . On the other hand, if  $r$  meets the robot-level constraints of  $t$ , then  $aff(r, t)$  decreases as the average capability surplus of  $r$  increases beyond the requirements of task  $t$ .

$$aff(r, t) = \begin{cases} -avg \{s_i^{(r)} - s_i^{(t)}\}, & \text{if } r \equiv t \\ i: |s_i^{(r)}| \geq |s_i^{(t)}| \\ -\infty, & \text{otherwise} \end{cases} \quad (17)$$

- **coalition-to-rule affinity:** For every rule in equations (13)-(15),  $C_2A_2$  has to generate all possible input reactant groups that satisfy the rule (as discussed in more detail in Section III-B). In our test scenario, all of these groups are comprised from the task associated with the rule in addition to a candidate robot coalition that is compatible with the task. As such, the affinity between a candidate coalition  $cc_t$  and a rule  $l$  is defined as the average robot-to-task affinity (equation (17)) over all robots in the coalition if  $output(l) = t$ , and  $-\infty$  otherwise:

$$aff(cc_t, l) = \begin{cases} avg \{aff(r, t)\}, & \text{if } output(l) = c_t \\ r \in cc_t \\ -\infty, & \text{otherwise} \end{cases} \quad (18)$$

Having defined the reaction rules and affinity formulae, we can now feed them into the reaction execution engine to obtain the solution. This particular problem has 608 conflict-free solutions, out of which only 55 (~9%) satisfy the resources needed by all three tasks. Figure 11 shows the possible objective values achievable by those 55 solutions and the number of occurrences of each objective. The results show that  $C_2A_2$  was able to converge to the second best solution, which is compared to the optimal solution in Table V. The table also shows the magnitude of unutilized resources on robots assigned by each solution to the three tasks.

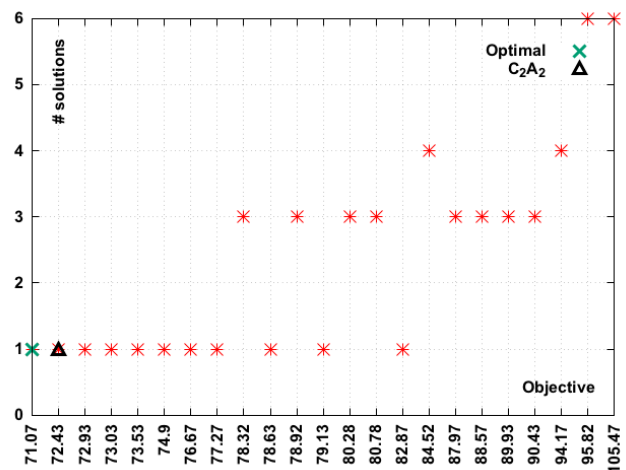


Figure 11. Number of conflict-free solutions for each objective value.

TABLE II. Robot capabilities used in test scenario, with baseline values for the functional elements specific to each capability.

Symbol	Description	Attributes
$s_1$	robot arm	$w_{lift} = 10kg$ (max. lifting capacity)
$s_2$	gripper	$w_{grip} = 20kg$ (max. object weight)
$s_3$	container	$w_{carry} = 50kg$ (max. payload)
$s_4$	camera	$a_{view} = 90^\circ$ (viewing angle) $d_{view} = 5m$ (visible range) $f_{sampling} = 5frame/s$ (sampling frequency)
$s_5$	sonar	$d_{det} = 5m$ (sensor range) $f_{det} = 40Hz$ (scan frequency)
$s_6$	mobility	$v_{max} = 0.6m/s$ (max. linear velocity) $\omega_{max} = 0.5\pi/s$ (max. angular velocity)

TABLE III. Tasks used in the test scenario and their robot-level and coalition-level constraints. The magnitude of each capability functional element is mapped to the range [0, 1], with 1 being the baseline value shown in Table II.

Symbol	Description	Robot-level Constraints	Coalition-level Constraints
$t_1$	area search and object manipulation	$1 \times s_4$ (camera) {0.8, 0.8, 0.5}	$1 \times s_1$ (robot arm) {0.5} $1 \times s_3$ (container) {0.5} $2 \times s_4$ (camera) {0.8, 0.8, 0.5}
$t_2$	area exploration	$1 \times s_4$ (camera) {0.8, 0.8, 0.5} $1 \times s_6$ (mobility) {0.8, 1}	$2 \times s_4$ (camera) {0.8, 0.8, 1}
$t_3$	cargo transportation	$12 \times s_5$ (sonar) {1, 1}	$1 \times s_2$ (gripper) {0.5} $2 \times s_3$ (container) {0.5} $2 \times s_4$ (camera) {0.8, 0.8, 0.5}

TABLE IV. Capability matrix of robots used in the test scenario.

Capability/ Robot	$s_1$ (robot arm)	$s_2$ (gripper)	$s_3$ (container)	$s_4$ (camera)	$s_5$ (sonar)	$s_6$ (mobility)
$r_1$	$1 \times \{0.5\}$		$1 \times \{0.5\}$	$1 \times \{0.8, 0.8, 0.5\}$	$16 \times \{1, 1\}$	$1 \times \{0.8, 1\}$
$r_2$		$1 \times \{0.6\}$		$1 \times \{0.8, 0.8, 0.5\}$	$16 \times \{1, 1\}$	$1 \times \{0.8, 1\}$
$r_3$	$1 \times \{0.5\}$		$1 \times \{1\}$		$16 \times \{1, 1\}$	$1 \times \{0.5, 0.8\}$
$r_4$				$1 \times \{0.8, 0.8, 0.5\}$	$16 \times \{1, 1\}$	$1 \times \{0.8, 1\}$
$r_5$				$1 \times \{0.8, 0.8, 1\}$	$14 \times \{1, 1\}$	$1 \times \{1, 1\}$
$r_6$		$1 \times \{1\}$	$1 \times \{1\}$		$14 \times \{1, 1\}$	$1 \times \{0.8, 1\}$
$r_7$				$1 \times \{1, 1, 0.5\}$	$14 \times \{1, 1\}$	$1 \times \{0.8, 1\}$
$r_8$	$1 \times \{0.5\}$			$1 \times \{1, 1, 0.5\}$	$14 \times \{1, 1\}$	$1 \times \{0.8, 1\}$
$r_9$		$1 \times \{0.3\}$		$1 \times \{0.8, 0.8, 1\}$	$14 \times \{1, 1\}$	$1 \times \{0.8, 1\}$
$r_{10}$	$1 \times \{1\}$			$1 \times \{0.8, 0.8, 0.5\}$	$8 \times \{1, 1\}$	$1 \times \{0.5, 0.8\}$

TABLE V.  $C_2A_2$  vs. optimal task-to-robot assignment.

	$C_2A_2$	Optimal Solution
$t_1$	$\{r_1, r_{10}\}$	$\{r_1, r_{10}\}$
$t_2$	$\{r_5, r_9\}$	$\{r_5, r_9\}$
$t_3$	$\{r_3, r_4, r_6, r_7\}$	$\{r_3, r_6, r_7, r_8\}$
Resource Surplus		
$s_1$	$1 \times \{1\}$ $1 \times \{0.5\}$	$1 \times \{1\}$ $2 \times \{0.5\}$
$s_2$	$1 \times \{0.5\}$ $1 \times \{0.3\}$	$1 \times \{0.1\}$ $1 \times \{0.5\}$
$s_3$	$2 \times \{0.5\}$	$2 \times \{0.5\}$
$s_4$	$1 \times \{0.2, 0.2, 0\}$	$2 \times \{0.2, 0.2, 0\}$
$s_5$	$64 \times \{1, 1\}$	$62 \times \{1, 1\}$
$s_6$	$4 \times \{0.8, 1\}$ $2 \times \{0.5, 0.8\}$ $1 \times \{0.2, 0\}$	$4 \times \{0.8, 1\}$ $2 \times \{0.5, 0.8\}$ $1 \times \{0.2, 0\}$
<b>Objective</b>	72.43	71.07

## V. CONCLUSION AND FUTURE WORK

In this paper we presented a novel implementation of a chemical reaction execution engine geared toward multi-mission pervasive computing applications. By utilizing the concept of chemical affinity between network nodes, or between nodes and certain tasks or missions, we demonstrated an approach by which the network as a whole can be steered toward convergence on a set of common goals through the distributed exchange of affinity values expressed on an individual basis. We showed how the problem can be represented as a Maximum-a-Posteriori assignment problem and how it can be solved efficiently using the Max-Product Belief Propagation algorithm after carefully constructing a probabilistic factor graph and designing the message update formulae for the problem. We validated the efficacy of our approach using simulation, and also more tangibly by applying it to the problem of resource-constrained task assignment.

As an ongoing effort to extend the work presented here, we are developing a formal framework for modeling various pervasive computing and Internet-of-Things applications, which will be responsible for abstracting the different physical and logical elements of the network as entities in the chemical domain. Furthermore, we are studying the effect of context on inter-reactant affinities, allowing the development of context-aware systems that can quickly adapt to their surroundings. Finally, we plan to utilize reinforcement learning techniques and exploratory self-adaptation, where the system associates past decisions with their effect on performance, enabling the system to self-optimize in anticipation of potential events expected to take place in the future.

## REFERENCES

- [1] M. ElGammal and M. Eltoweissy, "Chemistry-inspired, Context-Aware, and Autonomic Management System for Networked Objects," in *FUTURE COMPUTING, The Seventh International Conference on Future Computational Technologies and Applications*, 2015, pp. 38–47.
- [2] J. D. Park and A. Darwiche, "Solving MAP Exactly using Systematic Search," in *UAI'03: Proceedings of the Nineteenth Conference on Uncertainty in Artificial Intelligence*. Morgan Kaufmann Publishers Inc, Aug. 2002.
- [3] D. Koller and N. Friedman, *Probabilistic Graphical Models: Principles and Techniques*, ser. Adaptive Computation and Machine Learning. MIT Press, 2009.
- [4] J. Banâtre, A. Coutant, and D. Le Metayer, "A Parallel Machine for Multiset Transformation and its Programming Style," *Future Generation Computer Systems*, vol. 4, no. 2, 1988, pp. 133–144.
- [5] G. Berry and G. Boudol, "The Chemical Abstract Machine," *Proceedings of the 17th ACM SIGPLAN-SIGACT Symposium on Principles of Programming Languages*. POPL '90., 1992.
- [6] J. Bergstra and I. Bethke, "Molecular Dynamics," *The Journal of Logic and Algebraic Programming*, vol. 51, no. 2, 2002, p. 193–214.
- [7] G. Păun, "Membrane Computing," *Fundamentals of Computation Theory*, 2003.
- [8] M. Viroli and M. Casadei, "Biochemical Tuple Spaces for Self-organising Coordination," in *Proceedings of the 11th International Conference on Coordination Languages and Models (COORDINATION 2009)*, 2009, pp. 143–162.
- [9] P. Kreyssig and P. Dittrich, "On the Future of Chemistry-Inspired Computing," *Organic Computing — A Paradigm Shift for Complex Systems Autonomic Systems*, vol. 1, 2011, pp. 583–585.
- [10] V. Rajcsányi and Z. Németh, "The Chemical Machine: An Interpreter for the Higher Order Chemical Language," *Euro-Par 2011: Parallel Processing Workshops*, 2012.
- [11] C. Forgy, "Rete: A Fast Algorithm for the Many Pattern/Many Object Pattern Match Problem," *Artificial Intelligence*, vol. 19, no. 1, 1982.
- [12] D. T. Gillespie, "Exact Stochastic Simulation of Coupled Chemical Reactions," *The journal of physical chemistry*, 1977.
- [13] M. A. Gibson and J. Bruck, "Efficient Exact Stochastic Simulation of Chemical Systems with Many Species and Many Channels," *The Journal of Physical Chemistry*, vol. 104, no. 9, 2000, pp. 1876–1889.
- [14] A. Slepoy, A. P. Thompson, and S. J. Plimpton, "A Constant-time Kinetic Monte Carlo Algorithm for Simulation of Large Biochemical Reaction Networks," *The Journal of Chemical Physics*, vol. 128, 2008.
- [15] D. Pianini, S. Montagna, and M. Viroli, "Chemical-oriented Simulation of Computational Systems with Alchemist," *Journal of Simulation*, vol. 7, 2013, pp. 202–215.
- [16] M. Monti, L. Sanguinetti, C. F. Tschudin, and M. Luise, "A Chemistry-Inspired Framework for Achieving Consensus in Wireless Sensor Networks," *Sensors Journal, IEEE*, vol. 14, no. 2, 2014, pp. 371–382.
- [17] T. Meyer, "On Chemical and Self-healing Networking Protocols," Ph.D. dissertation, PhD Thesis, University of Basel, 2010.
- [18] M. Monti, T. Meyer, C. F. Tschudin, and M. Luise, "Stability and Sensitivity Analysis of Traffic-Shaping Algorithms Inspired by Chemical Engineering," *IEEE Journal on Selected Areas in Communications*, vol. 31, no. 6, 2013, pp. 1105–1114.
- [19] J. Pearl, "Reverend Bayes on Inference Engines: A Distributed Hierarchical Approach," in *AAAI*, 1982, pp. 133–136.
- [20] J. Banâtre, P. Fradet, and Y. Radenac, "Generalised Multisets for Chemical Programming," *Mathematical Structures in Computer Science*, Cambridge University Press, vol. 16, no. 04, 2006, pp. 557–580.
- [21] D. Dueck, "Affinity Propagation: Clustering Data by Passing Messages," Citeseer, 2009.
- [22] I. Givoni, "Beyond Affinity Propagation: Message Passing Algorithms for Clustering," Ph.D. dissertation, [tspace.library.utoronto.ca](http://tspace.library.utoronto.ca), University of Toronto, 2012.
- [23] S. S. Ponda, L. B. Johnson, and J. P. How, "Distributed chance-constrained task allocation for autonomous multi-agent teams," *2012 American Control Conference - ACC 2012*, 2012, pp. 4528–4533.
- [24] J. Chen and D. Sun, "Resource constrained multirobot task allocation based on leader–follower coalition methodology," *The International Journal of Robotics Research*, vol. 30, no. 12, Oct. 2011, pp. 1423–1434.
- [25] T. Mercker, D. W. Casbeer, P. T. Millet, and M. R. Akella, "An Extension of Consensus-Based Auction Algorithms for Decentralized, Time-Constrained Task Assignment," *2010 American Control Conference (ACC 2010)*, 2010, pp. 6324–6329.
- [26] S. Xu, "Energy-efficient Task Assignment of Wireless Sensor Network with The Application to Agriculture," *Iowa State University Digital Repository*, 2010.
- [27] C.-H. Fua and S. S. Ge, "COBOS: Cooperative Backoff Adaptive Scheme for Multirobot Task Allocation," *IEEE Transactions on Robotics*, vol. 21, no. 6, Dec. 2005, pp. 1168–1178.

## Unmanned Aerial Systems as Tools to Assist in Digitalized Decision Making

Major, Title of Docent, PhD Tapio Saarelainen

Army Academy  
Army Research and Development Division,  
Lappeenranta University of Technology  
Lappeenranta, Finland  
tapio.saarelainen@mil.fi  
tapio.saarelainen@lut.fi

**Abstract**—This paper presents an idea-phase introduction of how to utilize swarms of Unmanned Aerial Systems (UASs) to assist the overall capability in digitalized decision making at company level and below. In military operations, access to analyzed data is crucial in optimizing the performance of the troops. This need for data access applies also in civilian settings, and therefore, this paper briefly discusses some use cases of UASs in civilian environments. UASs are used as hub-stations and tools to gather data from the areas of interest and to increase Situational Awareness (SA). Autonomous or guided platforms built with commercially off the shelf (COTS) material, UASs remain inexpensive data collecting tools. As the tempo of operations increases, a sustained capability for accruing timely and accurate data from a designated area is necessary for improved digitalized decision making. The aim in examining technologies and principles applicable both in military and civilian data gathering is to illustrate their applicability in both of these environments.

**Keywords**-Unmanned Aerial Systems (UASs); dismantled company attack; real-time data; digitalized decision making.

### I. INTRODUCTION

This paper is an extended version of [1] and examines at an idea-stage the utilization of Unmanned Aerial Systems (UASs) in decision making, reconnaissance and monitoring by means of implemented sensors on UASs. This discussion comprises use cases drawn from both military and civilian contexts. The difference between Unmanned Aerial Vehicle (UAV) and Unmanned Aerial System (UAS) is slight but this slight difference is important in that UAS also refers to the ground systems and not just the flying component. The fast and reliable method of collecting data requires that the collected data are transmitted to the base-station as timely as possible. This ensures that the data are available for decision making purposes within a minimal delay. Moreover, industry and regulators have opted for UAS rather than UAV as the preferred term to detone Unmanned Aircraft or Aerial Systems as UAS encompasses all the aspects of deploying these aircraft rather than the mere platform.

Militaries all over the world continue developing methods for saving the lives of own troops. The reason for

this is the downsizing process of armies in western countries. In the environment where military operations are executed, a battlespace, the number of soldiers in combat units decreases, and simultaneously the number of personnel to take care of the logistics and maintenance issues increases as the maintenance of machinery utilized in the battlespace asks for ever increasing resources. The overall aim of militaries continues to be the sustained capability to improve operational performance despite the downsizing and minimized number of soldiers in combat. The remedy for this is an attempt to increase SA, which asks for the use of UASs to produce the required data for analyzing purposes.

In what follows, the preferred term is Unmanned Aerial Systems (UASs), including drones, unmanned aerial vehicles (UAVs), and remotely piloted aircraft (RPA), demonstrating the military use history that reflects this equipment's long-recognized potential in supporting warfighting efforts [2]. UASs represent systems that function as swarms and thereby enable effective collecting and transmitting of data.

UASs continue to be increasingly introduced in military operations. For instance, UASs exceed human-capability is that in Intelligence, Surveillance and Reconnaissance (ISR) [3], which involve dangers and unaffordable casualties. Without accrued knowledge from the Area of Interest (AOI), any army becomes incapacitated. Typically, UAS are utilized in operations that are characterized as being dull, dirty or dangerous (DDD). Also, UAS can be exploited in covert operations, and in research and environmentally critical roles. In addition, the economics of operation speak for the advantage of the UAS. Resorting to the performance of UAS can assist in minimizing human labour.

A company attack, typically a dismantled company attack, is a demanding military operation, which requires constant real-time data to allow executing all the phases of an operation to achieve the set goal. It comprises several phases of action, the first of which involves reconnaissance. An attacking unit must find out the composition and location of the opposite entity before a successful attack can be executed. Once the reconnaissance data have been gathered, the planning sequence of the operation begins by implementing the process of Military Decision Making

Process (MDMP). In this process, it is possible to benefit from automated assisting tools. When the MDMP has been carried out, it results in different types of Courses of Action (COAs). These COAs represent different alternatives to military commanders on how to organize the attack. Once the optimal COA has been chosen, the maneuver, dismounted company, attack can be ignited. A dismounted company attack is composed of the phases outlined in the following Figure 1: Assembly area, dismount line, line of departure, engagement, combat and the objective.

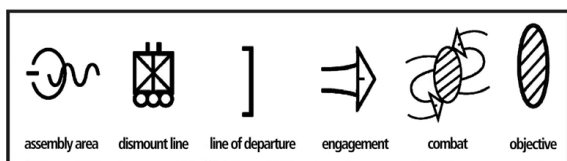


Figure 1. Dismounted company attack as a process [1].

To illustrate examining COAs, Figure 2 depicts two different types of COAs in a battlespace. The number of different COAs in real combat situation varies in that the number of COAs typically equals more than two, but to simplify things, in this case, there are only two COAs involved in the example depicted. In the first COA, the objective is to stop an armored enemy by deploying a flanking movement, whereas in the second COA, the objective is to destroy an enemy command post by direct engagement.

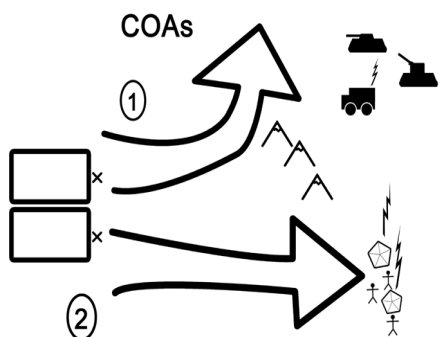


Figure 2. Different types of Courses of Action [1].

The utilization of UASs can be seen as having a central role when real-time data are required for rapid decision making. UASs can be viewed as a resource for military commanders in that UASs offer the advantage of surprise in an attack by producing the real-time data needed for decision making. If a commander fails in surprising the enemy, he or she loses the possibility to take the initiative in the operation. The ability to take and maintain the initiative is usually a prerequisite for a successful military operation, especially in a dismounted company attack. In order to facilitate an improved decision making process it is necessary to have access to the type of data that are necessary and most updated.

The utilization of UASs is necessary to get the correct information from enemy space as rapidly as possible in the

hectic tempo of operations, save soldiers' lives and support the morale of troops performing the manoeuvres in an operational area. Furthermore, the use of unmanned equipment can be seen as part of optimizing the existing resources of military units as machines ceaselessly continue fearless fighting.

When militarily utilized, UASs can be used for varying tasks: performing terrain reconnaissance in the area of objective, performing reconnaissance of the use of Nuclear, Biological and Chemical substances, maintaining reconnaissance engagement by providing data on enemy movements, and monitoring the actions of enemy troops (direction and speed of movement, location, size, formation, action). UASs can also be utilized in the targeting process in that UASs can be sent airborne to the designated areas for the reconnaissance and targeting of the potential enemy targets. UAVs can act as relay stations for sustaining the constant capability to communicate and control the troops and machines in the hostile area.

Collected data from the designated areas are utilizable in the MDMP that is linked to gaining SA and choosing between different COAs. These data can be collected more safely, if an appropriate number of UASs of the necessary type are available for these operations. Using UASs alongside with dismounted close combat soldiers to complement data gathering makes it possible to combine optimally the capabilities of soldiers and equipment. The latter can be sent out to the most dangerous locations while dismounted close combat soldiers remain in charge of the less lethal task, if ever possible in a battlespace.

The use of UASs gives an advantage for commanders. First, UASs can be sent to the areas of interest, days ahead, if required. UASs can be shut down or reactivated via electrical signals when necessary. This gives commanders the advantage to transport the UASs as reconnaissance resources to the designated areas timely at the chosen moment. When UASs have been flown to the area and shut down, they will not consume any energy, and the saved energy can be used at a chosen moment and in the wanted operation, which supports the own battle plan and own objectives. Commanders are able to plan these actions prior to execution and have UASs transported to the areas when deemed appropriate and safe. UASs can be ready and standing by in a chosen area, with the chosen sensors embedded in the UAS platform.

To summarize: commanders can benefit from the use of push and pull factors. Commanders can push the UASs to the optimal area of battlespace at a chosen moment. The optimized location of UASs may then guarantee the improved performance in own oncoming military maneuvers. The pull factor means pulling the data from the designated areas at a chosen moment. These data are pulled to increase the performance of own operations in analyzing the collected data. The collected data serve as raw material for defining SA and COP. The accrued data are utilized in the MDMP and in the process of choosing between different COAs.

A network structure offers a new and ubiquitous way to share and forward all kinds of data, including data collected

by various sensors, the Wireless Polling Sensor Network (WPSN) was introduced in [4]. Since nodes do not form a network per se but rather are polled by a selected node of the mobile network, they remain undetected due to their passive nature. Communication is critical in the execution process of command and control. When the possibilities offered by the Wireless Polling Sensor Network are taken into active use together with using One Time Pads (OTPs), two communication goals become achievable: the covert network and security in messaging. This is discussed more in Section VI.

When machines, such as UASs, are utilized, Service Oriented Architecture (SOA) becomes applicable. In digitized battlespace and in digitized operational planning, SOA is utilizable in allocating processes of own existing resources and optimizing the use of troops timely and in the correct operational area. SOA is also useful in offering assistance in the overall planning process. SOA can be used in optimizing the timing of the different actions, also while the dismounted company attack is in progress, and in automating the MDMP. By automating the MDMP and using UASs, commanders can save time, resources and lives as well as achieve the set objective.

In both military and civilian operations the need for updated analyzed data is equally important. The means utilized for collecting data on areas and targets of interest are identical as well.

The rest of this paper is organized as follows. Section II concentrates on the related work, Section III discusses the characteristics of Unmanned Aerial Systems, and Section IV targets the essence of practical communication. Section V deals with Wireless Polling Sensor Networks and the use of One Time Pads, Section VI deals with Military Decision Making Process, and Section VII tackles Situational Awareness and Common Operational Picture. Section VIII discusses the significance of sensors, and Section IX looks at SOA in relation to MDMP and reorganizing the chain of command in troops. Section X concentrates on possibilities offered by new technologies, Section XI comprises discussion, Section XII concludes with the results, and Section XIII addresses requirements for further studies.

The main contribution of this paper is the idea phase and conceptual level description of how the data accrued with the assistance of UASs can be implemented into a decision making process and how these collected and analyzed data in turn may enhance the results gained by means of a military decision making process. Also, improved situational awareness and common operational picture contribute in facilitating collective performance that can be identified as the overall performance capability in the execution of processes. Finally, this paper introduces idea phase methods on how to improve the process of automatic data gathering with the assistance of UAS and how to increase inputs towards automated decision making processes and towards automated military operations.

## II. RELATED WORK

The importance of UASs both in military and civilian environments has been recognized and several studies have

examined the overall performance of UASs in civilian settings. For instance, data acquisition for post-disaster assessment has been studied in [5]. Furthermore, [6] studied using UASs for inspecting structural damage caused by hurricane and concluded that UAVs have great potential for post-disaster data collection and assessment. The identified challenges included obstacle avoidance, site access, sensor coverage and weather conditions.

Moreover, civilian use cases of using UAVs include obtaining data on traffic trends and monitoring and controlling traffic in real-time to ease the traffic flows in risky areas, as indicated in [7]. In case of an emergency the pinpointed crash-site can be fast recovered and the injured evacuated.

UAVs have also been used for data acquisition for management and monitoring purposes in gas-pipeline inspection [8] with sustained UAV flying capacity for several hours.

Preparations for potential disaster-related usage of vision-based UAV navigation have been identified as an important factor in UAV navigation, see [9]. In this study, an algorithm was developed to identify structures within the UAV-collected imagery and navigation directives based on these structures were relayed back to the UAV.

The main challenges with UASs are linked with the limited communication ranges. This issue has been identified also in [1]. UASs have successfully been used in detecting different types of Points of Interests (POIs). The use of UASs in search and destroy missions has been challenging, as pointed out in [10]. The main challenges involve the communication process between the UASs [10]. The problem was solved by creating a new coalition formation algorithm to enhance the communication among the UASs.

In addition, UASs offer a more inexpensive solution than human-operated helicopters for monitoring high-voltage transmission lines [11].

As for the military use cases, several researchers have been studying the use of UASs in accruing data to support SA, COP and MDMP by increasing the performance of different types of networks. Moreover, the studies listed here have concentrated on increasing the speed, safety and capability to communicate in an improved manner.

As demonstrated in [12], ad-hoc networks can create a UAS access net ensuring communication among mobile or stationary users. These ad-hoc networks support Blue Force Tracking, as indicated in [13]. When UASs are equipped with Free Space Optics (FSO) communication links, operations can be executed by avoiding to become sensed by means of electrical reconnaissance detection, as concluded in [14]. FSO represents an optical communication technology that uses light propagating in free space to transmit data from point-to-point (and multipoint) by using low-powered infrared lasers, which can also be used for localization purposes, if range and orientation information is available. FSO-technology offers high-speed, up to 10 Gb, reliable and cost-effective connectivity for heterogeneous wireless services provision in both urban and rural deployments when Dense Wavelength Division Multiplexing (DWDM) is utilized in Radio-on-FSO (RoFSO) system.

In vision-based tracking, pan-tilt gimbaled cameras using Commercial off-the shelf (COTS) components can be used together with calculation algorithms and advanced controlling systems for integrated control of a UAS and an onboard gimbaled camera, see [15]. Along with the availability of both low-cost and highly capable COTS-based UASs and Unmanned Ground Vehicles (UGVs) and communications equipment, it is reasonable to apply quick and inexpensive means for surveillance, tracking and location purposes, as discussed in [16]. UASs of varying types and sizes can be used in aerial surveillance and ground target tracking, see [17]. To boost the performance of a single UAS, swarms of small UASs can rely on airborne MANETs, as indicated in [2]. Transmission antennas are significant in the process of operating UASs, as indicated in [18]. When swarms of UASs are utilized for navigation, localization and target tracking, information synchronization is important, as discussed in [19]. In present battlespace miniature UASs are becoming increasingly significant among surveillance applications, as shown in [20]. Remotely controlled UASs can act as an assisting tool in tracking and monitoring, as discussed in [15]. Remotely controlled UASs can enhance SA, Blue Force Tracking (BFT), thereby enforcing the probability of success in missions, even when operating beyond line-of-sight, see [21]. The means for exploiting UASs and UGVs in the processes of data collection and the distribution of an updated COP to be implemented in Shared SA are discussed in [22]. Battle Management Language (BML) can be seen as a common language enabler between machines and interfaces along with almost ubiquitous swarms of UASs [19]. For example, networks utilizing COTS components mounted on of UASs add survivability and remove the need for a line-of-sight connection, as described in [16].

This present paper examines how to facilitate a dismantled company attack with the use of UASs. This means aiming at optimizing the use of existing resources and automating an attack to the extent feasible. The objective is to contribute to the overall goal of increasing safety in military operations by means of improved use of resources resulting in decreasing numbers of casualties as well as increasing the tempo of own military operations.

The same calculation parameters and algorithms are utilizable both in military and civilian data collecting systems. This same applies to data transmitting systems.

### III. CHARACTERISTICS OF UNMANNED AERIAL SYSTEMS

Unmanned Aerial Systems utilized in a dismantled company attack can be autonomous or guided platforms built with COTS material ensuring the relatively low price tags on the UASs. The main function of UASs is to produce real-time data for commanders for decision making purposes. The use of swarms of UASs ensures the gathering of data behind the visual horizon. The distances between command link and the swarms of UASs are typically few kilometers. Once identified by the actions of an adversary, a UAS ends up becoming annihilated. Therefore, UASs have to be built to be disposable elements. When the UASs are used as swarms, the combat survivability of the system can be increased.

Some of the promising characteristics of the UASs involve long flight duration, improved mission safety, flight repeatability due to improving autopilots and reduced operational costs, especially in military environments, compared to manned aircraft. The potential advantages of an unmanned platform, however, depend on factors, such as aircraft and sensor types, mission objectives, and the UAS regulatory requirements for operations of a particular platform [2].

For the purposes of this paper, measuring the utilization of UASs in a dismantled company attack would require real functioning swarms of UASs. Creating a simulation to model a UAS assisted operation is at present, unfortunately, non-feasible on the grounds that neither funding nor facilities are available.

In Network Centric Operations (NCO) it is seminal to ensure identifying and defining relevant information to enable its distribution in the battlespace. This presupposes timely and secure information flow between own warriors and sensors [23]. UASs have to be used for collecting all the data available in the battlespace. Contemporary weapon systems require greater amounts of intelligence data at a higher accuracy level than ever before [13]. Since operations tend to be multi-national, different sensors and systems are required to communicate understandably between each entity. This means that all the participants representing different nations must agree on the wavelengths, frequencies, and waveforms to be utilized in the transmission processes between the sensors and base-stations. Various entities and nations typically utilize different types of signals and waveforms for varying reasons, and the utilization of the radio magnetic spectrum must be settled before a multi-national operation can be successfully executed. This is necessary to minimize instances of fratricide and collateral damage, which requires the maximized distribution of the updated COP. One solution for this involves utilizing Business Management Language (BML) [23].

As for the classification of UASs, the types of classifications vary depending on the source, as in [24]. A classification based on size includes the sub-classes of Small, Medium and Large UASs. The class of Small UASs can include Very Small UASs, which in turn can include Micro or Nano UASs and Mini UASs, whereas the categorization of UASs according to their travel ranges and endurance in the air include the following sub-classes developed by the US military: Very low cost close-range UASs, Close-range UASs, Short-range UASs, Mid-range UASs, and Endurance UASs. Table I below lists varying types of UASs.

Especially in civilian applications, UASs can be identified as collectors of data in ecological, meteorological, geological and human-induced disasters. UASs can be seen as versatile tools in data gathering for their flexibility, safety, ease of operation and relatively low-cost of ownership and operation. This facilitates UAS implementation in disaster situations, as described in [5].

This paper discusses only UASs because of their versatility compared to other Unmanned Vehicles (UVs), such as Unmanned Ground Vehicles (UGVs). When a small tactical level military unit, such as a company, is performing

a complicated maneuver, a dismantled company attack, the UASs represent the only reasonable type of UVs to be utilized.

The following Table I lists a classification of types of UASs built for varying purposes.

TABLE I. TYPES OF UASs

Type of UAS	Abbreviation	Altitude (meters)	Flight time / Distance (km)	Payload	Example of an UAS
Micro-Air Vehicle	MAV	Low <330 m	5 to 30 minutes / kilometers	10 – 200 grams	Mosquito, Carolo P50
Low-Altitude Short Endurance	LASE	<1000 m	1 to 2 hrs / few kilometers	200 – 500 grams	Dragon Flyer X6 VTOL
Low Altitude, Long Endurance	LALE	from 2000 to 4000 meters	several hours /tens of kilometers	up to several kilograms	RQ-11 Raven, Skylark
Medium Altitude Long Endurance	MALE	up to 9000 meters	+24 hrs / hundreds of kilometers	over 1000 kilograms	Ikhana, Heron 2, Predator B
High Altitude, Long Endurance	HALE	up to 20 kilometers	over 30 hrs / thousands of km:s	over 1000 kilograms	Global Hawk

UASs are capable of monitoring the designated target areas and transmitting real-time data to the base-station simultaneously when monitoring the area (see Figure 3).

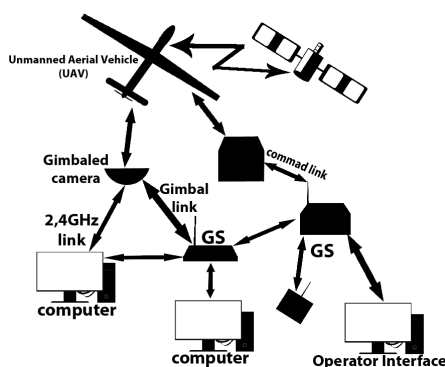


Figure 3. UASs and the data transmission [1].

When flight times are short, less than an hour, engines and sensors embedded into UASs can be powered by liquid fuel batteries to ensure adequate level of energy. Liquid Polymer (LiPo) batteries are utilizable for their capacity. Electrical surveillance components, guidance systems, and command systems depend on adequate electricity level.

Typically, the distance between a communication link and a swarm of UASs is few kilometers, and therefore 2.4 GHz Ultra-Wideband Network system between the communication link and the base station is applicable for these distances. The usual speed of swarms of UASs is tens of kilometers per hour. This is a chosen speed to balance the energy consumption and the range of transmission power and movement.

UASs are most versatile with their capability for quick deployment. UASs tend to be miniature-sized airplanes, drones and helicopters, weighing few kilograms. The range of these vehicles can vary from few hundred meters to few kilometers as can their mass and size. The same applies to the payload. The payload can be measured from tens of grams to few hundred grams depending on the use and measurements of UASs.

The typical payload of UASs can comprise varying sensors, such as: acoustic-, seismic-, magnetic-, visible image-, shortwave infrared (SWIR)-, thermal-, infrared-, low-light television (LLTV)-, and sensors for laser tracking and spotting, and for facial recognition. These sensor packages can be also deployed into the area of interest at a desired moment. If the area of interest is known well in advance, a UAS and the sensor package can be flown into the perimeter in advance and been dropped in the chosen area. In addition, a UAS can be guided close to the area of interest. The UAS can then be parked, for example, on rooftops and cliffs to wait for the command to start the reconnoitering mission. This saves time and positions the UAS in nearby perimeters of the desired area. The UASs remain hidden and hard to detect, and when detected, it is too late anyway.

In versatile combat situations, different types of Combat Information Systems (CISs) implemented by sensors are important parts of military command and control environment systems [25]. Raw reconnaissance data remain critical for creating a comprehensive Situational Awareness and Common Operational Picture. Without constant flow of intelligence and surveillance data, successful military operations cease from existing.

The significance and potential of miniature UASs has been discussed since the beginning of the past decade. Today, miniature fixed-wing UASs are mainly used to target drones, for surveillance, and as decoys [26].

Examples of target drones do not belong to the category of miniature fixed-wing aircrafts, but they are full-scale target drone types, such as MQM-117. Target UAV series include three members: MQM-117A, MQM-117B and MQM-117C.

In terms of reconnaissance drones, a famous example is RQ-11 Raven UAV. As for decoy drones, identifiable are Israeli manufactured Firebee 1241 and Scout.

For civilian purposes, the main uses of UASs include internal security, for instance border patrol, victim search and rescue, research, wildlife and land management, and agricultural maintenance processes.

#### IV. COMMUNICATION BETWEEN ENTITIES

The amount of data accrued via versatile sensors and tracking systems is vast. As a result, to distribute the location information filtered and fused through various systems remains a challenge. As said, warriors' main function remains to fight instead of double-checking the monitor of their palm-top or equivalent. Besides, there will always be disturbances in the electromagnetic spectrum, quality of service (QoS) and transmitting power along with the limited bandwidth set limitations to the ubiquitous communication

systems. However, the possibilities of battlespace communication are versatile, since almost all the sensors utilized are somehow linked together to facilitate BFT and Combat Identification (CID) and to improve COP and SA. UAS can be seen as a functional tool in the process of accruing data, see Figure 4.

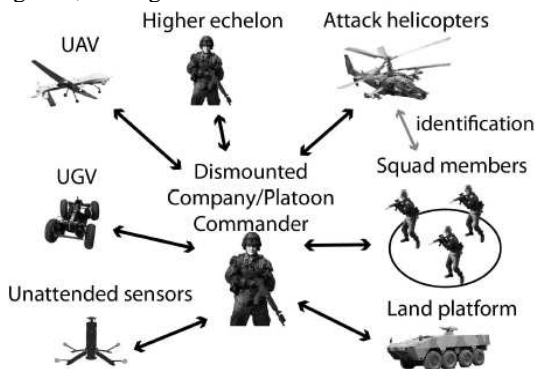


Figure 4. Data accruing process in brief.

When UASs are utilized in operations, the significance of communication links cannot be overemphasized. UAS are extensively used in exploration missions. They are used routinely to collect and send collected data back to ground station that provides real-time information on the covered area. Printed antennas can be seen as a solution in UASs. As described in [27], the significance of a functional printed antenna has been successfully tested and reported concerning a study in which printed antennas were used in computers for wireless local area network (WLAN) connectivity in the frequency of 2.4 GHz ISM (802.11b.g) and the 5 GHz (802.11a) bands. Printed patch antennas are widely utilized in automobiles as antennas for receiving signals of the global positioning system (GPS) and also in satellite digital audio radio systems (SDARS). These systems pose acceptable gain and radiation efficiency, as described in [28].

The capability to communicate between troops (soldiers) and machines (UASs) must be sustained throughout an operation. Without communication there is neither command nor control between the entities. Communication can be described as comprising three layers. These layers are sensor-layer, C<sup>4</sup>I<sup>2</sup>S layer and shooters layer. The layers are connected with the existing communication networks. Different layers are depicted in Figure 5.

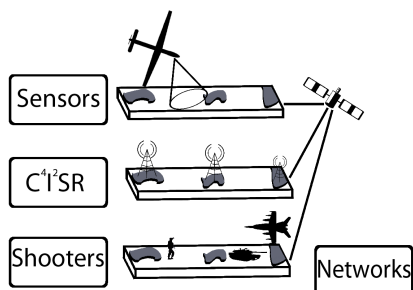


Figure 5. Communication network from sensor to shooter [1].

The depicted layers communicate and forward data via UAS-radios, which can utilize the output of GPS/GLONASS receivers for automatic position reporting. When Software Defined Radios (SDRs) are embedded onboard UASs, typical SDRs' features can be included into transmission protocols. These include: Multiband 30 – 512 MHz, multimode, multi-mission, software programmable architecture, Low Probability of Detection (LPD) and Low Probability of Identification (LPI), simultaneous voice and data, updated and analyzed data transfer from sensor to decision maker and onwards to the shooter applications. Lightweight UAS-implemented radios offer low consumption transceivers operating in the frequency of 2.4 GHz Industrial, Scientific and Medical (ISM) band. The use of this frequency offers very low Radio Frequency (RF) signature modulation scheme based on spread spectrum technology (DSSS) and provides a robust, reliable and low probability of detection time division multiple access (TDMA) waveform. Radios typically feature advanced encryption standard (AES) encryption providing a very high security level on the transferred audio and data systems, while security keys can be downloadable. UAS -radios can provide several tactical communication services: full-duplex voice conferencing, GPS reporting, e-mail, chat, file transfer, and real-time video streaming.

When properly adopted into active use, UASs can be seen as flying hubs or flying relay-stations, tools of communication. When UASs are used to secure communication, as depicted in Figure 5, the throughput of communication can be maximized. Furthermore, the swarms of UASs end up creating an own data communication system, as depicted in Figure 6. This ensures that the data transmission distances between UASs remain short and become operationally secure. This aids in meeting the requirements of Low-Probability of Detection (LPD) and Low-Probability of Identification (LPI). The described delicate system introduced is a new one and based on ideas that can be executed by utilizing existing COTS- technology [29].

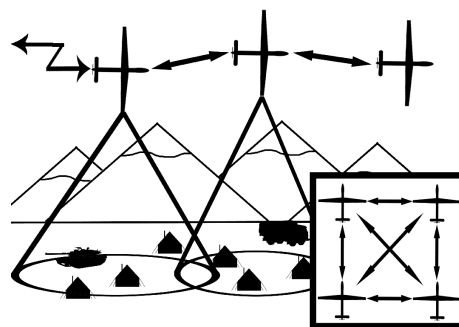


Figure 6. A data exchange process inside the swarm of UASs [1].

Figure 5 describes the idea of using UASs as swarms. The number of UASs used in each scenario varies depending on the commanded mission and its speed and other set requirements.

## V. WIRELESS POLLING SENSOR NETWORKS

A battlespace tends to be embedded with different types of sensors found from the soil, airborne or attached into various types of manned and unmanned vehicles. The utilization of Wireless Polling Sensor Network (WPSN) together with One-Time Pads (OTP)s can be viewed as one possible solution for the improvement of a communication system between sensors and UASs. In the case of UAVs and other easily captured nodes there is a special disadvantage in using ordinary crypto algorithms requiring a stored key. Furthermore, neither the time nor the computing power is available for asymmetric algorithms. A solution to this problem is presented by a novel idea of exchanging One-Time Pads and encrypting data with one of the OTPs. One-time pad (OTP), or Vernam's cipher, is a crypto algorithm where the key is as long as the plain text. The modern version of the algorithm simply takes a bitwise exclusive or of the key and the plain text. The idea is explained in [30].

The other OTP must be discarded for security reasons WPSN can be viewed as one possible solution when gathering data from different sensors and sensor networks. When a swarm of UASs is utilized in forming an ad-hoc network and polling a large number of fixed sensor nodes, a secure network system can be created. The WPSN system is more robust in the military environment than traditional Wireless Sensor Networks (WSNs). Although WSNs have been used for a long time, they demonstrate particular disadvantages. These include the fact that multi-hop transmission fails when nodes are destroyed in military environments, battery lifetime creates limitations, and security challenges remain unsolved. A WPSN has advantages in all of these areas compared to other proposed solutions. WPSN comprises a small mobile ad-hoc network of UASs and a high number of fixed ground-based sensors, which are periodically polled by the UASs.

The advantages concerning WPSN and OTP include that in the WPSN solution the fixed sensor nodes remain concealed, yet active, because the sensor nodes of WPSN do not communicate with each other but only respond to polling by the mobile nodes. The WPSN node communicates with a UAS through encrypted messages. Thereby, WPSN responds only after a UAS has submitted a polling request with a specific code. The routes of UVs can be fed into the systems early enough to gain the needed information from the designated areas [30].

When speaking about a battlespace and actions taking place in this hostile environment, it is mandatory that some of the UASs be shot down or destroyed by other means of contemporary warfare. This possibility must be recognized prior to engagement. UASs must be designed so that once malfunctioning, they will get automatically destroyed (software and hardware) to become instantly useless for the adversary. Yet, this destruction of one UAS does not jeopardize the concept of sustained secure communication, for the network composed by remaining UASs will reroute itself automatically.

By exploiting WPSN and OTP it is possible to utilize UASs as described above when gathering data both in

military and civilian environments. Especially the using of OTP increases operational security in both of these digitalized environments.

## VI. MILITARY DECISION MAKING PROCESS

In military operations performed at tactical level, i.e., battalion and below, the significance of tempo and timing becomes critical. In the MDMP all the raw data collected by UASs have to be analyzed and taken into account as they are directly connected with targeting systems, weapon selection processes, COP, SA and Control, Command, Computers, Recommunication, Information, Intelligence, Surveillance and Reconnaissance (C<sup>4</sup>I<sup>2</sup>SR).

Here, automation and mathematics can be seen as assisting tools in the process of making rapid and reliable decisions. When mathematical methodology is implemented, measuring the additive value model is the simplest and most commonly used mathematical model in multiple objective decision analysis. As described in [31], the additive value model is given by the equation:

$$v(x_j) = \sum_{i=1}^n w_i v_i(x_{ij}) \quad (1)$$

where

$v(x_j)$  is the total value of alternative  $j$ ,

$i=1$  to  $n$  are the value measures specified in the qualitative value model,

$x_{ij}$  is alternative  $j$ 's score (raw data) on value measure  $i$ ,

$v_i(x_{ij})$  is the single-dimensional value of alternative  $j$  on value measure  $i$ ,

and  $w_i$  is the swing weight of value measure  $i$ .

Equation (1) is the simplest and most commonly used mathematical model in multiple objective decision analysis.

Obviously, mathematics alone cannot solve the dilemma of making the correct operational decision quickly in a chaotic combat setting. When a decision is made between different COAs, mathematics and probability prognosis can only be seen as assisting tools. The human commander remains the only one who is responsible for sensible and applicable decision, which can be converted into commands to be issued and executed in an operation.

## VII. SITUATIONAL AWARENESS AND COMMON OPERATIONAL PICTURE

The term Situational Awareness has been given an apt definition in the Army Field Manual 1-02. SA can be understood as knowledge and understanding of the current situation, which promotes timely, relevant and accurate assessment of friendly, competitive and other operations within the battlespace in order to facilitate decision making. SA, furthermore, equals an informational perspective and skill that fosters an ability to determine quickly the context and relevance of events that is unfolding. The term SA

comprises three levels: 1) perception, 2) comprehension and 3) projection [32]. SA, or, the lack of it, remains critical in performing military operations successfully. The means to increase SA can and must be fostered and developed, since the loss or deterioration of SA results in inaccuracies, human errors, and eventual casualties and fratricide. The military operation in progress usually fails because of poor level of SA.

Situational Awareness has a strong relation to COP. COP represents an overall understanding of the prevailing situation in the battlespace. COP can be displayed on the screen of a computer or a digital device, and by using markers and traditional maps. COP features elements, such as individuals of friendly forces, neutral entities and the adversary, presented by symbols of various types.

To complete the list of phenomena affecting the MDMP, C<sup>4</sup>I<sup>2</sup>SR needs to be taken into account. UASs are utilized to assist the MDMP performed in C<sup>4</sup>I<sup>2</sup>SR environment. When combined together as swarms, UASs form tools for accruing data, forwarding and analyzing these data into the form of information to create COP and increase SA.

To sum up, all these listed elements are linked to the MDMP. The decisions made as part of the MDMP can also be seen as tools in targeting and weapon selection processes. Figure 7 explains the relations and functions inside MDMP when the use case is related to targeting and weapon selection systems. In the MDMP, the end-come is the optimal use of weapon systems to avoid collateral damage and fratricide.

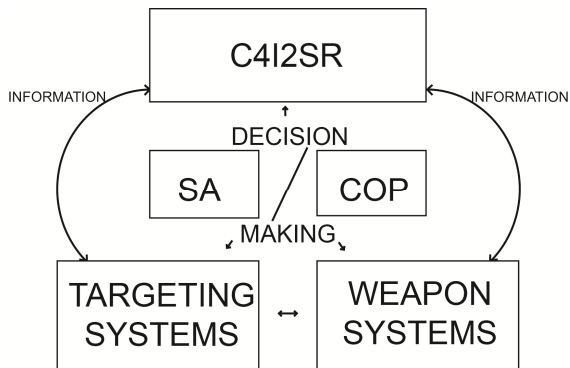


Figure 7. Decision making system in targeting and weapon systems [33].

### VIII. SENSORS

In order to achieve the set objective in a given military setting, it makes sense to utilize maximally the data produced by various types of sensors when accruing data from hostile environments. In some cases, especially when the weather conditions are challenging, for example, the wind speed exceeds 10 metres per second, the UASs cannot be used or they are too slow and there has to be an alternative possibility to deploy sensors for accruing real-time data. Some of these sensors can be deployed to the area of interest with the assistance of artillery fire produced by mortars or cannons. Rapidly deployable airborne sensors represent relatively inexpensive and versatile tools for low-level

battalion and company operations. As indicated in [33], light sensor munition can be deployed behind enemy lines, and an example of sensors' deployment, when UASs are not applicable, is Sensor Element Munitions (SEMs). SEMs can be manufactured of composites surfaced with materials capable of absorbing radar beams, making the SEM less visible in enemy counter-artillery radars. In any military operation, airborne sensors are important for missions, such as force protection, perimeter control and intelligence utilization, as discussed in [34]. Transmitting the accrued data to prevent cases of fratricide and to ensure success in operations presupposes optimal communications. WiMAX transmission offers applicable possibilities in forwarding collected data. The distances in the transmission process are relatively short, ranging from 1 kilometre to few kilometres in conditions of clear Line-Of-Sight.

The sensor package inside sensor element munitions is named Sensor Element (SE), which is made of COTS-products comprising sensors capable of sensing most of the phenomena occurring in the electromagnetic spectrum. Overall, COTS-products are relatively inexpensive and reliable in terms of function, as explained in [35]. Sensor Elements can contain the same sensors as UASs. The command post has the capability for the data fusion of all the accrued sensor information.

Once an SE is airborne, it immediately starts to transmit the gathered data to friendly troops either directly or, if the transmission distance exceeds the capability of the transmission unit, the SE transmits the data to another airborne device, which acts as a relay station in relation to own troops. The SE communicates with the receiver station and other sensor element packages over a 2.4 GHz Ultra-Wideband Network system. The accrued data are encrypted for security reasons. The composition of SEMs is depicted in Figure 8.

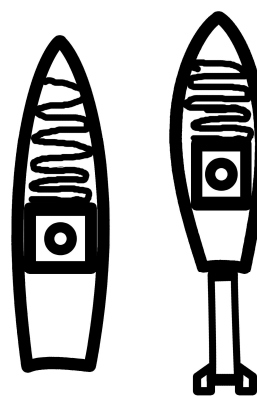


Figure 8. Structures of Sensor Element Munitions (SEMs): An artillery SEM (left), a mortar SEM (right) [33].

SEMs can be deployed to the target area with manned artillery weapons or unmanned remotely controlled pieces of artillery or by using mortars, as mentioned earlier. The process of deploying SEM to the area of interest is depicted in Figure 9. SEM ejects the Sensor Element, which in turn reports the gathered data to the base station [33].

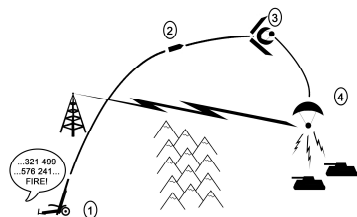


Figure 9. Process on how to deploy an SE to an enemy territory [33].

In Signature Prediction Process (SPP), described in [33], sensors accrue data and transmit these data for analysing centres. These data collected with SEMs are then verified with the data collected with other sensors in order to predict and anticipate the target and its actions. These data can be also utilized in analysing different possible courses of action and in the weapon selection process.

When we implement a weapon of any kind as part of the unmanned aerial system, we are dealing with an Unmanned Combat Aerial System (UCAS). The route planning of a UAS or Unmanned Combat Aerial System (UCAS) is in a significant role when an operation is in its planning stage. The same applies to the significance of algorithms in time limited operations, as indicated in [36]. The reconnoitering range tends to vary from one to few kilometers. When a dismounted company attack is supported with units of UASs tailored for Close-Air Support (CAS), the data exchange transmission process for the target data is depicted in Figure 10.

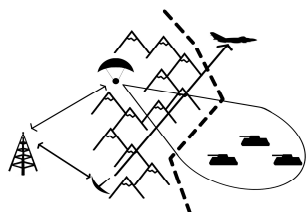


Figure 10. The process of detecting target to the shooter [33].

The UASs of CAS units optimize the speed and destruction power used in proximity to destroy the designated targets. When a small unit operates, it needs to achieve results in short time in order to maintain the initiative and reach the set objective. A company is a small military unit, which has to maximize the momentum offered by the performance produced by CAS units. UASs must be utilized as tools to evaluate the outcome of the executed CAS fire-mission. If the result of CAS fire-mission is reported not to fulfil the requirements set, the new round of CAS fire-mission must be performed to destroy the chosen target.

#### IX. SERVICE ORIENTED ARCHITECTURE

SOA offers a variety of possibilities to improve the performance in military operations. When UASs become more increasingly identified as an exploitable resource in the military data producing environment and as the inputs of the UASs become fully utilized operationally, SOA is going to

render itself useful for military commanders in executing military operations. SOA can be exploited when needing to reorganize the military organization after casualties affect the chain of command in a dismounted company. This process is described in [37]. Military operations nowadays usually demonstrate features of Network Centric Warfare (NCW) in which one key aspect is to be able to offer a valid and accurate COP for the operating troops in the battlespace. A basic requirement for a military commander is the ability to command the troops and sustain optimal SA and COP. An important aspect in distributing information in the battlespace is the amount and quality of information shared at different levels. SOA can be seen as a useful tool in distributing data in a preprogrammed manner. The amount of information allocated must be set to a level where the decision maker can perform timely and draw accurate conclusions. In the battlespace, the units suffer from casualties and the chain of command never remains intact.

A constructive idea in SOA is in its process ideology. In a dismounted company, the composition of the unit and its performance are critical in executing the operations. Military units suffer from casualties and their mathematical performance value tends to change in an unpredictable manner. The performance of a military organization, such as a dismounted infantry company, can be mathematically calculated as explained in [37]. Behind these mathematical values is a Psycho Physical Factor, described in [37]. The process of creating this factor is described in [38] and the formula may be useful in calculating the performance of a military unit.

The implementation of SOA is described in [37]. A key aspect in the presented architecture [37] is the dynamically changing architecture. Benefitting from the possibilities offered to orchestrate data and services with the assistance of SOA allows for improved performance in the execution of operations. SOA can be utilized in the process of choosing between different COAs. Eventually, the chosen COA will be fine-tuned into commands and manoeuvres of a dismounted company attack.

In applying SOA paradigms, loose coupling, dynamic binding and independency of development technologies, platforms and organizations, as well as locations, all these become advantages in that the use of SOA typically encourages reusing services. The identified assets belong to military units, but military units offer their responsibilities through services, and capability deployment requires invoking and integrating a number of services. Figure 11 depicts the relations of services, assets and capabilities of a military unit.

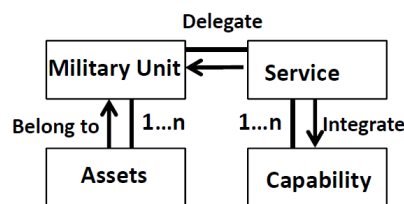


Figure 11. Conceptual model of C<sup>4</sup>I<sup>2</sup>SR capabilities based on SOA [39].

In a dismounted company attack, all operating military platoons use the same services and assets of a dismounted company. In this case, SOA itself offers a flexible approach to identify C<sup>4</sup>I<sup>2</sup>SR capabilities when several platoons benefit from the services and assets of a dismounted company. SOA enables a company to respond more quickly to the changing battlespace situations and requirements to execute the given missions in the given time and with the allocated resources.

X. POSSIBILITIES OF NEW TECHNOLOGIES

In order to be able to obtain depth of information, detailed digital data on the desired target, new technologies that render increasingly detailed information on the given targets become indispensable. These technologies include hyperspectral and multispectral imaging.

The classification of hyperspectral data by using statistical pattern recognition methods requires a lot of processing time. Image channels of the data are strongly correlated with each other. The classification and recognition of images requires algorithms of correct type. Hyperspectral images are produced by imaging spectrometers. Remote imaging has been utilized for scanning Earth and planetary surfaces. Typically, spectrometers are able to perform spectral measurements of bands, typically at least from 0.4 to 2.4 micrometers. The range represents visible through middle infrared wavelength ranges. Remote imagers in turn are designed to focus and measure the light reflects from many adjacent areas on the Earth's surface. The principle of spectrometer is presented in Figure 12.

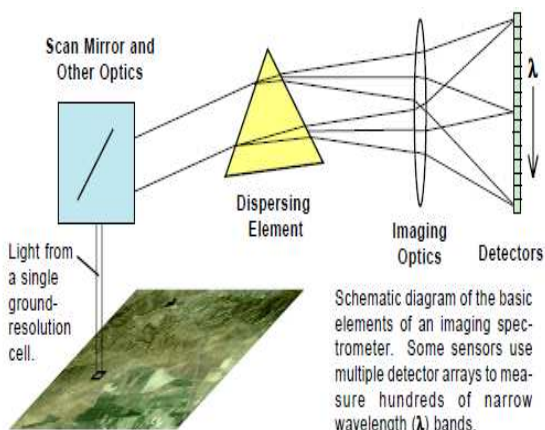


Figure 12. Functionality of an imaging spectrometer [40].

To interpret the scanned images, it is vital to understand spectral reflectance. As indicated in Figure 13, vegetation has higher reflectance in the near infrared range and lower reflectance of red light than soil [40].

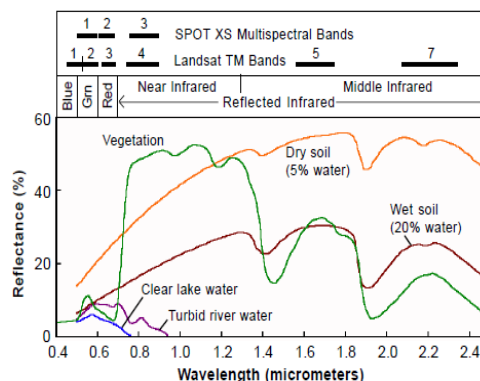


Figure 13. Representative spectral reflectance curves for several surface materials over the determined spectral range of visible light to reflected infrared [40].

Spectral libraries are important for they provide a source of reference spectra that can assist in the process of interpreting hyperspectral images. Imaging sensor converts detected radiance in each wavelength channel to an electric signal, which is then scaled and quantized into discrete integer values that represent encoded radiance values [40].

There are different strategies for image analysis. To interpret the collected data remains a challenge. Finding appropriate tools and approaches for visualizing and analyzing the essential information in a hyperspectral scene remains an area of active and constant research. Various countries and organizations have studied different approaches to solve the appropriate number of bands and wavelength ranges in order to improve the performance of spectrometers. The following Table II features the names of different types of sensors, organizations, number of bands used and wavelength ranges that have been identified.

TABLE II. A SAMPLE OF RESEARCH AND COMMERCIAL IMAGING SPECTROMETERS

A Sample of Research and Commercial Imaging Spectrometers				
Sensor	Organization	Country	Number of Bands	Wavelength Range (μm)
AVIRIS	NASA	United States	224	0.4 - 2.5
AISA	Spectral Imaging Ltd.	Finland	286	0.45 - 0.9
CASI	Itres Research	Canada	288	0.43 - 0.87
DAIS 2115	GER Corp.	United States	211	0.4 - 12.0
HYPMAP	Integrated Spectronics Pty Ltd	Australia	128	0.4 - 2.45
PROBE-1	Earth Search Sciences Inc.	United States	128	0.4 - 2.45

Hyperspectral image is comprised of several layers. Each layer contains data in certain wavelength. This is depicted in Figure 14.

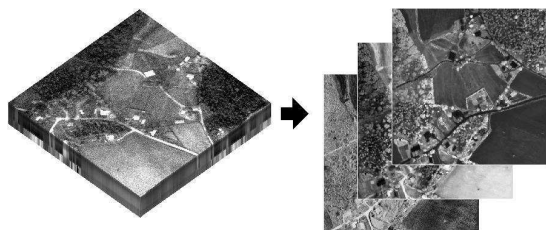


Figure 14. Hyperspectral image comprises several gray scale images that depict the same are in different wavelengths. [41].

Figure 15 features an image, in which steel rooftops are visible in white. The white color is visible in the process of interpreting the visual images provided by the sensors.



Figure 15. Steel roofs of buildings seen in white color [41].

One of the techniques used in UASs, laser scanning involves a scanning sensor transmitting thousands of pulses towards the target area (for example, terrain). The reflected echoes of pulses are then measured. Interpreting the collected images requires automatic classifiers. They search for artificial objects from the gathered data. In the future full waveform scanners are expected to produce more precise images from the scanned areas.

In thermal imaging sensor packages now weigh only 120 grams. The size and energy consumption of commercially produced sensors have decreased.

As indicated in [42], miniature size UASs, weighing few kilograms, equipped with payloads of hundreds of grams, are capable of performing reconnaissance operations performed during a short period of time. The typical Spatial Resolution (MS) is from one to twenty centimeters, when the flight-altitude remains below 500 meters as described in [42].

In practice, when two images, which have been taken from an identical area in a different time slot, are closely compared, it becomes possible to identify the changes. In doing so, changes surface concerning vehicles, pieces of artillery units, troops, and man-made bridges in the area of interest.

## XI. DISCUSSION

Although there are similarities between the military's operational requirements and those of the civilian UAS industry, standardization is still very much lacking. Yet, it is standardization that is required between the military settings and civilian UAS markets. This is because the equipment needs to be compatible and interoperable and used for data collecting jointly if necessary. Unless there are set standards, end-users of technology cannot benefit from the development of synthetic vision systems, sensors, flight hardware, advanced materials and robotic systems as none of these would be affordable.

As for the seminal terminology, definitions of UAS and UAV can be found in [43] and [44]. Obviously, academia and industry continue to affect the evolution of the terminology used. Also, when dealing with organizing services among different entities, Service Oriented Architecture is an important issue. As indicated in [45], SOA fosters loose coupling of software assets, reuse of software components, acceleration of time to market, and reduction of organizational spending. The object is to benefit from the data collected with the best solutions available to increase the operational performance in accessing services, and lastly, to increase the speed and safety of operations executed. .

The data produced by various multi-sensors can be utilized in the data refinery process to ease the recognition and identification process. This can be done with the assistance of data fusion processes by resorting to computer-programs designed for these data fusion processes [33]. In fact, when using the KNearest-Neighbour (KNN) algorithm, approximately 80 % of unknown target samples can be recognized correctly, when the known target classification accuracy remains above 95 %. This enables the use of the ATR and the Automatic Target Cues (ATC) [33].

As presented in publications [1], [33], the size and type of sensors have dramatically improved during past years. Sensors can be embedded inside artillery munitions or dispersed from aircraft. In some cases, helicopters can act as mother ships containing from tens to hundreds of small UASs and transport and drop them in designated areas for data accruing purposes.

When the UASs are successfully utilized in the different phases in a dismounted combat attack, the results can be optimally utilized. These gained results can be identified and evaluated in relation to the different stages of the process of a dismounted company attack. When the need of a requested service is identified, automated systems assist to fulfil the need of any type (need of data, resupply, firepower, evacuation).

UASs can be used for collecting updated and existing data and serving in the role of a radio transmission relay-link, as a flying hub-station and in assessing the impact of artillery fire. Using swarms of UASs enables quick, reliable and effective data collecting from a specified area. Furthermore, when UASs function as the communication link, the chain of command and control remains secure as regards communication.

By exploiting the data accessed by means of using UASs it is possible to enhance a dismounted military operation: readjusting the direction and action of combat units and increasing their speed. The communication between UASs and ground base-stations is encrypted. This ensures that the data collected and communication transmitted remain intact and coherent. UASs may fly via automated waypoints or serve as fighter-operated systems. UASs can be designed to be disposable, self-destroyable, once their task has been completed, or in case of malfunction, or if encountered by enemy. The use of SEMs becomes applicable in cases when the weather conditions are challenging, for example, the wind speed exceeds ten meters per second, or if data concerning a target must be rapidly accessed.

Compared to traditional WSN-systems, WPSN allows for improved security protocol in the communication between UASs and sensors. Data collecting systems gather raw data on battle space phenomena, for example, troop movements and action. These raw data feed the MDMP and facilitate speeding up the decision making. Using mathematical models and –programs produces improved SA and COP, compared to non-automatized human decision making performance. The improved SA and COP allow for significant increase in efficiency as regards planning and implementing the tactical use of destructive fire power.

As the raw data collected by UASs are already in electronic form, SOA can be utilized in planning, distributing and optimizing resources: evacuation, supplies, use of artillery fire. When the described systems for data collecting, analyzing, and communicating function as planned, it becomes possible to carry out an automated, computer-assisted attack as described in Figure 16. Utilizing FSO communication links fosters reliable, secure and coherent communication in command and control processes.

If and when all the accrued data can be properly processed and analyzed in MDMP with the assistance of SOA, the performance of troops can result in an automated dismounted company attack as depicted in Figure 16.

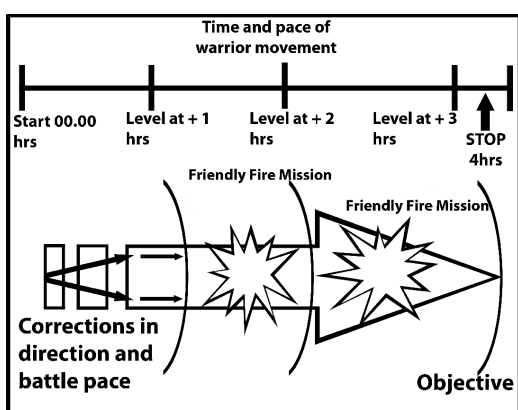


Figure 16. An automated attack operation. [1]

Figure 16 aims to visualize the goal of commanding military troops with the assistance of a computerized Artificial Intelligence (AI). The final commands for the military units to move and execute are given by a human

commander, not by a machine. UASs can be seen as tools in monitoring and assisting in an operation when re-adjusting its pace: If the pace of the units or an individual soldier is too slow, the data transmitted by UASs is utilized to fine-tune the speed and direction of the operating troops. The SA data acquired by means of UASs must be used in taking the initiative and translating it into success in battle and eventually meeting the set objectives of the given military operation.

As indicated in Figure 16 that features an automated military attack, similarly it is possible to control and command a search and rescue operation in a civilian setting, for example in a traffic crash. In other words, the executed operation is automated and sequenced. The use of mathematical classifiers is based on computational power and effective algorithms. The effective algorithms are utilizable both in military and civilian environments in that they do not separate environment-specific factors per se but rather merely calculate the values inserted in the algorithms regardless of the environment in question.

## XII. CONCLUSIONS

This paper examined how to utilize the real-time data collecting ability provided by UASs in order to improve the performance of a military performer and a civilian entity. This would require also standardizing the UASs to benefit both entities. The approach adopted is an idea-stage examination and as such aims to provide grounds for further discussion.

From a civilian perspective, the use of UAVs offers more cost-effective operational monitoring and management of natural resources. In flying low and slow and being comparatively affordable, UASs provide scientists with new opportunities for large scale appropriate measurement of ecological phenomena. This speeds up data gathering and saves natural resources in terms of energy consumption (aviation petroleum). The use of UASs does not disturb the balance of nature (animals, vegetation, birds migrating) more than using human-labor intense data gathering methods. From a military viewpoint, this paper relies on benefitting from the use of UASs as part of a dismounted company attack [1]. When doing so, it also points out the necessity of rapid data collection to support the fast MDMP.

According to the studies covered, it is important to continue doing research to improve the capabilities of data accruing with the assistance of UASs of various types. The variety and versatility of UASs continue to increase with UASs equipped with octo-rotors for superior maneuverability and stability as well as vertical take-off and landing. UASs are equipped with several types of sensor-packages depending on the data to be accrued. Also, the prevailing circumstances, such as mission duration and weather conditions, affect the equipping of UASs with bespoke sensor packages.

UASs are capable of producing high quality of data especially when platforms operate with low speed and in low altitude. Especially search and rescue missions benefit from mission effectiveness of the sensor and scanning systems, when sensors have enough time to monitor the areas beneath.

The UASs have to be able to communicate constantly with the base-station, and network reliability has to be ensured. The significance of connectivity presupposes that UASs must utilize suitable and reliable communication means and frequencies. Printed antennas have proved their efficiency in the frequency of 2.4 GHz ISM band. Embedded antennas provide several advantages for UASs, including reduced weight, lower manufacturing costs and lower drag.

The utilization and performance of UASs can be seen as data collectors in the battlespace. Sensors embedded into the UASs used can produce different types of data from the designated area. UASs can be deployed in most weather conditions and immediately when required, as there are no latency times. The data collected by UASs are then transmitted to the command posts. The collected real-time data remain critical for the MDMP. The data accrued must be in a pre-defined digitized form, which is applicable in digitized decision making systems exploited in the battlespace. The level and quality of SA continues to be critical at the dismounted close combat soldier level, whilst the level of COP plays an important role in command posts, where operations are planned, commanded and controlled.

Laser scanning and hyperspectral imaging offer new plausible means to accrue data from the battlespace. However, as these are technologies in-progress, uncertainty must be accepted.

The data for the MDMP are collected by using various types of sensors embedded into UASs and SEMs. The key issue is the speed of deploying the sensor package to the area. The prevailing combat situation in the battlespace determines the selecting of the type of UAS and sensor package embedded. The data accrued must be in a digitized form applicable in the software environment used. SOA can be used in re-organizing troops and allocating resources.

The ultimate goal of a dismounted company attack is to execute the mission with the resources allocated and to obtain the set objective. This asks for sustaining timely performance with a minimal number of casualties, decreased instances of fratricide and with the least possible amount of collateral damage. The objective is difficult to obtain, when relying on soldiers prone to erring. However, operational performance can be improved if the data collected by means of UASs are reliable and timely and can be adopted in active use to facilitate decision making. The possibility to use updated and analyzed data is vital for operations' success, especially in operations executed at a low operational level, such as a dismounted company attack. The utilization of these said data for decision making purposes may result in increased individual and collective performance capability in the executing of operations. With improved levels of SA and COP, operational security may be sustained.

When computers act as assisting tools both in the MDMP and its civilian equivalent offering suggestions as commands to the commander of attacking troops or, say, the staff in a search and rescue mission, the commander either approves or rejects the suggested commands. Thus, the role of a human decision maker remains critical in the chain of command.

### XIII. FUTURE WORK

Because Situational Awareness data remain vital in successful military and civilian operations, the reliable data must be gathered with all the possible means available. This applies to civilian cases of success as well. Attention must be paid to planning the utilization of UASs together with accounting for the operational security issues concerning using software and hardware in the battlespace and in, for example, civilian rescue operations.

Future work must be focused on system reliability and ease of use of selected tools to improve COP and SA in both civilian and military environments.

The usability of UASs to create a functional communication network requires field testing in combat exercise settings prior to any operational use. UASs have to be remotely destroyable both physically and digitally. The capability of UASs to self-destroy when malfunctioning or having been shot down must be tested. Other identified challenges are related to maintaining an adequate level of constant energy flow and protecting against violations caused by electronic warfare.

The use of SOA in assisting the MDMP has to be studied in combat exercise settings as well in order to gain realistic and relevant data on human commanders evaluating COAs when planning a dismounted company attack.

It is impossible to interpret digitized data without appropriate and suitable algorithms. Therefore, calculation power is needed to improve the performance of MDMP and the utilization of SOA. When appropriate solutions are designed to meet these challenges, the planning and execution capability of both military and civilian operations may significantly increase.

Obviously, this involves implementing technologies so that they conform to the requirements set by the given usage environment. Data gathering tools and mathematical algorithms operate on the same principles whether the operational environment is a military or civilian one. The key is to allow for reliable data gathering in all circumstances complemented by reliable data analyzing and utilizing as part of digitalized decision making. Prior to making decisions the decision maker needs to have timely and secure access to the most recent Situational Awareness concerning the Area of Interest. This may then optimize operational success and eventually bring about the desired end outcome.

### REFERENCES

- [1] T. Saarelainen, "Unmanned Aerial Vehicles as Assisting Tools in Dismounted Company Attack," in Proc. of NexComm, April 19 – 24, 2015, Barcelona, Spain, ISBN: 978-1-61208-396-4, pp. 19 – 27.
- [2] A. C. Watts, V. G. Ambrosia, and E. A. Hinkley, "Unmanned Aircraft Systems in Remote Sensing and Scientific Research: Classification and Considerations of Use," Remote Sens. 2012, vol 4, 1671-1692; doi:10.3390/rs4061671.
- [3] A. Kim, M. Kim, E. Puchaty, M. Sevcovic, and D. Delarentis, "A System-of-systems framework for the improved capability of insurgent tracking mission involving unmanned aerial vehicles," in Proc. of 5th International Conference in System

- of Systems Engineering, Loughborough, 2010, doi:10.1109/SYSOSE/2010.5544076, pp. 1 – 6.
- [4] T. Saarelainen and J. Jormakka, “C4I2SR Tools for the Future Battlefield Warriors,” in Proc. of IEEE International Conference on Digital Communications (ICDT) 13-19 June, 2009, Athens, Greece, pp. 38 – 43, doi:10.1109/ICDT.2010.15.
- [5] S. Adams, C. Friedland, and M. Levitan, “Unmanned Aerial Vehicle Data Acquisition for Damage assessment in hurricane events,” in Proc. of 8th International Workshop on Remote Sensing for Disaster Management, Tokyo, Japan, [https://blume.stanford.edu/sites/default/files/RS\\_Adams\\_Survey\\_paper\\_0.pdf](https://blume.stanford.edu/sites/default/files/RS_Adams_Survey_paper_0.pdf), accessed on Aug 30, 2015.
- [6] K. Pratt, R. Murphy, et al., “Requirements for semi-autonomous flight in miniature UAV for structural inspection,” Proc. in Association for Unmanned Vehicle Systems International, Orlando, Florida.
- [7] A. Puri, “A survey of unmanned aerial vehicles (UAV) for traffic surveillance,” [www.citeseerx.ist.edu/viewdoc/summary?doi=10.1.1.108.8384](http://www.citeseerx.ist.edu/viewdoc/summary?doi=10.1.1.108.8384), accessed on Aug 30, 2015.
- [8] D. Hausamann, W. Zirnig, et al., “Monitoring of gas transmission pipelines – A customer driven civil UAV application,” Proc. in 5th ONERA-DLR Aerospace Symposium, Toulouse, France, 2003.
- [9] S. Rathinam, Z. Kim, et al., “Vision based following of locally linear structures of using an unmanned aerial vehicle,” in Journal of Structure Systems, vol. 14, no.1, pp. 52 – 63, 2008.
- [10] J.M. George, P.B. Suit, J.B. Sousa, and F.L. Pereira, “Coalition formation with communication ranges and moving targets,” in Proc. of American Control Conference, June 30 – July 2, 2010, Baltimore, U.S.A., pp. 1605 – 1619, doi:10.1109/ACC2010.5531604.
- [11] J. Toth and A. Gilpin-Jackson, “Smart wiew for a smart grid – unmanned aerial vehicles for transmission lines,” in Proc. of the 1st International Conference on Applied Robotics for the Power Industry, 5 – 7 Oct. 2010, Montreal, QC, Canada, pp. 1 – 6, doi:10.1109/CARPL.20105624465.
- [12] S. Chaumette, R. Laplace, C. Mazel, and A. Godin, “Secure cooperative ad hoc applications within UAV fleets,” IEEE Conference on Military Communications Conference (MILCOM 2009), 18-21 Oct. 2009, Boston, MA, pp. 1 – 7, doi:10.1109/MILCOM.2009.5379819.
- [13] E. Loren, L. Riblett, and J. Wiseman, “TACKNET: Mobile ad hoc secure communications network,” in Proceedings of 41st Annual IEEE International Carnahal Conference on Security Technology, 8-11 October 2007, Ottawa, Ontario, Canada, pp. 156 – 162.
- [14] C. Chlestil et al., “Reliable optical wireless links within UAV swarms,” in Proceedings of Transparent Optical Networks, 18 – 22 June, 2006, Nottingham, Great-Britain, pp. 39 – 42, doi:10.1109/ICTON.2006.248491.
- [15] V.N. Dobrokhodov, I.I. Kaminer, K.D. Jones, and R. Ghabcheloo, “Vision-based tracking and motion estimation for moving targets using small UAVs,” in Proceedings of the 2006 American Control Conference Minneapolis, June 14 - 16, Minnesota, USA, pp. 1428 – 1433, doi:10.1109/ACC.2006.16564418.
- [16] D. Hague, H.T. Kung, and B. Suter, “Field experimentation of cots-based UAV networking,” in Proceedings of IEEE Conference on Military Communications (MILCOM2006), 23-25 Oct. 2006, pp. 1 – 7, doi:10.1109/MILCOM.2006.302070.
- [17] A. Ruangwiset, “Path generation for ground target tracking of airplane-typed UAV,” in Proceedings of the 2008 IEEE International Conference on Robotics and Biomimetics (ROBIO), Bangkok, Thailand, February 21 – 26, 2009, pp. 1354 – 1358, doi:10.1109/robio.2009.4913197.
- [18] C-M. Cheng, P-H. Hsiao, H.T. Kung, and D. Vlah, “Transmit antenna selection based on link-layer channel probing,” in Proceedings of IEEE Conference on World of Wireless, Mobile and Multimedia Networks, 18-21 June 2007, Cambridge, MA, U.S.A. pp. 1 – 6, doi:10.1109/WOWMOM.2007.4351703.
- [19] Y. Qu, Y. Zhang, and Q. Zhou, “Cooperative localization of UAV based on information synchronization,” in Proceedings of the 2010 IEEE International Conference on Mechatronics and Automation, August 4 – 7, 2010, Xi’an, China, pp. 225 – 230, doi:10.1109/ICMA.2010.5589081.
- [20] M. Pachter, N. Ceccarelli, and P.R. Chandler, “Vision-based target geo-location using camera equipped MAVs,” in Proceedings of 46th Conference on Decision and Control (CDC2007), 2007, pp. 2333 – 2338, doi:10.1109/CDC.2007.4434038.
- [21] B. Cummings, T. Zimmerman, B. Robinson, and M. Snyder, “Voice over blue force tracking,” in Proceedings of IEEE Conference on Military Communications Conference (MILCOM 2006), 23-25 Oct. 2006, Washington, DC, pp. 1 – 5, doi:10.1109/MILCOM.2006.302173.
- [22] J. Harrald and T. Jefferson, “Shared situational awareness in emergency management mitigation and response,” in Proceedings of 40th Annual Hawaii International Conference on System Sciences (HICSS 2007), Jan. 2007, Waikoloa, HI, pp. 23 – 23, doi:10.1109/HICSS.2007.481.
- [23] K. Rein, U. Schade, and M. Hieb, “Battle Management language (BML) as an enabler,” IEEE Conference on Communications, ICC’09, 14 – 18 June, Wachtberg, Germany, 2009, pp. 1 – 5.
- [24] Geospatial Applications of Unmanned Aerial Systems (UAS), “1.4 Classification of the Unmanned Aerial Systems,” <https://www.e-education.psu.edu/geog597g/node/5>, accessed on July 30, 2015.
- [25] S. Green and R. Watkin, “Information provision for the dismounted close combat soldier,” in Proc. of the 13th Conference on Information Fusion, 26 – 29 July 2010, Edinburgh, pp. 1 – 8, doi:10.1109/ICIF.2010.5712066.
- [26] G. Cai, K-Y. Lum, B. M. Chen, and T.H. Lee, “A brief overview on miniature fixed-wing unmanned aerial vehicles,” in Proc. of th 8th International Conference of Control and Automation, 9 – 11 June, 2010, Xiamen, pp. 285 – 290, doi:10.1109/ICCA2010.5524453.
- [27] M. S. Sharawi, O. A. Rawashdeh, and D. N. Anoi, “Evaluation and field testing of an embedded antenna in a small UAV wing structure,” in Proc. of Radio and Wireless Symposium, 10 – 14, Jan, 2010, New Orleans, LA, pp. 589 – 592, doi:10.1109/RWS.2010.5434138.
- [28] G. Austin et al., “Compact dual-band antenna for wireless access point,” Electronics Letters, vol 42, no. 9, April, 2006.
- [29] M. C. Zari et al., “Personnel identification system utilizing low probability-of-intercept techniques: prototype development and testing,” in Proceedings on The Institute of Electrical and Electronics Engineers 31st Annual 1997 International Carnahan Conference on Security Technology, 15-17 Oct 1997, Canberra, ACT, pp. 224 – 230, doi:10.1109/CCST.1997.626274.
- [30] J. Jormakka and T. Saarelainen, “UAV-based sensor networks for future force warriors,” International Journal On Advances in Telecommunications, vol 4, numbers 1 and 2, 2011, ISSN:1942-2601, pp. 58 – 71.
- [31] R. Dees, S. Nestler, R.Kewley, and K. Ward, “WholeSoldier performance: A value-focused model of soldier quality,” 77th MORS Symposium, WG20- Manpower and Personnel, 35 pages, 7 Dec 07, 21.6.2010, accessed on 5.2.2015.
- [32] Field Manual FM 1-02, [www.armypubs.army.mil/doctrine/Active\\_FM.html](http://www.armypubs.army.mil/doctrine/Active_FM.html) FM 1-02, accessed on 8.12.2012.

- [33] T. Saarelainen, "Targeting situational awareness beyond the event horizon by means of sensor element munition," ICDT 2012, The Seventh International Conference on Digital Telecommunications, pp. 8 – 14.
- [34] P. Buxbaum, "Denying access," Special Operations Technology, July 2010, Vol 8, Issue 5, pp. 26 – 27.
- [35] R. Kozma et al., "Multi-modal sensor system integrating COTS technology for surveillance and tracking," Radar Conference, 10-14 May 2010, pp. 1030 – 1035, doi 10.1109/RADAR.2010.5494467.
- [36] W. Xinzeng, C. Linlin, L. Junshan, and Y. Ning, "Route planning for unmanned aerial vehicle based on threat probability and mission time restriction," in Proc. of the Second International Geoscience and Remote Sensing Conference, 28 – 31 Aug. 2010, Qingdao, pp. 27 – 30, doi: 11.1109.IITA-GRS.2010.5603127.
- [37] T. Saarelainen and J. Timonen, "Tactical management in near real-time systems," IEEE International Multi-Disciplinary Conference on Cognitive Methods in Situation Awareness and Decision Support, (CogSIMA2011), Miami Beach, Florida, 22.-24 Feb 2011, U.S.A., pp. 240 – 247, 10.1109/COGSIMA.2011.5753452.
- [38] M. Phillips, "Air-to-Ground and ground-to-air communications," Military Technology, Vol XXXVII, Issue 6/2013, pp. 66 – 67.
- [39] Z. Ying, W. Zhixue, L. Xiaoming, and C. Li, "C4ISR capability analysis based on service-oriented architecture," The Fifth IEEE International Symposium on Service Oriented System Engineering, 2010, pp. 179 – 180, DOI 10.1109/SOSE.2010.41.
- [40] R.B. Smith, "Introduction to Hyperspectral Imaging," 5 January, 2012 <http://www.microimages.com>, accessed on June 30, 2015.
- [41] J. Lumme, "Vegetation and soil classification and analysis from imaging spectrometer data," Master's thesis, Helsinki University of Technology, 28 May 2004.
- [42] S. Nebiker, A. Annen, M. Scherrer, and D. Oesch, "A light-weight multispectral sensor for micro UAV – opportunities for very high resolution airborne remote sensing," [www.isprs.org/proceedings/XXXVII/congress/1\\_pdf/204.pdf](http://www.isprs.org/proceedings/XXXVII/congress/1_pdf/204.pdf), accessed on Aug 30, 2015.
- [43] <http://uavdesignguide.com/tag/what-is-the-difference-between-uav-and-uas/>, accessed on October 11, 2015.
- [44] [https://www.uavs.org/index.php?page=what\\_is](https://www.uavs.org/index.php?page=what_is), accessed on October 1, 2015
- [45] <http://www.sparxsystems.com/downloads/whitepapers/SOMF-2.1-Conceptualization-Model-Language-Specifications.pdf>, accessed on October 12, 2015.

# Structural Adaptation for Self-Organizing Multi-Agent Systems: Engineering and Evaluation

Thomas Preisler, Wolfgang Renz, and Tim Dethlefs

Multimedia Systems Laboratory  
Faculty of Engineering and Computer Science  
Hamburg University of Applied Sciences

Email: {thomas.preisler,wolfgang.renz,tim.dethlefs}@haw-hamburg.de

**Abstract**—Over one decade of research in engineering of self-organization (SO) has established SO as a decentralized way to develop self-adaptive systems. However, such SO systems may show unwanted behavior under certain conditions, e.g., a decrease of performance and/or starvation, even when apparently well-engineering. A promising concept to overcome such dynamical in-efficiencies in SO systems is to realize the dynamic exchange or reconfiguration of the coordination processes responsible for the self-organizing behavior in terms of a *structural adaptation*. In this paper, we propose an architecture and engineering approach to support the self-adaptive, structural exchange (or reconfiguration) of self-organizing coordination processes based on distributed Multi-Agent technology. Here, a sensor in each agent detects any decrease of specified SO performance indicators, which initiates a distributed adaptation process that allows the exchange (or reconfiguration) of the self-organizing coordination processes, enabling the system to adapt to changing conditions automatically. The proposed engineering approach is explained exemplarily and evaluated using a case study in which a set of autonomous robots is needed to be coordinated in order to achieve their collaborative goal of mining commodities. Based on two different coordination strategies, it will be shown how the autonomous entities benefit from self-organizing coordination processes that support the emergent formation of local mining groups among the robots, and how the concept of structural adaptation helps to overcome a failure that negatively influences these coordination processes by a dynamic exchange of the coordination processes.

**Keywords**—Self-Organizing Systems; Multi-Agent Systems; Structural Adaptation; Decentralized Coordination; Engineering Approach

## I. INTRODUCTION

A preliminary version of this article appeared as a conference paper [1]. This article extends the previous conference paper by giving a more detailed description of the both, the engineering approach as well as the evaluation of the proposed structural adaptations for self-organizing Multi-Agent Systems (MAS).

For self-organizing MAS the capability to adapt to a variety of (mostly external) influences, i.e., their *adaptivity*, is a key feature. In this context, adaptivity describes the ability of a system to change its structure respective behavior in response to external influences or altering demands. In addition, adaptive, self-organizing systems still strive towards reaching (initially defined) global goals. Looking in more detail at such adaptive systems, they reveal many different facets. According

to [2] it can be distinguished between *design-time* and *run-time* adaptivity, where the latter one is far more challenging. Figure 1 depicts even more dimensions of adaptive systems. It differentiates between approaches that only change system parameters in order to exhibit adaptive behavior and concepts that can even alter the whole structure respective replace certain components of the system. Furthermore, it distinguishes between approaches where the self-organizing behavior is achieved through centralized or decentralized control concepts. Thereby, it is differentiated between solutions where the adaptivity is managed manually or automatically by the system itself. The red dot shown in the figure ranks the proposed solution according to the different dimensions. Our approach is based on a decentralized architecture and emphasizes structure-based changes (while also supporting parameter-based ones). Possible adaptations are modeled manually at *design-time* and executes automatically at *run-time*. Therefore, the solution is ranked between manually and automatically adaptations.

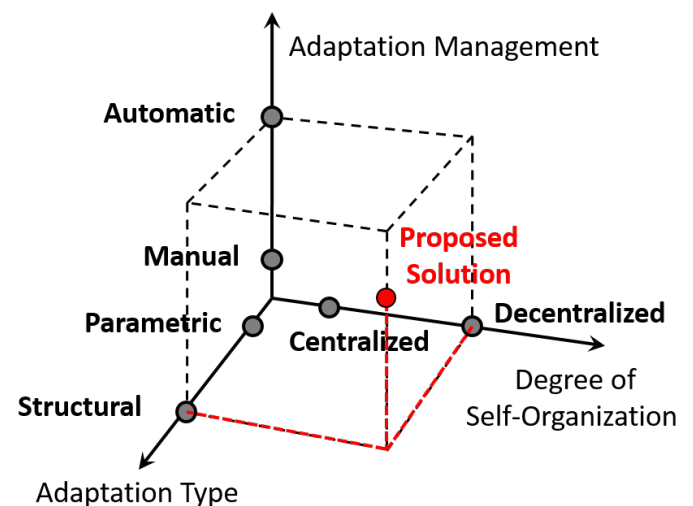


Figure 1. Dimensions of adaptive systems following [3].

Developing and operating systems that belong to this class of adaptive systems, i.e., self-organizing systems, is a challenging task. Firstly, it requires a systematic development approach that copes at all stages with three inherent characteristics of these systems: non-linear dynamics, stochastic behavior

and emergent phenomena. Secondly, it requires a modular system architecture which enables the adaptation of the structure at runtime using customizable and reusable coordination processes. These coordination processes can be understood as standalone design elements that equip a self-organizing system with a specific dynamic behavior. By exchanging these coordination processes at runtime, a distributed application can adapt not only its behavior but also its inherent structure. Thus, enabling the system to overcome problems like performance decrease or starvation, by adjusting the structure of its self-organizing processes automatically. The approach presented in this paper extends already established approaches for engineering self-organizing systems by introducing a system architecture that systematically enables structural adaptations for distributed systems with decentralized control mechanisms. It is conceptual comparable to the local reactive planning approach from the BDI (belief, desire, intention) agent software model [4], where an agent selects a plan based on local information and alternatives. In contrast, the proposed approach deals with systems that strive towards a distributed consensus on an application-global level to select and execute predefined structural adaptation plans. Thereby, each of the participating agents only relies on its local information in a decentralized way.

The remainder of this paper is structured as follows: Section II describes related work, followed by Section III where the properties and engineering challenges of self-organizing MAS are described. Section IV describes the core concepts of structural adaptations, the proposed architecture and description language as well as the adaptation algorithm. Section V introduces the *MarsWorld* scenario and describes two different coordination process manifestations as well as whose structural adaptation. The evaluation results of both the differences between the two coordination process manifestations and the impact of the structural adaptation are described in Section VI. Finally, Section VII concludes the paper.

## II. RELATED WORK

Current trends in computer science like mobile and ubiquitous computing in combination with an increasing diversification of hard- and software platforms challenge traditional engineering and operating approaches for distributed systems substantially. Years ago, such systems were mainly closed ones with a-priori known tasks, challenges, and users. Nowadays, with an increasing pervasiveness and distribution, they have turned into an integral part of the business world as well as the private life of many people. This evolution implicates new challenges for the engineering and operation of distributed systems. For instance, high and unpredictable dynamics, an increasing complexity, and the satisfaction of non-functional requirements like, e.g., robustness, availability, and scalability. Altogether, this requires a new generation of distributed systems that is capable of *adapting* its behavior *autonomously*.

This challenge is addressed by research areas like Autonomic [5] or Organic Computing [6] that aim at providing new approaches to solve it in a systematic fashion. They achieve it with different types of feedback loops, relying on (usually) centralized control elements. The authors of [7] identify feedback loops as the key design element within a distributed system in order to exhibit adaptivity. Here, feedback loops consist of three main components: *sensor*, *actuator* and

a *computing entity*. Sensors are in charge of observing the behavior and the (current) status of the system respective the environment it is situated in. Actuators can change the configuration of the system, which can either lead to *parametric* or *structural* changes. The computing entity that serves as a connector between the system input (sensor) and the output (actuator) can be very different with regards to its internal architecture and abilities [8]. For instance, the widespread autonomic control loop [5], which is based on a monitoring, analyzing, planning, executing and knowledge loop (MAPE-K), contains a centralized computing entity, which can be associated with an autonomic manager to software and hardware components in order to equip them with adaptive behavior. Contrasting to feedback loops, the authors of [9] introduce a policy-based approach where the non-functional concerns of an application are described as policies and the application adapts itself to changing conditions controlled by a centralized policy engine. Like the approach described in this paper, the work presented in [9] also focuses on a clean separation between the business-logic and the self-adapting fulfillment of non-functional requirements.

According to [10], this class of approaches, which introduce centralized control concepts, can be called *self-adaptive systems*. In contrast to this, there are approaches that aim at providing *automatically adaptive systems* which rely on decentralized architectures and utilize distributed feedback loops and coordination mechanisms. They are called *self-organizing systems* [10] and seem, due to their decentralized system architecture, to be better suited to deal with the aforementioned non-functional requirements. Also, the concept of self-organization has been observed in many other domains like, e.g., biology, physics, or sociology and has, furthermore, proven its applicability for distributed systems already before (as mentioned in e.g., [11] [12]).

In addition to the difference between centralized and decentralized feedback loops, another criterion targets the general applicability of existing approaches that aim at providing methods for structural adaptivity for distributed systems. According to [10], adaptivity defines a general system view that can be further decomposed into so called self-\* properties of distributed systems. Therefore, there are many approaches which target the provision of a subset of these properties [13] [14] [15]. Whereas these approaches reach good results with respect to specific aspects of adaptive behavior, they lack general methods and concepts that provide structural adaptivity in general. However, this limits the general applicability of these approaches and forces system developers to deal with (completely) different approaches if there is the requirement for more than just one type of adaptivity. Consequently, if a system requires different self-\* properties it has to incorporate different concepts and techniques which increases the complexity of related implementations considerably.

This could be improved by using approaches that are based on structural adaptivity. However, applying them to the concept of self-organization in decentralized systems is an ambitious task. Especially, the purposeful engineering of self-organizing systems is challenged by their inherent non-linear dynamics and the bottom-up development process. There is a lack of approaches (and corresponding implementations) that deal with the whole development process systematically. Approaches like [16] [17] focus mainly on early development

activities (e.g., requirement analysis or modeling), whereas approaches like [18] [19] provide basic implementation frameworks. Approaches like [20] [21] do provide a comprehensive development process but focus on self-adaptive systems based on centralized control concepts. An approach towards meta-adaptation support based on reusable and composable adaptation components is presented in [22]. The introduced *Transformer* framework constructs system global adaptation by contextually fusing adaptation plans from multiple adaptation components. Similar to the work presented in this paper, it focuses on decentralized structural adaptation for multiple purposes. While the work presented here focuses on a general engineering approach, the work presented in [22] focuses more on the conflict resolution between different adaptation behaviors. The authors of [23] introduce a decentralized planning approach for self-adaptation in multi-cloud environments. Thereby, they focus on the runtime management of Internet of Things oriented application deployed in multi-clouds. Decentralized self-adaptation is seen as a promising solution in order to maintain the applications for quality assurance. The presented approach tackles the uncertainty effect of adaptations on a specific layer, which may cause negative impacts on other layers. Therefore, they introduce a planning model and method to enable the decentralized decision making. The planning is formulated as a Reinforcement Learning problem [24] and solved using the Q-learning algorithm [25]. Contrasting, to the approach presented here where a general approach for the engineering of self-adaptation is envisioned, the approach presented by [23] focuses on solving the problem of self-adaptation in the specific context of multi-cloud environments.

In conclusion, it can be stated that there is a lack of approaches that combine the above mentioned aspects in order to support structural adaptivity as a basis for systematic development of generic self-organizing systems. Therefore, the following two sections introduce an approach based on the systematical engineering of self-organizing MAS, which supports the whole development process. It uses decentralized feedback structures and aims at supporting structural adaptivity in general.

### III. SELF-ORGANIZING MAS

The presented approach on structural adaptation of coordinations processes is based on previous work on self-organizing dynamics in MAS. Such a self-organizing dynamic is shown in the left side of Figure 2. The MAS exhibits a self-organizing dynamic that causes the system to adapt to external and internal influences. The self-organizing dynamic realizes the intended adaptivity of the software system and is mapped by decentralized coordination processes. The processes describe a self-organizing behavior that continuously structures, adapts and regulates aspects of the application. They instruct sets of decentralized coordination media and coordination enactments. Coordination enactments and media distinguish between techniques for the adaptation of system elements (local entity adaptation) and realizations of agent interactions (information propagation). Together, they control the microscopic activities of the agents, which on a macroscopic level lead to the manifestation of the intended self-organizing dynamic. The integration of the coordination enactments and media is prescribed by the coordination process definitions, which structure and instruct their operations. Thus, the self-organizing dynamic of the MAS is described by coordination

processes, which model the intended adaptivity of the system. On a technical level these processes instruct coordination enactments and media which realize the intended adaptivity.

Conceptually speaking, structural adaptations for self-organizing systems mean an adaptation of the coordination processes, as they describe the system's intended self-organizing dynamic. The right side of Figure 2 illustrates this concept. The MAS exhibits structural adaptations which influence and observe the self-organizing dynamic. Similar to the self-organizing dynamic, the structural adaptations are described by processes. They define adaptation conditions, which specify states of the system where the self-organizing dynamic should be altered. This alteration is realized by prescribed adaptation activities, which are triggered due to specified self-organization performance indicators. Ineffective coordination processes are deactivated if the system's behavior becomes deficient and, therefore other coordination processes are activated in exchange. This results in a structural adaptation of the coordination process composition. This means on a lower level, that if the system's behavior is not deficient but measured inefficient, the active coordination processes are reconfigured by parametric adaptations. The structural adaptation processes instruct adaptation enactments to monitor the agents with regard to the self-organization performance indicators. In both cases (structural or parametric adaptation), it is necessary that the system's entities find a consensus whether or not the adaptations should be performed. Therefore, a distributed voting method is utilized in order to find an agreement about the execution of the adaptation. In case of a positive one it is performed by manipulating the relevant coordination processes.

#### A. Coordination Enactment Architecture

The work on structural adaptations is based on a previously published tailored programming model for the software-technical utilization of coordination processes as reusable design elements [26]. The programming model provides a systematic modeling and configuration language called *MAS-Dynamics* and a reference architecture to enable the enactment of pre-described coordination models called *DeCoMAS* [27] (Decentralized Coordination for Multi-Agent Systems). The architecture is based on the clean separation of activities that are relevant for the coordination of agents and the system's functionality. Therefore, coordination processes can be treated as first class design elements that define application-independent coordination interdependencies. Figure 3 illustrates the layered structure of the coordination enactment architecture. The functionality of the MAS is mapped by the application layer. The coordination logic is realized as an underlying layer. This layer provides a set of coordination media, which provide the required coordination mechanisms. They build the infrastructure that allows the agents to exchange application independent coordination information and control the information dissemination. Thus, the coordination media are the technical realization of the previous described coordination processes. The agents communicate with the coordination media using their coordination enactments (cf. Figure 3(B)). The enactments influence and observe the agent activities (1) and exchange information that is relevant for the coordination via the coordination media (2). The local configuration of these activities, e.g., when to publish information and how

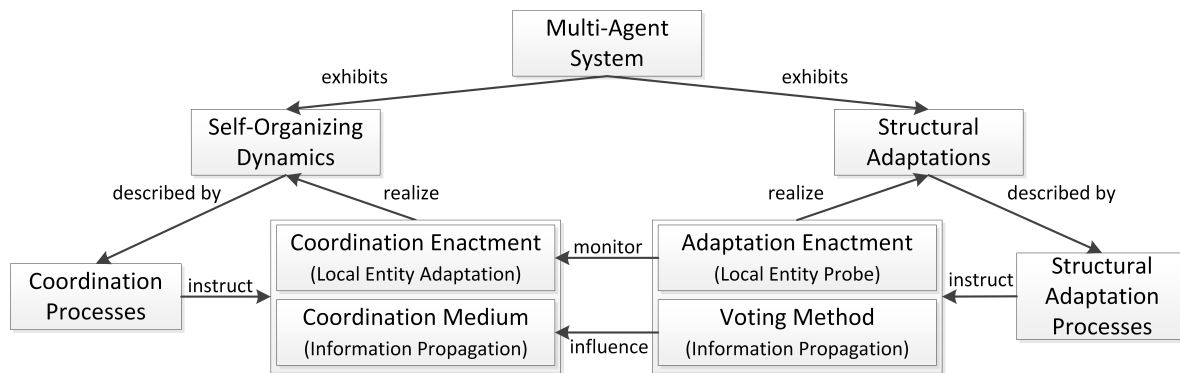


Figure 2. Structural adaptation processes exchange or reconfigure the coordination processes responsible for the self-organizing dynamics by monitoring self-organizational performance indicators.

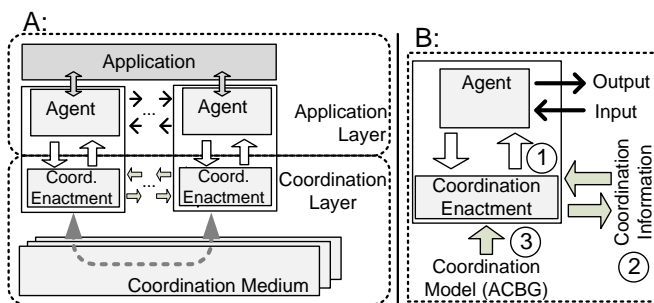


Figure 3. Coordination enactment architecture [29].

to process perceptions, is defined in a declarative, external coordination model (3) written in the *MASDynamics* language. Coordination is declaratively described to support the reuse of coordination pattern in different applications. This architecture focuses on the transparent separation of application and coordination logic, meaning that agent models are not modified by the coordination logic. This allows the supplement of coordination to existing applications. A recent example on how this architecture can be implemented to realize decentralized coordination in self-organizing systems based on Peer-to-Peer technology is described in [28].

### B. Engineering Self-Organizing MAS

The engineering of structural adaptations of coordination processes is part of an existing engineering approach for self-organizing MAS developed in the *SodekoVS* project [30]. Part of the project was the development of the *Coordination Enactment Architecture*. The project aimed at providing self-organizing processes as reusable elements that developers can systematically integrate into their applications. The utilization of self-organization in software engineering is addressed by providing a reference architecture to offer a conceptual framework for the configuration and integration of self-organizing processes. The integration is guided by adjusting methodical development procedures. Following this, coordination media are made available as middleware services. A minimal intrusive programming model allows developers to configure and integrate representations of nature-inspired coordination strategies into their applications. Figure 4 denotes the conceptual view on integrating self-organization. Incremental development activi-

ties are supplemented with activities that address the manifestation of self-organizing phenomena (I-V). While developers design the functionality of their applications, they revise the decentralized coordination of component activities in interleaved development activities. Supplements to the requirements activities (I) facilitate the description of the intended application dynamics. During analysis activities (II) it is examined which instances or combinations of coordination metaphors can lead to the required adaptivity. Design activities (III) detail the models of selected coordination strategies and configure the coordination media that are used for their realization. These activities prepare the implementation and integration (IV) of medium instances to be configured and accessed by a generic usage interface. Testing (V) activities are supplemented with a simulation-based validation that agent coaction meets the given requirements, i.e., manifests the intended adaptiveness. The whole development process, as described in [30], is designed as a iterative process. Based on the results of the simulation-based validation, the self-organized coordination processes are redesigned until they achieve the intended adaptivity. Either based on the validation results or as an result of the initial analysis it may be observed that certain coordination processes or certain process configuration are suitable for some conditions but become deficient or insufficient for others. In this case it is practical to utilize structural adaptations for the re-composition of coordination processes or, on a lower level, parametric adaptations for the reconfiguration of coordination parameters. The key challenge hereby is to identify these conditions that require a structural (or parametric) adaptation and map them to self-organizational performance indicators. As an addition to the existing engineering approach, this paper propagates anticipated structural adaptations. Following the same iterative approach as designing and implementing the coordination processes, the adaptations should also be designed and implemented in an iterative way. The conditions that require adaptations should be identified based on the requirements and analysis activities and redefined by the results of a simulation-based validation.

## IV. STRUCTURAL ADAPTATION OF COORDINATION PROCESSES

This section presents the structural adaptation architecture and an extension of the *MASDynamics* language for the declarative description of adaptations. The proposed architecture

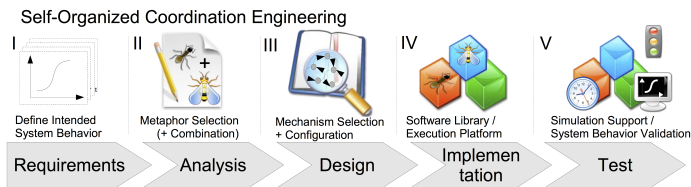


Figure 4. SodekoVS development activities following [30].

facilitates a voting algorithm that is used to find an agreement on possible adaptations which are then executed.

### A. Adaptation Architecture

The previous described Coordination Enactment Architecture is extended by the introduction of so called *Adaptation Enactments* in order to enable structural adaptations of coordination processes. Similar to the Coordination Enactments, that were introduced to equip applications with coordination capabilities, the Adaptation Enactments equip applications with the capability to structural adapt coordination processes at runtime. Figure 5 shows the extension of the Coordination Enactment Architecture. The Adaptation Enactments are part of the coordination layer and therefore independent from the system's functionality (supporting a clean separation between application and coordination logic). They observe the agents similar to the Coordination Enactments. But contrasting to the Coordination Enactments they do not influence the agents, but the coordination media, which are the technical realization of the coordination processes. As described before, the Coordination Enactments influence and observe the agent activities and exchange information relevant for coordination via a coordination medium. As shown in the figure, the Adaptation Enactments consists of two components. The *Monitor* observes specified self-organizing performance indicators, which are part of the agent, and in case of a decreased performance, determined by a specified condition, it initiates a voting process for a predefined structural adaptation. The *Service* is used as an interface for the distributed voting process. When the Adaptation Enactment Monitor of an agent observes a decreased performance, it initializes a distributed voting attempt and acts as leader of this vote. Utilizing the service interface it suggests an adaptation to the other agents. Based on their local information (state of the agent), the called Adaptation Enactment Services decide whether or not to agree on the proposed adaptation and inform the vote leader about their decision. The leader analyzes the received votes and decides if the required majority for the adaptation was reached. If so, the suggested adaptation is committed by activating or deactivating the affected coordination media, respectively by changing their coordination parameters.

### B. Adaptation Description

In order to describe structural adaptations, the *MASDynamics* language was extended to support the declarative description of possible adaptations. These adaptations are described at design time and executed at runtime. As described before, structural adaptations of coordination processes can be realized by exchange or reconfiguration of coordination processes. Therefore, the already realized description of coordination

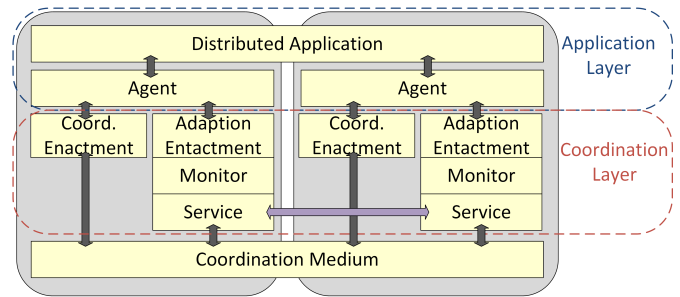


Figure 5. Structural Adaptation Architecture.

processes was extended to indicate whether or not a coordination process is active at start time. This allows developers to define multiple coordination processes with different behaviors at design time, from whom only a subset may be active at start time. Furthermore, the *MASDynamics* language was extended with the following elements to describe these possible adaptations:

The first part concerns the types of agents that are allowed to participate in the adaptation process. The *DeCoMAS* framework creates Adaptation Enactments for this types of agents, so they can be monitored with regards to specified performance indicators and are able to participate in the decision making process.

The second part concerns the actual adaptations. Each adaptation is identified by a unique *id* and a *reset* flag. The reset flags specifies if the performance indicator should be reset after a failed adaptation attempt. It can be used to prevent repeated adaptation attempts flooding the system, if only a subset of agents are subjected to bad performance indicators, while the majority of the systems still performs well and in that case would not agree on an adaptation. Further information in the adaptation description concerns the voting process. It includes a minimum total number of *answers* a vote leader awaits, before it starts to evaluate the results from an adaptation attempt it started. Also, the *quorum* that has to be reached, before a structural adaptation may be accepted is specified. A *timeout* after which the vote leader will start to evaluate the received answers even if it has not received all of the required answers can also be specified. Furthermore, it is possible to *delay* an adaptation attempt if specified. Also, an adaptation can be blocked for a certain amount of time at start time, to avoid oscillation problems (*startDelay*).

Besides the information concerning the adaptation process, the description also contains information about the affected coordination processes. This includes the *realization id* of the affected coordination process and the *information* if the process should be *activated* or *deactivated*, respective which *parameter* of the coordination process should be altered to which *value*. The last information needed for structural adaptations are the *constraints* regarding the agents state. For each agent type, they specify which *element* should be used as a self-organizing performance indicator. They contain a *condition* and a *threshold*. The condition is used by the Adaptation Enactment Monitor, to point out if the performance indicator has become deficient for the specified agent and, therefore, if an adaptation attempt should be started. When the Adaptation Enactment Service of an agent receives an adaptation request,

it uses the threshold to determine whether or not it should agree to the proposed adaptation. Therefore, the threshold allows the specification of an insufficient performance indicator that is not as strict as the actual condition, which would force the agent to start an adaptation attempt by itself. The threshold maps a negative trend allowing the agent to anticipate an insufficient performance. Listing 1 shows the XML Schema Definition (XSD) for the adaptation part of the *MASDynamics* language.

Listing 1. XSD for the adaptation part of the *MASDynamics* language.

```

1 <xs:schema attributeFormDefault="unqualified"
  elementFormDefault="qualified" xmlns:xs="http://
  www.w3.org/2001/XMLSchema">
2 <xs:element name="adaptation">
3 <xs:complexType>
4 <xs:sequence>
5 <xs:element name="realizations">
6 <xs:complexType>
7 <xs:sequence>
8 <xs:element name="realization" maxOccurs="unbounded
  " minOccurs="0">
9 <xs:complexType>
10 <xs:simpleContent>
11 <xs:extension base="xs:string">
12 <xs:attribute type="xs:string" name="id" use="optional
  "/>
13 <xs:attribute type="xs:string" name="activate" use="
  optional"/>
14 </xs:extension>
15 </xs:simpleContent>
16 </xs:complexType>
17 </xs:element>
18 </xs:sequence>
19 </xs:complexType>
20 </xs:element>
21 <xs:element name="constraints">
22 <xs:complexType>
23 <xs:sequence>
24 <xs:element name="constraint" maxOccurs="
  unbounded" minOccurs="0">
25 <xs:complexType>
26 <xs:simpleContent>
27 <xs:extension base="xs:string">
28 <xs:attribute type="xs:string" name="agent_id" use="
  optional"/>
29 <xs:attribute type="xs:string" name="element" use="
  optional"/>
30 <xs:attribute type="xs:string" name="type" use="
  optional"/>
31 <xs:attribute type="xs:byte" name="condition" use="
  optional"/>
32 <xs:attribute type="xs:byte" name="threshold" use="
  optional"/>
33 </xs:extension>
34 </xs:simpleContent>
35 </xs:complexType>
36 </xs:element>
37 </xs:sequence>
38 </xs:complexType>
39 </xs:element>
40 </xs:sequence>
41 <xs:attribute type="xs:string" name="id"/>
42 <xs:attribute type="xs:byte" name="answers"/>
43 <xs:attribute type="xs:float" name="quorum"/>
44 <xs:attribute type="xs:short" name="startDelay"/>
45 <xs:attribute type="xs:string" name="reset"/>
46 <xs:attribute type="xs:string" name="single"/>
47 </xs:complexType>
48 </xs:element>
49 </xs:schema>

```

### C. Adaptation and Voting Algorithm

The adaptation and voting process is illustrated as an UML Activity Diagram in Figure 6. The whole process is started when a self-organization performance indicator changes its value. Whenever such an event occurs the adaptation enactment's monitor checks the adaptation constraints. If a

constraint is fulfilled and no adaptation process with a higher priority is currently running, the according adaptation process is started. The priority of an adaptation process is determined by the hash value of the initiating agent's identifier. Due to the low probability of collisions in hash values, they can be used as unique identifiers in distributed systems where no global knowledge about all participating entities exists. By checking for an adaptation processes with a higher priority it is guaranteed that only one adaptation process is executed simultaneously. Therefore, interferences between these processes are prevented. If an adaptation constraint is fulfilled and no adaptation process with a higher priority is currently running, the monitor will call the remote voting services of all other agents. Then it waits until the required number of answers, as specified in the adaptation description, is received or until the timeout, also specified in the description, occurs.

A voting service that receives a voting request will check if it had already been suggested another adaptation with a higher priority, again to avoid inferences, in such a case it votes *no*. Otherwise, it checks its local value of the specified performance indicator against the threshold value. If the threshold is reached, a negative performance trend is recognized and the voting service agrees on the suggested adaptation by voting *yes*.

The monitor that proposed the adaptation waits until it has received the required number of answers or the timeout has occurred. Then it checks if the required majority, as specified in the adaptation description, was reached. The adaptation process is aborted in case of a timeout. When the monitor has received the required number of answers it evaluates them by counting the *yes* and *no* votes and calculating the ratio. If the ratio reaches or exceeds the required majority, the monitor commits the suggested adaptation. If not, it aborts the process. Again if adaptation process was interfered by a process with a higher priority it is aborted at this point. The proposed adaptation is committed by activating, respectively deactivating the distributed coordination by or by changing their configuration parameters via interfaces offered by the coordination media for such purposes.

## V. CASE STUDY: MARSWORLD

The MarsWorld scenario is based on a hypothetical application setting presented in [31]. A set of autonomous robots is sent to the planet Mars to mine ore. The mining process consists of three distinct activities:

- 1) *Analysis* of potential ore locations to verify the presence of ore.
- 2) *Mining* or *production* of the analyzed ore deposits.
- 3) *Transportation* of the mined ore to a homebase.

The robots in this scenario are controlled by software agents, which are specialized to perform one of the three distinct mining operations. The *Sentry* agents are equipped with sophisticated sensors to analyze potential ore locations, *Producer* agents have the capability to mine ore deposits at analyzed locations and the *Carry* agents can transport the mined ore to the homebase. Obviously, as none of the three agents types is able to mine alone, the agents need to work together to achieve their collaborative goal. Therefore, this scenario is chosen for the case study, as the agents require some sort of coordination in order to achieve their collaborative goal. The *Sentry* agents

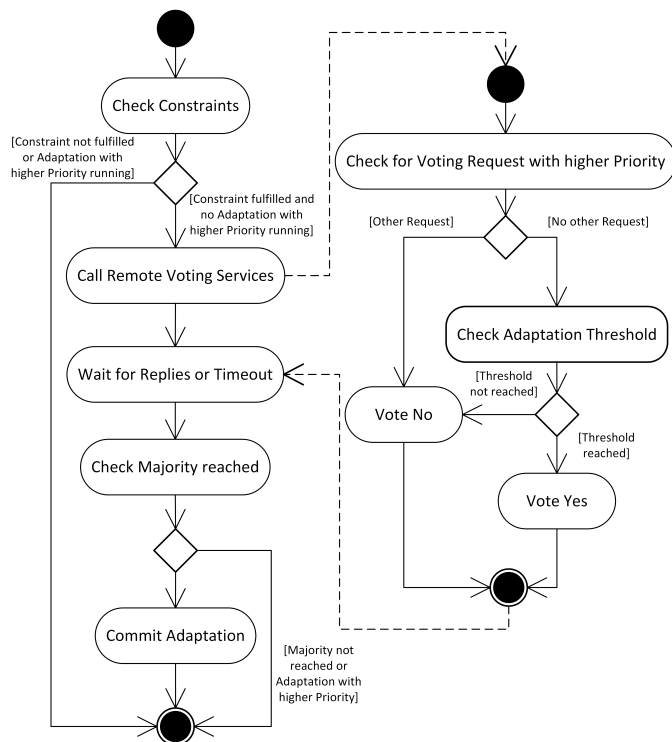


Figure 6. Adaptation and Voting Algorithm.

analyze potential ore deposits and inform the *Producer* agents whether or not ore can be mined there. The *Producers* mine the ore at the analyzed deposits and inform the *Carry* agents about it, so they can carry it to the homebase. Initially all agents explore the environment randomly. All agents are equipped with sensors to find potential ore deposits. If *Producer* or *Carry* agents encounter any potential deposits, they inform a *Sentry* agent. *Sentry* agents that have encountered a potential deposit or were informed about one, move towards the deposit and analyze it. When they have verified the presence of ore at the location they request a *Producer* agent to mine it. Accordingly, after mining the ore *Producers* request a *Carry* agent to transport it to the homebase.

#### A. Coordination

As the MarsWorld example exhibits no predefined organizational structure the agents need to be coordinated in order to achieve their collaborative goal. Three coordination process for the distribution of the required information can be derived from the described communication taking place among the agents:

- 1) Coordination information the *Producer* and *Carry* agents send to the *Sentry* agent, when they encounter potential ore deposits while exploring the environment.
- 2) Coordination information the *Sentry* agents send to *Producer* agents when they have analyzed a potential ore deposit and found ore to mine there.
- 3) Coordination information the *Producer* agents send to the *Carry* agents after they minded ore and it is now ready for transportation to the home base.

In order evaluate the impact of both, the self-organizing coordination processes and their structural adaptation two

different manifestations of the three described coordination processes are envisioned. The first one is based on a simple random selection approach and, therefore, does not exhibit any self-organizing behavior. In this case, each of the coordination processes randomly selects an agent of the required type and informs it about the sensed, analyzed or produced ore.

The second manifestation is based on a neighborhood approach. In this case, each coordination process selects the agent of the required type, which is nearest to the emitting agent. By selecting the nearest agent it is ensured that the informed agents have to travel the minimal distance to reach the designated destination. If the environment consists of multiple ore deposit clusters, characterized by a small distance between the deposits in the cluster and a large distance to the next cluster, this coordination approach leads to the self-organized formation of local mining groups among the agents. Thus, enabling the agents to organizes themselves in an emergent way.

Obviously, knowledge about the current positions of each agent is required by the coordination processes based on this approach. Therefore, the environment in this case study is equipped with a positioning service offering this information. The three coordination process realizations based on the neighborhood approach utilize this service in order to distribute the coordination messages to the nearest agent of the appropriate type. This results in the realizations of the following six coordination processes:

- *latest\_target\_seen\_random*: This coordination process informs a *Sentry* agent whenever a *Producer* or *Carry* agent has encountered a potential ore deposit. It randomly selects one of the *Sentry* agents and informs it. The *Sentry* agent adds the received location to its queue of locations which it has to analyze.
- *latest\_target\_analyzed\_random*: This coordination process randomly selects and informs one of the *Producer* agents if a *Sentry* agent has analyzed a potential ore deposit and actually found ore to mine there. The *Producer* agents adds the location to its queue of ore deposits to mine and eventually starts to mine it until the deposit is depleted.
- *latest\_target\_produced\_random*: This coordination process randomly selects and informs one of the *Carry* agents whenever a *Producer* agent has completely mined a ore deposit. The *Carry* agent adds the location to its queue of produced ore that is ready for transportation
- *latest\_target\_seen\_nearest*: Whenever a *Producer* or *Carry* agent has encountered a potential ore deposit, this coordination process selects the *Sentry* agent nearest to the location of the *Producer* or *Carry* agent and informs it about the deposit. The *Sentry* agent adds the location to its queue and eventually analyzes it.
- *latest\_target\_analyzed\_nearest*: After a *Sentry* has analyzed a potential ore deposit and actually found ore there, this coordination process selects the *Producer* agent nearest to the location and calls it to mine ore here.
- *latest\_target\_produced\_nearest*: When a *Producer* agent has completely depleted the ore deposit, this

coordination process selects and informs the *Carry* agent nearest to the location, so that it can transport the mined ore to the homebase.

Listing 2 shows the declarative description of the *latest\_target\_seen\_nearest* coordination process. It is written in the previously described *MASDynamics* configuration language. The listing shows that whenever the *callSentryEvent* is monitored in either a *Producer* or *Carry* agent, coordination information about this latest seen target is communicated to a *Sentry* agent. The according event is triggered inside a *Producer* or *Carry* agent whenever a potential ore deposit is found. Using the specified coordination mechanism, which is the technical realization of the previous described coordination medium concept, the nearest *Sentry* agent is selected as the receiver of the coordination information. The coordination mechanism is implemented as Java class and makes use of the positioning service offered by the environment in order to determine the nearest *Sentry* agent. When the *Sentry* agent receives the coordination information with the position of the potential ore deposit, the specified *latestTargetEvent* is triggered by its coordination enactment. This results in the location being added to the *Sentry*'s queue of location to analyze. The coordination process descriptions for the other coordination processes are constructed similar.

Listing 2. XML listing showing the declarative description of the coordination process realization for the *latest\_target\_seen\_nearest* process written in the *MASDynamics* language.

```

1 <realization id="latest_target_seen_nearest">
2 <from>
3 <agent_element element="callSentryEvent"
4   agent_id="Producer" type="INTERNAL_EVENT">
5   <parameter_mappings>
6     <mapping ref="latest_target" name="
7       latest_target"/>
8   </parameter_mappings>
9 </agent_element>
10 <agent_element element="callSentryEvent"
11   agent_id="Carry" type="INTERNAL_EVENT">
12   <parameter_mappings>
13     <mapping ref="latest_target" name="
14       latest_target"/>
15   </parameter_mappings>
16 </agent_element>
17 </from>
18 <mechanism_configuration
19   mechanism_id="sodekovs.marsworld.coordination.
20     NearestMechanism" agent_type="JADEX">
21 </mechanism_configuration>
22 <to>
23 <agent_element element="latestTargetEvent"
24   agent_id="Sentry" type="INTERNAL_EVENT">
25   <parameter_mappings>
26     <mapping ref="latest_target" name="
27       latest_target"/>
28   </parameter_mappings>
29 </agent_element>
30 </to>
31 <active>true</active>
32 </realization>

```

## B. Structural Adaptation

Arguably, the coordination process manifestations that are based on the neighborhood approach will perform better, as the formation of local mining groups around the ore clusters minimizes the distance the agents have to travel, before they can analyze, produce or transport ore. Therefore, it optimizes the overall mining efficiency. But these coordination processes depend on the positioning service offered by the environment. If this service fails, the coordination processes will not be able

to select the nearest agents, thus, they will not be able to inform the according agents. In such a case the application would benefit from the capability to structurally self-adapt and to switch to the random-selection based coordination process manifestations. The goal is to deactivate the location based coordination processes, when the positioning service offered by the environment fails. As compensation the random selection based coordination processes will be activated. The agents have no knowledge about the fact that the positioning service has failed in this scenario conception. But they can measure the time that has passed since they have received the last coordination information. If they have not received any messages within a given time, they assume that something went wrong and the positioning service is broken. In this example, an agent waits 20 seconds until it assumes a malfunction and initializes a voting process acting as leader.

Of course, it is possible that the agents have not received any coordination information within this time frame for other reasons, e.g., when the agents are exploring an area of the scenario where no other agents are exploring and, therefore, these agents are too far away from the emitting agents to be selected by the location based coordination processes. Therefore, the agents have to find an agreement, whether or not the coordination processes should be adjusted to overcome local phenomena.

Therefore, the voting algorithm described in Section IV-C is used by the agents to find an agreement on the adaptation. When an agent has not received any coordination information within the last 20 seconds (condition of the adaptation constraint) it starts the voting process and acts as the leader of it. Agents that have received a voting requests determine if they have received any coordination information within the last 15 seconds (adaptation threshold) and if so vote *yes*.

The threshold value expresses tendencies indicating a potential negative trend, so that agents can agree on a proposed adaptation before exhibiting a deficient behavior by themselves. In this case, they exhibit a potential negative trend and interpret it as an upcoming deficiency if an other agent proposes an adaptation and therefore, already has exhibited the deficiency. Of course, more complex conditions, as the time windows used in this example, are possible to model both the constraint (deficient behavior) and threshold (negative trend) values.

The agent, which started the voting process, waits until it has received all the voting results (this is a simplification because in this small scenario we neglect any message lost) and evaluates them. If the required majority of 75% has been reached, the structural adaptation is performed. At start time, the adaptation capability is blocked for 30 seconds, because it may take a while before the first potential ore deposits are sensed and, therefore, the system might adapt prematurely because of oscillation problems.

Listing 3 shows the declarative description of the structural adaptation for this example. It shows that the agent initiating the voting process awaits answers from 16 others (including itself) and that a quorum of 75% *yes*-Votes is required so that the adaptation is performed. The *startDelay* indicates that the adaptation enactment is blocked for the first 30 seconds. The *reset* flag appoints that the constraint value should not be reseted after a failed voting attempt and the *single* flag

asserts that the adaptation should only be performed once. Under the *realizations* tag it is described which coordination processes should be activated and deactivated if the adaptation is performed. The *constraints* describe which values in the participating agents should be monitored, in this case an BDI<sup>1</sup>-agent belief called *no\_msg\_received* that stores the information how much time has passed since the agent has received the last coordination information. As described before, the *condition* and *threshold* values are simple integer values in this example.

Listing 3. XML listing showing the declarative description of the structural adaptation for the MarsWorld example.

```

1 <adaptations>
2 <adaptation id="change-to-random" answers="16"
   quorum="0.75" startDelay="30000" reset="
   false" single="true">
3 <realizations>
4 <realization id="latest_target_seen_nearest"
   activate="false"/>
5 <realization id="latest_target_analyzed_nearest"
   activate="false"/>
6 <realization id="latest_target_produced_nearest"
   activate="false"/>
7 <realization id="latest_target_seen_random"
   activate="true"/>
8 <realization id="latest_target_analyzed_random"
   activate="true"/>
9 <realization id="latest_target_produced_random"
   activate="true"/>
10 </realizations>
11 <constraints>
12 <constraint agent_id="Producer" element="
   no_msg_received" type="BDI_BELIEF"
   condition="20" threshold="15"/>
13 <constraint agent_id="Carry" element="
   no_msg_received" type="BDI_BELIEF"
   condition="20" threshold="15"/>
14 <constraint agent_id="Sentry" element="
   no_msg_received" type="BDI_BELIEF"
   condition="20" threshold="15"/>
15 </constraints>
16 </adaptation>
17 </adaptations>

```

### C. Scenario Description

The following scenario was designed to measure and evaluate both, the differences between the self-organizing and the random-selection based coordination processes and the impact of the structural adaptation. Figure 7 shows the examined scenario. It is characterized by a  $2 \times 2$  dimension and contains 20 ore deposits with a total ore amount of 1000 ore units. As shown in the figure, the ore deposits are grouped together to local clusters. Each cluster contains 250 units of ore. The ore deposits in the left, top corner of the scenario are identified as cluster 1, the ore deposits in the right, top corner as cluster 2, the ore deposits in the left, bottom core as cluster 3 and the ore deposits in the right, bottom corner as cluster 4. The scenario was designed this way to highlight the self-organizing potential of the neighborhood-based coordination approach, allowing the agents to form local mining groups in a self-organized way. The homebase is located in the middle of the environment.

At the start of the application, all agents start from the homebase and begin to explore the environment randomly. When the *Sentry* agent encounters any ore deposit it starts to analyze it, while the *Producer* and *Carry* agents inform *Sentry*

<sup>1</sup>The belief-desire-intention agent model is developed for programming intelligent agents. Superficially characterized by the implementation of an agent's beliefs, desires and intentions, it uses these concepts to solve a particular problem in agent programming.

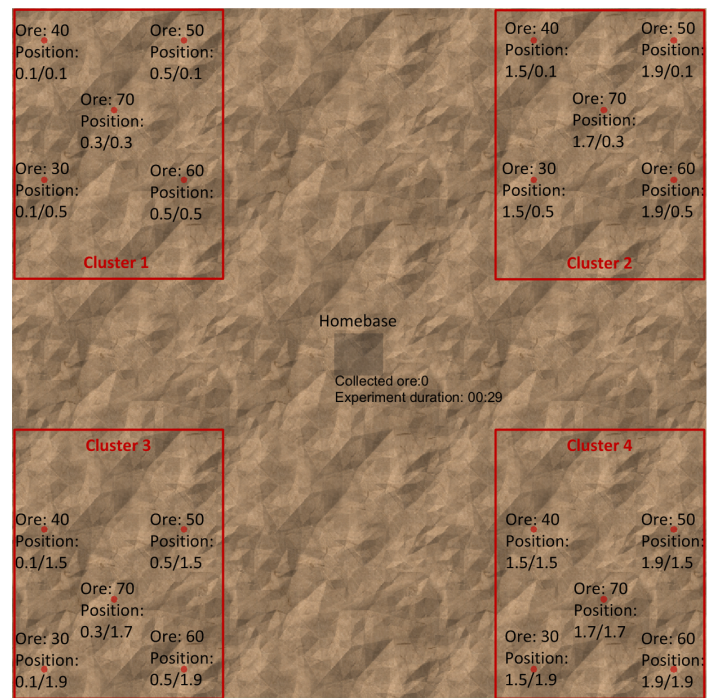


Figure 7. Screenshot of the MarsWorld scenario with highlighted ore clusters.

agents, based on the used coordination process, about sensed deposit. The scenario is finished when the complete amount of ore was mined and transported to the homebase. It is executed with the following amount and configuration of agents:

- *Sentry*: Amount 4, Vision 0.15, Speed 0.1
- *Producer*: Amount 4, Vision 0.1, Speed 0.1
- *Carry*: Amount 8, Vision 0.05, Speed 0.2, Capacity<sup>2</sup> 20

Figure 8 shows a running MarsWorld application based on this scenario. As shown in the figure, the agents were able to mine 150 units of ore after 59 seconds have passed. The shown scenario was executed with the neighborhood-based coordination process manifestations and at this point it seems that the agents have formed three local mining groups (black markers) while mining the ore clusters two, three and four.

## VI. EVALUATION

The realization of the MarsWorld scenario is based on the Jadex MAS platform [32]. The *Sentry*, *Producer* and *Carry* agents were realized as BDI-agents. At start time, all agents explore the environment randomly. Based on the coordination information they receive through to the coordination processes goals to analyze (*Sentry*), produce (*Producer*) or transport (*Carry*) ore are dispatched in the according agents.

In order to measure and evaluate the impact of both, the self-organizing coordination processes and the structural adaptation of these processes, the *MarsWorld* scenario was executed 50 times for each of the two different coordination process manifestations (neighborhood-based and random-selection) as

<sup>2</sup>The capacity denotes the maximum number of ore units a *Carry* agent can transport.

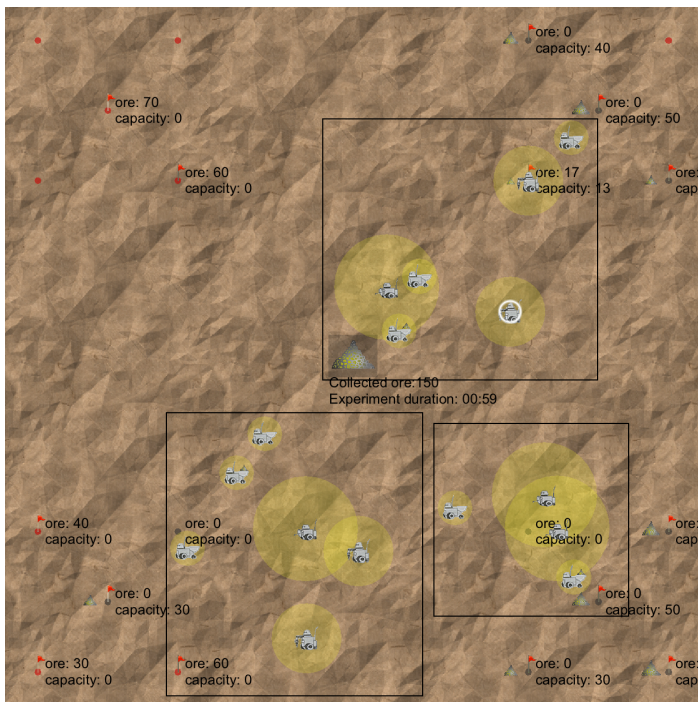


Figure 8. Screenshot of the running MarsWorld application with highlighted self-organizationally formed local groups.

well as for the structural adaptation. To automatically start the 50 simulation runs for each of the three described characteristics, a simulation management framework for agent based distributed systems [33] was used. Additionally, an evaluation framework for the automatically observation and evaluation of predefined system observables [34] was used.

The six different coordination processes were described declaratively using the *MASDynamics* language. As a technical realization two different coordination mechanisms were implemented. The first one randomly selects one agent of the appropriate type. This coordination mechanism was used by the three random-selection based coordination process manifestations. The other coordination mechanism used the positioning service offered by the environment to select and inform the nearest agent of the appropriate type. This coordination mechanism was used by the three neighborhood based coordination process manifestations.

#### A. Coordination

In order to evaluate the impact of the self-organization, the number of analyzed, produced and collected ore was observed in each of the 50 simulation runs for the neighborhood and random-selection based coordination process manifestations. Figure 9 shows the results of the analysis. The time passed is denoted on the x-axis in 1/10 seconds steps. The y-axis shows the percentage amount of ore that is analyzed, produced or collected. As described in Section V-C, the scenarios had a total amount of 1000 units of ore. Only the first 3 minutes of all simulation runs were observed, because this was the fastest time in which the scenario was completely depleted in all of the simulation runs and, therefore, the only period under observation that contains results for all simulation runs. The results of the neighborhood-based coordination process

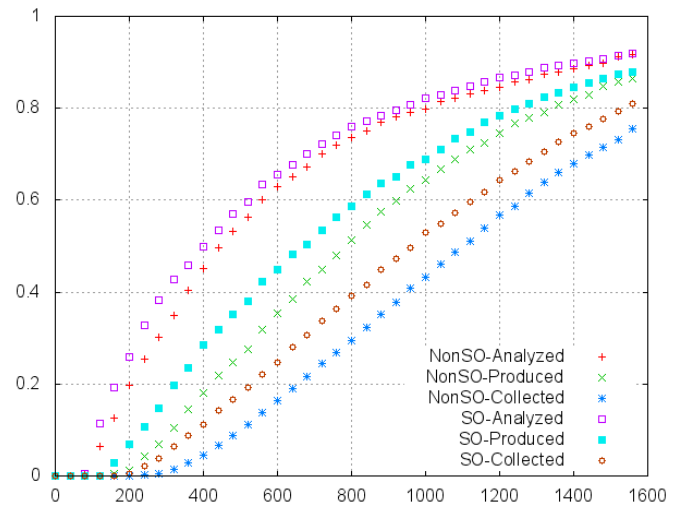


Figure 9. Evaluation of the coordination processes.

manifestations are identified by the *SO*-prefix in Figure 9 and the ones based on the random-selection coordination process manifestations by the *NonSO*-prefix.

The efficiency of the self-organization is shown in Figure 10. Again the x-axis denotes the passed time in 1/10 second steps and the y-axis shows the percentage efficiency of the self-organizing coordination processes over the non self-organizing ones. It shows how the self-organized coordination processes which enable the agents to form local mining groups by calling the nearest available agent of the required type increase the overall efficiency. On a more detailed view, the figure shows that the impact of the self-organization on the amount of analyzed ore is significantly less then the impact on the amount of produced and collected ore. This is because the *Sentry* agents are able to find potential ore deposits to analyze by themselves while they are exploring the environment randomly. Therefore, they do not necessarily rely on receiving coordination information about potential ore deposits. These information just helps the agents to find deposits faster. The *Producer* and *Carry* agents, on the other hand are only able to produce or carry ore when they have received a coordination information about an analyzed or mined deposit. Thus, their ability to produce or carry ore strongly depends on the coordination. Contrary, the *Sentry* agents are able to analyze ore without any coordination. Furthermore, the figure shows how the efficiency of the three self-organized coordination processes differs over time depending on the amount of ore that has already been analyzed, produced or carried.

#### B. Structural Adaptation

To measure the impact of the structural self-adaptation 50 simulation run were executed with the self-organizing coordination processes active at start time. After 60 seconds a failure in the positioning service of the environment was simulated. Thus, the self-organizing coordination processes relying on this service were no longer able to select the nearest appropriate agent and therefore, were not able to distribute coordination information anymore. As described before, the Adaptation Enactment was blocked for the first 30 seconds

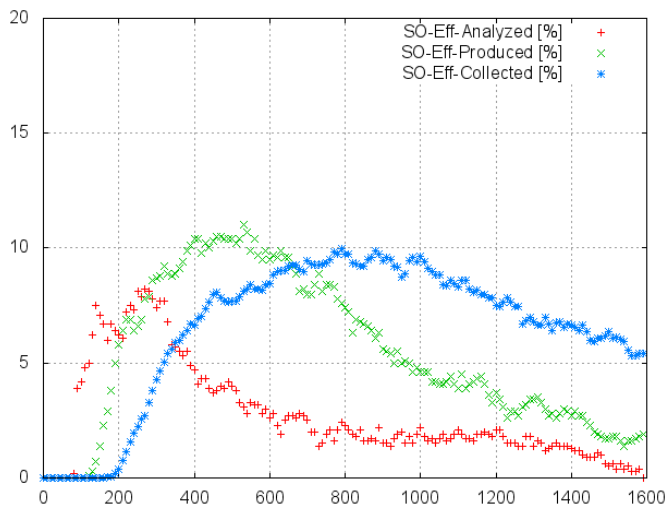


Figure 10. Efficiency of the self-organized coordination processes.

to overcome problems due to agents still exploring the environment without having sensed any potential ore deposits and therefore, not sending any coordination information. Figure 11 shows the evaluation results of the structural adaptation. Again the x-axis denotes the time in 1/10 second steps. The y-axis shows the total number of voting attempts, the percentage of simulated failures in the positioning service and the percentage of performed adaptations.

The figure shows how the simulated failure in the positioning service occurs after 60 seconds have passed (deviations are caused by inaccuracies of the MAS platform's clock service). First voting attempts can be observed after 50 seconds have passed, as this is the shortest possible time after which agents could notice not having received any coordination information within the last 20 seconds. As the figure shows, the percentage of voting attempts grows until in mean all systems have performed the structural adaptation. In this case the adaptation was configured to be a *unique* adaptation. So, after it was performed, no further voting attempts were started. The results also show that in approximately 15% of the simulation runs, the system adapted its structure before the actual failure occurred. As described before, the adaptation requires a majority of 75% percent of the agents agreeing on it. As the scenario consists out of 16 agents, 12 agents are required to vote for the adaptation. For the voting attempt to be started, at least one agent must not have received any coordination information within the last 20 seconds. In order to reach the required majority, this requires at least 11 agents not having received any coordination information within the last 15 seconds (the specified threshold value). Due to the random exploration of the environment this phenomena might occur before the simulated failure, if the agents have only sensed a few ore deposits. Combined with the formation of local self-organized mining groups, this can lead to a majority of agents that are not involved in any mining activities and, therefore, are not receiving any coordination information. These agents will interpret the absent of such messages as a potential failure in the coordination processes and thus, vote for the structural adaptation. A higher blocking time for the adaptation enactment at start time or higher constraint and threshold

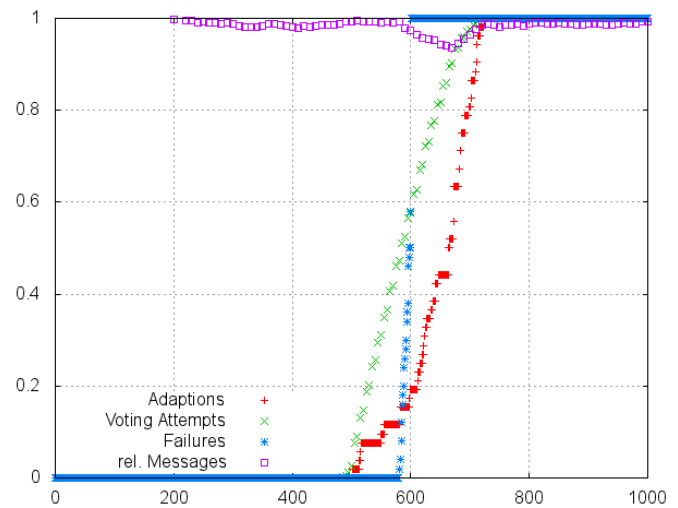


Figure 11. Evaluation of the structural adaptation.

values would lead to fewer premature adaptations. But on the other hand, that would also lead to a higher response time before the system adapts itself after a failure. As described in Section III-B, suitable adaptation parameters have to be identified as part of an iterative, simulation driven engineering approach.

Furthermore, the figure also shows the relative number of coordination messages from the defective scenarios, in relation to the number of coordination messages from the self-organized scenarios where no failure occurs and therefore, no adaptation was needed. The curved line shows that there is no deviation between the two scenarios until the failure occurs. When the failure occurs the number of messages slides down in relation to the failure-free scenario. After the structural adaptation took place, the number of messages rises up until the level of the failure-free scenario is reached again. This shows how the structural adaptation is able to repair a deficient behavior caused by an external failure.

## VII. CONCLUSION AND FUTURE WORK

In this paper, we presented an architecture and engineering approach for structural adaptations in self-organizing MAS to realize the dynamic exchange or reconfiguration of self-organizing coordination processes. It aims at supporting structural adaptations in general, rather than focusing on single self-\* properties. The approach consists of a generic system architecture that governs the development of self-organizing MAS and a description language that supports the declarative description of coordination processes and pre-described structural adaptations, which can be processed by the corresponding framework automatically. It is supported by an engineering process consisting of incremental development activities that are supplemented with activities that address the manifestation of self-organizing behavior. The approach supports the modularization of coordination, which enables reusability and interoperability of coordination processes. It propagates a clear separation between application functionality and coordination, allowing developers to implement coordination without the need to change the application's business logic. Furthermore, with the introduction of structural adaptations of coordination

processes it supports the self-adaptive structural exchange or reconfiguration of self-organizing processes. By detecting any decrease of specified SO performance indicators, the adaptation enactment extension initiates a distributed voting process, that allows for the exchange or reconfiguration of the self-organizing processes to adapt to changing conditions automatically. It is conceptual comparable to the reactive planning approach (local) from the BDI agent model, where an agent selects a plan based on local information and alternatives. In case of the proposed approach, the system as a whole strives towards a distributed consensus on application-global level to select and execute predefined structural adaptation plans. Thereby, each of the participating agents only relies on its local information.

The presented framework was used in the *MarsWorld* scenario to realize a collaborative application in which three different types of agents needed to be coordinated, in order to mine ore on Mars. This scenario was used to evaluate both the impact of self-organizing coordination processes and their structural adaptation. In order to show the impact of self-organizing behavior three different coordination processes in two different manifestations were implemented. A random-selection based manifestation and a proximity-based one. The later one allows the agents to form local mining groups in a self-organized way by exchanging coordination information with the nearest possible agent. For each of the two coordination process manifestations 50 simulation runs were performed and the number of analyzed, produced and collected ore was measured. Based on these results, it was shown that the application benefited from self-organizational behavior, as the self-organizing proximity-based coordination processes were more efficient in terms of processed ore over time than their non self-organizing counterparts. The impact of structural adaptations was shown by simulating a failure in the positioning service offered by the environment and used by the proximity-based coordination processes. The agents' Adaptation Enactments detected and interpreted the absence of coordination messages caused by the failure of the positioning service as a deficient behavior and agreed on a structural adaptation using a distributed voting approach. The deficient proximity-based coordination processes were deactivated and replaced by their random-selection based counterparts. Thus, we showed how the system was able to recognize the failure of the positioning service, by observing the absence of incoming coordination information and adapting its structure to repair itself. Furthermore, it was explained under which conditions the system adapted itself rightfully and which conditions may lead to premature adaptations due to misinterpretations of the absence of coordination information.

Future work aims at the reimplementation of both the decentralized coordination framework for MAS (*DeCoMAS*) as well as the structural adaptation extension. It is envisioned to realize a more general coordination framework that does not only supports MAS but component-based applications in general. Therefore, the focus will shift from the coordination of agents to the coordination of universal software components. This should support a broader range of applications and both unify and simplify the engineering and development process of self-organizing application relying on decentralized coordination processes. This new Decentralized Coordination Framework (*DeCoF*) will be used to realize the self-organizing

redistribution of bikes in a bike-sharing system as described in [35]. Based on the structural adaptations it shall be shown how the adaptation of different coordination processes optimizes the self-organizing redistribution of the bikes depending on the time of day and rush-hour situations.

#### ACKNOWLEDGMENT

The authors would like to thank Deutsche Forschungsgemeinschaft (DFG) for supporting this work through a research project on "Self-organization based on decentralized coordination in distributed systems" (SodekoVS).

#### REFERENCES

- [1] T. Preisler and W. Renz, "Structural adaptations for self-organizing multi-agent systems," in Seventh International Conference on Adaptive and Self-Adaptive Systems and Applications (ADAPTIVE), Nice, France, 2015, pp. 1–8.
- [2] K. Geihs, "Selbst-adaptive software," *Informatik-Spektrum*, vol. 31, 2008, pp. 133–145.
- [3] A. Vilenica, "Anwendungsentwicklung selbstorganisierender systeme: Systematische konstruktion und evaluierung," Ph.D. dissertation, Hamburg University, Department of Informatics, Vogt-Kölln-Str. 30, 22527 Hamburg, Germany, 12 2013.
- [4] A. S. Rao and M. P. George, "Bdi agents: From theory to practice," in Proceedings of the First International Conference on Multi-Agent Systems (ICMAS-95), 1995, pp. 312–319.
- [5] J. O. Kephart and D. M. Chess, "The vision of autonomic computing," *Computer*, vol. 36, no. 1, 2003, pp. 41–50.
- [6] J. Branke, M. Mnif, C. Müller-Schloer, H. Prothmann, U. Richter, F. Rochner, and H. Schmeck, "Organic computing - addressing complexity by controlled self-organization," in Proc. of the 2th Int. Symp. on Leveraging Appl. of Formal Methods, Verification and Validation, ser. ISOLA '06. IEEE Comp. Soc., 2006, pp. 185–191.
- [7] Y. Brun, G. Marzo Serugendo, C. Gacek, H. Giese, H. Kienle, M. Litoiu, H. Müller, M. Pezzè, and M. Shaw, "Software engineering for self-adaptive systems through feedback loops," B. H. Cheng, R. Lemos, H. Giese, P. Inverardi, and J. Magee, Eds. Berlin, Heidelberg: Springer-Verlag, 2009, ch. Engineering Self-Adaptive Systems through Feedback Loops, pp. 48–70.
- [8] J.-P. Mano, C. Bourjot, G. A. Lopardo, and P. Glize, "Bio-inspired mechanisms for artificial self-organised systems," *Informatica (Slovenia)*, vol. 30, no. 1, 2006, pp. 55–62.
- [9] L. Veiga and P. Ferreira, "Poliper: policies for mobile and pervasive environments," in Proceedings of the 3rd workshop on Adaptive and reflective middleware, ser. ARM '04. New York, NY, USA: ACM, 2004, pp. 238–243.
- [10] M. Salehie and L. Tahvildari, "Self-adaptive software: Landscape and research challenges," *ACM Trans. Auton. Adapt. Syst.*, vol. 4, May 2009, pp. 14:1–14:42.
- [11] M. Mamei, R. Menezes, R. Tolksdorf, and F. Zambonelli, "Case studies for self-organization in computer science," *J. Syst. Archit.*, vol. 52, no. 8, 2006, pp. 443–460.
- [12] T. D. Wolf and T. Holvoet, "A catalogue of decentralised coordination mechanisms for designing self-organising emergent applications," Dept. of Comp. Science, K.U. Leuven, Tech. Rep. CW 458, 8 2006.
- [13] D. Garlan, "Model-based adaptation for self-healing systems," in In Proceedings of the first workshop on Self-healing systems. ACM Press, 2002, pp. 27–32.
- [14] M. Smit and E. Stroulia, "Autonomic configuration adaptation based on simulation-generated state-transition models," in Software Engineering and Advanced Applications (SEAA), 2011 37th EUROMICRO Conf. on, 2011, pp. 175–179.
- [15] E. Yuan and S. Malek, "A taxonomy and survey of self-protecting software systems," in Software Engineering for Adaptive and Self-Managing Systems (SEAMS), 2012 ICSE Workshop on, June 2012, pp. 109–118.

- [16] M. Morandini, F. Migeon, M.-P. Gleizes, C. Maurel, L. Penserini, and A. Perini, "A goal-oriented approach for modelling self-organising mas," in Proceedings of the 10th International Workshop on Engineering Societies in the Agents World X, ser. ESAW '09. Berlin, Heidelberg: Springer-Verlag, 2009, pp. 33–48.
- [17] T. De Wolf and T. Holvoet, "Towards a methodology for engineering self-organising emergent systems," in Proc. of the 2005 conference on Self-Organization and Automatic Informatics (I). Amsterdam, The Netherlands: IOS Press, 2005, pp. 18–34.
- [18] G. Di Marzo Serugendo, J. Fitzgerald, and A. Romanovsky, "Metaself: an architecture and a development method for dependable self-\* systems," in Proc. of the 2010 ACM Symp. on Applied Comp., ser. SAC '10. New York, NY: ACM, 2010, pp. 457–461.
- [19] S.-W. Cheng, "Rainbow: cost-effective software architecture-based self-adaptation," Ph.D. dissertation, School of Computer Science, Carnegie Mellon University, Pittsburgh, PA, USA, May 2008.
- [20] K. Geihs, P. Barone, F. Eliassen, J. Floch, R. Fricke, E. Gjørven, S. Hallenstein, G. Horn, M. Khan, A. Mamelli, G. Papadopoulos, N. Paspallis, R. Reichle, and E. Stav, "A comprehensive solution for application-level adaptation," *Software: Practice and Experience*, 2008.
- [21] S. Hallsteinsen, K. Geihs, N. Paspallis, F. Eliassen, G. Horn, J. Lorenzo, A. Mamelli, and G. Papadopoulos, "A development framework and methodology for self-adapting applications in ubiquitous computing environments," *Journal of Systems and Software*, vol. 85, no. 12, Dec. 2012, pp. 2840–2859.
- [22] N. Gui and V. De Florio, "Towards meta-adaptation support with reusable and composable adaptation components," in Self-Adaptive and Self-Organizing Systems (SASO), 2012 IEEE Sixth International Conference on, Sept. 2012, pp. 49–58.
- [23] A. Ismail and V. Cardellini, "Decentralized planning for self-adaptation in multi-cloud environment," in *Advances in Service-Oriented and Cloud Computing*, ser. Communications in Computer and Information Science, G. Ortiz and C. Tran, Eds. Springer International Publishing, 2015, vol. 508, pp. 76–90. [Online]. Available: [http://dx.doi.org/10.1007/978-3-319-14886-1\\_9](http://dx.doi.org/10.1007/978-3-319-14886-1_9)
- [24] R. S. Sutton and A. G. Barto, *Reinforcement learning: An introduction*. MIT press Cambridge, 1998.
- [25] C. J. Watkins and P. Dayan, "Q-learning," *Machine learning*, vol. 8, no. 3-4, 1992, pp. 279–292.
- [26] J. Sudeikat and W. Renz, "MASDynamics: Toward systemic modeling of decentralized agent coordination," in *Komm. in Vert.Syst. (KiVS)*. Springer, 2009, pp. 79–90.
- [27] —, "Decomas: An architecture for supplementing mas with systemic models of decentralized agent coordination," in *IEEE/WIC/ACM International Conference on Web Intelligence*. IEEE, 2009, pp. 104 – 107.
- [28] T. Preisler, A. Vilenica, and W. Renz, "Decentralized coordination in self-organizing systems based on peer-to-peer coordination spaces," in *Works. on Self-organising, adaptive, and context-sensitive distributed systems (SACS)*, vol. 56, 2013.
- [29] A. Vilenica, J. Sudeikat, W. Lamersdorf, W. Renz, L. Braubach, and A. Pokahr, "Coordination in Multi-Agent Systems: A Declarative Approach using Coordination Spaces," in Proc. of the 20th European Meeting on Cybernetics and Systems Research (EMCSR 2010) - Int. Workshop From Agent Theory to Agent Impl. (AT2AI-7), R. Trappl, Ed. Austrian Soc. for Cyb. Studies, 4 2010, pp. 441–446.
- [30] J. Sudeikat, L. Braubach, A. Pokahr, W. Renz, and W. Lamersdorf, "Systematically Engineering Self-Organizing Systems : The SodekoVS Approach," *Electronic Communications of the EASST*, vol. 17, 2009, p. 12.
- [31] J. Ferber, *Multi-Agent Systems: An Introduction to Distributed Artificial Intelligence*, 1st ed. Boston, MA, USA: Addison-Wesley Longman Publishing Co., Inc., 1999.
- [32] L. Braubach and A. Pokahr, "Jadex active components framework - BDI agents for disaster rescue coordination," in *Software Agents, Agent Systems and Their Applications*, ser. NATO Science for Peace and Security Series - D: Information and Communication Security, M. Essaïdi, M. Ganzha, and M. Paprzycki, Eds. IOS Press, 2012, vol. 32, pp. 57–84. [Online]. Available: <http://dx.doi.org/10.3233/978-1-60750-818-2-57>
- [33] A. Vilenica and W. Lamersdorf, "Simulation management for agent-based distributed systems," in *Enterprise Information Systems*, J. Filipe and J. Cordeiro, Eds. Springer-Verlag, 3 2011, pp. 477–492.
- [34] —, "Benchmarking and evaluation support for self-adaptive distributed systems," in *The Sixth International Conference on Complex, Intelligent, and Software Intensive Systems (CISIS 2012)*, L. Barolli, F. Xhafa, S. Vitabile, and M. Uehara, Eds. IEEE Explore, 7 2012, pp. 20–27.
- [35] T. Preisler, T. Dethlefs, and W. Renz, "Data-adaptive simulation: Cooperativeness of users in bike-sharing systems," in *Proceedings of the Hamburg International Conference of Logistics*, W. Kersten, T. Blecker, and C. M. Ringle, Eds., vol. 20. epubli GmbH, 2015.

## Pedestrian Detection with Cascaded Part Model for Occlusion Handling

Yawar Rehman<sup>1</sup>, Irfan Riaz<sup>2</sup>, Fan Xue<sup>3</sup>, Jingchun Piao<sup>4</sup>, Jameel Ahmed Khan<sup>5</sup> and Hyunchul Shin<sup>6</sup>

Department of Electronics and Communication Engineering,

Hanyang University (ERICA Campus), South Korea

e-mail: {yawar<sup>1</sup>, irfancra<sup>2</sup>, fanxue<sup>3</sup>, jameel<sup>5</sup>}@digital.hanyang.ac.kr, {kcpark1011<sup>4</sup>, shin<sup>6</sup>}@hanyang.ac.kr

**Abstract**—Pedestrian detection in a crowded environment under occlusion constraint is a challenging task. We have addressed this task by exploiting the properties of a rich feature set, which gives almost all cues necessary for recognizing pedestrians. Such rich feature set results in higher dimensional feature space. We have used partial least square regression to map these higher dimensional features to a lower dimensional yet discriminative feature space. Part model is further applied to deal with occlusions. The proposed method gives the best reported results on INRIA pedestrian dataset with detection accuracy of 98% at  $10^{-4}$  False Positives Per Window (FPPW) and a miss rate of 31.62% at  $10^{-1}$  False Positives Per Image (FPPI). We have also demonstrated the effectiveness of our part model under partial and heavily occluded conditions. Our proposed system outperforms several state of the art techniques under various evaluation conditions of INRIA pedestrian database.

**Keywords**-Pedestrian detection; occlusion handling.

### I. INTRODUCTION

Recent advancements in computer vision show researchers interest in developing a system to detect pedestrians efficiently. Detecting pedestrian is a challenging problem and various methods have been proposed. The performance of the detector depends on how well the method works in complex environments such as crowded scenes, illumination variation, occlusion, and cluttering [1]. Extensive literature can be found on the problem of object detection. It all started with the revolutionary work of Viola and Jones (VJ) [2][3]. VJ used integral sums as features and developed adaboost as classifiers. VJ achieved 20% of miss rate at over 10 FPPI. Histogram of Oriented Gradients (HOG) [4] achieved the same miss rate at  $\sim 1$  FPPI and more recent methods [5][6] at equivalent miss rate achieved under  $10^{-1}$  FPPI (data obtained from [7][8]). With the passage of time, researchers have given importance to the rich feature sets. Wang [9] cascaded texture and HOG features and trained a linear Support Vector Machine (SVM) so that small feature blocks of SVM weights can handle occlusions. In contrast to Wang's approach (HogLbp), we combined gradient, texture and color features and trained the linear SVM in lower dimensional feature space using partial least squares regression. In addition to it, we have cascaded a part model instead of breaking the final feature vector into small feature blocks for occlusion handling. Felzenszwalb's [10] deformable part model (DPM) achieved two fold improvement over 2006 PASCAL best performance for pedestrian detection. Schwartz [11] solved the problem of human detection in reduced dimensional space. Their feature vector was composed of three concatenated features, i.e., Co-

occurrence matrices for texture information, Histogram of Oriented Gradients (HOG) for gradient information, and color information. Concatenation of these three features resulted in a feature vector of 170,820 dimensions. Partial Least Square (PLS) regression was used to reduce high dimensional feature space into discriminative reduced dimensional feature space. Quadratic Discriminant Analysis (QDA) model was used for classification. Kembhavi [12] also tackled vehicle detection problem in reduced dimensional space. They captured the color properties of the vehicle and its surroundings through color probability maps. Gradient information of the vehicle was captured using HOG and the pair of pixels method was used to extract structural properties. Concatenation of all these features resulted in the final feature vector of 70,000 dimensions. PLS regression was used for lower dimensional feature space and QDA model was trained as a classifier for finding objects of interest. Wang [13] handled object tracking as a classification problem and worked it out in reduced dimension by creating different PLS subspaces. They proposed an adaptive appearance model, which used different subspaces to handle variation of poses, occlusion, and cluttering. Haj [14] used discriminative properties of PLS lower dimensional space to solve the problem of head pose estimation. The author also compared different dimensionality reduction approaches and the result obtained from PLS regression was reported the best.

Dollár [15] proposed Aggregate Channel Features (ACF) and emphasized the importance of color features in the task of pedestrian detection. Author used boosted features for the task of pedestrian detection. Feature pool was created by using multiple channels such as gradient, intensity, and color features. Several first and second order features were calculated on a patch inside a detection window on different channels. Boosted classifier was trained as [2] on these features in order to classify the detection window while testing. Benenson [16] transferred computations from testing time to training time and proposed a pedestrian detector named "Very Fast". Lim [17] proposed a method "Sketch Tokens" to detect contour of the objects. Sketch tokens were used with ACF as additional features for pedestrian detection. Benenson [18] reported a set of experiments in the quest of strongest rigid detector, and proposed "Roerei" pedestrian detector. The detectors proposed in [16][17][18] followed the frame work of ACF for pedestrian detection and provided state of the art results. Our part model is also based on the structural design of [15].

The key contributions of the proposed method are the cascaded integration of the part model with the root model (which in terms suppresses the false positives and handle

occlusions) and the proposed formulation for switching between the root model and the part model (when occlusion hypothesis is verified) on the fly. The integration of both models help significantly in solving the occlusion cases and decreases the number of miss classifications, which improve the detection accuracy of the proposed system. And the switching formulation helps to commute the time for feature calculations of both models.

We demonstrate our proposed system on INRIA pedestrian database. INRIA pedestrian database was introduced by Dalal & Triggs [4] when their detector performed almost ideal on the first ever MIT pedestrian database. INRIA dataset is still not fully explored and rigorously used in pedestrian detection evaluation. It contains 2,416 training positive windows cropped from 614 frames and 1,126 testing positive windows cropped from 288 frames. Both windows and frames are included in INRIA database. Training and testing negative frames are provided separately in INRIA database. Our system achieved the accuracy of 91% at  $10^{-5}$  false positive per window (FPPW), 98% at  $10^{-4}$  FPPW [1] and a miss rate of 31.62% at  $10^{-1}$  FPPI. Our system consists of two main models, Partial Least Square (PLS) model and Part model (PM). Partial Least Square is a dimension reduction technique, which emphasizes supervised dimension reduction. PLS is helpful in providing discriminative lower dimensional feature space and avoiding the calculations containing thousands of extracted features. Part model ensures the search of a subject (i.e., pedestrian) in parts rather than to be searched as a whole. PM is helpful in handling occlusions. We have designed our part model as was described in [15].

## II. FEATURE EXTRACTION

We have used three types of features in PLS model, i.e., gradient features, texture features, and color features.

### A. Gradient Features

The first and foremost features that we have added in our feature set are gradient features. It is due to the fact that the research in object detection, specifically in human detection has increased significantly after the advent of HOG feature descriptor [4]. HOG was dedicated to human detection and it also provided the best results of its time.

For computing gradient features, we have used heavily optimized implementation of [15][19][20][21], which is similar to that of [4]. An image window is divided into 8x8 pixel blocks and each block is divided into 4 cells of 4x4 pixels. 9 bin HOG features per cell was then calculated obtaining 36 dimensional features per block. Each block is L2 normalized, which resulted 4 different normalizations per cell. It is useful because it makes HOG descriptor illumination invariant. HOG also shows rotation invariant properties as long as rotation is within the bin size. Clipping value of histogram bin is set to 0.2 and trilinear interpolation is used for the placement of gradients into their respective bins.

### B. Texture Features

The texture information provides better results particularly in case of face detection because of discriminative texture on

face (i.e., eyes, nose, mouth, etc). Including texture information in the pedestrian feature set will tend the system towards improvement in terms of detection because of the fact that there is a considerable amount of discriminative texture inside human contour.

We have used Local Binary Pattern (LBP) [22] to estimate texture features. LBP is a simple yet efficient technique for calculating texture in an image. It assigns the value '1' in 3x3 pixel neighborhood if each pixel's intensity value in the neighborhood is greater than or equal to the center pixel's intensity value, '0' is assigned, otherwise. There are many variants of LBP but we have used the most stable one, which was reported to achieve good results by many authors. 3x3 neighborhood produces 256 possible binary patterns, which are too many for making reliable texture feature descriptor but in 256 possible binary patterns there exist total of 58 patterns, which exhibit at most two bit-wise transitions from '0' to '1' or from '1' to '0'. These patterns are known as uniform patterns. Using uniform patterns instead of 256 patterns will remarkably reduce the texture feature vector size with marginal decrease in performance [22]. We have used the implementation of uniform patterns as was given by [23]. An image window is divided into the blocks of 8x8 pixels and for each block a 58 texture feature descriptor is calculated. The final texture feature set is obtained by concatenating features obtained from several blocks.

### C. Color Features

Color features play an important role in providing discriminative identities to objects. The dilemma is when talking about pedestrian detection, better recognition rates and efficiency by including color information is doubted by some researchers because of the variability in clothing color. Instead [11][15][24] showed the importance of color features in pedestrian detection.

We have taken the samples of pedestrians and non-pedestrians (i.e., non-humans) from INRIA database and converted into LUV color space. Our intuition of selecting LUV came from the result reported by [15], that LUV outperformed other color spaces by achieving an accuracy of 55.8% alone (i.e., not combined with other features) in pedestrian detection. PLS regression is applied on L, U, and V space separately. PLS regression components shows maximum inter-class and intra-class variance. Human contour can be seen as silhouette by plotting them. U space showed dominant (red) peak at head region in all three PLS components. It is because variance of the head region in an image with respect to the surrounding region was maximum. During experimentation, we tried to include only U space as color information, but accuracy has decreased. In our opinion, the decrease in accuracy was due to lack of color information, which also points to the fact that including color information plays a significant role in detection. We have exploited this by including LUV color space representation in our system.

The final feature vector reflecting different extracted information from an image window looks like:

$$F = [\text{Gradient Texture Color}] \quad (1)$$

### III. PARTIAL LEAST SQUARES MODEL

We have accumulated rich feature set for all possible cues of pedestrians, which resulted in high dimensional feature space. In our experiments, the number of samples used for training the classifier are less than the dimension of rich feature space. The phenomenon when data dimensions remains greater than the number of samples is known as multicollinearity. Partial least squares regression addresses the problem of multicollinearity and reduces data dimensions. PLS regression uses class labels for producing latent components that makes lower dimensional space more discriminative. An idea of constructing latent variables is summarized here, for details reader is encouraged to refer [25][26].

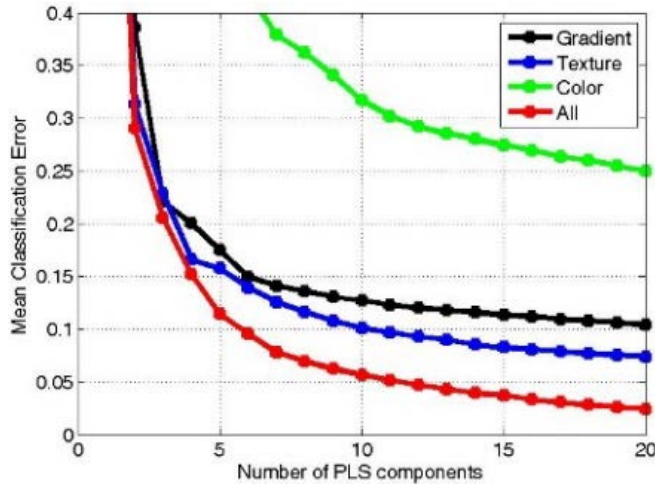


Figure 1. Mean square error vs PLS components

There are two popular variants of PLS, Non-iterative partial least square (NIPALS) and Simple partial least square (SIMPLS). They both differ in matrix deflation process. We used SIMPLS regression in our experiments. Let  $X^{N \times m}$  and  $Y^{N \times n}$  be the two blocks of variables. PLS models the relationship between the sets of variables by maximizing the covariance between them through latent variables.

$$X = TP^T + E \tag{2}$$

$$Y = UQ^T + F \tag{3}$$

Where  $T^{N \times p}$  and  $U^{N \times p}$  are score matrices;  $P^{m \times p}$  and  $Q^{n \times p}$  are loading matrices and  $E^{N \times m}$  and  $F^{N \times n}$  are residuals. The weight matrix in first iteration is calculated as,

$$w_1 = \bar{X}^T \bar{Y} / \|\bar{X}^T \bar{Y}\| \tag{4}$$

and till  $k^{th}$  iteration it is calculated as,

$$\bar{X}_k = \bar{X}_{k-1} - t_{k-1} p_{k-1}^T \tag{5}$$

Where  $t$  and  $p$  are the column vectors of matrix  $T^{N \times p}$  and  $P^{m \times p}$ , respectively, and  $k$  represents the number of PLS factors. The dimension of an input image  $x$  is reduced by projecting its feature vector on to the weight matrix obtained after  $k$  iterations, where columns of  $W = \{w_1, w_2, w_3, \dots, w_k\}$

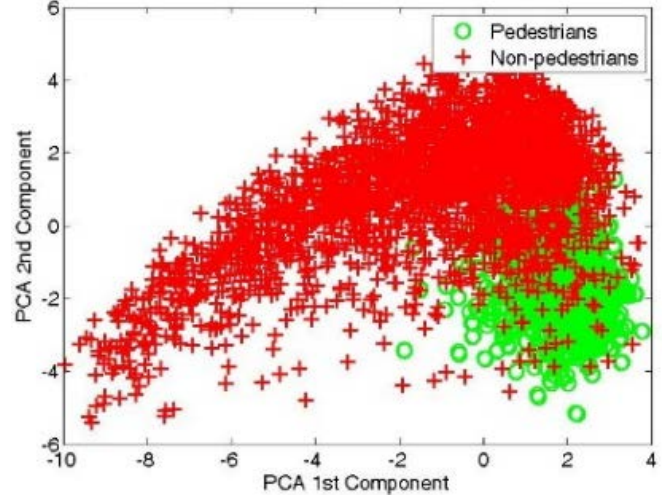


Figure 2. PCA lower dimensional space

represents PLS components. After projection, a low dimensional vector  $z^{1 \times k}$  is obtained.

Principal component analysis (PCA) is a well-known technique for dimension reduction. It also addresses multicollinearity problem, but does not consider class labels of data for dimension reduction. PLS is a supervised dimension reduction technique that considers class labels for dimension reduction. This enables PLS to produce highly discriminative reduced dimensional data as it is evident from Figures 2 and 3. We have plotted first two components of both dimension reduction techniques to show their discriminative power in lower dimensional space.

Our system extracts three cues from an image patch, which makes our high dimensional feature set. The total number of features extracted from an image patch are approximately fourteen thousand. With the help of PLS, we have reduced our feature set to only sixteen dimensions, which are the best representation of our high dimensional data. Figure 1 shows the mean classification error at different dimensions.

### IV. PART MODEL

Part models are generally used in pedestrian detection to handle occlusions. It is a common practice to divide human body into five parts (i.e., head, left torso, right torso, upper limbs, and lower limbs) and detect each part separately. Deformation schemes were also introduced by several authors in order to keep different parts glued together. In our case, we have used upper body part model. The model includes head, left torso, and right torso.

We argue that, using upper body parts as a whole will give more discrimination among features because hardly any other object is represented with this structure. The structure of head, shoulders, arms, and torso (all connected) gives more discriminative feature property rather than to search them individually. Furthermore, to avoid complex deformation schemes [10], using only upper body as a part model is the best choice.

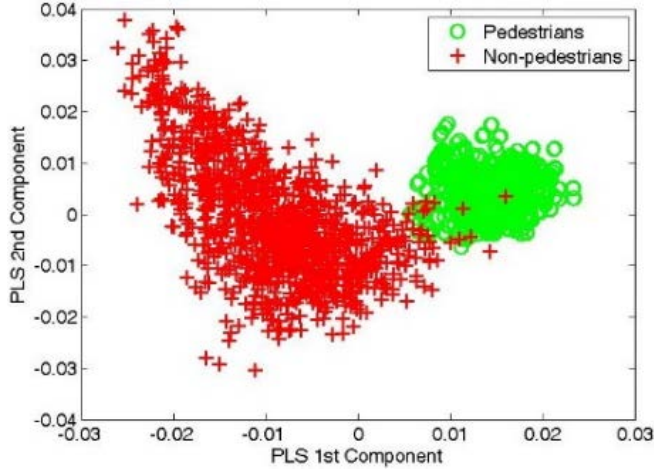


Figure 3. PLS lower dimensional space

P. Dollà reported in [27] that over 53% of the pedestrians are occluded in some frames and 19% of the pedestrians are occluded in all frames. The author underscores the importance of detecting occluded pedestrians by reporting that over 70% of the pedestrians are occluded in all frames. Author further reports that 97% of the occlusion belongs to a small subset out of hundreds of possible occlusion types. The pedestrians in this subset are occluded from lower torso to limbs region, which also seconds our rationale of using upper body model for occlusion handling.

In order to design the upper body model, we have used the frame work of Aggregate Channel Features (ACF). For an input image  $I$ , we compute gradient histogram, gradient magnitude and color channels. After computing channels, we sum block of pixels to make the aggregate channels. Thus, the aggregate channels are the single pixel look up tables of the computed channels. We finally vectorize the aggregate channels and give them to the decision tree classifier to differentiate upper body from the background.

We have used total of ten channels, six gradient histogram channels, one gradient magnitude channel and three color channels of LUV color space as shown in Figure 4. Six gradient histogram channels contain the high pixel values of only those pixel, which lie in the respective span of the gradient angles, the values of remaining pixels are assigned zero. First gradient channel contains the high values of pixels that lie in the range of  $0 \sim 30$  degrees, second gradient channel contains the high values of pixels that lie in the range of  $31 \sim 60$  and so on. Six gradient histogram channels covers the span of  $0 \sim 180$  degrees. Magnitude channel contains the magnitude values of all the pixels in an input image  $I$ . Gradient magnitude channel basically gives the information of a sudden change in intensities or edges. Color channels contain the three channels of LUV color space. The reason of using LUV color space was discussed in Section II. The gradient angles and magnitudes were calculated by using the following equations.

$$\nabla I = \begin{bmatrix} g_x \\ g_y \end{bmatrix} = \begin{bmatrix} \partial I / \partial x \\ \partial I / \partial y \end{bmatrix} \approx \begin{bmatrix} I(x+1, y) - I(x, y) \\ I(x, y+1) - I(x, y) \end{bmatrix} \quad (6)$$

$$M(x, y) = \sqrt{g_x^2 + g_y^2} \approx |g_x| + |g_y| \quad (7)$$

$$\phi(x, y) = \tan^{-1} \left( \frac{g_y}{g_x} \right) \quad (8)$$

This type of channel frame work is often called modern HOG features with color. Since features are designed in such a way that they should be easier for the classifier to learn. It is a common practice to choose a classifier first, and based on the properties of that classifier features are designed, and not vice versa. Adding color features along with gradient histogram and gradient magnitude channel tends to improve the performance of detector, because of similar variance of color in face and hand regions. Final feature vector contains the information of gradients histogram, magnitude, and color from head, shoulders, left, and right torso. Discussion on the training of the classifier for part model is presented in Section V.

## V. CLASSIFIERS

### A. Linear Support Vector Machine

We have used linear support vector machine (SVM) for training our root model (i.e., full body detector) and for detection purpose the famous sliding window technique have been used. The sliding window technique checks for the object of interest at every possible location. Because we have trained our linear SVM on a fixed scale, so we made the pyramid of test image, to make our detector scale invariant and reduced the search problem to a binary classification problem. We trained our linear SVM classifier as was described in [4] and using a template size of  $128 \times 64$  pixels.

For a robust binary classifier it is a common practice to use 'bootstrapping', which was introduced in [28]. The main idea behind this technique is to minimize the training data of negative images. First, a classifier is loaded with the cache of all positive and some negative examples and it is trained. Then the trained classifier is applied on the negative images from the natural dataset, i.e., the dataset does not contains object of interest. This is also known as "mining hard negatives". Classifier will produce some false positives in the current round, which are stored. Then the classifier is again trained with the cache of false positives in addition to its previous cache of positive and negative examples in the next round. This process may be repeated few times but over fitting should be avoided.

We have trained linear SVM with the help of afore mentioned discussion. We have loaded all the positive samples of the upper body and 5000 negative samples extracted randomly from the training negative images and positive windows provided in INRIA pedestrian database. We have set the bucket size of collecting negatives as 5000, and maximum negatives that can be collected as 10,000. In the 1<sup>st</sup> round of bootstrapping, our classifier has collected 5000 negative samples, making the total number of negatives 10,000. We have trained the classifier again with the positives and 10,000 negative samples, and ran it on the testing negative images. In the 2<sup>nd</sup> round of bootstrapping, our classifier has collected around 3000 negative samples, making the total number of hard negatives  $\sim 13,000$ . We

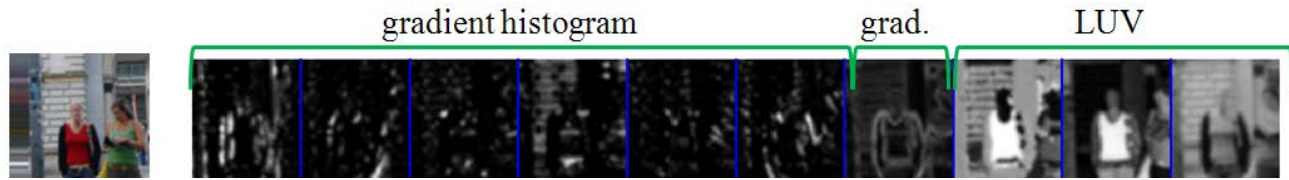


Figure 4. The computed gradient histogram, gradient magnitude and LUV color channels. The channels are computed on 128x64 pixel image. Six histogram channels, each containing high values of those pixels, which lie in the respective range. Gradient magnitude channel captures the edges as shown by the person upper body silhouette. L, U and V channel shows different shades of color in its domain. The input image on the left most is bigger in dimension and contains more background [15].

randomly choose 10,000 hard negatives out of 13,000 and train our classifier to initiate the next round of bootstrapping. In round 3, our classifier hardly collected  $\sim 100$  negative samples. We stop the training of the classifier after three rounds of bootstrapping.

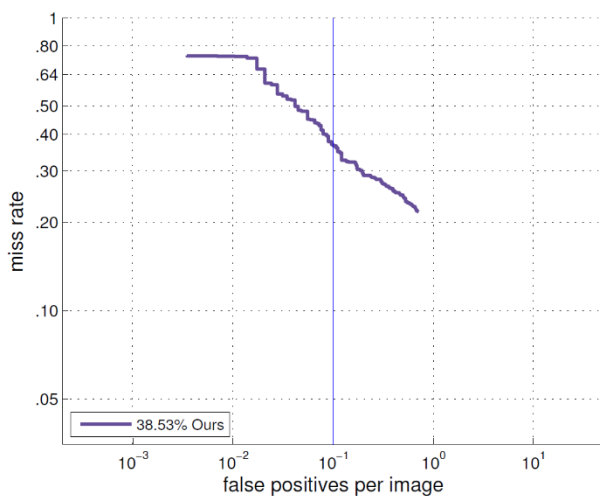


Figure 5. Missrate of our trained PLS person detector on INRIA dataset with 5000 bucket size and 10,000 total no. of negatives using FPPI evaluation metric.

It is necessary to fix the total number of negative that can be collected to avoid the over fitting problem. As SVM is a good memorizer, it over fits on the data when large number of negatives are added. An over fitted classifier will perform better on the training data but the accuracy of the same classifier will fall drastically if tested on a data other than training. We have fixed the total number of negative samples that can be collected to 10,000 and also introduced randomness in the selection of negative samples, which ensures that the classifier will only learn the features of object rather than to learn a particular pattern that yields high false positive rate in testing. We have achieved the miss rate of 38.53% at  $10^{-1}$  FPPI with our PLS person detector on INRIA dataset as shown in Figure 5. The reason for reporting our results in FPPI evaluation metric and FPPW metric is discussed in the Section VII.

By increasing the total number negatives that can be collected to 12,000 we have achieved the miss rate of 38.42% at  $10^{-1}$  FPPI as shown in Figure 6. By further altering the bucket size and increasing it to 6000, we have achieved the miss rate of 36.98% at  $10^{-1}$  FPPI as shown in Figure 7.

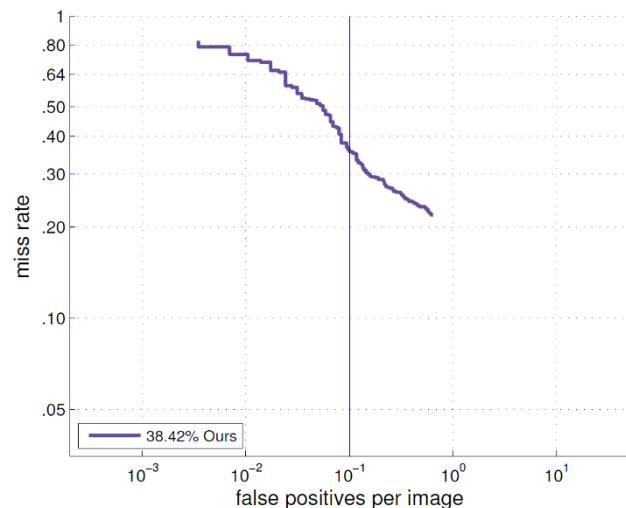


Figure 6. Missrate of our trained PLS person detector on INRIA dataset with 5000 bucket size and 12,000 total no. of negatives using FPPI evaluation metric.

### B. Adaboost

We have trained our upper body model for handling occlusions using adaptive boosting classifier (adaboost). It is a combination of several weak learner that we add up gradually at each stage to make a strong classifier in the end. Among various variants of adaboost, we have used discrete adaboost classifier.

Discrete adaboost is a technique for constructing strong classifier as a combination of several weak classifiers. We have used depth-2 decision trees as our weak classifiers, where each node is a decision stump, which is defined by a rectangular region on the aggregated channels. We perform four rounds of training, in the first round we have loaded 2416 positive samples and 5000 randomly collected negative samples from INRIA pedestrian dataset. We apply bootstrapping in other three rounds and increased the number of weak classifiers in each round (100, 400, 1000, and 2500).

Total of 5000 negative samples were allowed to be added in each round of bootstrapping and the maximum number of negative sample that can be added was set to 15,000. With these settings, the result of our upper body model combined with the PLS root model on INRIA pedestrian dataset is shown in Figure 9.

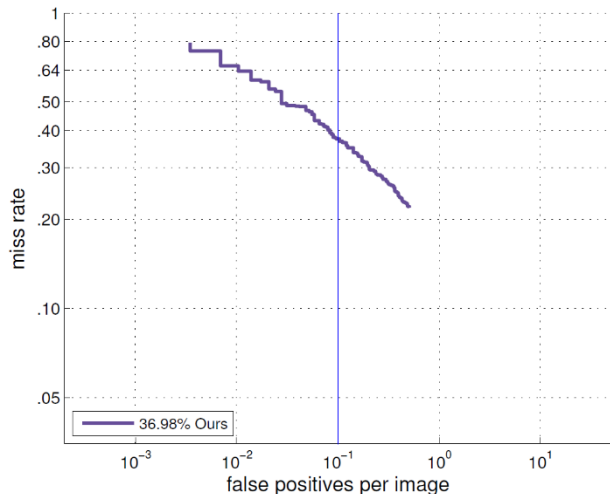


Figure 7. Missrate of our trained PLS person detector on INRIA dataset with 6000 bucket size and 12,000 total no. of negatives using FPPI evaluation metric.

### C. Model switching

Our proposed system demands the use of two different types of features and classifiers. We can calculate both type of features of an input image and then apply both the classifiers on their respective features to get the results. This is a simple but computationally expensive, exhaustive and sluggish way of achieving our goal. What we needed was a system that can switch between the feature calculation and weights of two different models (i.e., PLS & PM) at any location or at any scale on a testing image. We designed a simple conditional model for this task as follows.

We consider that our PLS root model linear SVM calculates the score using the following equation.

$$Y = \beta \cdot \varphi(x_p^s) + bias \quad (9)$$

Where ' $\beta$ ' represents SVM weight vector, ' $x$ ' represents the extracted features at a pyramid scale ' $s$ ' and position ' $p$ ' from an input image, ' $\varphi(\cdot)$ ' represents PLS dimension reduction function, ' $bias$ ' represents SVM bias term, and ' $Y$ ' is the calculated score by linear SVM.

We altered this equation in order to fulfil our needs of speed and to avoid useless computation. We introduced a variable ' $flag$ ', which will decide what features to calculate and, which models to activate using the following equation.

$$Y = (\beta \cdot \varphi(x_p^s) + bias) * flag \quad (10)$$

where

$$flag = \begin{cases} 0, & th1 < Y < th2 \\ 1, & th1 > Y > th2 \end{cases}$$

' $flag$ ' is a function of occlusion hypothesis and it can take only two values i.e., 0 or 1. We generate our occlusion hypothesis when the PLS root model classifier's score at scale ' $s$ ' and position ' $p$ ' lies between thresholds ' $th1$ ' and ' $th2$ '. Whenever this condition is satisfied, part model (upper body model) is activated and the aggregated channel features of the part model will be calculated at scale ' $s$ ' and position ' $p$ '. The decision of the part model classifier will be taken as the final decision. After that part model will be deactivated, and it will wait for the call of ' $flag$ ' to again activate.

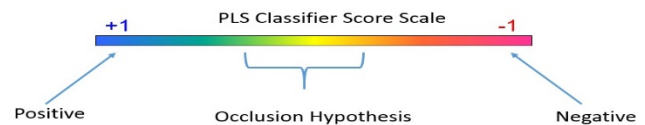


Figure 8. Heuristic for occlusion hypothesis

Combination heuristic of both models (PLS and part model) is discussed in Section VI.

### VI. PLS + PART MODEL (COMBINED MODEL)

Our approach for combining both models is based on simple heuristic. We have trained our classifier for PLS model on lower dimensional space, which is very discriminative in nature. Linear SVM trained on lower dimensional data classifies efficiently and separates humans from non-humans almost accurately. Upon careful analysis, we came to know that the samples that were incorrectly classified by linear SVM either positives or negatives, their score lie in the vicinity of '0'. We generate our occlusion hypothesis that if a sample ' $q$ ' whose predicted score value ' $v$ ' lie between ' $th1$ ' and ' $th2$ ', then it is considered to be an occlusion and upon meeting this condition our part model will be activated and final score ' $m$ ' returned by part model will be taken as true value of the sample ' $q$ '. The heuristic for occlusion hypothesis is shown in Figure 8. Figure 9 shows the miss rate of our combined model at  $10^{-1}$  FPPI on INRIA pedestrian database.

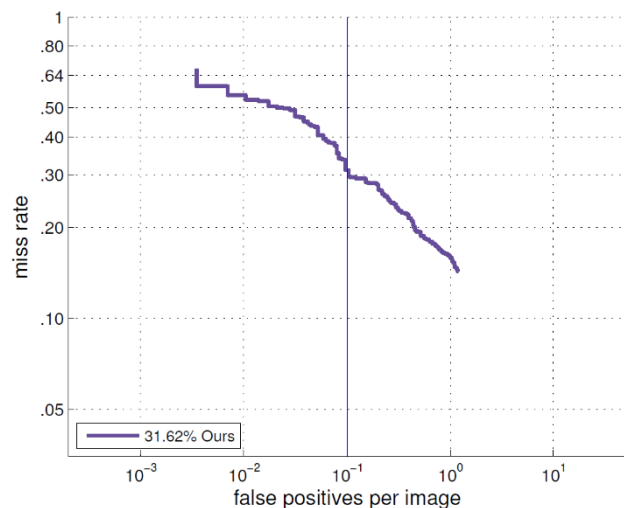


Figure 9. Missrate of our combined model at INRIA pedestrian dataset using FPPI evaluation metric.

### VII. EVALUATION METRICS

It is in common practice the results of object detection are reported in false positives per image (FPPI). As the INRIA dataset comes with test images as well as test windows, it will be unjust to report the results only in FPPI evaluation metrics. We have also reported our results in false positives per window (FPPW) metrics [1] as results in FPPW metrics were also reported by the dataset authors.

### A. FPPW

Several runs of the trained classifiers (on HOG, FHOG & our method) were stored by varying decision threshold. Then the plot between false positive rate ( $FPr$ ) and miss rate ( $Mr$ ) is drawn by using the following equations.

$$FPr = FP/(FP + TN) \quad (11)$$

$$Mr = FN/(FN + TP) \quad (12)$$

Where  $FPr$  represents false positive rate,  $FP$  represents false positives,  $TN$  represents true negatives,  $Mr$  represents miss rate,  $FN$  represents false negatives and  $TP$  represents true positives. The comparison between HOG, variant of HOG (FHOG) introduced by [10], and our method in terms of FPPW, is shown in Figure 10. Each of the classifier was trained as described in Section V. Our system gives accuracy of 90.5% at  $10^{-5}$  false positive per window (FPPW) and accuracy of 98.1% at  $10^{-4}$  FPPW. Testing was done on 1,126 positive cropped windows and 105,500 negative cropped windows from negative images provided by INRIA dataset.

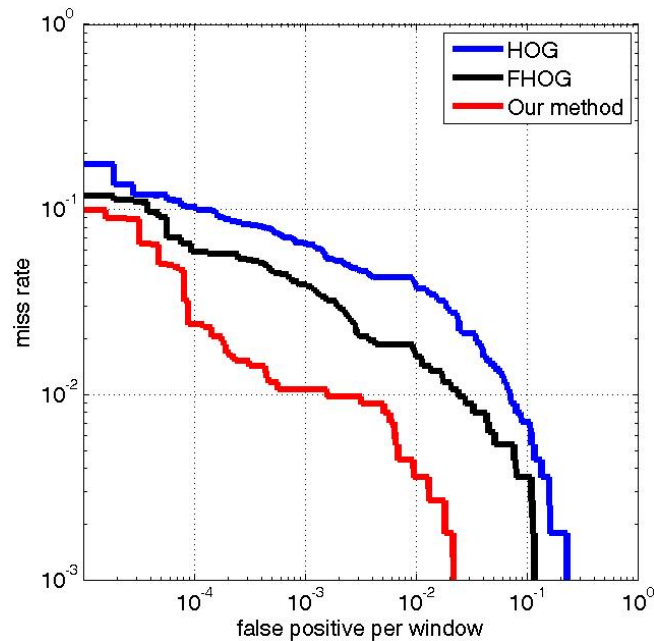


Figure 10. Comparison of our model with HOG and FHOG in FPPW evaluation metrics

### B. FPPI

We report the results of our detector in FPPI evaluation metrics on INRIA dataset. INRIA dataset consists of 288 testing images containing pedestrians varying in sizes, postures and occlusions. Some of the images contains pedestrians with challenging posture, cluttered environment and crowded scenes, which tends to induce occlusions. Performance of our detector under these challenging conditions can viewed in Figure 11. For the FPPI evaluation on INRIA dataset, we have used the improved labelling proposed in [29]. In improved labelling, pedestrians are mainly divided into seven classes. Three of those classes deals with occlusions, other three of them deals with the pedestrian

sizes and the remaining class includes all pedestrians irrespective of their occlusions and sizes. This labelling gives a good estimate of detector's performance in different conditions and scenarios. Table I shows the distribution of pedestrians according to their height in pixels and visibility.

TABLE I. DISTRIBUTION OF INRIA TESTING PEDESTRIAN SAMPLES

Type	Height (pixels)	Visibility (%)
Reasonable	50 ~ $\infty$	0.65 ~ $\infty$
Partially occ.	50 ~ $\infty$	0.65 ~ 1
Heavily occ.	50 ~ $\infty$	0.2 ~ 0.65
Large scale	100 ~ $\infty$	$\infty$ ~ $\infty$
Near scale	80 ~ $\infty$	$\infty$ ~ $\infty$
Medium scale	30 ~ 80	$\infty$ ~ $\infty$
All	20 ~ $\infty$	0.65 ~ $\infty$

Height of a pedestrian in an image is inversely proportional to distance between camera and the pedestrian. This can be modeled by using the following equation [27].

$$h \approx H f/d \quad (13)$$

Where  $h$  represents the pixel height of pedestrians,  $H$  is the actual height,  $f$  is the focal length of the camera used for recording images and  $d$  is the distance between camera and the pedestrian. Assuming pedestrian actual height  $H \approx 1.80$ m, camera focal length  $f \approx 1000$  we obtain  $d \approx 1800/h$  m. A camera mounted on a vehicle moving with the speed of 15 m/s ( $\approx 55$  km/h) on an urban road, a pedestrian of 100 pixels would be 18 m away and a pedestrian of 50 pixels would be 36 m away. It means that, if a pedestrian is standing 36 m away, it would take 2.4 seconds for a driver of a car moving at a speed of 55 km/h to react, which is reasonably good on an urban road. For the evaluation of our proposed detector, we fix the height range from 50 pixel to infinity, which is a reasonable choice under urban conditions. We have evaluated our detector's performance under different height and visibility range settings as shown in Table I. We have reported our results and its comparison with other techniques on INRIA dataset at  $10^{-1}$  FPPI (as indicated with blue line). We have adopted evaluation code from [30] available online.

## VIII. EXPERIMENTAL RESULTS

The comparison between HOG, variant of HOG (FHOG) introduced by [10], and our method is shown in Figure 10. Our system gives accuracy of 91% at  $10^{-5}$  false positive per window (FPPW) and accuracy of 98% at  $10^{-4}$  FPPW. Testing was done on 1,126 positive cropped windows and 105,500 negative cropped windows from negative images provided by INRIA dataset. According to the observations of [10], there are some cases in, which the use of light insensitive features will give benefit and in other cases the use of light sensitive features will give benefit. FHOG consists of 32 features. 13 of them are the representations of 36 HOG features in reduced dimensional space that are light insensitive features and remaining features are light sensitive features.

We can see in Figure 10 that FHOG clearly dominates HOG. On the other hand, our method achieved the best accuracy in comparison to HOG and FHOG. To our

knowledge, our system gives the best state of the art results at  $10^{-4}$  FPPW [1] on INRIA pedestrian database. In our opinion, the reason for achieving the best results on INRIA dataset in FPPW evaluation metrics is that our system was able to solve occluded cases with high confidence values, which in case of other state of the art detectors either produced false negatives or they might have corrected those cases with a lower confidence value. The time cost of projecting high dimensional feature vector onto the weight matrix and lacking of vertical occlusion handling can be counted as the limitations of the proposed system.

We also report our results in FPPI evaluation metrics. Our proposed system clearly dominates other state of the art methods, yielding the lowest miss rate at  $10^{-1}$  FPPI as shown in the following graphs.

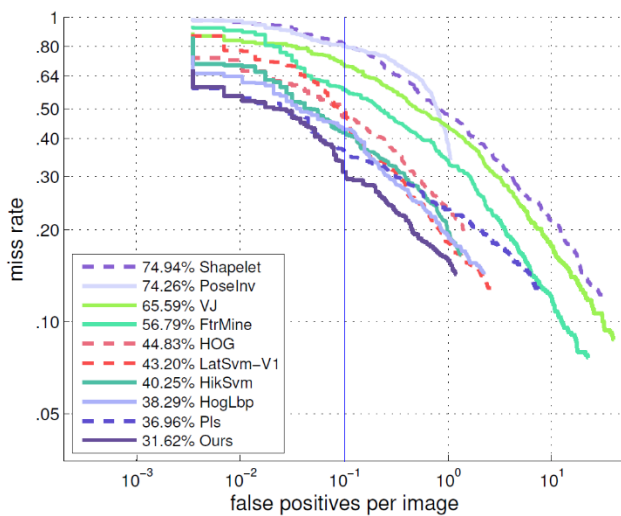


Figure 11. Miss rate vs FPPI under reasonable condition

As shown in Figure 11, our proposed detector achieved the miss rate of 31.62% at  $10^{-1}$  FPPI and dominated other state of the art detectors in reasonable condition. Under reasonable conditions, only those pedestrians are considered for evaluation whose height starts from 50 pixels to as much as maximum height of the frame with a visibility range of 65% and higher.

Figure 12 shows our proposed detector achieved the miss rate of 38.79% at  $10^{-1}$  FPPI and dominated other state of the art detectors in partial occlusion condition. Under partial occlusions, only those pedestrians are considered for evaluation whose height starts from 50 pixels to as much as maximum height of the frame with a visibility range from 65% to 100%.

Figure 13 shows our proposed detector achieved the miss rate of 69.60% at  $10^{-1}$  FPPI and dominated other state of the art detectors in heavy occlusion condition. HOG-LBP detector uses texture features, and detects the whole pedestrian in chunks. Whereas, our proposed upper body detector neither uses texture features nor uses full body information for occlusion handling. Under heavy occlusions, only those pedestrians are considered for evaluation whose height starts from 50 pixels to as much as

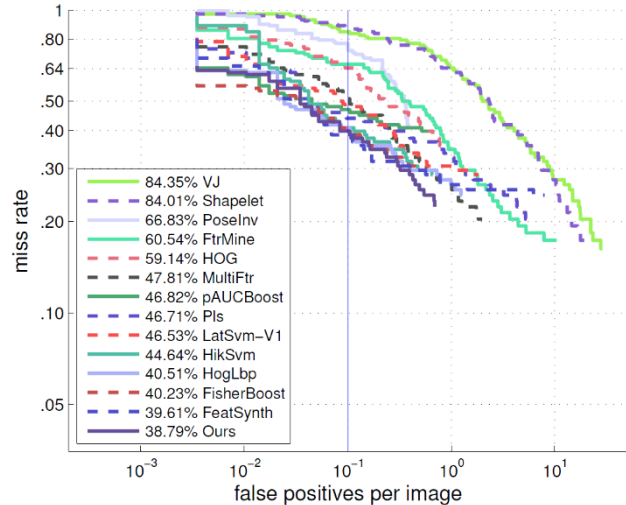


Figure 12. Miss rate vs FPPI under partial occlusions

maximum height of the frame with a visibility range from 20% to 65%.

Figure 14 shows our proposed detector achieved the miss rate of 21.38% at  $10^{-1}$  FPPI and dominated other state of the art detectors in large scale pedestrian condition. Under large scale pedestrian condition, only those pedestrians are considered for evaluation whose height starts from 100 pixels to as much as maximum height of the frame with a visibility of 100%.

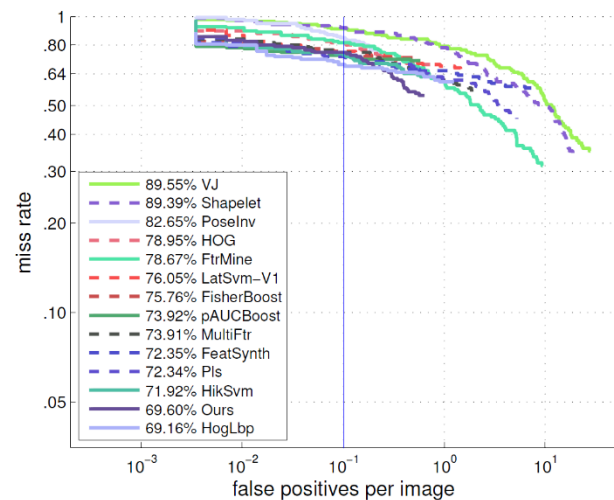


Figure 13. Miss rate vs FPPI under heavy occlusions

Figure 15 shows our proposed detector achieved the miss rate of 22.13% at  $10^{-1}$  FPPI and dominated other state of the art detectors in near scale pedestrian condition. Under near scale pedestrian condition, only those pedestrians are considered for evaluation whose height starts from 80 pixels to as much as maximum height of the frame with a visibility of 100%.

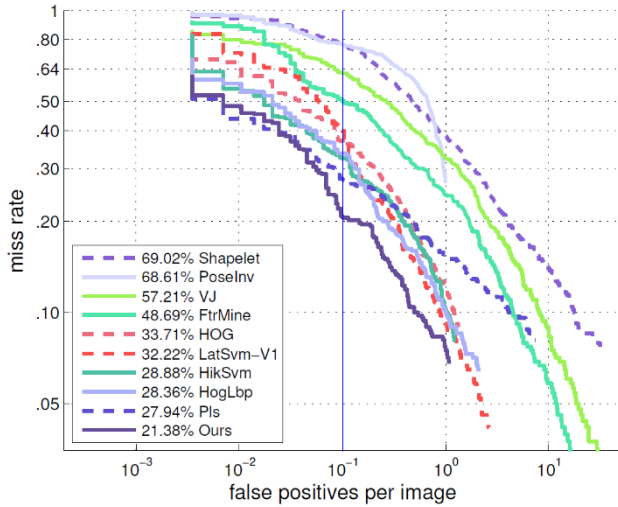


Figure 14. Miss rate vs FPPI of large scale pedestrians

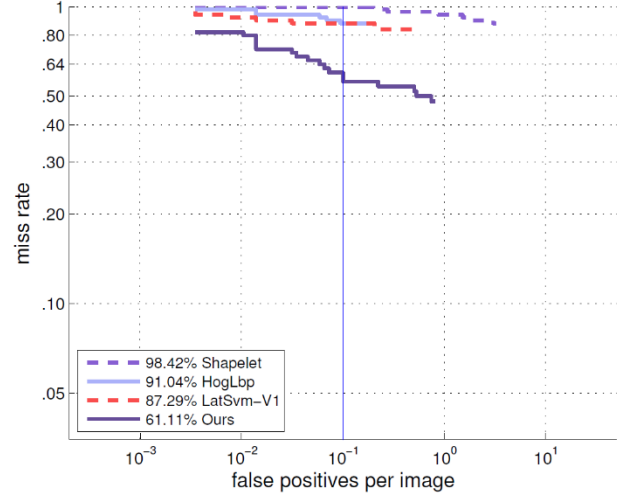


Figure 16. Miss rate vs FPPI of medium scale pedestrians

Figure 16 shows our proposed detector achieved the miss rate of 61.11% at 10<sup>-1</sup> FPPI and dominated other state of the art detectors in medium scale pedestrian condition. Results of only three detectors were available in medium scale pedestrian category. Under medium scale pedestrian condition, only those pedestrians are considered for evaluation whose height ranges from 30 pixels to 80 pixels with a visibility of 100%.

in more discriminative lower dimensional space. Part model is also integrated with our system for handling occlusions. We have achieved the detection rate of 98.1% at 10<sup>-4</sup> FPPW and 31.62% miss rate at 10<sup>-1</sup> FPPI on INRIA pedestrian database. We plan to further improve this detection rate in terms of FPPI by effectively adding another dimension of tracking and between-frames information into our system.

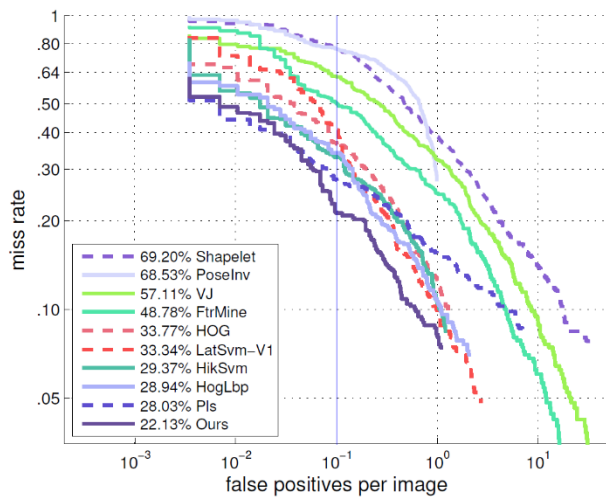


Figure 15. Miss rate vs FPPI of near scale pedestrians

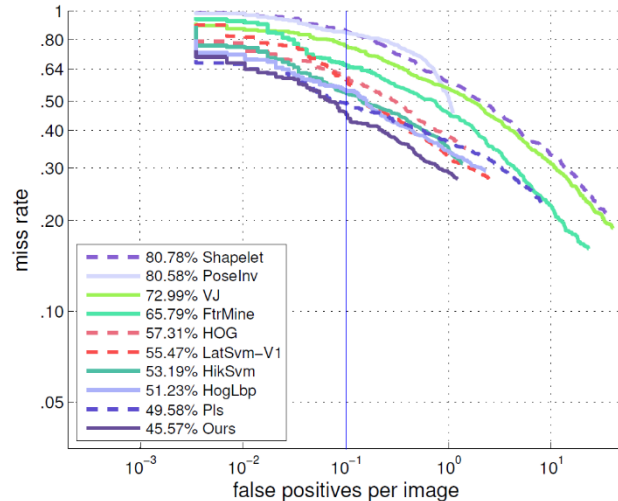


Figure 17. Miss rate vs FPPI of all condition

Figure 17 shows our proposed detector achieved the miss rate of 45.57% at 10<sup>-1</sup> FPPI and dominated other state of the art detectors in all condition. Under all condition, only those pedestrians are considered for evaluation whose height range is 20 pixels and higher with a visibility range of 65% and higher.

### IX. CONCLUSION

We have developed a system that is capable of detecting pedestrians via monocular camera images efficiently. With the help of PLS, we are able to represent our rich feature set

### ACKNOWLEDGMENT

This work was supported by the National Research Foundation of Korea (NRF) Grant funded by the Korean Government (MOE) (No. NRF-2013R1A1A2004421). Moreover, the authors Yawar Rehman, Irfan Riaz and Jameel Ahmed Khan are sponsored by “Higher Education Commission” (HEC) of the Government of Pakistan.



Figure 18. First three rows shows the results obtained from INRIA database and fourth row shows some results from ETH pedestrian database. The performance of our detector in occlusions, cluttered scenes, and pose variations, should be noted.

## REFERENCES

- [1] Y. Rehman, et al., "Pedestrian detection with occlusion handling," in Proc. PATTERNS 2015, pp. 15-20.
- [2] P. Viola and M. Jones, "Rapid Object Detection Using a Boosted Cascade of Simple Features," Proc. IEEE Conf. Computer Vision and Pattern Recognition (CVPR), 2001.
- [3] P. Viola, M. Jones, and D. Snow, "Detecting Pedestrians Using Patterns of Motion and Appearance," Int'l J. Computer Vision 2005, vol. 63, no. 2, pp. 153-161.
- [4] N. Dalal and B. Triggs, "Histograms of Oriented Gradients for Human Detection," Proc. IEEE Conf. Computer Vision and Pattern Recognition (CVPR), 2005.
- [5] P. Dollár, Z. Tu, P. Perona, and S. Belongie, "Integral Channel Features," Proc. British Machine Vision Conf. (BMVC), 2009.
- [6] R. Benenson, M. Mathias, R. Timofte, and L.V. Gool, "Pedestrian Detection at 100 Frames per Second," Proc. IEEE Conf. Computer Vision and Pattern Recognition (CVPR), 2012.
- [7] P. Dollár, C. Wojek, B. Schiele, and P. Perona, "Pedestrian Detection: An Evaluation of the State of the Art," IEEE Trans. Pattern Analysis and Machine Intelligence 2012, vol. 34, no. 4, pp. 743-761.
- [8] [www.vision.caltech.edu/Image\\_Datasets/CaltechPedestrians/](http://www.vision.caltech.edu/Image_Datasets/CaltechPedestrians/), 2014.
- [9] X. Wang, T. X. Han, and S. Yan, "An HOG-LBP human detector with partial occlusion handling," Computer Vision and Pattern Recognition (CVPR) 2009, pp. 32-39.
- [10] P. Felzenszwalb, D. McAllester, and D. Ramanan, "A discriminatively trained, multiscale, deformable part model," in Computer Vision and Pattern Recognition (CVPR) 2008, pp. 1-8.
- [11] W.R. Schwartz, A. Kembhavi, D. Harwood, and L.S. Davis, "Human detection using partial least squares analysis," Computer Vision and Pattern Analysis (CVPR) 2009, pp. 24-31.
- [12] A. Kembhavi, D. Harwood, and L.S. Davis, "Vehicle Detection Using Partial Least Squares," IEEE Trans. Pattern Analysis and Machine Intelligence 2011, vol.33, no.6, pp. 1250-1265.
- [13] Q. Wang, F. Chen, W. Xu, and M.-H. Yang, "Object Tracking via Partial Least Squares Analysis," IEEE Trans. on Image Processing 2012, pp. 4454-4465.
- [14] M.A. Haj, J. Gonzalez, and L.S. Davis, "On partial least squares in head pose estimation: How to simultaneously deal with misalignment," Computer Vision and Pattern Recognition (CVPR), 2012, pp. 2602-2609.
- [15] P. Dollár, R. Appel, S. Belongie, and P. Perona, "Fast Feature Pyramids for Object Detection," IEEE Trans. on Pattern Analysis and Machine Intelligence 2014, vol.36, no.8, pp. 1532-1545.
- [16] R. Benenson, M. Mathias, R. Timofte, and L.V. Gool, "Pedestrian detection at 100 frames per second," in Computer Vision and Pattern Recognition (CVPR) 2012, pp. 2903-2910.
- [17] J.J. Lim, C.L. Zitnick, and P. Dollár, "Sketch Tokens: A Learned Mid-level Representation for Contour and Object Detection," in Computer Vision and Pattern Recognition (CVPR) 2013, pp. 3158-3165.
- [18] R. Benenson, M. Mathias, T. Tuytelaars, and L.V. Gool, "Seeking the Strongest Rigid Detector," in Computer Vision and Pattern Recognition (CVPR) 2013, pp. 3666-3673.
- [19] P. Dollár, Z. Tu, P. Perona, and S. Belongie, "Integral Channel Features," Proc. British Machine Vision Conf. 2009.
- [20] P. Dollár, S. Belongie, and P. Perona, "Fastest Pedestrian Detector in the West," Proceedings of BMVC, 2010.
- [21] P. Dollár, R. Appel, and W. Kienzle, "Crosstalk Cascades for Frame-Rate Pedestrian Detection," Proceedings of ECCV, 2012.
- [22] T. Ojala, M. Pietikainen, and T. Maenpää, "Multiresolution gray-scale and rotation invariant texture classification with local binary patterns," IEEE Trans. On Pattern Analysis and Machine Intelligence 2002, vol.24, no.7, pp. 971-987.
- [23] A. Vedaldi and B. Fulkerson, "VLFeat: An Open and Portable Library of Computer Vision Algorithms," [Accessed from <http://www.vlfeat.org/>], 2008.
- [24] S. Walk, N. Majer, K. Schindler, and B. Schiele, "New features and insights for pedestrian detection," Computer Vision and Pattern Recognition (CVPR) 2010, pp. 1030-1037.
- [25] R. Rosipal and N. Kramer, "Overview and recent advances in partial least squares in Latent Structures Feature Selection," Springer Verlag, 2006.
- [26] S. Wold, "PLS for Multivariate Linear Modeling QSAR," Chemometric Methods in Molecular Design, 1994.
- [27] P. Dollár, C. Wojek, B. Schiele, and P. Perona, "Pedestrian Detection: An Evaluation of the State of the Art," IEEE Trans. on Pattern Analysis and Machine Intelligence 2012, vol.34, no.4, pp. 743-761.
- [28] S. Kah-Kay and T. Poggio, "Example-based learning for view-based human face detection," IEEE Trans. on Pattern Analysis and Machine Intelligence 1998, vol.20, no.1, pp. 39-51.
- [29] M. Taiana, J. Nascimento, and A. Bernardino, "An Improved Labelling for the INRIA Person Data Set for pedestrian Detection," Pattern Recognition and Image Analysis 2013, vol. 7887, pp. 286-295.
- [30] Accessed from, [www.vision.caltech.edu/](http://www.vision.caltech.edu/), 2015.

## Improving Energy Awareness Integrating Persuasive Game, Feedback, and Social Interaction into the Novel Ener-SCAPE Application

Diego Arnone, Alessandro Rossi  
Research and Development Laboratory  
Engineering I.I. S.p.A.  
Palermo, Italy

email: [diego.arnone@eng.it](mailto:diego.arnone@eng.it), [alessandro.rossi@eng.it](mailto:alessandro.rossi@eng.it)

Marzia Mammina  
DemetriX S.r.l.  
Palermo, Italy  
email: [marzia.mammina@demetrix.it](mailto:marzia.mammina@demetrix.it)

Enrico Gabriele Melodia  
Pidiemme Consulting S.r.l.  
Bagheria, Italy  
email: [e.melodia@pdm-c.it](mailto:e.melodia@pdm-c.it)

Sandra Elizabeth Jenkins  
Engineering Systems Division, Technology and Policy  
Program '14  
Massachusetts Institute of Technology  
Cambridge, MA, USA  
email: [sandjenkins@gmail.com](mailto:sandjenkins@gmail.com)

**Abstract**— Ener-SCAPE is a novel work in progress software framework made up of a persuasive game, a graphical interface to monitor energy usage and a tool for social interaction, which aims to improve the energy consumption awareness of its users at home as well as in the workplace. The game uses a common “escape room” game approach, tailoring the game archetype to focus on energy efficiency and energy consumption awareness. The monitoring interface allows the users to monitor some predefined energy efficiency indexes. The tool for social integration helps users to build social awareness. Users play the game by trying to exit from a virtual home or office by solving energy puzzles, working to improve their energy savings in their real environment, and sharing their acquired knowledge and experiences. Ener-SCAPE implements a unique feedback mechanism based on real energy consumption that leads consumers to apply what they have learned from the virtual reality of the game into their daily real lives. An important aspect of this work is that it merges different elements, which emerged as successful in achieving improved energy awareness, i.e., feedback mechanisms, serious games and social interaction.

**Keywords**—energy awareness; serious game; educational game; escape room game; energy efficiency; feedback mechanism; social network interaction.

### I. INTRODUCTION

This work is the extension of a study [1] that presents the design of a novel application and related underlying software framework whose main aim is to decrease the energy consumption levels both at home and in the office by increasing the consumption awareness of energy users. With respect to the previous study, this work presents an expanded literature review, the software framework is described in depth, the business model for the possible development of Ener-SCAPE as a product to market is showed, and suggestions for future works are presented. The main target of both works is reducing energy consumption caused through or careless energy use.

Energy consumption is steadily increasing worldwide, despite mitigation efforts, particularly in those countries that are experiencing a great economic growth. This is a global issue for environmental protection, as well as an economic and political issue, for countries that depend on foreign energy suppliers.

Many solutions are being proposed and implemented in order to address increasing energy consumption, such as incentives for renewable energy sources, new technologies for highly efficient buildings, new technologies for more efficient appliances, and more sustainable transportation.

People consume energy every day, not only for their basic needs, but also for making their lives more enjoyable, comfortable and improving their standard of living. Thus, if people are not driven to save energy and encouraged to improve their energy consumption behaviour in their everyday lives, lifestyle choices may frustrate savings coming from aforementioned engineering solutions [1][2][3]. Despite efforts to improve energy efficiency, the aggregate energy consumption behaviour in the transportation and residential sectors is responsible for a significant percentage of the overall energy consumption worldwide. Studies conducted in various countries have concluded that 26% to 36% of residential energy consumption is a result of household behaviour [2]. For example, behavioural change in the use of standby equipment can lead to energy saving up to 35% [4]. For this reason, the energy policy adopted by many countries is focused on Energy Consumption Awareness (ECA). The main factors that may influence energy consumption behaviours of citizens are environmental education, real time control of energy consumption, involvement of young people, and overall greater energy consumption awareness. Thus, ECA policies can be strategic for energy consumption reductions.

With the growing number of products and devices in homes and offices, keeping up-to-date with energy efficiency measures may be a difficult task. However, as more devices

are able to communicate with each other, consumers will be able to look for more innovative and accessible ways to manage and learn about energy efficiency. Nevertheless, this kind of knowledge is a necessary but not sufficient condition for energy saving [5]. Indeed, studies generally demonstrate that information can increase knowledge, but has minimal effects on behaviour [6]. In order to reach significant savings, knowledge must be associated with energy awareness, motivational factors (such as curiosity), cost considerations, and willingness [7]. As a consequence, citizens should be "energy aware" in order to change their behaviour and save energy.

Behaviours improving energy efficiency are generally seen as factors reducing comfort. Actually, this is a misconception and people do not have to give up activities or their standard of living to save energy. On the contrary, new technologies and more effective behaviour will allow citizens to do more: improving their living conditions without compromising their standards. Furthermore, energy efficiency improvement can also lead to lower costs and greater sustainability, which is another important opportunity to stimulate economic growth.

This work aims to complement and build upon current initiatives. The goal of the novel proposed application is to improve the energy consumption awareness of people both at home and in the office, by employing three features: (i) a well-known and successful game model, (ii) a real-time intuitive feedback on consumption and (iii) a close collaboration with other players/consumers.

In Section II, the state of the art on feedback impacts, persuasive games, and social interaction on energy awareness is reported. In Section III, the different EnerSCAPE applications are fully described. In Section IV, the scheduled experimentation plan is described. In Section V, the business model is explained. In Section VI, the conclusion and details of future works are given.

## II. LITERATURE REVIEW

In the last few years several institutions, including the European Union (EU), have become increasingly committed to promoting a higher awareness of energy consumption. For this purpose, the EU has launched several initiatives and published several documents, especially directed at children and adolescents. Both in the EU and in the United States, labels reporting the energy consumption of household appliances have been introduced to inform consumers in a simple and direct way about energy efficiency of products [8][9]. In addition, information campaigns for raising awareness in energy consumption have spread. These actions produce long-term results, in particular, those focused on children [10].

But in order to obtain immediate results, feedback on consumption is frequently adopted to improve energy awareness. In the few last years, several studies have analysed the effectiveness of feedback as a tool for promoting energy savings at home. They generally report savings in a wide range (from 1.1% to over 20%) but usual savings are between 5% and 12% [11][12]. Fischer [11] lists the relevant features of feedback that may determine its

effectiveness: frequency, duration, content, breakdown, medium and way of presentation, comparison, and combination with other instruments. The study shows that the most successful results come from feedback that is given frequently over a long period of time, provides an appliance-specific breakdown, is presented in a clear and appealing way, and uses computerised and interactive tools [11]. In order to promote energy savings, the consumers should first be made aware of the amount of energy they are consuming, so that they can then learn how they can improve their behaviour. Users should identify potential savings in their environment, by knowing how and where energy is actually used: this requires users to be aware not only of the overall energy consumption reported in their bills, but also at the appliance level. Reinhart et al. [13] have designed a system, called Ubiquitous Smart Energy Management (USEM), which is not only a simple automated solution to reduce electricity usage, but also provides detailed energy consumption information and incorporates mobile tools to assist and encourage users at improving their energy consumption behaviour. Some research projects, e.g., BeAware [14], or commercial products, e.g., Ecosphere [15], aim at motivating users to be more responsible in their use of electric appliances by showing real-time energy consumption feedback through intuitive user interfaces. Recent studies prove that this kind of feedback is enough, by itself, to reduce consumption by 15% [16]. Feedback can stimulate energy conservation only with the presence of motivational factors, cost considerations and altruistic or environmental concerns [12]. Some studies in the literature [17][18] show that the custom and real-time feedback on energy consumption is effective in consumption reduction.

Persuasive technologies have proven useful in modifying behaviours related to energy usage. A potential way to drive awareness is through the so called "serious games", i.e., interactive virtual simulations whose main purpose is the development of user abilities and skills in a simulated environment with the aim of apply them in the real world. Recent studies suggest that the effectiveness of learning increases when it is active, experiential, situated, problem-based, and provides immediate feedback [19]. Indeed, literature proves that serious games can influence people change behaviours and attitudes in the areas of health, public policy, education and training [20], and notably for our purposes, energy [21]. Additionally, environmental awareness and attitudes toward environmental preservation can be promoted by simulation games [22]. Finally, simulation games can efficiently guide players with improving their environmental knowledge, attitudes, and behaviour [7].

Many serious games have been developed with the aim to increase knowledge and awareness about ecological and energy issues. Ecoville [23] is an interactive game, where the mission is to build a sustainable energy community constrained by resource, pollution and budget limits, by handling the energy balance, CO<sub>2</sub> emissions, garbage disposal, etc. EnerCities [24] further develops the concept: in this game, based on the Theory of Planned Behaviour [25], players have to balance three variables: population,

planet, and profit. Power Agent [26] and Power Explorer [27] are two “pervasive games” that put family members in competition to reduce the domestic consumption as measured by sensors, pointing out the difference between player and non-player behaviours through an avatar helping to convey best practices in energy efficiency.

Even though there have been relatively good results, serious games still remain a “niche” field. The main limits to their popularity are their target audience (scholars and families, often very different from the average users and far from the gaming community), as well as the perception that educational games are boring, and also the lack of entertainment features that characterize traditional games. Moreover, the majority of serious games produced so far come from research projects, thus, there is not a large library of commercial games on the market, and the genre has not generated significant results in terms of revenue and profits.

In the recent years, some projects combining feedback mechanism and serious gaming have been developed with the purpose of promoting behavioural changes in energy consumption at home. As part of the EU funded project SOFIA [28], a product implementing game elements was designed for families with children with the aim of improving environmentally responsible behaviour in domestic energy consumption. Furthermore, Yang et al. [7] have developed a system called Energy CONservation PET (ECOPET): using a game-based learning strategy, with the help of a pet avatar, players are encouraged to use home-energy efficiently. The main distinctive feature of these last two products is the in-game implementation of a feedback mechanism, which helps learners to use electric appliances properly [7][28].

Finally, it is worth highlighting the social nature of this topic. Recent studies have showed that “energy consumption is a social and collective process rather than individual” [29]. A social debate, for example, by way of social network, can make people build common awareness. People, initially reluctant to change their behaviour, can be motivated to act in a more responsible way by interaction with other people. Several years ago, Mankoff et al. [30] already demonstrated a motivational effect for saving energy by integrating energy usage feedback to the MySpace social network. Similarly, Foster et al. [31], by means of a novel Facebook application, have demonstrated that energy consumption can be reduced through social encouragement and competition. Obviously, only exchanging ideas or opinions is not enough to raise awareness and change people behaviours. Real consumption measurements play a fundamental role in allowing people to change their behaviour in a more conscious way [29]. Petkov et al. [32] have expanded the idea of social comparison with their social application EnergyWiz, which allows users to compare their energy usage with their own history and the history of other users.

The goal of this work is to exploit the potentiality supplied by feedback, serious games, and social interaction

in a novel software framework, named Ener-SCAPE, which integrates all these aspects to improve the ECA of its users.

### III. ENER-SCAPE

Ener-SCAPE is a software framework composed of a persuasive game, a monitoring tool for energy consumption that processes and shows data coming from a sensing infrastructure, and a tool for social interaction. It mainly aims at improving the awareness of energy consumers both in their homes and in buildings where they usually work.

The core of Ener-SCAPE is the game. The name itself recalls the game genre since it is based on: the “room escape”, or “escape games” [33], which is a subgenre of the well-known point-and-click adventure games. In the game, players are tasked with escaping from an apartment or an office by solving rebus puzzles, through the use of specific information and the implementation of strategies. The escape game paradigm has been chosen because it allows the game to be located in a place similar to the one where people should put into practice what they have learned. Moreover, making users explore the house while trying to escape allows them to face realistic situations. Most of the suggestions for a better ECA are related to common energy loads from devices that can be found in most houses and offices. Additionally, working with virtual environments allows game designers to make the game experience more exciting, emotionally compelling and to provide new elements. In this way, information and sensations experienced are remembered and allow the player to sharpen their perception, attention and memory by promoting behavioural changes through “learning by doing” [34].

#### A. Framework Architecture

The logical architecture is subdivided into four layers: the Security Layer, Business Layer, Data Layer, and Presentation Layer. A graphical representation is provided in Figure 1.

The Security Layer implements all checks needed to authenticate users and authorise access to resources. The application is accessible both from personal computers (PC) and mobile devices (tablets, smartphones), after user authentication. The OAuth v2.0 [35] protocol has been chosen to securely share user data with the Ener-SCAPE applications: monitoring data are exchanged anonymously with a token identifying the user.

The Business Layer implements the business logic of the whole system and the data processing that leads to the results that will be provided to the users through the dashboard. The logical components of the Business Layer are grouped by their functions:

- Notification Management, whose purpose is to provide a service for the exchange of real-time notifications between the various architectural components, according to the Publish/Subscribe pattern;
- User Management, which represents the logical group of software components in charge of managing the basic user information (creation, editing, profiling), as well as the interaction with the Social Community;

- Energy Management, which comprises the components that acquire data from sensors and the components that retrieve consumption data from a remote database for all requests from users through the monitoring dashboard;
- Game Management, which manages the logic of the Ener-SCAPE game and provides all the functional components, from loading the assets of the game, to the client-side components at Presentation Layer;
- Smart Advice Management, which groups all the infrastructure components that are responsible for the production of Smart Advice, i.e., personalised pieces of advice aiming at reducing energy consumption;
- CEP Management, which comprises the components that deal with the Complex Event Processing (CEP) in real-time, to increase the situation awareness of the users and to support their decisions.

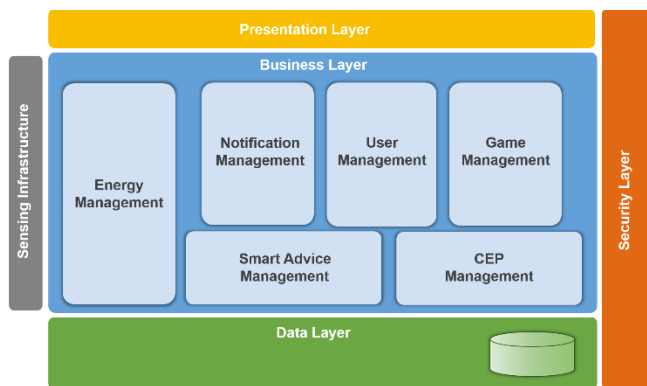


Figure 1. Ener-SCAPE high level architecture.

The Data Layer is the layer where interactions with the data storage are performed.

Finally, the Presentation Layer represents the application user interfaces (game, dashboard for monitoring energy performance, interface to interact with social networks).

All the taxonomic and non-taxonomic relationships between entities within the Ener-SCAPE application domain have been modelled in the Ener-SCAPE Ontology. This ontology is also at the basis of the feedback system to the end users aimed at increasing, in a personalised way, awareness of the impact of energy consumption actions. Feedback is made available to users on the monitoring dashboard in form of contextualised hints, or Smart Advice. The identification of the more appropriate piece of advice to be made available to the user is based on the real-time identification of contextual information: the advice is presented as one or more “hints” depending on user-specific factors, such as the type of dwelling and the consumption of electrical energy, as well as on environmental factors, such as climatic conditions during the period under observation. For example, in a region where the weather is warmer than expected, a user whose energy consumption during summer is higher than what has been forecasted, could be informed that the increase in consumption is probably because of the increased use of air conditioning in their home. In addition, a

suggestion may be offered for improving the use of the air conditioning in order to reduce energy consumption. The production of personalised recommendations is done through semantic technologies. Circumstances relevant to users are described through Ontology Web Language (OWL) assertions. The different contexts that can be adapted to the user are logically organised according to a tree and each context is identified by a set of characteristics, such as type of dwelling where the user lives and the number of people living in the same house. The tips are then associated with one or more nodes in the tree. The task of determining what recommendations are appropriate for a given user is delegated to an ontological reasoner [18]. Hints proposed to the user have been gathered by seeking suggestions aiming at energy saving and efficiency on websites of institutions, government agencies, and consumer groups, as suggested in [3].

The CEP is a technology that enables processing and combining events from multiple sources to detect occurrences of special events that require a response from a system or from a human operator [36]. CEP is, therefore, a useful tool to increase the Situation Awareness, i.e., the awareness of the context. The use of CEP techniques in Ener-SCAPE, applied to consumption data and to the user profile, is a crucial step for the Energy Consumption Awareness. The CEP in Ener-SCAPE arises also as a valuable tool to report to end users (consumers, energy manager) criticalities and malfunctioning. Figure 2 shows the CEP architecture in Ener-SCAPE.

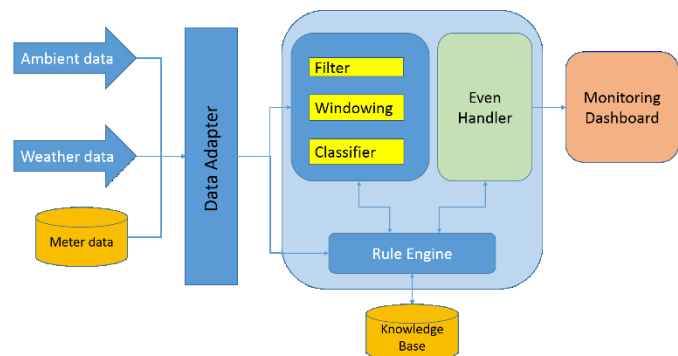


Figure 2. CEP architecture in Ener-SCAPE.

Two versions of the software framework are being developed: one related to a home environment and the other related to a building/campus environment. Both versions include and integrate the applications mentioned before: a dashboard for monitoring real energy consumption, which shows performance indicators and hints to improve performance; the escape game with two different approaches that will be described later; and the tool for integration with social networks (Facebook/Twitter/Google+) to allow collaboration between players/consumers.

The innovative aspect of the proposed approach is a simple but effective mechanism to integrate the three applications with the aim of converting existing successful

models to an “edutainment” (education and entertainment) function.

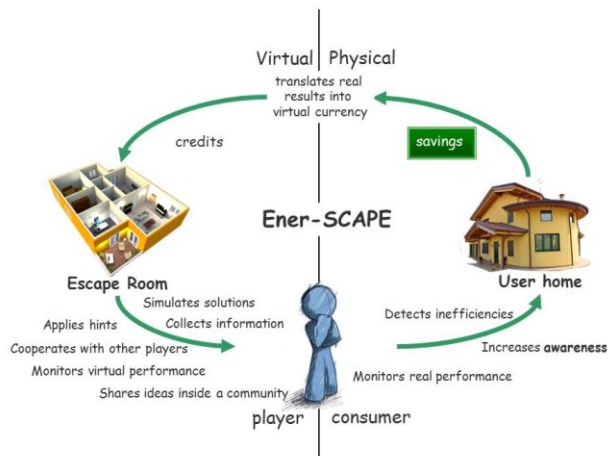


Figure 3. Ener-SCAPE approach to energy consumption awareness (home environment).

The cornerstone of the Ener-SCAPE game, as previously introduced, is essentially to escape from a house (or a building in the second version of the game) as in any escape room game. Escaping can only be achieved by solving a sequence of rebus puzzles (find items, combine them, use them, look for clues, piece together clues, gather information, find combinations, compose puzzles, solve riddles, etc.). The main feature of the game lies in the themes of each action: eco-sustainability, savings, efficiency, and energy-awareness. Moreover, effectiveness in acquiring ECA is given by the feedback from the real world. The game is integrated with a very simple and intuitive monitoring tool, which processes the data collected through a sensing infrastructure and allows consumers to see their real energy performance. The application allows the users to compare their current energy consumption with historical average values.

While playing, users acquire information (gained from the game or the social networks where they get useful tips for solving puzzles) that can also be used in the real world. The ultimate aim of the game is impacting consumer behaviour in their real lives. The monitoring dashboard provides a means to measure performance improvement, which is then translated into virtual currency that can be spent in the game to ease the escape. In order to facilitate the solution of a rebus puzzle, the users can utilise the virtual currency obtained from social network interactions. Indeed, users can cooperate with other consumers in specific social network groups: each consumer builds his or her own reputation by cooperating with the community in solving the escape room rebuses as well as in achieving better energy performance in the real world. A domain expert rewards the acquired reputation by assigning virtual currency to be spent in the game.

In this way, users at home will strive to improve their behaviour by trying to reach the optimal values of real

performance indexes. Before addressing the optimal performance, the system proposes intermediate targets and rewards their achievements by assigning virtual currency to be spent in the game. In order to measure real performance, the user must install “off-the-shelf” sensors; solutions based on Non-Intrusive Appliance Load Monitoring (NIALM) are being taken into account as possible alternatives. Therefore, as can be seen in Figure 3, Ener-SCAPE implements a virtuous cycle that allows the consumer to learn how to efficiently use energy simply by playing the game. At home, the user can save or waste energy. Then, the dashboard graphically represents the real performances based on data coming from a sensing infrastructure installed in the home. The transition from the physical world to the virtual one corresponds to the translation of the real results into virtual currency, which in turn affects the consumer’s ability to solve the rebuses in the virtual escape room. Finally, the beneficial cycle results in simulated solutions, information the user collects, applied hints, cooperation with other players, monitoring virtual performance, and sharing ideas inside a community. In this way, players may become consumers with increased energy consumption awareness that can help them to detect inefficiencies and improve their energy behaviour.

The game environment has been designed to be as graphically attractive as possible. In order to reach a good quality in architectural rendering, the free interior design software application Sweet Home 3D has been used [37].

Finally, the application was designed to be used on both PC and mobile devices, such as smartphones and tablets, in order to meet the requirements of usability and to avoid limiting the game to a single kind of device. Figure 4 shows a mock-up of the game in the tablet version in the home environment. On the right, there is a basket where discovered items are collected; at the bottom, there are some widgets where players can view their virtual and real performances, as well as their scores and hints. Figure 5. Mock-up of the dashboard (tablet version) in the home environment.

Figure 5 shows a mock-up of the dashboard in the tablet version in the home environment. The monitoring interface includes diagrams that give the users a representation of their consumption and performance. The user can select the time horizon, which can be daily, weekly, monthly or annually: the data will be temporally aggregated based on the selected time horizon. The user can also select the unit of energy consumption: kilowatt hours (kWh), EUR (€), grams of CO<sub>2</sub> (g CO<sub>2</sub>), tonnes of oil equivalent (TOE). Users can compare their current consumption with the ideal average consumption for similar classes of consumers, previously profiled, and can check any possible abnormalities in their consumption caused by inefficiencies (see Figure 5). In the current version of the service platform, users are profiled on the basis of static information: e.g., in the home environment, size and type of the house, number, age and educational qualification of occupants, etc. This classification is probably not enough to catch the living style of users. Therefore, we are investigating how to model some aspects of the lifestyle that can be used as parameters,

deduced dynamically from historical measurements, for user clustering.



Figure 4. Mock-up of the game (tablet version) in the home environment.

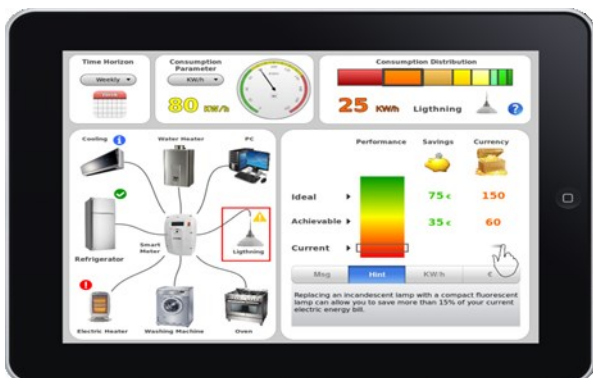


Figure 5. Mock-up of the dashboard (tablet version) in the home environment.

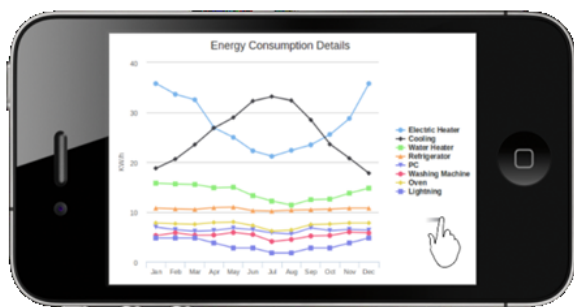


Figure 6. Energy consumption diagrams (smartphone version).

The access to energy consumption and performance values is enabled in multiple ways: by selecting household appliances in the star structure that represents the set of monitored devices (Figure 5), or by selecting a consumption category (e.g., heating, lighting, appliances, sockets, etc.).

Ener-SCAPE includes a feedback system to the end users, both in the home and in the building/campus contexts, in a personalised way to increase the awareness of the impact of their energy consumption actions. This approach is used in several ways and in a dedicated manner for the different actors in the system, e.g., suggesting:

- in the home environment, which appliance the user is using or has just used, and which device has exceeded a fixed threshold;
- inside the building/campus, the ineffective use of heating systems in relation to the outside temperature.

The feedback is made available to users on the dashboard in the form of “hints” (see Figure 5).

The monitoring dashboard shows the consumption trends, both cumulatively and per device. Users can also compare their current consumption with their historical consumption, as showed in Figure 6 and Figure 7 that depict the dashboard for smartphones.

The game version for an office environment (see Figure 8 for a mock-up of the PC version) has only one significant difference from the one for the home environment: it is an escape game played in teams. Thus, we had the chance to exploit the potentiality of collaborative learning in serious games [38]. Moreover, teams play against one another. In this way, we had also the chance to take advantage from recent studies results: Cagiltay et al. [39] have showed that creating a competition environment in a serious game makes motivation of learners improve significantly.

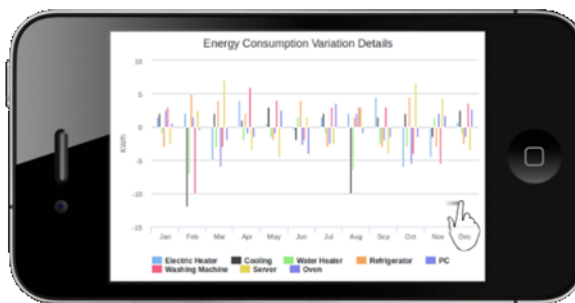
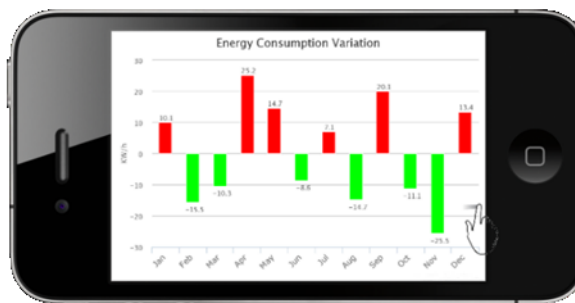


Figure 7. Energy consumption variation diagrams (smartphone version).

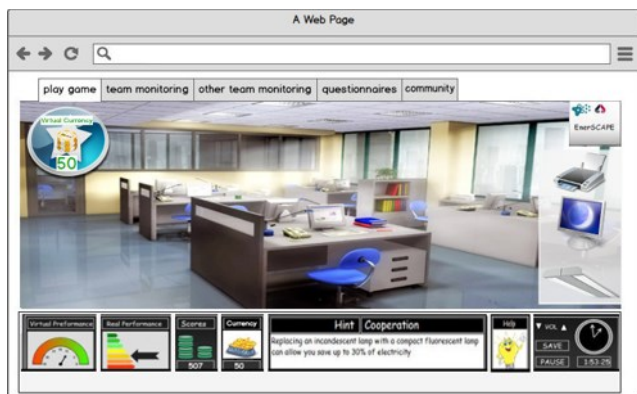


Figure 8. Mock-up of the game (PC version) in the building environment.

So, when motivation increases, learners tend to be more involved with the issue [40].

The basic idea of the game is identical to the one proposed for the home environment, but with the inclusion of other actors besides the previous single user/player: the energy manager (responsible for the coordination, management and efficient use of energy resources in the building/campus) and other users/players who live in the same environment and are energy consumers. In this case, as previously said, a mechanism for collaboration (among users belonging to the same team) and competition (with the other groups/teams of users) has been implemented. Members of the same team can exchange tips, information, and objects in the virtual world where they move. Every player can constantly see not only the results of his/her team but also the results of other teams. In order to improve the energy performance in the building(s), the energy manager will oversee the progress of the game, suggesting changes in behaviour, recommending precautions, or imposing guidelines. Furthermore, as in the home environment case, the user may take advantage of social networks as an important resource to acquire information and to earn virtual currency.

The beneficial cycle previously described for the office environment is represented in Figure 9.

Ener-SCAPE is currently in development but a complete and working prototype is already available for testers. Figure 10, Figure 11, Figure 12, and Figure 13 show some snapshots of the game and the monitoring tool for the PC version of Ener-SCAPE.

Figure 14 represents the Domain Expert interface: by accessing the application, a Domain Expert can interact with the Community through the major social networks (Twitter, Facebook, and Google+). When some members of the Community emerge by merit, for having provided useful pieces of advice and/or effective solutions, either for the game or for improving the performance in the real world, the Domain Expert can assign virtual currency to them.

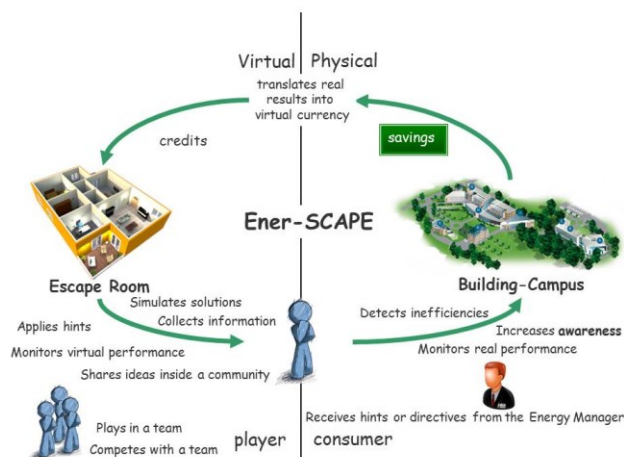


Figure 9. Ener-SCAPE approach to energy consumption awareness (building environment).

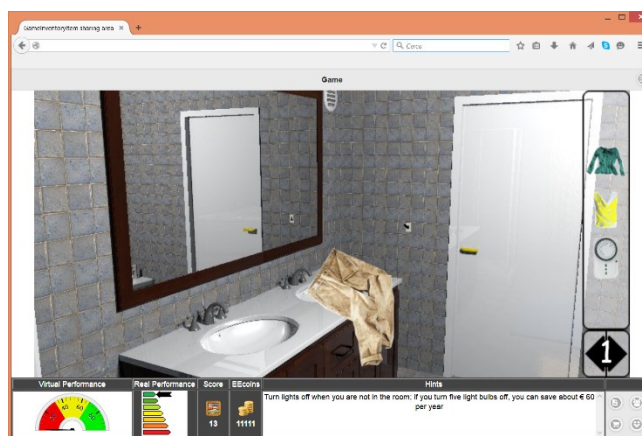


Figure 10. Snapshot of the game in the home environment for PC version

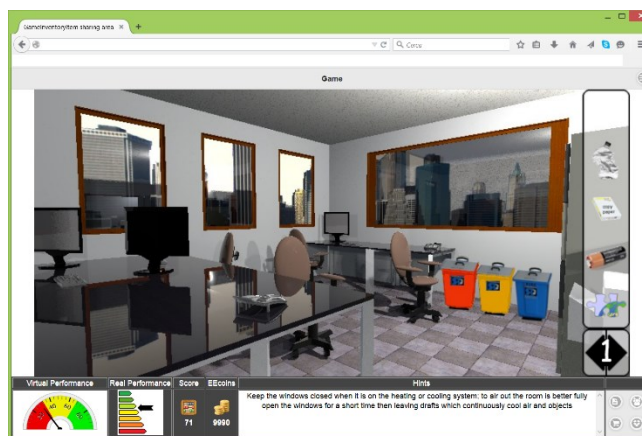


Figure 11. Snapshot of the game in the building environment for PC version.

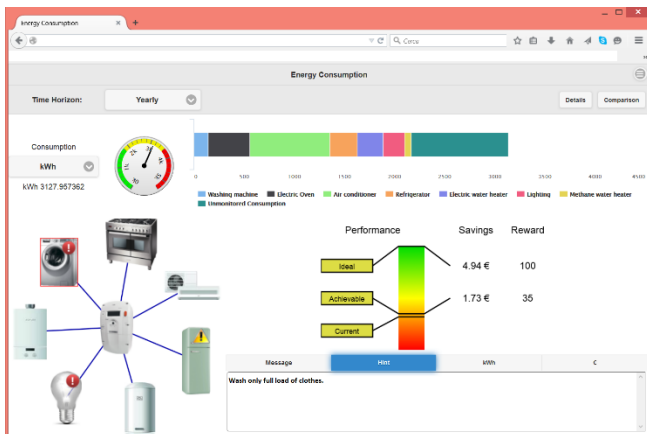


Figure 12. Snapshot of the monitoring dashboard for PC version.

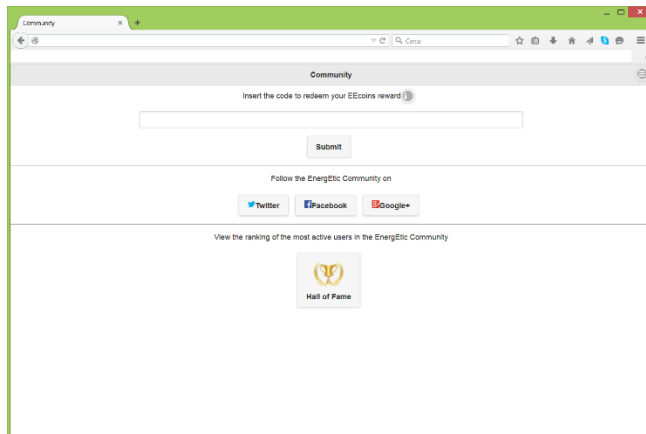


Figure 15. Player interface to redeem reward codes and to interact with the Community.

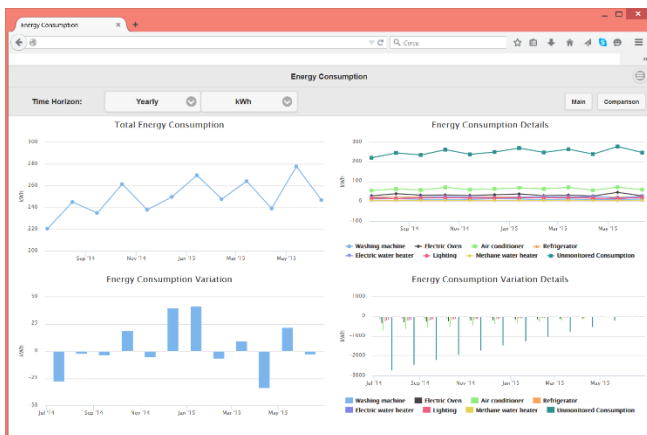


Figure 13. Energy consumption graphics in the version for PC.

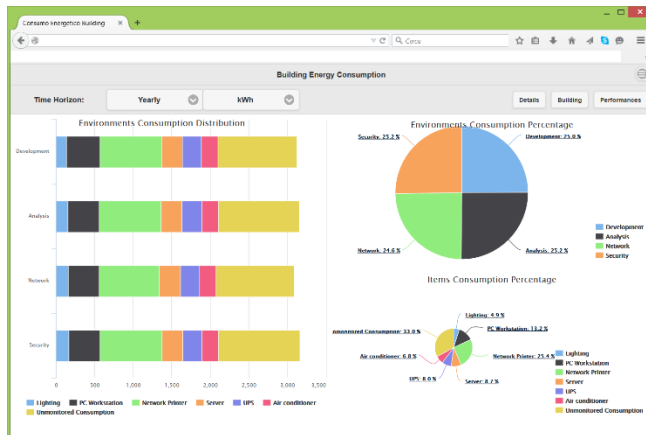


Figure 16. Energy Manager interface (PC version).

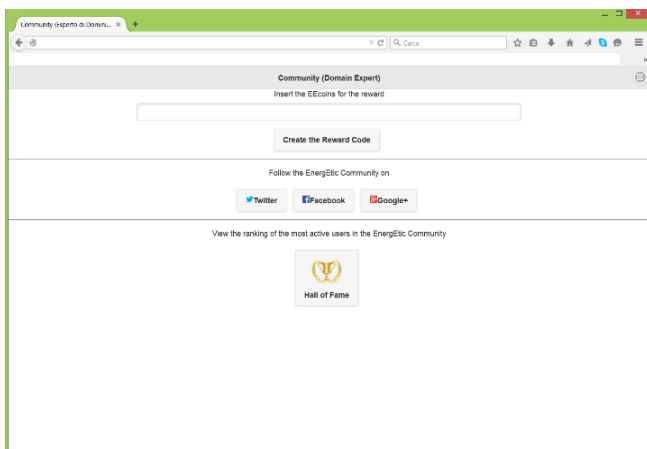


Figure 14. Domain Expert interface (PC version).

With this aim, the system generates the corresponding Reward Code (a string that is sent to the user through channels external to the application, e.g., via email, through the systems of internal chat on Facebook or Google+) for cashing in the virtual currency.

Figure 15 depicts the interface for the players to redeem the Reward Codes and to interact with the Community.

As the consumer user, the Energy Manager is provided with an interface that displays information to monitor consumption, cumulative or per device, from which he can deduce actions to induce improvements in energy efficiency, savings and economic sustainability (Figure 16).

#### IV. EXPERIMENTATION PLAN

In the light of a scientific validation of Ener-SCAPE, we intend to proceed with an experimentation phase aiming at gathering real data to evaluate the effectiveness of Ener-SCAPE. During the experimentation phase, we intend to evaluate both the home and the office version, adequately tailoring an experimentation plan. The home experimentation plan foresees the distribution of Ener-SCAPE and the sensing system to 20 users, chosen among the ones who will

join the Ener-SCAPE public site and fill out the intention form for participating in the experimentation, including profiling data. The received applications will be then analysed and the users will be selected so as to have a statistical sample as diverse as possible. The office experimentation plan will be carried out at Engineering Ingegneria Informatica S.p.A. premises in Palermo, Italy.

In order to evaluate the results of this experimentation phase, a set of metrics has been identified and divided into quantitative metrics and qualitative metrics.

Quantitative metrics measure the effects of greater energy awareness. No preliminary consumption baseline is provided for the evaluation of the performance: users are clustered on the basis of a set of parameters (age, job, education, skills, etc.) provided during the preliminary registration phase. Their performance, both in home and in building/campus environment, are evaluated at a well-defined set of time slots (hour, day, week, month, etc.) and compared to their own past average values (starting from the beginning of the experimentation) or to the values of users belonging to the same cluster (e.g., the best user, the average one or the worst one). In order to have a greater persistence of the results, a massive amount of information must be acquired and assimilated slowly, so as to have a significant impact on the lifestyle of the consumer, rather than only on the performance recorded during the experimental period. The impact of Ener-SCAPE is expected to increase slowly with time, so that the comparison to the average performance, in the first part of the use of the application, can be considered as the comparison to the baseline.

TABLE I. INDIRECT QUALITATIVE METRICS

Application	Metrics
Feedback (monitoring)	Response to interaction Real-time perception Dashboard reliability Usefulness of shown information Completeness of shown information User-friendliness
Game (the escape room)	Compliance to the Escape Room paradigm Perception of the entertaining aspect Appreciation of the entertaining aspect Perception of the educational aspect Appreciation of the educational aspect Appreciation of the graphical aspect <i>Appreciation of the team based Escape Room</i> <i>Appreciation of the competition mechanism</i> <i>Appreciation of the collaborative mechanism</i>
Social (community)	Usefulness of support to the community Reliability of information from the community Fairness of ranking mechanism

Qualitative metrics are subdivided into indirect metrics, aimed at assessing the user perception of the Ener-SCAPE application, and direct metrics, aimed at evaluating the effectiveness of Ener-SCAPE by evaluating the sensitivity acquired by the user in the field of eco-sustainability. In both cases, it has been decided to proceed by administering questionnaires to the users. In TABLE I, a list of indirect metrics are provided; specific metrics pertaining only to the business/campus case are reported in italic.

At the end of the experimentation phase, all the data collected will be analysed to evaluate the impact of Ener-SCAPE on the energy awareness.

## V. BUSINESS MODEL

In recent years, big companies such as Google Inc. and Microsoft Corp. developed their own energy management tools. Both the initiatives have failed and their projects were closed after few years [41][42]. One reason can be found in the early stage of the market when the products were launched (2009). Indeed, very few smart meters and smart grid networks had been installed in those years. Additionally, Google and Microsoft probably did not follow the right distribution strategy, building only few partnerships with strategic partners. Starting from these two cases, and considering a possible launch of Ener-SCAPE into the market, we had the chance to develop new business models to avoid past mistakes.

Following the Business Model Canvas [43], we can analyse the possible development of Ener-SCAPE as a product to market. To do so, we have to consider separately the two versions of the software framework. The home version has individual users interested in energy and environmental issues, or interested in escape room games, as possible customers. Indeed, the game can be the driver to spread ECA even among people not directly interested in it. As a value proposition, Ener-SCAPE can increase ECA in an appealing and fresh way. Increasing the energy efficiency at home, users can save their money and respect the environment. We have identified two distribution channels: online selling in a dedicated web site or by partnership with a specialised third party as producers/sellers of energy sensing systems, energy retailers, energy service companies, consumers' associations, etc. We think that revenue could be produced after a year of software engineering and testing, during which the following resources will be utilised: software engineers, relational resources and technical resources. After this first phase, the promotion activity and a constant maintenance will be crucial. We have identified the following cost items: product realisation, promotion, maintenance, direct and indirect selling.

We have also done a business model of the building/campus version of Ener-SCAPE. Medium or large companies interested in their energy saving are possible customers of the product. The value proposition is the chance to save money consuming less energy. Distribution channels could include a direct sales force or selling by distributors/partners. The revenue plan is substantially the same as the plan seen for the Ener-SCAPE home version. Indeed, key resources, activities and cost structure are shared for both versions of the product. In the end, we can summarise that starting with relatively small investments, mostly concentrated in the first year, two marketable products may be obtained with good chance to generate incomes.

Finally, the reference market of Ener-SCAPE is in energy management software. Today, energy monitoring systems are offered by many big multinational companies such as

IBM Corporation, CISCO Systems, Inc., and the General Electric Company. However, this market is constantly developing, primarily due to the birth of the “Internet of Things” [44] and automation systems [45], and secondarily due to the great attention this market is calling. Despite the large amount of players, today there is no evidence that a product like Ener-SCAPE is already on the market. The distinctive feature is the simultaneous presence of a persuasive game in the form of an escape room game, a monitoring interface for the electric consumption and a tool for the integration with social networks. As a matter of fact, Ener-SCAPE strength lies in the cooperation of these three elements, to reach the same goal: providing the users with a greater ECA to get a better energy efficiency, save money and natural resources, and improve their lives.

## VI. CONCLUSION AND FUTURE WORK

This work proposes a pervasive and multi-platform application to improve energy consumption awareness. Following the results of a number of previous works found in the literature and analysed in depth, Ener-SCAPE has designed and developed an energy-aware application integrating successful elements for achieving energy consumption awareness: serious games, real time and detailed feedback on energy consumption and motivational factors coming from the social interaction in a community. In order to pave the way for possibly launching the application into the market, an experimentation phase has been scheduled inside the business plan. Corroborated by the use of elements that individually have been proven effective in increasing ECA, which have emerged as well known and widely utilized, we are confident on the effectiveness of this ongoing work.

Besides what is already planned, the monitoring tool can be extended and improved. Citizens consume not just electricity at their homes but also gas, water, and heat. Thus, the Ener-SCAPE monitoring interface could be enriched to evaluate all of these additional areas of consumption. In regards to the game, other exploratory works could be done with information and visualisation techniques. As an example, the home version could be expanded from a single player into a multiplayer game, by taking into consideration other households. The single user approach could be changed into a team-based one; trying to increase the ECA in all the household with a collaborative (and not only competitive) version of the game. This enhancement is supported by recent studies demonstrating that family relationships and dynamics have a lot of influence on ECA improvement [15]. Moreover, the age of the users and the contingent presence of children at home have been demonstrated as affecting the levels knowledge in energy related issues inside families [46].

## ACKNOWLEDGMENT

This work is part of “ENERGETIC – Tecnologie per l’Energia e l’Efficienza Energetica” project, co-funded by MIUR (Italian Ministry for Education, University and

Research) by means of the national Program PON R&C 2007-2013, project, PON02\_00\_355\_3391233C.

## REFERENCES

- [1] D. Arnone, A. Rossi, E. G. Melodia, M. Mammina, and S. E. Jenkins, “Ener-SCAPE: A Novel Persuasive Game to Improve the Energy Consumption Awareness,” The Fifth International Conference on Smart Grids, Green Communications and IT Energy-aware Technologies (Energy 2015), IARIA, May 2015, pp. 24-28, ISSN: 2308-412X.
- [2] L. Adua, “To cool a sweltering earth: does energy efficiency improvement offset the climate impacts of lifestyle?” *Energy Policy*, Vol. 38 (10), pp. 5719–5732, Oct. 2010, doi: 10.1016/j.enpol.2010.05.021.
- [3] C. Wilson, “Evaluating communication to optimise consumer-directed energy efficiency interventions,” *Energy Policy*, Vol. 74, pp. 300–310, Sep. 2014, doi: 10.1016/j.enpol.2014.08.025.
- [4] T. Dietz, G. T. Gardner, J. Gilligan, P. C. Stern, and M. P. Vandenbergh, “Household actions can provide a behavioural wedge to rapidly reduce US carbon emissions,” *Proc. Nat. Acad. Sci. USA*, Vol. 106 (44), pp. 18452–18456, Oct. 2009, doi: 10.1073/pnas.0908738106.
- [5] G. T. Gardner and P. C. Stern, “Environmental problems and human behaviour,” (2nd ed.). Boston, 2002, MA: Pearson Custom.
- [6] P. C. Stern, “Contributions of psychology to limiting climate change,” *Am. Psychol.*, Vol. 66 (4), pp. 303–314, Jun. 2011, doi: 10.1037/a0023235.
- [7] J. C. Yang, K. H. Chien, and T. C. Liu, “A digital game-based learning system for energy education: an Energy COnservation PET,” *Turkish Online Journal of Educational Technology*, Vol. 11 (2), pp. 27-37, Apr. 2012, Online ISSN: 1303-6521.
- [8] New EU Energy Label, “Home page,” [Online]. Available: <http://www.newenergylabel.com/index.php/start/> [retrieved: July, 2015].
- [9] Energy Star, “Home page,” [Online]. Available: <http://www.energystar.gov/> [retrieved: July, 2015].
- [10] EUROPEAN COUNCIL - 25/26 MARCH 2010 - Europe 2020: a New European Strategy for Jobs and Growth. [Online]. Available: <http://register.consilium.europa.eu/pdf/en/10/st00/st00007.en10.pdf> [retrieved: July, 2015].
- [11] C. Fischer, “Feedback on household electricity consumption: a tool for saving energy?,” *Energy. Effic.*, Vol. 1 (1), pp. 79-104, Feb. 2008, doi: 10.1007/s12053-008-9009-7.
- [12] A. Nilsson, C. Jakobsson Bergstad, L. Thuvander, D. Andersson, K. Andersson, and P. Meiling, “Effects of continuous feedback on households’ electricity consumption: potentials and barriers,” *Appl. Energ.*, Vol. 122, pp. 17–23, Feb. 2014, doi: 10.1016/j.apenergy.2014.01.060.
- [13] F. Reinhart, K. Schlieper, M. Kugler, E. Andre, M. Masoodian, and B. Rogers, “Fostering Energy Awareness in Residential Homes Using Mobile Devices,” The Fourth International Conference on Smart Grids, Green Communications and IT Energy-aware Technologies (Energy 2014), IARIA, Apr. 2014, pp. 35-43, ISSN: 2308-412X.
- [14] BeAware, “Home page,” [Online]. Available: <http://www.energyawareness.eu/beaware/> [retrieved: July, 2015].
- [15] S. Snow, D. Vyas, and M. Brereton, “When an eco-feedback system joins the family,” *Pers. Ubiquit. Comput.*, Online ISSN 1617-4917, Feb. 2015, doi: 10.1007/s00779-015-0839-y.

- [16] S. D'Oca, S. P. Corgnati, and T. Buso, "Smart meters and energy savings in Italy: determining the effectiveness of persuasive communication in dwellings," *Energy Res. Soc. Sci.*, Vol. 3, pp. 131–142, Sept. 2014, doi: 10.1016/j.erss.2014.07.015.
- [17] S. Darby, "The effectiveness of feedback on energy consumption. A review for DEFRA of the literature on metering, billing and direct displays," Environmental Change Institute, University of Oxford, Apr. 2006, [Online]. Available: <http://www.eci.ox.ac.uk/research/energy/electric-metering.php>.
- [18] P. Chaussecourte, B. Glimm, I. Horrocks, B. Motik, and L. Pierre, "The Energy Management Adviser at EDF," *Proc. 12th International Semantic Web Conference (ISWC 2013)*, Oct. 2013, pp. 49–64, doi: 10.1007/978-3-642-41338-4\_4.
- [19] E. A. Boyle, T. M. Connolly, and T. Hainey, "The role of psychology in understanding the impact of computer games," *Entertain. Comput.*, Vol. 2 (2), pp. 69–74, Jan. 2011, doi: 10.1016/j.entcom.2010.12.002.
- [20] T. M. Connolly, E. A. Boyle, E. MacArthur, T. Hainey, and J. M. Boyle, "A systematic literature review of empirical evidence on computer games and serious games," *Comput. Educ.*, Vol. 59, pp. 661–686, Sept. 2012, doi: 10.1016/j.compedu.2012.03.004.
- [21] U. Dorji, P. Panjaburee, and N. Srisawasdi, "A learning cycle approach to developing educational computer game for improving students' learning and awareness in electric energy consumption and conservation," *J. Educ. Techno. Soc.*, Vol. 18 (1), pp. 91–105, Jan. 2015, Online ISSN: 1436-4522.
- [22] M. Torres and J. Macedo, "Learning sustainable development with a new simulation game," *Simulat. Gaming*, Vol. 31 (1), pp. 119–126, Mar. 2000, doi: 10.1177/104687810003100112.
- [23] Ecoville, [Online]. Available: <http://www.ecovillejeu.com> [retrieved: July, 2015].
- [24] EnerCities, "Home page," [Online]. Available: <http://www.enercities.eu> [retrieved: July, 2015].
- [25] I. Ajzen, "The theory of planned behavior," *Organ. Behav. Hum. Dec. Proc.*, vol. 50 (2), pp. 179–211, Oct. 1991, doi: 10.1016/0749-5978(91)90020.
- [26] A. Gustafsson, M. Bång, and C. Katzeff, "Evaluation of a Pervasive Game for Domestic Energy Engagement Among Teenagers," *ACM CIE*, vol. 7 (4), art. 54, Dec. 2009, doi: 10.1145/1658866.1658873.
- [27] A. Gustafsson, M. Bång, and M. Svahn, "Power Explorer – a casual game style for encouraging long term behavior change among teenagers," *Proc. The International Conference on Advances in Computer Entertainment Technology (ACE '09)*, pp. 182–189, Oct. 2009, doi: 10.1145/1690388.1690419.
- [28] W. Willemsen, J. Hu, G. Niezen, and B. van der Vlist, "Using game elements to motivate environmentally responsible behaviour," *Game and Entertainment Technologies (GET 2011)*, IADIS.
- [29] L. S. G. Piccolo, C. Baranauskas, M. Fernandez, H. Alani, and A. De Liddo, "Energy consumption awareness in the workplace: technical artefacts and practices," *XIII Brazilian Symposium on Human Factors in Computer Systems (IHC 14)*, pp. 27–31, Oct. 2014.
- [30] J. Mankoff, D. Matthews, S. R. Fussell, and M. Johnson, "Leveraging social networks to motivate individuals to reduce their ecological footprints," *Proc. The 40th Hawaii International Conference on System Sciences (HICSS 2007)*, pp. 87–96, Jan. 2007.
- [31] D. Foster, S. Lawson, M. Blythe, and P. Cairns, "Wattsup?: Motivating reductions in domestic energy consumption using social networks," *Proc. The 6th Nordic Conference on Human-Computer Interaction: Extending Boundaries (NordiCHI '10)*, pp. 178–187, Oct. 2010.
- [32] P. Petkov, F. Köbler, M. Foth, and H. Krcmar, "Motivating domestic energy conservation through comparative, community-based feedback in mobile and social media," *Proc. The 5th International Conference on Communities and Technologies (C&T '11)*, pp. 21–30, June 2011.
- [33] H. T. Hou and Y. S. Chou, "Exploring the technology acceptance and flow state of a chamber escape game - Escape the Lab© for learning electromagnet concept," *Proc. The 20th International Conference on Computer in Education (ICCE 2012)*, Asia-Pacific Society for Computers in Education, Nov. 2012, pp. 38–41.
- [34] R. C. Schank, T. R. Berman, and K. A. Macpherson, "Learning by doing" Instructional-design theories and models: A new paradigm of instructional theory 2, 1999, pp. 161–181.
- [35] OAuth 2.0, "About OAuth 2.0 page", [Online]. Available: <http://oauth.net/2/> [retrieved: July, 2015].
- [36] O. Etzion and P. Niblett, "Event Processing In Action," Manning Publications Co. Greenwich, CT, USA 2010, ISBN: 1935182218 9781935182214.
- [37] Sweet Home 3D, "Home Page," [Online]. Available: <http://www.sweethome3d.com/> [retrieved: July, 2015].
- [38] J. Sánchez and R. Olivares, "Problem solving and collaboration using mobile serious games," *Comput. Educ.*, Vol. 57, pp. 1943–1952, Apr. 2011, doi: 10.1016/j.compedu.2011.04.012.
- [39] N. E. Cagiltay, E. Ozcelik, and N. S. Ozcelik, "The effect of competition on learning in games," *Comput. Educ.*, Vol. 87, pp. 35–41, Apr. 2015, doi: 10.1016/j.compedu.2015.04.001.
- [40] E. Ozcelik, N. E. Cagiltay, and N. S. Ozcelik, "The effect of uncertainty on learning in game-like environments," *Comput. Educ.*, Vol. 67, pp. 12–20, Sept. 2013, doi: 10.1016/j.compedu.2013.02.009.
- [41] C. Nuttall, "Google's mission falters on health, energy," *The Financial Times*, Financial Times Tech Blog, 25 Jun. 2011 [Online]. Available: <http://blogs.ft.com/tech-blog/2011/06/googles-mission-falters-on-health-energy/> [retrieved: July, 2015].
- [42] C. Nuttall, "Microsoft shutters Hohm," *The Financial Times*, Financial Times Tech Blog, 30 Jun. 2011 [Online]. Available: <http://blogs.ft.com/tech-blog/2011/06/microsoft-shutters-hohm/> [retrieved: July, 2015].
- [43] A. Osterwalder and Y. Pigneur, "Business model generation: a handbook for visionaries, game changers and challengers," John Wiley & Sons, Jul. 2010.
- [44] J. Gubbia, R. Buyab, S. Marusica, and M. Palaniswamia, "Internet of Things (IoT): A vision, architectural elements, and future directions," *Future Gener. Comp. Sy.*, Vol. 29 (7), Sept. 2013, pp. 1645–1660, doi: 10.1016/j.future.2013.01.010.
- [45] A. Alkar and U. Buhur, "An internet based wireless home automation system for multifunctional devices," *IEEE Trans. Consumer Electronics*, Vol. 51 (4), pp. 1169–1174, Nov. 2005, doi: 10.1109/TCE.2005.1561840.
- [46] I. Vassileva and J. Campillo, "Increasing energy efficiency in low-income households through targeting awareness and behavioral change," *Renew. Energ.*, Vol. 67, pp. 59–63, Dec. 2013, doi: 10.1016/j.renene.2013.11.046.

# Round-Trip Engineering Approach to Keep Activity Diagrams Synchronized with Source Code

Keinosuke Matsumoto, Ryo Uenishi, and Naoki Mori  
 Department of Computer Science and Intelligent Systems  
 Graduate School of Engineering, Osaka Prefecture University  
 Sakai, Osaka, Japan  
 email: {matsu, uenishi, mori}@cs.osakafu-u.ac.jp

**Abstract**—Methods for introducing business logic changes and new implementation methods into software should be flexible. Model driven development is regarded as one of the most flexible development methods. The user expects source code to be generated from the models. However, the models and the source code generated from them become unsynchronized if the code is changed. To solve this problem, a round-trip engineering (RTE) approach was proposed that has a feature that keeps the models synchronized with the source code. Tools that provide RTE exist, but almost all of them are applicable only for static diagrams. In this study, RTE is directly adapted to activity diagrams as a type of dynamic diagram. A method is proposed for realizing an RTE approach that keeps activity diagrams synchronized with the source code. The results of application experiments confirmed that the transformation rate of the models and source code is satisfactory. Thus, the success of the proposed RTE approach was verified.

**Keywords**—round-trip engineering; model; reverse engineer; activity diagram; model driven development.

## I. INTRODUCTION

This paper is based on one [1] presented at ICAS 2015. Model driven architecture (MDA) [2][3] is attracting attention as an approach that can flexibly handle changes in business logics or new software technologies [4][5]. Its core data are models that serve as software design diagrams. It includes features for transforming the models to various types of models and for automatic source code generation [6][7][8][9][10].

The development and standardization of MDA is being advanced by the Object Management Group (OMG). However, the models and the source code generated from them become unsynchronized if the code is changed. To solve this problem, round-trip engineering (RTE) [11][12][13][14] was proposed. RTE includes a feature that keeps the models synchronized with the source code. Therefore, the consistency between them can be maintained. Tools that provide RTE exist, but almost all of them are applicable only for static diagrams, such as class and component diagrams. Therefore, it is necessary to adapt RTE to dynamic diagrams.

In this study, RTE is adapted to activity diagrams as a type of dynamic diagram. A method is proposed to realize RTE for activity diagrams and source code [15][16]. Activity diagrams are defined in Unified Modeling Language (UML) and express the flows of activities. They can also describe

the contents of methods, unlike sequence diagrams. Further, they can express processes hierarchically and are used widely from upper to lower processes of software development. For transforming activity diagrams to source code, the proposed method analyzes the XML metadata interchange (XMI) [17] of the activity entities. XML is a markup language that defines a set of rules for encoding documents in a format that is both human- and machine-readable. XMI is a standard for exchanging metadata information. Conversely, for transforming source code to activity diagrams, the proposed method analyzes the abstract syntax tree (AST) [18] of the source code. In the mutual transformation process, an intermediate representation is used. It has a hierarchical structure and corresponds to both activity diagrams and source code. For this reason, XMI can easily be transformed to an AST and vice versa. For describing conditional branches and loop statements, activity diagrams use the same elements. They cannot be transformed to source code in their existing form. Therefore, a method for analyzing them and transforming one into the other is developed that distinguishes the conditional branches and loop statements. A successful transformation rate of the models and source code was confirmed. Thus, the validity of the proposed method was verified.

The contents of this paper are as follows. In Section II, related work is described. In Section III, the proposed method is explained. In Section IV, the results of application experiments conducted to confirm the validity of the proposed method are given. Finally, in Section V the conclusion and future work are presented.

## II. RELATED WORK

This section describes work related to this study.

### A. Abstract Syntax Tree

The AST, which belongs to the Eclipse AST implementation, is a directed tree that shows the syntactic analysis results of source code. It is also used to create byte code from the source code as the internal expression of a compiler or interpreter. An AST provides the ASTParser class, which changes source code into an AST. Many types of nodes can be defined by the AST. An AST node can be searched by using the ASTVisitor class corresponding to one of the design patterns [19]. The visitor design pattern allows an algorithm to be separated from the object structure on

which it operates. A practical result of this separation is that new operations can be added to existing object structures without modifying the structures. An example of an AST is shown in Figure 1. A detailed analysis can be performed by changing the AST levels.

*B. Consistency among Software Documentations and Source Code*

Many approaches, such as those proposed in [20][21], manage consistency and synchronization between software documentation and source code. In particular, RTE refines intermediate results by editing requirement definitions, design plans, and source code alternately. In general, if either the models or code is changed, the RTE automatically reflects the change in the other entity. RTE has a feature that keeps the models synchronized with the source code. An outline of RTE is shown in Figure 2.

Tools, such as UML Lab [22] and Fujaba [23][24], were proposed to maintain the consistency of models and source code. In these tools, a template for generating source code is described by a template description language. Source code can be automatically generated from models by using the template and these tools allow the source code and static diagrams, such as class diagrams and component diagrams, to be refactored synchronously. They also perform code generation and reverse engineering in real time. However, they cannot handle dynamic diagrams, such as activity diagrams, that can describe the behavior of a system. Although Fujaba considers activity diagrams,

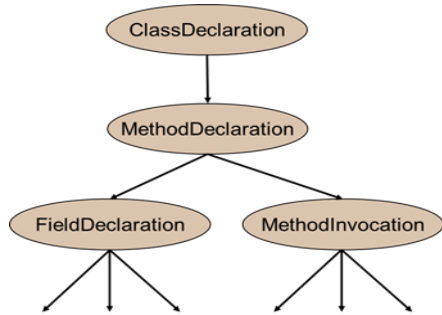


Figure 1. Example of AST.

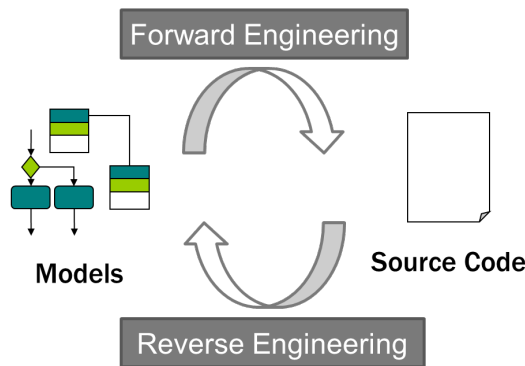


Figure 2. Outline of RTE.

it does not address them directly. In contrast, our approach can handle activity diagrams directly.

III. PROPOSED METHOD

In this section, the proposed transformation method from activity diagrams to source code and from source code to activity diagrams is described. Activity diagrams mainly describe the behaviors of a system using nodes and edges. A content of action is described in a node. The flow of a series of actions is expressed by connecting nodes by edges. An activity diagram is described for each method in class diagrams in the proposed method. Figure 3 shows the basic concept of the proposed method.

*A. Transformation from Activity Diagram to Source Code*

A specific transformation flow from activity diagrams to source code is as follows.

1) *XMI Analysis of Activity Diagram*: An activity diagram is expressed in XMI form as a UML file. It begins with a start node and ends with a final node, following nodes or groups through edges. Nodes have information about the actions or controls of the activity diagram. Edges have information about the control flows in the form of attributes and subelements. Group is a tag that has nodes and edges of a subactivity as subelements. Each tag is given an id to discriminate it from other tags. Table I shows the nodes used by an activity diagram.

2) *Transformation from XMI to Intermediate Representation*: Node and edge tags have a transition starting id and targeting id, respectively. Using these ids, the flow of actions of an activity diagram can be extracted as a sequence of ids. The activity diagram can be transformed from XMI to an intermediate representation by replacing the ids with the corresponding nodes extracted from the XMI analysis. The intermediate representation is a sequence of nodes as the flow of actions. The reason for introducing the intermediate representation is that it facilitates the transformation of XMI to source code and vice versa. Figure 4 shows a metamodel of intermediate representation and Figure 5 shows an example of intermediate representation.

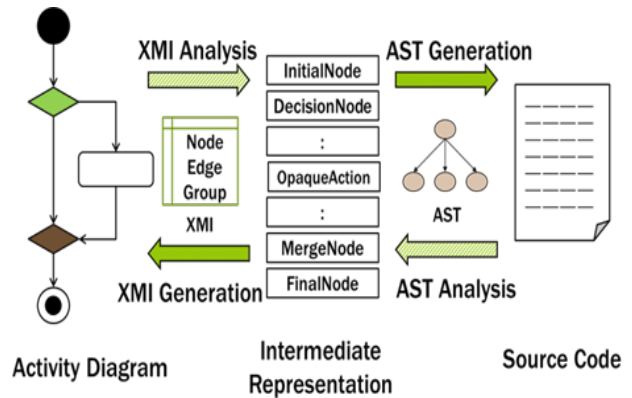


Figure 3. Schematic diagram of the proposed method.

Figure 6 shows an image of this transformation.

3) *Transformation from Intermediate Representation to AST:* By analyzing the flow of the actions of an intermediate representation, it can be transformed into an AST. The intermediate representation is analyzed in order from the beginning. According to the corresponding nodes, it is necessary to extract information, such as a branch and loop, from the representation structure. For example, a branch has

TABLE I. NODES USED BY AN ACTIVITY DIAGRAM

Tag	Node
Node tag	ActivityInitialNode
	ActivityFinalNode
	CallBehaviorAction
	CallOperationAction
	DecisionNode
	LoopNode
	MergeNode
	OpaqueAction
Group tag	StructuredActivityNode
Edge tag	ControlFlow

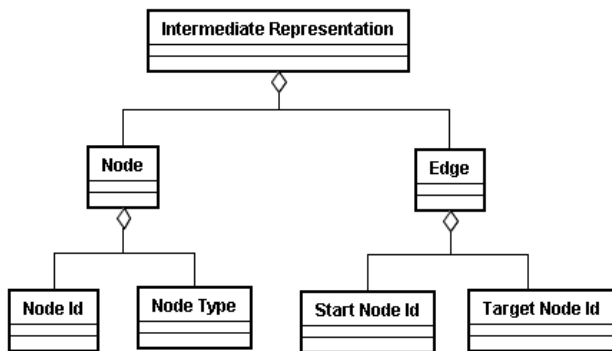


Figure 4. Metamodel of intermediate representation.

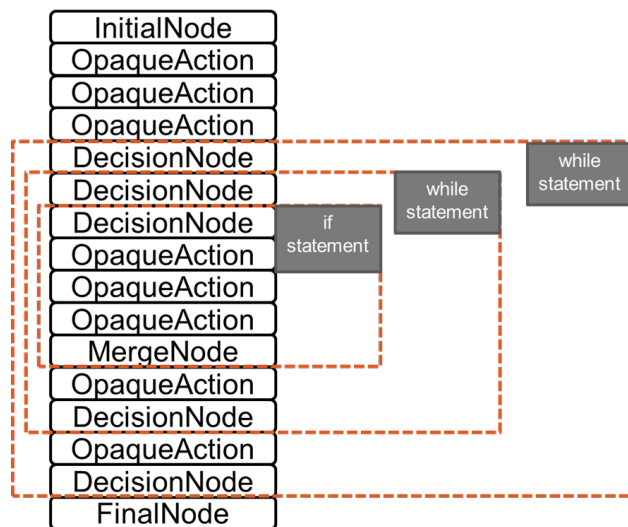


Figure 5. Example of intermediate representation.

a structure embraced by Decision node and Merge node, but a loop has a structure embraced by Decision nodes. In order to distinguish such structures, a stack that stores the ids of Decision nodes is created. If a Decision node is extracted, the id is pushed to the stack immediately. It is a branch if a Merge node is extracted before a subsequent Decision node is extracted. If a Decision node is extracted and its id is the same id as that popped from the stack, then it is a loop. Otherwise, a new Decision node is extracted and its id is stacked. Figure 7 shows this transformation.

4) *Transformation from an AST to Source Code:* The target source skeleton code is transformed from class diagrams by using Acceleo templates for classes. Acceleo [25] is the Eclipse Foundation's open-source code generator that provides templates for skeleton code. Transformed activity diagrams and classes of a target source skeleton code are expressed by an AST. A method having a name that is identical to that of an activity diagram can be searched by using ASTVisitor class. The method code transformed from the AST of the activity diagram is added to the method body to which it corresponds in the target source skeleton code for every activity diagram.

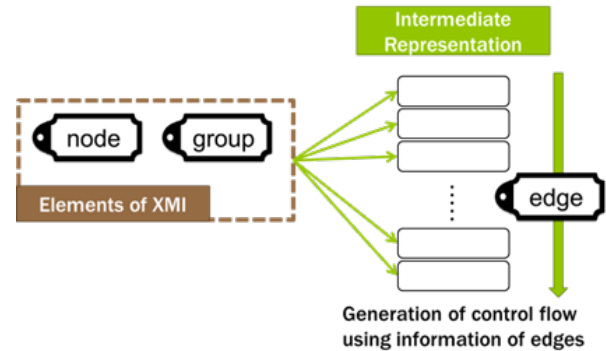


Figure 6. From XMI to intermediate representation.

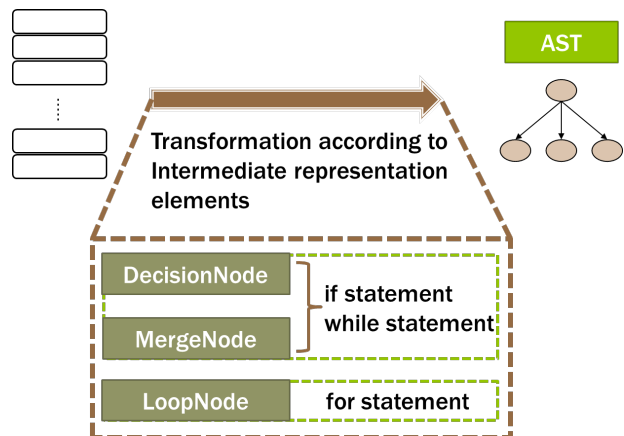


Figure 7. From intermediate representation to AST.

**B. Transformation from Source Code to Activity Diagram**

The specific flow of transformation from source code to activity diagrams is as follows.

1) *AST Analysis of Source Code*: The ASTParser class transforms source code into an AST, and the ASTVisitor class searches AST nodes to handle. These are defined as an AST library. The structure of the source code is analyzed by using these classes.

2) *Transformation from AST to Intermediate Representation*: The required information is extracted by analyzing the AST. Whenever an AST node is searched, the information on the AST node is saved in detail. Required AST nodes are the DeclarationStatement node (such as variables and call of methods) IfStatement node, WhileStatement node, ForStatement node, and so on. The flow of the processing is almost the same as that of the transformation from the XMI of an activity diagram to intermediate representation. Figure 8 shows this transformation.

3) *Transformation from Intermediate Representation to XMI*: A sequence of ids can be extracted from nodes, groups, and edges in the transformation from activity diagrams to source code. If this transformation is executed in reverse, nodes, groups, and edges are generated by analyzing the flow of actions. Specifically, nodes or groups are generated for each action of the intermediate representation. They are transformed to XML according to the action type. Simultaneously, the edges that connect nodes or groups are



Figure 8. From AST to intermediate representation.

generated. A transition starting id and targeting id can be generated from the sequence of intermediate representation. By generating Decision or Merge nodes expressing branches or loops, a stack that is similar to that of the transformation from activity diagrams to intermediate representation is used.

4) *Adding XMI to Activity Diagram*: Generated nodes, groups, and edges are added to the XMI file of an activity diagram. In the case of an addition, the user refers to the activity diagram in the package where the source code is located. If the diagram already exists, the addition is performed after deleting the contents of the existing file; otherwise, the addition is performed after generating a new diagram.

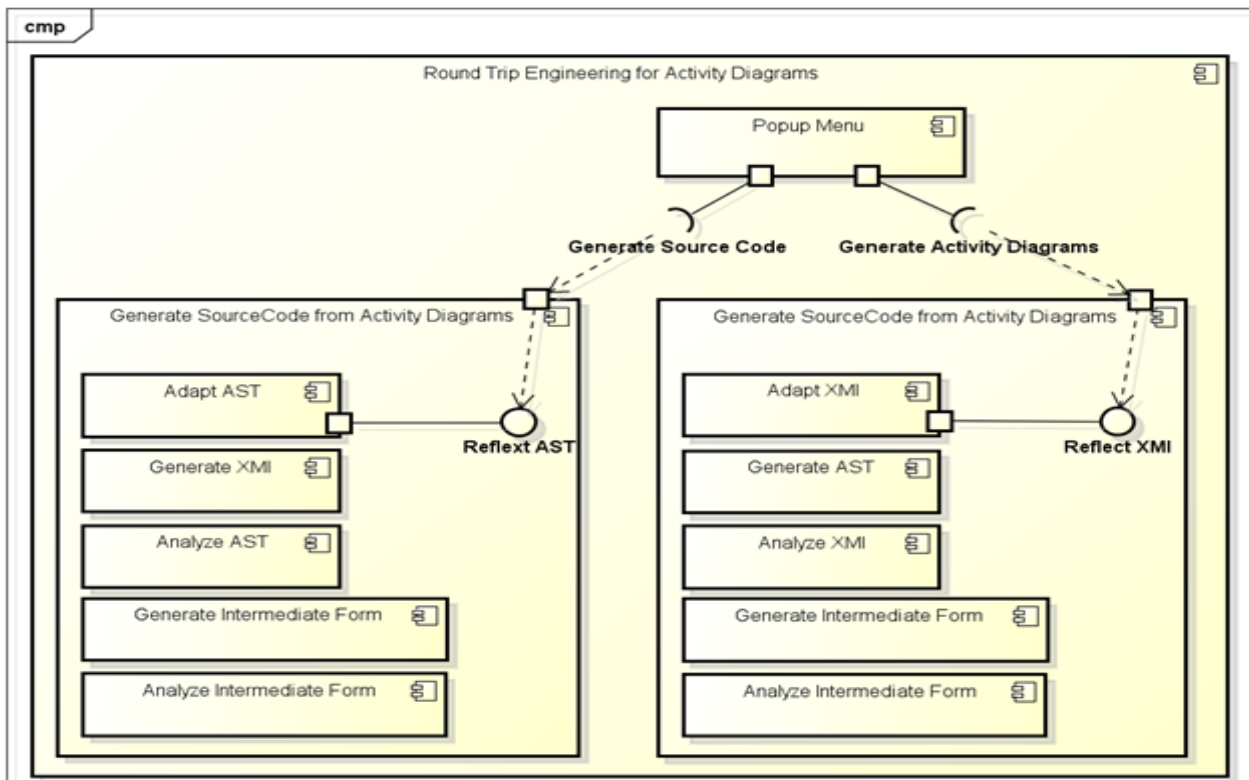


Figure 9. Plug-ins of the proposed method.

powered by Astah

C. Implementation of the Proposed Method

The plug-in shown in Figure 9 was implemented in order to realize the proposed method using the integrated development environment, Eclipse [26]. The details of the plug-in are as follows.

1) *Reflection of Activity Diagrams in Source Code:* The pop-up menu for source code is opened and a dialog reflecting activity diagrams is called. In the dialog, the target activity diagram can be chosen from a selection dialog. An activity that has already been selected can also be made a target in its existing form. Two or more activity diagrams can be chosen from a selection dialog. When an activity diagram is reflected in the source code, the signature of a method is created from the activity diagram. If the signature may agree with that of the method in the target source code, processing is added in the method body.

2) *Reflection of Source Code in Activity Diagrams:* The pop-up menu for an activity diagram is opened and a dialog reflecting the source code is called. In the dialog, the target source code can be chosen from a selection dialog. A source

code that has already been selected can also be made a target in its existing form. When the activity diagram is created, a folder with the name of the target source code is formed in the same package as that which includes the source code. Each activity diagram is created for every method of the source code in the folder. If an activity diagram already exists, overwrite preservation is conducted.

IV. EVALUATION OF THE PROPOSED APPROACH

The proposed method was applied to sample systems to confirm its validity.

A. Transformation Rate

The transformation rate was computed by comparing the number of XMI nodes of the activity diagrams. The objects that were compared were the handwritten activity diagrams and the activity diagrams automatically generated from the source code. The AST and XMI nodes were utilized as an index of whether the transformation had succeeded. The equations for calculating the rate of transformation are as follows.

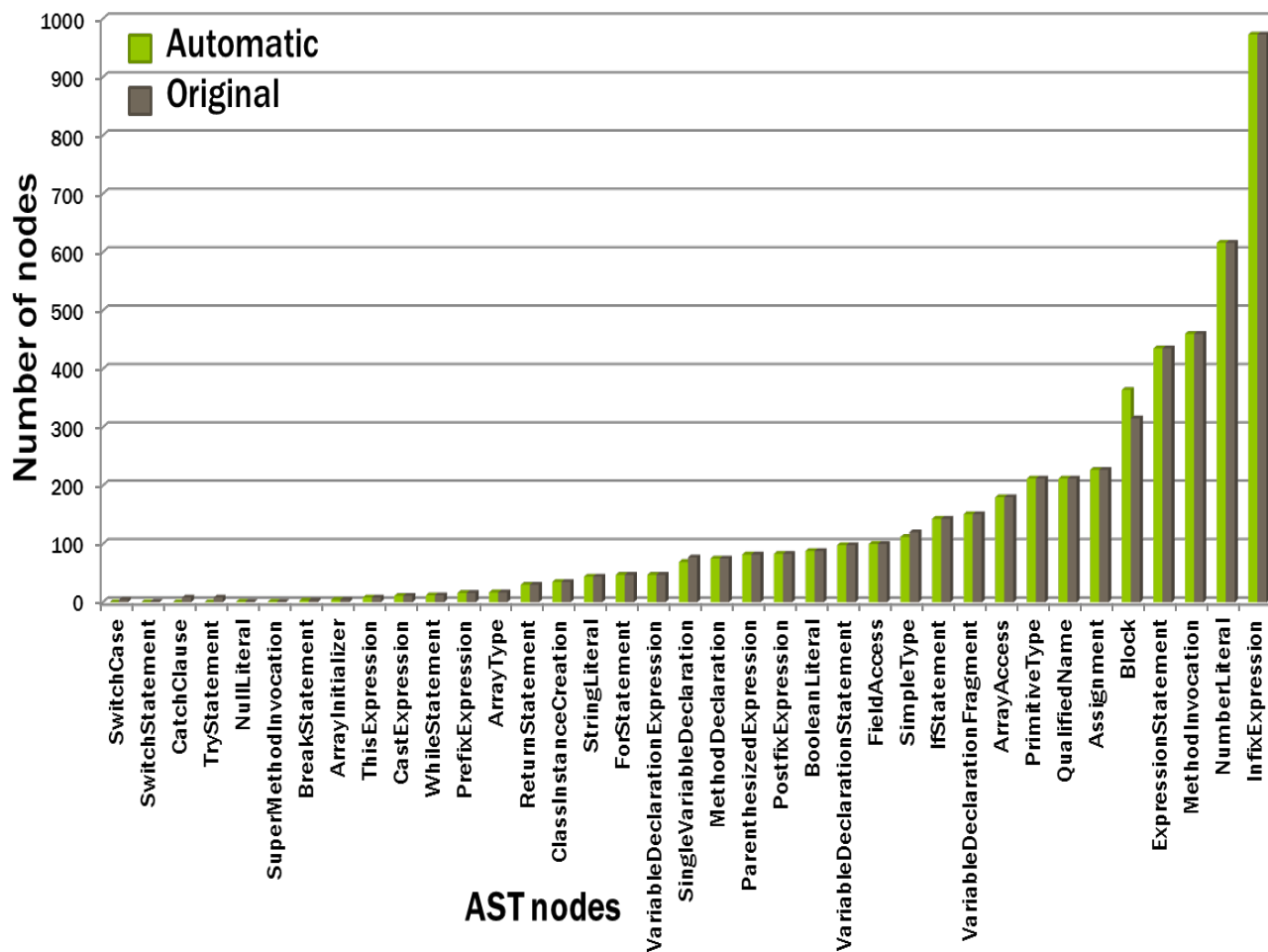


Figure 10. Comparison results of AST nodes.

TABLE II. COMPARISON OF THE NUMBER OF XMI NODES

XMI node	Automatic	Original	Difference
group	47	47	0
packagedElement	75	75	0
guard	155	159	-4
operation	198	198	0
elementImport	300	300	0
importedElement	300	300	0
edge	1137	1142	-5
node	1367	1369	-2

TABLE III. COMPARISON OF THE NUMBER OF AST NODES

AST node	Automatic	Original	Transformation rate (%)
SwitchCase	0	4	0
CatchClause	0	8	0
TryStatement	0	8	0
NullLiteral	1	1	100
SuperMethodInvocation	1	1	100
BreakStatement	3	3	100
ArrayInitializer	4	4	100
ThisExpression	8	8	100
CastExpression	11	11	100
WhileStatement	12	12	100
PrefixExpression	16	16	100
ArrayType	17	17	100
ReturnStatement	30	30	100
ClassInstanceCreation	35	35	100
StringLiteral	44	44	100
ForStatement	47	47	100
VariableDeclarationExpression	47	47	100
SingleVariableDeclaration	69	77	89.6
MethodDeclaration	75	75	100
ParenthesizedExpression	82	82	100
PostfixExpression	83	83	100
BooleanLiteral	88	88	100
VariableDeclarationStatement	98	98	100
FieldAccess	100	100	100
SimpleType	112	120	93.3
IfStatement	147	143	97.2
VariableDeclarationFragment	151	151	100
ArrayAccess	180	180	100
QualifiedName	212	212	100
PrimitiveType	215	212	98.6
Assignment	227	227	100
Block	368	315	83.2
ExpressionStatement	435	435	100
MethodInvocation	460	460	100
NumberLiteral	616	616	100
InfixExpression	977	973	99.6
Total	4971	4944	99.5

$$[1 - \{\text{abs}(NA_g - NA_o) / NA_o\}] * 100 \quad (1)$$

where  $NA_g$  and  $NA_o$  are the number of AST nodes of generated source code and the original source code, respectively.

$$[1 - \{\text{abs}(NX_g - NX_o) / NX_o\}] * 100 \quad (2)$$

where  $NX_g$  and  $NX_o$  are the number of XMI nodes of generated source code and original source code, respectively.

### B. Transformation of Hunter Game

The proposed method was applied to a hunter game [27][28]. Both the activity diagrams and source code of the hunter game were available. The number of AST nodes of the original hunter game is 4971. Figure 10 shows the comparison results of the number of AST nodes.

A handwritten activity diagram was transformed into source code and the source code was transformed in reverse into an activity diagram. The two activity diagrams were compared. Tables II and III show a comparison of the number of XMI and AST nodes, respectively.

The XMI nodes that were not transformed can be seen in Table II. There are three types of nodes: guard, edge, and node. A switch statement cannot be described in an activity diagram, but the same processing can be described by using if statements. Guard nodes also decreased in the same number as the switch cases in the generated activity diagrams. The number of edges in connection with them also decreased.

Table III shows the comparison results of AST nodes. The total transformation rate is 99.5%. There are no differences between nodes that in fact express processing, "group," "edge," and "node." This is because only the processing that can be expressed in an activity diagram is expressed in the source code generated from the activity diagram. According to the number of nodes, it was determined that the transformations were successful.

Since there are many kinds of AST nodes, the number of nodes of every type should be compared. The

TABLE IV. COMPARISON OF THE NUMBER OF AST NODES

AST node	Automatic	Original	Difference
ActivityParameterNode	69	69	0
Activity	75	75	0
MergeNode	102	102	0
DecisionNode	114	114	0
InitialNode	118	118	0
ActivityFinalNode	118	118	0
StructuredActivityNode	141	141	0
Expression	159	159	0
CallOperationAction	192	198	-6
PrimitiveType	300	300	0
OpaqueAction	515	509	+6

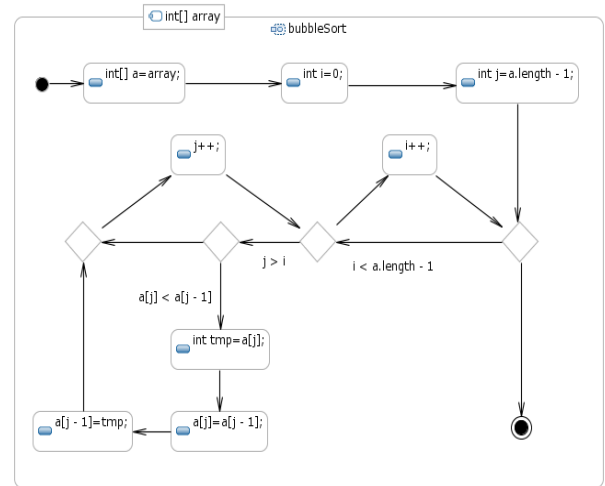
transformation rate is shown in Table IV. Only the number of the node type CallOperationAction decreased. CallOperationAction is an AST node that calls a method. The reason why the number of this node decreased is that the calling method part was not appropriately determined. OpaqueAction expresses the processing that cannot be expressed by the AST nodes. Therefore, OpaqueAction expresses the processing that CallOperationAction should originally express. It can be affirmed that the mutual transformation of activity diagrams was successful.

C. RTE of Activity Diagrams

RTE of activity diagrams and source code was performed using the proposed method. A bubble sort algorithm was used as an example. Figure 11 shows its activity diagram and the source code generated from the diagram. After adding a change (modification, addition, and deletion) to the source code, an activity diagram was generated from the changed source code. It was verified that the generated activity diagram reflected the added change.

1) Code Modification: A modification was added to the generated source code. Items to be modified were variable value, variable name, and loop statement (while statement to for statement). A new activity diagram was generated from the modified source code by the proposed method. Figures 12-13 show the modified source code and activity diagrams for the modifications of variable name and loop statement, respectively. The figures show that the modifications were reflected in the activity diagrams.

2) Code Addition: Code was added to the source code and a new activity diagram was generated from the added source code using the proposed method. Figures 14-15 show the added source code and the activity diagrams for the



```
void bubbleSort(int[] array) {
    int[] a = array;
    int i = 0;
    int j = a.length - 1;
    while (i < a.length - 1) {
        while (j > i) {
            if (a[j] < a[j - 1]) {
                int tmp = a[j];
                a[j] = a[j - 1];
                a[j - 1] = tmp;
            }
            j++;
        }
        i++;
    }
}
```

Figure 11. Original activity diagram and its source code.

```
void bubbleSort(int[] array) {
    int[] a = array;
    int i = 0;
    int j = a.length - 1;
    while (i < a.length - 1) {
        while (j > i) {
            if (a[j] < a[j - 1]) {
                int tmp2 = a[j];
                a[j] = a[j - 1];
                tmp2 = a[j - 1];
            }
            else {
                j++;
            }
        }
        i++;
    }
}
```

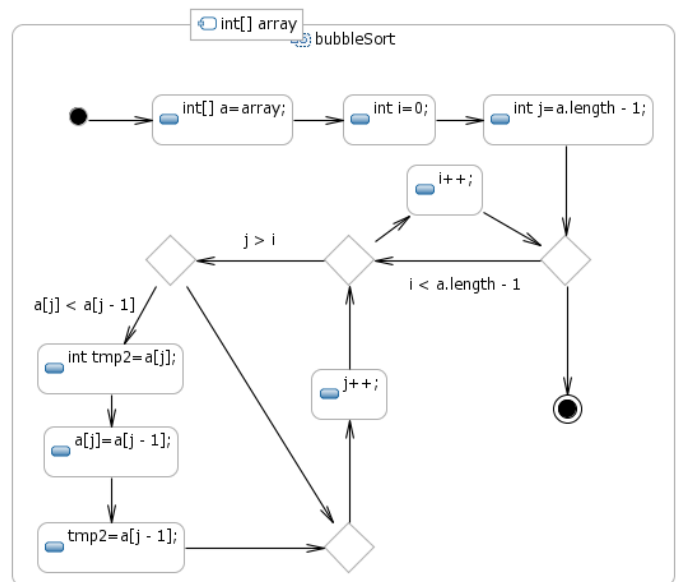


Figure 12. Modified variable code and activity diagram.

addition of a loop statement and if statement. The figures show that the addition was reflected in the activity diagrams as intended.

3) *Code Deletion:* Code was deleted from the

generated source code and a new activity diagram was generated from the deleted source code using the proposed method. Figure 16 shows the deleted source code and the activity diagram for deletion of the if statement. The figure shows that the deletion was reflected in the activity diagram.

```

void bubbleSort(int[] array) {
> int[] a = array;
> int i = 3;
> int j = a.length - 1;

> for (i = 0; i < a.length; i++) {
> > for (j = 0; j < i; j++) {
> > > int tmp = a[j];
> > > a[j] = a[j - 1];
> > > tmp = a[j - 1];
> > }
> }
}
    
```

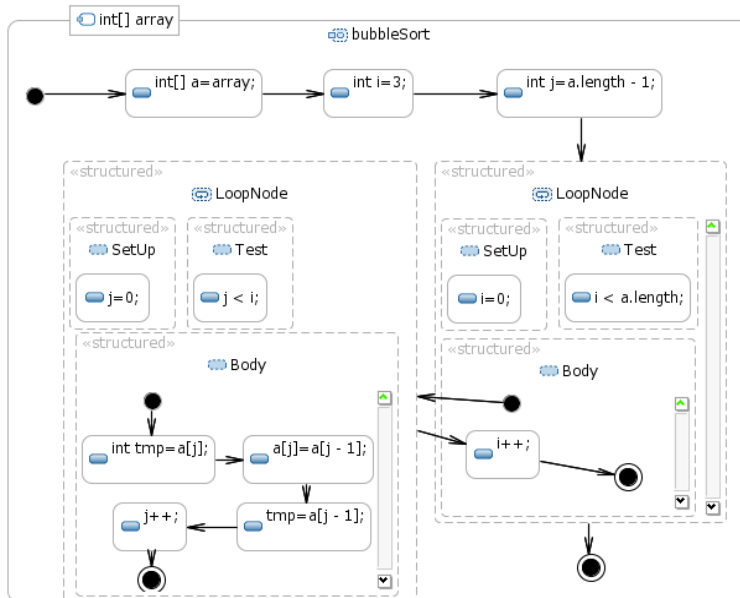


Figure 13. Modified source code and activity diagram.

```

public void bubbleSort(int[] array) {
> int[] a = array;
> int i = 0;
> int j = a.length - 1;
> while (i < a.length - 1) {
> > while (j > i) {
> > > if (a[j] < a[j - 1]) {
> > > > int tmp = a[j];
> > > > a[j] = a[j - 1];
> > > > a[j - 1] = tmp;
> > > > } else {
> > > }
> > > j++;
> > }
> > i++;
> }
> for (int k = 0; k < array.length; k++)
> > System.out.println(k);
}
    
```

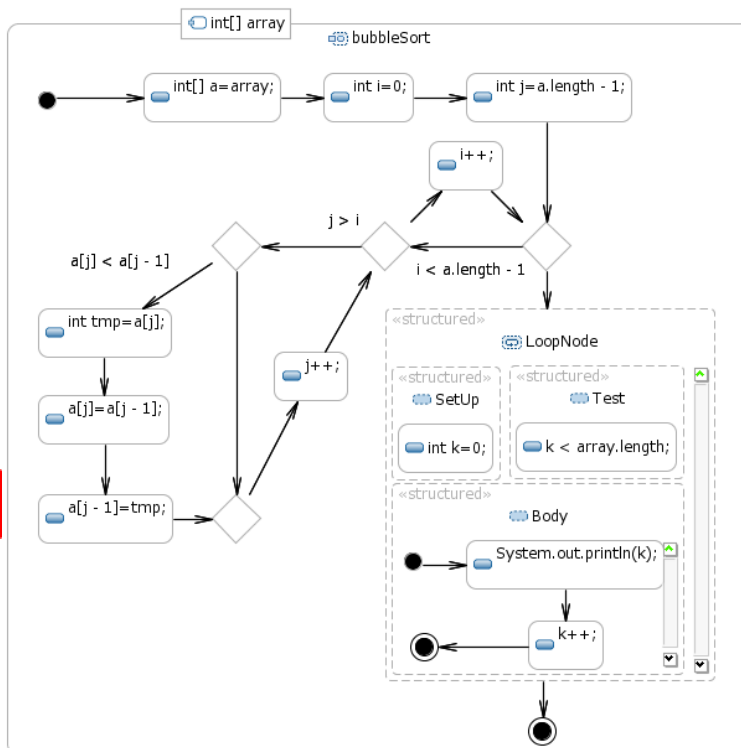


Figure 14. Added source code and activity diagram.



activity diagrams that can be handled by this approach are as follows. They consist of actions of the same granularity, and they do not include many multilayered group nodes.

Since activity diagrams cannot yet handle switch and try-catch statements, the definition of these description methods and increasing the number of convertible elements are important future work.

#### ACKNOWLEDGMENT

This work was supported in part by JSPS KAKENHI Grant Number 24560501.

#### REFERENCES

- [1] K. Matsumoto, R. Uenishi, and N. Mori, "A round-trip engineering method for activity diagrams and source code," Proc. of the Eleventh International Conference on Autonomic and Autonomous Systems (ICAS 2015), IARIA, May 2015, pp. 24-29, ISBN: 978-1-61208-405-3.
- [2] S. J. Mellor, K. Scott, A. Uhl, and D. Wiese, MDA Distilled: Principles of Model Driven Architecture, Addison Wesley Longman Publishing Co., Inc. Redwood City, CA, 2004.
- [3] S. Beydeda, M. Book, and V. Gruhn, Model-Driven Software Development, Springer Berlin Heidelberg, 2005.
- [4] M. J. Escalona and G. Aragón, "NDT: A model-driven approach for Web requirements," IEEE Transactions on Software Engineering, vol. 34, no. 3, 2008, pp. 377-390.
- [5] G. Casale, D. Ardagna, M. Artac, F. Barbier, E. Di Nitto, A. Henry, G. Iuhasz, C. Joubert, J. Merseguer, V. I. Munteanu, J. F. Pérez, D. Petcu, M. Rossi, C. Sheridan, I. Spais, D. Vladušić, "DICE: Quality-driven development of data-intensive cloud applications," Proc. of the Seventh International Workshop on Modeling in Software Engineering (MiSE 2015), May 2015, pp. 1-6.
- [6] A. Uhl, "Model-Driven development in the Enterprise," IEEE Software, January/February 2008, pp. 46-49.
- [7] R. F. Paige and D. Varró, "Lessons learned from building model-driven development tools," Software System Model, vol. 11, 2012, pp. 527-539.
- [8] N. Condori-Fernández, J. I. Panach, A. I. Baars, and T. Vos, Ó. Pastor, "An empirical approach for evaluating the usability of model-driven tools," Science of Computer Programming, vol. 78, no. 11, 2013, pp. 2245-2258.
- [9] K. Matsumoto, T. Maruo, M. Murakami and N. Mori, "A graphical development method for multiagent simulators," modeling, simulation and optimization - focus on applications, Shkelzen Cakaj, Eds., March 2010, pp. 147-157, INTECH, ISBN 978-953-307-055-1.
- [10] K. Matsumoto, T. Mizuno, and N. Mori, "A method of applying component-based software technologies to model driven development," Proc. of the Third International Conference on Intelligent Systems and Applications (INTELLI 2014) IARIA, June 2014, pp. 54-59, ISBN: 978-1-61208-352-0,
- [11] N. Medvidovic, A. Egyed, and D. S. Rosenblum, "Round-trip software engineering using UML: From architecture to design and back," Proc. of the 2nd Workshop on Object Oriented Reengineering, 1999, pp.1-8.
- [12] U. Aßmann, "Automatic roundtrip engineering," Electronic Notes in Theoretical Computer Science, vol. 82, 2003, pp. 33-41.
- [13] A. Henriksson and H. Larsson, "A definition of round-trip engineering," Technical Report, University of Linköping, Sweden, 2003.
- [14] M. Antkiewicz and K. Czarnecki, "Framework-specific modeling languages with round-trip engineering," in Model Driven Engineering Languages and Systems, Springer Berlin Heidelberg, 2006, pp. 692-706.
- [15] A. K. Bhattacharjee and R. K. Shyamasundar, "Activity diagrams: A formal framework to model business processes and code generation," Journal of Object Technology, vol. 8, no. 1, January-February 2009, pp. 189-220 .
- [16] Pakinam N. Boghdady, Nagwa L. Badr, Mohamed Hashem, and Mohamed F. Tolba, "A proposed test case generation technique based on activity diagrams," International Journal of Engineering & Technology IJET-IJENS vol. 11, no. 3, 2011, pp. 35-52.
- [17] XML metadata interchange. XMI: [Online]. Available from: <http://www.omg.org/spec/XMI/2015.11.24>.
- [18] I. Neamtiu, J. S. Foster, and M. Hicks, "Understanding source code evolution using abstract syntax tree matching," ACM SIGSOFT Software Engineering Notes, vol. 30, no. 4. ACM, 2005, pp. 1-5.
- [19] E. Gamma, R. Helm, R. Johson, and J. Vlissides, Design patterns: Elements of reusable object-oriented software, Addison-Wesley, 1995.
- [20] A. Cicchetti, D. D. Ruscio, R. Eramo, and A. Pierantonio, "Automating co-evolution in model-driven engineering," Proc. of the 12th International Enterprise Distributed Object Computing Conference (EDOC'08), IEEE, September 2008, pp. 222-231.
- [21] Roberto E. Lopez-Herrejon and Alexander Egyed, "C2mv2: Consistency and composition for managing variability in multi-view systems," Proc. of the 15th European Conference on Software Maintenance and Reengineering. IEEE, 2011. pp. 347-350.
- [22] Unified Modeling Language Lab. UML Lab: [Online]. Available from: <http://www.uml-lab.com/en/uml-lab/2015.11.24>.
- [23] U. A. Nickel, J. Niere, J. P. Wadsack, and A. Zündorf, "Roundtrip engineering with Fujaba," Proc. of the Second Workshop on Software-Reengineering (WSR), Bad Honnef, 2000, pp. 1-4.
- [24] L. Geiger and A. Zundorf, "Tool modeling with Fujaba," Electronic Notes in Theoretical Computer Science, vol. 148, 2006, pp. 173-186.
- [25] Acceleo: [Online]. Available from: <http://www.eclipse.org/acceleo/> 2015.11.24.
- [26] Eclipse: [Online]. Available from: <https://www.eclipse.org/home/index.php> 2015.11.24.
- [27] M. Benda, V. Jagannathan, and R. Dodhiawalla, "On Optimal Cooperation of Knowledge Sources," Technical Report, BCS-G 2010-28, Boeing AI Center, 1985.
- [28] K. Matsumoto, T. Ikimi, and N. Mori, "A switching Q-learning approach focusing on partial states," Proc. of the Seventh IFAC Conference on Manufacturing Modelling, Management, and Control, June 2013, pp. 982-986, Saint Petersburg, Russia.

## Considerations for Proposed Compatibility Levels for 9-150 kHz Harmonic Emissions Based on Conducted Measurements and Limits in the United States

Elizabeth A. Devore, Adam Birchfield, S. Mark Halpin

Department of Electrical and Computer Engineering

Auburn University, AL USA

ead0012@auburn.edu, abb0017@auburn.edu, halpism@auburn.edu

**Abstract**— A key enabling component of the Smart Grid is communications. Of particular interest is power line communications where very little additional infrastructure is needed to establish communication links. In the very vast majority of cases, smart meters will be located in the low voltage environment and therefore must be designed to operate properly in the presence of disturbance levels bounded by established compatibility levels. Without standardized limits for emissions in this frequency range, levels can and have reached the point where smart meter communication disturbances have been reported. The International Electrotechnical Commission's Technical Committee 77, Sub-Committee 77A, Working Group 8 is presently tasked with developing compatibility levels for disturbances in the frequency range 2-150 kHz. This range is particularly important given that numerous smart meter products are designed to communicate in this band. Communication failures, thought to be due to higher-frequency harmonics, have been reported in the literature and demonstrated in tests conducted in Europe. All of this information is being considered by Working Group 8 and is reflected in a proposed compatibility level curve for this higher frequency range. However, only limited (if any) work has been done in North America. In the United States, there are no defined compatibility levels for 2-150 kHz, but there are limits for voltage notches in IEEE Standard 519. In this paper, compatibility level curves proposed by European utilities and end-user equipment manufacturers are used to evaluate the results of initial product testing in the 120 V three-wire low-voltage environment commonly found in North America. Further consideration is given to the measurement, propagation, and summation of disturbances at higher frequencies based on a model developed for the line(s) between in-service equipment and the service point where smart meters are connected. The results of the analysis show that the total level of disturbance further exceeds the proposed CL curve when the tested equipment is in service and that measurements taken at the public supply terminals represent measurements taken at the service point.

**Keywords** – smart meters; power line communication; high-frequency harmonics; EMC standardization; commutation notches.

### I. INTRODUCTION

In this paper previous work on the possible impacts of high-frequency harmonic emissions on smart meter communications [1] is extended. Smart meters are typically connected directly at the low-voltage (LV) point of service for an end user. These meters make the traditional direct

measurements of voltages and currents and compute power and energy consumption for billing purposes. Of course, smart meters are also capable of characterizing the quantities measured such as harmonic content and voltage excursions. All of these evaluations/calculations are done locally at the meter point. When these meters and their enhanced capabilities are integrated into a coordinated communication and control system, the smart grid is born. Without data sharing and communications, there would be no smart grid. Therefore, disturbances in meter communications must be considered.

Smart meter communication approaches can be broadly divided into two categories: wired and wireless. Recognition and tolerance of the background environment and disturbances for wireless systems are covered by numerous applicable standards for wireless communications. Similar standards for wired systems exist for higher frequencies (generally above 150 kHz) and lower frequencies (generally below 2 or 3 kHz), but no consensus presently exists in the range 2-150 kHz [2]. This frequency range includes the bands used by most smart meter manufacturers for communications via the power line (PLC). Nonexistent compatibility levels (CLs) and limits in the 2-150 kHz range have resulted in smart meter development without regard to standardized background emission levels and problems are beginning to appear [3]. Other problems in addition to PLC failures have also been attributed to harmonics in this range [4]–[6]. All industry stakeholders have recognized the need for rapid standardization, and numerous activities across Europe have resulted in proposed standards. Concerns related to PLC systems are most often the main focus for wired systems [3], [7]–[9].

Working Group (WG) 8 of the International Electrotechnical Commission (IEC) Technical Committee (TC) 77, Sub-Committee (SC) 77A is specifically charged with reviewing and evaluating the results of these ongoing activities and developing consensus CLs in the 2-150 kHz frequency range [10]. This task is complicated by the fact that numerous end-use products produce emissions in this frequency range, usually due to the common use of various high switching frequency power converter designs required to meet energy efficiency requirements [7], [11]. These high-frequency emissions are produced by end-use equipment categories ranging from entertainment (e.g., televisions and displays) to lighting (compact fluorescent and LED ballasts and controls). Other sources of high-frequency emissions include voltage-source inverters used in motor drives and a

number of distributed generation sources that are or could be interfaced with the public network. Active infeed converters (AICs), normally using high switching frequencies, are used to integrate energy from these sources (e.g., solar panels, fuel cells, or wind turbines) to the power supply system to be made available for other consumers. Distributed energy sources use AICs to synchronize voltages and currents to the power system or to exchange electrical energy between energy storage devices (e.g., batteries) and the system or end-use equipment. AICs also provide the possibility of adjusting the fundamental and controllable harmonic components that feed into or are taken from the power line, which in effect generates high frequency distortion. It is possible for AICs to be used to mitigate pre-existing harmonics in the power system [12] if they are controlled as an active filter. All of these emissions combine in the LV network serving the end-user facility and the cumulative emission levels could reach values such that interference with smart meter communications occurs. Alternatively, these high-frequency emissions could essentially circulate between local-area direct-connected devices, resulting in very little impact on the supply system [13]–[15].

In the United States, the only standard that pertains to disturbances in the 2-150 kHz range is IEEE Standard 519-2014 [16]. According to Standard 519, a notch is the result of disturbances in the normal voltage waveform that lasts less than 0.5 cycles, and is initially of opposite polarity than the waveform. Therefore, the area of this notch is subtracted from the normal waveform. These notches are often caused by rectifiers and other nonlinear devices, resulting in higher order harmonics. In order to avoid issues related to these notches, a total allowable notch area for LV systems is set. IEEE Standard 519 only contributes to limits regarding a single disturbance source, while the goal of WG8 is to set maximum acceptable levels for the sum of all disturbances at the point of common coupling (PCC), located between the smart meter and the LV system. There are no standards in the United States that deal with the cumulative sum of disturbances from all high frequency disturbing sources.

In this paper, proposed CLs are compared to emission testing results for some 120 V products in common use in North America so that postulates can be developed regarding how multiple disturbance-producing products in the 9-150 kHz range might summate at the point of service where the smart meter is located. In order to obtain reliable information from smart meters, high frequency disturbances must be managed. Therefore, the aim of this work is to present disturbance measurements that must be considered for the design and operation of smart meters using PLC. For measurements, focus is given to the 9-150 kHz frequency range because it has been recommended that different effects and limiting factors may be present for the frequency ranges 2-9 kHz and 9-150 kHz [17]. Related works are disclosed in Section II. The set-up used for measuring emissions levels is explained in Section III. In Section IV, proposed CLs are introduced. Further, in Section V, limits based on maximum notch area and notch depth set in IEEE Standard 519 for voltage notches are used to consider individual disturbance sources with regard to the proposed CLs. In Section VI,

results of tests to assess high-frequency disturbance propagation in 120 V, three-wire LV systems are presented and compared to proposed CLs. In Section VII, a model for the line between the public supply terminals (where emissions were measured) and the PCC is considered in order to posit how the disturbances from multiple end-user pieces of equipment sum at each location. Finally, conclusions and future work are provided in Section VIII.

## II. RELATED WORKS

To date, all testing, research, and evaluation of high-frequency harmonic product emissions has been focused on products used in European LV networks. This may primarily be a result of the common use of PLC for smart meter communication in European countries [3]. Published results of the similarities and differences of multiple product tests investigating voltage emissions have not been found in these works. Instead, previous testing has been focused on specific equipment, namely lighting, such as touch dimmer lamps [4] and fluorescent lamps [13], or on current distortion of various appliances [19].

Further, none of these works provide a solution to the problem, rather the data is used to assist in creating standards.

Smart meter manufacturers stand to benefit from truly international specified standards that can be used on a global scale. In order to accomplish this, information on products and standards used in North American LV networks is required. The work presented in the following sections is intended to contribute to the European works and aid in the development and acceptance of international standards for high frequency harmonic disturbances for PLC.

## III. TEST AND MEASUREMENT APPROACH

All measurements were carried out on 120 V equipment and systems using a 100 MHz digitizing oscilloscope with built-in signal processing functions including Fourier analysis. Spectral analysis was also conducted off-line using digitized data transferred from the oscilloscope to a local computer. The tests were carried out using a 120 V supply taken directly from the local public network. Equipment was connected to the 120 V public supply source using a standard three-wire cable rated for continuous operation at 120 V, 15 A. Measurements are taken at two locations: (1) the supply terminals,  $M_1$ , and (2) the load equipment connection point,  $M_2$ . Voltage signals were the only quantities that were measured; current emissions were not considered in this work. The setup is shown in Figure 1.

As required by electrical codes in the United States, the public supply point is grounded at the point of service only. The equipment under test (EUT) is grounded by connection back to the single ground point at the service; this ground conductor is specifically required to be isolated from the normal current-carrying conductors. Because smart meters will communicate using the power conductors and not the ground, the emission levels produced at the EUT terminals and the supply voltage terminals are measured between the

two power conductors rather than from either conductor to the ground.

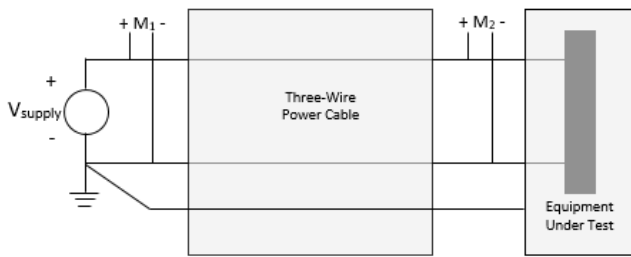


Figure 1. Test and Measurement Setup

Measurements are made at the points  $M_1$  and  $M_2$  as shown in Figure 1. The measured emission levels at  $M_2$  with and without the EUT in operation can be used to evaluate the emissions due solely to the operation of the EUT. The measured levels at  $M_1$  with and without the EUT in operation can be used to evaluate the propagation of emissions from the EUT to the supply point. Of course this propagation is a direct function of the frequency response of the power cable and the impedance of the supply system along with any other connected equipment [13]–[15]. While theoretical models can be developed for simple cases, this task can become difficult and inaccurate for realistically complex systems and is best assessed via direct measurement of input and output characteristics (e.g., at  $M_2$  and  $M_1$ ).

Typical emission levels in the range 9-150 kHz are on the order of a few millivolts (mV) and are commonly expressed in the unit “decibel-microvolt” ( $\text{dB}\mu\text{V}$ ) where  $20 \text{ dB}\mu\text{V} = 10 * 1 \mu\text{V} = 10 \mu\text{V}$ ,  $40 \text{ dB}\mu\text{V} = 100 * 1 \mu\text{V} = 100 \mu\text{V}$ , etc. A decibel (dB) is the logarithmic unit representing the ratio between two quantities, and  $\text{dB}\mu\text{V}$  represents the ratio between the measured voltage emissions and  $1 \mu\text{V}$ . Expressed in this common  $\text{dB}\mu\text{V}$  unit, typical emission levels in the frequency range of interest will be around 80-100  $\text{dB}\mu\text{V}$  (10-100 mV). Plotting the magnitude in  $\text{dB}\mu\text{V}$  allows possibly large variations in ratios to be plotted on a common scale. Of course, these emission levels will only be encountered at the specific frequencies at which they are produced; much lower levels, typically 40-60  $\text{dB}\mu\text{V}$ , will be present over the majority of the frequency range of interest. In order to resolve these small spectral components with sufficient accuracy using a typical oscilloscope/spectrum analyzer, it is necessary to remove the power frequency component from the measured signal before it is processed by the spectrum analyzer. This removal process requires an analog filter of band-stop or high-pass design to eliminate the power frequency signal or pass without attenuation the higher frequencies of interest, respectively.

A high-pass design was chosen for the measurements reported in this work and a custom design was conceived and implemented to avoid any over-dependence on commercial products. In addition, it is difficult to select any particular commercially-available product based on accuracy, performance, or other criteria because no standardized

interface coupling exists [18]. The analog filter design is shown schematically in Figure 2.

Because the filter is a custom design, it is necessary to validate the expected high-pass frequency characteristics and verify that the power frequency component, in this case at 60 Hz, will be sufficiently attenuated. The simulated frequency response characteristic of the filter is shown in Figure 3. It is clear from Figure 3 that the filter delivers a significant attenuation at the power frequency and corresponding low-frequency harmonics whereas the response is essentially flat with minimal attenuation in the frequency range of interest (9-150 kHz). The frequency response was further verified by measurement of the frequency response of the constructed filter. The result is shown in Figure 4 and verifies the essentially flat characteristic and minimal attenuation in the 9-150 kHz range.

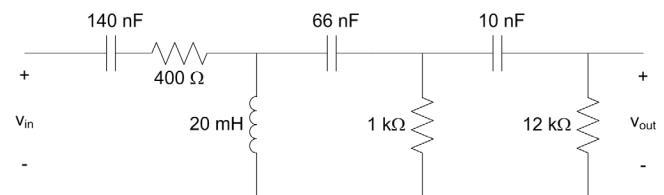


Figure 2. Filter Design and Parameters

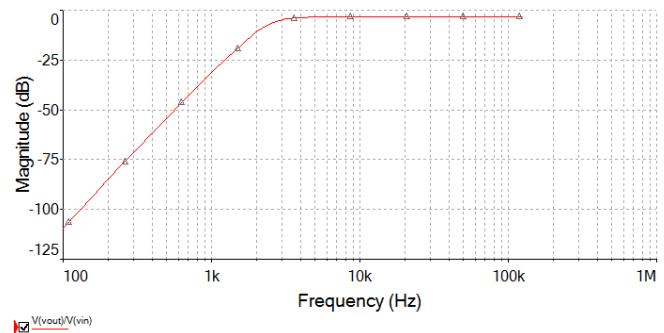


Figure 3. Simulated Frequency Response of Custom Filter

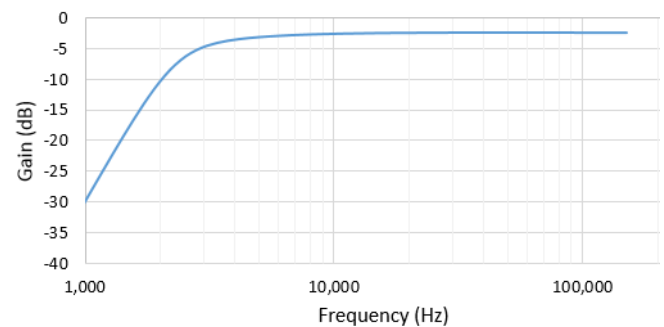


Figure 4. Measured Frequency Response of Custom Filter

IV. COMPATIBILITY LEVELS

A CL is the level of disturbance above which problems (e.g., communication interference) are expected to occur. Two CL curves have been proposed in Europe. One of the proposed CL curves made by European utilities is shown in Figure 5. Shown in the plot are the proposed maximum allowable peak levels in dBμV for the 3-150 kHz frequency range. The CL curve proposed by European manufacturers is given in Figure 6. The maximum allowable emissions are again given in dBμV, based on peak values, for the 9-150 kHz frequency range.

Considering both figures, the primary discrepancy between the proposed curves lies in the 9-50 kHz range. The communication issues cited by European utilities have played a major role in the development of CLs. As a result, the utilities' CL curve will be used as the primary reference for evaluation of the measurements discussed in this paper.

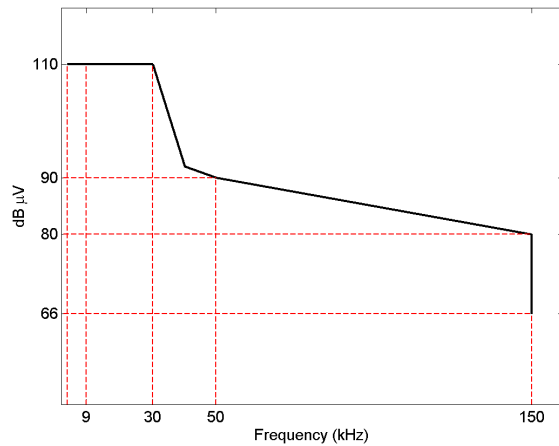


Figure 5. Utility Proposed Compatibility Levels

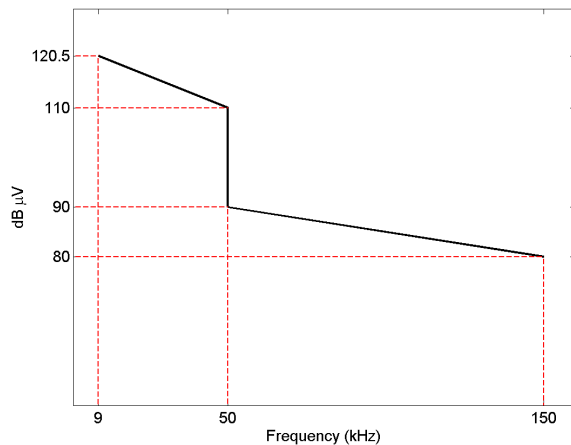


Figure 6. Manufacturer Proposed Compatibility Levels

V. COMMUTATION NOTCH LIMITS

In order to consider the CLs proposed in Europe, CLs based on established standards in North America should be considered if they exist. Unfortunately, only limits for specific disturbance sources exist in IEEE Standard 519 and these do not represent the total, maximum disturbance level that is defined by CLs. The ultimate objective, of course, is for the limits for individual disturbing sources to result in a total summated disturbance level, considering all disturbance sources, which does not exceed the maximum permissible total disturbance levels, which define the CLs.

The limits for commutation notches provided in IEEE Standard 519-2014 are shown in Table I and are based on the variables defined in Figure 7. Based on Figure 7,  $f(t)$  was written for a 50 Hz sinusoidal waveform, considering the general system notch area and depth from Table I. The notch area was normalized as a 1V system by dividing by 480V. In order to plot the magnitude,  $f(\omega)$ , for the frequency range 2-150 kHz, the Fourier series was calculated. Figure 8 is the plot of the results for the Fourier series and the European utility proposed CLs, both given in dBμV based on peak values. Both the CLs and the notch limits drop off as frequency increases. However, the IEEE limits are based solely on commutation notches, and are intended to be applied to a specific disturbance. The CL curve is representative of the maximum permissible value for the sum of all disturbances seen at the PCC.

TABLE I. RECOMMENDED LIMITS ON COMMUTATION NOTCHES[16]

	<i>Special applications</i> <sup>a</sup>	<i>General system</i>	<i>Dedicated system</i> <sup>b</sup>
Notch depth	10%	20%	50%
Notch area ( $A_N$ ) <sup>c,d</sup>	16400	22800	36500

- a. Special applications include hospitals and airports.
- b. A dedicated system exclusively supplies a specific user or user load.
- c. In volt-microseconds at rated voltage and current.
- d. The values for  $A_N$  have been developed for 480 V systems. It is necessary to multiply the values given by V/480 for application at all other voltages.

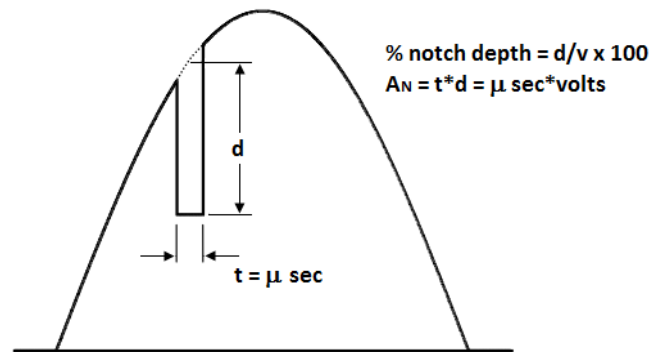


Figure 7. Definition of Notch Depth and Notch Area [16]

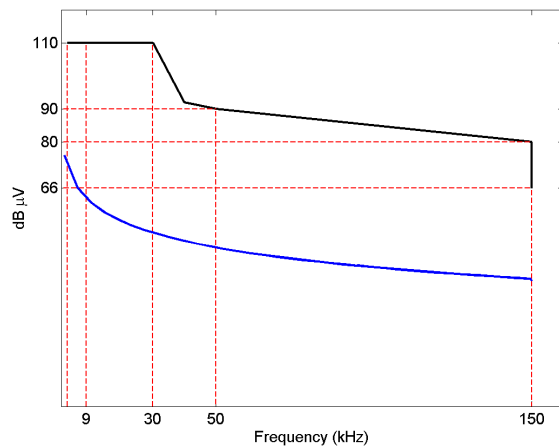


Figure 8. Utility Proposed CL vs. Commutation Notch Limits

## VI. MEASUREMENT RESULTS COMPARED TO PROPOSED COMPATIBILITY LEVELS

Measurements were conducted at  $M_1$  and  $M_2$  in Figure 1 using the high-pass filter of Figure 2, the digitizing oscilloscope, and off-line computer-based spectral analysis. Measurements were initially performed at  $M_1$  with no EUT operating in order to establish a baseline condition. To recognize and evaluate expected variations in background emission levels over time, the baseline evaluations were conducted over a 72 hr period including a normal workday, multiple nighttime periods, an end-of-week day, and a holiday. These results are shown in Figure 9, averaged over a period defined by a particular date and hour-of-day range as shown in the figure. The magnitude of the recorded measurements were RMS values, with units  $\text{dB}\mu\text{V}_{\text{RMS}}$ . In order to compare the proposed CLs on the same scale, the RMS values were converted to peak values by  $\text{dB}\mu\text{V}_{\text{peak}} = (1.414) * \text{dB}\mu\text{V}_{\text{RMS}}$ . The task of multiplying peak values by 1.414 was achieved by adding 3dB to the measurements.

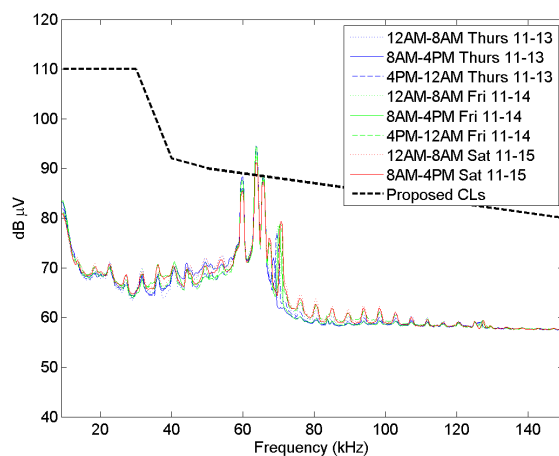


Figure 9. 72 hr Background Emission Levels

It is clear from Figure 9 that the variations in background emission levels are not overly significant. It is equally clear that there are significant background emissions in the frequency range 60-70 kHz that either exceed or nearly exceed the utility's proposed CL curve. The background emission levels in Figure 9 can be used during the emission assessment of various operating EUTs. These longer-time background levels are also useful for evaluating potential measurement errors; erroneous measurements would likely deviate significantly from the established background levels.

Two major categories of consumer products were tested in this work: lighting and televisions (displays). Measurements were taken on both ends of the supply cable impedance (approximately 30.5m long power cable as previously described) and with and without the EUT in operation. For the cases with the EUT disconnected, measurements were made both before and after the EUT connection and operation so that the reference levels immediately before and after each test could be known and, for validation purposes, compared to the longer-time results of Figure 9 as appropriate.

The results of two compact fluorescent lamp (CFL) tests are shown in Figure 10 (a) and (b). These results clearly show that one of the CFLs produces a noticeable emission around 120 kHz whereas the other tested lamp provides an attenuating effect around 80 kHz at the EUT terminals but not at the supply terminals. From these two tested lamps, it does not appear reasonable to make generalizations. However, comparing the test results to the proposed CL curve, it is clear that disturbance levels still exceed the proposed CL between 60-70 kHz. In this case, the 3-5  $\text{dB}\mu\text{V}$  increase in magnitude in the 60-70 kHz range represents the additive effects of end-user devices and is indicative of the emission level of the EUT.

The results of four LED lamp tests are shown in Figure 11 (a)-(d). These results show the effects of a general change with some increases and some decreases (a) and (d), an increasing change in background emissions (b), and the effects of a decreasing change in background emissions (c). For all the tested LED lamps, there does not appear to be a significant impact on emissions relative to the background levels at either the source or load terminals. Again, all of the tested LED lamps contribute to exceeding or nearly exceeding the proposed CL curve in the 60-70 kHz frequency range for each of the tests conducted. In tests (b) and (c), before the reference and after, respectively, have a lower emission level than measurements taken while the EUT was in service for the entire band of interest.

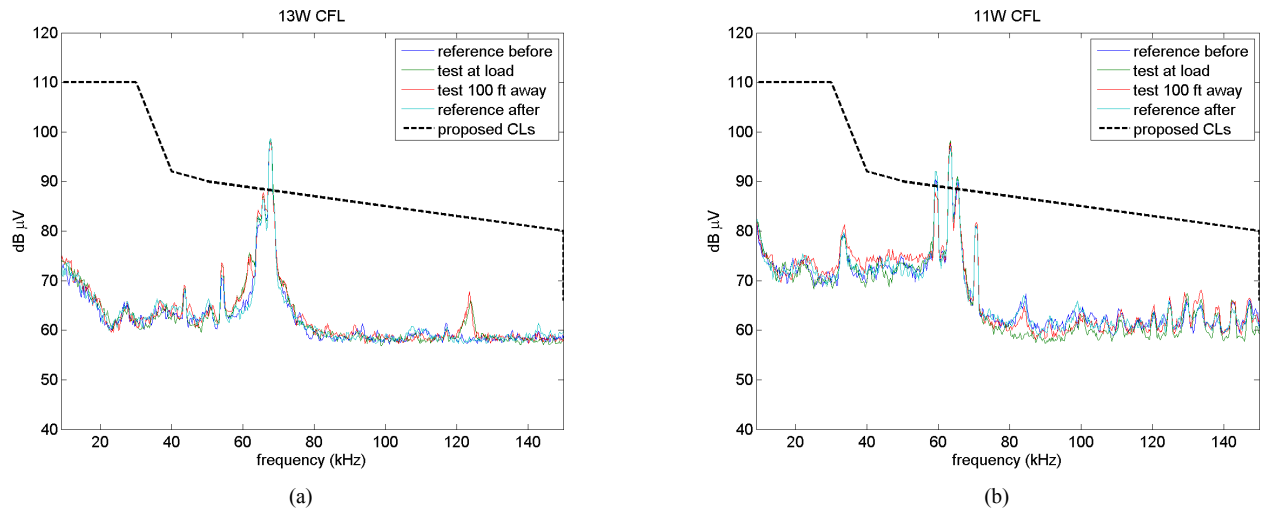


Figure 10. CFL Test Results vs. Utility Proposed CL

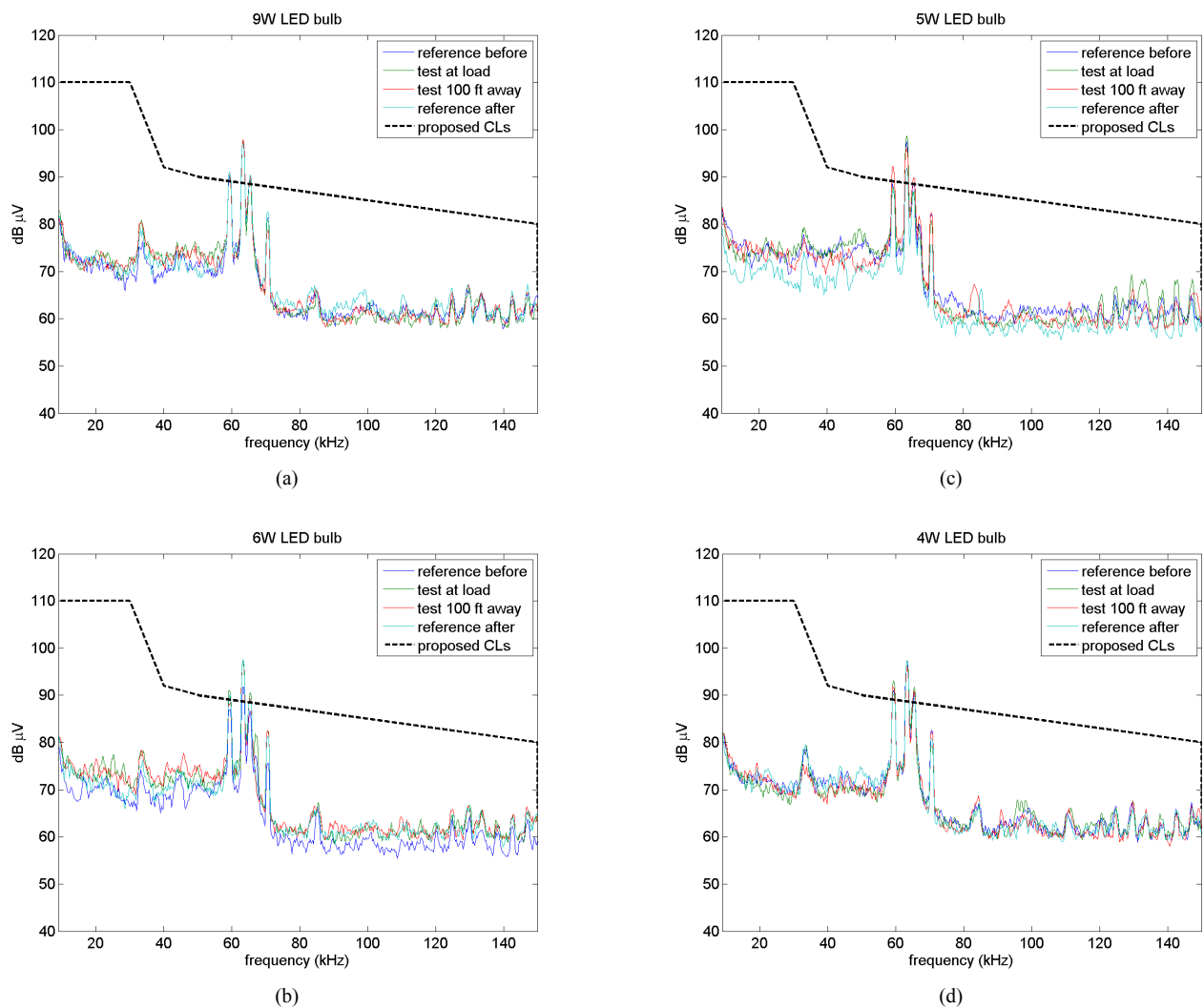


Figure 11. LED Test Results vs. Utility Proposed CL

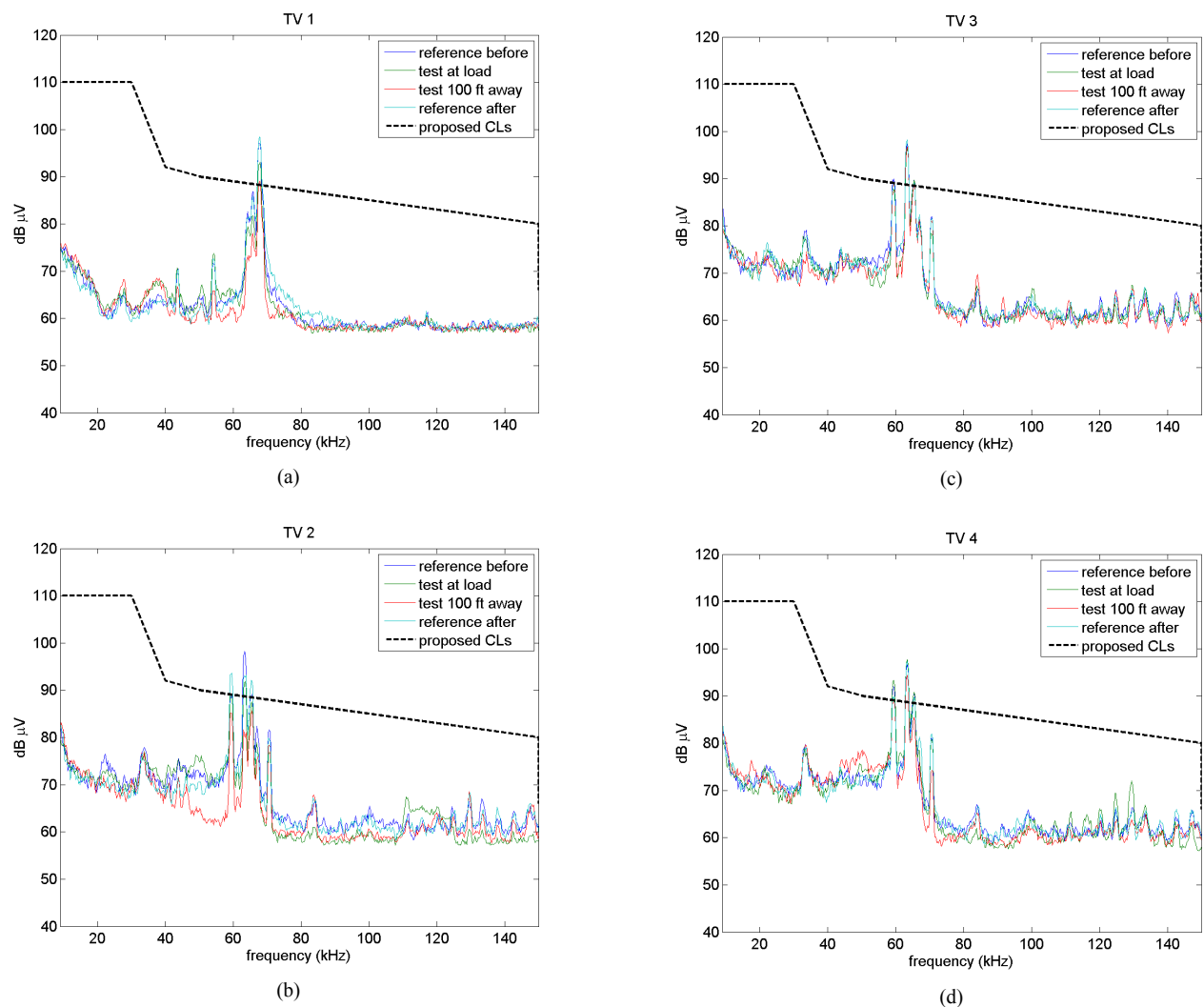


Figure 12. Television/Monitor Test Results vs. Utility Proposed CL

The results of four television/display tests are shown in Figure 12 (a)-(d). Tests (b) and (d) show some amplification and attenuation effects of the power cable, particularly around 40-60 kHz and 110-120 kHz (b), and 120-130 kHz (d). The other two tests do not appear to have any single dominant features but it is clear that the emission levels change with and without the EUT in operation in all cases. Again, all tests show that disturbance levels in the 60-70 kHz band exceed the utility proposed CL curve.

It should be clearly noted that the results shown in Figures 10-12 show the total emission levels with and without the EUT in service. While a comparison of the “with” and “without” results gives some indication of the emissions produced by a particular EUT, this type of general observation is not sufficient in many areas, particularly in standardization related to equipment emission limits and possibly installation-level emission limits. With regard to installation-level emission limits, such as those in IEC Standard 61000-3-6, it will be necessary to develop applicable summation laws that can be used as a first

approximation to separate individual emission contributions from a measured total emission level. Such a summation law could, for example, be used to identify (approximately) the emissions produced by the EUTs in Figures 10-12 from the total measured levels.

At this time, no summation law exists in the 2-150 kHz band and general comparisons with and without the EUT in service are the only things possible. However, the commutation notch limits shown in Figure 8, based on IEEE Standard 519, can be used to consider the maximum limits allowed for specific equipment. The allotted limits for individual equipment can then be used to define a summation law for this higher frequency range. None of this work can be completed until CLs for the 2-150 kHz range are defined.

Further, in order to measure total disturbances based on allotted established limits, it is necessary to develop testing and measurement specifications that are applicable to the general 2-150 kHz band similar to those which exist for products for frequencies below 2-3 kHz as specified in IEC Standards 61000-3-2 and 61000-3-12. The measurements

shown in Figures 9-12 were taken at the user supply terminals, not at the PCC. In order to establish proper measurement specifications at the PCC, the lines between the PCC and the user supply terminals (where these measurements were taken) must be characterized.

VII. LINE MODELING

In order for the values measured at the supply terminals to reflect the values measured at the PCC, it is necessary to multiply measured data at the public supply point by the transfer function of the line. The transfer function was determined by measuring a 50ft (approximately 15.24m), Romex 12-3 (12 gauge, 3 conductor) indoor non-metallic wire using an impedance analyzer. This wire was chosen because it is commonly used in the United States to wire residential indoor branch circuits for outlets, switches, and other loads.

The analyzer was set up so that a signal input and output were measured on opposite ends between two of the Romex wire conductors. The analyzer was set to measure  $V_{out}/V_{in}$  ( $V_2/V_1$ ) over the frequency range 2-150 kHz. The results are shown in Figure 13. In order to determine resonances that occur in the line, the measurements were conducted in the 2 kHz-20 MHz frequency range. Inspection of the measurements shows that resonance does not occur, and the gain is approximately 1V/V, in the 2-150 kHz range.

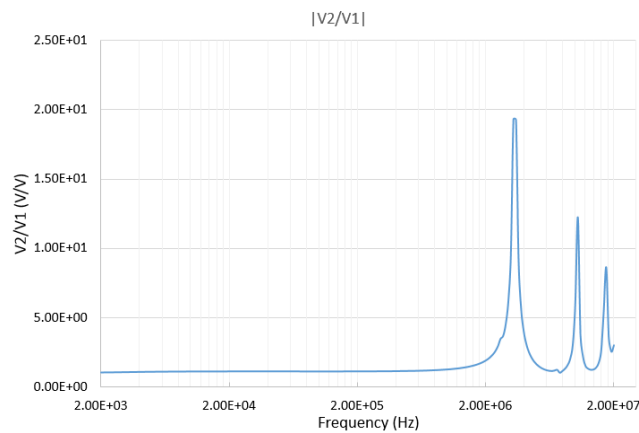


Figure 13. Measured Transfer Function for 12-3 Romex Wire

In order to verify these measurements, equivalent, per-meter, RLC parameters were calculated to determine the resonant frequency. The series dc conductor resistance  $R$ , series inductance  $L$ , and shunt capacitance  $C$  parameters were calculated using (1), (2), and (3) based on single line calculations [20]. According to [21], it is important to note that resonances at high frequencies cause issues. However, the length of the line is important when considering line modeling. The resonant frequency ( $f_0$ ) based on the calculated LC values (for the entire 15.24m line) is approximately 2.8 MHz. Recognizing the free space for conductors to move in the Romex wire, the measured

distance between conductors ( $D$ ) is not exact. Considering the measured transfer function in Figure 13, the calculated value for  $f_0$  is reasonable.

$$R_{dc} = \frac{\rho l}{A} \tag{1}$$

$$L = \frac{\mu}{2\pi} \ln \frac{D}{r'} \tag{2}$$

$$C = \frac{2\pi\epsilon}{\ln(\frac{D}{r'})} \tag{3}$$

Also, based on the calculations and measurements, it is reasonable to assert that for short lines such as those used in residential homes in the United States (for example, 100ft or 30.5m), a single, equivalent RLC circuit is sufficient for modeling the line between the supply terminals and the PCC. This assertion is based on the electrical wavelength,  $\lambda$ , for this line. The wavelength (4) is approximately  $1.5 \times 10^5 \text{m} - 2 \times 10^3 \text{m}$  from 2-150 kHz for velocity ( $v$ ) equal to the speed of light. Assuming an electrically short line is  $\lambda/4$ , wiring used in residential buildings can be assumed to be electrically short and modeled using a single RLC line model rather than a distributed parameter line model. This assumption is true even for velocity ( $v$ ) much less than the speed of light.

$$\lambda = \frac{v}{f} \tag{4}$$

It is clear from these results that the measurements taken at the public supply terminals represent measurements taken at the service point where any smart meter would likely be located. This is true because the characteristics of the line between the two points is essentially flat for the 2-150 kHz range of interest. As a result, development of standardized measuring techniques for high-frequency harmonics can be considered at the public supply terminals.

VIII. CONCLUSIONS

The emission levels for some consumer equipment typically used in North America were compared to proposed CLs for high-frequency emissions. The results of the analysis show that the total level of disturbance further exceeds the proposed CL curve when the tested equipment is in service. Although there are variations in the recommendations made by European manufacturers, the existing difference in proposed CLs in the 9-50 kHz range between the utilities and manufacturers is not significant because neither level is exceeded with or without the tested equipment in service. For both the manufacturer and utility proposed CL, disturbance levels with and without tested equipment in service exceed the limits in the 60-70 kHz range.

If either of the European proposed CL curves were to be adopted in the United States, filtering would be required in order to reduce the harmonic levels that surpass the defined CLs in the 60-70 kHz range. Specifically, filters added on

equipment or at the PCC can help reduce undesired harmonics to a value below the chosen CL curve. Although PLC is not (currently) the dominant communication technique used for smart meter communication in North America, it is still of interest for North America to follow future proposals made by the IEC and European utilities and manufacturers in order to prepare for alternative metering methods that may be used in the future. Further, the limits based on IEEE Standard 519 notch commutations is important to consider regarding a developed summation law for lower frequency harmonics once a CL curve is established. The summation law from IEC Standard 61000-3-6 should be evaluated for 2-150 kHz in order to determine if the same law may be applied to harmonics above the 50<sup>th</sup> order.

The evaluation of individual EUTs and the averaged day/time background disturbance levels measured confirm that individual products can add to background emission levels. Although, based on measurements and calculations performed, it is reasonable to assume that the measurements taken at the supply terminals are the same as measurements taken at the meter, further tests examining multiple products and additional measurements made at the PCC will be necessary for future consideration of CLs in the 9-150 kHz range.

#### ACKNOWLEDGMENT

The initial work for this project was conducted as a student project at Auburn University [1]. Mr. Birchfield is carrying out his graduate studies at The University of Illinois Urbana-Champaign.

#### REFERENCES

- [1] M. Arechaveleta, S.M. Halpin, A. Birchfield, W. Pittman, W.E. Griffin, and M. Mitchell, "Potential Impacts of 9-150 kHz Harmonic Emissions on Smart Grid Communications in the United States," 5<sup>th</sup> International Conference on Smart Grids, Green Communications, and IT Energy-Aware Technologies (Energy 2015), May 2015, pp. 59-64.
- [2] R. Burkart and J.W. Kolar, "Overview and Comparison of Grid Harmonics and Conducted EMI Standards for LV Converters Connected to the MV Distribution Grid," 1<sup>st</sup> Power Electronics South America Conference and Exhibition, September 2012.
- [3] P. Pakonen, S. Vehmasvaara, M. Pikkarainen, B.A. Siddiqui, and P. Verho, "Experiences on Narrowband Powerline Communication of Automated Meter Reading Systems in Finland," Electric Power Quality and Supply Reliability Conference (PQ), June 2012.
- [4] M. Pikkarainen, S. Vehmasvaara, B.A. Siddiqui, P. Pakonen, and P. Verho, "Interference of touch dimmer lamps due to PLC and other high frequency signals," Electric Power Quality and Supply Reliability Conference (PQ), June 2012.
- [5] G.A. Franklin, "A Practical Guide to Harmonic Frequency Interference Affecting High-Voltage Power-Line Carrier Coupling Systems," IEEE Transactions on Power Delivery, April 2009, pp. 630-641.
- [6] B. Gustavsen, "Study of Transformer Resonant Overvoltages Caused by Cable-Transformer High-Frequency Interaction," IEEE Transactions on Power Delivery, April 2010.
- [7] S.M. Bashi, A.U.M Al-Abulaziz, and N.F. Mailah, "Effects of High Power Electronics Converters on PLC Signals," Journal of Applied Sciences, January 2006, pp. 1888-1891.
- [8] S.K. Ronnberg, M.H.J. Bollen, and M. Wahlberg, "Interaction Between Narrowband Power-Line Communication and End-User Equipment," IEEE Transactions on Power Delivery, August 2011, pp. 2034-2039.
- [9] E. de Jaeger, H. Renner, and K. Stockman, "Special Report-Session 2: Power Quality and Electromagnetic Compatibility," 22<sup>nd</sup> International Conference on Electricity Distribution (CIRED), June 2013.
- [10] D. Heirman, "EMC Standards Activity," IEEE Electromagnetic Compatibility Magazine, January 2014.
- [11] J. Luszcz, "High Frequency Harmonics Emission of Modern Power Electronic AC-DC Converters," 8<sup>th</sup> International Conference on Compatibility and Power Electronics, June 2013, pp. 269-274.
- [12] IEC/TS 62578 Ed.2, "Power electronics systems and equipment - Operation conditions and characteristics of active infeed converter (AIC) applications including design recommendations for their emission values below 150 kHz," March 2014.
- [13] E.O.A Larsson, C.M. Lundmark, and M.H.J. Bollen, "Distortion of Fluorescent Lamps in the Frequency Range 2-150 kHz," 7<sup>th</sup> International Conference on Harmonics and the Quality of Power, September 2006.
- [14] S. Ronnberg, M. Wahlberg, M. Bollen, A. Larsson, and M. Lundmark, "Measurements of Interaction Between Equipment in the Frequency Range 9 to 95 kHz," 20<sup>th</sup> International Conference on Electricity Distribution (CIRED), June 2009.
- [15] D. Frey, J.L. Schanen, S. Quintana, M. Bollen, and C. Conrath, "Study of High Frequency Harmonics Propagation in Industrial Networks," 2012 International Symposium on Electromagnetic Compatibility, September 2012.
- [16] IEEE Std 519<sup>TM</sup>-2014, IEEE Recommended Practice and Requirements for Harmonic Control in Electric Power Systems.
- [17] A. Larsson, "High-frequency Distortion in Power Grids due to Electronic Equipment," Licentiate thesis, Dept. Applied Physics and Mech. Eng., Luleå Univ. of Tech., Luleå, Sweden, 2006.
- [18] M. Coenen and A. van Roermund, "Conducted Mains Test Method in 2-150 kHz Band," 2014 International Symposium on Electromagnetic Compatibility, September 2014, pp. 601-604.
- [19] B. Sudiarto, A.N. Widyanto, and H. Hirsch, "Current Distortion Characteristics of Some Home Appliances in Distorted Voltage Environment for Frequency Range of 2-150 KHz," International Conference on Renewable Energies and Power Quality (ICREPO'14), April 2014.
- [20] C.A. Gross, "Transmission Lines" in *Power System Analysis*, 2<sup>nd</sup> ed. New York: Wiley, 1986, pp. 100-114.
- [21] R. Langella, L. Nunges, F. Pilo, G. Pisano, G. Petretto, S. Scalfari, and A. Testa, "Preliminary Analysis of MV Cable Line Models for High Frequency Harmonic Penetration Studies," Power and Energy Society General Meeting, July 2011

## Evaluation of an Integrated Testbed Environment for the Web of Things

Mina Younan  
 Computer Science Department  
 Faculty of Computers and Information  
 Minia University  
 Minia, Egypt  
 E-mail: [mina.younan@mu.edu.eg](mailto:mina.younan@mu.edu.eg)

Sherif Khattab, Reem Bahgat  
 Computer Science Department  
 Faculty of Computers and Information  
 Cairo University  
 Giza, Egypt  
 E-mails: [{s.khattab, r.bahgat}@fci-cu.edu.eg](mailto:{s.khattab, r.bahgat}@fci-cu.edu.eg)

**Abstract** – Sensor networks research is still active due to the proliferation of devices equipped with sensors and actuators. Although simulators (e.g., Cooja) and Web sites (e.g., Thingspeak) allow building Internet of Things (IoT) and Web of Things (WoT) applications, they are not compatible with many testing purposes, especially for the WoT. Younan et al recently proposed a testbed architecture for the WoT. It augments IoT by Web applications and allows for generating datasets and using them offline and online. In this paper, we present an evaluation of the WoT testbed by empirically measuring the accuracy of the generated dataset and by qualitatively comparing the testbed to the state-of-the-art in WoT and IoT measurement platforms.

**Keywords** – *Internet of Things (IoT); Web of Things (WoT); Entities of Interest (EoIs); Testbed evaluation.*

### I. INTRODUCTION

Nowadays research in the area of Wireless Sensor Networks (WSN) sheds the light on the role of simulators and testbeds to enhance the research results [1]. This is gaining importance due to the increasing number of devices and things connected to the Internet, which is expected to reach the order of billions by 2020 [2][3] as soon as the Internet Protocol (IP) becomes the core standard in the fields of embedded devices. As a result, the number of human Internet users may well be less than the number of devices connected to it.

Research on the Internet of Things (IoT) focuses on the infrastructure needed for connecting things and devices to the Internet. IoT addresses the connectivity challenge by using IP and IPv6 for embedded devices (i.e., 6LoWPAN) [4]. IoT devices, sensors and actuators, allow the state of things (e.g., places and other devices) to be inferred [3][5]. In a sense, IoT devices convert things to Smart Things (SThs) and things' environments to smart spaces. Entities of Interest (EoIs), things, devices, resources, discovery, and addressing are main terms in the IoT [6].

On the other hand, the Web of Things (WoT) "virtualizes" the IoT infrastructure and focuses on the application layer needed for building useful applications over the IoT layer. Services, such as searching for SThs and EoIs, in addition to Web-based applications for controlling

and monitoring services in smart spaces using friendly user interfaces, are core power features in the WoT.

Muhammad et al. [7] summarize the differences between emulators, simulators, and physical testbeds. They conclude that physical testbeds provide more accurate results. For instance, MoteLab [5] is a testbed for WSNs. It addresses challenges related to sensors' deployment and the time consumed for building a WSN. It features a Web application to be accessed remotely. The need for WSN testbeds is highlighted by challenges and research topics, which shed light on a specific set of features to be embedded within the testbed and its tools [7][8].

However, there has been no general method for testing and benchmarking research in the WoT [1][7][8][9], especially for searching in the WoT. The problem of how to find SThs and EoIs with their dynamic states that change according to environment events [10][11] has sheer importance in drawing conclusions, deductions, and analysis in various fields. In the WoT search problem, not only datasets about sensor readings are needed, but integrating the readings with information and meta-data about the underlying infrastructure is needed as well.

In our previous work [1], a testbed architecture for the WoT is proposed, which achieves the integration between the sensors' readings and the underlying infrastructure. The testbed addresses the general needs of WoT testing and focuses on the Web search problem and its related issues, such as crawling (i.e., preparing WoT pages for crawling). The testbed can be used as a WoT application, which monitors real devices in real-time and can be used as a WoT simulator to do the same process on WoT datasets instead of devices. It aims at collecting datasets that contain information about things (i.e., properties and readings) formatted using multiple markup languages. The collected datasets are designed to help in testing in many problem domains [10][12].

In this paper, we present a detailed analysis of the testbed presented in [1] using a case study on crawling the WoT. Empirical evaluation of the WoT testbed is presented and its features are discussed in the light of other IoT and WoT testbeds in the literature. In particular, the accuracy of the dataset is measured and evaluated; this is important in order to make accurate decisions about the states of the

simulated EoIs specially that most of the EoIs' states depend on the synchronization of more than one STh reading. For completeness, the testbed architecture and its implementation are also described in this paper.

The remainder of the paper is organized as follows. In the next section, the related work regarding the creation of searchable IoT and WoT domains using IoT and WoT simulators and datasets is discussed. Discussion of IoT and WoT testbeds is presented in Section III. Section IV describes the testbed architecture of [1] and its implementation, followed by the evaluation of the dataset's time-accuracy in Section V. A case study is presented in Section VI. Finally, conclusions and important ideas for future work are presented in Section VII.

## II. RELATED WORK

In the light of the WoT challenges and dataset requirements discussed in [1], this section discusses the usage of sensor datasets in the literature. To summarize our observations, if the research is only interested in values measured by sensors or in states of EoIs (e.g., being online or offline), then the used dataset is based on the WoT level (dynamic information), whereas if the research is interested in the sensor network infrastructure, then the used dataset is based on the IoT level (static information). Because the SThs may be movable objects, i.e., their location may be changing frequently, and then the research may need an additional type of information, which is called quasi-dynamic information about SThs. In this case, such a property about SThs will be considered as a special type of their readings (dynamic information). An integrated dataset contains information about both sensor readings and network infrastructure, that is, it is based on both IoT and WoT levels.

Several studies [7][8][9][13] discuss and compare between existing simulators and testbeds using general criteria, such as the number of nodes, heterogeneity of hardware, and mobility, but none of them discusses WoT features, such as STh's logical path, supported formats in which EoIs' states are presented, and accuracy of the datasets generated by the testbeds. In the next section, we present a comparison of testbeds and measurement platforms that combines both IoT and WoT features.

### A. IoT Simulation

There is no general way for simulating IoT [7][9][13]. Moreover, there are situations in which simulators and real datasets containing raw information (e.g., sensor readings [14]) or information about the IoT layer are not enough for modeling an environment under testing, as the datasets miss the sense of one or more of the challenges mentioned earlier and thus, miss the main factors for accurate WoT evaluation. Also, many datasets are not actually related to the problem under investigation, but were generated for testing and evaluating different algorithms or methods in other researches. For instance, an evaluation of WSNs'

simulators according to a different set of criteria, such as the Graphical User Interface (GUI) support, the simulator platform, and the available models and protocols, concludes that there is no general way for simulating WSNs, and hence IoT and WoT [9][13]. None of these criteria address the previous challenges. So, it is desirable to embed the unique IoT and WoT challenges within the datasets and to make simulators support as much of these challenges.

**WSN Simulators.** Several studies [7][9][13] summarize the differences between existing simulators according to a set of criteria. The Cooja simulator gives users the ability to simulate WSNs easily using a supported GUI [9][13] and different types of sensors (motes) for different sensor targets. Sensor applications are written in the nesC [15] language after being built in the TinyOS [16] (e.g., the RESTful client server application [17]). However, there are limitations and difficulties for testing the extensible discovery service [12] and sensor similarity search [18] in Cooja, because there is no information about the network infrastructure and entities. In particular, static information about sensors is written in different formats, and schematics information of the buildings and locations of sensors can be presented.

**WSN Physical Testbeds.** Physical testbeds produce accurate research results [7]. Different testbeds are found in this field due to different technologies and network scales. MoteLab [5] supports two ways for accessing the WSNs, (1) by retrieving stored information from a database server (i.e., offline) and (2) by direct access to the physical nodes deployed in the environment under test (i.e., online). However, the WoT challenges mentioned previously are not fully supported in MoteLab. User accessibility in MoteLab is similar to what is done in the testbed proposed in [1].

SmartCampus [19] tackles gaps of experimentation realism, supporting heterogeneity (devices), and user involvement [8] in IoT testbeds. CookiLab [20] gives users (researchers) the ability to access real sensors deployed in Harvard University. However, it does not support logical paths as a property for sensor nodes and entities (WoT features).

Nam et al. [21] present an Arduino [22] based smart gateway architecture for building IoT, which is similar to the architecture of the testbed environment proposed in [1] (e.g., periodic sensor reporting). They build an application that discovers all connected Arduinos and lists the devices connected on each Arduino. However, the framework does not cover all scenarios that WoT needs, especially for searching. For example, information of logical paths and properties of entities and information of the devices that the components simulate or measure are missing.

At Intel Berkeley research lab [14], 54 sensors were deployed, and sensor readings were recorded in the form of plain text. The dataset includes information about the sender, the receiver, probability of successful sending (i.e., some sensor readings were missed) and a quasi-dynamic

information about sensors (coordinates). However, the time accuracy of the dataset was not measured.

### B. WoT Simulation

Using websites (e.g., [23][24][25]), a WoT environment can be built online by attaching STHs like Arduinos [22]. These websites monitor the states of devices and provide RESTful services (GET, PUT, UPDATE, DELETE) [26] for uploading and accessing reading feeds. Moreover, the values (sensor readings) are visualized for users. The services of the aforementioned websites are similar to services of the testbed environment in [1]. However, these websites are limited by available service usage and formats of the responses, which are hardcoded and embedded within the website code or at least not exposed to users. The testbed architecture in [1], which is built specially for testing WoT, provides more general services, such as monitoring live information fed from attached STHs, visualizing sensor readings and states of EoIs over time, controlling actuators, triggering action events, and periodic sensor reporting.

### C. Service Architecture for WoT

Web services are considered as the main method for accessing WoT devices [27]. Mayer et al. [28] propose a hierarchical infrastructure for building WoT to enhance the performance of the searching service. The searching scenario starts by getting a list of sensors that can answer a query according to their static properties and predicted values. Then, the identified sensors are queried to check their current values, which are used for ranking the search results. The searching scenario is integrated into the proposed testbed.

Mayer and Guinard [12] and Mayer [29] implement an algorithm, called extensible discovery service [12], for solving the problem of using multiple formats (e.g., Microformats and Microdata) in the WoT. They implement their algorithms as a Web application that asks the users about a sensor page URL and retrieves information about devices if and only if the page is written in one of a set of pre-defined formats. However, their work does not result in a dataset. The proposed testbed in [1] allows such an algorithm to be tested to measure its performance. The required dataset contains sensor information written in different formats so that the algorithm is tested in parsing and retrieving information about sensors and entities.

The present paper substantially extends the work presented in [1] by discussing WoT testbed features in the light of other IoT and WoT testbeds in the literature, considering testbed evaluation by measuring the dataset time accuracy, and presenting a case study for crawling the WoT.

To summarize, up to our knowledge, none of the previously proposed testbeds fulfills the full requirements for testing and evaluating the Web search process in the WoT. The proposed testbed environment in [1] aimed at

filling this gap. It is not the main focus of the testbed to be yet another WSN testbed but to integrate WoT and IoT features for virtualizing things and entities, retrofitting on the benefits of existing physical testbeds [1]. Making decisions about EoIs' states depends on more than one sensor reading, so evaluation of datasets generated by the testbed focuses on the time accuracy (synchronization time) and dataset integrity, as will be indicated in details in Section V.

## III. COMPARISON OF STATE-OF-THE-ART IOT AND WOT TESTBEDS

From WSN to the IoT, and then moving forward to the WoT, one purpose is sought for, that is monitoring and controlling the surrounding environment. All of these platforms have the same network infrastructure, but data manipulation (accessing and representing sensory data) differs from one platform to another according to the user interests. WSN testbeds aim at improving algorithms and solutions for resource constrained devices, while IoT testbeds aim at integrating these devices (STHs) into globally interconnected networks [8]. The main goal of the WoT testbeds, including the integrated WoT testbed [1], is to improve the usability of the information produced by the IoT and to provide more services that raise this usability by increasing the primary beneficiaries of the WoT technologies. The information generated from the testbeds can be widely used in different industries if and only if people and machines can understand this information.

Different criteria have been set for WSN and IoT testbed assessment and evaluation [7][8][13]. Because WoT is the application layer on top of IoT that presents sensory data in an abstract form using available web tools and services, most of the future requirements described in [8] are important to be hosted in WoT testbeds. Federation is one of the most important factors that have to be met in WoT testbeds, whereby WoT testbeds host more than one WoT system for evaluating many services such as a searching service. Another requirement is heterogeneity of connected devices and formats that are embedded in web pages to represent STHs. Heterogeneity of data formats means that WoT systems hosted in a single testbed can use different pages with different formats. Semantic technologies in testbeds enhance the scale and heterogeneity requirements.

Different studies have defined different criteria sets for comparing testbeds in WSN and IoT [7][8][9]. In the light of those studies, the proposed testbed should cover most of existing IoT testbeds' features in addition to other WoT requirements, such as accessing data through RESTful services, getting high-level states instead of raw sensory data, and searching in real-time for STHs and EoIs.

The comparison of testbeds in this section is divided into two main categories according to the testbed architecture: (1) infrastructure layer and (2) software layer, where testing and evaluation services are done.

### A. Elements of the infrastructure layer

Elements of this layer concerning the IoT environment are as follows:

1) *the number of nodes and possibility of discovering new nodes (scalability)*: the number of nodes in WSN testbeds should be more than 10, but in IoT it should be more than 1000. Because WoT is a layer above the IoT, as it was mentioned previously, then the SThs number should be sufficiently large. WoT testbed could be accessed offline and online. So, deploying additional SThs can be done manually by registering the STh's in online mode using simple GUI, or dynamically when the gateways receive acknowledgement messages from the SThs. In addition to the GUI that testbed supports for giving users the ability to add additional devices online like Thingspeak and Xively,

sharing datasets that simulate physical components (accessing WoT testbed in offline mode) gives users the ability to virtually increase the deployed number of SThs.

2) *the environment properties*: environment properties relate to a certain physical phenomenon (e.g., temperature, light, and humidity). The WoT testbed supports virtual environment in offline mode, whereby real-time information was generated from real SThs and stored in dataset files.

3) *availability and portability*: this element means the ability to deploy and re-deploy the testbed in different places. The WoT testbed is a physical testbed as well as a simulator, whereby it can be used for monitoring one place or environment (online or offline). Monitoring other places needs node preparation, using the same software for configuring, discovering devices, and collecting data from them.

TABLE I. A COMPARISON BETWEEN WSN/IOT TESTBEDS AND SIMULATORS AND THE WOT TESTBED PROPOSED IN [1].

Criteria		Current WSN/IoT/WoT Testbeds and Simulators		Integrated WoT Testbed [1]
Scalability	Number of deployed nodes	Simulators	Testbeds	<ul style="list-style-type: none"> <li>▪ Prototype is done over 30 sensor nodes.</li> <li>▪ For enhancing scalability, testbed supports:               <ul style="list-style-type: none"> <li>○ GUI for registering additional SThs</li> <li>○ Sharing datasets</li> </ul> </li> </ul>
		Possibility to discover new nodes	Manually.	
Environment		Produce randomly-modeled information (e.g., Cooja [17])	Physical testbeds produce real information (e.g., MoteLab [5]).	<ul style="list-style-type: none"> <li>▪ Physical environment in online mode.</li> <li>▪ Virtual environment in offline mode</li> </ul>
Availability/Portability		By sharing saved simulation projects.	Difficult to move from one place to another	It is a physical testbed and simulator in one (online or offline).
Hardware/Software heterogeneity		E.g., Cooja [17] <ul style="list-style-type: none"> <li>▪ Add different types of motes in the same experiment</li> <li>▪ All motes write their information in the same format.</li> </ul>	E.g., MoteLab [5]	<ul style="list-style-type: none"> <li>▪ Different SThs' types.</li> <li>▪ Different formats (i.e., different WoT environments are deployed in one testbed)</li> </ul>
Repeatability/Reproducibility		Save projects	Users have to build new applications to work on these datasets generated from physical testbeds	<ul style="list-style-type: none"> <li>▪ Run in offline mode on the generated datasets.</li> <li>▪ No need to build new applications to work on the datasets.</li> </ul>
Real-time Information		Random information	Real-time information	<ul style="list-style-type: none"> <li>▪ Real-time information</li> <li>▪ Datasets (historical data) are written in multiple formats.</li> </ul>
WoT	Dataset sharing	share saved projects (e.g., Cooja [17])	share results and evaluation measurements through web applications (e.g., MoteLab [5])	<ul style="list-style-type: none"> <li>▪ Output of the testbed is simple to be manipulated with other testbeds.</li> <li>▪ It supports RESTful services to publish data directly in a simple way.</li> </ul>
	User involvement	<ul style="list-style-type: none"> <li>▪ Users intervene deeply</li> <li>▪ Environmental conditions are absent (Thingspeak [24] and Xively [23] achieve this target but in limited formats).</li> </ul>	<ul style="list-style-type: none"> <li>▪ Working interactively through a web application or published APIs</li> <li>▪ Scheduling 'batch' tasks to be executed on the testbeds (e.g., MoteLab [5]).</li> </ul>	Users can: <ul style="list-style-type: none"> <li>▪ deploy nodes manually or automatically</li> <li>▪ generate datasets by selecting criteria or rules on the DsC application.</li> </ul>
	SThs attributes	<ul style="list-style-type: none"> <li>▪ Static attributes are like serial and model numbers and brand.</li> <li>▪ Dynamic attributes are like the physical location (longitude and latitude).</li> </ul>		Support logical path as a main SThs attribute.
	SThs Formats	Most of them support a single format.		Generate different types of SThs formats (Microdata, Microformats, and RDF).

4) *the hardware heterogeneity*: the ability to include different types of sensors. The WoT testbed supports different types of devices in different formats.

*B. Elements of the software layer:*

Elements of this layer concerning the WoT environment are as follows:

- 1) *software heterogeneity*: the ability to run the testbed on multiple operating systems and to support multiple formats for SThs data and definitions.
- 2) *re-usability (repeatability and reproducibility)*: the ability to save an experiment to rerun it later.
- 3) *real-time information*: measures if the testbeds produce imitative information (as in simulators) or real information in the real-time (as in physical testbeds).
- 4) *WoT features*: WoT features include data sharing, user involvement, GUI, RESTful APIs, STh’s attributes and formats. These features identify the tasks that the users can do on testbeds, the possibility to support data visualization (high-level knowledge), and the possibility to share datasets. In the WoT testbed, users can deploy nodes manually (configuring SThs and EoIs using a GUI) or automatically when SThs receive acknowledgement messages, they also generate datasets by selecting criteria or rules on the DsC application. On the other hand, Users intervene deeply in simulators, whereby they build networks and create sensor nodes or channels, but environment conditions in simulators are absent. Xively [23] and Thingspeak [24] achieve this target but support less accessibility for resources in limited formats. When users work on physical testbeds, they have two choices: (1) working interactively on the

physical testbed, which monitors and controls a certain environment, through a web application or published APIs or (2) scheduling ‘batch’ tasks to be executed on the testbeds (e.g., MoteLab [5]).

From Table I, we argue that WoT research needs a special type of testbeds, of which is the integrated WoT testbed [1], to support absent WoT features needed to leverage existing testbeds to the WoT level.

IV. THE INTEGRATED WOT TESTBED

The proposed testbed architecture in [1] transforms the physical control of devices in a surrounding physical environment to an emulated control for those devices keeping the same sense of events and features that existed in the physical environment. These events and features are embedded in datasets that can be later replayed. The proposed architecture has two modes of operation: online and offline (Figure 2). In online mode, datasets are generated, “real” physical information is recorded, and a Web application offers WoT services by accessing the real devices for monitoring and controlling them. In offline mode, the Web application accesses the datasets to replay the events monitoring information.

A. Testbed Architecture

The testbed architecture, shown in Figure 1 (b), is divided into five parts, as follows.

**An IoT infrastructure** (e.g., modeling a smart home) is shown in step 1 Figure 1 (b). To build the IoT [31], the steps are briefly as follows. First, things are converted to SThs by attaching smart equipment (e.g., sensors and actuators), as shown in Figure 1 (a). Second, the static and dynamic information of SThs is described. SThs representation

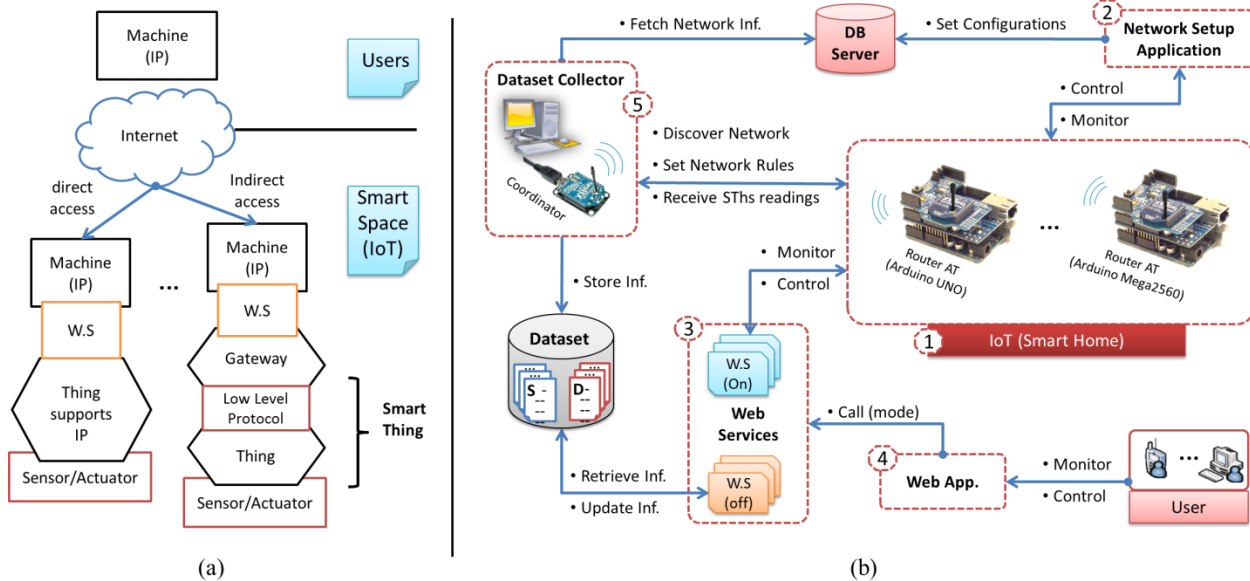


Figure 1. Testbed Architecture: (a) Integrating smart things (SThs) in the IoT - (b) Testbed environment architecture for simulating a physical environment .

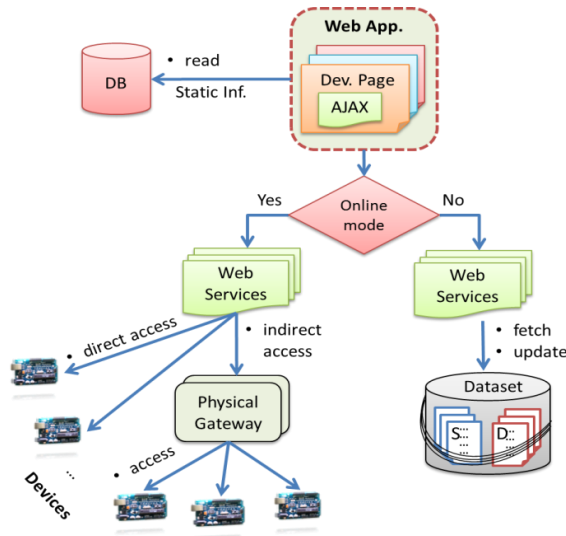


Figure 2. Testbed operation modes: Web services fetch data from real devices and gateways (online mode), or from dataset files (offline mode).

specifies URLs to invoke STHs services and their parameters and response format [29]. Third, RESTful APIs for accessing the STHs are built. Fourth, communication protocols between STHs and gateways are developed. Fifth, the STHs are connected to the Internet using physical and virtual gateways. STHs integration is done in the form of (1) direct integration, for STHs that support IP address for connection or (2) indirect integration using gateways, for STHs that use low-level protocols [32][33].

**Network setup application** (step 2 in Figure 1 (b)), after building IoT, a program is built for configuring the IoT network. It assigns locations to STHs in the hierarchical structure of the simulated building or environment shown in Figure 3. This allows for using the generated logical path as attributes for the STH.

**Web services for each device** (step 3 in Figure 1 (b)) are used for executing WoT services directly and for feeding back users with information about STHs, such as indicated in Figure 1 (a). The web services are hosted on machines that support IP connection, either the STH itself or a physical gateway for accessing STHs that use low-level protocols.

A **Web application** (step 4 in Figure 1 (b)) offers WoT services like monitoring and controlling. The application loads information by calling web services, which pull information from devices (online mode) or from WoT dataset files (offline mode), as shown in Figure 2.

The **dataset collector (DsC)**, the last component in the testbed architecture (step 5 in Figure 1 (b)), works as shown in Figure 4 (b), it discovers all available gateways and list of devices (SThs) connected on each one, sets rules by which data are collected from them, and sets the format by which the datasets are generated. As shown in Figure 4 (a), each discovered gateway waits for a discovery request from the

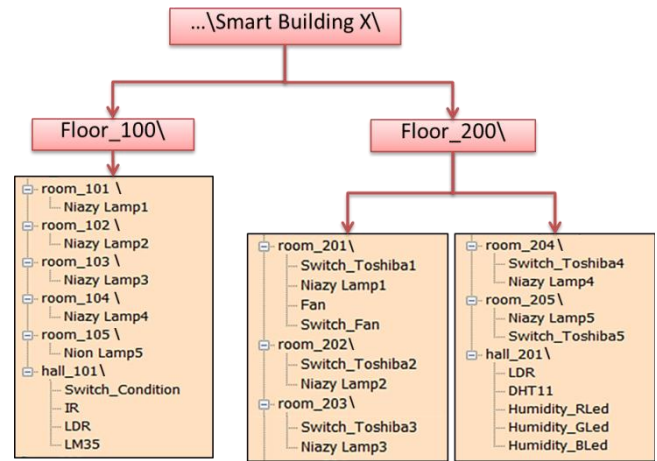


Figure 3. WoT graph for locating devices at specific paths in the hierarchical structure of a building.

DsC and replies with a message that contains its identification information in the form *id\_name-type* (e.g., 2\_Arduino-Mega2560). A gateway also sends an acknowledgement message (Ack) to inform the DsC that it has set all required rules successfully. Finally, a gateway sends a message that contains all required information about STHs' states as specified in the rules sent by the DsC.

**B. Testbed Implementation**

According to the testbed architecture presented in the previous section, the testbed implementation was done along four axis [1]; building IoT infrastructure and implementing network setup application were done in the first axis, building WoT application and related web services were done in the second axis, DsC was implemented in the third axis, and finally the dataset files

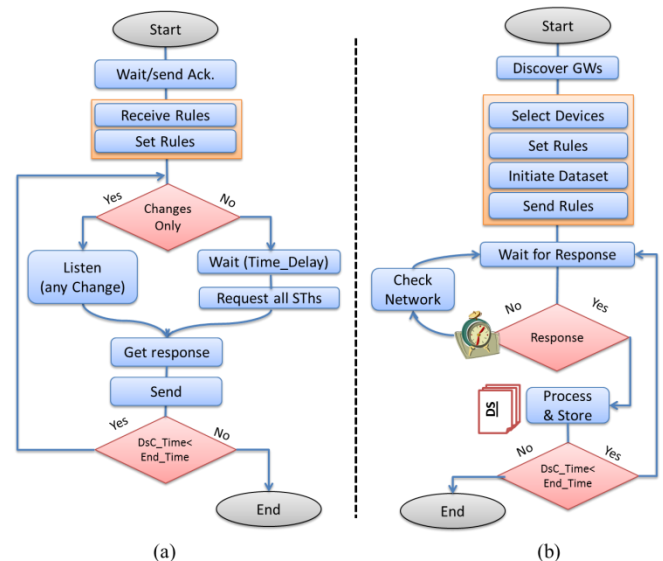


Figure 4. Time accuracy for a dataset generated by the integrated WoT testbed using rule *EstimatedTime\_All\_Network* (pull).



Figure 5. Locating and configuring a fan device at logical path 'floor\_100/room\_102.'

were generated.

### 1) Building the IoT infrastructure

This step will be executed the first time around; but, if a dataset that is generated by this testbed exists, then building WoT begins from the next step by attaching the dataset with the web application to work in offline mode. Building the IoT infrastructure was done in a simple way [27][34] using widely-available components. The SECE server [21] gets information from the IoT according to events and actions that happen in the environment. It offers the collected information in a friendly user interface. A testbed environment for the WoT is built using these connections.

Building the IoT infrastructure [31][35] was done in five steps, as mentioned above. Connecting devices and entities to the internet is done after converting them to STHs and EoIs, the network setup application is used for configuring the STHs and EoIs, where each STH and EoI has a unique URL following the hierarchical structure shown in Figure 3. Whereas it is desirable to build IoT using devices that support direct IP connection rather than devices that support only low-level protocols, the latter devices needed gateways for integrating them into the IoT. The IoT infrastructure was built using Arduinos, on which sensors and actuators were connected. Arduino has two interfaces: a Serial Peripheral Interface (SPI) bus and an Internal Integrated Circuit (I2C), which allows modules, like Ethernet and Secure Digital (SD) cards, to communicate with the microcontroller [35]. The Arduinos connected more than one device using digital and analog pins. In a sense, the Arduinos acted as physical gateways and IP addresses were set for them. They were attached to the network using Ethernet or XBee [34][36] [37] connections. Digi's Configuration and Test Utility Software (Digi's X-CTU) [38] was used to interface with radio's firmware of connected XBee modules.

Table II lists the components that were used for building a simple instance of the testbed. A large number of components, which could be connected on Arduinos are

available and have different purposes. They could be used for building more complex testbed instances with different targets.

**Network setup application** was written in C# for locating, managing and configuring resources for each virtual gateway. A virtual gateway represents a location, such as floor\_100 and floor\_200. For example, Figure 5 shows the process of adding a new device to the testbed using the application. Logical paths in the building hierarchical structure are very important for accessing devices

TABLE II. SET OF COMPONENTS (SENSORS, ACTUATORS, AND GATEWAYS) USED FOR BUILDING AN INSTANCE OF THE PROPOSED WoT TESTBED.

Component	Description
Arduinos(2)	Microcontrollers of type UNO & Mega-2560
ENC28J60 (2)	Arduino Ethernet module for accessing Arduinos through the internet (New versions of Arduinos support Ethernet connection using an Ethernet Shield).
Zigbee modules (3)	Type (XBee series 2) – network connections (Zigbee protocol is used for wireless network connections)
Zigbee Usb-Shield	For connecting Zigbee module with computer - acts as a base station (Coordinator)
Zigbee Arduino Shield (2)	Connecting Zigbee modules to Arduinos
LM35	Temperature Sensor
DHT11	Temperature and Humidity Sensor
LEDs (10)	Light actuators (Red, White, Green)
LDR (2)	Photo Cell/Photo Diode for light detection
IR & TV remote	Remote control circuit
Fan	Small Fan (operates at 3-5 V)
Switches (10)	Tactile push switches
Resistors	For LDR, LED, etc. 150Ω : 10KΩ
Bread Boards (2) & Jumper wire packs	Connecting Arduinos and components

The **protocols**, written in Arduino Sketches [22], were used to get and set the state of devices that are connected to the Arduinos, whereby get and set requests were sent within the body of the protocol messages. When the special symbol '#' is found within the body of the message, as shown in Figure 6, the spider gets the current device's states. The crawling case involved only getting information, not controlling or changing device states.

### 2) From IoT to WoT

Building Web pages in the testbed followed standard features for dealing with dynamic information. The common way for developing dynamic websites depends on AJAX. AJAX is used for live update of some parts in the sensor's pages. The dynamic parts typically include STHs readings or entity states, which indirectly depend on sensor readings [23][24].

However, pages with dynamic content built using AJAX cannot be crawled by traditional search engine crawlers.

```

void loop()
{ ...
  else if(strcmp(buffer,"GET# ") == 0)
    send_sr_get(client);
  else if(strcmp(buffer,"POST# ") == 0)
    send_sr_post(client);
  ...
}
void send_sr_get (EthernetClient client)
{
  // send a standard http response header
  client.println("HTTP/1.1 200 OK");
  client.println("Content-Type: text/html");
  client.print("Value of ");
  client.print(default_Dpin);
  client.print(" is ");
  client.print(digitalRead(default_Dpin));
  ...
}

```

Figure 6. Device network protocol for handling incoming requests of monitoring, controlling, and crawling services (RESTful service).

Some search engines, such as Google, suggest practical solutions for optimizing the crawling process [39] of dynamic content. Alternative URLs that lead to pages with static information are indexed by default or instead of pages that contain dynamic information. According to Google optimization rules, Web sites in our testbed use AJAX in some parts in device's web page but for crawling, corresponding Web services are accessed instead to get current STh value or EoI state, in addition to all possible states with corresponding occurrence probabilities. Another technique not implemented in our testbed is to render pages on the fly (i.e., crawlers have browsing processes embedded in their code [40]). Still, it is difficult to crawl pages that need to send some data first before loading their content. Moreover, the time consumed by the crawling process itself becomes high and the crawling process needs to be done frequently; information in WoT may be updated in less than a minute.

Using Ethernet, RESTful APIs can access Arduino components. Devices are programmed as *clients* to push sensor data to services and as *services* to enable remote control of devices over the Web. Because it is desirable to have a Web page for each device and because Arduino acts as a gateway for managing at least one component, a website is built and can be hosted on an SD card connected to the Arduino. The website is accessed using an IP address, assigned to the Arduino. Another alternative is to host the website on a different server for adding more capabilities like storage capacity. In the latter case, Arduinos are accessed using RESTful APIs. The selection of either alternative is determined by the amount of information that needs to be stored and accessed over time.

Two steps were done to add WoT layer to the testbed. First, a **Web application** was written in Asp.Net (Figure 7). The main services of the Web application are monitoring sensors, controlling actuators, triggering action events, and periodic sensor reporting [21][31][33]. The WoT



Figure 7. Web pages of virtual gateways get their information from a database server. Sensor Web pages get their information either from direct access to devices or from the offline dataset.

application was built according to the building hierarchical structure configured by the Network setup application. The homepage shows general information and allows users to perform general tasks, such as monitoring room status. The user selects a logical path to browse, then, for each room, a list of devices and their states appear. The user selects a device to access. The device page loads the RESTful services dynamically using Web Services Description Language (WSDL) [41] according to the Arduino IP and selected device ID. Second, a set of **Web services** were written in C#. The Web application loads the available RESTful services dynamically for each device. A special tag 'GET#' is added as an additional service that is executed by default for the device webpage. The crawling process returns the current sensor value or the state of the device and all possible states with their probabilities.

### 3) Dataset Collector

In Figure 8, using Zigbee connection, the WoT coordinator (gateway that acts as a base station) discovers all available gateways, getting a list of connected devices on

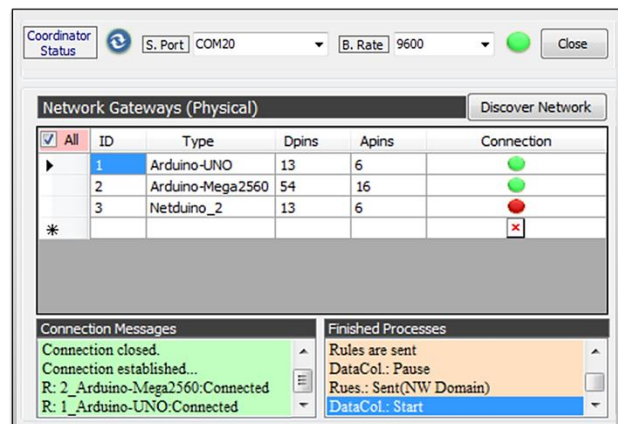


Figure 8. DsC discovers gateways in the WoT and loads their static information (e.g., number of digital and analogue pins).

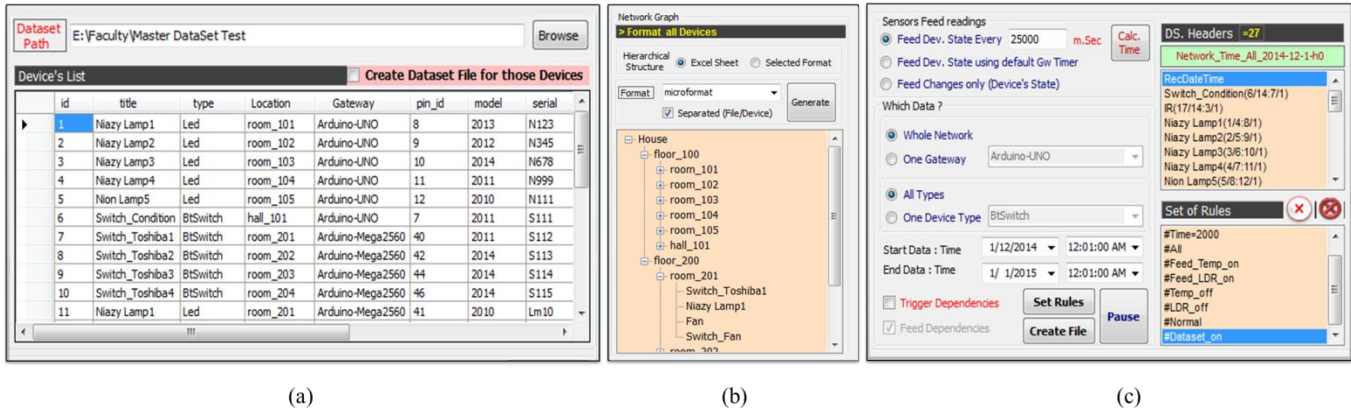


Figure 9. Dataset collector: (a) DsC loads list of devices connected on discovered gateways in the WoT . (b) Static information about the IoT testbed are generated in different formats. (c) Rules are defined to control the way gateways send dynamic information (readings).

each gateway (Figure 9 (a)). The DsC application generates files written in different formats for the static information of the IoT testbed including the building hierarchy and the devices located in the hierarchy (Figure 9 (b)). The dynamic information is collected using a set of rules, such as shown in Figure 9 (c). The rules instruct the gateways to send back specific information about a specific list of devices according to a specific action or event done by other devices. The gateways feed the DsC with device readings according to these rules. If the rule *ChangesOnly* is selected, the DsC stores only changes on device state. If the rule *TimeSlot* was selected, the DsC stores periodical feeds of device state. One of the most important rules is that if a certain device type is selected for analysis of device readings and making decisions according to the analysis results, rules can be set to collect data from all devices of that type across all the gateways in WoT.

4) Generated Dataset Files

A simple dataset was generated by the testbed according

```
<div class = "hproduct ">
  <span class = " fn">22_Fan</span>
  <span class = " identifier">,
    <span class = " type ">Fan</span> Sfan123
    <span class = " value ">0</span>
  </span>
  <span class = " category ">
    <a href =http://www.XXX.com rel = " tag"> Fan </a>
  </span>
  <span class = " brand ">Brand Name</span>
  <span class = " description "> characterized by ...
  </span>
  <span class = " Photo ">Fan</span>
  <a href =http://www.XXX.com/?s=wsn
    class = " URL">
    More information about this device.
  </a>
</div>
```

Figure 10. Static information about a fan written in Microformats.

to the rules: (1) *every\_2500 ms* for updating dataset every 2500 millisecond (i.e., DsC pulls information from the network), it could be replaced by rule *ChangesOnly* for storing changes on devices' states only (i.e., devices push information to DsC), (2) *All\_Network* for pulling information from all discovered gateways in the network, (3) *All\_types* means all devices on selected gateways, (4) *2014-12-1-h0\_to\_2015-1-1-h0* for storing dataset from 1/12/2014 to 1/1/2015, and (5) *TD* for triggering all dependences related to selected devices. The dataset generated according to limited time slot (date and time) by DsC, as shown in Figure 9 (b), contains static information about IoT infrastructure and dynamic information about sensing and actuating activities.

The static information of each device, such as logical path and device type, is stored in a file named using the device ID, the EoI ID, and device name (e.g., *22\_9\_Fan*). Static information about a fan written in Microformats is shown in Figure 10.

The dynamic information, such as sensor readings, is stored in a file named using the collection-rule title and the date and time of collection (e.g., *Network\_Time\_All\_2014-12-1-h0*). This file contains readings collected from all devices in the WoT testbed. A subset of data stored in that file would look like Table III, where monitoring is set to rule *time only*.

TABLE III. SAMPLE READINGS GENERATED FROM ALL SENSORS OF TYPE 'LAMP' IN THE ENTIRE NETWORK AS A TIME SERIES. CONSUMED VOLTAGES ARE MAPPED FROM (0:5) TO (0:255).

Time	XLamp2 (2/5:9/1)	XLamp3 (3/6:10/1)	XLamp4 (4/7:11/1)	XLamp5 (8/8:12/1)
03:01 PM	66	77	83	71
03:02 PM	66	80	83	68
03:04 PM	66	68	65	69
03:06 PM	67	71	69	67
03:08 PM	68	80	85	70
...	...	...	...	...
10:12 PM	65	80	85	70

As being mentioned earlier, sensor definition contains information about the sensor in order to be accessed easily through the WoT application. In sensor definition: 'Xlamp2(2/5:9/1)', X is sensor's brand name, lamp2 is sensor title, (2/5) is the virtual location sensor id and hosting room id, and (9/1) is the physical location where 9 is pin number and 1 is gateway id. Column 'Time' is the response time. Arduinos support 5 Voltages as maximum; they convert voltage range (0:5V) to be (0:255) using built in analog to digital converter. Values recored for each sensor definition, are current voltages consumed by that sensor (0 : 255).

## V. WOT TESTBED EVALUATION

In this section, the proposed WoT testbed in [1] is evaluated in terms of the dataset accuracy. We start by presenting the used metrics and the experiment setup. Then, we describe experiment results and summarize our observations.

### A. Dataset accuracy

Running the testbed in online mode produces dynamic information in real time about STHs and EoIs located in the surrounding environment. On the contrary, when running the testbed in offline mode, it produces simulated dynamic information; information about STHs and EoIs retrieved from the attached dataset is real but not in the real time. In other words, the dataset was generated previously by the testbed and saved, then attached to the testbed to simulate the environment.

Two factors affect dataset accuracy: (1) the number of messages that are lost between the gateway and the DsC and (2) the *time accuracy* of the STHs' values that are recorded in the dataset. In general, *time accuracy* is defined as the difference of time between the actual time at which a STH has the value X or an EoI is in state X and the time at which this information is recorded in the dataset. As such, the time accuracy is important to be measured for making accurate decisions, especially when decisions depend on synchronizing multiple STHs' readings or EoIs' states.

The time accuracy is affected by message latency, which is defined as the time consumed to send a data message between a gateway and the DsC. The latency is directly influenced by the message size, the distance between sender and receiver, and the baud rate (link bandwidth). Other indirect factors should also be considered: network topology and covered area (out-of-range nodes can send still their information if all or some nodes are configured with mesh capabilities), protocols and modules (e.g., XBee and Wifi), and capabilities of DsC for handling and processing all incoming messages from all connected devices.

Thereby, the time latency of a STH's message  $L_{STh}(msg)$  is defined as:

$$L_{STh}(msg) = T_C + T_R \quad (1)$$

where  $T_C$  is the time for communication between the DsC and the gateway and  $T_R$  is the time for handling and processing the incoming message by the DsC (i.e., parsing and analyzing an incoming message then recording STHs' values in the dataset). Boonsawat et al. [37] calculate the pulling time delay using the function *millis()* of the Arduino library, which returns the number of milliseconds since the Arduino board began running the current program (last reset) [22], it is used for realizing the distance between the coordinator and the end-devices [37].

Practically, estimating the actual reading time of a STH can be done in two ways: (1) STHs send actual time (sensing time) included in their messages after clock synchronization between discovered gateways and the DsC (clock synchronization can be done using the *DateTime* library [42]) and (2) calculating the time that the message consumes starting from its initialization to its recording. In the case of periodical requests, DsC firstly sends rules to selected gateways so that they adjust their configurations. After that, gateways send STHs' readings periodically according to the time defined in the DsC rules. The DsC sends requests every X seconds to all discovered gateways and waits for them to send their messages back. In that case, message latency is equal to the difference in time between message receiving time at the DsC and request sending time at the DsC as well. For example, if request sending time is 14:22:20 and message receiving time is 14:22:25, then the latency is 5 seconds.

Gateway latency,  $L_{Gw}$ , is computed as the average of all latencies that have occurred in all messages of all STHs connected to the gateway. We are using the average as an example statistic for simplicity; for more accurate results, the 50<sup>th</sup> percentile or the interquartile mean can be used instead, using straightforward modification in the equations.

$$L_{Gw} = \frac{1}{k} * \sum_{j=1}^k \left( \frac{1}{n_j} * \sum_{i=1}^n L_{STh_j}(msg_i) \right) \quad (2)$$

where  $k$  is the number of STHs connected to the gateway and  $n_j$  is the number of recorded values for STH  $j$ . the formula  $\left( \frac{1}{n_j} * \sum_{i=1}^n L_{STh_j}(msg_i) \right)$  represents the average latencies for STH  $j$ . In the case of datasets generated by pulling (the rule *EstimatedTime\_All\_Network*), the value of  $n_j$  should be identical for all STHs on each gateway. Then, Equation (2) becomes:

$$L_{Gw} = \frac{1}{n*k} * \sum_{j=1}^k \sum_{i=1}^n L_{STh_j}(msg_i) \quad (3)$$

Message Integrity Error (*MsgIE*) is the ratio between the number of received messages by the DsC and the number of sent messages by the gateways.

$$MsgIE = 1 - \left( \frac{\sum_{i=1}^l r_{GW_i}}{l * \left( \frac{t_f - t_s}{p} \right)} \right) \quad (4)$$

where  $l$  is number of discovered gateways in the testbed,  $r_{GW_i}$  is the number of messages sent by gateway  $GW_i$  (in the pulling case, all gateways ideally send an equal number of messages),  $t_s$  is the start recording time,  $t_f$  is the finish recording time ( $t_s$  and  $t_f$  are in milliseconds), and  $p$  is the interval for sending and receiving messages periodically. The formula  $\left( l * \frac{t_f - t_s}{p} \right)$  represents the number of messages that should be received and handled by the DsC when there is no error.

Synchronizing DsC's clock with all discovered gateways produces no clock synchronization errors. In that case, the actual reading time of each STh reading can be written inside the message and recorded into the dataset. But, when messages do not contain the reading time due to difficulties in clock synchronization, then the receiving time is used to estimate the STh reading time. So, the Synchronization Time Error (*SynTE*) is computed as follows:

$$SynTE = 1 - \left( \frac{1}{l * p} * \sum_{i=1}^l L_{GW_i} \right) \quad (5)$$

where  $L_{GW_i}$  is the latency of gateway  $i$ ,  $l$  the number of discovered gateways in the WoT testbed, and  $p$  the interval between two consecutive messages that come from the same gateway (i.e., gateway waits the time interval  $p$  to send one message containing all SThs' readings).

Because dataset Accuracy ( $AC_{DS}$ ) depends on two factors as mentioned above (time accuracy in which STh reading is written and integrity of dataset contents), then  $AC_{DS}$  is computed by the following equation:

$$AC_{DS} = \left( 1 - (SynTE + MsgIE) \right) * 100 \quad (6)$$

### B. Experiment setup

A large number of SThs in the WoT testbed produces less dataset accuracy due to network communication overhead and overwhelming the capabilities of the DsC to handle and process all incoming messages. Receiving a single message from each gateway (responsible for a group of SThs) is more desirable and is adopted in our testbed.

Evaluation of the WoT testbed was done by running the DsC application on a machine (base-station) with 8 GB RAM and core-i5 CPU running at 2.3 GHz. The DsC and gateways send and receive at a baud rate of 9600 bps. The first gateway (of type Arduino-Uno) is at a distance of 10m from the DsC, the second gateway (of type Arduino-Mega256) is at a distance of 15m, and the third one (of type Netduino2) is connected directly to the DsC through the SPI bus. All nodes in the testbed instance were configured in a

#Received Msgs	#Recorded Msgs	Recording Time	Receiving Time	Latencies msc.	Syn. Accuracy
1103 msg.(s)	19 row(s)	0.480027	15.780903	12296.993351	98.9861419...
R: 1_Arduino-UNO:@1.@@0.@1.0.0.0.1.@72.@87,					
R: 1_Arduino-UNO:@1.@@0.@1.0.0.0.1.@70.@87,					
R: 2_Arduino-Mega2560:@0.0.0.0.0.@1.@1.0.0.1.1.1.1.@264.@21.30,					
R: 1_Arduino-UNO:@1.@@0.@1.0.0.0.1.@72.@87,					
R: 2_Arduino-Mega2560:@0.0.0.0.0.@1.@1.0.0.1.1.1.1.@265.@21.30,					
R: 1_Arduino-UNO:@1.@@0.@1.0.0.0.1.@70.@87,					
R: 2_Arduino-Mega2560:@0.0.0.0.0.@1.@1.0.0.1.1.1.1.@264.@21.30,					
R: 1_Arduino-UNO:@1.@@0.@1.0.0.0.1.@72.@87,					
R: 2_Arduino-Mega2560:@0.0.0.0.0.@1.@1.0.0.1.1.1.1.@264.@21.30,					
R: 1_Arduino-UNO:@1.@@0.@1.0.0.0.1.@70.@87,					

Figure 11. Time accuracy for a dataset generated by the integrated WoT testbed using rule *EstimatedTime\_All\_Network* (pull).

star topology, so the maximum number of nodes in each path is 2 and the number of edges is one (i.e., a direct link between the DsC and each gateway in the network). The gateway of type Arduino-Uno had message size  $\approx 6$  bytes and Arduino-Mega  $\approx 10$  bytes.

Two fundamental approaches were used for getting sensor data in the testbed, pull and push [10], represented as the rules *EstimatedTime\_All\_Network* and *ChangesOnly*, respectively. In this paper, we focus more on the pull approach and measure the time accuracy as the time interval between reading and recording SThs' values. We note that the rule *EstimatedTime\_All\_Network* (pull) generates more data and is expected to affect the time accuracy more than the *ChangesOnly* rule; the dataset from pull contains the information generated by the rule *ChangesOnly* (push) in addition to repetitions of steady readings over the time.

### C. Results using *EstimatedTime\_All\_Network* rule

DsC pulls SThs' information by implementing the rule *EstimatedTime\_All\_Network* to generate a dataset for all connected devices on all the discovered gateways. Each discovered gateway in the WoT periodically sends one message every 1000 ms containing all SThs' values (i.e., the expected number of messages that all selected gateways can send is not known at the beginning).

Figure 11 shows the number of received messages, the number of recorded messages, the time consumed in the last recording process, the latency (in milliseconds) of the last message, the sum of latencies (in milliseconds) of all messages from all gateways, and the current synchronization accuracy of all SThs' readings. The list of devices connected to each gateway is shown in Figure 3, where 1\_Arduino-Uno represents Floor\_100 and 2\_Arduino-Mega2560 represents Floor\_200. The two gateways send a sequence of SThs' readings. The message fields from 1\_Arduino-Uno are switches, fans, last IR signal, LEDs, LDR, and temperature (LM35) and for 2\_Arduino-Mega2560 switches, fans, LEDs, LDR, humidity/temperature (DHT11). Message fields are separated by the special character @. Empty message fields indicate that no value was available. For switches, fans, and LEDs, a value of 1 corresponds to the ON state and a value of 0 to OFF.

As shown in Figure 11, the DsC received two messages back-to-back from the gateway 1\_Arduino-Uno. This was due to gateway 1\_Arduino-Uno being closer to the DsC than the other gateway as indicated by a stronger Received Signal Strength Indicator (RSSI). RSSI was measured in decibels using Digi's X-CTU software to determine signal noise, and its value ranges from 0 to 120; the closer it is to zero, the stronger is the signal.

Figure 11 shows an example of applying Equation (6) to calculate the  $AC_{DS}$ . In this experiment,  $p=1000$  ms,  $t_s=05:01:10$  and  $t_f=05:10:22$ . The total number of received messages from all gateways was 1103 messages, and the total latency time was approximately 12297 ms, yielding about 11.14 ms of latency per message. The latency included the processing time at the DsC for each received message and the network delay. The testbed produced the dataset with  $AC_{DS} \approx 98.98\%$ , where  $SynTE = 0.999\%$  and  $MsgIE = 0.011\%$ . We note that when reading time is sent with STHs' values, then  $SynTE=0\%$ , but the message size will increase, which in turn may increase message loss rate and  $MsgIE$ . Results of [43] confirm our measurements.

#### D. Results using ChangesOnly rule

When the *ChangesOnly* rule is used, message size has a direct relation to the number of STHs that detect change at the same time or within the same check period. This is because STHs push their information only when certain changes happen in their states and gateways check periodically for changes in STHs' values. The maximum message size is reached when all STHs of a certain gateway detect change at the same time, which is equivalent to the message size in the pull approach.

We ran an experiment in which gateways check STHs' values for change every 1000 ms. we found that most of the time message size was small, so we decided to send the reading time within the message. Implementing the system this way produced  $SynTE = 0\%$  with a small  $MsgIE$  and with small message parsing and processing overhead at the DsC. Because the expected number of messages is not known at the beginning,  $MsgIE$  can be measured using Equation 4 provided that all gateways send their total number of sent messages periodically in SYNC messages.

#### E. Results Discussion

As can be concluded from the previous results, dataset accuracy depends on the network overhead, which in turn depends on the pull period,  $p$ , and on the number of gateways and STHs in the testbed. The DsC application allows for setting the pull period, as shown in Figure 9 (c). If the number of STHs is too large and state changes occur only sporadically affecting a limited number of STHs then it is desirable to use the *ChangesOnly* rule to produce more accurate and smaller dataset.

As mentioned previously, there are two methods to estimate actual STH reading time. The first method requires clock synchronization between the DsC and all testbed

gateways. STHs' readings are recorded in the dataset with the time written within the message. But recording the reading time within the message increases message size and time required for parsing and analyzing the message body, which then causes increased network overload, especially when the number of gateways and STHs connected to them is large. The messages thus come from gateways with low RSSI and can be lost easily. The first method is desirable if accuracy of data synchronization is critical, especially when the *ChangesOnly* rule is used for dataset generation.

The second method consumes less time for parsing and analyzing message body and reduces message size. It can be used with the *EstimatedTime\_All\_Network* rule. If dataset accuracy is not critical or time scale of reading accuracy is larger than that of which latency occurs (e.g., if device synchronization is sensitive on the days' time scale and the delay in recording messages is in seconds or minutes), then the second method can be used. The second method can be augmented by a mechanism to estimate message latency using echo request and reply.

Table IV summarizes the differences between the two methods.

TABLE IV. COMPARISON OF ACTUAL STH READING-TIME ESTIMATION METHODS.

Criteria	in-message	calculated
Main idea	Synchronizing DsC's clock with all selected gateways	Computing time difference between reading time and recording time
Reading and receiving time delay	<ul style="list-style-type: none"> <li>▪ Reading time is sent within the message body.</li> <li>▪ Recording time= reading time</li> </ul>	<ul style="list-style-type: none"> <li>▪ Recording time = actual reading time + latency</li> </ul>
Dataset accuracy	depends only on $MsgIE$ , which depends mainly on weak RSSI	depends on $SynTE$ and $MsgIE$
Dataset error in the pull case	Dataset accuracy is estimated using Equation (6)	
	$SynTE = 0\%$	$SynTE$ is estimated using Equation (5)
Dataset error in the push case	<ul style="list-style-type: none"> <li>▪ All gateways send their total number of sent messages to measure <math>MsgIE</math> using Equation (4).</li> </ul>	
	$SynTE = 0\%$	$SynTE$ is estimated using Equation (5)
Pros	More accurate	<ul style="list-style-type: none"> <li>▪ Smaller messages</li> <li>▪ faster message parsing and analysis</li> </ul>
Cons	<ul style="list-style-type: none"> <li>▪ Larger messages (by about 2 bytes)</li> <li>▪ slower message parsing and analysis</li> </ul>	$SynTE > 0\%$

## VI. CASE STUDY

In this section, a case study of the proposed WoT testbed is described.

#### A. Using WoT Dataset for information analysis

Using the generated dataset, researchers can analyze sensor data collected using multiple controlled scenarios. A

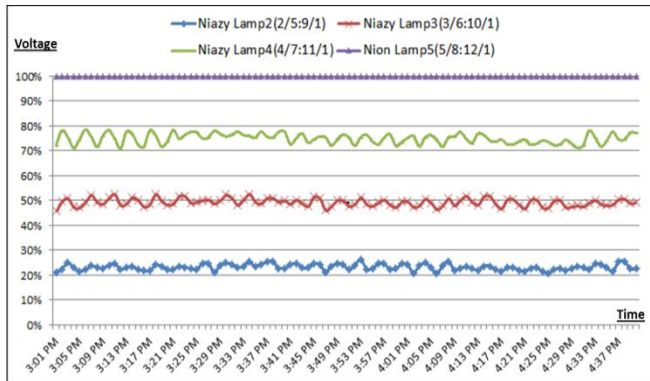


Figure 12. A graph generated out of a dynamic data file collected from devices of the same type (lamp in this graph). Voltages consumed by devices are represented in percentage at Y axis.

lot of experiment scenarios can be achieved on the testbed, such as comparing the state of devices on certain gateways (e.g., gateways of a room), comparing state of devices on all gateways (e.g., all gateways of a building), getting live time of each device and high level power consumption in daily live to provide suggestions related to energy efficiency achievement (i.e., Energy awareness through interactive user feedback). Figure 12 shows a comparison between devices of type 'Lamp' for analysis of power consumption. Y-axis represents consumed voltages percent and X-axis represents time.

Estimation on timing accuracy of the data hasn't been measured yet, but after enlarging WoT scale, DsC can estimate timing accuracy by calculating request and receive time for each device. In general, such a dataset, especially composed of dynamic information, will be helpful for computing Fuzzy-based sensor similarity [18], and for running prediction algorithms on real information that are used in searching about STHs and EoIs in the WoT. Providing information about STHs and EoIs in multiple formats with additional attributes like logical paths expands experimental work in this area.

### B. Browsing WoT

Building simple and physical WoT (offline or online) will be helpful and more accurate than using simulators. Figure 2 shows a scenario of calling RESTful web services for pulling information about buildings and their devices from the generated dataset (offline). Sensor pages call Web services that fetch information from a dataset file 'Network\_Time\_All\_2014-12-14-h17.xlsx' using command of type *OleDbCommand*. Web services called in the testbed (Figure 2) execute the command string shown in Figure 13. 'Device\_Header' and 'Sheet\_Title' were sent by calling pages to the Web service *monitoring*. The special character @ before variables 'Date\_1' and 'Date\_2' means that they are initiated within the Web service.

```
Select [Device_Header]
From [Sheet_Title]
Where [RecDateTime] = (Select min ([RecDateTime])
From [Sheet_Title]
Where [RecDateTime]
Between @Date_1 and @Date_2)
```

Figure 13. Accessing dataset files using web services (offline mode): Selecting column 'Device\_Header' from sheet 'Sheet Title' where its time = current system time (hours and minutes) using *OleDbCommand*.

### C. Crawling and indexing WoT

Preparing WoT pages for crawling and indexing improves searching results. To this end, the crawling process should be tested at first, after that comes determining which information should be indexed and how to index such large and dynamic information to satisfy different kinds of queries where initiators of those queries could be human users or machines. For testing WoT crawling, the web spider starts with crawling EoI's page then recursively follows all links of devices (get list of devices' URLs) and so on to stop with links of device's services (get list of device's services by parsing its Web Services Description Language (WSDL)). Most of device's links are links to RESTful services that return results directly.

As mentioned before, AJAX needs special type of web crawlers that either emulates Web browsers by loading pages then executing the AJAX parts on the fly or forwards requests to default pages (pages with static information). To demonstrate benefits of the proposed testbed in testing the WoT, the .Net Crawler [44] was directed to the Web page, shown in Figure 7, to test the ability of crawling the WoT. Result of crawling process, as shown in Figure 14 (a), is a list of rooms' URLs [45]. For each room's URL, the crawler recursively crawled list of devices' URLs [46]. All rooms' pages, list of devices for each room, and device's details (properties and RESTful services) were reached recursively from home page URL [47]. Crawling RESTful services like POST and GET requests were developed and a sample of its execution is shown in Figure 14 (b). Getting service URL now is available using WSDL, like what is Google did [39], services are overridden to get dynamic information (state) about the static information (default pins), so the optimization here is not to forward request for static page to get static information but to forward request for static list of devices to get their dynamic information.

Ostermaier et al. [10] construct a real-time search engine for the WoT called Dyser, preparing sensor pages that should be indexed with static information about sensors (e.g., type) and dynamic information (in the form of possible states and its prediction model). Like Dyser, the proposed testbed prepares sensor pages and entity pages to provide static information about themselves and dynamic information in the form of possible states with dynamic probabilities calculated by prediction model (e.g., Markov).

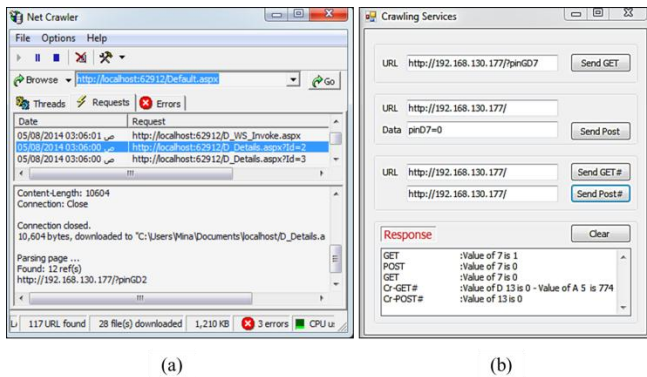


Figure 14. A Web spider case study for the WoT testbed. (a) Crawling pages of virtual gateways. (b) Crawling RESTful services that are loaded dynamically using WSDL.

Dyser prototype supports only probabilities of the possible states not the prediction model itself as indicated in its architecture.

According to the methodology used for searching for STHs and EoIs, information should be prepared. For instance, in the case of integrating the WoT with traditional search engines, semi-static information about the WoT should be written in rich format. Microformats and Microdata are embedded in HTML pages (WoT pages). But, in the case of special search engines that support queries written in SPARQL query language, information should be stored as RDF triples.

#### D. Reusing Testbed for Different IoT

The proposed testbed architecture allows the implementation of different purposes in the WoT. If someone has to operate the testbed for a certain environment (for example, energy saving of smart home, detect something unacceptable happening at a shopping mall, etc.), and because the proposed testbed operates in two modes (online and offline), then reusing this testbed depends on the operation mode.

For online mode, new IoT infrastructure, which is built by attaching resources support information about measuring physical phenomena and actuating EoIs, is replaced by the IoT part shown in Figure 1 (b) and registered by Network setup application. New IoT should speak the same language as the DsC (gateways make it easy for supporting heterogeneity in devices).

For offline mode, such as shown in Figure 15, because the dataset represents the IoT itself where it hosts information about STHs, EoIs, and sensing and actuating processes, then IoT part will be replaced by that dataset to be accessed by web services as indicated in Figure 2. So, offline mode could be used for retesting previously built IoT. Moreover, it could be used like Docklight [48] for discovering nodes in the network and testing packet transfer

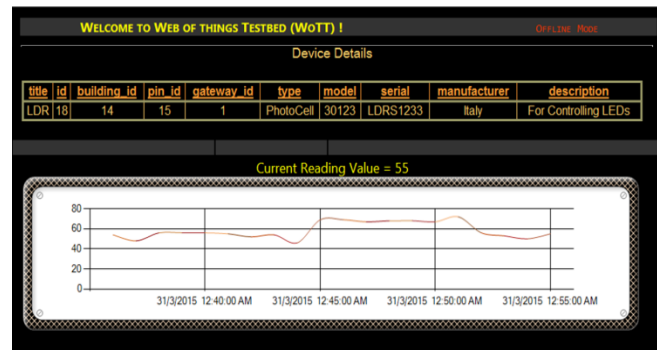


Figure 15. Testbed is running in offline mode (attaching IoT dataset).

delay between the coordinator and endpoint nodes in a star topology.

#### VII. CONCLUSION AND FUTURE WORK

WoT has become one of the most trendy research directions due to facilities and services provided in many domains. Sensors can provide great benefits if their readings are presented in a meaningful and friendly way to users and machines. Searching for STHs and EoIs is one of the most important services in the WoT. In this work, we presented an evaluation of our integrated WoT testbed architecture by empirically measuring the dataset accuracy of the generated dataset and by qualitatively comparing our testbed to the state-of-the-art in WoT and IoT measurement platforms. The dataset generated from the testbed is expected to help research on the crawling, indexing, and searching processes in WoT. From the evaluation results, we argue that dataset quality depends on time accuracy of STHs' readings.

An interesting problem for direct future work is how to enable the DsC to help testbed users to calculate an optimal time interval for receiving and processing messages, according to message size, the number of discovered gateways in the testbed, and the number of STHs connected to them, with the goal of increasing accuracy of the dataset.

The problem of searching for STHs and EoIs depends on the standardization of formats used for representing STHs properties and services they offer. So, providing semantic discovery services based on the application of multiple discovery strategies [12] and enriching STHs meta-data may enhance the performance of searching services in the WoT. Creating standardized RESTful service description embedded in HTML using microdata is feasible and desirable [29]. Still, a few important issues remain here: security in the WoT, the methodologies by which WoT builders select an appropriate topology to cover an environment with certain conditions, achieving high performance and high accuracy, whereby the key service in the WoT is to give users the ability to get interesting knowledge in quickly, accurately and in an abstract form, and how to index WoT data streams.

## REFERENCES

- [1] M. Younan, S. Khattab, and R. Bahgat, "An Integrated Testbed Environment for the Web of Things," in ICNS 2015 : The Eleventh International Conference on Networking and Services, ISBN: 978-1-61208-404-6, Rome, Italy, May, 2015, pp. 69-78.
- [2] M. Blockstrand, T. Holm, L.-Ö. Kling, R. Skog, and B. Wallin. (2011, Feb.) Operator opportunities in the internet of things – getting closer to the vision of more than 50 billion connected devices. [Online]. [http://www.ericsson.com/news/110211\\_edcp\\_244188811\\_c](http://www.ericsson.com/news/110211_edcp_244188811_c)
- [3] L. Coetzee and J. Eksteen, "The Internet of Things – Promise for the Future ? An Introduction," in IST-Africa Conference, Gaborone, May 2011, pp. 1-9.
- [4] WS4D Initiative. (2010, Aug.) WS4D-uDPWS - The Devices Profile for Web Services (DPWS) for highly resource-constrained devices. [Online]. <http://code.google.com/p/udpws/wiki/IntroductionGeneral>
- [5] G. Werner-Allen, P. Swieskowski, and M. Welsh, "MoteLab: A Wireless Sensor Network Testbed," in Information Processing in Sensor Networks, 2005. IPSN 2005. Fourth International Symposium on, Boise, ID, USA, 2005, pp. 483-488.
- [6] S. Haller, "The Things in the Internet of Things," Poster at the (IoT 2010). Tokyo, Japan, vol. 5, no. 26, p. 4, Nov. 2010.
- [7] I. Muhammad, A. Md Said, and H. Hasbulla, "A Survey of Simulators, Emulators and Testbeds for Wireless Sensor Networks," in nformation Technology (ITSim), 2010 International Symposium in, vol. 2, Kuala Lumpur, June 2010, pp. 897-902.
- [8] A. Gluhak, S. Krco, M. Nati, D. Pfisterer, N. Mitton, and T. Razafindralambo, "A Survey on Facilities for Experimental Internet of Things Research.," IEEE Communications Magazine, Institute of Electrical and Electronics Engineers (IEEE), no. <10.1109/MCOM.2011.6069710>. <inria-00630092>, pp. 58-67, 2011, 49 (11).
- [9] J. Miloš , N. Zogović, and G. Dimić, "Evaluation of Wireless Sensor Network Simulators," in the 17th Telecommunications Forum (TELFOR 2009), Belgrade, Serbia, 2009, pp. 1303-1306.
- [10] B. Ostermaier, B. M. Elahi, K. Römer, M. Fahrmaier, and W. Kellerer, "A Real-Time Search Engine for the Web of Things," in The 2nd IEEE International Conference on the Internet of Things (IoT), Tokyo, Japan, Nov. 2010, pp. 1-8.
- [11] shodan search engine. [Online]. [www.shodanhq.com](http://www.shodanhq.com), (Accessed: 10 April 2015).
- [12] S. Mayer and D. Guinard, "An Extensible Discovery Service for Smart Things," in Proceedings of the 2nd International Workshop on the Web of Things (WoT 2011), ACM, San Francisco, CA, USA, June 2011, pp. 7-12.
- [13] H. Sundani, H. Li, V. K. Devabhaktuni, M. Alam, and P. Bhattacharya, "Wireless Sensor Network Simulators - A Survey and Comparisons," International Journal Of Computer Networks (IJCN), vol. 2, no. 6, pp. 249-265, Feb. 2011.
- [14] P. Bodik, C. Guestrin, W. Hong, S. Madden, M. Paskin, and R. Thibaux. (2004, Apr.) Intel Lab Data. [Online]. <http://www.select.cs.cmu.edu/data/labapp3/index.html>, (Accessed: 10 April 2015).
- [15] D. Gay, P. Levis, D. Culler, E. Brewer, M. Welsh, and R. von Behren, "The nesC language: A holistic approach to networked embedded systems," in PLDI '03 Proceedings of the ACM SIGPLAN 2003 conference on Programming language design and implementation, New York, NY, USA, May 2003, pp. 1-11.
- [16] P. Levis, S. Madden, J. Polastre, R. Szewczyk, K. Whitehouse, and A. Woo, "TinyOS: An Operating System for Sensor Networks," in Ambient Intelligence, W. Weber, J. M. Rabaey, and E. Aarts, Eds. Springer Berlin Heidelberg, 2005, ch. 2, pp. 115-148.
- [17] h. b. T. AS IS. Contiki: The Open Source OS for the Internet of Things. [Online]. <http://www.contiki-os.org/>
- [18] C. Truong, K. Romer, and K. Chen, "Sensor Similarity Search in the Web of Things," in In World of Wireless, Mobile and Multimedia Networks (WoWMoM), 2012 IEEE International Symposium, San Francisco, CA, June 2012, pp. 1-6.
- [19] M. Nati, A. Gluhak, H. Abangar, and W. Headley, "SmartCampus: A user-centric testbed for Internet of Things experimentation," in Wireless Personal Multimedia Communications (WPMC), 2013 16th International Symposium on, Atlantic City, NJ, June 2013, pp. 1-6.
- [20] G. Mujica, V. Rosello, J. Portilla, and T. Riesgo, "Hardware-Software Integration Platform for a WSN Testbed Based on Cookies Nodes," in IECON 2012 - 38th Annual Conference on IEEE Industrial Electronics Society , Montreal, QC, October. 2012, pp. 6013-6018.
- [21] H. Nam, J. Janak, and H. Schulzrinne, "Connecting the Physical World with Arduino in SECE," Computer Science Technical Reports, Department of Computer Science, Columbia University, New York, Technical Reporting CUCS-013-13, 2013.
- [22] Arduino. [Online]. <http://www.arduino.cc/>, (Accessed: 10 April 2014).
- [23] I. LogMeIn. Xively. [Online]. <http://www.Xively.com> , (Accessed: 10 April 2014).
- [24] Powered by ioBridge. ThingSpeak- The open data platform for the Internet of Things.. [Online]. <http://www.thingspeak.com>, (Accessed: 10 April 2015).
- [25] X. Inc. (2012, Jan.) XMPro Internet of Things. [Online].

- <http://xmpro.com/xmpro-iot/>, (Accessed: 10 April 2015).
- [26] Dr. M. Elkstein. (2014, Nov.) Learn REST: A Tutorial. [Online]. <http://rest.elkstein.org/2008/02/what-is-rest.html> , (Accessed: 10 April 2015).
- [27] C. Pfister, "The Internet of Things," in *Getting Started with the Internet of Things: Connecting Sensors and Microcontrollers to the Cloud*, B. Jepson, Ed. United States of America.: O'Reilly Media, Inc., 2011, ch. 4, pp. 29-41.
- [28] S. Mayer, D. Guinard, and V. Trifa, "Searching in a Web-based Infrastructure for Smart Things," in *Proceedings of the 3rd International Conference on „the Internet of Things (IoT 2012)*, IEEE, Wuxi, China, October 2012, pp. 119-126.
- [29] S. Mayer, "Service Integration - A Web of Things Perspective," in *W3C Workshop on Data and Services Integration*, Citeseer, Bedford, MA, USA, October 2011, pp. 1-5.
- [30] SensLab. [Online]. <http://www.senslab.info>.
- [31] D. Guinard, "A Web of Things Application Architecture - Integrating the Real-World into the Web," PhD Thesis, Computer Science, Eidgenössische Technische Hochschule ETH Zürich, Zürich, 2011.
- [32] D. Guinard, V. Trifa, S. Karnouskos, and D. Savio, "Interacting with the SOA-Based Internet of Things: Discovery, Query, Selection, and On-Demand Provisioning of Web Services," *Services Computing, IEEE Transactions on*, vol. 3, no. 3, pp. 223-235, Sep. 2010.
- [33] D. Guinard and V. Trifa, "Towards the Web of Things: Web mashups for embedded devices," in *in Workshop on Mashups, Enterprise Mashups and Lightweight Composition on the Web (MEM 2009)*, in *proceedings of WWW (International World Wide Web Conferences)*, Madrid, Spain, 2009, p. 15.
- [34] R. Faludi, *Building Wireless Sensor Networks*, 1st ed., B. Jepson, Ed. Tokyo, United States of America: O'Reilly Media, Inc., 1005 Gravenstein Highway North, Sebastopol, CA 95472., 2011.
- [35] A. McEwen and H. Cassimally, *Designing the Internet of Things*, 1st ed., C. Hutchinson, Ed. John Wiley & Sons, November 2013, <https://books.google.com.eg/books?id=oflQAQAAQBAJ>.
- [36] Digi International Inc. Official XBee website- Connect Devices to the Cloud. [Online]. <http://www.digi.com/xbee>, (Accessed: April 2015).
- [37] V. Boonsawat, J. Ekchamanonta, K. Bumrunghket, and S. Kittipiyakul, "XBee wireless sensor networks for temperature monitoring.," in *the second conference on application research and development (ECTI-CARD 2010)*, Chon Buri, Thailand, May, 2010, pp. 221-226.
- [38] Digi International Inc. Digi. [Online]. <http://www.digi.com/products/xbee-rf-solutions/xctu-software/xctu>, (Accessed: November 2015).
- [39] Google. (2010, Jan.) Search Engine Optimization (SEO) - Starter Guide
- [40] P. Suganthan G C, "AJAX Crawler," in *Data Science & Engineering (ICDSE), 2012 International Conference on*, IEEE, Cochin, Kerala, July 2012, pp. 27-30.
- [41] wikipedia, Web Services Description Language. [Online]. [http://en.wikipedia.org/wiki/Web\\_Services\\_Description\\_Language](http://en.wikipedia.org/wiki/Web_Services_Description_Language), (Accessed: November 2014).
- [42] M. Margolis. *Electronic Projects Components Available WorldWide (PJRC)-DateTime Library*. [Online]. [https://www.pjrc.com/teensy/td\\_libs\\_DateTime.html](https://www.pjrc.com/teensy/td_libs_DateTime.html), (Accessed: April 2015).
- [43] G. Randolph and N. Hirsch. (2010, Mar.) PIC32MX: XBee Wireless Round-trip Latency. [Online]. [http://hades.mech.northwestern.edu/index.php/PIC32MX:\\_XBee\\_Wireless\\_Round-trip\\_Latency](http://hades.mech.northwestern.edu/index.php/PIC32MX:_XBee_Wireless_Round-trip_Latency)
- [44] H. Mostafa. (2006, Mar.) Code Project. [Online]. <http://www.codeproject.com/Articles/13486/A-Simple-Crawler-Using-C-Sockets>, (Accessed: 10 April 2015).
- [45] [http://localhost:62912/R\\_Devices.aspx?Id=4](http://localhost:62912/R_Devices.aspx?Id=4), (Accessed: 10 November 2015)
- [46] [http://localhost:62912/D\\_Details.aspx?Id=1](http://localhost:62912/D_Details.aspx?Id=1), (Accessed: 10 November 2015)
- [47] <http://localhost:62912/Default.aspx>, (Accessed: 10 November 2015)
- [48] Flachmann und Heggelbacher GbR. (2015, Aug.) docklight. [Online]. <http://docklight.de/>, (Accessed: 10 November 2015)

# Quality of Service Based Event Stream Processing Systems in Smart Grids

Epal Njamen Orleant

Grenoble INP, LIG  
Saint Martin d'Hères, France

Email: [orleant.epal-njamen@imag.fr](mailto:orleant.epal-njamen@imag.fr)

Lourdes Martinez

Grenoble INP, LIG  
Saint Martin d'Hères, France

Email: [martinez@imag.fr](mailto:martinez@imag.fr)

Christine Collet

Grenoble INP, LIG  
Saint Martin d'Hères, France

Email: [christine.collet@grenoble-inp.fr](mailto:christine.collet@grenoble-inp.fr)

Genoveva Vargas-Solar

CNRS, LIG-LAFMIA  
Saint Martin d'Hères, France  
Email: [genoveva.vargas@imag.fr](mailto:genoveva.vargas@imag.fr)

Christophe Bobineau

Grenoble INP, LIG  
Saint Martin d'Hères, France  
Email: [christophe.bobineau@grenoble-inp.fr](mailto:christophe.bobineau@grenoble-inp.fr)

**Abstract**—This paper presents an approach for composing event streams based on quality of service requirements (QoS) of smart grids. The approach consists of an event stream model, composition strategies guided by QoS such as memory consumption, event priority and notification latency. Model and strategies are implemented by a distributed event stream processing system consisting of execution units that can be deployed across a smart grid. The paper describes implementation issues and experimental results.

**Keywords**—Complex event processing; Quality of service; Smart Grids.

## I. INTRODUCTION

Smart grids are complex networks vastly instrumented with intelligent electronic devices (sensors, smart meters, actuators, etc.), network communication and information technologies. Devices emanate huge amounts of data that can be exploited for a wide range of applications like network traffic analysis, automation of operational control, prevention or detection of dysfunctions, etc. Strategies to handle asynchronous data collection, data transfer, and real-time data notification and processing are critical for achieving smart grid monitoring.

Those data can be considered as events that refer to happenings of interest produced within the system environment. The capacity to monitor and supervise a smart grid relies on processing low level events in order to infer higher level events semantically richer and more useful for end user applications [1]. This process includes events filtering, aggregation, correlation, windowing, etc. Infrastructures able to achieve these computations on events are referred to as complex event processing systems like [2–6].

For example, let us consider that a smart meter produces an event of type CoverOpenAlert when its cover is opened, and a sensor produces an event of type BadVoltage when it detects an abnormal voltage on the electrical line. An application may be interested in the sequence of CoverOpenAlert and a BadVoltage occurring at the same place, within a two minutes time window. This pattern detects suspicious activities (MeterSuspected event type) on smart meters. The detection

of such a high level event includes event filtering (type and attribute based filtering), windowing and temporal correlation.

In these situations, devices may notify events to a remote Information System (IS) able to perform complex events processing. The IS sends commands (with or without human intervention) to certain devices for reacting to the reported events. The dialog IS - devices may take considerable time, thus hindering real-time requirements. An intuitive manner for alleviating this problem is to inject certain intelligence into devices, such that they can react to situations without some external intervention. Thus, (total or partial) event processing should be distributed among the smart grid devices. An inherent consequence is the necessity to deploy event processing systems in distributed architectures. The latter must efficiently achieve event processing while adapting to their environment in terms of the multiplicity of data sources (sensors, smart meters, existing databases, etc.) and smart grid QoS requirements.

*a) Multiplicity of data sources:* Distributed systems like smart grids consist of different types of components that can act as event producers or consumers, with different interaction modes (synchronous or asynchronous, push or pull based style), as illustrated by sensors, smart meters, existing databases. The diversity of interaction modes, coupled with the difference in data formats make it difficult to integrate events from different producers for event processing purposes.

*b) Quality of service (QoS):* The need to detect and notify complex events from basic events is sometimes correlated with some quality of service requirements like memory consumption, network occupancy, event priority, notification latency, etc. The extension of event models towards more flexible and QoS oriented event models requires an analysis and the semantics that should be given to the events, and of their associated processing strategies. This requires dissociating the modeling of event and the application design and, the proposal of methods that allow to define event types independently of the management issues (detection, production, notification). Therefore, it is required to adapt the event models to smart grid characteristics. On the other hand, those QoS requirements generally constrain the way the event processing must be

achieved. More precisely, event processing must be achieved on each device considering its memory availability.

Existing systems are limited in the sense that they do not fully satisfy QoS requirements for event processing. The problem we address in this paper can be summarized as follows: given smart grid needs in terms of event composition and QoS, how to provide the complex event processing system that best fulfills expected QoS requirements?

Our approach considers an event based abstraction of smart grids functions and services. This abstraction allows to reason on the smart grid in terms of event streams that are generated by smart grid components. In order to identify relevant or critical situations (complex events) among those event streams, we propose a distributed complex event processing architecture. The event processing logic is implemented as a network of operators executed by distributed event processing units. We also propose strategies applicable to event processing units in order to address the following QoS dimensions: event priority, memory occupation and notification latency.

The remainder of the paper is organized as follows: Section II presents the related work. Section III presents the overview of our approach for QoS based complex event processing in smart grids. Section IV describes the proposed model and system architecture for QoS based event processing. Section V discusses how to specify QoS requirements and introduces the QoS adoption strategies. These strategies are presented in Section VI and Section VII. Section VIII discusses the experimental results. Finally, Section IX concludes the paper.

## II. RELATED WORK

Many works have been achieved on event streams analysis and composition, and many event processing systems have been proposed so far [2–6], either for centralized or distributed architectures.

In centralized architectures, produced events are processed by a single node acting as an event processing server [3][5][6][7][8]. In this approach, event streams must be routed to the server node. This potentially increases the latency of the event processing, and overloads the network and server, which risks to become a point of failure. Therefore, this approach is not suited for distributed contexts.

In distributed architectures, the event processing logic is performed by a set of distributed communicating nodes, each one achieving a part of the work. This offers a better scalability and availability than centralized approaches. Some distributed event processing systems are [2][4][9][10]. In this category, we distinguish between clustered and in-network architectures. In clustered architectures, the event processing is realized in a clustered environment [4][11], whereas in-network architectures allows to distribute the event processing over a large number of nodes within a network topology [9][2]. This work aims to propose an in-network event stream processing systems for smart grid that deals with QoS.

Behnel et al. [12] and Appel et al. [13] identify some QoS dimensions (latency, priority, etc.) relevant for distributed event processing, but they do not propose mechanisms for their adoption. However, some other systems provide QoS support. They optimize the query processing according to a particular objective, and differs from each other by the adopted QoS dimensions. For example, [2] focuses on reducing

the network traffic whereas [9] studies energy consumption. In wide networking environments, it is not reasonable to expect that all applications share the same objective. In our approach, we identify a set of QoS properties relevant for event processing in smart grids, and we study their adoption by the event processing system.

A survey on the QoS requirements of smart grid communication systems is presented in [14]. It focuses on the functionalities that have to be provided by smart grid communication infrastructures in order to address application requirements. Sun et al. [15] propose to add QoS by providing differentiated service for data traffic with different priority at the MAC (Media Access Control) layer. GridStat [16] is a publish-subscribe middleware framework designed to meet the QoS requirements for the electric power grid. It manages network resources to provide low-latency, reliable delivery of information produced anywhere on the network and sent to multiple other points. In our work, we assume the existence of QoS support at the networking layer (e.g. message priority) on which a complex event processing system dealing with event priority, memory occupation and notification latency can be proposed for smart grids.

## III. APPROACH OVERVIEW

Figure 1 summarizes our approach to integrate complex event processing technologies into smart grids. It consists in three layers of abstraction, namely smart grid, event streams, and event processing network layers.

- The smart grid layer consists in the real physical smart grid architecture, which includes telecommunication based devices such as smart meters, sensors, data concentrators, etc. Those devices are connected by communication networks technologies including power line, wireline or wireless communications [17]. The smart grid is described in terms of information being used and exchange between functions, services and components. This layer of abstraction is referred to as the *Information layer* in the smart grid reference architecture model [18]. In our approach, information is seen as events that happen within the smart grid.
- The event streams layer considers that data generated by smart grids components are event streams. In this layer, smart grid components act as sources, which can generate different types of events in a continuous manner. The event model considered in this work is presented in Section IV.
- The event processing network layer consists in a set of distributed event processing units that are connected by event channels. This network is created according to complex event subscriptions. It may be deployed across multiple distributed computers, software artifacts and physical networks. The complex event subscriptions are tagged with applications QoS requirements such as event priority and notification latency. Those QoS requirements have to be translated into constraints applicable to event processing units at execution time. In addition to constraints derived from applications requirements, inherent constraints to the smart grid infrastructure also must be taken into consideration, such as limitations on computational

resources (i.e., memory and CPU) and / or communication networks (i.e., network occupation).

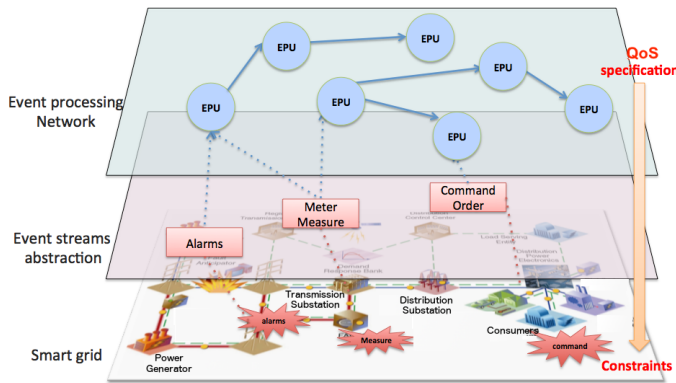


Figure 1. Approach overview

#### IV. MODEL AND ARCHITECTURE

This section presents the event model (event type and event stream), and the runtime architecture of our approach (event processing network).

##### A. Event model

1) *Event type and event instance*: An event type represents a class of significant facts (events) and the context under which they occur. The definition of an event type includes the attributes presented in Table I.

TABLE I. EVENT TYPE ATTRIBUTES

Name	Type
typeName	String
producerID	String
detectionTime	Number
productionTime	Number
notificationTime	Number
receptionTime	Number
priority	Number
context	Set<Attribute >

The *typeName* attribute refers to the name of the event type. The *producerID* attribute refers to the id of the entity who produced the event instance. The *detectionTime* attribute refers to the time at which the event instance has been detected by a source. The *productionTime* attribute refers to the time at which the event has been produced (as a result of a processing on others events) by an event processing unit. The *notificationTime* attribute refers to the time at which the event is notified to interested consumers. The *receptionTime* refers to the time at which the event is received by an interested consumer. The *priority* attribute represents the priority value associate to the event instance. The context (*context* attribute) of an event type defines all the attributes that are particular to this event type. They represent the others data manipulated by the producer, which are relevant to this event type. For example, the context of a *MeterMeasure* event type generated by a smart meter includes the *voltage* and *current* attribute.

An event type can be simple or composite. Simple event types are event types for which instances are generated by producers (sensors, smart meters, etc.). They are not generated

from the processing of other events. In the example considered in Section I, *BadVoltage* and *CoverOpenAlert* are simple event types. More generally in a smart grid, the event types include *Alarms*, *MeterMeasure* and *SensorMeasure* generated by electric devices and such as smart meters and sensors, and *Command*, *ControlOrder*, *ControlAction* generated by utility applications.

Complex (or composite) event types are event types for which instances are generated as a result of event processing. Reference [19] includes a set of operators applicable to events. They capture particular situations (relevant or critical) that can be inferred from occurrences of others events. Those situations have to be notified to utility applications, such that the system can be automatically or manually controlled. In the same example, *MeterSuspected* is a complex event type. Complex event types can also capture aggregated values, like the daily electricity consumption of a household. This can be product of the aggregation of the *MeterMeasure* event instances included on a one-day window.

An event instance (or simply event) is an occurrence of an event type. The event instance defines the value associated to each attribute of the event type. For example, the event occurrence *e* with attributes presented in Table II denotes an event instance of type *MeterMeasure*, which has been produced by producer *meter1* at time 1, notified at time 2, received at time 3, which has a priority value 3, and for which the voltage and current values are 220 and 3, respectively.

TABLE II. EVENT INSTANCE

Name	Type
typeName	'MeterMeasure'
producerID	'meter1'
detectionTime	1
productionTime	1
notificationTime	2
receptionTime	3
priority	3
voltage	220
current	3

2) *Event stream*: An event stream is a continuous, append-only sequence of events. We note  $Stream(s, T)$  the stream of events of type T generated by the source s. If S is a set of sources, then  $\{\cup Stream(s, T), s \in S\}$  defines a stream of events of type T, denoted  $Stream(T)$ .

##### B. Event processing network

As introduced in Section III, the event processing logic is implemented by the event processing units. The runtime deployment of event processing units with associated event channels is called the event processing network [20][21]. This is illustrated in Figure 2.

The general vision of our QoS based complex event processing system can be briefly described as follows: applications subscribe to composite events by issuing complex event patterns to the system, this must also include the specification of the associated QoS requirements. The system then deploys a set of distributed event processing units, which apply different strategies to meet QoS requirements during event processing. Complex events produced by the event processing units are notified to consumers. In a smart grid, such an infrastructure can act as a middleware on which utility applications rely

for detecting interesting or critical situations (sensors errors, alarms, etc.) over the electrical grid, and at the same time, rely on some QoS guarantees (e.g., priority, notification latency, etc.).

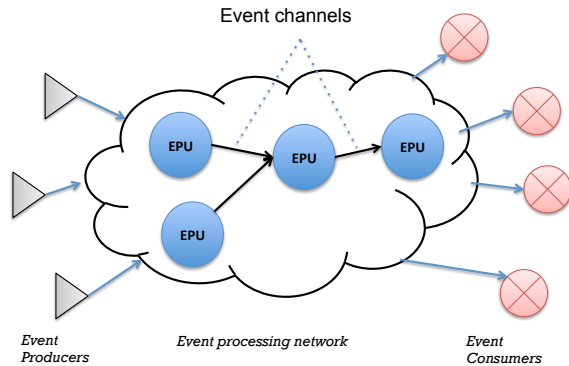


Figure 2. Event processing network

1) *Event processing unit*: An event processing unit can be defined by three types of components (see Figure 3):

- a set of input queues, on which parts of input event streams are maintained.
- an operator, which implements a three step event processing logic: *fetch-produce-notify*. In the first step (fetch), some events are selected from the input queues and marked as ready to be used to produce new composite events. In the second step (produce), the events selected at the first step are used to produce new composite events according to the operator semantic. The produced complex events are stored in the output queue. In the third step (notify), events in the output queue are notified either, to another event processing units or to the interested consumers.
- an output queue, which contains events to be notified.

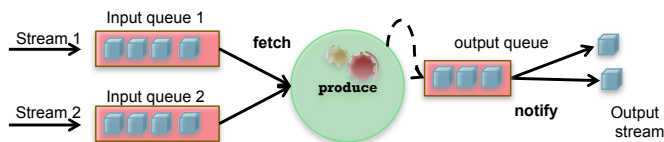


Figure 3. Event processing unit

2) *Event channel*: Event processing units communicate through event channels. Event channels are means of conveying events [22]. This can be done via standard tcp or udp connections, or higher level communication mechanisms like publish/subscribe [23] or group communication [24] provided by a middleware layer.

### C. Architecture

The architecture of the proposed QoS based event processing system is depicted at Figure 4. It consists of four layers described as follows.

- the application layer consists of two types of components: event producers (sensors, smart meters, etc.),

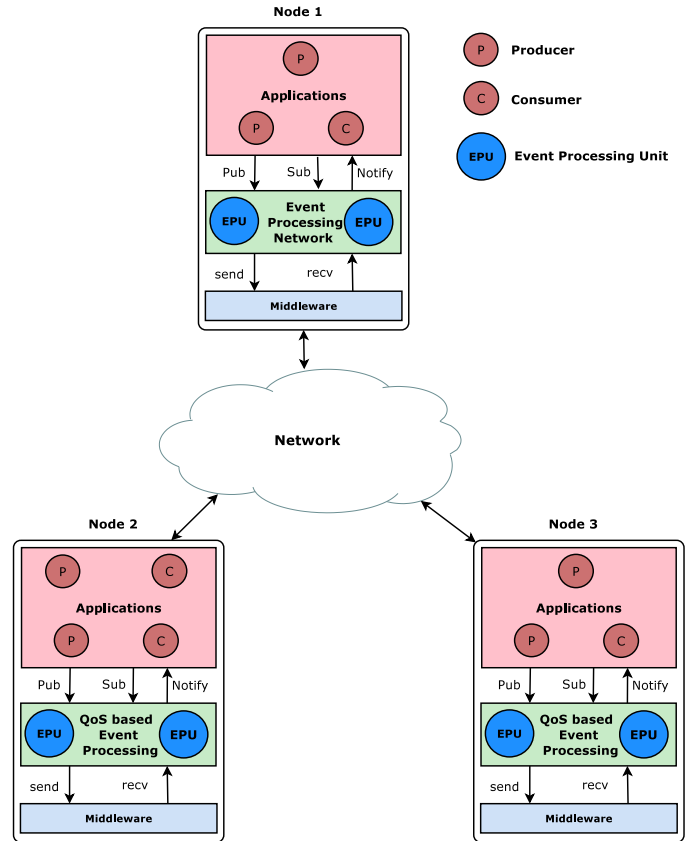


Figure 4. System architecture

and event consumers that subscribe to complex event patterns having specific QoS requirements.

- the event processing network layer consists of a set of distributed event processing units that communicate among them via event channels.
- the middleware layer provides a high level communication mechanism to event processing units. This can be publish/subscribe [23][16] or group communication services [24]. It relies on the underlying network layer.
- the network layer ensures messages delivery from one destination to another.

## V. QOS SUPPORT IN EVENT PROCESSING

The need to detect and notify complex events from basic events is sometimes correlated with some QoS requirements. The QoS dimensions we address in this paper are event priority, notification latency and memory occupation. Those QoS requirements are either imposed by smart grid applications (event priority, notification latency), or by the execution environment (memory occupation).

1) *Event priority*: Event priority defines a priority order between events. In some contexts, events may have different priorities that have to be captured at event processing runtime. For example, in a smart grid, a BadVoltage event can be

higher priority than a CoverOpenAlert event. Events that have a higher priority have to be processed and notified earlier than less priority events.

2) *Memory occupation*: Smart grid devices may have different memory capacity. To adapt event processing to the memory capacity of devices, it must be a way to specify the maximum memory occupation incurred by an event processing unit at execution time. The memory occupation constraint gives an upper bound of the number of events that an event processing unit can maintain at execution time.

3) *Notification latency*: In the common practice for power device protection, the circuit breaker must be opened immediately if the voltage or current on a power device exceeds the normal values. The notification latency of an event is the time elapsed between its production and its notification to interested consumers (end users or event processing units). The notification latency constraint imposed on an event processing unit defines an upper bound on the notification latency of events produced by that event processing unit.

#### A. QoS expressions

Each QoS requirement is associated to a specific value domain. Below we specify the value domains corresponding to the introduced QoS requirements:

- $D_{latency}$  denotes the notification latency domain. Latency is a measure of time that adopts a numeric value expressed as either, a positive integer or a positive fraction. Therefore, a latency value belongs to the domain of real numbers  $\mathbb{R}^+$ . Thus, we can say that  $D_{latency} \subseteq \mathbb{R}^+$ . We also assume that the arithmetic and comparison operations that can be applied on real numbers also can be applied among values belonging to  $D_{latency}$ . For instance, intuitively a low latency is preferable than a high latency, thus it can be desirable to compare latency values using the comparison operators less than (<), and less than or equal to ( $\leq$ ).
- $D_{priority}$  denotes the event priority domain. An event instance is associated to a priority level that varies according to the event type. A priority level is represented with a positive integer value. Therefore, we consider that a priority value belongs to the domain of natural numbers  $\mathbb{N}$ ; thus,  $D_{priority} \subseteq \mathbb{N} \leq n$ . We assume that we can use comparison or arithmetic operators on latency values. The priority is a heavily restricted bounded QoS requirement, priority = 1 denotes the highest priority and priority = n denotes the lower priority. The equal to (=) operator is required to associate an event to a priority level.
- $D_{memocc}$  denotes the memory occupation domain. We express the memory occupation in terms of number of events, for this reason, such a requirement adopts an integer positive value thus belonging to the domain of natural numbers  $\mathbb{N}$ . We state that  $D_{memocc} \subseteq \mathbb{N} \leq m$ . Where the comparison operator less than or equal to ( $\leq$ ) specifies an upper bound and m specifies the maximum memory capacity of the current device.

Let us assume that  $D$  is the set of the considered QoS domains, thus  $D = D_{latency} \cup D_{priority} \cup D_{memocc}$ . Given a domain  $D_Q$ , we assume a function  $name(D_Q)$  that returns the domain name, a function  $operator(D_Q)$  that returns the set of

related operators, and a function  $value(D_Q)$  that returns the set of possible values.

For instance, let us consider the domain  $D_{latency}$ , thus:

- $name(D_Q) = \text{notification latency}$
- $operator(D_Q) = \text{greater than } (>), \text{ greater than or equal to } (\geq), \text{ less than } (<), \text{ less than or equal to } (\leq), \text{ equal to } (=), \text{ not equal to } (\neq)$
- $value(D_Q) = \mathbb{R}^+$ , this is the set of all positive real numbers

1) *Atomic QoS expression*: An atomic QoS expression  $\alpha$  specifies a QoS requirement. It is of the form  $(n, \Theta, v)$ , where

- $n$  denotes a domain  $D_Q$ , where  $D_Q \in D$
- $\Theta \in operator(D_Q)$  and,
- $v \in value(D_Q)$

For instance, the atomic QoS expression (notification latency,  $\leq$ , 2000 ms) specifies that the latency for notifying an event must be equal than or less to 2000 milliseconds.

2) *Complex QoS expression*: A complex QoS expression  $\epsilon$  specifies multiple QoS requirements. Assuming that an atomic QoS expression specifies a QoS requirement, thus a complex QoS expression results from the conjunction of two or more atomic QoS expressions. The definition of a complex QoS expression is as follows:

- If  $\alpha_1$  and  $\alpha_2$  are atomic QoS expressions then  $\alpha_1 \cup \alpha_2$  is a complex QoS expression  $\epsilon_1$ .
- Let us suppose that the complex QoS expression  $\epsilon_2$  results from the conjunction  $\alpha_1 \cup \alpha_2 \cup \alpha_3$  of atomic expressions.
- Thus,  $\epsilon_2$  results from the conjunction  $\epsilon_1 \cup \alpha_3$ .
- A complex QoS expression results from the conjunction of two or more QoS atomic expressions, or other complex expressions.

The QoS expression (notification latency,  $\leq$ , 2000 ms)  $\cup$  (event priority, =, 1) specifies that the notification latency must be less than or equal to 2000 milliseconds, and in addition, the highest priority level (i.e., priority = 1) is required.

#### B. QoS adoption

QoS expressions are translated into constraints that have to be satisfied by the runtime environment. In order to address those QoS requirements, we propose:

- an event processing units placement algorithm that ensures load balance between the available processing devices while minimizing the end to end latency. For simplicity, we will refer to this problem as the operators placement problem, since the placement of an event processing unit is the same as the placement of the operator it implements.
- a strategy applicable to event processing units allowing to ensure that high priority events will be processed and notified earlier than less priority events.

VI. OPERATOR PLACEMENT

Event stream processing operators can be deployed in several ways on smart grid devices. Operators placement may considerably impact the quality of service. For instance, deploying operators on a single node may potentially minimize the latency of events processing, since it avoids the time spent to communicate among several nodes. However, concentrating the process on one node may overflow its memory capacity, thus resulting in the violation of a QoS requirement (i.e., memory occupation). This section presents a QoS adoption strategy that addresses the operator placement problem.

A. Problem definition

Operators placement refers to the (close to) optimal selection of the physical nodes hosting the operators in an event processing network in order to satisfy a predefined global cost function. Operators placement is an instance of a more general task-assignment problem that addresses the (close to) optimal assignment of  $m$  tasks to  $n$  processors in a network, which has an  $O(n^m)$  complexity. The operator placement problem is NP-complete.

The operator placement algorithm takes as input a specification of a physical network topology  $T = \{N, E\}$ , which consists in a set of computing nodes  $N$  and their links  $E$ . The operator placement also requires a specification of the resources (i.e., memory and CPU) available on each node, and the latency of communication links. Figure 5 shows an example of network topology that comprises 9 computing nodes, each communication link being labeled with its corresponding latency. Table III shows the resources availability on each computing node. In order to specify the exact value of CPU rate available on each node, we specify a coefficient that indicates how fast is that node compared to a reference node for which the CPU coefficient is 1. For example, node  $n_1$  is two times slower than node the reference node  $n_7$ , and node  $n_8$  is three times faster than node  $n_7$

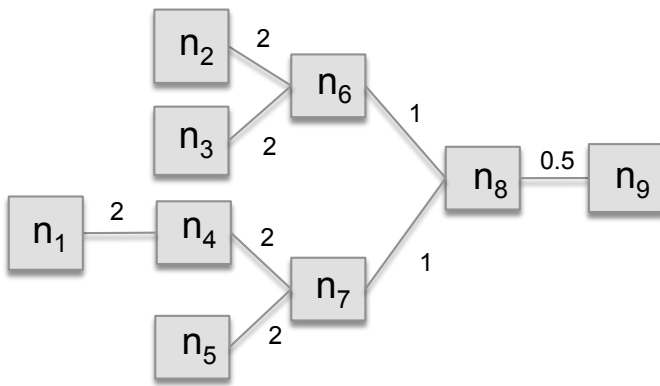


Figure 5. A physical network topology

The operator placement algorithm also takes as input an event processing graph  $EPG = \langle \theta, A \rangle$ , which consists in a set of event streams producers  $P \in \theta$ , a set of stream processing operators  $O \in \theta$  and a set of event stream consumers  $C \in \theta$ .  $A$  represents the set of edges that connect the operators in  $O$ . Figure 6 shows an example of an event processing graph, where  $P_1$  and  $P_2$  are two producers,  $C_1$  is a consumer,  $o_1, o_2, o_3$  and  $o_4$  are stream processing operators. The operators are

TABLE III. RESOURCES AVAILABILITY ON NETWORK NODES

Node	Memory	CPU coefficient
$n_1$	10	1/2
$n_2$	10	1/2
$n_3$	15	1/2
$n_4$	12	1/2
$n_5$	10	1/2
$n_6$	10	1/2
$n_7$	50	1
$n_8$	60	3
$n_9$	30	2

associated with measures or estimates of demand, such as the memory and CPU time that each operator expects for processing a single input event. Table IV shows the estimates associated to operators  $o_1, o_2, o_3$  and  $o_4$ .

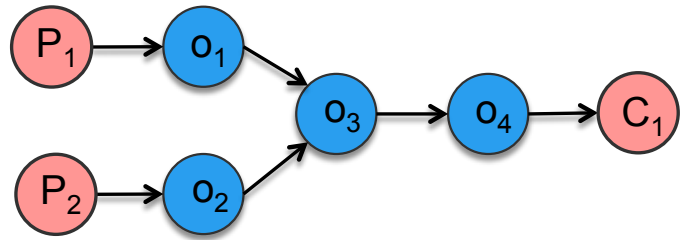


Figure 6. An event processing graph

TABLE IV. ESTIMATES OF THE OPERATORS RESOURCES REQUIREMENTS

Operator	Memory	Execution time
$o_1$	8	4
$o_2$	12	5
$o_3$	10	6
$o_4$	20	9

The output of the operator placement algorithm is a mapping function  $\lambda$  that associates to each operator the node on the network topology in which it should be hosted. Figure 7 shows a possible operator placement, where operators  $o_1, o_2, o_3$  and  $o_4$  are mapped to nodes  $n_6, n_4, n_8$  and  $n_8$ , respectively.

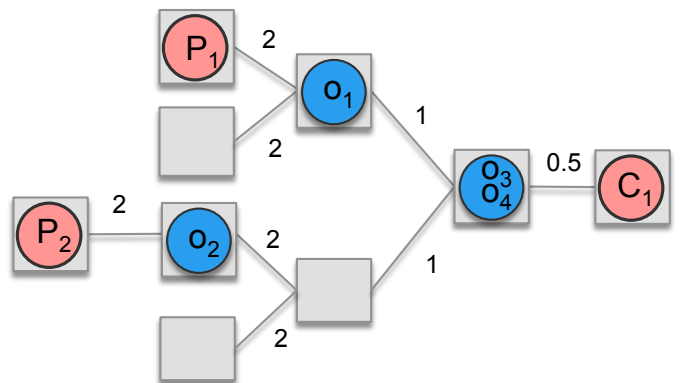


Figure 7. Example of operators placement.

We assume that each producer and each consumer is restricted to a permanent physical network node. Operators can be placed on arbitrary nodes having enough available resources for their execution. In general, a placement algorithm assigns

operators to processing nodes in a way that satisfies a set of specified constraints and optimize a given objective function. In our setting, the constraint is to ensure that no processing node is overloaded beyond its memory capacity. The objective function is the expected end-to-end latency between producers and consumers.

### B. Problem formalization

In order to formally define the issue of operators placement, let us consider the notations presented in Table V.

TABLE V. NOTATIONS

Operator	Execution time
$o$	event processing operator
$n$	network node
$init$	initial mapping of producers and consumers
$time(o)$	execution time of $o$ on a reference node
$mem(o)$	memory required by operator $o$
$p(o, n)$	execution time of $o$ on node $n$
$cpuCoeff(n)$	CPU coefficient of node $n$
$amem(n)$	memory available on a node $n$
$lat(e)$	latency of the network link $e$
$netPath(n_i, n_j)$	the network path between nodes $n_i$ and $n_j$
$c(a)$	latency of the communication between operators connected by the edge $a$
$\lambda(o)$	the mapped location of operator $o$

We formalize the operator placement problem as follows:

$$\underset{\lambda}{\text{minimize}} \quad cost(\lambda) = \sum_{o \in \Theta} p(o, \lambda(o)) + \sum_{a \in A} c(a) \quad (1)$$

subject to:

$$\lambda(o) = init(o), \text{ if } o \in P \cup C \quad (2)$$

$$\forall n \in N \quad \sum_{o: \lambda(o)=n} mem(o) \leq amem(n) \quad (3)$$

where

$$p(o, n) = \frac{time(o)}{cpuCoeff(n)} \quad (4)$$

$$c(a) = \begin{cases} 0 & \text{if for } a = (o_i, o_j), \lambda(o_i) = \lambda(o_j) \\ \beta(a) & \text{otherwise} \end{cases} \quad (5)$$

$$a = (o_i, o_j), \beta(a) = \sum_{e_i \in netPath(\lambda(o_i), \lambda(o_j))} lat(e_i) \quad (6)$$

Equation (1) states the cost of an operator mapping  $\lambda$ , which is the estimated end-to-end latency incurred by  $\lambda$ . It is calculated as the sum of the latency due to event processing (first part) and the latency due to the network communication (second part). Equation (2) states that the mapping should be consistent with respect to the initial mapping of producers and consumers. Equation (3) states that the mapping should be defined such that no processing node is overloaded beyond its memory capacity. Equation (4) shows the formula that allows to compute the processing time of a mapped operator. Equations (5) and (6) show how to compute the network latency incurred by inter operator communications. By using these formulas, we can compute the cost of the operators mapping presented in Figure 7.

First, note that this mapping is valid, since it does not violate (2) and (3). Following (4), we compute  $p(o, \lambda(o))$  for

operators  $o_1$  to  $o_4$  as 8, 10, 2 and 3, respectively. The latency of event processing is then 23.

Now let us compute the latency due to inter-operator communications. For the edge  $(P_1, o_1)$ , it equals 2. For the edge  $(P_2, o_2)$ , it also equals 2. For the edge  $(o_1, o_3)$ , it equals 1. For the edge  $(o_2, o_3)$ , it equals 2+1, so 3. For the edge  $(o_3, o_4)$  it equals 0. For the edge  $(o_4, C_1)$ , it equals 0.5. The latency incurred by inter operator communication is then 7.5. Thus, the total cost of the operator mapping is  $cost(\lambda) = 23+7.5 = 30.5$ .

### C. Brute force approach

The operator placement problem can be modelled as a constraint satisfaction problem (CSP). CSPs are mathematical problems defined as a set of objects whose state must satisfy a number of constraints. The constraints that we consider are defined by (2) and (3), and are similar to the constraint defined by the bin packing problem, where items of different volumes must be packed into a finite number of bins, each with a given volume. For the purpose of operator placement, the bins represent the processing nodes, and their size represents their memory capacity. The items represent the operators, and their volume represents their memory occupation. We can now rely on a CSP solver to find the set of valid mappings according to the bin packing constraint. The optimal mapping is the one with the minimum cost among the set of valid mappings, as shown in the following algorithm.

```

OpPlacement(EventProcessingGraph epg, NetworkTopology topo, InitialMapping init)
 $\lambda_{opt} \leftarrow null$ ;
 $solver \leftarrow BinPackingSolver()$ ;
 $solver.constructBinPackingConstraint(epg, topo, init)$ ;
if  $solver.hasSolution()$  then
   $\lambda \leftarrow solver.nextSolution()$ ;
   $c \leftarrow cost(\lambda)$ ;
   $\lambda_{opt} \leftarrow \lambda$ ;
  while  $solver.hasSolution()$  do
     $\lambda \leftarrow solver.nextSolution()$ ;
     $c_2 \leftarrow cost(\lambda)$ ;
    if  $c_2 < c$  then
       $c \leftarrow c_2$ ;
       $\lambda_{opt} \leftarrow \lambda$ ;
    end if
  end while
end if
return  $\lambda_{opt}$ ;

```

### D. Greedy approach

The *OpPlacement* algorithm browses the whole space of correct solutions (with respect to the bin packing constraint) in order to find the optimal one. Then, it follows a brute force approach. Because of its exponential complexity, the *OpPlacement* algorithm fails to produce a result in an acceptable period of time for large event processing graphs and network topologies. In order to deal with such large inputs, we propose a greedy approach for operator placement. The idea of this approach is to incrementally map parts of the event processing graph on specific parts of the network topologies, combining found solutions, till all operators are mapped. There are two main aspects that have to be considered here in order to apply this approach. First, it should be specified how to

compute parts of the event processing graph. Then, it should be specified how to compute the part of the network topology where a computed part of the event processing graph should be mapped. In order to do that, we rely on the following hypothesis on event processing graph and network topology respectively:

- *Hypothesis 1*: there is one consumer for each input event processing graph. This reduces the complexity of the problem, since considering many consumers in the event processing graph will lead to multi optimization with respect to each consumer, especially when some consumers share the same part of the event processing graph.
- *Hypothesis 2*: the network topology has a tree structure. This is consistent with electrical grid topologies, which are generally designed under a tree structure.

1) *Computing subgraphs of the event processing graph:*

Given the original event processing graph, a subgraph will consist of intermediates operators that are reachable from a given producer to the consumer  $c$ . Therefore, they will be the same number of subgraph than the number of producers in the original graph. In the following, we assume the existence of a function  $subgraph(EPN, P_i)$  that computes the subgraph associated to the producer  $P_i$ . For example, considering the event processing graph in Figure 8, the result of the function  $subgraph(EPN, P_2)$  is the subgraph that consists of the set of nodes  $\theta' = \{P_2, o_2, o_3, o_4, c\}$  and the set of edges  $A' = \{(P_2, o_2), (o_2, o_3), (o_2, o_4), (o_3, c), (o_4, c)\}$ .

2) *Computing a subgraph of the network topology:* Once we compute a subgraph  $subgrap(EPN, P_i)$  of an event processing graph for a given producer  $P_i$ , we need to compute the subgraph of the network topology where it should be mapped. In order to do that, we consider the mapped location of the producer  $P_i$  and the one of consumer  $c$  as defined by the initial mapping  $init$ . The resulting subgraph is the one that includes the nodes in the path between  $init(P_i)$  and  $init(c)$ . Since the network topology is a tree, there is only one path between  $init(P_i)$  and  $init(c)$ . Then, the size of the subgraph is of the order of  $O(\log(n))$ , where  $n$  corresponds to the number of nodes in the original network topology. We assume that this subgraph is computed by the function  $subgraphTopo(T, n_i, n_j)$ .

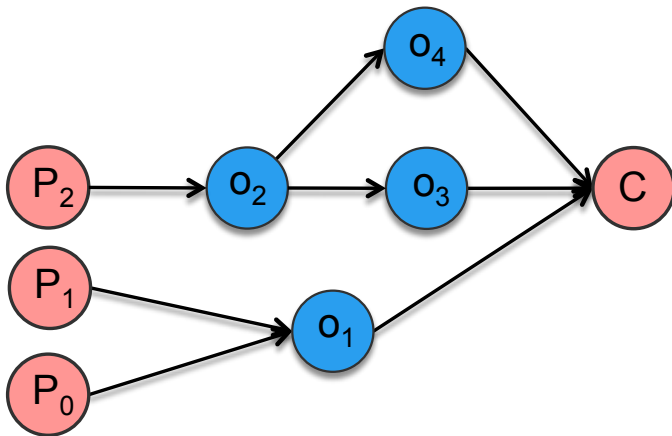


Figure 8. Event processing graph

For example, considering the network topology in Figure 9, and assuming that the producer  $P_2$  and the consumer  $c$  are initially mapped at nodes  $n_6$  and  $n_{10}$ , respectively, the result of the function  $subgraphTopo(T, n_6, n_{10})$  is the subgraph that consists in the set of nodes  $N' = \{n_6, n_8, n_9, n_{10}\}$  and the set of edges  $E' = \{(n_6, n_8), (n_8, n_9), (n_9, n_{10})\}$ .

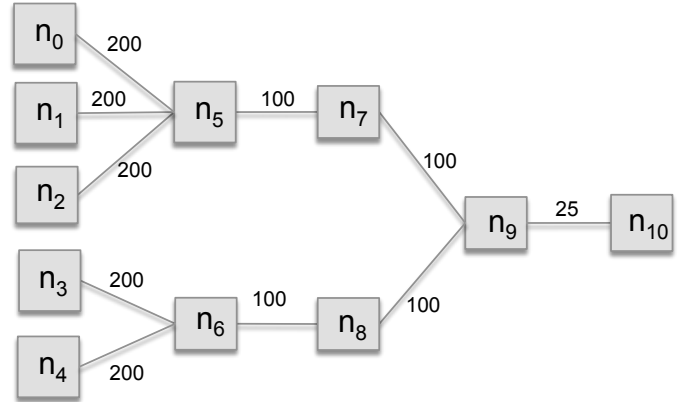


Figure 9. Network topology

3) *Greedy algorithm:* The greedy version of the algorithm is presented as follows.

```

OpPlacementGreedy(EventProcessingGraph epg, Network-
Topology topo, InitialMapping init)
λ ← init;
for each producer  $P_i$  in epg do
     $epg' \leftarrow subgraph(epg, P_i)$ ;
     $topo' \leftarrow subgraphTopo(topo, init(P_i), init(c))$ ;
     $\lambda' \leftarrow OpPlacement(epg', topo', \lambda)$ ;
    if  $\lambda' \neq null$  then
         $\lambda \leftarrow \lambda \cup \lambda'$ ;
        for each operator  $o$  in  $epg'$  do
            if  $o$  is not mapped then
                mark  $o$  as mapped;
                update the available memory in  $\lambda(o)$ ;
            end if
        end for
    else
        return null;
    end if
end for
return λ;
    
```

The *OpPlacementGreedy* algorithm achieves local optimization for each computed subgraph of the original event processing graph. At each step, the solution is combined with the previously found solutions and the result is used like the initial mapping for others iterations. As it finds solutions during subgraph mappings, it marks all non-mapped operators as mapped, and continues till all subgraphs are mapped. If the mapping of a subgraph of the original event processing graph fails, the algorithm stops and the mapping is considered as failed.

VII. DEALING WITH EVENT PRIORITY

The QoS requirements concerning memory occupation and latency have already been addressed by the operators placement algorithm presented in the previous section. However,

the event priority still remains for being attended, this section presents a proposal to deal with this requirement.

As stated in Section IV, any instance of an event type has a priority attribute to which an integer value must be assigned (See Table I). The priority value of a simple event is defined by its producer, whereas the priority value of a composite event is computed as the maximum priority of its operand events. The higher is the priority value associated to an event instance, the higher is the event priority. Events are inserted into input and output queues according to their priority. Input and output queues are priority-based FIFO structures with limited capacity. The priority relation  $\prec$  is defined as follows:  $e_i \prec e_j \rightarrow e_i.priority < e_j.priority \vee e_i.priority = e_j.priority \wedge e_j.detectionTime \leq e_i.detectionTime$

The  $\prec$  relation ensures that high priority events will be notified early compared to less priority events. As consequence, the notification of a less priority event can be postponed for a significant amount of time. This issue, that we refer to as the starvation problem, is stated more precisely as follows: an event in the output queue may suffer the starvation problem with respect to the notification step, if after a significant number of notifications  $k$ , the event is still in the output queue, due to its priority that is less compared to that of inserted events.

To solve the starvation problem, we associated to each event in the output queue a time to live value  $tll$  that is initialized to an integer  $k$ . At each notification step, the  $tll$  value of each event decreases and the events for which the  $tll$  value equals zero are notified. For the event priority defined by applications to be really effective, there are also some assumptions that have to be made on the underlying layers of the event processing runtime. More precisely, the middleware layer must provide a FIFO delivery mechanism, allowing to convey events while preserving their notification order such as in [24] [25].

## VIII. EXPERIMENTAL EVALUATION

We focused our experiments to the evaluation of the operator placement algorithm. We developed our algorithm using Java programming language. We rely on the Jacop CSP solver [26] to implement the bin packing constraint. For our experiments, we defined different types of devices (smart meters, data concentrators, sensors, etc.) with different resource profiles. A resource profile is defined by a memory capacity and a CPU coefficient. Based on this, we generated network topologies with various sizes, and containing devices with different defined profiles. The latency of the communication links among the different devices was fixed too. We followed the same idea with operators. We defined different kind of operators with memory and CPU time requirements. We generated event processing graphs of different sizes, and comprising the specified operator types.

We conducted a first experiment to compare the results of the greedy algorithm with those of the brute force algorithm. More precisely, we focused on the algorithm execution time, and the quality of resulting operator placement, which is captured by its cost. We generate 20 different inputs for the algorithm, each consisting in a network topology and an event processing graph. Each network topology consisted in 15 nodes, and the number of operators in each event processing graphs ranged from 7 to 10. For each input, we

executed the *OpPlacement* algorithm (brute force) and the *OpPlacementGreedy*. We choose to run this experiment over a small network topology and small event processing graphs in order to make sure that the optimal solution can be calculated.

We compared first the execution time of the algorithms. The result is depicted at Figure 10, which presents for each of the 20 executions (x axis), the time duration (y axis) of the brute force algorithm, and the time duration of the greedy algorithm. Clearly, the greedy algorithm performs faster than the brute force algorithm, being in average one order of magnitude faster.

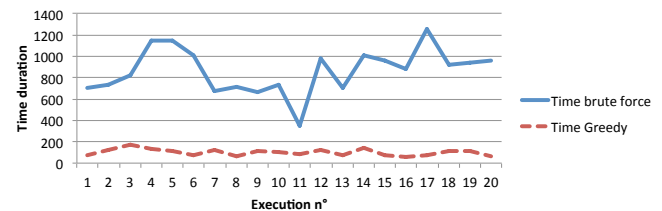


Figure 10. Operator placement execution time: comparison between brute force and greedy algorithm

Figure 11 compares the cost of operator placement computed by the greedy algorithm with the optimal one, computed by the brute force algorithm. We can observe that the cost of the operator mapping computed by the greedy algorithm is generally close to the optimal one. Even more interesting, for this experiment, the accuracy of the greedy approach (computed as the percentage of optimal solutions that were found) was 55%.

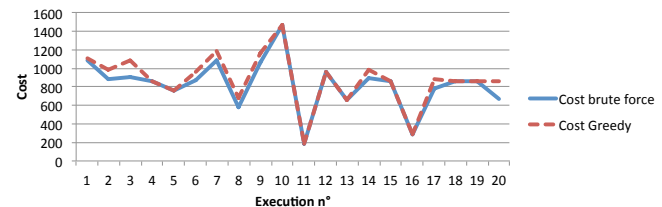


Figure 11. Cost of operator placement: comparison between brute force and greedy algorithm

We conducted another experiment in order to test how the greedy algorithm behaves on large event processing graphs. We execute the algorithm over a network topology consisting in 50 nodes. The size of event processing graphs ranged from 15 to 110 nodes. It is worth to mention that the brute force approach was not able to compute the optimal result here, due to its time complexity. Figure 12 presents the result of this experiment. We notice that the time duration of the greedy algorithm does not necessarily increases when the size of the event processing graph grows. In fact, the structure of the event processing graph is another factor that impacts the performance of the algorithm. In event processing graphs for which operators are highly connected, the subgraph associated to a producer can have a high number of operators. Therefore, the time to compute the mapping of that subgraph can be longer. For example, in the experiment, the event processing graphs having size 45 and 60 were dense, this explains the peaks we observed in the duration time.

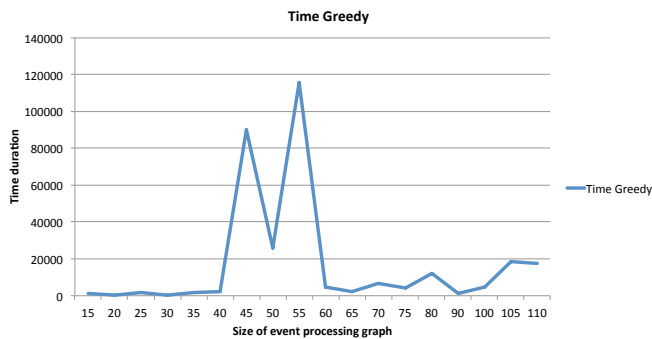


Figure 12. Scale up of the greedy algorithm

## IX. CONCLUSION

This paper shows that monitoring of smart grids can be done using an event based approach where event streams generated by distributed sources are processed by distributed event processing units. Such units may produce complex events indicating situations of interest that are notified to consumers. Since the invocation of business, critical processes is now triggered by events. The QoS of the event processing infrastructure becomes a key issue. We have identified key QoS dimensions relevant to smart grids, namely event priority, memory occupation and notification latency. We proposed a brute force algorithm for deploying event stream operators in a network topology, considering memory occupation and latency. To overcome the time complexity of the brute force approach, we propose a greedy algorithm for operator placement. The experiments shown that, while performing faster than the brute force approach, the greedy algorithm provides good quality solutions. We also proposed a strategy to deal with event priority.

We are currently developping a simulation platform to demonstrate our approach. The simulation platform allows to represent a smart grid topology and an event processing network. In addition, it implements the proposed strategies for QoS adoption. On the other hand, we are working on the specification of a real smart grid use case. The simulation platform will leverage the implementation and validation of the proposed use case.

Network occupation is another QoS dimension relevant to smart grids that was not addressed in this work. As future work, it would be interesting to integrate network occupation as another constraint in our model. The proposed QoS based event stream processing approach can be associated with a language for describing complex event composition with related QoS. This will also be studied in future works.

## ACKNOWLEDGMENT

This work was carried out as part of the SOGRID project ([www.so-grid.com](http://www.so-grid.com)), co-funded by the French agency for Environment and Energy Management (ADEME) and developed in collaboration between participating academic and industrial partners.

## REFERENCES

[1] O. Epal, C. Collet, and G. Vargas, "Towards a Quality of Service Based Complex Event Processing in Smart Grids," in Proceedings of the 5<sup>th</sup> International Conference

on Smart Grid, Green Communication and IT Energy-aware Technologies (ENERGY). International Academy, Research and Industry Association, May 2015, pp. 1–4.

[2] G. Cugola and A. Margara, "Raced: An adaptive middleware for complex event detection," in Proceedings of the 8<sup>th</sup> International Workshop on Adaptive and Reflective Middleware, ser. ARM '09. New York, NY, USA: ACM, 2009, pp. 5:1–5:6.

[3] "Homepage of Esper," 2015, URL: <http://esper.codehaus.org/> [accessed: 2015-03-27].

[4] "Homepage of TIBCO StreamBase," 2015, URL: <http://www.streambase.com/> [accessed: 2015-03-27].

[5] D. Gyllstrom, E. Wu, H.-J. Chae, Y. Diao, P. Stahlberg, and G. Anderson, "SASE: complex event processing over streams," in Proceedings of the 3<sup>rd</sup> Biennial Conference on Innovative Data Systems Research (CIDR), 2007, pp. 407–411.

[6] "Homepage of Oracle CEP," 2015, URL: <http://www.oracle.com/> [accessed: 2015-03-26].

[7] A. J. Demers, J. Gehrke, B. Panda, M. Riedewald, V. Sharma, and W. M. White, "Cayuga: A general purpose event monitoring system." in Proceedings of the 5<sup>th</sup> Biennial Conference on Innovative Data Systems Research (CIDR). [www.cidrdb.org](http://www.cidrdb.org), January 2007, pp. 412–422.

[8] D. Luckham, "Rapide: A Language and Toolset for Simulation of Distributed Systems by Partial Orderings of Events," Stanford University, Tech. Rep., 1996.

[9] O. Saleh and K.-U. Sattler, "Distributed complex event processing in sensor networks," in Proceedings of the 2013 IEEE 14<sup>th</sup> International Conference on Mobile Data Management - Volume 02, ser. MDM '13. IEEE Computer Society, June 2013, pp. 23–26.

[10] P. R. Pietzuch, B. Shand, and J. Bacon, "A framework for event composition in distributed systems," in Proceedings of the ACM/IFIP/USENIX International Conference on Middleware, ser. Middleware '03, vol. 2672. Springer-Verlag New York, Inc., 2003, pp. 62–82.

[11] "Storm: Distributed and fault-tolerant real-time computation," 2013, URL: <http://storm.incubator.apache.org/> [Accessed: 2015-11-10].

[12] S. Behnel, L. Fiege, and G. Mühl, "On quality-of-service and publish-subscribe," in Proceedings of the International Conference on Distributed Computing Systems, 2006, pp. 1–6.

[13] S. Appel, K. Sachs, and A. Buchmann, "Quality of service in event-based systems," in Proceedings of the CENTRAL EUROP Workshop (CEUR), vol. 581, 2010, pp. 1–5.

[14] Y.-h. Jeon, "QoS Requirements for the Smart Grid Communications System," Journal of Computer Science and Network Security, vol. 11, no. 3, 2011, pp. 86–94.

[15] W. Sun, X. Yuan, J. Wang, D. Han, and C. Zhang, "Quality of Service Networking for Smart Grid Distribution Monitoring," in Proceedings of the 1<sup>st</sup> IEEE International Conference on Smart Grid Communications, 2010, pp. 373–378.

[16] H. Gjermundrød, D. E. Bakken, C. H. Hauser, and A. Bose, "GridStat: A flexible QoS-managed data dissemination framework for the power grid," IEEE Transactions on Power Delivery, vol. 24, no. 1, 2009, pp. 136–143.

- [17] W. Wang, Y. Xu, and M. Khanna, "A survey on the communication architectures in smart grid," *Computer Networks*, vol. 55, no. 15, Oct. 2011, pp. 3604–3629.
- [18] Smart Grid Coordination Group, "Smart grid reference architecture," 2012, URL: <http://ec.europa.eu/> [accessed: 2015-03-27].
- [19] G. Cugola and A. Margara, "Processing flows of information: From data stream to complex event processing," *ACM Computing Surveys*, vol. 44, no. 3, 2012, pp. 15:1–15:62.
- [20] L. Perrochon, W. Mann, S. Kasriel, and D. C. Luckham, "Event Mining with Event Processing Networks," pp. 474–478, 1999.
- [21] G. Sharon and O. Etzion, "Event-processing network model and implementation," *IBM Systems Journal*, vol. 47, no. 2, 2008, pp. 321–334.
- [22] "Event processing glossary version 2.0," 2011, URL: <http://www.complexevents.com> [accessed: 2015-03-27].
- [23] P. T. Eugster, P. A. Felber, R. Guerraoui, and A.-M. Kermarrec, "The many faces of publish/subscribe," *ACM Computing Surveys*, vol. 35, no. 2, 2003, pp. 114–131.
- [24] G. V. Chockler and R. Vitenberg, "Group Communication Specifications : A Comprehensive Study," *ACM Computing Surveys*, vol. 33, no. 4, 2001, pp. 427–469.
- [25] A. Malekpour, A. Carzaniga, G. T. Carughi, and F. Pedone, "Probabilistic FIFO Ordering in Publish/Subscribe Networks," in *Proceedings of the 10<sup>th</sup> International Symposium on Network Computing and Applications*. Ieee, augst 2011, pp. 33–40.
- [26] "Homepage of JaCoP," 2015, URL: <http://jacop.osolpro.com> [accessed: 2015-03-26].

# Map-Cache Synchronization and Merged RLOC Probing Study for LISP

Vladimír Veselý, Ondřej Ryšavý

Department of Information Systems

Faculty of Information Technology, Brno University of Technology (FIT BUT)

Brno, Czech Republic

e-mail: {ivesely, rysavy}@fit.vutbr.cz

**Abstract**—Locator/Id Separation Protocol is alternative routing paradigm, which tries to solve limitations (cumbersome support of mobility, multihoming, inbound traffic engineering, renumbering and rapid growth of default-free zone routing tables) of traditional TCP/IP routing model. The presented work deals with a map-cache synchronization and merged RLOC probing, which are outlined and evaluated as possible solutions improving performance and reducing the overhead of LISP. The proposed extension is evaluated using simulation model built for OMNet++ tool.

**Keywords**-LISP; VRRP; map-cache synchronization; RLOC probing; OMNet++

## I. INTRODUCTION

This paper extends our previous work published in [1] and [2]. We refined implementation of previously developed simulation modules; we designed and investigated two merged RLOC algorithms; and we conducted new measurements.

**Locator/ID Separation Protocol (LISP)** development started after IAB Workshop in 2006 as a response to problems described in RFC 4984 [3] and RFC 6227 [4]. LISP should reduce default-free zone (DFZ) routing table growth, stop prefix deaggregation, allow easier multihoming and mobility without the Border Gateway Protocol (BGP). LISP can be deployed transparently without any changes needed for hosts or domain-name system (DNS). LISP is agnostic to any network protocol and support not only IPv4 and IPv6 but any other future protocol operating on L3. LISP provides communication with the legacy non-LISP world because transition mechanism is an integral part of LISP specification. Nevertheless, the enterprise is always skeptical and slow when adopting a new technology. Hence, it is a great research challenge to investigate LISP features using modeling and simulation as the referential testbed tools producing meaningful outcomes.

IP address functionality is dual. It serves for identification (“which device is it?”) and localization (“where is the device?”) purposes. The consequence of this overloading is the inability to build scalable and long-term effective DFZ routing system. The main idea behind LISP is to remove this duality so that there are networks doing routing either based on locators (i.e., transit networks like DFZ) or identifiers (i.e., edge end networks). LISP accomplishes this by splitting the IP addresses into two distinct namespaces:

- **Endpoint Identifier (EID)** namespace (so called LISP site), where each device has unique address;
- **Routing Locator (RLOC)** namespace with addresses intended for localization. There is also a non-LISP namespace where direct LISP communication is (even intentionally) not supported.

Apart from namespaces, there also exist: a) specialized routers (called **tunnel router** a.k.a. **xTR**) spanning between different namespaces; b) dedicated devices maintaining mapping system; and c) proxy routers allowing communication between LISP and the non-LISP world).

A LISP mapping system performs lookups to retrieve a set of RLOCs for a given EID. Tunnel routers between namespaces utilize these EID-to-RLOC mappings to perform map-and-encapsulation (see RFC 1955 [5]). The original (inner) header (with EIDs as addresses) is encapsulated by a new (outer) header (with RLOCs as addresses), which is appended when crossing borders from EID to RLOC namespace. Whenever a packet is crossing back from RLOC to EID namespace, the packet is decapsulated by stripping outer header off. Figure 1 shows LISP architecture components including xTRs.

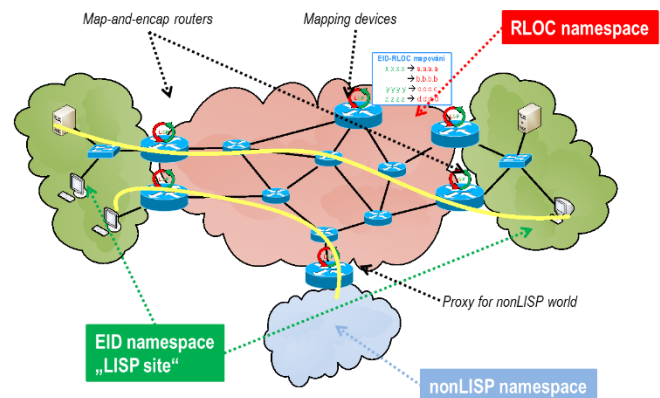


Figure 1. LISP reference model

Queries performing EID-to-RLOC mapping are data-driven. This behavior means that a new data transfer between LISP sites may require a mapping lookup, which causes that data dispatch is stopped until a mapping is retrieved. This behavior is analogous to the DNS protocol and allows LISP to operate a decentralized database of EID-to-RLOC mappings.

Replication of the whole (potentially large-scale) database is unnecessary because mappings are accessed on-demand, just like as in DNS a host does not need to know complete domain database. Tunnel routers maintain **map-cache** of recently used mappings to improve a performance of the system.

LISP is being successfully deployed in enterprise networks, and one of its most beneficial use-cases is for data-centers networking. An important feature of any data center is its ability to maintain high-availability of provided services. This goal is accomplished mainly with redundancy. In the case of the outage, service delivery is not affected because of redundant links, devices and power sources. **Virtual Router Redundancy Protocol (VRRP)** is among related protocols and technologies guaranteeing redundancy and helping to achieve high-availability.

VRRP is widely adopted protocol providing redundancy of default gateway (a crucial L3 device that serves as exit/entry point to a given network). VRRP is IETF's response for Cisco's proprietary Hot Standby Routing Protocol (HSRP) and Gateway Load Balancing Protocol (GLBP) delivering same goals. VRRP combines redundant first hop routers into virtual groups. One master router forwards clients' traffic within each group, where backup routers are checking master's liveness ready to substitute it. Switching to a new active router is transparent from the host's perspective thus no additional configuration or special software is needed.

The Automated Network Simulation and Analysis (ANSA) project aims to develop a variety of RFC-compliant simulation models to provide researchers and network administrators with a reliable verification tool. This paper provides more detail description of implemented and further refined simulation models, which create a part of the ANSA project and which extend the functionality of the INET framework version 2.4 in OMNeT++.

This paper has the following structure. The next section describes the design of relevant LISP and VRRP models. Section III deals with a map-cache synchronization mechanism – how synchronization works, how it is implemented and how it should aid devices to run LISP and VRRP simultaneously. Section IV presents validation scenarios for outlined implementations and shows promising results backing up improvement's impact on LISP operation. The paper is summarized in Section V together with the unveiling of our plans.

## II. IMPLEMENTATION

### A. LISP – A Theory of Operation

LISP is being codified within IETF [6]. The main core and functionality are described in RFCs 6830-6836.

LISP supports both IPv4 and IPv6. Moreover, LISP is agnostic to address family thus it can seamlessly work with any upcoming network protocol. Transition mechanisms are part of the protocol standard. Hence, LISP supports communication with the legacy non-LISP world. LISP places additional UDP header succeeded by LISP header between inner and outer header. LISP uses reserved port numbers – 4341 for data traffic and 4342 for signaling.

Basic components of the LISP architecture are **Ingress Tunnel Router (ITR)** and **Egress Tunnel Router (ETR)**. Both are border devices between EID and RLOC space; the only difference is in which direction they operate. The single device could be either ITR-only or ETR-only or ITR and ETR at the same time (thus abbreviation xTR). ITR is the exit point from EID space to RLOC space, which encapsulates the original packet. This process may consist of querying mapping system followed by updating local map-cache, where EID-to-RLOC mapping pairs are stored for a limited time to reduce signaling overhead. ETR is the exit from RLOC space to EID space, which decapsulates packet. Outer header, auxiliary UDP, and LISP headers are stripped off. ETR handles registering all LISP sites (their EID addresses) and by which RLOCs they are accessible. If we inspect structure of LISP packet somewhere in RLOC space then:

- Inner header source IP = sender's EID address;
- Inner header destination IP = receiver's EID address;
- Outer header source IP = ITR's RLOC address;
- Outer header destination IP = ETR's RLOC address.

LISP mapping system consists of two components – **Map Resolver (MR)** and **Map Server (MS)**. Looking for EID-to-RLOC mapping is an analogous process as DNS name resolution (see Figure 2). In the case of DNS, the host asks its DNS resolver (configured within OS) which IP address belongs to a given FQDN. DNS server responds with a cached answer or delegates the question recursively or iteratively to another DNS server according to the name hierarchy. For LISP, querier is ITR that needs to find out, which RLOCs could be used to reach a given EID. ITR has preconfigured MR, which is bothered each time mapping is needed. Just as in the case of DNS, mapping queries are data-driven. This means that data transfer between LISP sites initiates mapping process and data itself are postponed until a mapping is discovered. Map-cache on each ITR holds only those records that are actively needed for ongoing traffic.

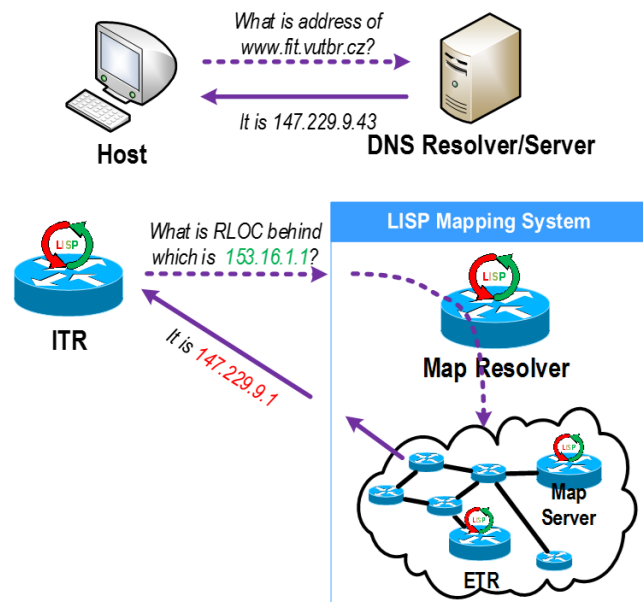


Figure 2. Comparison between DNS and LISP mapping system

The list below contains all LISP control messages responsible for mapping systemsignalization.

- *LISP Map-Register* – Each ETR announces LISP site(s) to the map server utilizing this message. Each registration contains authentication data and the list of mappings and their properties.
- *LISP Map-Notify* – UDP cannot guarantee message delivery. The map server may optionally (when the proper bit is set) confirm a reception of *LISP Map-Register* with this message.
- *LISP Map-Request* – ITR generates this request whenever it needs to discover current EID-to-RLOC mapping and sends a message to preconfigured MR.
- *LISP Map-Reply* – This is a solicited response from the mapping system to the previous request and contains all mappings of RLOCs to a certain EID together with their attributes. Each ITR has its map-cache where the reply information is stored for a limited time and used locally to reduce the signalization overhead of mapping system. Moreover, the mapping system generates *LISP Negative Map-Reply* as a response whenever a given identifier is not the EID, and thus proxy routing for non-native LISP communication must occur.

A map resolver processes ITR’s *LISP Map-Requests*. Either the map resolver responds with *LISP Negative Map-Reply* if queried address is from a non-LISP world (not EID), or *LISP Map-Requests* is delegated further into a mapping system to the appropriate map server.

Every map server maintains **mapping database** of LISP sites that are advertised by *LISP Map-Register* messages. If the map server receives *LISP Map-Request* then: a) either the map server responds directly to querying ITR; or b) the map server forwards request towards designated ETR that is registered to a map server for the target EID. xTRs perform **RLOC probing** (checking of non-local locator liveness) in order to always use current information.

Each RLOC is accompanied by two attributes – priority and weight. **Priority** (one-byte long value in the range from 0 to 255) expresses each RLOC preference. The locator with the lowest priority is preferred for outer header address. Priority value 255 means that the locator must not be used for traffic forwarding. Incoming communication may be load-balanced based on the **weight** value (in the range from 0 to 100) between multiple RLOCs sharing the same priority. Zero weight means that RLOC usage for load-balancing depends on ITR preferences.

The following demonstration should help the reader to get more familiar with LISP data traffic. Figure 3 depicts two LISP sites (“Site A” using EID prefix 100.0.0.0/24 and “Site B” with prefix 200.0.0.0/24) that are interconnected via RLOC space composed of five ISP networks. PC-A with address 100.0.0.99 wants to perform unicast data transfer to PC-B with address 200.0.0.99. EIDs are transparent for hosts and end-stations do not concern about LISP routing. The steps necessary to complete this scenario are following:

- #1) DNS resolver returns EID as IP address associated with PC-B (e.g., pc.siteb.com A 200.0.0.99);

- #2) The packet traverses “Site A” until it reaches xTR-A2. This router acts as ITR and prepares appropriate outer header for encapsulation. RLOC is looked up in map-cache based on destination EID 200.0.0.99, and RLOC 4.0.0.1 is chosen due to the lowest priority;
- #3) Packet traverses RLOC space with 2.0.0.1 as source and 4.0.0.1 as destination RLOC in the outer header and with 100.0.0.99 as the source and 200.0.0.99 as destination EID in the inner header.
- #4) The packet is routed via ISPs until it reaches xTR-B2’s interface with address 4.0.0.1. This router performs decapsulation and forwards packet to “Site B” based on destination EID address;
- #5) The packet is delivered to PC-B having the same structure (single IP header, EIDs as addresses) as it was in #1. LISP functionality is transparent to end-point devices and non-LISP routers.

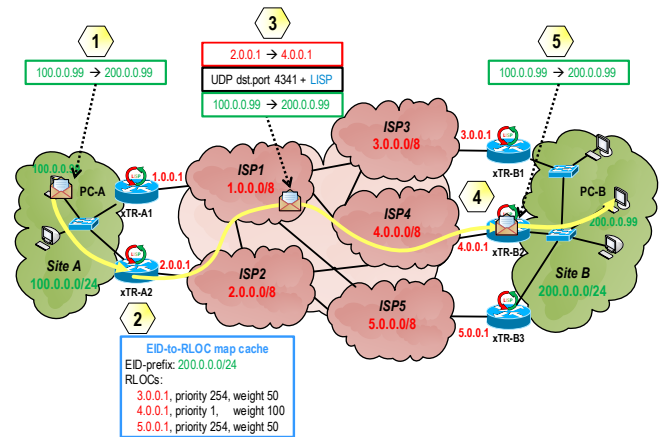


Figure 3. Illustrative LISP unicast data transfer

### B. LISP – Design of a Simulation Module

A simulation model of LISP xTR, MR and MS functionality is currently implemented as LISPRouting compound module. It consists of five submodules that are depicted in Figure 4 and described in Table I below. Implementation is in full compliance with definitions from RFC 6830 [7] and RFC 6833 [8].

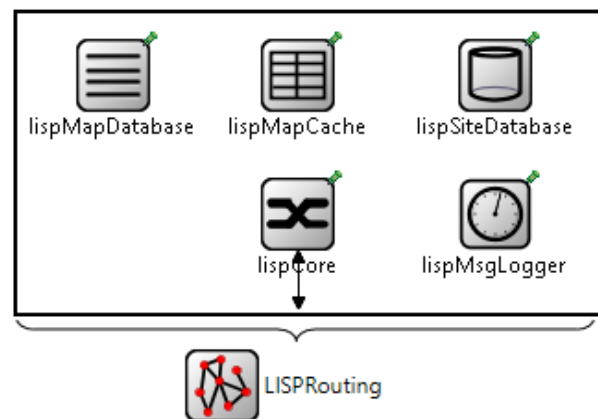


Figure 4. LISPRouting module structure

All LISP abstract data structures and settings can be configured statically (using XML file before simulation beginning). Map-cache and map/site database are implemented using generic class `LISPMapStorage` that is extended via C++ inheritance to accommodate different requirements of each control plane component. Every `LISPMapStorage` contains the ordered list of `LISPMapEntry` instances.

TABLE I. DESCRIPTION OF LISPRROUTING SUBMODULES

Name	Description
<code>lispCore</code>	The module handles LISP control and data traffic. It independently combines the functionality of ITR, ETR, MR and MS. This involves: encapsulation and decapsulation of data traffic; ETR site registration and MS site maintenance; ITR performing lookups; MR delegating requests.
<code>lispMapDatabase</code>	Each xTR maintains the configuration of its LISP sites (i.e., which RLOCs belong to a given EID or which local interfaces are involved in LISP) that is used by control-plane during registration or for RLOC probing.
<code>lispMapCache</code>	Local LISP map-cache that is populated on demand by routing data traffic between LISP sites. Each record (EID-to-RLOC mapping) has its separate handling (i.e., expiration, refreshment, availability of RLOCs).
<code>Lisp SiteDatabase</code>	MS's database that maintains LISP site registrations by ETRs. It contains site-specific information (e.g., shared key, statistics of registrars and most importantly known EID-to-RLOC mappings).
<code>lisp MsgLogger</code>	This module records and collects statistics about the LISP control plane operation, e.g., number, types, timestamps and length of messages.

### C. VRRP – Theory of Operation

VRRP specification is publicly available as RFC standard – RFC 3768 [9] describes IPv4-only VRRPv2 and RFC 5798 [10] describes dual IPv4+IPv6 VRRPv3. VRRPv2 routers send control messages to multicast address 224.0.0.18. VRRPv3 routers use ff02::12 for IPv6 communication. VRRP has its own reserved IP protocol number 112.

Clustered redundant routers form a VRRP group identified by **Virtual Router ID (VRID)**. Within the group, a single router (called **Master**) is elected based on announced **priority** (a number in the range from 1 to 255). Higher priority means a superior willingness to become Master, zero priority causes the router to abstain from being Master. In the case of equal priority, binary higher IP address serves as tie-breaker. VRRP election process is always preemptive (unlike to non-preemptive HSRP or GLBP). Preemption means that the router with the highest priority always wins to be the Master no matter whether the group already have other Master elected. Only Master actively forwards traffic. Remaining routers (called **Backups**) are just listening and checking for Master's keep-alive messages.

Hosts have configured virtual IP address as their default gateway. Only Master responds to *ARP Requests* for this IP. This IP address has assigned reserved MAC address –

00:00:5e:00:01:\$\$ for VRRPv2 and 00:00:5e:00:02:\$\$ for IPv6 (where \$\$ is VRID). Whenever VRRP group changes to a new Master, *ARP Gratuitous Reply* is generated in order to rewrite association between the interface and reserved MAC in CAM table(s) of switch(es). This allows transparent changing of Masters for hosts during the outage.

VRRP has only one type of control message – *VRRP Advertisement*. If Master is not elected, then, VRRP routers exchange advertisements to determine which one is going to be a new Master. If Master is already elected, then, only Master is sending *VRRP Advertisements* to inform Backup routers that it is up and correctly running. *VRRP Advertisement* is generated whenever advertisement timer (*AT*) expires (by default every 1 second). If this interval is set to a lower value, then, Master's failure is detected faster but protocol overhead increases. Master down interval (*MDI*) resets with each reception of an advertisement message. Backup, which expires the *MDI* sooner, becomes a new Master. Value of *MDI* depends on priority of each VRRP router according to (1). The highest (best) priority Backup times out first (because of the lowest *skew time*) and thus takes over role as a new Master before others.

$$MDI = 3 \times AT + \frac{skew\ time}{256 - priority} \quad (1)$$

### D. VRRP – Design of Simulation Module

VRRP version 2 is implemented as `VRRPv2` compound module connected with `networkLayer`. The module is a container for dynamically created instances of `VRRPv2VirtualRouter` during simulation startup. Each instance handles particular VRRP group operation on a given interface. Its structure is depicted in Figure 5, and a brief description of the functionality follows in Table II. Both modules together implement full-fledged VRRPv2 with the same finite-state machine (FSM) as in [9]. VRRP FSM's states *Init*, *Backup* and *Master* reflect VRRP router role and govern control message generation and processing.

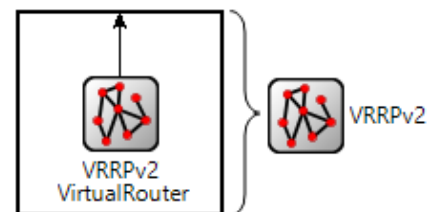


Figure 5. VRRP modules structure

TABLE II. DESCRIPTION OF VRRP MODULES

Name	Description
<code>VRRPv2</code>	Responsible for the creation of <code>VRRPv2VirtualRouters</code> according to the startup configuration and forwarding VRRP messages to/from them between appropriate gates.
<code>VRRPv2 VirtualRouter</code>	This module governs <i>VRRP Advertisements</i> processing, the transition between states and directs ARP for a single VRRP group.

### III. CONTRIBUTION

This section identifies our contribution that we made to LISP specification. The contribution consists of providing efficient solutions to two of LISP known problems, namely, Site-Based State Synchronization Problem and Locator Path Liveness Problem.

Assume multiple redundant routers are acting as first hops in the high-availability scenario like in Figure 6. Those routers are simultaneously clustered into VRRP groups and act as LISP's xTRs – they run LISP and VRRP at the same time. The performance of map-and-encap depends on the fact whether xTR's map-cache contains valid EID-to-RLOC mapping or not. Dispatched data traffic drives map-cache record creation. If map-cache misses the mapping, then, a mapping system needs to be asked, and initiating data traffic is meantime dropped. This fact is illustrated in Figure 6 for EID address y.y.y.y. On the one hand, packets (with y.y.y.y as destination) can traverse ITR1 without any problem (locator is present in map-cache) but on the other hand, same packets are discarded on ITR2, which misses the mapping. Packet dropping is a valid step as long as the mapping is not discovered because *map-and-encap* cannot occur without proper information. The rationale behind this behavior is the same as in the case of ARP throttling [11], where any triggering traffic should be discarded to protect control-plane processing and prevent superfluously recurrent mapping system queries.

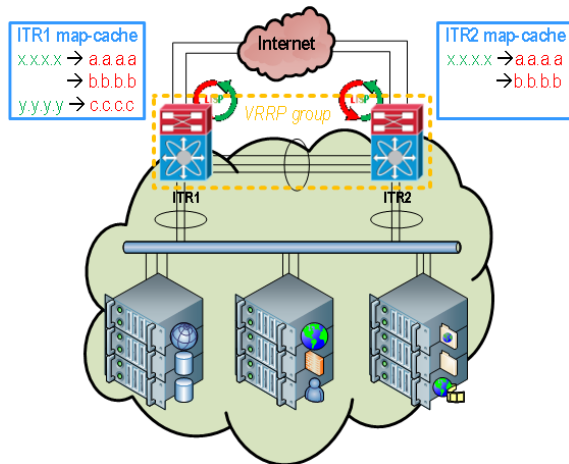


Figure 6. Site-Based State Synchronization Problem illustration

Each xTR has own map-cache, and its content may differ even within the same LISP site because different traffic may initialize various cache record. Hence, xTRs can easily experience severe packet drops and LISP control message storms due to the map-cache misses when Master change occurs within VRRP group. This is known as **Site-Based State Synchronization Problem**. If we have two or more redundant xTRs, then we want to reduce packet drops as much as possible during the intermittent phase of switching to a new active device. xTR outage leads to the off-site signaling storm (lots of *LISP Map-Request/Reply* messages being exchanged) and dispatching delay for ordinary traffic.

This problem is described as the one of LISP weak-points in [12] and theoretically investigated in [13]. The viable

solution would be to provide map-cache content synchronization that should minimize map-cache misses upon failure. We present our solution addressing this problem based on this assumption.

We have decided to implement it as a technique maintaining synchronized map-caches within a predefined **synchronization set (SS)** of ITRs. Any solicited *LISP Map-Reply* triggers synchronization process among SS members.

SS members are identified and reached using the IP address. Following strategies might be used when choosing appropriate SS member address:

- SS address comes from non-LISP world – Either IP address should be loopback or address of dedicated interconnection shared by all SS members. In the first case, unique device loopbacks need to employ additional routing. In the second case, the additional port for the dedicated connection is seldom available. Also, tracking of SS member needs additional LISP control plane updates;
- SS address comes from LISP world:
  - SS address is RLOC – SS membership is bound to the operability of a given RLOC interface, but this has negative implications for the situation, where xTR has more than one RLOC available. Although, it is easy to track SS member status using return value of RLOC probing;
  - SS address is EID – The best option reflecting LISP's ideology. EID as SS address should be reachable via direct routing (xTRs share common EID segment) or unless all RLOCs to this EID are down (which could be also used to track peer synchronization status).

Each record in the map-cache is equipped with a time-to-live (TTL) parameter. TTL expresses for how long the record is considered to be valid and usable for map-and-encap. By default, every record uses the same initial TTL value. Map-caches within SS must maintain the same TTL on shared records; otherwise, a loss of synchronization might occur (on some ITRs, identical records could expire because of no traffic demands). Either SS membership may be completely stateless, or SS member may maintain a state of its synchronization peers. This allows sending of partial synchronization updates. We have implemented two modes of synchronization:

- 1) *Naïve* – The whole content of map-cache is transferred to SS. All mappings are then updated according to the new content and TTLs are reset. This approach works fine, but it obviously introduces significant transfer overheads;
- 2) *Smart* – Only a record that caused synchronization is transferred. Moreover, we adhere to the following policy. When TTL expires, the ITR must check record usage during the last minute (one minute should be a period long enough to detect ongoing communication). If the mapping has not been used, then, it is removed from the cache. Otherwise, its state is refreshed in a query followed by the necessary data synchronization.

Both approaches guarantee that devices within SS could forward rerouted LISP data traffic without a packet loss because they share the same content as ITR's map-cache of the former Master device.

The proposed solution employing synchronization defines a new mechanism that introduces two new control messages (one carries synchronization data, another optionally acknowledges successful synchronization):

- *LISP CacheSync* – Message contains map-cache records that are being synchronized and authentication data protecting SS members from spoofed messages;
- *LISP CacheSync Ack* – Because LISP leverages UDP, it cannot guarantee message delivery. However, we decided to employ the same principle as for *LISP Map-Register* and *LISP Map-Notify*. Hence, *LISP CacheSync* delivery may be optionally confirmed by echoing back *LISP CacheSync Ack* message.

The following discussion explains the issues related to the reuse of existing LISP mechanism and advocates the proposed extension. The first approach would be to alter existing *LISP Map-Requests* by forcing included map-reply record field to contain more than one record. However, this approach is unreliable because it lacks acknowledgment scheme. The second approach would be to leverage so-called **Solicit-Map-Request (SMR)**. SMR is a mechanism how ETRs may rate-limit requests and notify ITRs about mapping change. When mapping changes, ETR starts to send *LISP Map-Request* (with the SMR-bit set) to ITRs with which it recently exchanged data. Then, ITR generates SMR-invoked *LISP Map-Request* to discover new mapping. If we want to use SMR to push new mappings into ITR's map-cache, then the best way seems to be extending the functionality of MR (see [13]). However, this approach yields significant off-site signalization.

**Locator Path Liveness Problem** concerns whether a destination locator is reachable via a particular source locator. This ensures the existence of bi-directional connectivity between a given pair of locators. A problem relevant to LISP is depicted in , where *xTR-A1* asks for "Site B" locators. In this case, two locators are available (1.0.0.1 and 2.0.0.1). *xTR-A1* chooses the second one as a destination address for packets. If the link between *ISP1* and *ISP2* goes (un)intentionally down, 2.0.0.1 is not reachable anymore, and *xTR-A1* must somehow find out this fact.

The simple method for Locator Path Liveness detection does not scale well in large networks because the reachability of every destination locator must be probed against every source locator of a given device. Complexity of such a task is generally  $O(n \times m)$ , where  $n$  is a number of source and  $m$  a number of destination locators. However, instead of brute-force probing some hints might be used to mitigate (but not to avoid) such complexity, e.g., piggybacking, timeouts, knowing of underlying routing, or positive feedback from control protocol messages.

To make Locator Path Liveness Problem even more complicated, let us imagine a situation when the LISP site has two or more ITRs with different destination locator reachability. One ITR has connectivity, and another has not

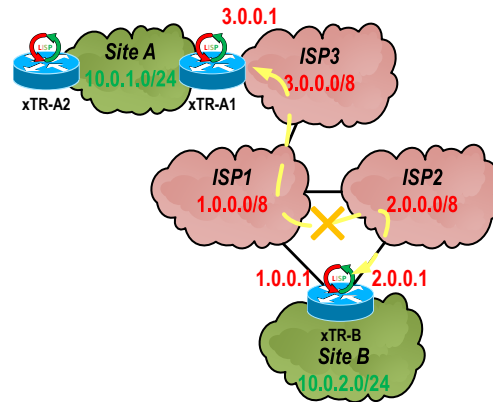


Figure 7. Locator Path Liveness Problem illustration

(e.g., *xTR-A1* and *xTR-A2* on ). Hence, all packets processed by that ITR is going to be discarded somewhere in topology. Because of LISP transparency, neither routing protocol nor hosts have capabilities to detect this issue and inform LISP devices accordingly.

In order to find a remedy for this problem, we focused on the behavior of Cisco referential implementations and their RLOC probing algorithm checking locator reachability. ITR is probing assigned locators for each configured EID. This is in compliance with [7], but it leads to repeated check of the same locator multiple times, which represents a significant overhead larger networks.

We decided to reduce protocol overhead by merging EIDs to check locator liveness with single RLOC probe that we call **merged RLOC probing**. This method is based on the following assumption: "If the same locator is reachable for one EID then it would also be reachable for other EID." Hence, the router can generate only one RLOC probe during a single liveness checking period. If it receives a positive *LISP Map-Reply Probe*, it may consider probed locator as alive for all EIDs in map-cache that are using it. More sophisticated approach is to perform the following steps:

- 1) On the sender side, check liveness of a given locator with a single *LISP Map-Request Probe* containing one or more query records. Each query record specifies cached EID that uses probed RLOC;
- 2) On the receiver side, respond with *LISP Map-Reply Probe* that includes locator status updates for all queried EIDs contained in request (or only subset of those EIDs that are in up state);
- 3) Back on the sender, refresh a locator status of relevant EIDs in map-cache according to answer(s) in reply.

Above described mechanism is compatible with RFC description and does not need any protocol extensions. Yet, it preserves the accuracy of Cisco's RLOC probing algorithm but with only single RLOC probe exchanged.

We have integrated all above described algorithms – *Cisco's, Simple* and *Sophisticated* – in our LISP simulation module and perform their evaluation as described further.

#### IV. TESTING

In this section, we provide information regarding: a) validation of LISP and VRRP simulation models (the goal

is to build reliability of implemented simulation models); and b) evaluation of map-cache synchronization and merged RLOC probing (the goal is to show the impact of deployed techniques on LISP operation).

Validation is based on the comparison (i.e., message order and timestamps) of behavior with the referential implementation. Therefore, we have built exactly the same real network topologies as for simulations. We captured and analyzed relevant messages exchanged between devices for both LISP and VRRP functionality. We compared the results with the behavior of an implementation running on Cisco routers (namely C7200 with IOS version c7200-adventerprisek9-mz.152-4.M2) and host stations.

A. LISP Functionality

We have verified LISP implementation on the topology depicted in Figure 8. Simulation network contains two sites – green areas “Site A” (interconnected by switch S1, bordered by xTR\_A1 and xTR\_A2) and “Site B” (interconnected by S2, bordered by xTR\_B1 and xTR\_B2). The topology contains router MRMS, which acts as MR and MS for both sites. IPv4 only capable core (red area) is simulated by a single Core router. Static routing is employed to achieve mutual connectivity across the core. HostA and HostB are dual-stack devices, where HostA is scheduled to ping HostB after second successful site registration (at t=70s). MRMS is allowed to proxy-reply on mapping requests for “Site A”. All RLOCs are configured with priority 1 and weight 50 to achieve equal load balancing for incoming traffic.

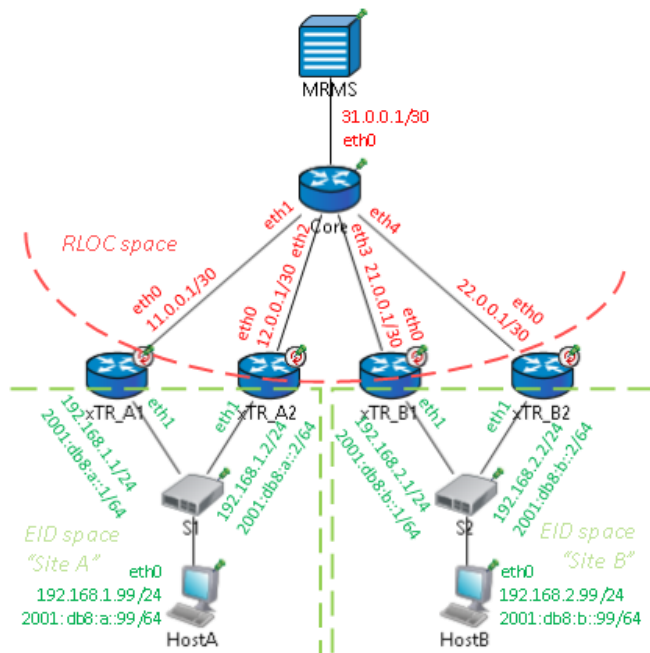


Figure 8. LISP testing topology

Testing scenario beginning is aligned with initialization of xTR\_A1’s LISP process that freshly starts after the reboot. The list of important phases is briefly described below:

- #1) First of all, each ETR starts RLOC probing, which is a polling mechanism that checks the reachability of announced locators. Each ETR sends *LISP Map-Request* with a probe-bit set on to queried RLOC address (e.g., xTR\_A1 is probing xTR\_A2’s locator 12.0.0.1). Neighboring xTR\_\* then responds with *LISP Map-Reply* with probe-bit set announcing a state of its RLOC interface. This process repeats by default every minute. The lower RLOC probe timer is, the sooner RLOC outage is detected but protocol’s overhead increases. Also, Cisco’s LISP implementation queries same RLOC for each assigned EID.
- #2) ETRs send registration about their EID sites towards MS. Each xTR\_\* generates *LISP Map-Register* message. Registration process repeats every 60 seconds in order to keep mappings up-to-date. *LISP Map-Register* contains all EID-to-RLOC mapping properties (i.e., EID, TTL, RLOC statuses, and attributes). For phase #2 illustration, Figure 9 shows xTR\_B1’s “Site B” registration after #1.

```

SiteDatabase (std::list<LISPSite>)
├── SiteDatabase[2] (LISPSite)
│   └── [1] = Site B, key: "HesloB"
│       Maintained EIDs>
│       192.168.2.0/24
│       2001:db8:b::/64
│       Registered ETRs>
│       ETR 21.0.0.1, last at: 60.000018339999
│       2001:db8:b::/64, expires: 86460.000018339999, state: c
│       21.0.0.1 (up) pri/wei=1/50 Local
│       22.0.0.1 (up) pri/wei=1/50
│       192.168.2.0/24, expires: 86460.000018339999, state: c
│       21.0.0.1 (up) pri/wei=1/50 Local
│       22.0.0.1 (up) pri/wei=1/50
    
```

Figure 9. xTR\_B1’s registration of "Site B"

- #3) HostA initiates ping to HostB’s address 2001:db8:b::99. *ICMP Echo Request* is delivered to xTR\_A1 (hosts default gateway), where it triggers LISP query because that particular EID-to-RLOC mapping is currently unknown. The first ping is dropped due to that. xTR\_A1 sends *LISP Map-Request* to MS. MRMS performs a lookup on its site database and delegates request to one of the designated ETRs, in this case, xTR\_B1. xTR\_B1 responds with *LISP Map-Reply* with current mapping (two RLOCs 21.0.0.1 and 22.0.0.1 belong to EID 192.168.2.0/24). Figure 10 illustrates this result.

```

MappingStorage (std::list<LISPMapEntry>)
├── MappingStorage[2] (LISPMapEntry)
│   [0] = <unspec>/0, expires: never, state: incomplete, action: send-map-request
│   [1] = 2001:db8:b::/64, expires: 86470.000085239999, state: complete, action: no-action
│       21.0.0.1 (up) pri/wei=1/50
│       22.0.0.1 (up) pri/wei=1/50
    
```

Figure 10. Content of xTR\_A1’s map-cache after phase #3

- #4) The second ping arrives on xTR\_A1. Because the mapping is known, it is encapsulated with an outer

header as LISP carrying data (marked *LISP Data* message) and sent to one of  $xTR\_B^*$  after random selection of equally preferred locators. In our case, *LISP Data* is delivered to  $xTR\_B2$  where original ping is decapsulated and forwarded further to end destination.  $HostB$  responds with *ICMP Echo Reply* that is passed to its default gateway ( $xTR\_B1$ ). Over here the same process as in #4 repeats – ping is dropped, and mapping query triggered. Only this time, MS replies directly to *LISP Map-Request*. MRMS is allowed to send *LISP Map-Reply* instead of designated ETR because of proxy-reply for “Site A”. Figure 11 shows the result.

```

MappingStorage (std::list<LISPMapEntry>)
├── MappingStorage[2] (LISPMapEntry)
│   ├── [0] = <unspec>/0, expires: never, state: incomplete, action: send-map-request
│   └── [1] = 2001:db8::/64, expires: 86472.000160199999, state: complete, action: no-action
│       ├── 11.0.0.1 (up) pri/wei=1/50
│       └── 12.0.0.1 (up) pri/wei=1/50

```

Figure 11. Content of  $xTR\_B1$ 's map-cache after phase #4

#5) Third and other consecutive pings pass without experiencing any drop because both default gateways have proper EID-to-RLOC mappings.

Phases of LISP operation are compared to simulation and real network in Table III. For clarity and due to limited space, only some messages are recorded for #1, #2 and #3. Nevertheless, omitted messages do not show significant deviations.

TABLE III. TIMESTAMP COMPARISON OF LISP MESSAGES

Phase	Message	Sender	Simul. [s]	Real [s]
#1	<i>LISP Map-Req. Probe</i>	$xTR\_A1$	0.000	0.000
	<i>LISP Map-Rep. Probe</i>	$xTR\_A2$	0.000	0.063
#2	<i>LISP Map-Register</i>	$xTR\_A1$	60.000	60.567
#3	<i>ICMP Echo Request</i>	HostA	70.000	70.000
	<i>LISP Map-Request</i>	$xTR\_A1$	70.000	70.361
	<i>LISP Map-Reply</i>	$xTR\_B1$	70.000	70.460
#4	<i>ICMP Echo Request</i>	HostA	72.000	71.931
	<i>LISP Data</i>	$xTR\_A1$	72.000	71.944
	<i>ICMP Echo Reply</i>	HostB	72.000	71.962
	<i>LISP Map-Request</i>	$xTR\_B1$	72.001	72.852
	<i>LISP Map-Reply</i>	MRMS	72.001	72.889
#5	<i>ICMP Echo Request</i>	HostA	74.000	74.011
	<i>ICMP Echo Reply</i>	HostB	74.001	74.177

### B. VRRP Functionality

We have verified VRRP functionality on the topology depicted in Figure 12. Simulation network contains two VRRP routers (GW1 and GW2) clustered in VRID 10. A single switch (SW) interconnects devices on the local segment. Host (Host) and router (ISP) pair substitute communication outside LAN. Both VRRP routers are configured with the default priority, default AT value and virtual default-gateway IP address set to 192.168.10.254.

For this test, we scheduled that original Master (GW2) would go down (at  $t=20s$ ) and back up (at  $t=30s$ ). Meantime, Host starts pinging (at  $t=10s$ ) Internet address 33.33.33.33 every second where traffic goes via virtual default

gateway. Scenario beginning (phase #1 at  $t=0s$ ) is aligned with initialization of VRRP process.

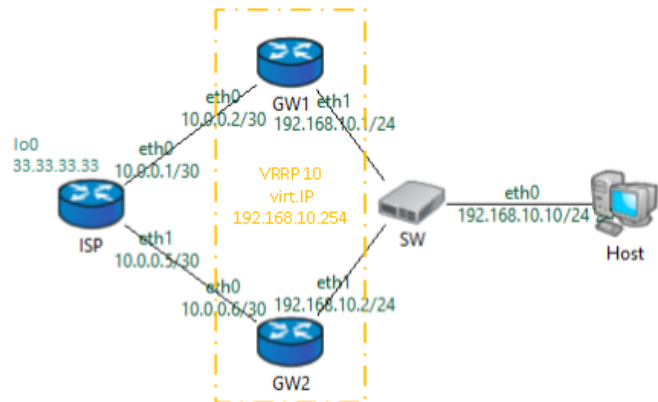


Figure 12. VRRP testing topology

Test goes through following phases:

- #1) Both GW1 and GW2 immediately transit from *Init* state to *Backup* and are waiting to hear *VRRP Advertisement* from potential Master.
- #2) They both expire *MDI* at the same time ( $t=3.609275$ , equation (1) yields the same result) and transit to *Master* state. This allows them to send their own *VRRP Advertisement* and discover each other. They compare announced properties in advertisement with their own VRRP settings. GW2 becomes a new Master. Despite having same priority (value 100), GW2 address 192.168.10.2 is higher.
- #3) If Host wants to ping 33.33.33.33, then, the traffic needs to go via default-gateway and Host requests IP-to-MAC mapping with the help of *ARP Request*. The message is delivered to GW1 and GW2, but only GW2 responds with *ARP Reply* because it is Mater. Subsequently, endless ping passes through GW2.
- #4) GW2 failure occurs, and GW1 seizes to receive *VRRP Advertisements*. GW1's *MDI* expires and next GW1 becomes a new Master sending its own *VRRP Advertisements*. But before that, GW1 sends *ARP Gratuitous Reply* in order to change CAM of SW. Meantime, pings are being dropped since moment of failure until GW1 is elected.
- #5) Pings pass through SW towards GW1 and ISP.
- #6) GW2 goes up and transits after *MDI* from *Init* to *Backup*. Then, GW2 transits from *Backup* to *Master* state. GW2 sends its own *VRRP Advertisement*, which is superior to ones from GW1, and *ARP Gratuitous Reply* for virtual default-gateway 192.168.10.254. Immediately when GW1 hears GW2's advertisement, GW1 abdicates for being Master router and transits to *Backup* state.

The comparison between timestamps and message confluence can be observed in Table IV.

TABLE IV. TIMESTAMP COMPARISON OF VRRP MESSAGES

Phase	Message	Sender	Simul. [s]	Real [s]
#2	VRRP Advertisement	GW1	3.609	3.612
	VRRP Advertisement	GW2	3.609	4.367
	VRRP Advertisement	GW2	4.609	5.286
#3	ARP Request	Host	10.000	10.000
	ARP Reply	GW2	10.000	10.034
	ICMP Echo Request	Host	10.000	10.986
#4	VRRP Advertisement	GW1	23.219	23.655
	ARP Gratuitous Reply	GW1	23.219	23.643
#6	VRRP Advertisement	GW2	33.718	33.612
	ARP Gratuitous Reply	GW2	33.718	33.611

Please notice that Cisco's VRRP implementation sends two *ARP Gratuitous Replies* before any VRRP advertisement. After we had observed this, we implemented another FSM in our VRRP module to accommodate this behavior. However, the routing outcome from Host perspective is same no matter on chosen FSM.

### C. Impact of Map-Cache Synchronization

There are two goals behind the following test. The first one is to show the impact of synchronization on a packet drop rate and map-cache misses. The second one is to enumerate the burden of deploying map-cache synchronization on the control plane. A scenario is focused on cache misses due to the missing mapping rather than expired ones because of default TTL (1 day). Five minutes time slot with the single VRRP Master outage is the simplest illustration of how to compare the impact of map-cache synchronization.

We prepared simulation topology that contains a single LISP site with two routers ( $xTR1$  and  $xTR2$ ), which provide highly-available VRRP default-gateway for two hosts interconnected by switch SW. Host1 and Host2 are pinged IPv4 EIDs (172.16.[0-19].0/24) randomly thus generating traffic that triggers LISP mapping system queries. All routing is done statically. Hence, there is no need to employ routing protocol on Core router. We prepared special  $xTR$  called  $xTR\_Responder$  that: a) registers destination EIDs; and b) responds to hosts ICMP messages. The whole topology is depicted in Figure 13.

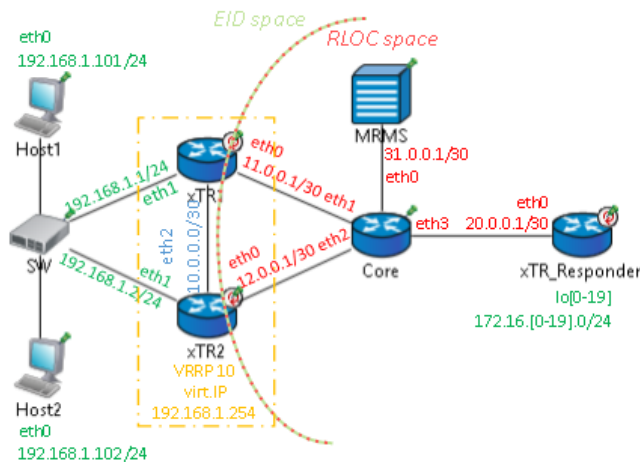


Figure 13. LISP testing topology for map-cache synchronization

During the outage, all  $xTR1$ 's interfaces shutdown (i.e., they are physically disconnected from the network). Yet, the  $xTR1$ 's control plane is operational – generating scheduled LISP messages that are not being delivered. We scheduled following phases for the test run:

- #1) At first, all  $xTRs$  register their EIDs. In the case of  $xTR\_Responder$ , EID space is modeled with the help of loopback interfaces – twenty of them ranging with addresses from 172.16.0.0/24 to 172.16.19.0/24 reachable via single RLOC 20.0.0.1. In case of  $xTR1$  and  $xTR2$ , EID 192.168.1.0/24 is reachable via two RLOCs 11.0.0.1 and 12.0.0.1.
- #2)  $xTR1$  and  $xTR2$  form VRRP group with VID 10 and virtual address 192.168.1.254, which is used by Host1 and Host2 as default-gateway.  $xTR1$  is Master because of higher priority ( $xTR1$  has 150,  $xTR2$  only 100) as long as it is operational.
- #3) Host1 starts pingging ten random EIDs in range from 172.16.0.0/24 to 172.16.9.0/24. Because EIDs are chosen randomly, they may be duplicate. Each first ICMP packet causes mapping query and is dropped.
- #4) Then,  $xTR1$  failure occurs right before a new LISP registration (at  $t=119s$ ). Hosts traffic is diverted to a new VRRP Master, which is  $xTR2$ .
- #5) After #4, also Host2 starts to ping ten random EIDs from 172.16.10.0/24 to 172.16.19.0/24. Same duplicity rule as in #3 applies.
- #6)  $xTR1$  recovers from the outage at  $t=235s$  and once again all hosts traffic goes through it.

Depending on map-cache synchronization type, additional map-cache misses might occur.  $xTR1$  and  $xTR2$  synchronized themselves via their RLOCs (11.0.0.1 for  $xTR1$  and 12.0.0.1 for  $xTR2$ ).

The scenario has been tested with three simulation configurations each representing different map-cache synchronization technique:  $\alpha$ ) no synchronization at all (default LISP behavior);  $\beta$ ) *naïve* mode; and  $\gamma$ ) *smart* mode. Impact on map-cache is summarized in Table V for all previously mentioned different configuration runs. Fewer map-cache misses are considered better.

We do not employ LISP synchronization acknowledgment scheme for  $\beta/\gamma$ -runs, the impact of acks is analyzed later. The scenario offers testing of all three kinds of addressed for SS member identification – e.g., nonLISP with 10.0.0.0/30; RLOC with 11.0.0.1 and 12.0.0.1; and EID with 192.168.1.1 and 192.168.1.2) with same results. Nevertheless, we use EIDs as the most feasible options. Before interpreting the results, please note that Host1 randomly (using same seeds for all three runs) chose eight different EIDs, Host2 six EIDs, totally fourteen distinct ping destinations.

TABLE V. MAP-CACHE MISSES IN SCENARIO WITH ONE OUTAGE

Phase	$\alpha$ cache misses		$\beta$ cache misses		$\gamma$ cache misses	
	$xTR1$	$xTR2$	$xTR1$	$xTR2$	$xTR1$	$xTR2$
#3	8	0	8	0	8	0
#5	0	14	0	6	0	6
#6	14	0	0	0	0	0
<b>Total</b>	22	14	8	6	8	6

Without any synchronization, traffic diversion to a new VRRP Master always causes misses due to unknown mappings. We can see this in phases #5 and #6 for  $\alpha$ -run, when the router starts to dispatch LISP data with the empty map-cache.

If the synchronization is employed, then, only new destinations lead to map-cache miss. This is because a new VRRP Master already has mappings discovered by neighbor  $xTR$ . Hence, there is a difference in phase #5 for  $\alpha$ -run (empty cache) and  $\beta/\gamma$ -runs (cache in sync with SS member).  $\beta$ - and  $\gamma$ -runs are equal in the number of cache misses, but  $\gamma$ -run is more effective in protocol overhead. The difference (36 cache misses versus 14) would be even more significant in the case of multiple VRRP Master outages. Please note that every map-cache miss is also connected with the data packet drop.

In order to compare synchronization modes, we conducted measurement taking into account all LISP control messages processed by `lispCore` module, namely their packet sizes. We assume that larger size is always a greater burden for router's control plane processing. Figure 14 shows the results ( $\alpha$ -run = blue crosses,  $\beta$ -run = green triangles,  $\gamma$ -run = red circles), where each symbol represents one LISP control message.

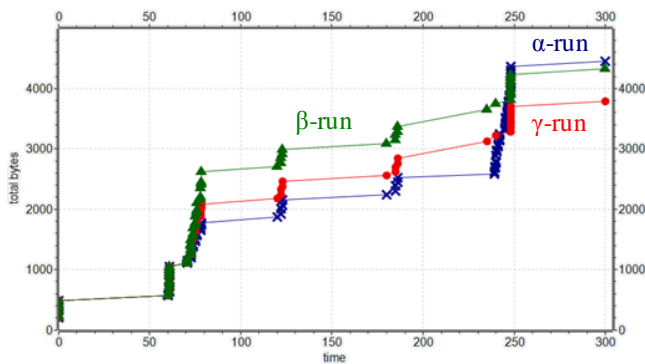


Figure 14.  $xTR1$ 's LISP control messages occurrence and total processed byte size in scenario with single outage

We can see that *smart* outperforms *naïve* because it is less intensive while only single mapping is transferred during synchronization, not a whole map-cache. Moreover, both synchronization modes are better than no synchronization on protocol overhead because they decrease the number of mapping queries (i.e., exchanged messages count). The difference is not that significant on Figure 14, especially between naïve and no sync mode. However, it is getting more obvious as the number of VRRP outages increases. Following table and figure prove this claim for the same topology but with two  $xTR1$  outages – phases #4 and #6 repeat twice.

TABLE VI. MAP-CACHE MISSES IN SCENARIO WITH TWO OUTAGES

Phase	$\alpha$ cache misses		$\beta$ cache misses		$\gamma$ cache misses	
	$xTR1$	$xTR2$	$xTR1$	$xTR2$	$xTR1$	$xTR2$
#3a	8	0	8	0	8	0
#5a	0	14	0	6	0	6
#6a	14	0	0	0	0	0
#5b	0	0	0	0	0	0
#6a	14	0	0	0	0	0
<b>Total</b>	<b>36</b>	<b>14</b>	<b>8</b>	<b>6</b>	<b>8</b>	<b>6</b>

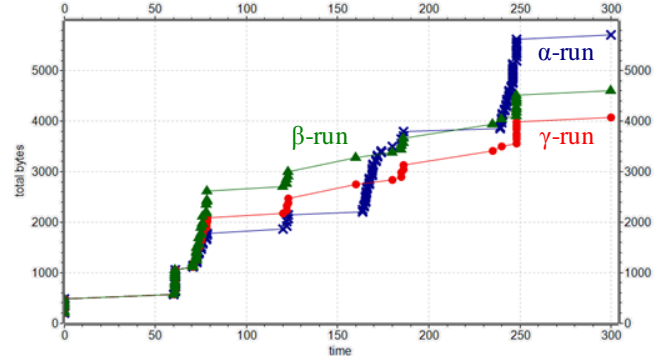


Figure 15.  $xTR1$ 's LISP control messages occurrence and total processed byte size in scenario with two outages

Repetition of phases 4), 5) and 6) is denoted in Table VI with letters: “a” for the first outage; and “b” for the second outage. In Table VI, we can observe that a total number of cache misses for  $\alpha$ -run has increased by 14.  $xTR1$  had gone down (losing its map-cache content), then went back (repopulating map-cache once again with 14 EIDs) and then this cycle repeats once again. For  $\beta$ -run and  $\gamma$ -run, additional outages pose no change, because  $xTR1$  completely synchronizes itself with  $xTR2$  ( $xTR2$  sends the whole map-cache as soon as it detects the status of the one of  $xTR1$ 's RLOCs up), when it is once again operational. Figure 15 shows an increase in a number of processed LISP control message for no synchronization, where impacts of other synchronization techniques remain same.

LISP synchronization acknowledgment mechanism poses an additional control plane burden. In order to evaluate acknowledgment impact, we conducted measurement on the same topology with two outages. The results in a number of processed LISP control messages bytes are depicted in Figure 16 and can be compared with Figure 14.

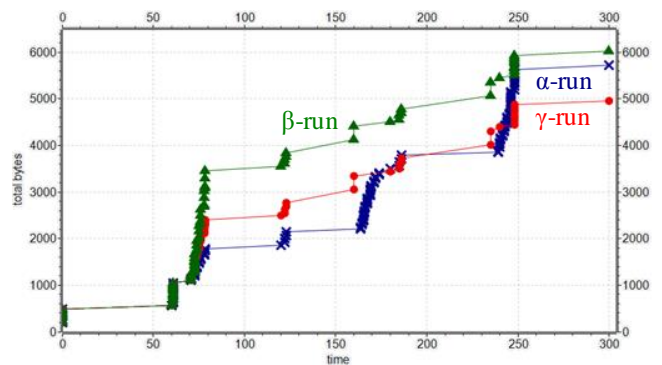


Figure 16.  $xTR1$ 's LISP control messages occurrence and total processed byte size in scenario with two outages + acknowledgments

It is apparent that protocol overhead on the number of messages has increased. In the case of no synchronization, it slightly outperforms naïve mode by a total size of processed bytes. However, the smart mode still has the best characteristic even with enabled acknowledgments. Once again, we can expect that additional outages or more EID ping destinations would influence results in favor of  $\beta/\gamma$ -runs over  $\alpha$ -run (see Figures 17 and 18).

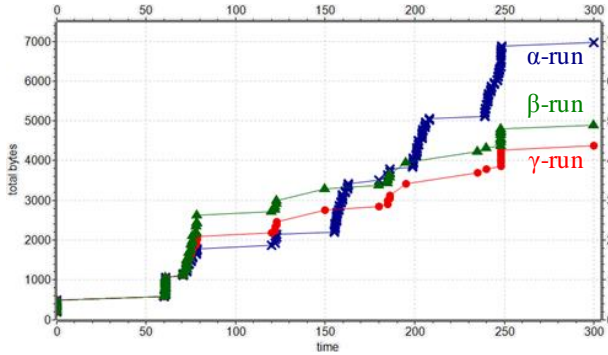


Figure 17. xTR1’s LISP control messages occurrence and total processed byte size in scenario with three outages

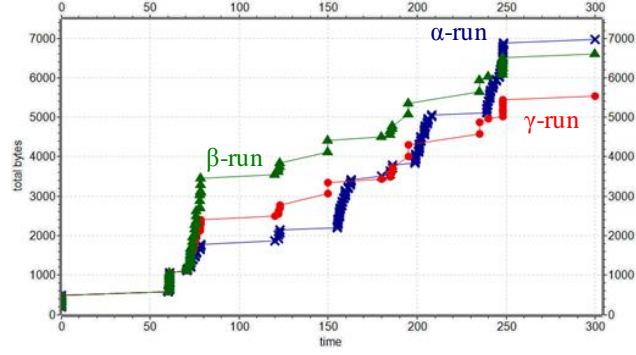


Figure 18. xTR1’s LISP control messages occurrence and total processed byte size in scenario with three outages with ack

TABLE VII. xTR1’S STATISTICS FOR DIFFERENT MAP-CACHE SYNCHRONIZATION SCENARIOS

single xTR1 outage scenario									single xTR1 outage with sync ack scenario								
α			β			γ			α			β			γ		
miss	cnt	size	miss	cnt	size	miss	cnt	size	miss	cnt	size	miss	cnt	size	miss	cnt	size
22	81	4 458	8	62	4 328	8	62	3 796	22	81	4 458	8	71	5 458	8	71	4 394
two xTR1 outages scenario									two xTR1 outages with sync ack scenario								
α			β			γ			α			β			γ		
miss	cnt	size	miss	cnt	size	miss	cnt	size	miss	cnt	size	miss	cnt	size	miss	cnt	size
36	109	5 718	8	63	4 614	8	63	4 082	36	109	5 718	8	73	6 030	8	73	4 966
three xTR1 outages scenario									three xTR1 outages with sync ack scenario								
α			β			γ			α			β			γ		
miss	cnt	size	miss	cnt	size	miss	cnt	size	miss	cnt	size	miss	cnt	size	miss	cnt	size
50	137	6 978	8	64	4 900	8	64	4 368	50	137	6 978	8	75	6 602	8	75	5 538

Table VII summarizes the evaluation of map-cache synchronization techniques. The table shows  $\alpha/\beta/\gamma$ -run (i.e., none, *naïve* and *smart* sync) statistics for different scenarios (one/two/three outage(s) with or without acknowledgment). xTR1’s statistic numbers are depicted with following column meanings: “miss” as the number of map-cache miss occurrence; “cnt” as the total count of LISP control plane messages sent and received; “size” as processed messages count by LISP control plane measured in total byte size. We added to Table VII also same statistics section for a scenario with three outages in order to analyze trends. Results show a linear growth in complexity.

D. Impact of Merged RLOC Probing

The goal of the following subsection is to measure the impact of merged RLOC probing on control plane processing.

We took the previous topology and adjusted it; see the result in Figure 19. Currently, it contains a LISP site with just one xTR router and one end-device called Host1. More important are LISP sites that are reachable via xTR\_Responder1 and xTR\_Responder2. We simulate multiple EID networks reachable via the same xTRs with the help of loopback interfaces. Each xTR\_Responder has forty loopbacks with EID addresses in the range of 172.16.[0-39].0/24. Each EID is being registered towards MRMS as reachable via xTR\_Responder1’s RLOC 21.0.0.1 and xTR\_Responder2’s RLOC 22.0.0.1. VRRP functionality on xTR is disabled because it is not needed for this scenario. Host1 might randomly generate ICMP traffic towards destination EIDs, but this is not necessary for merged RLOC

probing analysis. All communicating parties are interconnected via Core employing static routing configuration.

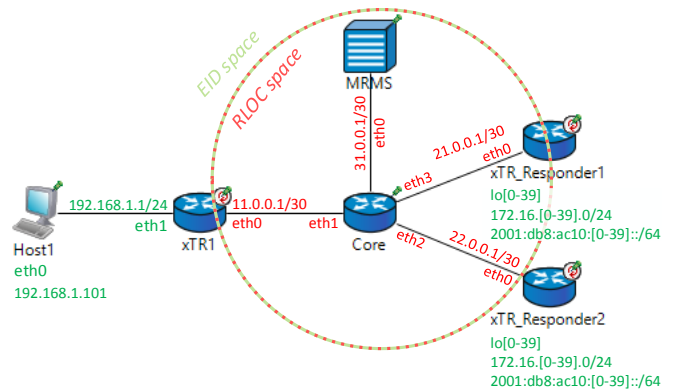


Figure 19. LISP testing topology for merged RLOC probing

RLOC probing starts immediately after LISP routing control plane is initialized. Following phases occur no matter on used RLOC probing algorithm:

- #1) Probing xTR sends *LISP Map-Request Probe* to RLOC address for a given set of EIDs;
- #2) Probed xTR responds with *LISP Map-Reply Probe* announcing that RLOC is up;
- #3) In case that *LISP Map-Request Probe* was not replied, probing xTR repeats the probe at time  $t_{next} = t_{last} + 2^{numOfRetries}$ , where  $t_{last}$  is the last time probe was sent and  $numOfRetries$  is number of retry attempts to send this probe. After by default three

unsuccessful *LISP Map-Request Probe*, mark RLOC as down and schedule next probe after 60 seconds.

Optional phase #3) behavior is solely based on Cisco implementation observations. Also Cisco's LISP implementation has some other specifics: a) postponed start of first EID registration ( $t + 60$  seconds since control plane initialization); b) postponed start of RLOC probing for IPv6 RLOCs ( $t + 30$  since the first IPv4 probe). We have integrated this behavior into the LISP simulator. However, we are not employing it in order to provide better readability of this scenario's results.

Those phases repeat by default every minute in order to keep RLOC reachability up-to-date. This interval could be decremented to a lower value, but protocol overhead increases in an inverse relationship.

Measurement is focused on a number of *LISP Map-Request/Reply Probes* exchanged between *xTR\_Responder1* and *xTR\_Responder2* and the amount of corresponding bytes processed by *xTR\_Responder1*'s LISP control plane. We assume that five minutes simulation time is a period long enough to show the trend of each RLOC probing algorithm. During this period, five RLOC probe batches occur. Except mandatory EID registrations, no other LISP control traffic is spoiling the results.

We have conducted two simulation scenarios in order to observe complexity trends. The first one is for the topology with forty different EIDs (twenty IPv4 172.16.[0-19].0/24 and twenty IPv6 2001:db8:ac10:[0-19]::/64) on *xTR\_Responders* reachable via RLOCs 21.0.0.1 and 22.0.0.1, the second with eighty different EIDs (forty IPv4 172.16.[0-39].0/24 and forty IPv6 2001:db8:ac10:[0-39]::/64). All three algorithms are evaluated separately as different configuration simulation runs - Cisco's default algorithm as  $\delta$ -run, simple as  $\epsilon$ -run and sophisticated as  $\lambda$ -run algorithm variants of merged RLOC probing.

TABLE VIII. XTR\_RESPONDER1'S STATISTICS FOR DIFFERENT RLOC PROBING ALGORITHM SCENARIOS

40 EIDs scenario					
$\delta$		$\epsilon$		$\lambda$	
cnt	size	cnt	size	cnt	size
805	55 500	25	8 520	25	28 530
80 EIDs scenario					
$\delta$		$\epsilon$		$\lambda$	
cnt	size	cnt	size	cnt	size
1 605	110 900	25	15 920	25	56 330

Total count of sent and received LISP control messages are shown in Table VIII with following meaning of columns: "cnt" as the total count of LISP control plane messages sent and received; "size" as the amount processed messages by LISP control plane measured in total byte size.

Apart from five *LISP Map-Register*, *xTR\_Responder1* five times: a) sends *LISP Map-Request Probe* and receives *LISP Map-Reply Probe*; b) receives *xTR\_Responder2*'s probes and responds to them with replies. It is apparent that count of exchanged messages is drastically lower when using any merged RLOC probing algorithm. Cisco's algorithm generates RLOC probe for each EID-to-RLOC mapping,

which means forty/eighty *LISP Map-Request Probe* and forty/eighty *LISP Map-Reply Probe* messages per single phases #1 and #2 occurrences. Opposite to that any merged RLOC algorithm exchanges only single *LISP Map-Request/Reply Probe* pair between *xTR\_Responders*.

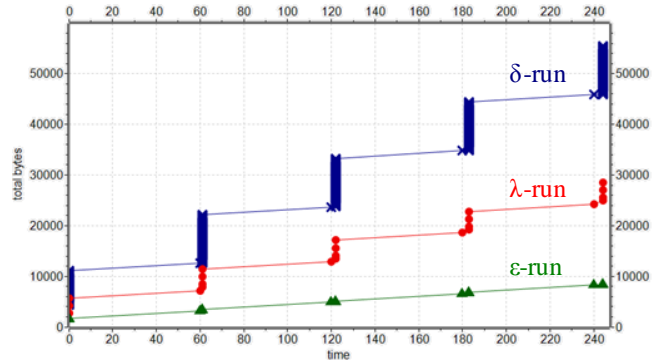


Figure 20. xTR1's LISP control messages occurrence and total processed byte size in scenario with two outages

In Figure 20, we can see that *simple* algorithm ( $\epsilon$ -run = green triangles) has the lowest protocol overhead measured in the total amount of bytes processed by *xTR\_Responder1*. This is because each probe carries only single EID chosen in a round-robin fashion, where successful reception of *LISP Map-Reply Probe* refreshes RLOC state for all EIDs that are using it. In case of *sophisticated* algorithm ( $\lambda$ -run = red circles), all relevant EIDs are packed in a single probe, thus, (significantly) increasing its size but still half of Cisco's ( $\delta$ -run = blue crosses) total processed byte size. On the other hand, *simple* merged RLOC probing algorithm might seem to be too simple and lacking of accuracy if we want the use-case where the same RLOC is up for some EIDs, and down for another EIDs. In that case, *sophisticated* variant offers the same functionality but with better granularity. Because scenarios are linearly dependent, the only difference between forty and eighty EIDs scenario graphs is in Y-axis values and a higher amount of RLOC probe (symbol) occurrences.

## V. CONCLUSION

In this paper, we presented a detailed description of LISP and VRRP technologies. We proposed and tested two LISP improvements - map-cache synchronization and merged RLOC probing - aimed to achieve a better routing performance (primarily in high-availability use-cases).

We evaluated proposed improvements using newly implemented models in OMNeT++ simulator tool. Validation of these models against a real-life topology shows the acceptable precision in terms of time accuracy. However, simulation results are affected by a simpler simulated control-plane (without any potential processing delay of the real router). Hence, some simulation timestamps in Table III and IV are below one millisecond difference.

Previously, LISP map-cache performance have been evaluated employing high-level simulation that is not taking into account protocol implementation specifics [14]. Hence, one of the goals of our work was to provide the community

with a simulation tool with a near-real implementation behavior. Results from simulations show that deployment of map-cache synchronization techniques has a positive impact on data packet-loss and a total number of map-cache misses. Moreover, synchronization decreases LISP signaling overhead (i.e., no need to query mapping system for forgotten map-cache entries). *Smart* mode map-cache synchronization yields the best results.

We investigated Cisco's RLOC probing algorithm used to verify locator reachability. Cisco's algorithm has disputable scalability mostly because of periodical polling. We developed two new RLOC probing variants that aim to be more efficient (even though they still use polling). Simulation tests show that both of them significantly reduces the number of exchanged *LISP Map-Reply/Request Probes*, thus reducing LISP protocol overhead. *Sophisticated* merged RLOC probing algorithm provides the same reliability as Cisco's version, but it utilizes only the half of Cisco's bandwidth in bytes processed by the control plane.

Among our plans with further investigation of LISP is to add support for proxy xTR functionality and recognize more LISP control flags (like SMR bits). We would like to use further our LISP simulation modules and test effectiveness of different distributed mapping systems (e.g., LISP-ALT, LISP-DDT). Also, we would like to upgrade VRRP to support IPv6 addresses and all features of VRRP version 3.

All source codes could be downloaded from GitHub repository [15]. Real packet captures and simulation datasets for the results reproduction could be investigated from Wiki of the repository mentioned above. More information about ANSA project is available on its homepage [16].

#### ACKNOWLEDGMENT

This work was supported by following organizations and research grants:

- FIT-S-14-2299 supported by Brno University of Technology;
- IT4Innovation ED1.1.00/02.0070 supported by Czech Ministry of Education Youth and Sports.

#### BIBLIOGRAPHY

- [1] V. Veselý and O. Ryšavý, "Locator/Id Split Protocol Improvement for High-Availability Environment," in ICNS 2015 - Proceedings of 11th Conference on Networking and Services, pp. 61-67, Rome, Italy, 2015.
- [2] V. Veselý, M. Marek, O. Ryšavý and M. Švéda, "Multicast, TRILL and LISP Extensions for INET," International Journal On Advances in Networks and Services, vol. 7, no. 3&4, pp. 240-251, 2014.
- [3] D. Meyer, L. Zhang and K. Fall, "RFC 4984: Report from the IAB Workshop on Routing and Addressing," September 2007. [Online]. Available: <http://tools.ietf.org/html/rfc4984>. [Accessed 6<sup>th</sup> December 2015].
- [4] T. Li, "RFC 6227: Design Goals for Scalable Internet Routing," May 2011. [Online]. Available: <http://tools.ietf.org/html/rfc6227>. [Accessed 6<sup>th</sup> December 2015].
- [5] R. Hinden, "RFC 1955: New Scheme for Internet Routing and Addressing (ENCAPS) for IPNG," June 1996. [Online]. Available: <http://tools.ietf.org/html/1955>. [Accessed 6<sup>th</sup> December 2015].
- [6] IETF, "Locator/ID Separation Protocol (lisp)," 15<sup>th</sup> September 2015. [Online]. Available: <http://datatracker.ietf.org/wg/lisp/charter/>. [Accessed 15<sup>th</sup> September 2015].
- [7] D. Farinacci, V. Fuller, D. Meyer and D. Lewis, "RFC 6830: The Locator/ID Separation Protocol (LISP)," January 2013. [Online]. Available: <http://tools.ietf.org/html/rfc6830>. [Accessed 6<sup>th</sup> December 2015].
- [8] V. Fuller and D. Farinacci, "RFC 6833 - Locator/ID Separation Protocol (LISP) Map-Server Interface," January 2013. [Online]. Available: <https://tools.ietf.org/html/rfc6833>. [Accessed 6<sup>th</sup> December 2015].
- [9] R. Hinden, "RFC 3768: Virtual Router Redundancy Protocol (VRRP)," April 2004. [Online]. Available: <https://tools.ietf.org/html/rfc3768>. [Accessed 6<sup>th</sup> December 2015].
- [10] S. Nadas, "RFC 5798: Virtual Router Redundancy Protocol (VRRP) Version 3 for IPv4 and IPv6," April 2010. [Online]. Available: <https://tools.ietf.org/html/rfc5798>. [Accessed 6<sup>th</sup> December 2015].
- [11] R. Froom, E. Frahim and B. Sivasubramanian, CCNP Self-Study: Understanding and Configuring Multilayer Switching, Cisco Press, 2005.
- [12] D. Saucez, O. Bonaventure, L. Iannone and C. Filsfils, "LISP ITR Graceful Restart," December 2013. [Online]. Available: <https://tools.ietf.org/html/draft-saucez-lisp-ittr-graceful-03>. [Accessed 6<sup>th</sup> December 2015].
- [13] D. Saucez, J. Kim, L. Iannone, O. Bonaventure and C. Filsfils, "A Local Approach to Fast Failure Recovery of LISP Ingress Tunnel Routers," NETWORKING 2012, vol. 7289, no. ISBN: 978-3-642-30044-8, pp. 397-408, May 2012.
- [14] J. Kim, L. Iannone and A. Feldmann, "A deep dive into the LISP cache and what ISPs should know about it," NETWORKING 2011, vol. 6640, no. ISBN: 978-3-642-20756-3, pp. 367-378, 2011.
- [15] GitHub, "kvetak/ANSA," December 2013. [Online]. Available: <https://github.com/kvetak/ANSA/wiki>. [Accessed 6<sup>th</sup> December 2015].
- [16] Brno University of Technology, "ANSA Wiki | Main / HomePage," January 2014. [Online]. Available: <http://nes.fit.vutbr.cz/ansa/pmwiki.php>. [Accessed 6<sup>th</sup> December 2015].



[www.iariajournals.org](http://www.iariajournals.org)

**International Journal On Advances in Intelligent Systems**

🔗 issn: 1942-2679

**International Journal On Advances in Internet Technology**

🔗 issn: 1942-2652

**International Journal On Advances in Life Sciences**

🔗 issn: 1942-2660

**International Journal On Advances in Networks and Services**

🔗 issn: 1942-2644

**International Journal On Advances in Security**

🔗 issn: 1942-2636

**International Journal On Advances in Software**

🔗 issn: 1942-2628

**International Journal On Advances in Systems and Measurements**

🔗 issn: 1942-261x

**International Journal On Advances in Telecommunications**

🔗 issn: 1942-2601